Raimondo Manca
Sally McClean
Christos H Skiadas
Editors

New Trends in Stochastic Modeling & Data Analysis

ISAST 2015

New Trends in Stochastic Modeling and Data Analysis

Edited by

Raimondo Manca-Sally McClean-Christos H Skiadas

ISAST 2015

Raimondo Manca-Sally McClean-Christos H Skiadas
Editors

New Trends in Stochastic Modeling and Data Analysis

ISBN (print) 978-618-5180-06-5
ISBN (e-book) 978-618-5180-10-2

Preface

This is the first book devoted to the 3rd Stochastic Modeling Techniques and Data Analysis (SMTDA) International Conference held in Lisbon, Portugal, June 11-14, 2014. Revised and expanded forms of papers from the conference presentations are included.

SMTDA main objective is to publish papers, both theoretical or practical, presenting new results having potential for solving real-life problems. Another important objective is to present new methods for solving these problems by analyzing the relevant data. Also, the use of recent advances in different fields is promoted such as for example, new optimization and statistical methods, data warehouse, data mining and knowledge systems, computing-aided decision supports and neural computing.

The first Chapter includes papers on Asymptotic Analysis of Stochastic Systems with Complex Structure, whereas contributions on Markov and semi-Markov models are included in the second Chapter.
Papers on Clustering and Partitioning for particular cases are included in the third Chapter, and papers on Survival Analysis and Branching Processes are presented in the fourth Chapter.
Papers on Stochastics methods and techniques are presented in the fifth Chapter along with Data Analysis papers included in the sixth Chapter.
Chapter seven includes papers on Demography and Related Applications, whereas Stochastic Processes, Copulas and Actuarial Applications are analyzed in Chapter eight.

Many thanks to the authors for their contribution and our sincere thanks to the referees to their hard work and dedication in providing an improved book form. We acknowledge the valuable support of the SMTDA committees and the secretariat. We are happy for editing another book of the SMTDA series.

November 2015

Raimondo Manca, *"La Sapienza" University, Rome, Italy*

Sally McClean, *University of Ulster, UK*

Christos H Skiadas, *ManLab, Technical University of Crete, Chania, Greece*

Contents

1 CHAPTER

Asymptotic Analysis of Stochastic Systems with Complex Structure

On the Models and Methods Discussed in the Chapter "Asymptotic Analysis of Stochastic Systems with Complex Structure"

Ekaterina Bulinskaya

Department of Mathematics and Mechanics, Lomonosov Moscow State University, Moscow, Russia
(E-mail: ebulinsk@yandex.ru)

Abstract. The chapter under consideration consists of 4 papers. They are devoted to investigation of complex stochastic models arising in various applications of Probability Theory such as Queueing, Insurance, Computer Science, Particle Population Dynamics etc. We discuss below the models and methods used for investigation of their behavior.
Keywords: Asymptotics, Dividends, Front propagation, Lévy processes, Multi-channel queueing system, Optimization, Reinsurance, Stability, Stochastic boundedness, Synchronization, Unreliable servers.

1 Introduction

The chapter contains four papers. All of them are written by professors of Lomonosov Moscow State University and its alumni.

The common feature of the papers is the complex structure of the models under consideration. Moreover, the first and second papers treat the so-called input-output models. In the former case input is formed by customer arrivals and output is the flow of the served customers. In the latter case the premium inflow constitutes the system input whereas the policyholders indemnification and dividends represent the output. The third and fourth papers deal with particles evolution. In the former case this evolution is described by Lévy processes whereas in the latter case the underlying process is a branching random walk on a lattice. It is interesting to mention that the synchronization is used in the first and third papers, whereas the second and fourth papers deal with different types of operators.

2 Main part

Below we discuss each paper separately, stressing the methods used for investigation and their role in further research. Some unsolved problems are mentioned as well.

New Trends in Stochastic Modeling and Data Analysis (pp. 3-12)
Raimondo Manca - Sally McClean - Christos H Skiadas (Eds)

2.1 Queueing systems

The first paper is "Stability analysis of multi-server discrete-time queueing systems with interruptions and regenerative input flow" by L.G.Afanasyeva and A.Tkachenko. The authors consider a multi-channel system with heterogeneous unreliable servers and regenerative input flow.

The class of regenerative flows contains a vast collection of processes widely used in queueing theory. It includes, for example, Markov arrival process (MAP), Markov modulated process (MMP), semi-Markov modulated process (SMMP) and many others. We mention in passing that a doubly stochastic Poisson process with a random intensity is regenerative, hence, it is a member of this class as well.

Each server may suffer a breakdown and be repaired. It is supposed that breakdown epochs form a renewal process and the processes corresponding to different servers are independent and do not depend on the input flow. Different servers have different distributions of service times. Thus, the servers are heterogeneous from the reliability and service time view-points.

If a server is occupied at the time of breakdown the customer service is immediately interrupted. There exist various types of service discipline, after the server repair, treated e.g. in Gaver[17]. The most frequently used ones are *preemptive resume* service discipline and *preemptive repeat different* discipline. In the former case service continues after interruption whereas service is repeated from the start in the latter case. The service time after interruption is independent of the original service time. In the paper under consideration the second discipline is investigated. It is also supposed that all the random variables specifying the model (interarrival times, regeneration periods of the input flow, service times, the lengths of server on and off periods) have discrete distributions, possible values being $1, 2, \ldots$. In other words, a discrete-time queueing system is studied.

The main result of the paper is a necessary and sufficient condition for stochastic boundedness of the process describing the number of customers in the system. Note that, under assumption of general service distribution and introduced above service discipline, this condition cannot be expressed in terms of means of the random variables describing the system. Gaver[17] has established the same condition for a more simple model $M|G|1|\infty$ supposing additionally that the service availability time is exponentially distributed and the server breakdown can occur only during a customer service. Introduction of an important notion called completion time lets reduce the investigation of systems with interruption to the study of the classical $M|G|1|\infty$ system without interruptions.

The queueing systems with interruptions can model many real situations. The service interruption may be the result of resource sharing, servers breakdown or arrival of priority customer to be served immediately. There exit a lot of papers devoted to this subject. Thus, a survey of recent results in this domain can be found in Krishnamoorthy *et al.*[25]

The early works on queues with interruptions involved the use of integral equations and Laplace transforms. Later on, supplementary variable tech-

nique was employed, and models were analyzed with the help of Markov renewal theory, see, e.g., Pyke[43]. Introduction of phase-type distributions and matrix-analytic method by Neuts[39], [40] generalized Poisson/exponential assumptions of arrivals and service times for interruption models. More recently, Balcioglu *et al.*[8] approximated $GI|D|1$ queue with correlated server breakdowns and preemptive resume discipline by the corresponding system having the interruption process with (independent) hyper-exponentially distributed on-times and general off-times. Multiple servers queues with breakdowns are studied by Mitrany and Avi-Itzhak[32] and Neuts and Lucantoni[41]. Both contributions consider a Poisson arrival and breakdown processes and exponential service times.

Although systems with interruption are investigated since the middle of the last century, see, e.g., White and Christie[49], according to our knowledge, the stability conditions are not yet proved in general case. Such conditions are not straightforward, typically the queueing systems are not work-conserving and therefore not always stable when the server capacity exceeds the arrival load.

The sufficient conditions for stability of $GI|G|m|\infty$ system were established in Morozov *et al.*[38] under the following assumptions. All the servers have the same exponentially distributed service time and input flow is recurrent. As shown in the paper under consideration, this sufficient condition is wide away from the necessary one in many real situations.

A powerful approach to obtain stability conditions for systems with interruptions is synchronization method combined with the regenerative theory. In the paper by Afanasyeva and Bashtova[1] the coupling method was implemented for asymptotic analysis of the single-server system with a regenerative input. A similar approach was applied to study the stability condition of the multi-channel system with heterogeneous servers and a regenerative input flow in a random environment, see Tkachenko[48]. It was supposed that all servers get out of the order simultaneously.

The model treated in the paper by L.G.Afanasyeva and A.Tkachenko (this chapter) is characterized by new interesting features. It deals with a sufficiently general input flow, the servers are heterogeneous, the server may fail at any time, not only during the customer service, the on- and off-intervals, in each cycle, can be dependent.

Moreover, the authors concentrate on the conditions of stochastic boundedness of the process representing the total number of customers in the system. This lets obtain the estimate of system capacity, that is, the upper bound of input intensity providing the stochastically bounded queue. Such an approach allows to avoid the introduction of any additional suppositions.

Assumption of aperiodicity of all the renewal processes describing the model is quite natural since the investigation is based on the theory of discrete renewal processes. The main idea of the proofs is synchronization of renewal processes determining the system performance. The authors study the counting processes $N_i(t)$, $i = 0, 1, \ldots, m$, here $N_0(t)$ has unit jumps at the regeneration points of the input flow, whereas $N_i(t)$ jumps at times of the ith server breakdown. A synchronization point signifies that all these processes have a jump. It is established that intervals between two neighboring synchronization points have

a finite expectation. The process $Y(t)$ is the number of customers which could be served up to time t were the system never empty. The synchronization points are the regeneration points for the process $Y(t)$, since the service discipline is preemptive repeat different.

The traffic coefficient is the ratio of expectations of increments, on synchronization intervals, of input flow and process $Y(t)$. The numbers of customers in the system at synchronization times form an imbedded Markov chain. The Foster criterium lets establish that this chain is stochastically bounded if the traffic coefficient is less than 1. It follows immediately that the number of customers in the system is also stochastically bounded. If the imbedded Markov chain is irreducible and aperiodic then it is ergodic, hence by the Smith theorem one proves the stability of the process, that is, existence of the proper limit distribution. The stochastic unboundedness of the customers number in the system, for the traffic coefficient greater or equal to 1, is proved by construction of majorizing processes.

The sufficient conditions of system stability are established for the case of traffic coefficient less than 1. Some examples are also treated. The paper ends by discussion of the obtained necessary and sufficient condition of stochastic boundedness. It turned out that if the service time variance is greater than the square of its expectation, than under some additional assumptions the condition of stability for the case of preemptive repeat different service discipline is weaker than for the case of preemptive resume service discipline and visa verse. That means it is reasonable to interrupt sometimes the service and begin it once again to increase the system capacity. Here naturally arise some optimization problems.

2.2 Dividends and reinsurance

The second paper is "Optimization of Multi-Component Insurance System with Dividend Payments" by E.Bulinskaya and A.Muromskaya. It deals with optimization of insurance company performance in the framework of cost approach, see, e.g., Bulinskaya[13].

It is well known that since the seminal work of Lundberg[29] which appeared in 1903, the reliability (or safety) approach consisting in the study of ruin probability has dominated in actuarial sciences. The explanation is obvious, the primary goal of any insurance company is indemnification of the losses suffered by its policyholders.

However being a corporation insurance company has a secondary but very important goal, namely, payment of dividends to its shareholders. Hence, in 1957 de Finetti[16] proposed to deal with maximization of expected discounted dividends paid until the ruin time, thus introducing the cost approach. He used the barrier strategy for the simple model described by the random walk with jumps ± 1 and obtained the optimal dividend barrier. An interesting discussion of this model one can find in Gerber and Shiu[21], see also the monographs by Bühlmann[14] and Gerber[20].

The *barrier* strategy means that whenever the (modified) company surplus reaches a prescribed barrier $b > 0$ all the overflow is paid as dividends. It is

shown in Gerber[19] that barrier dividend payments form a complete family of Pareto-optimal dividends.

A natural generalization of the barrier strategy is a *threshold* one. To diminish the ruin probability one pays the dividends with a constant rate a (lesser then the rate of premium inflow) all the time the surplus is above a fixed threshold b. It is proved, see, e.g., Jeanblanc-Picqué and Shiryaev[22], that the barrier strategy is optimal in the class of threshold ones for a diffusion model. There also exists a possibility to choose several thresholds b_i and corresponding payment intensities a_i, see, e.g., Badescu *et al.*[7].

For a classical reserve process Gerber[18] has shown that optimal strategy can be found in the class of *band* strategies. Such a strategy is characterized by three sets A, B and C which partition the state space of the reserve process. Each set is associated with a certain dividend payment as follows: if the current surplus $x \in A$, then every incoming premium is paid out; if $x \in B$, then a lump sum is paid out moving the current reserve to the closest point in A that is smaller than x; if $x \in C$ then no dividend is paid.

We mention also the simple *impulse-type* strategy. One chooses two levels b_1 and b_2 with $0 \leq b_1 < b_2$ and uses the following rule for dividend payments: if the surplus is above or equal to b_2, then the amount $b_2 - b_1$ is paid out immediately; if the surplus is below b_2, nothing is done until the reserve reaches the level b_2 again. Such dividend strategies naturally arise in diffusion models with dividend transaction costs, as stated in Albrecher and Thonhauser[5].

The most frequently studied models are the classical Cramér-Lundberg model dealing with a compound Poisson process and its diffusion approximations. The rigorous description of dividend strategies can be found in a very useful survey by Albrecher and Thonhauser[4], see also references therein.

Recently, the models described by Lévy processes became very popular, see, e.g., Loeffen[27,28]. Furthermore, the optimality of barrier strategy was established for spectrally negative Lévy processes in Loeffen[26] and Yin and Wang[54].

Along with dividend strategy the control parameters of insurer are the initial company surplus and premium inflow rate. Moreover, nowadays reinsurance is a necessary condition for the stable performance of any insurance company notwithstanding its size. So, there appeared some papers dealing with dividends and reinsurance, see, e.g. Azcue and Muler[6], Karapetyan[24], Mnif and Sulem[33].

In contrast to these papers treating the excess of loss reinsurance with unlimited liability of reinsurer the paper by Bulinskaya and Muromskaya (this chapter) deals with the case of limited liability l. It is supposed that the claim process is a compound Poisson with claim amounts having exponential or uniform distribution. The authors study a barrier strategy, since it has already been proved that in the Brownian motion setting and in Cramér-Lundberg model (without reinsurance) with exponentially distributed claims an optimal dividend strategy is a barrier one, see, e.g., Loeffen[26].

The mathematical tools used for investigation are integro-differential and differential equations combined with optimization methods. Under a mild restriction that the dividend barrier is less than the retention level d an explicit

form of the optimal barrier b_l^* is obtained for exponential claim distribution. It is also proved that b_l^* is monotone decreasing in l and increasing in d. The conditions on the model parameters for validity of inequalities $0 < b_l^* < d$ are established as well.

For the uniform distribution under the similar assumptions it turned out that the optimal dividend barrier is equal to the initial company surplus. So the authors plan to study more general dividend strategies mentioned above. It will be reasonable to apply the stochastic dynamic programming, see, e.g., Scmidli[44].

2.3 Synchronization problems

The third paper "Multidimensional Synchronization Models Based on Lévy Processes" written by A.Manita is devoted to stochastic N-component synchronization systems $(x_1(t), \dots, x_N(t))$, $x_j \in \mathbb{R}^d$, whose dynamics is described by Lévy processes and synchronizing jumps.

The main idea of synchronization is the coordination of events to operate a system in unison. Synchronization models are very popular in physics, biology, data communication, as well as in various fields of mechanical and electrical engineering (see, e.g., Pikovsky *et al.*[42], Strogatz[46], Bertsekas and Tsitsiklis[9], Blekhman *et al.*[10]). Among these models there is a special class of multicomponent systems that are using a message passing mechanism (Jefferson and Witkowski[23]) to share information between interacting components. The first rigorous study of the message passing mechanism was presented in Mitra and Mitrani[31] for some 2-dimensional stochastic system. Nowadays, the multidimensional generalizations of this probabilistic model are of importance to different modern applications in computer science such as asynchronous argorithms, wireless networks, clock synchronization problem etc. (see, e.g., Sundararaman *et al.*[47] or Simeone *et al.*[45]).

The current paper significantly generalizes results of Manita[30]. It is proved that symmetric models reach synchronization in a stochastic sense: differences between components $d_{kj}^{(N)}(t) = x_k(t) - x_j(t)$ have limits in distribution as $t \to \infty$. Moreover, the paper contains conditions of existence of natural (intrinsic) space scales for large synchronized systems. The intrinsic space scales correspond to sequences $\{b_N\}$ such that $d_{kj}^{(N)}(\infty)/b_N$ converge in law as $N \to \infty$. This problem appears to be deeply related to asymptotic properties of the Lévy processes defining the free dynamics of components. The present study contributes much to the understanding of behavior of synchronization models with large number of components. The class of systems considered in this paper includes both Markov and non-Markov models and covers many important examples of one-component dynamics. Proofs are using advanced techniques related to domains of attraction of stable laws and to superposition of renewal processes. The model of the preceding paper Manita[30] being a system of N Brownian particles with synchronization admits the calculation of distribution of $d_{kj}^{(N)}(t)$ in an explicit form. It is not the case for non-Markov models of the present paper where results on the law of $d_{kj}^{(N)}(t)$ have a form of limit theorems as $t \to \infty$ and $N \to \infty$.

2.4 Particle population dynamics

The applications of spectral theory of convolution operators with multi-point perturbation to study of particle population dynamics are considered in the paper "The Propagating Front of Particle Population in Branching Random Walks" by S. Molchanov and E. Yarovaya. The paper extends the latest investigations of the authors (Molchanov and Yarovaya[34–37]) and their talks at the 3rd International Conference on Stochastic Modeling Techniques and Data Analysis (SMTDA 2014).

Continuous-time branching random walks with finite set of generation centers, sources of branching, on multidimensional lattices $\mathbf{Z}^d$ may be used as a model of particle population dynamics, see, e.g., Yarovaya[51]. The dynamics of such processes is usually described in terms of birth, death and walks of particles on the lattice. Continuous random trajectories on $\mathbf{R}^d$ were considered by Cranston *et al.*[15] in the context of the theory of phase transitions for homopolymers. The evolution of such processes depends on the structure of a medium and the spatial dynamics, see, e.g., Albeverio *et al.*[3], Bogachev and Yarovaya[11,12], Yarovaya[50] for details. The structure of the medium is defined by the offspring reproduction law at generation centers situated at the lattice points, as shown in Yarovaya[51].

These and some other models of branching random walks were primarily studied under assumption that the variance of random walk jumps is finite, see, e.g., Yarovaya[52] where phase transitions for various models of branching random walks depending on the lattice dimension were obtained.

The goal of this paper is to understand how the limiting behavior of the jump intensities, and in particular the "finiteness" of their variance, influences the properties of the branching random walk.

One of the first steps in this direction is undertaken in Yarovaya[52,53] where the branching random walk has infinite variance of jumps. The global limit theorems on the convergence of multidimensional random walks with heavy tails to stable state are obtained in Agbor *et al.*[2]. In the present paper the authors consider four classes of the intensities of jumps describing the behavior of a random walk. Namely, they deal with four types of tails: very light, subexponential, of moderate power and heavy. The limit structure of the particle population inside of the propagating front is determined by the properties of the underlying random walk, see, e.g., Molchanov and Yarovaya[34–37]. The key role in investigation of such structures plays the study of the Green function whose properties are closely related to the spectral properties of the operator determining the law of an underlying random walk. Using these results the limit structure of the particle population inside of the propagating front is investigated.

3 Conclusion

All the authors have enjoyed the participation in a well organized 3rd SMTDA conference and would like to thank the Editors for invitation to write the papers contained in this Chapter. We hope that this introductory paper has

also contributed to deeper understanding of the discussed problems, whereas the additional references (not pretending on completeness) will be useful for a reader interested in the investigation of complex systems.

Acknowledgement. The research was partially supported by RFBR grant 13-01-00653.

References

1. L. Afanasyeva and E. Bashtova. Coupling method for asymptotic analysis of queues with regenerative input and unreliable server. *Queueing Systems*, 76, **2**, 125–147, 2014.
2. A. Agbor, S. Molchanov and B. Vainberg. Global limit theorems on the convergence of multidimensional random walks to stable. *ArXiv.org e-Print archive, May* arXiv:1405.2487, 2014.
3. S. Albeverio, L. Bogachev, and E.Yarovaya. Asymptotics of branching symmetric random walk on the lattice with a single source. *Comptes Rendus de l'Academie des Sciences, Paris, series I.*, 326, 975–980, 1998.
4. H. Albrecher and S. Thonhauser. Optimality results for dividend problems in insurance. *Rev. R. Acad. Cien. Serie A. Mat.*, 103, 2, 295–320, 2009.
5. H. Albrecher and S. Thonhauser. Some remarks on an impulse control problem in insurance, Preprint, University of Lausanne, 2009.
6. P. Azcue and N. Muler. Optimal reinsurance and dividend distribution policies in the Cramér-Lundberg model. *Math. Finance*, 15, 2, 261308, 2005.
7. D.S. Badescu, S. Drekic and D. Landriault. On the analysis of a multi-threshold Markovian risk model. *Scand. Act. J.*, 4, 248–260, 2007.
8. B. Balcioglu, D. L. Jagerman, and T. Altiok. Approximate mean waiting time in a GI/D/1 queue with autocorrelated times to failures. *IIE Transactions*, 39, **10**, 985–996, 2007.
9. D. P. Bertsekas and J. N. Tsitsiklis. *Parallel and Distributed Computation: Numerical Methods*. Athena Scientific, Belmont, 1987.
10. I. I. Blekhman, A. L. Fradkov, O. P. Tomchina, and D. E. Bogdanov. Self-synchronization and controlled synchronization: general definition and example design. *Mathematics and Computers in Simulation*, 58, 4–6, 367–384, 2002.
11. L. Bogachev and E. Yarovaya. Moment analysis of a branching random walk on a lattice with a single source. *Doklady Akademii Nauk*, 363, 439–442, 1998.
12. L. Bogachev and E. Yarovaya. A limit theorem for a supercritical branching random walk on $\mathbf{Z}^d$ with a single source. *Uspekhi Mat. Nauk*, 53, 229–230, 1998.
13. E. Bulinskaya. On a cost approach in insurance. *Surveys of Applied and Industrial Mathematics*, 10, 2, 276–286, 2003.
14. H. Bühlmann. *Mathematical Methods in Risk Theory*. Springer-Verlag, Berlin, Heidelberg, New York, 1970.
15. M. Cranston, L. Koralov, S. Molchanov and B. Vainberg. Continuous model for homopolymers. *J. Funct. Anal.*, 256, 8, 2656–2696, 2009.
16. B. De Finetti. Su unimpostazione alternativa della teoria collettiva del rischio. *Transactions of the XVth congress of actuaries*, 2, 433–443, 1957.
17. D. P. Gaver Jr. A waiting line with interrupted service, including priorities. *Journal of the Royal Statistical Society, Series B*, 73–90, 1962.
18. H. U. Gerber. Entscheidungskriterien für den zusammengesetzten Poisson-prozess. *Schweiz. Aktuarver. Mitt.*, 1, 185–227, 1969.

19. H. U.Gerber. The dilemma between dividends and safety and a generalization of the Lundberg-Cramér formulas. *Scand. Actuar. J.*, 1, 46–57, 1974.
20. H. U. Gerber. *An Introduction to Mathematical Risk Theory.* S.S. Huebner Foundation Monograpgh Series No. 8. Homewood, IL: Irwin, 1979.
21. H. U. Gerber and E.S.W. Shiu. Optimal dividends: analysis with Brownian motion. *North American Actuarial Journal*, 8, 1, 1–20, 2004.
22. M. Jeanblanc-Picqué and A. N. Shiryaev. Optimization of the flow of dividends. *Russian Math. Surveys*, 50, 257–277, 1995.
23. D. Jefferson and A. Witkowski. An approach to performance analysis of timestamp-driven synchronization mechanisms. In: *Proceedings of the third annual ACM symposium on Principles of distributed computing*, 243–253. ACM Press, New York, 1984.
24. N. V. Karapetyan. Dividends and reinsurance. *Proceedings of the 6th International Workshop on Simulation*, VVM com.Ltd, 47–52, 2009.
25. K. Krishnamoorthy, P.K. Pramod, and S.R. Chakravarthy. Queues with interruptions: a survey. *TOP*, 1-31, 2012.
26. R. Loeffen. On optimality of the barrier strategy in de Finetti's dividend problem for spectrally negative Lévy processes. *Ann. Appl. Probab.*, 18, 5, 1669–1680, 2008.
27. R. L. Loeffen. An optimal dividends problem with transaction costs for spectrally negative Lvy processes. *Insurance: Mathematics and Economics*, 45, 1, 4148, 2009.
28. R. Loeffen. An optimal dividends problem with a terminal value for spectrally negative Lévy processes with a completely monotone jump density. *J. Appl. Probab.*, 46, 1, 85–98, 2009.
29. F. Lundberg. *Approximerad framställning av sannolikhetsfunktionen. Aterförsäkring av kollektivrisker*, Akad. Afhandling. Almqvist o. Wiksell, Uppsala, 1903.
30. A. Manita. Intrinsic space scales for multidimensional stochastic synchronization models. In: J. R. Bozeman, V. Girardin, and C. H. Skiadas, Eds. *New Perspectives on Stochastic Modeling and Data Analysis*, ISAST, Athens, Greece, 271–282, 2014.
31. D. Mitra and I. Mitrani. Analysis and optimum performance of two message-passing parallel processors synchronized by rollback. *Performance Evaluation*, 7, 2, 111–124, 1987.
32. I. L. Mitrany and B. Avi-Itzhak. A many-server queue with service interruptions. *Operations Research*, 16, 3, 628–638, 1968.
33. M. Mnif, and A. Sulem. Optimal risk control and dividend policies under excess of loss reinsurance. *Stochastics*, 77, 5, 455–476, 2005.
34. S. A. Molchanov and E. B. Yarovaya. Limit theorems for the Green function of the lattice Laplacian under large deviations of the random walk. *Izvestiya RAN: Mathematics*, 76, 6, 1190–1217, 2012.
35. S. A. Molchanov and E. B. Yarovaya. Branching processes with lattice spatial dynamics and a finite set of particle generation centers. *Doklady Akademii Nauk*, 86, 2, 1–4, 2012.
36. S. A. Molchanov and E. B. Yarovaya. Population Structure inside the Propagation Front of a Branching Random Walk with Finitely Many Centers of Particle Generation. *Doklady Akademii Nauk*, 86, 3, 1–4, 2012.
37. S. A. Molchanov and E. B. Yarovaya. Large Deviations for a Symmetric Branching Random Walk on a Multidimensional Lattice. *Proceedings of the Steklov Institute of Mathematics*, 282, 186–201, 2013.

38. E. Morozov, D. Fiems, and H. Bruneel. Stability analysis of multiserver discrete-time queueing systems with renewal-type server interruptions. *Performance Evaluation*, 68, 12, 1261–1275, 2011.
39. M. F. Neuts, *Matrix-geometric solutions in stochastic models: an algorithmic approach*. Courier Dover Publications, 1981.
40. M. F. Neuts, *Structured stochastic matrices of M/G/1 type and their applications*. Marcel Dekker, New York, 1989.
41. M. F. Neuts and D. M. Lucantoni. A markovian queue with n servers subject to breakdowns and repairs. *Management Science*, 25, 9, 849–861, 1979.
42. A. Pikovsky, M. Rosenblum, and J. Kurths. *Synchronization: A Universal Concept in Nonlinear Sciences*. Cambridge University Press, 2001.
43. R. Pyke. Markov renewal processes: definitions and preliminary properties. *The Annals of Mathematical Statistics*, 1231–1242, 1961.
44. H. Schmidli. *Stochastic Control in Insurance. Probability and Its Applications*. Springer, London, 2008.
45. O. Simeone, U. Spagnolini, Y. Bar-Ness, and S. H. Strogatz. Distributed synchronization in wireless networks. *IEEE Signal Processing Magazine*, 25, 5, 81–97, 2008.
46. S. H. Strogatz. *Sync: The Emerging Science of Spontaneous Order*. Hyperion, 2003.
47. B. Sundararaman, U. Buy, and A. D. Kshemkalyani. Clock synchronization for wireless sensor networks: A survey. *Ad Hoc Networks (Elsevier)*, 3, 281–323, 2005.
48. A. V. Tkachenko. Multichannel queueing systems in a random environment. *Moscow University Mathematics Bulletin*, 1, 53–57, 2014.
49. H. White, L. Christie. Queueing with preemptive priorities or with breakdown. *Oper. Res.*, 6, 1, 79–95, 1958.
50. E. Yarovaya. *Branching Random Walks in Nonhomogeneous Medium*, Moscow State University Press, Moscow, 2007.
51. E. Yarovaya. Branching Random Walks with Several Sources. *Mathematical Population Studies*, 20, 14–26, 2013.
52. E. Yarovaya. Branching Random Walks with Heavy Tails. *Communications in Statistics - Theory and Methods*, 42, 16, 2301–2310, 2013.
53. E. Yarovaya. Criteria for Transient Behavior of Symmetric Branching Random Walks on Z and Z^2. In: J. R. Bozeman, V. Girardin, and C. H. Skiadas, Eds. *New Perspectives on Stochastic Modeling and Data Analysis*. 283–294, 2014.
54. C. Yin and C. Wang. Optimality of the barrier strategy in de Finetti's dividend problem for spectrally negative Lévy processes: An alternative approach. *Journal of Computational and Applied Mathematics*, 2009. doi:10.1016/j.cam.2009.07.051.

Stability Analysis of Multi-Server Discrete-Time Queueing Systems with Interruptions and Regenerative Input Flow

Larisa G. Afanasyeva[1] and Andrey Tkachenko[2]

[1] Lomonosov Moscow State University, Department of Mathematics and Mechanics, 119991, Leninskie Gory, Moscow, Russia
(E-mail: l.g.afanaseva@yandex.ru)
[2] National Research University Higher School of Economics, Department of Applied Economics, 101000, Myasnitskaya Ulitsa, Moscow, Russia
(E-mail: tkachenko_av@hse.ru)

Abstract. This paper is focused on a discrete-time multichannel queueing system with heterogeneous servers, regenerative input flow and interruptions. The breakdowns of servers may occur at any time even if they are not occupied by customers. Consecutive moments of breakdowns are defined by a renewal process. We consider the preemptive repeat different service discipline. Exploiting coupling method the necessary and sufficient stability condition for the system is established.
Keywords: Multichannel system, Regenerative flow, Stability, Interruption, Vacation, Unreliable servers.

1 Introduction

Queueing systems in which servers may be not available for operation arise naturally as models of many computer, communication and manufacturing systems. Service interruptions may result from resource sharing, server breakdowns, priority assignment, vacations, some external events, and others. For instance, for queueing systems with preemptive priority discipline service interruptions for the low priority customers occur when a high priority customer arrives during a low priority customer's service time. Therefore, there is significant interest in the investigation of queueing systems with service interruptions.

This study is focused on a queueing system with a regenerative input flow and heterogeneous servers that suffer independent interruptions. Service times are generally distributed. The breakdowns of the servers may occur at any time even if they are not occupied by customers. Consecutive moments of breakdowns are defined by a renewal process. We consider the preemptive repeat different service discipline, so the service is repeated from the start with different independent service time after restoration of the server, see Gaver[8].

Systems with unreliable servers have been intensively investigated for a long time and were focused on the single-server case. There are some review papers,

New Trends in Stochastic Modeling and Data Analysis (pp. 13-26)
Raimondo Manca - Sally McClean - Christos H Skiadas (Eds)

that cover most of the literature in these sphere. Results concerning systems with servers vacations can be found in Doshi[6] and Ke *et al.*[11]. The problems of servers breakdowns and their solutions are presented in Krishnamoorthy *et al.*[12]. There are some other papers with extensive literature survey as well, see, e.g., Pechinkin *et al.*[17], Morozov *et al.*[15].

One of the powerful approaches to obtain stability conditions for systems with interruptions is synchronization method combined with the regenerative theory. This method was used in Morozov *et al.*[15] to study the multichannel queueing system with identically distributed service times by different servers, renewal input flow, alternating renewal-type servers' interruptions for the discrete-time case. Authors established some sufficient conditions of stability for the preemptive repeat different and preemptive resume service disciplines. In the paper Afanasyeva and Bashtova[2] the coupling method was implemented for asymptotic analysis of the single-server system with a regenerative input. A similar approach was applied to obtain the stability condition of the multichannel system with heterogeneous servers and a regenerative input flow in a random environment by Tkachenko[19]. It was supposed that all servers get out of the order simultaneously.

In this paper we consider the multichannel model with interruptions in a discrete-time case. The necessary and sufficient condition of the stability is established. The key element of our analysis is synchronization of processes under consideration. This method is based on the regeneration property of the input flow and renewal structure of processes describing the servers' breakdowns, see Afanasyeva and Bashtova[2].

The paper is organized as follows. The model is described in detail in Section 2. In Section 3 we introduce auxiliary service flows and define the traffic rate. Synchronization of input and service flows is constructed in Section 4, whereas Section 5 is devoted to the (in)stability problem. In Section 6 we provide some comments. The further research directions are discussed in the final section Conclusion.

2 Model description

We consider a system with m heterogeneous servers and a common queue. Service times of customers by the ith server constitute a sequence $\{\eta_{i,n}\}_{n=1}^{\infty}$ of independent identically distributed (iid) random variables that do not depend on input flow and service times by other servers. Let $B_i(t)$ be a distribution function (d.f.) of $\eta_{i,n}$ and $b_i = \mathbf{E}\eta_{i,n} < \infty$ $(i = \overline{1,m})$. We assume that servers may be unavailable for service from time to time. The breakdowns of the servers may occur at any time even if they are not occupied by customers. Let $\{s_{i,n}^{(2)}\}_{n=0}^{\infty}$ be breakdown epochs and $\{s_{i,n}^{(1)}\}_{n=1}^{\infty}$ restoration epochs for the ith server. Here $0 = s_{i,0}^{(2)} < s_{i,1}^{(1)} < s_{i,1}^{(2)} < s_{i,2}^{(1)} \ldots$. Then $u_{i,n}^{(1)} = s_{i,n}^{(1)} - s_{i,n-1}^{(2)}$ and $u_{i,n}^{(2)} = s_{i,n}^{(2)} - s_{i,n}^{(1)}$ represent the lengths of the nth blocked and nth available period of the ith server respectively $(i = \overline{1,m})$. The sequence $\{u_{i,n}^{(1)}, u_{i,n}^{(2)}\}_{n=1}^{\infty}$ consists of iid random vectors (for all $i = \overline{1,m}$) that do not depend on the input

flow and service times. However, for each n and i,random variables $u_{i,n}^{(1)}$ and $u_{i,n}^{(2)}$ are not assumed to be independent. Let $u_{i,n} = u_{i,n}^{(1)} + u_{i,n}^{(2)}$ be the length of the nth cycle for server i. A cycle consists of a blocked period followed by an available period. We assume that $\mathbf{E}u_{i,n}^{(1)} = a_i^{(1)} < \infty$, $\mathbf{E}u_{i,n}^{(2)} = a_i^{(2)} < \infty$, $a_i = a_i^{(1)} + a_i^{(2)}$ $(i = \overline{1,m})$. Server is free if it is neither serving a customer nor interrupted. If server becomes free and there are customers in the queue, a new customer enters the server. It is possible that more than one server becomes free simultaneously. Then customer in the queue chooses an idle server according to some algorithm, possibly random. For definiteness we assume that a customer chooses a free server with the least number. It is possible that an unavailable period may start while a customer is receiving service. Then service of the customer is immediately interrupted. There are various disciplines for continuation of the service after server restoration, see, e.g., Gaver[8]. Here we consider preemptive repeat different service discipline, i.e. service is repeated from the start and the service time after restoration is independent of the original service time. We assume that customers remain with the same server until service completion. In order to ensure the service process for the ith server we have to assume that $\mathbf{P}(\eta_{i,1} \le u_{i,1}^{(2)}) > 0$ for all $i = \overline{1,m}$. If this condition is not fulfilled for some server i, then the ith server has to be excluded since it is always busy by service of the single customer.

We assume that the input flow $X(t)$ is a regenerative one. For further use we give

Definition 1. A stochastic flow $X(t)$ is called *regenerative* if there is an increasing sequence of random variables $\{\theta_i,\ i \ge 0\}, \theta_0 = 0$ such that the sequence $\{\varkappa_i\}_{i=1}^{\infty} = \{X(\theta_{i-1}+t) - X(\theta_{i-1}), \theta_i - \theta_{i-1}, t \in [0, \theta_i - \theta_{i-1})\}_{i=1}^{\infty}$ consists of independent identically distributed random elements.

The random variable θ_i is said to be the ith regeneration point of $X(t)$ and $\tau_i = \theta_i - \theta_{i-1}$ is the ith regeneration period $(i = 1, 2, \ldots)$. Let $\xi_i = X(\theta_i) - X(\theta_{i-1})$ be the number of customers arriving during the ith regeneration period. Assume that $\tau = E\tau_1 < \infty$, $a = E\xi_1 < \infty$. The limit $\lambda_X = \lim_{t\to\infty} \frac{X(t)}{t}$ with probability one (w.p.1) is called the *intensity* of $X(t)$. It is easy to prove that $\lambda_X = \frac{a}{\tau}$ (see, e.g., Afanasyeva and Bashtova[2]). The class of regenerative flows contains most of fundamental flows that are exploited in the queueing theory. First of all, the doubly stochastic Poisson process (for definition see, e.g., Grandell[9]) with stochastic regenerative intensity is regenerative one. There are many other examples of the regenerative flows, for instance, semi-Markovian, Markov-modulated, Markov-arrival, and other processes, see Afanasyeva *et al.*[4]. Important properties of regenerative flows are given in Afanasyeva and Bashtova[2].

We consider a discrete-time system, i.e. time is divided into fixed length intervals or slots and all arrivals, departures, interruptions (restorations) are synchronized with respect to slot boundaries. Moreover, in the case of some events synchronization at one slot these events are ordered as follows: arrival, departure, and interruption (restoration). System is observed at the end of a slot, when all events of the slot are realized.

3 Auxiliary processes

In this section we define auxiliary processes $Y_i(t)$ ($i = \overline{1,m}$) that will be exploited for asymptotic analysis of the system stability. We think of $Y_i(t)$ ($i = \overline{1,m}$) as the number of customers, that can be served by the ith server if there is no empty queue in the system within interval $[0,t]$. In order to construct the processes $Y_i(t)$ we introduce the collection $\left\{\{\eta_{i,n}^{(j)}\}_{n=1}^{\infty}\right\}_{j=1}^{m}$ of independent sequences $\{\eta_{i,n}^{(j)}\}_{n=1}^{\infty}$ consisting of iid random variables with d.f. $B_i(x)$. Let $K_{i,j}(t)$ be the counting process associated with the sequence $\{\eta_{i,n}^{(j)}\}_{n=1}^{\infty}$, i.e. $K_{i,j}(t) = \max\{k : \sum_{n=1}^{k} \eta_{i,n}^{(j)} \le t\}$ ($K_{i,j}(0) = 0$) and $\mu_i(t)$ be the number of cycles for the ith server during $[0,t]$, i.e. $\mu_i(t) = \max\{j : \sum_{n=1}^{j} u_{i,n} \le t\}$ ($\mu_i(0) = 0$). Then the process $Y_i(t)$ is defined by the relation

$$Y_i(t) = \sum_{j=1}^{\mu_i(t)} K_{i,j}\left(u_{i,j}^{(2)}\right) + K_{i,\mu_i(t)+1}\left(\max\left[0, t - s_{i,\mu_i(t)+1}^{(1)}\right]\right). \tag{1}$$

By $H_i(t)$ we denote the renewal function for $K_{i,j}(t)$, i.e. $H_i(t) = \mathbf{E}K_{i,j}(t)$.

Lemma 1. *There exists the limit*

$$\lim_{t\to\infty} \frac{Y_i(t)}{t} = \frac{\mathbf{E}H_i(u_{i,n}^{(2)})}{a_i} = \lambda_{Y_i} \text{ w.p.1.}$$

Proof. Putting $g_i(n) = \sum_{j=1}^{n} K_{i,j}(u_{i,j}^{(2)})$ we get from (1) the evident inequalities

$$g_i(\mu_i(t)) \le Y_i(t) \le g_i(\mu_i(t)+1). \tag{2}$$

Since $K_{i,j}(u_{i,j}^{(2)})$ is a sequence of iid random variables with a finite mean, we have $n^{-1}g_i(n) \xrightarrow[n\to\infty]{} \mathbf{E}H_i(u_{i,j}^{(2)})$ w.p.1 by strong law of large numbers (SLLN). Besides, it follows from the renewal theory that $t^{-1}\mu_i(t) \xrightarrow[t\to\infty]{} a_i^{-1}$ w.p.1. In view of independence of $\{\{\eta_{i,n}^{(j)}\}_{n=1}^{\infty}\}_{j=1}^{m}$ and $\{u_{i,n}^{(1)}, u_{i,n}^{(2)}\}_{n=1}^{\infty}$ one can easily obtain the convergence

$$\frac{g_i(\mu_i(t))}{\mu_i(t)} \xrightarrow[t\to\infty]{} a_i^{-1}\mathbf{E}H_i(u_{i,1}^{(2)}) \quad \text{w.p.1.}$$

Now the proof of the lemma follows from (2). □

Let $Y(t) = \sum_{i=1}^{m} Y_i(t)$ be the number of customers served by the system during $[0,t]$ under assumption that the queue is not empty within this interval. From Lemma 1 we have

$$\lambda_Y = \lim_{t\to\infty} \frac{Y(t)}{t} = \sum_{i=1}^{m} \frac{\mathbf{E}H_i(u_{i,1}^{(2)})}{a_i} \quad \text{w.p.1.} \tag{3}$$

We think of λ_X and λ_Y as the arrival and service rate respectively. Intuitively, it is clear that traffic rate ρ of the system has to be determined as

$$\rho = \frac{\lambda_X}{\lambda_Y} = \frac{\lambda_X}{\sum_{i=1}^{m} a_i^{-1} \mathbf{E} H_i(u_{i,1}^{(2)})}. \tag{4}$$

The main stability result consists of the formal proof of this fact. Key element of our analysis is synchronization (coupling) of renewal processes $Y_i(t)$ $(i = \overline{1,m})$ and regenerative input flow $X(t)$.

4 Synchronization of renewal points for input and service flows

First we prove a lemma for general regenerative aperiodic flows in a discrete-time case. Let $Z_1(t)$ and $Z_2(t)$ be independent regenerative flows with regeneration points $\{\theta_{1,j}\}_{j=1}^{\infty}$ and $\{\theta_{2,j}\}_{j=1}^{\infty}$ respectively $(\theta_{i,0} = 0; i = 1, 2)$. As usually, aperiodicity means that the greatest common divisor (GCD)

$$GCD\,\{k : \mathbf{P}(\theta_{i,1} = k) > 0\} = 1, \quad i = 1, 2. \tag{5}$$

Define common points of regeneration for $Z_1(t)$ and $Z_2(t)$ by the relation

$$T_k = \min\{\theta_{1,j} > T_{k-1} : \bigcup_{l=1}^{\infty} \{\theta_{2,l} = \theta_{1,j}\}\}, \quad T_0 = 0.$$

Lemma 2. *Let condition* (5) *be fulfilled and* $\mathbf{E}(\theta_{i,1}) < \infty$ *(*$i = 1, 2$*). Then the sequence* $\{T_k\}_{k=1}^{\infty}$ *consists of regeneration points for* $Z_1(t)$ *and* $Z_2(t)$ *and*

$$\mathbf{E}T_1 = \mathbf{E}\theta_{1,1} \cdot \mathbf{E}\theta_{2,1} < \infty. \tag{6}$$

Proof. Since the first statement follows from the construction of T_k we prove (6). Put

$$\nu_k = \min\{j > \nu_{k-1} : \bigcup_{l=1}^{\infty} \{\theta_{1,j} = \theta_{2,l}\}\}, \quad \nu_0 = 0,$$

so that $T_k = \theta_{1,\nu_k}$. Then $\{\nu_k - \nu_{k-1}\}_{k=1}^{\infty}$ is a sequence of iid random variables and in accordance with Wald's identity $\mathbf{E}T_1 = \mathbf{E}\theta_{1,1} \cdot \mathbf{E}\nu_1$ (see, e.g., Feller[7]). Therefore, we need to prove the finiteness of $\mathbf{E}\nu_1$. Let $h_2(t)$ $(h(t))$ be the mean number of renewals up to time t for the renewal process $\{\theta_{2,n}\}_{n=1}^{\infty}$ $(\{\nu_k\}_{k=1}^{\infty})$, so that $h_2(t) = \sum_{l=0}^{\infty} \mathbf{P}(\theta_{2,l} = t)$ and $h(t) = \sum_{k=0}^{\infty} \mathbf{P}(\nu_k = t)$. Taking into account (5) we get from Blackwell's theorem (see, e.g., Thorisson[18])

$$h_2(t) \xrightarrow[t\to\infty]{} \frac{1}{\mathbf{E}\theta_{2,1}}, \quad h(t) \xrightarrow[t\to\infty]{} \frac{1}{\mathbf{E}\nu_1}. \tag{7}$$

In view of $Z_1(t)$ and $Z_2(t)$ independence

$$h(j) = \mathbf{P}\{\bigcup_{l=0}^{\infty} \{\theta_{1,j} = \theta_{2,l}\}\} = \mathbf{E}\left(\sum_{l=0}^{\infty} \mathbf{P}\{\theta_{1,j} = \theta_{2,l} | \theta_{1,j}\}\right) = \mathbf{E}h_2(\theta_{1,j}). \tag{8}$$

Since $\theta_{1,j} \xrightarrow[j\to\infty]{} \infty$ w.p.1, then $h_2(\theta_{1,j}) \xrightarrow[j\to\infty]{} \frac{1}{\mathbf{E}\theta_{2,l}}$ w.p.1. Thus from (7), (8) and Lebesgue's dominated convergence theorem we obtain $\mathbf{E}\nu_1 = \mathbf{E}\theta_{2,1} < \infty$. □

In the model under consideration we have $m+1$ regenerative flows $X(t)$, $Y_i(t)$ $(i = \overline{1,m})$ with points of regeneration $\{\theta_j\}_{j=1}^{\infty}$ and $\{s_{i,j}^{(2)}\}_{j=1}^{\infty}$ respectively. To exploit Lemma 2 for synchronization of these processes we introduce the following counting processes

$$N_0(t) = max\{k : \theta_k \le t\},$$
$$N_i(t) = max\{k : s_{i,k}^{(2)} \le t\}, \quad i = \overline{1,m}.$$

We need the additional assumption.

Condition 1. The counting processes $N_0(t)$ and $N_i(t)$ $(i = \overline{1,m})$ are aperiodic.

Let us define subsequence $\{T_k\}_{k=0}^{\infty}$ of the sequence $\{\theta_j\}_{j=1}^{\infty}$ by the recurrent relation

$$T_k = min\{\theta_j > T_{k-1} : \bigcap_{j=1}^{m}\{N_i(\theta_j) - N_i(\theta_j - 1) > 0\}\}, \quad (T_0 = 0). \qquad (9)$$

In other words, T_k is a point of regeneration of $X(t)$ such that all the servers get out of the order simultaneously at this moment. Hence, $\{T_k\}_{k\ge 0}$ are the common regeneration points for the input flow $X(t)$ and $N_i(t)$ $(i = \overline{1,m})$. Since we consider the preemptive repeat different service discipline then $\{T_k\}_{k\ge 0}$ is a sequence of regeneration points for $Y_i(t)$ and $Y(t)$ as well. Moreover, from Lemma 2 we obtain

$$\mathbf{E}T_1 = \frac{1}{\mathbf{E}\tau_1}\prod_{i=1}^{m} a_i^{-1} < \infty.$$

Thus we have constructed the sequence of common regeneration points for the processes $X(t)$ and $Y(t)$. Set $\Delta_k^X = X(T_k) - X(T_{k-1})$, $\Delta_k^Y = Y(T_k) - Y(T_{k-1})$.

Lemma 3. *Let Condition 1 be fulfilled. Then the traffic rate of the system defined by* (4) *is equal to*

$$\rho = \frac{\mathbf{E}\Delta_k^X}{\mathbf{E}\Delta_k^Y}.$$

Proof. Since $\{T_k\}_{k\ge 0}$ is a sequence of regeneration points for $X(t)$ and $Y(t)$ and $\mathbf{E}T_1 < \infty$ it follows that sequences $\{\Delta_k^X\}_{k\ge 0}$ and $\{\Delta_k^Y\}_{k\ge 0}$ consist of iid random variables with finite means. Let $\mu(t) = \max\{k : T_k \le t\}$. From the renewal theory and SLLN we have

$$\lambda_X = \lim_{t\to\infty}\frac{X(t)}{t} = \lim_{t\to\infty}\left(\frac{\mu(t)}{t}\frac{1}{\mu(t)}\sum_{k=1}^{\mu(t)}(X(T_k) - X(T_{k-1})) + \frac{X(t) - X_{T_{\mu(t)}}}{t}\right) =$$

$$= \frac{\mathbf{E}\Delta_k^X}{\mathbf{E}T_1}, \text{ w.p.1.}$$

The same arguments yield $\lambda_Y = \frac{\mathbf{E}\Delta_k^Y}{\mathbf{E}T_1}$, so that $\rho = \frac{\lambda_X}{\lambda_Y} = \frac{\mathbf{E}\Delta_k^X}{\mathbf{E}\Delta_k^Y}$. □

5 Stability results

Let $Q(t)$ be the number of customers in the system (including customers in servers and queue) at instant t.

Definition 2. The process $\{Q(t), t \geq 0\}$ is called *stochastically bounded* if for any $\varepsilon > 0$ there exists $y < \infty$ such that for any $t > 0$

$$\mathbf{P}\{Q(t) < y\} > 1 - \varepsilon.$$

Otherwise we say that $Q(t)$ is stochastically unbounded. This definition is close to the notion of *tightness* used in Pang and Whitt[16] .

Theorem 1. *Let Condition 1 be fulfilled. Then*

- $Q(t) \xrightarrow[t\to\infty]{} \infty$ *w.p.1 if* $\rho > 1$,
- $Q(t) \xrightarrow[t\to\infty]{P} \infty$ *if* $\rho = 1$.
- $Q(t)$ *is stochastically bounded if* $\rho < 1$.

Here ρ *is defined by* (4).

Proof. Denote by $\widetilde{Y}_i(t)$ the number of customers served by the ith server during the interval $[0, t]$ and $\widetilde{Y}(t) = \sum_{i=1}^{m} \widetilde{Y}_i(t)$, $\widetilde{\Delta}_n^Y = \widetilde{Y}(T_n) - \widetilde{Y}(T_{n-1})$. Employing the approach proposed by Borovkov[5] and developed by Iglehart and Whitt[10] we can choose service times from the collection $\{\{\eta_{i,n}^{(j)}\}_{n=1}^{\infty}\}_{j\geq 1}$ in such a way that $\widetilde{Y}_i(t) \leq Y_i(t)$ w.p.1 $(i = \overline{1, m})$. Therefore,

$$\widetilde{Y}(t) \leq Y(t) \text{ and } \widetilde{\Delta}_n^Y \leq \Delta_n^Y \ w.p.1. \tag{10}$$

Consider the case $\rho > 1$. Taking into account (10) we have

$$Q(t) \geq Q(0) - Y(t) + X(t),\ t \geq 0 \ w.p.1. \tag{11}$$

From (4), we get $\lambda_X > \lambda_Y$. Thus in view of definitions of λ_X, λ_Y and (11) we obtain the first statement of the theorem.

Let $\rho = 1$. Consider the embedded process $q_n = Q(T_n)$ and denote $Z_k = \sum_{j=1}^{k}(\Delta_j^X - \Delta_j^Y)$ $(Z_0 = 0)$. We define the auxiliary sequence $\{q_k^-\}_{k\geq 0}$ by the relation

$$q_k^- = \max[0,\ q_{k-1} + \Delta_k^X - \Delta_k^Y],\ q_0^- = 0.$$

Then $q_k \geq q_k^-$ w.p.1 and (see Afanaseva[1]) the following inequality is fulfilled in distribution

$$q_k^- = \max[q_0 + Z_k,\ \max_{1\leq j\leq k} Z_j],\ Z_k = \Delta_k^X - \Delta_k^Y.$$

If $\rho = 1$, it follows from Lemma 3 that $\mathbf{E}\Delta_j^X = \mathbf{E}\Delta_j^Y$. Therefore, $\{Z_k\}_{k\geq 0}$ is a random walk with zero drift. Hence, except when $\Delta_j^X = \Delta_j^Y = c$ w.p.1 (c is a constant) $\max_{1\leq j\leq k} Z_j \xrightarrow[k\to\infty]{P} \infty$ (see, e.g. Feller[7]). This means that $q_k \xrightarrow[k\to\infty]{P} \infty$ and the second statement of theorem holds.

Now let $\rho < 1$. Consider the ith server. We assume that service times of customers processing during the kth available period $[s_{i,k}^{(1)}, s_{i,k}^{(2)}]$ $(k = 1, 2, \ldots)$ are consequently selected from the sequence of iid random variables $\{\eta_{i,n}^{(k)}\}_{n\geq 1}$. Let us recall that process $Y_i(t)$ is defined by the same sequence on the kth cycle with the help of (1). Introduce the event

$$A_n = \{Q(t) \geq m \text{ for all } t \in [T_{n-1}, T_n]\}. \tag{12}$$

Then

$$\Delta_n^Y \mathbf{I}(A_n) = \widetilde{\Delta}_n^Y \mathbf{I}(A_n), \tag{13}$$

where $\mathbf{I}(A)$ is the indicator of event A. Now we introduce the embedded process $x_n = (q_n, e_1(n), \ldots, e_m(n)), n \geq 0$, where $e_i(n) = 1$ if there is a customer on the ith server at time T_n and $e_i(n) = 0$ otherwise. Hence $e_i(n) = 1$ for all $i = \overline{1,m}$ if $q_n \geq m$. In view of interruption discipline and properties of the synchronization epochs $\{T_n\}_{n\geq 1}$ the process $\{x_n\}_{n\geq 1}$ is a Markov chain with countable set of states $\mathfrak{K} = \{\{0\}; (j, e_1, \ldots, e_m), j = \overline{1, m-1}, e_i \in \{0; 1\}; j, j \geq m\}$. Let $\mathfrak{K}_\mathfrak{o}$ be the set of unessential states and $\mathfrak{K}_\mathfrak{j}$ $(j = \overline{1,r})$ irreducible classes of communicating states. From the condition $\mathbf{E}\Delta_j^X < \mathbf{E}\Delta_j^Y$ it follows that for any $j_0 \in \mathfrak{K}$ one can find t_0 such that $\mathbf{P}(Q(t_0) < m | Q(0) = j_0) > 0$. Therefore there exist k_0 and n_0 such that $\mathbf{P}(q_{n_0} < m + k_0 | q_0 = j_0) > 0$ for any $j_0 \in \mathfrak{K}$. It provides the finiteness of the number of classes r, so we have

$$\mathfrak{K} = \mathfrak{K}_\mathfrak{o} \bigcup_{j=1}^{r} \mathfrak{K}_\mathfrak{j}.$$

Consider the first class $\mathfrak{K}_\mathfrak{1}$. Assume that it is aperiodic. Then for any $x \in \mathfrak{K}_\mathfrak{1}$, $y \in \mathfrak{K}_\mathfrak{1}$ there exists

$$\lim_{n\to\infty} \mathbf{P}(x_n = x | x_0 = y) = \pi_x^{(1)}. \tag{14}$$

If

$$\sum_{x\in\mathfrak{K}_\mathfrak{1}} \pi_x^{(1)} = 1 \tag{15}$$

then q_n is stochastically bounded under condition that $q_0 \in \mathfrak{K}_1$. Let us show that (15) is fulfilled employing Foster's criterion (see, e.g., Meyn and Tweedie[13]). We define the test function $f(q, e_1, \ldots, e_m) = q$. It is sufficient to show that for some $\varepsilon_1 > 0$ there exists $M_{\varepsilon_1} > m$ such that

$$\mathbf{E}(f(x_n) - f(x_{n-1}) | x_{n-1} = x) < -\varepsilon_1 \tag{16}$$

for all $x = (q, e_1, \ldots, e_m)$ with $q > M_{\varepsilon_1}$. Taking into account (13) we get

$$\begin{aligned} q_n = q_{n-1} + \Delta_n^X - \widetilde{\Delta}_n^Y = q_{n-1} + \Delta_n^X - \widetilde{\Delta}_n^Y \mathbf{I}(A_n) - \widetilde{\Delta}_n^Y \mathbf{I}(\overline{A}_n) \leq \\ \leq q_{n-1} + \Delta_n^X - \Delta_n^Y \mathbf{I}(A_n) = q_{n-1} + \Delta_n^X - \Delta_n^Y + \Delta_n^Y \mathbf{I}(\overline{A}_n). \end{aligned} \tag{17}$$

From the assumption $\rho < 1$ we have

$$E\Delta_k^X - E\Delta_k^Y = -\delta < 0. \tag{18}$$

Note that for any $\varepsilon > 0$ there exists M_ε such that $\mathbf{P}(A_n) < \varepsilon$ if $q_{n-1} > M_\varepsilon$ w.p.1. Therefore, in view of integrability of random variables Δ_n^Y, one may choose M_δ such that $\mathbf{E}\Delta_n^Y \mathbf{I}(\overline{A}_n) < \frac{\delta}{2}$ if $q_{n-1} > M_\delta$. Thus, we obtain from (17) and (18)

$$\mathbf{E}(f(x_n) - f(x_{n-1})|x_{n-1} = x) < E\Delta_n^X - E\Delta_n^Y + \frac{\delta}{2} = -\frac{\delta}{2}$$

if $x_{n-1} > M_\delta$, that proves (16).

Let $\mathfrak{K}_1$ be a periodic class with a period h. Then we consider a sequence $\{\widetilde{x}_n^{(l)}\}_{n\geq 1}$ $(l = \overline{0, h-1})$, where $\widetilde{x}_n^{(l)} = x_{nh+l}$. It is well-known (see, e.g., Feller[7]) that Markov chain $\{\widetilde{x}_n^{(l)}\}_{n\geq 1}$ is irreducible and aperiodic. Arguing as above we prove that $\widetilde{q}_n^{(l)} = q_{nh+l}$ is stochastically bounded as $n \to \infty$.

We can similarly prove stochastic boundedness of q_n for initial state $x_0 = (q_0, e_1(0), \ldots, e_m(0)$ from any other class $\mathfrak{K}_i$ $(i = \overline{2, r})$. Since the number of classes r is finite we conclude that q_n is stochastically bounded as $n \to \infty$ for any initial state of Markov chain $x_0 \in \mathfrak{K}$. Hence, the process $Q(t)$ is also stochastically bounded. □

Remark 1. Let us note that the first statement of Theorem 1 is not based on the regenerative property of $X(t)$. It is sufficient to assume that there exists $\lim_{t\to\infty} t^{-1}X(t) = \lambda_X$ w.p.1 $(0 < \lambda_X < \infty)$.

Remark 2. So far we considered zero-delayed regenerative flows $X(t)$ and $Y_i(t)$ assuming that

$$\mathbf{P}(\theta_0 = 0) = \mathbf{P}(s_{i,0}^{(2)} = 0) = 1, \ (\overline{i = 1, m}).$$

Let this condition be not fulfilled and consider delayed regenerative flows. For the validity of Theorem 1 we have only to claim

$$\mathbf{P}(\theta_0 < \infty) = \mathbf{P}(s_{i,0}^{(2)} < \infty) = 1, \ (\overline{i = 1, m}),$$

since its proof is based on results of Lemmas 1 – 3 true for delayed regenerative flows as well.

For the next theorem we recall definition of the ergodicity.

Definition 3. Process $\{Q(t), \ t \geq 0\}$ is *ergodic* one if for any initial state $Q(0)$ there exists

$$\lim_{t\to\infty} \mathbf{P}\{Q(t) \leq x\} = F(x),$$

where $F(x)$ is a distribution function and it does not depend on $Q(0)$.

Theorem 2. *Let Condition 1 be fulfilled and Markov chain $\{x_n\}_{n\geq 1}$ be an irreducible and aperiodic one. Then*

- $Q(t) \xrightarrow[t\to\infty]{} \infty$ *w.p.1 if* $\rho > 1$.
- $Q(t) \xrightarrow[t\to\infty]{P} \infty$ *if* $\rho = 1$.
- $Q(t)$ *is ergodic if* $\rho < 1$.

Proof. The first statement of the theorem follows from Theorem 1. Consider the other cases. The set of states $\mathfrak{K}$ of Markov chain $\{x_n\}_{n\geq 1}$ may have some unessential states but all the essential states organize the unique class $\mathfrak{K}_1$ of communicating states. Let $\rho < 1$. It follows from Theorem 1 that there exists the limit (14), where $\pi_x^{(1)} > 0$ for $x \in \mathfrak{K}_1$ and (15) is fulfilled, i.e. the Markov chain $\{x_n\}_{n\geq 1}$ is ergodic. Let us take a state $j_0 \in \mathfrak{K}_1$, $j_0 \geq m$ and assume that $x_0 = j_0$. Denote $\nu_{j_0} = \min\{n > 0 : x_n = j_0\}$, so that ν_{j_0} is the time of the return to the state j_0. Since Markov chain $\{x_n\}_{n\geq 1}$ is ergodic, it follows that $\mathbf{E}\nu_{j_0} < \infty$. Now consider $Q(t)$. Note that $Q(t)$ is a regenerative process and T_n is a point of the regeneration of $Q(t)$ if $q_n = Q(T_n) = j_0$. Let $\widetilde{\tau}_{j_0}$ be the time of return to the state j_0 for $Q(t)$, i.e.

$$\widetilde{\tau}_{j_0} = \min\{t > 0 : Q(t) = j_0\},$$

under assumption that $Q(0) = j_0$. Since $\mathbf{E}(T_n - T_{n-1}) = \mathbf{E}T_1 < \infty$ (Lemma 2) from Wald's identity we have $\mathbf{E}\widetilde{\tau}_{j_0} = \mathbf{E}T_1\mathbf{E}\nu_{j_0} < \infty$. Besides, from any initial state the process $Q(t)$ gets into j_0 in finite time w.p.1. Also we remark that condition (5) holds for $\widetilde{\tau}_{j_0}$. Therefore, one can exploit Smith's theorem to prove the third statement of the theorem. Finally, note that if $\rho = 1$ and $Q(t)$ is stochastically unbounded, then $\mathbf{E}\widetilde{\tau}_{j_0} = \infty$ and $Q(t) \xrightarrow[t\to\infty]{P} \infty$ that proves the second statement of the theorem. □

Conditions of Theorem 2 can be provided in various ways. Below we give two examples which are important from applied point of view. Let $r_i = \min\{j : \mathbf{P}(\eta_{i,1} = j) > 0\}$ $(i = \overline{1,m})$, $r_0 = \max_{i=\overline{1,m}} r_i$.

Condition 2. There exist $k \geq 0$ and j_1 such that one of the following inequalities holds

$$(i) \quad \mathbf{P}\left(\xi_1 = k,\ t_i - t_{i-1} \geq r_0\ (i = \overline{2,k}),\ \tau_1 = j,\ j - t_k \geq r_1\right) > 0 \text{ for all } j \geq j_1,$$
$$(ii) \quad \mathbf{P}\left(\xi_1 = k,\ t_i - t_{i-1} \geq r_0\ (i = \overline{2,k}),\ \tau_1 = j,\ j - t_k < r_1\right) > 0 \text{ for all } j \geq j_1.$$

Here t_i is arrival instant of the ith customer $(i = \overline{1,k})$. One can easy verify that for any initial state $x_0 \in \mathfrak{K}$ we have $\mathbf{P}(x_1 = \{0\}|x_0) > 0$ under Condition 2(i) and $\mathbf{P}(x_1 = \{1,1,0,\ldots,0\}|x_0) > 0$ under Condition 2(ii). Therefore, Markov chain $\{x_n\}_{n\geq 1}$ is irreducible and aperiodic. The same result is true under

Condition 3. $\mathbf{P}(\xi_1 = 0, \tau_1 > 0) > 0$ and $GCD\{j : \mathbf{P}(\tau_1 = j|\xi_1 = 0) > 0\} = 1$.

Example 1. Here we consider the discrete modification of Markov Arrival Process as an input flow $X(t)$. Let $y(t)$ be an ergodic Markov chain with finite number of states, stationary distribution $\{\pi_k\}_{k=1}^N$ and matrix of transition probabilities $\{P_{i,j},\ i,j = \overline{1,N}\}$. We assume that $0 < P_{i,i} < 1\,(i = \overline{1,N})$. New customer arrives when $y(t)$ changes its state. Then the intensity of $X(t)$ is defined as follows

$$\lambda_X = \sum_{k=1}^{N} \pi_k(1 - P_{k,k}).$$

Regeneration points of $X(t)$ are the instants when $y(t)$ gets into the state $\{1\}$ from any state $i \neq 1$, i.e.

$$\theta_n = \min\{t > \theta_{n-1} : y(t) = 1, y(t-1) \neq 1\},\ \theta_0 = 0,\ y(0) = 1.$$

The number of customers arriving during the kth regeneration period is defined by the relation

$$\xi_k = X(\theta_k) - X(\theta_{k-1}).$$

Therefore for any $l < j$ we have

$$\mathbf{P}\left(\xi_1 = 2,\ t_1 = l,\ t_2 = \tau_1 = j\right) = (P_{1,1})^{l-1} \sum_{k \neq 1} P_{1,k} (P_{k,k})^{j-1-l} P_{k,1} > 0.$$

Thus Condition 2 (ii) holds.

Example 2. Now we consider the discrete modification of the Markov Modulated Process as an input flow $X(t)$. Let $y(t)$ be an ergodic Markov chain with finite number of states, stationary distribution $\{\pi_k\}_{k=1}^N$ and matrix of transition probabilities $\{P_{i,j},\, i,j = \overline{1,N}\}$. We assume that $0 < P_{i,i} < 1\,(i = \overline{1,N})$. The input flow is defined as follows. If $y(t) = j$ then a new customer arrives at time t with probability α_j and $0 < \alpha_j < 1$ $(j = \overline{1,N})$. Then the intensity λ_X of the flow $X(t)$ is given by the relation

$$\lambda_X = \sum_{j=1}^{N} \alpha_j \pi_j.$$

Assume that $y(0) = j$ and define points of regeneration for $X(t)$ by the relation

$$\theta_n = \min\{t > \theta_{n-1} : X(t) = j\}, \theta_0 = 0.$$

Since $\alpha_j \in (0,1)$ and $P_{j,j} > 0$ it is evident that Condition 3 holds.

Remark 3. Let us remark that the sufficient condition of stability for a system with recurrent input flow, $b_i = b$ $(i = 1\overline{1,m})$ and preemptive repeat different service discipline was obtained in Morozov *et al.*[15]. This condition in our terms has a form

$$\lambda_X < \sum_{i=1}^{m} \frac{a_i^{(2)} - b}{a_i b}. \tag{19}$$

One can easily see that (19) is a corollary of the condition $\rho < 1$ where ρ is defined by (4). Indeed, taking into account the well-known inequality (see, e.g. Feller[7])

$$H_i(t) \geq \frac{t}{b_i} - 1, \quad t \geq 0$$

we get from (4) and Theorem 2 the following sufficient condition of stability

$$\lambda_X < \sum_{i=1}^{m} \frac{a_i^{(2)} - b_i}{a_i b_i}.$$

This condition is the same as (19) when $b_i = b$ $(i = \overline{1,m})$.

6 Comments

Generally speaking the traffic coefficient (4) cannot be expressed in terms of moments of the arrival, service and interruption processes. But under some additional assumptions concerning the distributions of service times and available periods one can obtain sufficient condition of stability in terms of moments, due to the asymptotic expansion for renewal functions $H_i(t)$ $(i = \overline{1,m})$, see Feller[7],

$$H_i(t) = \frac{t}{b_i} + \frac{\sigma_i^2 - b_i^2}{2b_i^2} + R_i(t),$$

where $\sigma_i^2 = Var(\eta_{i,1})$ and $R_i(t) \xrightarrow[t\to\infty]{} 0$. Let $\sigma_i^2 > b_i^2$ for all $i = \overline{1,m}$. Then there exists $\delta_1 < \frac{1}{2}$ and t_δ such that under assumption $\mathbf{P}(u_{i,1}^{(2)} > t_\delta \ (i = \overline{1,m})$ the sufficient condition has the form

$$\lambda_X < \sum_{i=1}^{m} \frac{a_i^{(2)}}{a_i b_i} + \delta_1 \sum_{i=1}^{m} \frac{\sigma_i^2 - b_i^2}{b_i^2 a_i}. \tag{20}$$

Analogously, if $\sigma_i^2 < b_i^2$ $(i = \overline{1,m})$ and $u_{i,1}^{(2)}$ is large enough w.p.1, then for some $\delta_2 > \frac{1}{2}$ the sufficient condition has the form

$$\lambda_X < \sum_{i=1}^{m} \frac{a_i^{(2)}}{a_i b_i} - \delta_2 \sum_{i=1}^{m} \frac{b_i^2 - \sigma_i^2}{b_i^2 a_i}. \tag{21}$$

Note that for preemptive resume service discipline, when the service is continued after interruption, sufficient condition of stability is given by the inequality

$$\lambda_X < \sum_{i=1}^{m} \frac{a_i^{(2)}}{a_i b_i}. \tag{22}$$

For a single-server queue this fact was proved in Afanasyeva and Bashtova[2] and for multichannel systems with recurrent input flow and $b_i = b$ $(i = \overline{1,m})$ in Morozov[14]. The proof for the model under consideration can be realized by analogy with proof of Theorem 1. Comparing (20), (21), and (22) we see that (under some additional assumptions) the capacity of the system with preemptive repeat different service discipline is greater (less) than for preemptive resume service discipline when $\sigma_i^2 > b_i^2$ $(\sigma_i^2 < b_i^2)$ for all $i = \overline{1,m}$. Besides, for the case $a_i^{(2)} = a_i$ $(i = \overline{1,m})$, i.e. there are no blocked periods but there are interruptions of service, we have

$$\lambda_X < \sum_{i=1}^{m} b_i^{-1} + \delta_1 \sum_{i=1}^{m} \frac{\sigma_i^2 - b_i^2}{b_i^2 a_i},$$

when $\sigma_i^2 > b_i^2$ $(i = \overline{1,m})$. For systems without interruptions the necessary and sufficient condition of stability has the form obtained in Afanasyeva and Tkachenko[3]

$$\lambda_X < \sum_{i=1}^{m} b_i^{-1}.$$

Again we see that if $\sigma_i^2 > b_i^2$ $(i = \overline{1,m})$ interruptions and independent repetition of service from the start can increase the capacity of the system.

7 Conclusion

In this paper we focus on a multichannel discrete-time queueing system with heterogeneous unreliable servers and a regenerative input flow. Although queueing systems with service interruptions have been investigated since late 1950's, to the best of our knowledge, stability conditions were not yet formally proved for these systems with non-geometric (non-exponential in continuous time case) parameters. The model under consideration is similar to the system that was investigated in Morozov *et al.*[15]. However, there are essential differences that lead to consideration of different processes. Firstly, we employ the regenerative flow as an input flow. Secondly, servers of the system may be heterogeneous. We have considered the preemptive repeat difference service discipline. In this paper the necessary and sufficient condition for stability of the queue-length process is established, whereas in Morozov *et al.*[15] only sufficient condition for this service discipline is proved. Certainly, exploiting the same technique, stability theorems for preemptive resume service discipline may be also proved. The synchronization method enables us to obtain stability results for continuous-time case as well.

Acknowledgements. This paper is partially supported by the Russian Foundation For Basic Research grant 13-01-00653.

References

1. L. Afanaseva. Queuing Systems with Cyclic Control Processes. *Cybernetics and Systems Analysis*, 41, **1**, 43–55, 2005.
2. L. Afanasyeva and E. Bashtova. Coupling method for asymptotic analysis of queues with regenerative input and unreliable server. *Queueing Systems*, 76, **2**, 125–147, 2014.
3. L. Afanasyeva and A. Tkachenko. Multichannel queueing systems with regenerative input flow. *Theory of Probability & Its Applications*, 58, **2**, 174–192, 2014.
4. L. Afanasyeva, E. Bashtova, and E. Bulinskaya. Limit theorems for semi-Markov queues and their applications. *Communications in Statistics-Simulation and Computation*, 41, **6**, 688–709, 2012.
5. A. A. Borovkov. Some limit theorems in the theory of mass service, II multiple channels systems. *Theory of Probability & Its Applications*, 10, **3**, 375–400, 1965.
6. B. T. Doshi. Queueing systems with vacations a survey. *Queueing Systems*, 1, **1**, 29–66, 1986.
7. W. Feller, *An introduction to probability theory and its applications*, 2nd ed. New York, NY, USA: Wiley, 1957.
8. D. P. Gaver Jr. A waiting line with interrupted service, including priorities. *Journal of the Royal Statistical Society. Series B (Methodological)*, 73–90, 1962.
9. J. Grandell, *Doubly Stochastic Poisson Processes*, 1976th ed. Springer, 1976.
10. L. D. Iglehart, W. Whitt. Multiple channel queues in heavy traffic I. *Advances in Applied Probability*, 2, **1**, 150–177, 1970.

11. J. C. Ke, C. H. Wu, and Z. G. Zhang. Recent developments in vacation queueing models: a short survey. *International Journal of Operations Research*, 7, **4**, 3–8, 2010.
12. A. Krishnamoorthy, P. K. Pramod, and S. R. Chakravarthy. Queues with interruptions: a survey. *TOP*, 1–31, 2012.
13. S. P. Meyn and R. L. Tweedie, *Markov chains and stochastic stability.* Cambridge University Press, 2009.
14. E. Morozov and R. Delgado. Stability analysis of regenerative queueing systems. *Automation and Remote Control*, 70, **12**, 1977–1991, 2009.
15. E. Morozov, D. Fiems, and H. Bruneel. Stability analysis of multiserver discrete-time queueing systems with renewal-type server interruptions. *Performance Evaluation*, 68, **12**, 1261–1275, 2011.
16. G. Pang, R. Talreja, and W. Whitt. Martingale proofs of many-server heavy-traffic limits for Markovian queues. *Probability Surveys*, 4, 193–267, 2007.
17. A. V. Pechinkin, I. A. Sokolov, and V. V. Chaplygin. Multichannel queueing system with refusals of servers groups. *Informatics and its Applications*, 3, **3**, 4–15, 2009.
18. H. Thorisson. A complete coupling proof of Blackwell's renewal theorem. *Stochastic Processes and their Applications*, 26, 87–97, 1987.
19. A. V. Tkachenko. Multichannel queueing systems in a random environment. *Moscow University Mathematics Bulletin*, 1, 53–57, 2014.

Optimization of Multi-Component Insurance System with Dividend Payments

Ekaterina Bulinskaya and Anastasia Muromskaya

Department of Mathematics and Mechanics,
Lomonosov Moscow State University
119991 Moscow, Russia
(E-mail: ebulinsk@yandex.ru)

Abstract. We study a model of insurance company performance with dividends payment and reinsurance. The claim process is supposed to be compound Poisson. The company uses the barrier dividend strategy. In contrast to previous research the non-proportional excess of loss reinsurance treaty with limited liability of reinsurer is applied. The optimal dividend barrier, providing the maximal value of expected discounted dividends paid until ruin, is obtained for exponential and uniform claim distributions under some additional assumptions.
Keywords: Dividends, Reinsurance, Limited liability, Optimization.

1 Introduction

It is well known that the primary task of any insurance company is indemnification of its policyholders losses. Hence, many researchers have investigated the ruin probability of insurance company. In other words, a so-called reliability approach has dominated for a long time in actuarial sciences.

However, being a corporation, the insurance company needs to pay dividends to its shareholders. Thus, in 1957 De Finetti[4] proposed a new approach. Namely, he initiated the study of expected discounted dividends until the company ruin. The aim was to choose a dividend strategy providing the maximal value of the above mentioned dividends. Review of the results in this domain one can find in the papers by Abrecher and Thonhauser[1] and Avanzi[2]. We mention also the investigations by Gerber *et al.*[6] and Gerber and Shiu[7] which are generalized in our work.

Nowadays reinsurance is widely used for stabilization of any insurance company performance. So we consider below a multi-component system taking into account not only dividends payment but reinsurance as well. In contrast to the papers by Karapetyan[8] and Mnif and Sulem[9], where excess of loss reinsurance with unlimited liability of reinsurer was treated, we study the case of limited liability. The optimal barrier strategy of dividends payment is established for the exponential and uniform claim distributions under some additional assumptions.

New Trends in Stochastic Modeling and Data Analysis (pp. 27-42)
Raimondo Manca - Sally McClean - Christos H Skiadas (Eds)

The paper is organized as follows. In Section 2 we give the model description recalling some results obtained for the company not using reinsurance. The excess of loss reinsurance with limited liability of reinsurer is treated in Section 3. In the first subsection we find the optimal dividend barrier for the case of exponential claims whereas the uniform distribution is considered in the second subsection. In Section 4 we give comments and discuss further research directions.

2 Model description

At first we present some results obtained previously for the classical Cramér-Lundberg model by other researchers. In the framework of this model the insurance company surplus at time t (without dividends payment) is as follows:

$$U(t) = U(0) + ct - S(t),\ t \geq 0.$$

Here $\{S(t), t \geq 0\}$ is a compound Poisson process with intensity λ. The claim amounts are independent nonnegative identically distributed random variables with probability density $p(y)$. Premiums are acquired continuously at the rate $c = (1+\theta)\lambda p_1$ where $\theta > 0$ and $p_1 = \int\limits_0^\infty yp(y)dy$ is the expected claim value.

To study the insurance company performance and dividend payments denote by $D(t)$ the total dividends paid until t. Then

$$X(t) = U(t) - D(t)$$

is the company surplus at time t and

$$T = \inf\{t:\ X(t) < 0\}$$

is the ruin time of the company.

Dividends are paid according to some strategy. There exist a lot of possible dividends strategies. However we are going to consider only barrier strategies with barrier level b. Such a strategy means that there is no dividend payment if $X(t) < b$, whereas the payment intensity equals c if $X(t) = b$ (see Fig. 1). We assume that $X(0) = x \leq b$, hence, $X(t)$ never exceeds b.

Let $V(x,b) = E\left[\int\limits_0^T e^{-\delta t} dD(t)\right]$ be the expected discounted dividends under barrier strategy with parameter b, whereas $x = U(0)$ denotes the initial company surplus, $0 \leq x \leq b$. Then, according to Gerber *et al.*[6], $V(x,b)$, as a function of x, satisfies the following equation

$$cV'(x,b) - (\lambda+\delta)V(x,b) + \lambda \int\limits_0^x V(y,b)p(x-y)dy = 0,\quad 0 < x < b, \qquad (1)$$

with the boundary condition

$$V'(b,b) = 1. \qquad (2)$$

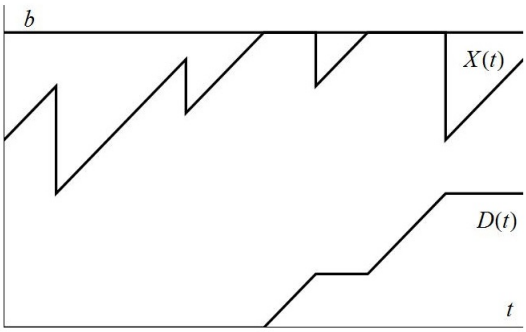

Fig. 1. Company surplus and dividends under barrier strategy

The exponential distribution with parameter β was also treated in Gerber *et al.*[6]. They have found the explicit form of $V(x,b)$ for this distribution. For this purpose the operator $\left(\frac{d}{dx}+\beta\right)$ was applied to all the summands of equation (1). (We are going to use such a method treating the case with reinsurance). Thus,

$$V(x,b) = C_0 e^{rx} + C_1 e^{sx}, \quad 0 \le x \le b.$$

Here the coefficients $r > 0, s < 0$ are the roots of the characteristic equation

$$(1+\theta)p_1\xi^2 + (\theta-\alpha)\xi - \alpha\beta = 0,$$

where $\alpha = \frac{\delta}{\lambda}$. The coefficients C_0 and C_1 were obtained using the boundary condition (2) and substitution of $V(x,b)$ in the initial equation (1). Hence,

$$C_0 = \frac{r+\beta}{\nu(b)}\ , \quad C_1 = -\frac{s+\beta}{\nu(b)}$$

with

$$\nu(b) = re^{rb}\,(r+\beta) - se^{sb}\,(s+\beta)\ .$$

It was shown as well that the barrier strategy with parameter b^* satisfying $\nu'(b^*) = 0$ is optimal, that is, maximizes the expected dividends $V(x,b)$ paid until ruin. So, for exponential claim distribution it is not difficult to find the optimal barrier

$$b^*(r,s) = \frac{1}{r-s}\ln\frac{s^2(s+\beta)}{r^2(r+\beta)}\ .$$

The aim of our investigation is obtaining of the solution of equation (1) for various claim distributions in case of excess of loss reinsurance with limited liability of reinsurer. Moreover, it is also interesting to get the optimal value of parameter b, providing maximum of $V(x,b)$.

3 Excess of loss reinsurance with limited liability of reinsurer

In addition to usual XL reinsurance treaty with retention d we assume that reinsurer has a liability limit l. Let X be the initial claim size of direct insurer

then his payment under the above mentioned treaty is

$$X_l = \min(d, X) + \max(X - l - d, 0),$$

whereas the reinsurer's payment is equal to

$$X'_l = \min(\max(X - d, 0), l).$$

Denote by $F_l(x)$ the distribution function of insurer's payment in the framework of reinsurance treaty. Then $F_l(x)$ has the form presented by Fig. 2 if the initial claim had an absolutely continuous distribution. Here the initial claim distribution function $F(x)$ is depicted by the dash line and the boldface line represents the corresponding distribution after reinsurance.

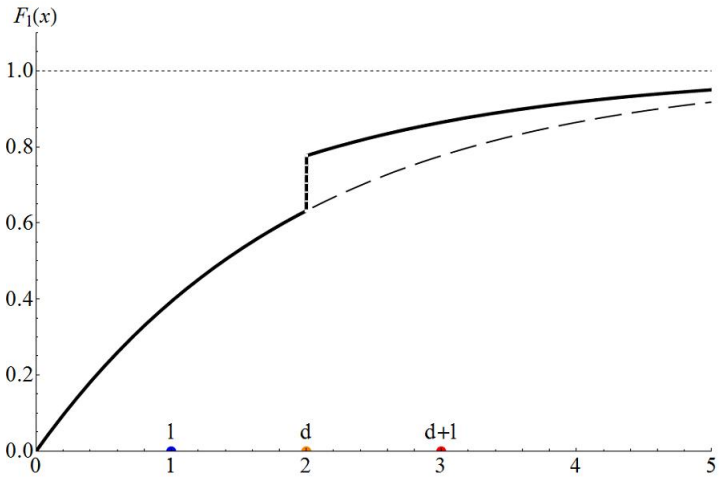

Fig. 2. Insurer's distribution function

Let us suppose that direct insurer and reinsurer use for premiums calculation the expected value principle with loads θ and θ_1 respectively (and $\theta_1 > \theta > 0$). Then the insurer's premium net of reinsurance c_l has the form

$$c_l = \lambda(1+\theta)p_1 - \lambda(1+\theta_1)\int_d^{d+l}(1 - F(x))\,dx.$$

Theorem 1. *The integro-differential equation for total discounted dividends until ruin, under reinsurance treaty, $V(x, b, d, l)$ can be written for $0 < x < d$ as follows*

$$\tilde{c}_l V'(x, b, d, l) - (1+\alpha)V(x, b, d, l) + \int_0^x V(y, b, d, l)p(x - y)\,dy = 0 \qquad (3)$$

and for $d \le x < b$

$$\tilde{c}_l V'(x,b,d,l) - (1+\alpha)V(x,b,d,l) + \int_{x-d}^{x} V(y,b,d,l)p(x-y)\,dy$$
$$+ V(x-d,b,d,l)(F(d+l)-F(d)) + \int_{0}^{x-d} V(y,b,d,l)p(l+x-y)\,dy = 0. \quad (4)$$

Here $\tilde{c}_l = \frac{c_l}{\lambda}$ *and* $\alpha = \frac{\delta}{\lambda}$. *The boundary condition has the form*

$$V'(b,b,d,l) = 1. \quad (5)$$

Proof. Proceeding along the same lines as in Gerber *et al.*[6] one obtains the following equation

$$c_l V'(x,b,d,l) - (\lambda+\delta)V(x,b,d,l)$$
$$- \lambda \int_{0}^{x} V(y,b,d,l)\,dF_l(x-y) = 0, \quad 0 < x < b, \quad (6)$$

and boundary condition (5).

We can transform the integral term in the left-hand side of equation (6) putting $x - y = t$

$$-\lambda \int_{0}^{x} V(y,b,d,l)\,dF_l(x-y) = \lambda \int_{0}^{x} V(x-t,b,d,l)\,dF_l(t)$$
$$= \begin{cases} \lambda \int_{0}^{x} V(x-t,b,d,l)\,dF(t), & \text{for } 0 < x < d, \\ \lambda \int_{0}^{d} V(x-t,b,d,l)\,dF(t) + \lambda V(x-d,b,d,l)(F_l(d) - F_l(d-0)) \\ \quad + \lambda \int_{d}^{x} V(x-t,b,d,l)dF(l+t), & \text{for } d \le x < b. \end{cases} \quad (7)$$

We assume here that $b > d$. If $b \le d$, we are going to consider only $x < d$.

We begin by treating the case $0 < x < d$. Since

$$\lambda \int_{0}^{x} V(x-t,b,d,l)dF(t) = \lambda \int_{0}^{x} V(y,b,d,l)p(x-y)dy,$$

one deduces that, for $x < d$, equation (6) is equivalent to (3).

Hence, the equation for $V(x,b,d,l)$ in interval $x \in (0,d)$ is similar to (1). Moreover, these two equations have only different intensities of premium acquirement.

Now turn to the case $d \le x < b$. First of all, we use the following transformations of two terms in the right-hand side of (7) for $d \le x < b$:

$$\lambda \int_0^d V(x-t,b,d,l)dF(t) = \lambda \int_x^{x-d} V(y,b,d,l)dF(x-y)$$
$$= -\lambda \int_x^{x-d} V(y,b,d,l)p(x-y)\,dy = \lambda \int_{x-d}^{x} V(y,b,d,l)p(x-y)\,dy$$

and

$$\lambda \int_d^x V(x-t,b,d,l)\,dF(l+t) = \lambda \int_d^x V(x-t,b,d,l)p(l+t)dt$$
$$= \lambda \int_0^{x-d} V(y,b,d,l)p(l+x-y)\,dy.$$

Note also that the following equality

$$F_l(d) - F_l(d-0) = F(d+l) - F(d)$$

is valid. Dividing both sides of (6) by λ and putting $\tilde{c}_l = \frac{c_l}{\lambda}$ we get the new equation

$$\tilde{c}_l V'(x,b,d,l) - (1+\alpha)V(x,b,d,l) - \int_0^x V(y,b,d,l)\,dF_l(x-y) = 0, \quad d \le x < b.$$

Due to equality (7) and the described above transformations, this equation takes the form (4). This ends the proof. □

The next step is to get instead of integro-differential equations (3) and (4) the second order differential equations and solve them.

3.1 Exponential claim distribution

Further we concentrate on the case of exponential claim distribution with parameter β and obtain the following result.

Theorem 2. *For $0 < x < d$ the function $V(x,b,d,l)$ satisfies the second order differential equation*

$$\tilde{c}_l V''(x,b,d,l) + (\beta\tilde{c}_l - (1+\alpha))V'(x,b,d,l) - \alpha\beta V(x,b,d,l) = 0, \qquad (8)$$

whereas for $d \le x < b$ one has

$$\tilde{c}_l V''(x,b,d,l) + (\beta\tilde{c}_l - (1+\alpha))V'(x,b,d,l) - \alpha\beta V(x,b,d,l)$$
$$= -e^{-\beta d}F(l)V'(x-d,b,d,l). \qquad (9)$$

Here $\tilde{c}_l = \frac{1}{\beta}\left((1+\theta) + (1+\theta_1)e^{-\beta d}(e^{-\beta l} - 1)\right)$.

Proof. The first case is $0 < x < d$. We apply the operator $(\frac{d}{dx} + \beta)$ to all the summands of equation (3) and easily get, as in Gerber *et al.*[6], expression (8).

For exponential distribution

$$\tilde{c}_l = (1+\theta)p_1 - (1+\theta_1)\int_d^{d+l} e^{-\beta x}\,dx = \frac{1}{\beta}\left((1+\theta) + (1+\theta_1)e^{-\beta d}(e^{-\beta l} - 1)\right)$$

and

$$\beta\tilde{c}_l - (1+\alpha) = (\theta - \alpha) + e^{-\beta d}(1+\theta_1)(e^{-\beta l} - 1)\ .$$

Now we turn to the domain $d \le x < b$ and apply the operator $\left(\frac{d}{dx} + \beta\right)$ to equation (4). The operator is separately applied to each summand. For the first one we get

$$\left(\frac{d}{dx} + \beta\right)[\tilde{c}_l V'(x,b,d,l)] = \tilde{c}_l V''(x,b,d,l) + \beta\tilde{c}_l V'(x,b,d,l),$$

the second one yields

$$\left(\frac{d}{dx} + \beta\right)[-(1+\alpha)V(x,b,d,l)] = -(1+\alpha)V'(x,b,d,l) - \beta(1+\alpha)V(x,b,d,l).$$

For the third term we have

$$\left(\frac{d}{dx} + \beta\right)\int_{x-d}^{x} V(y,b,d,l)p(x-y)\,dy$$

$$= \left(\frac{d}{dx} + \beta\right)\int_0^x V(y,b,d,l)p(x-y)\,dy - \left(\frac{d}{dx} + \beta\right)\int_0^{x-d} V(y,b,d,l)p(x-y)\,dy.$$

Then applying the operator $\left(\frac{d}{dx} + \beta\right)$ and simultaneously using the relation $p'(x) = -\beta p(x)$, we obtain

$$\left(\frac{d}{dx} + \beta\right)\int_0^x V(y,b,d,l)p(x-y)dy = \beta V(x,b,d,l).$$

Next, we transform the integral

$$\left(\frac{d}{dx} + \beta\right)\int_0^{x-d} V(y,b,d,l)p(x-y)dy = V(x-d,b,d,l)p(x-x+d)$$

$$+\int_0^{x-d} V(y,b,d,l)p'(x-y)dy + \beta\int_0^{x-d} V(y,b,d,l)p(x-y)dy = V(x-d,b,d,l)p(d),$$

getting

$$\left(\frac{d}{dx}+\beta\right)\int\limits_{x-d}^{x} V(y,b,d,l)p(x-y)dy = \beta V(x,b,d,l) - V(x-d,b,d,l)p(d).$$

For the fourth term we have the following expression

$$\begin{aligned}&\left(\frac{d}{dx}+\beta\right)[V(x-d,b,d,l)(F(d+l)-F(d))]\\ &= V'(x-d,b,d,l)(F(d+l)-F(d)) + \beta V(x-d,b,d,l)(F(d+l)-F(d)).\end{aligned}$$

The last term gives

$$\begin{aligned}\left(\frac{d}{dx}+\beta\right)\int\limits_{0}^{x-d} V(y,b,d,l)p(l+x-y)dy &= V(x-d,b,d,l)p(l+x-x+d)\\ + \int\limits_{0}^{x-d} V(y,b,d,l)p'(l+x-y)dy + \beta\int\limits_{0}^{x-d} V(y,b,d,l)p(l+x-y)dy&\\ = V(x-d,b,d,l)p(l+d).&\end{aligned}$$

After summation of all the obtained expressions we get

$$\begin{aligned}&\tilde{c}_l V''(x,b,d,l) + \beta\tilde{c}_l V'(x,b,d,l) - (1+\alpha)V'(x,b,d,l) - \beta(1+\alpha)V(x,b,d,l)\\ &+ \beta V(x,b,d,l) - V(x-d,b,d,l)p(d) + V'(x-d,b,d,l)(F(d+l)-F(d))\\ &+ \beta V(x-d,b,d,l)(F(d+l)-F(d)) + V(x-d,b,d,l)p(l+d) = 0.\end{aligned}$$

Using the relations $F(x) = 1 - e^{-\beta x}$ and $p(x) = \beta e^{-\beta x}$, after some transformations we finally establish the desired equation (9). □

Now we are able to prove the following result.

Theorem 3. *For the exponential claim distribution the optimal dividends barrier, under excess of loss reinsurance treaty with limited liability of reinsurer and assumption* $0 < x \le b < d$*, is given by*

$$b_l^* = b^*(r_l, s_l) = \frac{1}{r_l - s_l}\ln\frac{s_l^2(s_l+\beta)}{r_l^2(r_l+\beta)}\ . \tag{10}$$

Here $r_l > 0, s_l < 0$ *are the roots of the characteristic equation*

$$\tilde{c}_l\xi^2 + (\beta\tilde{c}_l - (1+\alpha))\,\xi - \alpha\beta = 0. \tag{11}$$

Proof. Obviously, for $0 < x \le b < d$ the solution of equation (8) has the form

$$V(x,b,d,l) = E_0(b,d,l)e^{r_l x} + E_1(b,d,l)e^{s_l x}.$$

As in case without reinsurance we establish that

$$E_0(b,d,l) = \frac{r_l+\beta}{\nu_l(b,d,l)}\ , \quad E_1(b,d,l) = -\frac{s_l+\beta}{\nu_l(b,d,l)}\ ,$$

where

$$\nu_l(b,d,l) = r_l e^{r_l b}\,(r_l+\beta) - s_l e^{s_l b}\,(s_l+\beta)\ .$$

Minimizing this expression we obtain that the optimal dividends barrier has the form (10). □

Now we prove some corollaries useful for investigation of system stability.

Corollary 1. *Parameters r_l and s_l are monotone increasing in l and decreasing in d.*

Proof. Recall that for the exponential claim distribution we have

$$\tilde{c_l} = \frac{1}{\beta}\left[(1+\theta) - (1+\theta_1)e^{-\beta d}(1-e^{-\beta l})\right].$$

It is clear that $\tilde{c_l}$ decreases in l and increases in d. Now we verify the monotone dependence on l and d of the roots of characteristic equation (11).

The discriminant $D = (\beta\tilde{c_l} - (1+\alpha))^2 + 4\alpha\beta\tilde{c_l}$, therefore

$$s_l = \frac{-\sqrt{D} - \beta\tilde{c_l} + (1+\alpha)}{2\tilde{c_l}} = \frac{(1+\alpha)-\sqrt{D}}{2\tilde{c_l}} - \frac{\beta}{2}.$$

First of all we find the derivative of s_l with respect to $\tilde{c_l}$

$$(s_l)'_{\tilde{c_l}} = \left(\frac{(1+\alpha)-\sqrt{D}}{2\tilde{c_l}}\right)'_{\tilde{c_l}} = \frac{-D'_{\tilde{c_l}}\tilde{c_l} - 2\sqrt{D}(1+\alpha-\sqrt{D})}{4{\tilde{c_l}}^2\sqrt{D}}$$
$$= \frac{(\alpha\beta\tilde{c_l} - \beta\tilde{c_l} + (1+\alpha)^2) - \sqrt{D}(1+\alpha)}{2\sqrt{D}{\tilde{c_l}}^2}.$$

The Vieta formulas lead us to conclusion that

$$r_l + s_l = \frac{(1+\alpha)-\beta\tilde{c_l}}{\tilde{c_l}} = \frac{1+\alpha}{\tilde{c_l}} - \beta.$$

After differentiation in $\tilde{c_l}$ and using the expression of $(s_l)'_{\tilde{c_l}}$ we get

$$(r_l+s_l)'_{\tilde{c_l}} = (r_l)'_{\tilde{c_l}} + \frac{(\alpha\beta\tilde{c_l} - \beta\tilde{c_l} + (1+\alpha)^2) - \sqrt{D}(1+\alpha)}{2\sqrt{D}{\tilde{c_l}}^2} = -\frac{1+\alpha}{{\tilde{c_l}}^2}.$$

Hence,

$$(r_l)'_{\tilde{c_l}} = \frac{-(\alpha\beta\tilde{c_l} - \beta\tilde{c_l} + (1+\alpha)^2) - \sqrt{D}(1+\alpha)}{2\sqrt{D}{\tilde{c_l}}^2}.$$

For all the admissible parameters values

$$(\alpha\beta\tilde{c_l} - \beta\tilde{c_l} + (1+\alpha)^2)^2 < (\sqrt{D}(1+\alpha))^2 = D(1+\alpha)^2.$$

Since $-\sqrt{D}(1+\alpha)$ is negative, the numerator in expression of $(r_l)'_{\tilde{c_l}}$ is negative for all values of $-(\alpha\beta\tilde{c_l}-\beta\tilde{c_l}+(1+\alpha)^2)$. Thus, we obtained inequality $(r_l)'_{\tilde{c_l}} < 0$. Similar arguments are valid for $(s_l)'_{\tilde{c_l}}$, that is, $(s_l)'_{\tilde{c_l}} < 0$. Hence, we come to the conclusion that r_l and s_l are monotone decreasing in $\tilde{c_l}$, therefore r_l and s_l are monotone increasing in l and decreasing in d. □

Now we consider the conditions for $b_l^* > 0$.

Corollary 2. *Conditions* $(1+\theta)+(1+\theta_1)e^{-\beta d}(e^{-\beta l}-1) > (1+\alpha)^2$ *and* $b_l^* > 0$ *are equivalent.*

Proof. We have established that b_l^* has the form (10).

Clearly, $b_l^* > 0 \Leftrightarrow s_l^2(s_l+\beta) > r_l^2(r_l+\beta)$. Since r_l and s_l are the roots of the characteristic equation (11), we can write

$$\tilde{c_l} r_l^2 + (\beta\tilde{c_l} - (1+\alpha))r_l - \alpha\beta = 0, \quad \tilde{c_l} s_l^2 + (\beta\tilde{c_l} - (1+\alpha))s_l - \alpha\beta = 0.$$

It follows immediately

$$r_l^2 = \frac{\alpha\beta - (\beta\tilde{c_l} - (1+\alpha))r_l}{\tilde{c_l}},$$

whence

$$\begin{aligned} r_l^2(r_l+\beta) &= \frac{\alpha\beta - (\beta\tilde{c_l} - (1+\alpha))r_l}{\tilde{c_l}}(r_l+\beta) \\ &= \frac{r_l(\alpha\beta - \beta(\beta\tilde{c_l} - (1+\alpha))) + \alpha\beta^2 - r_l^2(\beta\tilde{c_l} - (1+\alpha))}{\tilde{c_l}} \\ &= \frac{r_l(\tilde{c_l}\alpha\beta - \tilde{c_l}\beta(\beta\tilde{c_l} - (1+\alpha))) + \alpha\beta(\alpha+1) + r_l(\beta\tilde{c_l} - (1+\alpha))^2}{\tilde{c_l}^2} \\ &= \frac{((1+\alpha)^2 - \beta\tilde{c_l})r_l + \alpha\beta(\alpha+1)}{\tilde{c_l}^2}. \end{aligned}$$

Thus, we obtained the expression of the form $\frac{Ar_l+B}{\tilde{c_l}^2}$. Analogously, for $s_l^2(s_l+\beta)$ one gets the following presentation

$$s_l^2(s_l+\beta) = \frac{As_l + B}{\tilde{c_l}^2}$$

with the same A and B. Therefore $b_l^* > 0 \Leftrightarrow s_l^2(s_l+\beta) > r_l^2(r_l+\beta) \Leftrightarrow As_l + B > Ar_l + B \Leftrightarrow A(s_l - r_l) > 0$. We know that $s_l - r_l < 0$. Hence,

$$A = -\beta\tilde{c_l} + (1+\alpha)^2 < 0 \;\Leftrightarrow\; (1+\theta)+(1+\theta_1)e^{-\beta d}(e^{-\beta l}-1) > (1+\alpha)^2 \;\Leftrightarrow b_l^* > 0. \square$$

Now we are able to study monotonicity of b_l^* in l and d and condition $b_l^* < d$.

Corollary 3. *The following conditions*

1. $\alpha \in (0; 0.5)$,
2. $(1+\alpha)^2 < 1+\theta < \min\left(3 - 1.5\alpha; (1+\alpha)^2(1-\alpha)^{-1}\right)$,
3. $d > \max\left(-\frac{1}{\beta}\ln\left(\frac{(1+\theta)-(1+\alpha)^2}{1+\theta_1}\right); b^*\right)$

are sufficient for $b_l^* < d$. *Furthermore,* b_l^* *is monotone decreasing in* l *and increasing in* d.

Proof. We have already established that

$$\beta\tilde{c_l} > (1+\alpha)^2 \;\Leftrightarrow\; b_l^* > 0.$$

This inequality for $\beta\tilde{c}_l$ will be the first assumption for the study of monotonicity of b_l^* in l and d.

Now consider separately each factor in (10) and write the conditions of their monotonicity in l and d. We begin by treating $r_l - s_l$. Clearly the fraction $(r_l - s_l)^{-1}$ will be changing in opposite direction.

$$(r_l - s_l)'_{\tilde{c}_l} = (r_l)'_{\tilde{c}_l} - (s_l)'_{\tilde{c}_l} = \frac{-(\alpha\beta\tilde{c}_l - \beta\tilde{c}_l + (1+\alpha)^2)}{\tilde{c}_l{}^2\sqrt{D}}.$$

Here we denote by D the discriminant of characteristic equation (11). The denominator in the right-hand side of the equality is always positive. Therefore

$$(r_l - s_l)'_{\tilde{c}_l} < 0 \;\Leftrightarrow\; \beta\tilde{c}_l(\alpha - 1) + (1+\alpha)^2 > 0.$$

This inequality is fulfilled either for $\alpha > 1$ or for $\beta\tilde{c}_l < (1+\alpha)^2(1-\alpha)^{-1}$. Under such assumptions $(r_l - s_l)^{-1}$ grows in $\tilde{c}_l$, hence, it diminishes in l and grows in d. This is the second condition of b_l^* monotonicity.

Next, we deal with the second factor in (10). The logarithm is a monotone increasing function, so we consider only its argument

$$\left(\frac{s_l^2(s_l+\beta)}{r_l^2(r_l+\beta)}\right)'_{\tilde{c}_l} = \frac{s'_l(3s_l^2 + 2s_l\beta)(r_l^3 + r_l^2\beta) - r'_l(3r_l^2 + 2r_l\beta)(s_l^3 + s_l^2\beta)}{(r_l^3 + r_l^2\beta)^2}.$$

The denominator of this fraction is always positive. We have already obtained two inequalities $(s_l)'_{\tilde{c}_l} < 0$ and $(r_l)'_{\tilde{c}_l} < 0$. The factors $(r_l^3 + r_l^2\beta)$ and $(3r_l^2 + 2r_l\beta)$ are positive, because r_l is a positive root of characteristic equation (11). Due to $s_l + \beta > 0$, we have $(s_l^3 + s_l^2\beta) > 0$. Thus, for $3s_l^2 + 2s_l\beta < 0$, the derivative of the logarithm's argument will be positive and it will monotone grow in $\tilde{c}_l$. Note that

$$3s_l^2 + 2s_l\beta < 0 \;\Leftrightarrow\; s_l(3s_l + 2\beta) < 0 \;\Leftrightarrow\; s_l > -\frac{2}{3}\beta.$$

Using the expression of s_l, we rewrite the last inequality in the form

$$\frac{-\sqrt{(\beta\tilde{c}_l - (1+\alpha))^2 + 4\alpha\beta\tilde{c}_l} - \beta\tilde{c}_l + (1+\alpha)}{2\tilde{c}_l} > -\frac{2}{3}\beta,$$

getting after some transformations the third condition of b_l^* monotonicity, namely, $\beta\tilde{c}_l < 3 - 1.5\alpha$.

Hence, we can rewrite the list of conditions for b_l^* monotonicity in l and d as follows

1. $\beta\tilde{c}_l > (1+\alpha)^2$
2. either $\alpha > 1$ or $\beta\tilde{c}_l < (1+\alpha)^2(1-\alpha)^{-1}$
3. $\beta\tilde{c}_l < 3 - 1.5\alpha$.

For simultaneous validity of conditions 1 and 3 we need the fulfillment of the following inequality $(1+\alpha)^2 < 3-1.5\alpha$, which is true for $0 < \alpha < 0.5$. It means, in condition 2 we can take only $\beta\tilde{c}_l < (1+\alpha)^2(1-\alpha)^{-1}$. Thus, instead of three conditions we obtain only one of the form

$$(1+\alpha)^2 < \beta\tilde{c}_l < \min\left(3-1.5\alpha; (1+\alpha)^2(1-\alpha)^{-1}\right).$$

It follows immediately that inequality $(1+\alpha)^2 < (1+\alpha)^2(1-\alpha)^{-1}$ must be true as well. Since it is fulfilled for all $\alpha \in (0,1)$, condition $0 < \alpha < 0.5$ is sufficient.

Finally, under assumptions

$$(1+\alpha)^2 < \beta\tilde{c}_l < \min\left(3-1.5\alpha; (1+\alpha)^2(1-\alpha)^{-1}\right) \text{ and } \alpha \in (0; 0.5) \qquad (12)$$

one has $b_l^* > 0$, moreover, b_l^* is monotone decreasing in l and increasing in d.

Recall that $\beta\tilde{c}_l$ is monotone decreasing in l. Therefore, if $\lim_{l\to\infty} \beta\tilde{c}_l > (1+\alpha)^2$, the same is true for all $l \geq 0$. Thus, we must have the following condition

$$\lim_{l\to\infty} \beta\tilde{c}_l = (1+\theta) - (1+\theta_1)e^{-\beta d} > (1+\alpha)^2.$$

This inequality is valid if $1+\theta > (1+\alpha)^2$ and $d > -\frac{1}{\beta}\ln\left(\frac{(1+\theta)-(1+\alpha)^2}{1+\theta_1}\right)$. Remark that $-\frac{1}{\beta}\ln\left(\frac{(1+\theta)-(1+\alpha)^2}{1+\theta_1}\right) > 0$ if $\theta_1 > \theta$ (this condition is valid for our model). Thus, if $d > -\frac{1}{\beta}\ln\left(\frac{(1+\theta)-(1+\alpha)^2}{1+\theta_1}\right)$, then $\beta\tilde{c}_l > (1+\alpha)^2$ for all $l \geq 0$.

Analogously, $\beta\tilde{c}_l$ increases in d. Therefore, if $\beta\tilde{c}_l > (1+\alpha)^2$ for $d = 0$, the same inequality is valid for all $d \geq 0$. For $d = 0$ we have

$$\begin{aligned}
&(1+\theta) + (1+\theta_1)(e^{-\beta l} - 1) > (1+\alpha)^2 \\
&\qquad \Leftrightarrow\ (1+\theta_1)(e^{-\beta l} - 1) > (1+\alpha)^2 - (1+\theta) \\
&\qquad\qquad \Leftrightarrow\ e^{-\beta l} > \frac{(1+\alpha)^2 + \theta_1 - \theta}{1+\theta_1} \\
&\qquad\qquad\qquad \Leftrightarrow\ l < -\frac{1}{\beta}\ln\left(\frac{(1+\alpha)^2 + \theta_1 - \theta}{1+\theta_1}\right).
\end{aligned}$$

Note that $-\frac{1}{\beta}\ln\left(\frac{(1+\alpha)^2+\theta_1-\theta}{1+\theta_1}\right) > 0$ for $(1+\theta) > (1+\alpha)^2$ and is defined for $\theta_1 > \theta$ (in this case the argument of logarithm is positive). Above we have made the same assumptions.

Summing up, if $l < -\frac{1}{\beta}\ln\left(\frac{(1+\alpha)^2+\theta_1-\theta}{1+\theta_1}\right)$ and $(1+\theta) > (1+\alpha)^2$, then $\beta\tilde{c}_l > (1+\alpha)^2$ for all $d \geq 0$.

Now turn to the condition $\beta\tilde{c}_l < \min\left(3-1.5\alpha; (1+\alpha)^2(1-\alpha)^{-1}\right)$. We have already established that $\beta\tilde{c}_l$ decreases in l and increases in d. So if for

$l = 0$ (or $d \to \infty$) we have $\beta\tilde{c}_l < \min\left(3 - 1.5\alpha; (1+\alpha)^2(1-\alpha)^{-1}\right)$, then the same inequality will be valid for all nonnegative l (or d). For $l = 0$ (or $d \to \infty$) the inequality under consideration has the form

$$1 + \theta < \min\left(3 - 1.5\alpha; (1+\alpha)^2(1-\alpha)^{-1}\right).$$

Thus, the following conditions

1. $\alpha \in (0; 0.5)$,
2. $(1+\alpha)^2 < 1 + \theta < \min\left(3 - 1.5\alpha; (1+\alpha)^2(1-\alpha)^{-1}\right)$,
3. $d > -\frac{1}{\beta}\ln\left(\frac{(1+\theta)-(1+\alpha)^2}{1+\theta_1}\right)$

are sufficient for monotone decreasing of b_l^* in l, $l \geq 0$. Moreover, for $l = 0$ we get $b_l^* = b^*$, where b^* corresponds to the functioning without reinsurance. That means, $b_l^* \leq b^*$ for all $l \geq 0$ (see Fig. 3). So assuming $d > b^*$, we get $d > b_l^*$ for all $l \geq 0$. Hence, we established the sufficient conditions for validity of the desired inequality $d > b_l^*$. □

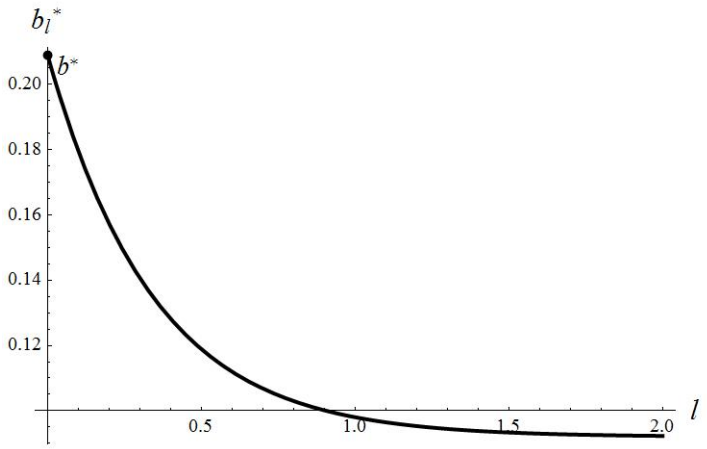

Fig. 3. Monotonicity of b_l^* in l.

We assumed $\beta = 3$, $\lambda = 0.5$, $x = 0.1$, $\delta = 0.1$, $\theta = 0.6$, $\theta_1 = 0.85$, $d = 1$, $b = 1$ drawing graphic in Fig. 3.

Remark. Similarly one can get the following slightly different sufficient conditions for validity of $d > b_l^*$:

1. $\alpha \in (0; 0.5)$,
2. $(1+\alpha)^2 < 1 + \theta < \min\left(3 - 1.5\alpha; (1+\alpha)^2(1-\alpha)^{-1}\right)$,
3. $l < -\frac{1}{\beta}\ln\left(\frac{(1+\alpha)^2+\theta_1-\theta}{1+\theta_1}\right)$
4. $d > b^*$.

3.2 Uniform distribution of claims

Assume the claims to be uniformly distributed on the interval $[0; h]$. It is reasonable to suppose that $d + l < h$.

Theorem 4. *For $0 < x < d$ the function $V(x, b, d, l)$ satisfies the second order differential equation*

$$\tilde{c}_l V''(x, b, d, l) - (1 + \alpha)V'(x, b, d, l) + \frac{1}{h}V(x, b, d, l) = 0, \tag{13}$$

whereas for $d \le x < h - l$ one has

$$\tilde{c}_l V''(x, b, d, l) - (1+\alpha)V'(x, b, d, l) + \frac{1}{h}V(x, b, d, l) + \frac{l}{h}V'(x-d, b, d, l) = 0 \tag{14}$$

and for $h - l \le x < b$

$$\tilde{c}_l V''(x, b, d, l) - (1 + \alpha)V'(x, b, d, l) + \frac{1}{h}V(x, b, d, l) + \frac{l}{h}V'(x - d, b, d, l) - \frac{1}{h}V(x - (h - l), b, d, l) = 0. \tag{15}$$

Here $\tilde{c}_l = (1 + \theta)\frac{h}{2} - l(1 + \theta_1)(1 - \frac{2d+l}{2h})$.

Proof. The first case is $0 < x < d$. For such x, the application of operator $\frac{d}{dx}$ to equation (3) taking into account equality $p(t) = \frac{1}{h}$ for $t \in (0, d)$ yields (13). For uniform distribution of claims we have

$$\tilde{c}_l = (1 + \theta)p_1 - (1 + \theta_1)\int_d^{d+l}(1 - F(x))dx = (1 + \theta)\frac{h}{2} - l(1 + \theta_1)(1 - \frac{2d + l}{2h}).$$

The second case corresponds to $d \le x < h - l$. Inserting the uniform distribution function $F(t)$ in (6), dividing by λ and using transformation (7) we get

$$\tilde{c}_l V'(x, b, d, l) - (1 + \alpha)V(x, b, d, l) + \int_0^d V(x - t, b, d, l)d\frac{t}{h} + V(x - d, b, d, l)\left(\frac{d + l}{h} - \frac{d}{h}\right) + \int_d^x V(x - t, b, d, l)d\frac{l + t}{h} = 0.$$

Application of operator $\frac{d}{dx}$ provides (14).

The last case corresponds to $h - l \le x < b$. Here (6) has the form

$$\tilde{c}_l V'(x, b, d, l) - (1 + \alpha)V(x, b, d, l) + \int_0^d V(x - t, b, d, l)d\frac{t}{h} + V(x - d, b, d, l)\left(\frac{d + l}{h} - \frac{d}{h}\right) + \int_d^{h-l} V(x - t, b, d, l)d\frac{l + t}{h} = 0.$$

After application of $\frac{d}{dx}$ we get the desired result (15). □

Now we are able to prove the following result.

Theorem 5. *If the claim distribution is uniform on interval* $[0, h]$ *and the roots of characteristic equation corresponding to differential equation* (13) *are real then the optimal dividend barrier* b *under assumption* $0 < x \leq b < d$ *is equal to initial capital of insurance company* x*.*

Proof. Obviously, for $0 < x \leq b < d$ the solution of equation (13) has the form

$$V(x, b, d, l) = U_0(b, d, l)e^{p_l x} + U_1(b, d, l)e^{q_l x} = \frac{p_l e^{p_l x} - q_l e^{q_l x}}{p_l^2 e^{p_l b} - q_l^2 e^{q_l b}},$$

where $p_l > q_l > 0$ are the roots of the characteristic equation

$$\tilde{c}_l \xi^2 - (1 + \alpha)\xi + h^{-1} = 0.$$

We assume here that $D = (1 + \alpha)^2 - 4\tilde{c}_l h^{-1} > 0$.

Thus the optimal barrier should be equal to

$$b_l^* = \frac{1}{p_l - q_l} \ln \frac{q_l^3}{p_l^3}, \tag{16}$$

however it is not difficult to establish that $b_l^* < 0$. That means, the function $V(x, b, d, l)$ has no local maximum for $b \in (0, d)$ and the optimal dividend barrier b is equal to x. □

Remark. For further investigation of the model we provide the following algorithm of $V(x, b, d, l)$ calculation for $d \leq x < b$ (see also Fig. 4)

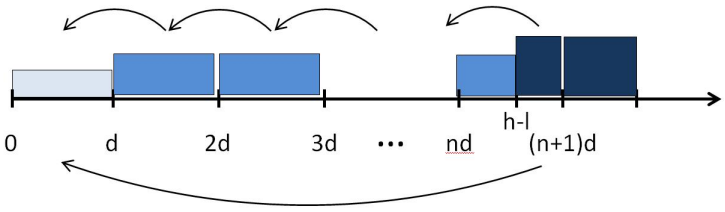

Fig. 4. Scheme of $V(x, b, d, l)$ calculation

1. Find expression of $V(x, b, d, l)$ on interval $(0, d)$.
2. Let $h - l \in (nd, (n + 1)d]$ for $n = 1, 2, \ldots$. The form of the function on half-interval $[kd, (k+1)d)$ for $1 \leq k \leq n-1$ can be obtained using its form on half-interval $[(k - 1)d, kd)$ and equation (14), the same is true for the last half-interval $[nd, h - l)$.
3. For $x \in [h-l, (n+1)d)$ according to (15) the function $V(x, b, d, l)$ depends on $V'(x-d, b, d, l)$ and $V(x-(h-l), b, d, l)$. The same is true for $x \geq (n+1)d$. Similarly, for $h - l \leq x < b$ we use the expression of the function on two previous half-intervals.

4 Comments

For the exponential and uniform claim distributions, we have considered the barrier dividends strategy and obtained the form of optimal barrier level b_l^* for the model with limited reinsurer's liability l in the excess of loss reinsurance treaty having retention d. It was additionally supposed that one is interested only in barriers $b \in (0, d)$. The restrictions on the model parameters for the fulfillment of such a condition in the case of exponential distribution were established. The set $[d, \infty)$ will be treated in the forthcoming publication. For the uniform distribution we treated only the case of characteristic equation with real roots. The case of complex roots will be presented in the other paper along with threshold and band strategies, as well as different value functions (for definitions see, e.g. the useful survey by Albrecher and Thonhauser[1]).

We plan also to study the modification of the model proposed by Dickson and Waters[5] and developed further by Gerber *et al.*[6]. Namely, it will be assumed that in case of ruin the shareholders pay out the deficit in order to enable the company to function further. Another research direction is to take into account the transaction costs associated with dividends payment, see, e.g., Paulsen[10], or possibility of bank loans, see Bulinskaya[3].

Acknowledgement. The research was partially supported by RFBR grant 13-01-00653.

References

1. H. Albrecher and S. Thonhauser. Optimality results for dividend problems in insurance. *Rev. R. Acad. Cien. Serie A. Mat.*, 103, 2, 295–320, 2009.
2. B. Avanzi. Strategies for dividend distribution: a review. *North American Actuarial Journal*, 13, 2, 217–251, 2009.
3. E. Bulinskaya. Asymptotic analysis of insurance models with bank loans. In: J. R. Bozeman, V. Girardin, and C. H. Skiadas, Eds. *New Perspectives on Stochastic Modeling and Data Analysis*, ISAST, Athens, Greece, 255–270, 2014.
4. B. De Finetti. Su un'impostazione alternativa della teoria collettiva del rischio. *Transactions of the XVth International Congress of Actuaries*, 2, 433–443, 1957.
5. D. C. M. Dickson and H. R. Waters. Some optimal dividends problems. *Astin Bull.*, 34, 1, 49–74, 2004.
6. H. U. Gerber, E. S. W. Shiu and N. Smith. Maximizing dividends without bankruptcy. *ASTIN Bulletin*, 36, 1, 5–23, 2006.
7. H. U. Gerber, E. S. W. Shiu. On optimal dividend strategies in the compound Poisson model. *North American Actuarial Journal*, 10, 2, 76–93, 2006.
8. N. V. Karapetyan. Dividends and reinsurance. *Proceedings of the 6th International Workshop on Simulation*, VVM com.Ltd, 47–52, 2009.
9. M. Mnif, and A. Sulem. Optimal risk control and dividend policies under excess of loss reinsurance. *Stochastics*, 77, 5, 455–476, 2005.
10. J. Paulsen. Optimal dividend payments until ruin of diffusion processes when payments are subject to both fixed and proportional costs. *Adv. in Appl. Probab.*, 39, 3, 669–689, 2007.

Multidimensional Synchronization Models Based on Lévy Processes

Anatoly Manita

Department of Probability, Faculty of Mathematics and Mechanics,
Lomonosov Moscow State University, 119991, Moscow, Russia
(E-mail: manita@mech.math.msu.su)

Abstract. We present an overview of a new approach to constructing probabilistic synchronization models based on Lévy dynamics of components. These models are very flexible from the viewpoint of applications and convenient for analytic study. We consider generally non-Markov N-component systems $x(t) = (x_1(t), \dots, x_N(t))$, $t \in \mathbb{R}_+$, with pairwise synchronizing interaction. We prove theorems about a long time synchronization (when $t \to +\infty$) and provide an answer to the question: what is a typical magnitude of desynchronization errors in large synchronized systems. It is discovered that the answer is deeply related to asymptotic properties of the Lévy processes defining the free dynamics of components.
Keywords: Stochastic synchronization, non-Markov models, intrinsic space scales, Lévy processes, domain of attraction of stable laws, superposition of renewal processes, Laplace transform, Lévy jump-diffusions.

1 Introduction

Stochastic processes with synchronization arise as a natural mathematical framework for analytical study of some applied models in computer science (Bertsekas and Tsitsiklis[3], Simeone *et al.*[26]) that are using the message passing mechanism (Jefferson and Witkowski [8]) to share information between components. In series of papers (Manita and Shcherbakov[19], Manita and Malyshev[12], Malyshkin[13], Manita[20,14,15]) probabilistic synchronization models were treated as multiparticle systems with a special synchronizing interaction. In purely probabilistic terms, such models may be regarded as special perturbations of multidimensional random walks.

The present paper is devoted to a very wide class of multicomponent systems which includes as particular cases the models of Manita[20,14,15,18]. Our aim is to generalize results on intrinsic space scales obtained in Manita[18] for symmetric systems of Brownian particles with pairwise synchronization. More precisely, the model of Manita[18] was a Markov process $x(t) = (x_1(t), \dots, x_N(t))$, $x_j(t) \in \mathbb{R}$, $t \in \mathbb{R}_+$, with components evolving as independent Brownian motions with constant diffusion coefficient $\sigma > 0$ except at random times T_1, T_2, ... of synchronization jumps. The sequence $\{T_n\}$ was assumed to be a Poisson flow

New Trends in Stochastic Modeling and Data Analysis (pp. 43-57)
Raimondo Manca - Sally McClean - Christos H Skiadas (Eds)

of intensity $\delta > 0$. The synchronizing interaction means that at any epoch T_n (independently of other synchronization epochs) the system chooses at random a pair of components (j_1, j_2) and then the component j_2 instantly changes its state to the value x_{j_1}:

$$x_{j_2}(T_n + 0) = x_{j_1}(T_n), \qquad x_j(T_n + 0) = x_j(T_n), \quad j \neq j_2. \tag{1}$$

For brevity we will refer to this system as "$\mathcal{BM}_N(\sigma, \delta)$-model". The pairwise synchronizing interaction (1) can be interpreted as follows: the component j_1 generates a message containing information about its current state x_{j_1} and sends it to the component j_2; the message reaches the destination instantly; after receiving the message the component j_2 reads it and adjusts its state x_{j_2} to the value x_{j_1} recorded in the message. It was proved that the $\mathcal{BM}_N(\sigma, \delta)$-model reveals a nice long-time behavior. Namely, distances between components $d_{jk}^{(N)}(t) = x_j(t) - x_k(t)$ have limits in law as $t \to \infty$. One may say that the system reaches synchronization in a stochastic sense. Moreover, it was shown in Manita[18] that rescaled distances $d_{jk}^{(N)}(\infty)/\sqrt{(N-1)N}$ are distributed according to the symmetric Laplace law with variance σ^2/δ. Since this distribution does not depend on N one comes to the conclusion that a natural space scale for the synchronized N-component system $\mathcal{BM}_N(\sigma, \delta)$ is of order N.

Multicomponent models $x(t) = (x_1(t), \dots, x_N(t))$ of the present paper generalize the $\mathcal{BM}_N(\sigma, \delta)$-model of Manita[18] in several directions. First we let components x_j take their values in $\mathbb{R}^d$ with $d \geq 1$. Secondly, we assume that the free dynamics of components is governed by Lévy processes with values in $\mathbb{R}^d$. In other words, the Brownian motion used in the $\mathcal{BM}_N(\sigma, \delta)$-model is replaced by more general and more flexible dynamics. Lévy processes have independent and stationary increments. Probability distributions of these increments may have heavy tails. This is important for many modern applications that demand a heavy-tailed modeling, e.g., data networks, the Web, etc. We will also see that stable Lévy processes and domains of attractions of stable laws play an exceptional role in asymptotic analysis of the synchronized system with large number of components. Thirdly, we make assumptions about the sequence $\boldsymbol{T} = \{T_n\}$ of synchronization epochs which are more natural in the context of multicomponent systems. It is assumed that each component j generates messages at epochs of some renewal process $\boldsymbol{\tau}^{(j)} = \left\{\tau_m^{(j)}\right\}$. Thus now the point process $\{T_n\}$ is the superposition of N independent renewal processes: $\boldsymbol{T} = \cup_j \boldsymbol{\tau}^{(j)}$. In general, this superposition is not a renewal process and therefore an analysis of $\boldsymbol{T} = \{T_n\}$ is a difficult task. Hence the present paper proposes a wide class of generally non-Markov synchronization models and this is also interesting for many applications. It is worth mentioning that the subclass of Markov multicomponent models driven by stable Lévy processes plays a special role in our study. Some results related to non-Markov models with large number of components hold only in an asymptotic sense while the same results for the Markov case can be obtained for any N in explicit form.

2 General synchronization models

We define a special continuous time stochastic process $x(t) = (x_1(t), \dots, x_N(t))$ with values in $\left(\mathbb{R}^d\right)^N$ and call it a general N-component model with pairwise synchronization.

Construction. In order to construct this model we fix, on some probability space $(\Omega, \mathcal{F}, \mathsf{P})$, the following triplet (a,b,c).

(a) $x_1^\circ(t), \dots, x_N^\circ(t)$ are N independent Lévy processes with values in $\mathbb{R}^d$;

(b) a set of N independent renewal processes $\boldsymbol{\tau}^{(k)} = \left\{\tau_m^{(k)}\right\}_{m=1}^{\infty}$, $k = 1, \dots, N$,

$$0 < \tau_1^{(k)} < \tau_2^{(k)} < \cdots \tag{2}$$

and a routing matrix $R = (r_{ij})_{i,j=1}^N$, $r_{ii} = 0$, $r_{ij} \geq 0$, $\sum_{j=1}^N r_{ij} = 1$;

(c) an initial configuration $x(0) = (x_1(0), \dots, x_N(0)) \in \mathbb{R}^{Nd}$.

Main assumption is that $(x^\circ(t),\, t \geq 0)$, $(\boldsymbol{\tau}^{(j)},\, j = \overline{1, N})$ and $x(0)$ *are independent.*

The process $x^\circ(t) = (x_1^\circ(t), \dots, x_N^\circ(t))$, $t \in \mathbb{R}_+$, will be called a free dynamics of independent components. Consider $\boldsymbol{T} = \cup_j \boldsymbol{\tau}^{(j)}$, a superposition of the renewal processes $\boldsymbol{\tau}^{(j)}$,

$$0 = T_0 < T_1 < T_2 < \cdots ,$$

and call $T = \{T_n\}_{n=1}^{\infty}$ a sequence of synchronization epochs.

We always assume that inter-event intervals of any renewal process $\boldsymbol{\tau}^{(j)}$ have *continuous* distributions. All further assumptions about the triplet (a,b,c) will be given later. Now we define the process $x(t) = (x_1(t), \dots, x_N(t))$.

$\diamondsuit$ Between epochs of the point process $\{T_n\}$ increments of any component $x_j(t)$ are the same as increments of the process $x_j^\circ(t)$ (free dynamics):

$$x(t) - x(0) = x^\circ(t) - x^\circ(0), \quad t \in (0, T_1],$$

$$x(t) = x(T_n + 0) + (x^\circ(t) - x^\circ(T_n + 0)) \qquad t \in (T_n, T_{n+1}],$$

$\diamondsuit$ At any epoch T_n there is an instantaneous interaction between components. The transition $x(T_n) \mapsto x(T_n + 0)$ is called a synchronizing jump and is defined as follows. For any point T_n there exists a unique (random) pair (j_1, m), $j_1 \in \{1, \dots, N\}$, $m \in \mathbb{N}$, such that $T_n = \tau_m^{(j_1)}$. It means that at time T_n the particle j_1 sends a message to some other particle j_2 which is chosen independently with probability $r_{j_1 j_2}$. This message provokes the synchronizing jump $x(T_n) \mapsto x(T_n + 0)$ according to the rule (1).

Free dynamics. By assumption (a) $x_1^\circ(t), \dots, x_N^\circ(t)$ are independent Lévy processes. We recall basic definitions and introduce some notation. Readers are refered to Sato[25] and Applebaum[1] for more details. A stochastic process $\left(x_j^\circ(t),\, t \in \mathbb{R}_+\right)$ is called a Lévy process if

- it starts from the origin: $x_j^\circ(0) = 0 \in \mathbb{R}^d$,

- it has independent and stationary increments,
- it is stochastically continuous.

Let y_1 and y_2 be two vectors in $\mathbb{R}^d$, $y_m = (y_m^1, \dots, y_m^d)$, $m = 1, 2$. Denote by $\langle y_1, y_2 \rangle$ their scalar product, i.e., $\langle y_1, y_2 \rangle = \sum_{l=1}^d y_1^l y_2^l$. It is well known that increments of a Lévy process are infinitely divisible. Let $\phi^j(t-s;\lambda)$ be characteristic function of the increment $x_j^\circ(t) - x_j^\circ(s)$:

$$\phi^j(t-s;\lambda) = \mathsf{E} \exp\left(i \left\langle \lambda, x_j^\circ(t) - x_j^\circ(s) \right\rangle\right), \qquad 0 \le s \le t, \qquad \lambda \in \mathbb{R}^d.$$

The classical result states that $\phi^j(t;\lambda) = e^{t\boldsymbol{\eta}_j^\circ(\lambda)}$ with some function $\boldsymbol{\eta}_j^\circ : \mathbb{R}^d \to \mathbb{C}$ having the Lévy-Khinchine form. For such Lévy process $\left(x_j^\circ(t),\, t \ge 0\right)$ we will use a short notation $x_j^\circ \sim \mathcal{LP}\left(\boldsymbol{\eta}_j^\circ\right)$.

We see that the set of Lévy exponents $\left\{\boldsymbol{\eta}_j^\circ(\lambda),\ j = 1, \dots, N\right\}$ completely determines free dynamics $x^\circ(t)$ of our model. Note that the class of the component dynamics $x_j^\circ(t)$ driven by Lévy processes contains many important examples. Among them we have d-dimensional *Brownian motions* with constant drifts and continuos time *random walks* in $\mathbb{R}^d$ or $\mathbb{Z}^d$. Choosing appropriate distributions of jumps we can easily model different heavy-tail cases. Details can be found in Section 5.

Epochs of interaction. As it was assumed above each component k has its own sequence of times (2) when it sends messages to other particles. For convenience we put $\tau_0^{(k)} \equiv 0$. Put $\Delta_n^{(k)} = \tau_n^{(k)} - \tau_{n-1}^{(k)}$. We assume that the random variables $\left(\Delta_n^{(k)},\, n \in \mathbb{N}\right)$ are independent and identically distributed. This means that $\boldsymbol{\tau}^{(k)} = \left\{\tau_m^{(k)}\right\}_{m=1}^\infty$ is an ordinary renewal process. Let $F_k(s) = \mathsf{P}\left\{\Delta_n^{(k)} \le s\right\}$ be a cumulative distribution function (c.d.f.) of inter-event intervals for the flow $\boldsymbol{\tau}^{(k)}$. By assumption all $F_k(s)$ are continuous. We see that the synchronization between components is completely determined by the functions $F_k(s)$, $k = 1, \dots, N$, and the matrix $R = (r_{ij})_{i,j=1}^N$.

Non-Markov and Markov models. To specify parameters of the general synchronization model $x(t) = (x_1(t), \dots, x_N(t))$ we will use notation

$$\mathcal{GG}_N\left(\left\{\boldsymbol{\eta}_j^\circ\right\}_{j=1}^N; \{F_j\}_{j=1}^N, R\right).$$

The first letter "$\mathcal{G}$" stands for a general Lévy process as free dynamics, the second "$\mathcal{G}$" stands for a general inter-event distribution. Note that $x(t)$ is not a process with independent increments and in general it is not a Markov process. The lack of Markov property is explained by the complicated structure of the sequence $\{T_n\}$.

However there is an important exclusion. If all $F_k(s)$ correspond to exponential distributions,

$$F_k(s) = \left(1 - \exp\left(-s/m_k\right)\right)_+, \qquad m_k > 0, \tag{3}$$

then $x(t)$ is a Markov process. Indeed, in this case the point process $\{T_n\}$ is a Poisson flow as the superposition of independent Poisson flows $\left\{\tau_n^{(j)}\right\}$, $j = \overline{1,N}$. We will denote the Markov model by $\mathcal{GM}_N\left(\left\{\boldsymbol{\eta}_j^\circ\right\}_{j=1}^N; \{m_j\}_{j=1}^N, R\right)$.

3 Symmetric models: main results

In this paper we mainly study *symmetric* synchronization models.

Symmetry assumptions. The model $\mathcal{GG}_N\left(\left\{\boldsymbol{\eta}_j^\circ\right\}_{j=1}^N; \{F_j\}_{j=1}^N, R\right)$ will be called *symmetric* if it satisfies the following *additional* assumptions.

Free dynamics. All functions $\boldsymbol{\eta}_j^\circ$, $j = \overline{1,N}$, defining the independent Lévy processes $x_j^\circ(t)$ are equal, i.e., $\boldsymbol{\eta}_j^\circ(\lambda) = \boldsymbol{\eta}^\circ(\lambda)$.

Synchronization epochs. $F_j(y) = F(y)$ for all $j = \overline{1,N}$.

Routing matrix. Senders choose destinations for their messages uniformly: $r_{jk} = 1/(N-1)$ for all $k \neq j$, $r_{jj} = 0$.

In other words, in the symmetric model all components are identical and their evolution follows the same probabilistic rules with the same parameters.

Initial distribution. Assume that distribution of $x(0)$ is invariant with respect to permutations of indices. Note that the case when all components start from the origin, i.e., $x_i(0) = 0 \quad \text{for all} \quad i = 1, \ldots, N$, is a particular example of this assumption.

If all above symmetry assumptions hold then for all $t > 0$ the distribution of the N-component system $x(t)$ remains invariant with respect to permutations of indices. In such case we will call the process $x(t)$ a symmetric synchronization model. In general, the symmetric model $x(t)$ is not Markov nor semi-Markov stochastic process. The only exception is the situation (3).

The *general symmetric* model will be denoted by $\mathcal{GGS}_N(\boldsymbol{\eta}^\circ; F)$. For *Markov symmetric* model we use notation $\mathcal{GMS}_N(\boldsymbol{\eta}^\circ; m)$ where m is the mean of the exponential distribution with c.d.f. $F(s) = (1 - \exp(-s/m))_+$.

Technical assumptions about F.

Assumption P1. The c.d.f. F is absolutely continuous:

$$F(s) = \mathsf{P}\left\{\Delta_n^{(k)} \leq s\right\} = \int_0^s p(s')\, ds', \qquad s \geq 0,$$
$$F(s) = 0, \qquad p(s) = 0, \qquad s < 0.$$

Note that this assumption concerns only inter-event intervals in each renewal process $\left\{\tau_n^{(j)}\right\}$. The point process $\{T_n\}$ is very complicated.

Consider the Laplace transform of the function $p(s)$:

$$p^*(z) = \int_0^{+\infty} e^{-zs} p(s)\, ds, \qquad z \in \mathbb{C}.$$

Since $p(s)$ is a probability density function (p.d.f.) its Laplace transform $p^*(z)$ is well defined at least in the complex half-plane $\{z:\ \mathrm{Re}\, z \geq 0\}$ (see, e.g., Cox[5]). It is readily seen from the Lebesque domination theorem that $p^*(a+i0) \to 0$ as $a \to +\infty$, $a \in \mathbb{R}$.

Assumption P2. The p.d.f. $p(s)$ is such that its Laplace transform $p^*(z)$ is a rational function.

An important role of distributions with rational Laplace tranform for the queueing theory was discovered by Cox in [4]. Now it is known (see, e.g., Assmussen and Bladt [2]) that probability distributions satisfying the Assumption P2 are exactly the ME (matrix-exponential) distributions.

It follows from Assumption P2 that $p^*(z)$ can be represented as a proper fraction $p^*(z) = \frac{P(z)}{Q(z)}$ where $P(z)$ and $Q(z)$ are some polynomials such that $\deg P < \deg Q$. It is easy to see that all poles z_i of $p^*(z)$ have *strictly negative* real parts ($\mathrm{Re}\, z_i < 0$). Assumption P2 implies the existence of an exponential moment $\mathsf{E} \exp\left(\delta \Delta_n^{(k)}\right) < \infty$ for some $\delta > 0$. We will use notation m for the mean: $m = \mathsf{E}\, \Delta_n^{(k)} = \int s\, p(s)\, ds$.

The function $p(s)$ is a probability density hence $p^*(0) = 1$. If $p(s)$ satisfies Assumption P2 then the equation

$$1 - p^*(z) = 0 \tag{4}$$

has a finite number of roots. Let $\{r_0, r_1, \ldots, r_q\}$, $r_0 = 0$, be the set of different roots of the equation (4). It is easy to show that all numbers $r_1, \ldots, r_q$ belong to the subplane $\mathrm{Re}\, z < 0$.

Assumption P3. The roots $r_1, \ldots, r_q$ are **simple** that is $(p^*)'(r_j) \neq 0$.

Assumption P3 is not necessary for the main results but it makes some proofs shorter.

Long time synchronization. Due to the stochastic nature of the free dynamics our stochastic system will never reach the *perfect synchronization regime* when states of all components $x_1(t)$, ..., $x_N(t)$ become equal after some (possibly random) time t_0. But we may expect a long time stabilization of synchronization errors in the distributional sense. To get some control over magnitudes of the synchronization errors we consider differences $d_{jk}^{(N)}(t) = x_j(t) - x_k(t)$ between states of any pair (j,k) at time t. By the symmetry assumptions the characteristic function of $d_{jk}^{(N)}(t)$,

$$\chi_N(t;\lambda) = \mathsf{E} \exp\left(i \left\langle \lambda, x_j(t) - x_k(t) \right\rangle\right), \qquad \lambda \in \mathbb{R}^d, \tag{5}$$

does not depend on j and k. Let a probability measure $P_{N,t}$ on $\left(\mathbb{R}^d, \mathcal{B}(\mathbb{R}^d)\right)$ be the distribution of $d_{jk}^{(N)}(t)$.

Theorem 1 *Let $x(t)$ be a symmetric synchronization model and let Assumptions P1 and P2 hold. Then for any fixed N the distribution of $d_{jk}^{(N)}(t) = x_j(t) - x_k(t)$ has a (weak) limit as $t \to \infty$:*

$$P_{N,t} \xrightarrow{w} P_{N,\infty}\,.$$

This theorem follows from the Lévy continuity theorem (Theorem 3.6.2 in Lukacs[11]) and the next lemma.

Lemma 1 *For any fixed N the family of characteristic functions $\{\chi(t;\lambda)\}_{t\geq 0}$ convergences to some function $\chi_N(\infty;\lambda)$ as $t\to+\infty$ and, moreover, this convergence is uniform in $\lambda\in\mathbb{R}^d$.*

It is well known (Lukacs[11, Th. 3.6.2]) that the function $\chi_N(\infty;\lambda)$ is the characteristic function of the limiting distribution $P_{N,\infty}$.

Proofs use a special representation of $\chi(t;\lambda)$ which is based on an averaging over the synchronization epochs $\{T_q\}$. For Markov synchronization models this representation is reduced to an explicit form and provides a relatively short proof of Lemma 1. The proof is very similar to Manita[18] and a conclusion for the *Markov* symmetric synchronization model $\mathcal{GMS}_N(\boldsymbol{\eta}^\circ;m)$ is the following: the function $\chi_N(t;\lambda)$ satisfies the linear first order differential equation

$$\frac{d}{dt}\,\chi_N(t;\lambda)=-q_N(\lambda)\,\chi_N(t;\lambda)+w_N, \tag{6}$$

where

$$w_N=\frac{2}{(N-1)m},\qquad q_N(\lambda)=\boldsymbol{\eta}(\lambda)+w_N,\qquad \boldsymbol{\eta}(\lambda):=-2\,\mathrm{Re}\,\boldsymbol{\eta}^\circ(\lambda).$$

Note that $\boldsymbol{\eta}(\lambda)\geq 0$. Hence Lemma 1 easily follows from this equation and we get the following important statement.

Theorem 2 *For the Markov symmetric synchronization model $\mathcal{GMS}_N(\boldsymbol{\eta}^\circ;m)$*

$$\chi_N(\infty;\lambda)=\frac{1}{1+\frac{1}{2}(N-1)m\boldsymbol{\eta}(\lambda)}\,. \tag{7}$$

This theorem generalizes the result obtained in Manita[18] for the $\mathcal{BM}_N(\sigma,\delta)$-system to the case of Markov models with arbitrary Lévy-driven free dynamics.

It is important to note that for *non-Markov* models the function $\chi_N(t;\lambda)$ does not satisfy to any differential equation. As it is seen from Manita[17] the limiting characteristic function $\chi_N(\infty;\lambda)$ does not have such elegant and explicit form as in the Markov case. Nevertheless, for the general symmetric model $\mathcal{GGS}_N(\boldsymbol{\eta}^\circ;F)$ satisfying to Assumptions P1 and P2 one can get the following representation

$$\chi_N(\infty;\lambda)=\frac{2}{(N-1)m}\int_0^\infty du\,e^{-u\boldsymbol{\eta}(\lambda)}\left(\varphi_2(u,k_N)\right)^{N-1}\varphi(u,k_N)\,. \tag{8}$$

Here $k_N=1-2/(N(N-1))$, $\varphi(u,v)=\mathsf{E}\,v^{\Pi_u}$ is the generating function for Π_u, the number of renewals on $[0,u]$ in the *ordinary* renewal process with the inter-event distribution F, and $\varphi_2(u,v)$ is the generating function for the number of renewals on $[0,u]$ for the *stationary* renewal process in which the distribution of the first interval Δ_1 differs from F and is given by

$$\mathsf{P}\left(\Delta_1\leq s\right)=\frac{1}{m}\int_0^s\left(1-F(w)\right)\,dw\,. \tag{9}$$

A derivation of the formula (8) consists of a chain of lemmas. Some of them are related to synchronized jumps and are similar to corresponding lemmas in Manita[18]. Other lemmas deal with the point process $\{T_q\}$ which is the superposition of independent renewal processes. Details of proofs can be found in Manita[17].

Systems with large number of components. For non-Markov models the function $\chi_N(\infty;\lambda)$ cannot be given in such simple form as (7). Therefore it is interesting to study its asymptotic properties when the number of components tends to infinity.

Theorem 3 *Consider a general symmetric model $\mathcal{GGS}_N(\boldsymbol{\eta}^\circ;F)$ satisfying Assumptions P1-P3. The characteristic function $\chi_N(\infty;\lambda)$ admits the following representation*

$$\chi_N(\infty;\lambda)=\frac{1}{1+\theta_{1,N}\boldsymbol{\eta}(\lambda)}+\theta_{2,N}(\lambda).$$

Here $\boldsymbol{\eta}(\lambda)=-2\operatorname{Re}\boldsymbol{\eta}^\circ(\lambda)$, the real sequence $\{\theta_{1,N}\}$ is such that $\theta_{1,N}\sim\frac{1}{2}mN$ as $N\to\infty$ and the sequence of functions $\{\theta_{2,N}(\lambda)\}$ vanishes uniformly in λ:

$$\sup_{\lambda\in\mathbb{R}^d}|\theta_{2,N}(\lambda)|\to 0\qquad(N\to\infty)\,.$$

The proof is given in Manita[17]. It is based on using the Laplace transform for generating functions and on analysis of singularities of rational complex functions related to the representation (8). The key problems are to find singularities giving the principal asymptotics and to control coefficients in decomposions because they depend on N.

4 Intrinsic scales of synchronized systems

When we consider a symmetric synchronization system with large number of components N we may ask about a proper space scale which depends on N and corresponds to typical values of the synchronization errors $d_{jk}^{(N)}$. It appears that probabilistic properties of the free dynamics have an important impact on the typical scale of the synchronized system.

Markov models with stable free dynamics. To explain an idea of intrinsic space scales we begin with the following explicit result which holds for any finite $N\geq 2$.

Theorem 4 *Let a Markov N-component symmetric synchronization model $\mathcal{GMS}_N(\boldsymbol{\eta}^\circ;m)$ be such that its free dynamics $x^\circ(t)$ is an α-*stable *Lévy process, $0<\alpha\leq 2$. Then for any fixed N the distribution of rescaled differences $d_{jk}^{(N)}(\infty)/\left(N-1\right)^{1/\alpha}$ does not depend on N.*

This statement follows from Theorem 2. Indeed, if the Lévy process $\mathcal{LP}\left(\boldsymbol{\eta}^\circ\right)$ is *α-stable* then $-\boldsymbol{\eta}(\lambda)=2\operatorname{Re}\boldsymbol{\eta}^\circ(\lambda)$ is the Lévy exponent of some *symmetric α-stable* Lévy process $\mathcal{LP}\left(-\boldsymbol{\eta}\right)$. Therefore $n\boldsymbol{\eta}(\lambda/n^{1/\alpha})\equiv\boldsymbol{\eta}(\lambda)$ for any

$n \in \mathbb{N}$. Hence characteristic function of $d_{jk}^{(N)}(\infty)/\left(N-1\right)^{1/\alpha}$ is equal to $\left(1+\frac{1}{2}m\boldsymbol{\eta}(\lambda)\right)^{-1}$. This result can be interpreted as follows: typical distances between components in the synchronized system are of order $\left(N-1\right)^{1/\alpha} \sim N^{1/\alpha}$.

Theorem 4 generalizes results of the paper Manita[18] where the role of the α-stable free dynamics was played by Brownian motions with $\boldsymbol{\eta}^{\circ}(\lambda) = -\frac{1}{2}\sigma^2\lambda^2$, $\alpha = 2$, $d = 1$. Indeed, we have equivalence of the following models

$$\mathcal{GMS}_N(-\frac{1}{2}\sigma^2\lambda^2; m) = \mathcal{BM}_N(\sigma, N/m).$$

Using self-similarity of the Wiener process one can derive that the intrinsic scale of $\mathcal{BM}_N(\sigma, N/m)$ is $N^{1/2}$ times smaller than the intrinsic scale of the model $\mathcal{BM}_N(\sigma, m^{-1})$ studied in Manita[18] and discussed in Introduction of the present paper.

Free dynamics attracting to stable laws. The Markov assumption is essential for Theorem 4. For the non-Markov case similar results hold only in asymptotic form as $N \to \infty$ (see Theorem 5 below). It is very important to point out that asymptotical results are also valid under conditions weaker than stability of free dynamics. Namely, it is sufficient to assume that free dynamics are taken from domains of attraction of stable laws. This permits to cover a great number of interesting examples.

Recall that stable laws are the only possible limiting distributions of scalar-normalized sums of i.i.d. random vectors. It is well known (Samorodnitsky and Taqqu[24]) that the definition of a stable law in $\mathbb{R}^d$ can be given in the following equivalent form: *a random vector $U \in \mathbb{R}^d$ is stable if it has a domain of attraction, i.e., if there is a random vector V and sequences of positive numbers $\{b_n\}$ and nonrandom vectors $\{C_n\}$, $C_n \in \mathbb{R}^d$, such that*

$$\frac{V_1 + \cdots + V_n}{b_n} + C_n \xrightarrow{d} U \tag{10}$$

where $V_1, \ldots V_n, \ldots$ are independent copies of V and the notation $\xrightarrow{d}$ denotes convergence in distribution. In this case the random vector V is said to be in the *domain of attraction* of the stable vector U and the short notation $V \in \mathbf{DOA}(U)$ is used. If the normalizing sequence $\{b_n\}$ has the form $b_n = n^{1/\alpha}$ for some $\alpha \in (0, 2]$ one says that V belongs to the *domain of normal attraction* of U and writes $V \in \mathbf{DONA}(U)$. Sometimes we put in these notation distributions instead of random vectors. Evidently, $\mathbf{DOA}(U) \supset \mathbf{DONA}(U) \ni U$. More details about domains of attractions of stable laws can be found in Gnedenko and Kolmogorov[7] and Meerschaert and Sikorskii[22].

In the sequel we use a short notation $U \sim \mathcal{S}\left(\alpha, \boldsymbol{\zeta}_U(\lambda)\right)$ to say that a random vector $U \in \mathbb{R}^d$ is stable with the index of stability $\alpha \in (0, 2]$ and characteristic function $\boldsymbol{\psi}_U(\lambda) = \exp \boldsymbol{\zeta}_U(\lambda)$.

Now let us introduce additional assumptions on the free dynamics $x^{\circ}(t) = (x_1^{\circ}(t), \ldots, x_N^{\circ}(t))$ of the symmetrical model $\mathcal{GGS}_N(\boldsymbol{\eta}^{\circ}; F)$.

Assumption D. There exists a stable law $\mathcal{S}(\alpha, \boldsymbol{\zeta}^\circ(\lambda))$ in $\mathbb{R}^d$ such that $x_j^\circ(1) \in \mathbf{DOA}(\mathcal{S}(\alpha, \boldsymbol{\zeta}^\circ(\lambda)))$ for any component j.

Assumption DN. There exists a stable law $\mathcal{S}(\alpha, \boldsymbol{\zeta}^\circ(\lambda))$ in $\mathbb{R}^d$ such that $x_j^\circ(1) \in \mathbf{DONA}(\mathcal{S}(\alpha, \boldsymbol{\zeta}^\circ(\lambda)))$ for any j.

Theorem 5 *Consider the symmetric synchronization model $\mathcal{GGS}_N(\boldsymbol{\eta}^\circ; F)$. Let Assumption D hold with some $\boldsymbol{\zeta}^\circ(\lambda)$ and some normalizing sequence $\{b_n\}$. Rescale the system $x(t) = (x_1(t), \dots, x_N(t))$ as follows*

$$y^{(N)}(t) = \frac{x(t)}{b_N}, \qquad y^{(N)}(t) = \left(y_1^{(N)}(t), \dots, y_N^{(N)}(t)\right).$$

Let $Q_{N,t}$ be the probability law of the rescaled differences $y_j^{(N)}(t) - y_k^{(N)}(t)$. Then for any fixed $N \geq 2$ a weak limit of $Q_{N,t}$ exists,

$$Q_{N,t} \xrightarrow{w} Q_{N,\infty} \quad as \quad t \to +\infty.$$

The limit of characteristic function of the distribution $Q_{N,\infty}$ has the explicit form

$$\int_{\mathbb{R}^d} \exp\left(i \langle \lambda, y \rangle\right) Q_{N,\infty}(dy) \to \frac{1}{1 + \frac{1}{2} m \boldsymbol{\zeta}(\lambda)} \quad as \quad N \to \infty \tag{11}$$

where $\boldsymbol{\zeta}(\lambda) := -2 \operatorname{Re} \boldsymbol{\zeta}^\circ(\lambda)$, $\lambda \in \mathbb{R}^d$.

We have an immediate corollary of this theorem under the stronger condition that the synchronized system $x(t)$ satisfies Assumption DN with respect to some stable law $\mathcal{S}(\alpha, \boldsymbol{\zeta}^\circ(\lambda))$. In this case $b_n = n^{1/\alpha}$ and the statement of Theorem 5 is true for the rescaled synchronization system

$$y^{(N)}(t) = \frac{x(t)}{N^{1/\alpha}}, \qquad y^{(N)}(t) = \left(y_1^{(N)}(t), \dots, y_N^{(N)}(t)\right).$$

Hence we see that distances between components in the synchronized system are of order $N^{1/\alpha}$ provided the free dynamics belongs to the domain of normal attraction of an α-stable law in the sense of Gnedenko and Kolmogorov[7].

Note also that the Lévy continuity theorem and (11) imply the weak convergence of $Q_{N,\infty}$ to some probability law $Q_{\infty,\infty}$ in $\mathbb{R}^d$ having the characteristic function $\left(1 + \frac{1}{2} m \boldsymbol{\zeta}(\lambda)\right)^{-1}$.

To derive Theorem 5 from Theorem 3 it is sufficient to show that

$$\forall \lambda \in \mathbb{R}^d \qquad n \boldsymbol{\eta}(\lambda / b_n) \to \boldsymbol{\zeta}(\lambda) \qquad (n \to \infty). \tag{12}$$

Details are given in Manita[17].

Limiting laws. Note that the limiting characteristic function in (11) has the form

$$\frac{1}{1 - \log \phi(\lambda)}, \qquad \lambda \in \mathbb{R}^d, \tag{13}$$

where $\phi(\lambda)$ is a characteristic function of some symmetric α-stable distribution. It follows from Mittnik and Rachev[23, Prop. 1] that the laws with characteristic

functions (13) are exactly the class of symmetric *geometric stable distributions* (GSDs). The GSDs are obtained as limiting laws of appropriately normalized *random* sums of i.i.d. random vectors in $\mathbb{R}^d$ where the *number* of summands is *geometrically distributed* and independent of the summands.

There are several remarkable examples among the limiting laws (11). Before discussing them we need to recall some classical results about representation of stable laws. It is known (Applebaum[1]) that characteristic function of a *symmetric* α-stable law has the following form

- for $0 < \alpha < 2$ (the *heavy tail* case):

$$e^{-\boldsymbol{\zeta}(\lambda)} = \exp\left(-\int_{S^{d-1}} |\langle\lambda,\xi\rangle|^{\alpha}\,\nu(d\xi)\right)$$

  where S^{d-1} is the unit sphere in $\mathbb{R}^d$ and ν is some finite measure on S^{d-1},
- for $\alpha = 2$ (the *Gaussian* case):

$$e^{-\boldsymbol{\zeta}(\lambda)} = \exp\left(-\langle A\lambda,\lambda\rangle/2\right)$$

  where A is a positive definite symmetric $d \times d$ matrix.

Corresponding formula for d-dimensional rotationally invariant α-stable laws, $0 < \alpha \le 2$, is simpler:

$$e^{-\boldsymbol{\zeta}(\lambda)} = \exp\left(-c^{\alpha}\,|\lambda|^{\alpha}\right), \qquad c > 0, \quad \lambda \in \mathbb{R}^d, \quad |\lambda| = \sqrt{\langle\lambda,\lambda\rangle}\,.$$

In particular, in dimension $d = 1$ the limiting law $Q_{\infty,\infty}$ in (11) has characteristic function

$$\frac{1}{1 + c^{a}\,|\lambda|^{a}}\,, \qquad \lambda \in \mathbb{R}, \tag{14}$$

with some $0 < a \le 2$, $c > 0$. This is characteristic function of the famous symmetric Linnik distribution first introduced in Linnik[10] and usually denoted as $\mathcal{L}_{a,c}$. It is known (see, e.g., Kotz *et al.*[9]) and Lukacs[11]) that this distribution is unimodal, absolutely continuous, geometric stable and infinitely divisible. If $0 < a < 2$ then the Linnik distribution has heavy tails (see, e.g., Erdogan and Ostrovskii[6] or Kotz *et al.*[9]): $q^{a}\mathsf{P}\left(\mathcal{L}_{a,c} > q\right) \sim \text{const}$ as $q \to +\infty$. For $a = 2$ the law (14) is the Laplace distribution. Note that in Manita[17] it was already proved that the Laplace distribution is the limiting law for the $\mathcal{BM}_N(\sigma,\delta)$-model.

5 Examples

It is very useful to illustrate the result of Theorem 5 by different concrete examples of free dynamics.

Free dynamics of the Gaussian type. Let $x_j^\circ(t)$, $j=\overline{1,N}$, satisfy equations

$$d\,x_j^\circ(t)=\sigma dB_j(t)+b\,dt,$$

where σ is a real $d\times d$ matrix, $b\in\mathbb{R}^d$ and $B_j(t)=(B_j^1(t),\dots,B_j^d(t))\in\mathbb{R}^d$ are independent standard d-dimensional *Brownian motions*. Any $x_j^\circ(t)$ is a Lévy process $\mathcal{LP}(\boldsymbol{\eta}^\circ)$ with the Lévy exponent $\boldsymbol{\eta}^\circ(\lambda)=i\,\langle b,\lambda\rangle-\frac{1}{2}\left\langle\sigma\sigma^T\lambda,\lambda\right\rangle$. Obviously, Assumption DN holds for $\mathcal{S}\left(2,-\frac{1}{2}\left\langle\sigma\sigma^T\lambda,\lambda\right\rangle\right)$. Therefore $\boldsymbol{\zeta}(\lambda)=\left\langle\sigma\sigma^T\lambda,\lambda\right\rangle$. Moreover, in this example we have even more favorable fact than an attraction to a stable law. Namely, any difference $d_{jk}^{(N)}(t)=x_j(t)-x_k(t)$ is already a *stable* Lévy process $\mathcal{LP}(-\boldsymbol{\eta})$ with $\alpha=2$ and $\boldsymbol{\eta}(\lambda)=\left\langle\sigma\sigma^T\lambda,\lambda\right\rangle$. This means that for the Markov model we can directly apply Theorem 4. For the general model we have from Theorem 5 that the proper scaling for $d_{jk}^{(N)}(t)$ is $N^{-1/2}$. Denoting the law of $d_{jk}^{(N)}(t)/N^{1/2}$ by $Q_{N,t}$ we conclude that the *weak* limit $Q_{\infty,\infty}=\underset{N}{w\text{-lim}}\,\underset{t\to+\infty}{w\text{-lim}}\,Q_{N,t}$ exists and the characteristic function corresponding to the law $Q_{\infty,\infty}$ is

$$\frac{1}{1+\frac{1}{2}m\left\langle\sigma\sigma^T\lambda,\lambda\right\rangle},\qquad\lambda\in\mathbb{R}^d.\tag{15}$$

One-dimensional random walks. Let $d=1$ and the free dynamics of each component $x_j^\circ(t)$ be a continuous time symmetric *random walk* with the Markov generator

$$(Lf)(y)=\beta\int_{\mathbb{R}}\left(f(y+q)-f(y)\right)\,\mu(dq),\qquad f\in C_b(\mathbb{R},\mathbb{R}).\tag{16}$$

Here $\beta>0$ is the intensity of jumps and $\mu(dq)=\frac{1}{2}a\,|q|^{-1-a}\,1_{\{|q|\geq 1\}}dq$ is the distribution of an individual jump $x\mapsto x+q$. Please, note once more that if the sequence $\{T_n\}$ is considered under general assumptions then the synchronization system $x(t)$ is not Markov while the free dynamics $x^\circ(t)$ is a Markov process.

The jump distribution $\mu(dq)$ has the "Pareto tails" and, as it is shown in Manita[17], the conditions of Theorem 5 can be easily checked. We present a summary of that analysis. Let ξ be a random variable with distribution $\mu(dq)$. If $a>2$ then ξ has a finite variation $D_0=\mathrm{Var}\,(\xi)=a/(a-2)$. It follows from (16) that $x_j^\circ(t)$ is a compound Poisson process, i.e., $x_j^\circ(t)\sim\sum\limits_{r=1}^{N_\beta(t)}\xi_r$ where $(N_\beta(t),\,t\geq 0)$ is the Poisson process with intensity β and $\xi_1,\dots,\xi_r,\dots$ are independent copies of ξ. It can be shown that $x_j^\circ(1)\in\mathbf{DONA}\,(\mathcal{N}(0,D))$ where $D=\beta a/(a-2)>0$. Hence Assumption DN holds with $\boldsymbol{\zeta}^\circ(\lambda)=-\frac{1}{2}D\lambda^2$, $\alpha=2$, and we can apply Theorem 5. It is readily seen that $\boldsymbol{\zeta}(\lambda)=D\lambda^2$. The distribution $Q_{N,t}$ of rescaled differences $d_{jk}^{(N)}(t)/\sqrt{N}$ converges in two subsequent limits $\underset{N}{w\text{-lim}}\,\underset{t\to+\infty}{w\text{-lim}}\,Q_{N,t}$. The limiting law $Q_{\infty,\infty}$ has characteristic function $(1+\frac{1}{2}mD\lambda^2)^{-1}$ which corresponds to the Laplace distribution with

density

$$p_L(y) = \frac{1}{2c_0}\, e^{-|y|/c_0}, \qquad -\infty < y < +\infty, \quad c_0 = \sqrt{\frac{mD}{2}}\,.$$

If $0 < a < 2$ (the *heavy tail* case) then $x_j^\circ(1)$ also belongs to the domain of normal attraction of some symmetric a-stable law and Assumption DN holds. Again Theorem 5 implies that rescaled differences $d_{jk}^{(N)}(t)/N^{1/a}$ converge in law as $t \to \infty$ to some distribution $Q_{N,\infty}$. The sequence $Q_{N,\infty}$ converges as $N \to \infty$ to a law with characteristic function having the form (14) for some $c = c(a, \beta, m) > 0$. Hence we obtain the symmetric Linnik distribution as a limiting law of rescaled differences between components.

Multi-dimensional random walks with heavy-tailed jumps. To generalize the previous one-dimensional example we consider a special subclass of *random walks* $x_j^\circ(t)$ in $\mathbb{R}^d$, $d \geq 2$, with generator

$$(Lf)(y) = \beta \int_{\mathbb{R}^d} (f(y+q) - f(y))\ \mu(dq), \qquad f \in C_b(\mathbb{R}^d, \mathbb{R}).$$

We restrict ourself to consideration of power law jumps and use some results from Meerschaert and Sikorskii[22, § 6.4]. Let $\xi \in \mathbb{R}^d$ denote a random vector with distribution $\mu(dq)$, $q \in \mathbb{R}^d$: $\mathsf{P}(\xi \in G) = \mu(G)$ for any Borel set $G \in \mathcal{B}(\mathbb{R}^d)$. It can be represented as $\xi = W\Theta$ where W is a scalar random variable and $\Theta \in S^{d-1}$ is a random vector taking values on the unit sphere in $\mathbb{R}^d$. Assume that W and Θ are independent, and

$$\mathsf{P}(W > R) = CR^{-\alpha}, \qquad R \geq R_0 > 0, \qquad \mathsf{P}(W \geq 0) = 1,$$

$$\mathsf{P}(\Theta \in B) = M(B), \qquad B \in \mathcal{B}(S^{d-1}),$$

where $C > 0$ is some constant, $C \leq R_0^\alpha$, and $M(\cdot)$ is a probability measure on S^{d-1}. It was explained in Manita[17] that in the *heavy tail* case $\alpha \in (0, 2)$ Assumption DN holds for some stable law $\mathcal{S}(\alpha, \boldsymbol{\zeta}^\circ(\lambda))$ with the stability index α. Moreover,

$$\boldsymbol{\zeta}(\lambda) = -2\,\mathrm{Re}\,\boldsymbol{\zeta}^\circ(\lambda) = 2C\,K_\alpha \int_{S^{d-1}} |\langle \lambda, \theta \rangle|^\alpha\ M(d\theta)$$

for some $K_\alpha > 0$. Applying Theorem 5 we see that the intrinsic space scale is of order $N^{1/\alpha}$. The distribution $Q_{\infty,\infty}$ has the characteristic function

$$\frac{1}{1 + \frac{1}{2} m \int_{S^{d-1}} |\langle \lambda, \theta \rangle|^\alpha\ \nu_\alpha(d\theta)}$$

where $\nu_\alpha(d\theta) = 2C\,K_\alpha M(d\theta)$.

If $\alpha \geq 2$ then the corresponding analysis is based on the multi-dimensional Central Limit Theorem. The normalizing sequence is $b_N = N^{1/2}$ and Assumption DN holds for d-dimensional Gaussian law. The final result is similar to (15). We omit details.

6 Conclusions and future studies

In this paper we proposed a large class of multicomponent stochastic synchronization systems which dynamics is based on Lévy processes. We showed that many important examples of one-component dynamics can be considered in this framework. We hope that our approach will be useful in constructing new probabilistic models of synchronizations for various modern applications. It can also help to develop non-Markov modifications of already existing models such as Manita[16] and Manita[21].

We presented rigorous results on asymptotic properties of synchronization systems with large number of components. These results provide an important information about typical magnitudes of desynchronization errors in synchronized systems.

The present study can be continued and extended in several directions. Our method can be adapted to synchronization models driven by Lévy jump-diffusions which are very polular in different application areas. Our Theorem 5 can be generalized to cover dynamics attracting to multivariate *operator stable* laws, see Manita[17]. Another important axis of the future research is a behavior of non-symmetric synchronization models.

This work was supported by the Russian Foundation for Basic Research (grant 12-01-00897).

References

1. D. Applebaum. *Lévy Processes and Stochastic Calculus*. Cambridge University Press, 2004.
2. S. Asmussen and M. Bladt. Renewal theory and queueing algorithms for matrix-exponential distributions. In A. S. Alfa and S. R. Chakravarthy, editors, *Matrix-analytic methods in stochastic models*, pages 313–341. Dekker, New York, 1996.
3. D. P. Bertsekas and J. N. Tsitsiklis. *Parallel and Distributed Computation: Numerical Methods*. Athena Scientific, Belmont, 1987.
4. D. R. Cox. A use of complex probabilities in the theory of stochastic processes. *Mathematical Proceedings of the Cambridge Philosophical Society*, 51, 313–319, 1955.
5. D. R. Cox. *Renewal Theory*. Methuen, 1962.
6. M. B. Erdogan and I. V. Ostrovskii. Analytic and asymptotic properties of generalized Linnik probability densities. *Journal of Mathematical Analysis and Applications*, 217, 2, 555–578, 1998.
7. B. V. Gnedenko and A. N. Kolmogorov. *Limit distributions for sums of independent random variables*. Addison-Wesley, 1968.
8. D. Jefferson and A. Witkowski. An approach to performance analysis of timestamp-driven synchronization mechanisms. In *Proceedings of the third annual ACM symposium on Principles of distributed computing*, pages 243–253. ACM Press, New York, 1984.
9. S. Kotz, T. Kozubowski, and K. Podgorski. *The Laplace Distribution and Generalizations: A Revisit With Applications to Communications, Exonomics, Engineering, and Finance*. Birkhäuser Boston, 2001.
10. Yu. V. Linnik. Linear forms and statistical criteria, I, II. *Ukr. Mat. Zhurnal*, 5, 207–290, 1953.

11. E. Lukacs. *Characteristic Functions*. Griffin, London, 1970.
12. V. Malyshev and A. Manita. Phase Transitions in the Time Synchronization Model. *Theory of Probability and its Applications*, 50, 1, 134–141, 2006.
13. A.G. Malyshkin. Limit dynamics for stochastic models of data exchange in parallel computation networks. *Problems of Information Transmission*, 42, 3, 234–250, 2006.
14. A. Manita. Brownian Particles Interacting via Synchronizations. *Communications in Statistics - Theory and Methods*, 40, 19-20, 3440–3451, 2011.
15. A. Manita. On Markovian and non-Markovian Models of Stochastic Synchronization. In *Proceedings of The 14th Conference "Applied Stochastic Models and Data Analysis" (ASMDA)*, pages 886–893, Roma, 2011.
16. A. Manita. Clock synchronization in symmetric stochastic networks. *Queueing Systems*, 76, 2, 149–180, 2014.
17. A. Manita. Intrinsic scales for high-dimensional Lévy-driven models with non-Markovian synchronizing updates. *Arxiv.Org*, 1409.2919, 1–50, 2014.
18. A. Manita. Intrinsic space scales for multidimensional stochastic synchronization models. In J. R. Bozeman, V. Girardin, and C. H. Skiadas, editors, *New Perspectives on Stochastic Modeling and Data Analysis*, pages 271–282. ISAST, 2014.
19. A. Manita and V. Shcherbakov. Asymptotic analysis of a particle system with mean-field interaction. *Markov Processes and Related Fields*, 11, 3, 489–518, 2005.
20. A. D. Manita. Stochastic Synchronization in a Large System of Identical Particles. *Theory of Probability and its Applications*, 53, 1, 155–171, 2009.
21. L. Manita. Controlling of clock synchronization in WSNs: structure of optimal solutions. *Arxiv.Org*, 1408.1434, 1–14, 2014.
22. M. M. Meerschaert and A. Sikorskii. *Stochastic Models for Fractional Calculus*. De Gruyter, 2011.
23. S. Mittnik and S. T. Rachev. *Alternative multivariate stable distributions and their applications to financial modelling*, pages 107–119. Birkhäuser Boston, 1991.
24. G. Samorodnitsky and S. Taqqu. *Stable Non-Gaussian Random Processes: Stochastic Models with Infinite Variance*. Taylor & Francis, 1994.
25. K. Sato. *Lévy Processes and Infinitely Divisible Distributions*. Cambridge University Press, 1999.
26. O. Simeone, U. Spagnolini, Y. Bar-Ness, and S. H. Strogatz. Distributed synchronization in wireless networks. *IEEE Signal Processing Magazine*, 25, 5, 81–97, 2008.

The Propagating Front of the Particle Population in Branching Random Walks

Stanislav Molchanov[1] and Elena Yarovaya[2]

[1] Department of Mathematics, University of North Carolina, Charlotte, USA
(E-mail: smolchan@uncc.edu)
[2] Department of Probability Theory, Faculty of Mechanics and Mathematics, Lomonosov Moscow State University, Moscow, Russia
(E-mail: yarovaya@mech.math.msu.su)

Abstract. Spectral properties of linear operators play an important role in the theory of branching random walks. The dynamics of such processes is usually described in terms of birth, death, and walks of particles on the lattice. We consider models of branching random walks under different assumptions about the tails of underlying random walks. Resolvent analysis of bounded symmetric operators with multi-point potential generating continuous-time branching random walks on d-dimensional lattices with a finite set of branching sources has allowed to study large deviations for branching random walks in a number of works of the authors. Using these results the limit structure of the particle population inside of the propagating front is investigated. A special attention is paid to the case when the spectrum of an evolution operator of mean numbers of particles contains only one positive isolated eigenvalue.
Keywords: Branching Random Walks, Evolution Operator, Green Functions, Large Deviations, Front.

1 Introduction

In the paper we summarize some recent studies of the branching random walk with a compactly supported birth rate potential. Under various assumptions about the tails of underlying random walks we investigate the propagating front of the particle population trying to present the complete "picture" of arising phenomena. To simplify the exposition, we formulate only the principal results and ideas skipping technical details and possible generalizations.

Let us formulate the problem. On the lattice $\mathbb{Z}^d$ we consider the branching random walk, similar to the Kolmogorov-Petrovsky-Piskunov (KPP) model, see Kolmogorov *et al.*[10]. The central object here is the point field $n(t, x, y)$, $t \geq 0$, $y \in \mathbb{Z}^d$, where $n(t, x, y)$ is the number of particles at the point $y \in \mathbb{Z}^d$ and time $t \geq 0$, provided that at the start a single particle is located at the point $x \in \mathbb{Z}^d$, that is, $n(0, x, y) = \delta(x - y)$.

New Trends in Stochastic Modeling and Data Analysis (59-73)
Raimondo Manca - Sally McClean - Christos H Skiadas (Eds)

The initial particle performs the symmetric random walk $x(t)$ with the generator $\mathcal{L}$ defined by

$$(\mathcal{L}f)(x) = \sum_{z \neq 0} (f(x+z) - f(x))\, a(z),$$

that acts on the space $l^p(\mathbb{Z}^d)$, $1 \leq p \leq \infty$, and has the following properties: $a(z) = a(-z)$ (symmetry: i.e., $\mathcal{L} = \mathcal{L}^*$ in $l^2(\mathbb{Z}^d)$); $\sum_{z \neq 0} a(z) = -a(0) = 1$ (normalization: the total intensity of jumps is 1); for every $z \in \mathbb{Z}^d$ there exists a set of vectors $z_1, z_2, \ldots, z_k \in \mathbb{Z}^d$, such that $z = \sum_{i=1}^k z_i$ and $a(z_i) > 0$ for $i = 1, 2, \ldots, k$ (irreducibility), for details see Yarovaya[19].

For a random walk $x(t)$ with the generator $\mathcal{L}$, the time τ spent by a particle at a point x is exponentially distributed with parameter 1; at time $\tau + 0$ the particle jumps to a point $x + z$ with intensity $a(z)$, which determines the distribution of the jump of the process.

In addition, for any time interval $(t, t + dt)$ each particle at $x \in \mathbb{Z}^d$ in the population independently of others can split in two particles, located at the same point. Later on these two particles (the parental one and the offspring) evolve independently of each other according to the same law as the initial particle.

The rate of splitting is presented in the form $V(x)dt = \beta V_0(x)dt$, where β is the coupling constant, and $V_0(\cdot)$ is a function subjected to the normalization

$$\max_{x \in \mathbb{Z}^d} V_0(x) = 1.$$

The central assumption is the finiteness of the support $\operatorname{supp} V$ of the function V: there are finitely many points $x_1, x_2, \ldots, x_N \in \mathbb{Z}^d$, where $V_0(x) > 0$ and, say, $V_0(x_1) = V_0(x_2) = \cdots = V_0(x_m) = 1$, $m \leq N$. They form $\operatorname{supp} V$, whereas $V_0(x) \equiv 0$ if $x \notin \operatorname{supp} V$.

One can consider more general schemes of the branching (more than one offspring or non-local but fast decreasing potential $V_0(\cdot)$, etc.) but we will concentrate on the simplest case. The theory also can include the mortality rate, as in Yarovaya[18,19], but again for transparency we exclude it. More details can be found in Molchanov and Yarovaya[13–16].

Consider the generating function

$$u := u_z = u_{z_1,\ldots,z_l}(t, x, y_1, \ldots, y_l) = \mathbf{E}_x z_1^{n(t,x,y_1)} \cdots z_l^{n(t,x,y_l)},$$

where $y_1, \ldots, y_l$ are different points of the lattice $\mathbb{Z}^d$ and $z_1, \ldots, z_l$ are complex variables. For the evolution of u the standard calculation gives the KPP-type equation

$$\partial_t u = \mathcal{L}u + \beta V_0(\cdot)(u^2 - u),$$

where

$$u_{z_1,\ldots,z_l}(0, x, y_1, \ldots, y_l) = \begin{cases} z_i, & x = y_i,\ i = 1, \ldots, l, \\ 1, & x \neq y_1, \ldots, y_l. \end{cases}$$

This case differs from the classical KPP-situation in two ways, namely, we have the lattice $\mathbb{Z}^d$ instead of the continuum $\mathbb{R}^d$ and a convolution bounded symmetric operator $\mathcal{L}$ instead of the Laplacian Δ.

Differentiating $u_{z_1,\dots,z_l}(t,x,y_1,\dots,y_l)$ in variables z_j, $j=1,\dots,l$, we get the moment equations. The simplest one is the equation for the first moment. If $m_1(t,x,y)=\mathsf{E}_x n(t,x,y)$ then

$$\begin{cases} \partial_t m_1 & = \mathcal{H}_\beta m_1, \\ m_1(0,x,y) & = \delta(x-y), \end{cases} \tag{1}$$

where the Hamiltonian $H_\beta = \mathcal{L}+\beta V_0(\cdot)I$ is a bounded self-adjoint operator on $l^2(\mathbb{Z}^d)$. For more details about the properties of the operator H_β see Molchanov and Yarovaya[16], Yarovaya[18,20]. For the mixed second moment

$$m_2(t,x,y_1,y_2)=\mathsf{E}_x n(t,x,y_1)n(t,x,y_2), \quad y_1\neq y_2,$$

the relevant equation has the form

$$\begin{cases} \partial_t m_2(t,x,y_1,y_2) = \mathcal{H}_\beta m_2 + 2\beta V_0(x) m_1(t,x,y_1) m_1(t,x,y_2), \\ m_2(0,x,y_1,y_2) \quad = \delta(x-y_1)+\delta(x-y_2). \end{cases}$$

Equations for all higher order moments can be obtained in a similar way, see, e.g., Yarovaya[18]. For any moment

$$m_k(t,x,y_1,\dots,y_l)=\mathsf{E}_x n^{j_1}(t,y_1)\dots n^{j_l}(t,y_l)$$

of order k depending on several points $y_1,\dots,y_l$, where $j_1+\dots+j_l=k$, the related equation has the form

$$\begin{cases} \partial_t m_k(t,x,y_1,\dots,y_l) = \mathcal{H}_\beta m_k + g_k(m_1,\dots,m_{k-1}), & k\geq 2, \\ m_k(0,x,y_1,\dots,y_l) \quad = \delta(x-y_1)+\dots+\delta(x-y_l), \end{cases}$$

where g_k is a polynomial of order k depending on the moments m_j, $j\leq k-1$. Here all the moment equations include the Hamiltonian H_β.

Let us consider the fundamental solutions of two closely related parabolic problems:

$$\begin{cases} \partial_t p(t,x,y) = (\mathcal{L}p)(x), \\ p(0,x,y) = \delta(x-y). \end{cases}$$

Here $p(t,x,y)=\mathsf{P}_x(x(t)=y)=p(t,0,y-x)=p(t,0,x-y)$ is the transition probability of the underlying random walk $x(t)$.

The second Schrödinger parabolic problem contains information about the first moment.

$$\begin{cases} \partial_t m_1 & = \mathcal{H}_\beta m_1, \\ m_1(0,x,y) & = \delta(x-y), \end{cases}$$

Due to the Feynman-Kac formula one has

$$m_1(t,x,y)=p(t,x,y)\mathsf{E}_x\left[e^{\beta\int_0^t V(x_s)\,ds} \mid x(t)=y\right],$$

hence, $m_1(t,x,y)\geq p(t,x,y)$. Of course, the fundamental solution $m_1(t,x,y)$ is not translation invariant. For fixed t, x and very large $|y|$ one expects that

$p(t,x,y) \sim m_1(t,x,y)$. An asymptotic analysis of $p(t,x,y)$ and $m_1(t,x,y)$ will be given below.

Let us note that using these results and Duhamel's formula for semigroups

$$\mathsf{P}_t = e^{t\mathcal{L}}, \quad \mathsf{M}_t = e^{t\mathcal{H}_\beta},$$

one can calculate moments. Let $n(t,x,\Gamma) = \sum_{y\in\Gamma} n(t,x,y)$, $\Gamma \in \mathbb{Z}^d$, then for $m_1(t,x,\Gamma)$ we get

$$m_1(t,x,\Gamma) = (\mathsf{P}_t \boldsymbol{I}_\tau)(x) = \sum_{y\in\Gamma} p(t,x,y).$$

For the equation

$$\partial_t u = (\mathcal{L}u)(x) + f(t,x), \quad u(0,x) = 0,$$

we have by Duhamel's formula

$$u(t,x) = \int_0^t ds(\mathsf{P}_{t-s} f)(s,x).$$

Similarly for

$$\partial_t u = \mathcal{H}_\beta u + f(t,x), \quad u(0,x) = 0,$$

we have

$$u(t,x) = \int_0^t (\mathsf{M}_{t-s} f)(s,x) ds.$$

2 Spectral theory of the operator $\mathcal{H}_\beta$

The operator $\mathcal{H}_\beta$ is a bounded self-adjoint operator on $l^2(\mathbb{Z}^d)$. Its spectrum consists of two components: the absolutely continuous spectrum located in $[-\min_\kappa \widehat{a}(\kappa), 0]$ where $\widehat{a}(\kappa) = \sum_{x\neq 0} a(x)\cos(\kappa,x)$ for $\kappa \in [-\pi,\pi]^d$, and the finite discrete spectrum $\sigma_d(\mathcal{H}_\beta)$ belonging to the positive part of the λ-axis. Detailed analysis of the properties of the operator $\mathcal{H}_\beta$ for different types of branching random walks can be found in Yarovaya[20] and Molchanov and Yarovaya[13].

The absolutely continuous spectrum can be described in terms of the general scattering theory (see, e.g., Shaban and Vainberg[17]) which includes the irradiation conditions on the infinity. For the applications to the population dynamics, the most important part of the spectrum of the operator $\mathcal{H}_\beta$ is its discrete spectrum $\sigma_d(\mathcal{H}_\beta)$, see Cranston *et al.*[4] and Yarovaya [21]. It contains no more than N positive eigenvalues λ_j, $j \geq 0$, since $\beta V_0(x)$ is the rank N perturbation of the operator $\mathcal{L}$ with a purely absolutely continuous spectrum, see Yarovaya [20]. If β is very large then $\sigma_d(\mathcal{H}_\beta)$ consists of N nonnegative eigenvalues $\lambda_0 > \cdots > \lambda_{N-1} > 0$. It is true for instance, if $\beta \min_{\mathrm{supp}\, V} V_0(x) > \|\Delta\|_2$. The situation of small β is more interesting.

Theorem 1. *If the underlying random walk $x(t)$ is recurrent then $\sigma_d(\mathcal{H}_\beta) \neq \emptyset$ for any $\beta > 0$. In particular, there exists a simple leading eigenvalue $\lambda_0(\beta, V_0) > 0$ for which the corresponding eigenfunction $\psi_0(x, \beta)$ is strictly positive.*

If the underlying random walk $x(t)$ is transient then there exists a value $\beta_{cr} > 0$, such that for

- *$\beta \leq \beta_{cr}$ the positive discrete spectrum is empty: $\sigma_d(\mathcal{H}_\beta) = \emptyset$;*
- *$\beta > \beta_{cr}$ there exists at least one leading eigenvalue $\lambda_0(\beta, V_0) > 0$ corresponding to eigenfunction $\psi_0(x, \beta) > 0$.*

Remark 1. If the underlying random walk $x(t)$ on $\mathbb{Z}^d$ is transient and $\beta = \beta_{cr}$ then there may exist an eigenvalue $\lambda_0(\beta_{cr}, V_0)$, which is equal to 0. As was shown in Yarovaya[18], for branching random walks with a finite variance of jumps such an eigenvalue $\lambda_0(\beta_{cr}, V_0) = 0$ exists if and only if $d \geq 5$.

Let us present an algorithm for calculating the eigenvalue $\lambda_0(\beta, V_0)$ in the transient case.

By definition, for a number $\lambda > 0$ to be an eigenvalue of the operator $\mathcal{H}_\beta$, it is necessary and sufficient that there exists a nonzero element $\psi \in l^2(\mathbb{Z}^d)$ satisfying the equation

$$(\mathcal{H}_\beta \psi)(x) = (\mathcal{L}\psi)(x) + \beta V_0(x)\psi(x) = \lambda\psi(x).$$

Rewrite the last equation in the form

$$(\mathcal{L} - \lambda I)\psi(x) = -\beta \sum_{j=1}^{N} V_0(x_j)\delta(x - x_j)\psi(x_j). \tag{2}$$

Let us recall that the solution of the equation

$$(\mathcal{L} - \lambda I)\psi(x) = -\delta(x - y),$$

is called the Green function

$$G_\lambda(x, y) = \int_0^\infty e^{-\lambda t} p(t, x, y)\, dt.$$

Then from (2) one can deduce that

$$\psi(x) = \beta \sum_{j=1}^{N} V_0(x_j) G_\lambda(x, x_j)\psi(x_j),$$

and by taking the vector x from $\operatorname{supp} V$, i.e. $x = x_1, \ldots, x_N$, we get the linear system

$$\psi(x_i) = \beta \sum_{j=1}^{N} V_0(x_j) G_\lambda(x_i, x_j)\psi(x_j) = (\mathcal{A}(\lambda, \beta)\psi)(x_i).$$

Consider now a square $N \times N$ matrix

$$\mathcal{A}(\lambda, \beta) = [a_{ij}] = [\beta V_0(x_j) G_\lambda(x_i, x_j)],$$

which has strictly positive elements. Then the Perron-Frobenius theorem ensures the existence of a strictly positive simple eigenvalue $\mu_0(\lambda,\beta)$ with the corresponding positive eigenvector $\psi_0(x_j)$, $j=1,\dots,N$. These objects are analytically depend on β and λ, see Kato[9]. Since $G_\lambda(\cdot,\cdot)\le\frac{1}{\beta}$ then the eigenvalue $\mu_0(\lambda,\beta)$ decreases in the first variable and increases in the second one. It is also clear that $\mu_0(\lambda,\beta)\to 0$, as $\lambda\to\infty$, for any fixed $\beta>0$.

Let us note that for a fixed β the leading eigenvalue $\lambda_0(\beta,V_0)$ of the operator $\mathcal{H}_\beta$ is a root of the equation

$$\mu_0(\lambda,\beta)=1$$

or of the equation

$$\det(\mathcal{A}(\lambda,\beta)-I)=0,$$

which can be written in the form

$$\det\begin{bmatrix}\beta V(x_1)G_\lambda(x_1,x_1)-1 & \cdots & \beta V(x_1)G_\lambda(x_1,x_N)\\ \beta V(x_2)G_\lambda(x_2,x_1) & \cdots & \beta V(x_2)G_\lambda(x_2,x_N)\\ \cdots & \cdots & \cdots\\ \beta V(x_N)G_\lambda(x_N,x_1) & \cdots & \beta V(x_N)G_\lambda(x_N,x_N)-1\end{bmatrix}=0$$

or

$$\det\begin{bmatrix}G_\lambda(x_1,x_1)-\frac{1}{\beta V_0(x_1)} & \cdots & G_\lambda(x_1,x_N)\\ G_\lambda(x_2,x_1) & \cdots & G_\lambda(x_2,x_N)\\ \cdots & \cdots & \cdots\\ G_\lambda(x_N,x_1) & \cdots & G_\lambda(x_N,x_N)-\frac{1}{\beta V_0(x_N)}\end{bmatrix}=0,$$

where $G_\lambda(x_i,x_i)=G_\lambda(0,0)$, $i=1,2,\dots,N$.

The last equation is useful in the situation when $\mid x_j-x_i\mid\gg 1$, i.e., the generating centers have small interaction. In this situation one can use the Gershgorin theorem, see, e.g., Gantmacher[5], which implies that all the eigenvalues $\lambda_j>0$ belong to the unity of the intervals

$$G_\lambda(0,0)\in\left[\frac{1}{\beta V_0(x_1)}+\tilde\delta(\lambda),\frac{1}{\beta V_0(x_1)}-\tilde\delta(\lambda)\right],$$

$$\dots$$

$$G_\lambda(0,0)\in\left[\frac{1}{\beta V_0(x_N)}+\tilde\delta(\lambda),\frac{1}{\beta V_0(x_N)}-\tilde\delta(\lambda)\right],$$

where $\tilde\delta=\min_i\sum_{j:j\ne i}G_\lambda(x_i,x_j)$. We have no possibility to discuss here in more detail these pure analytical problems .

Let $\mu_0(0,\beta)$ be the leading eigenvalue of $\mathcal{A}(0,\beta)=[\beta V_0(x_j)G_0(x_i,x_j)]$, $i,j=1,2,\dots,N$. If $G_0(\cdot,\cdot)=\infty$, i.e., the random walk is recurrent then $G_\lambda\uparrow\infty$, as $\lambda\downarrow 0$, and $\mu_0(0,\beta)=+\infty$ implies that for any $\beta>0$ there exists a positive ground state energy (see Shaban and Vainberg[17]) $\lambda_0(\beta)>0$ with positive eigenfunction $\psi_{\lambda_0}(x)=A(\lambda_0,\beta)\psi$.

Assume that the random walk is transient, i.e., $G_\lambda(x,y)\to G_0(x,y)<\infty$, as $\lambda\downarrow 0$. We have for $G_0(x,y)=G_0(0,x-y)$ the following Fourier representation

$$\widehat{G}_\lambda(0,\kappa)=\sum_{x\in\mathbb{Z}^d}e^{i(x,\kappa)}G_\lambda(0,x)=\frac{1}{\lambda+(1-\widehat{a}(\kappa))},\quad \kappa\in[-\pi,\pi]^d=T^d.$$

and $\widehat{G}_\lambda(0,\kappa) \to \widehat{G}_0(0,\kappa) = \frac{1}{1-\widehat{a}(\kappa)}$, as $\lambda \downarrow 0$, i.e.,

$$G_0(0, y-x) < \infty \Longleftrightarrow \int_{T^d} \frac{d\kappa}{1-\widehat{a(\kappa)}} < \infty.$$

In particular if $\sum_{x\in\mathbb{Z}^d} |x|^2 a(x) < \infty$ then $\widehat{a}(\kappa) = 1 - o(|\kappa|^2)$ and the random walk is transient in dimensions $d \geq 3$ and recurrent for $d = 1$ and $d = 2$. The condition $1 - \widehat{a}(\kappa)) = o(|\kappa|^\alpha)$, $\alpha < d$, is sufficient for the transitivity in dimensions $d = 1$ and $d = 2$. These conditions are not only sufficient but close to the necessary ones. Let us point out that for $d \geq 3$ any random walk on $\mathbb{Z}^d$ is transient with a finite or infinite second moment.

For the matrix $\mathcal{A}(0,\beta) = [\beta V_0(x_j) G_\lambda(x_i, x_j)]$ we have $\|\mathcal{A}\|_\infty = o(\beta)$ as $\beta \to 0$. It means that $\mu_0(0,\beta) < 1$ for small β, i.e., $\lambda_0(\beta)$ does not exist. The critical value β_{cr} is given by the relation $\mu_0(0,\beta_{cr}) = 1$: for $\beta > \beta_{cr}$ the leading positive eigenvalue $\lambda_0(\beta) > 0$ of the Hamiltonian $\mathcal{H}_\beta$ exists, for $\beta \leq \beta_{cr}$ it does not exist.

Let us consider other eigenvalues $\lambda_j(\beta)$, $\beta > 0$, of the Hamiltonian $\mathcal{H}_\beta$. Like before, they can be defined in terms of the eigenvalues $\mu_j(\lambda,\beta)$, $j \geq 1$, of the matrix $\mathcal{A}(\lambda,\beta)$. The last asymptotic matrix in fact has only real eigenvalues since

$$a_{ij} = \frac{1}{V_0(x_i)} \beta V_0(x_i) G_\lambda(x_i, x_j) V_0(x_j),$$

i.e., a_{ij} is symmetric in $\mathbb{R}^N$ with respect to the following dot-product in $\mathbb{R}^N$:

$$(x, y)_V = \sum_{j=1}^{N} x_j y_j V(x_j).$$

The equation for λ_j has a form $\mu_j(\lambda,\beta) = 1$.

It is not difficult to prove that in the case $\beta > \beta_{cr}$ the number $N = N(\beta)$ of the positive eigenvalues of the operator $\mathcal{H}_\beta$ grows when the parameter β increases.

Let us denote by β_1 the critical value of the parameter β such that for $\beta_{cr} < \beta < \beta_1$ the operator $\mathcal{H}_\beta$ has only one eigenvalue (the ground state energy). Here $\beta_{cr} = 0$ if $x(t)$ is recurrent and $\beta_{cr} > 0$ for the transient $x(t)$.

Consider the case when $\beta_{cr} < \beta < \beta_1$, and solve the first moment equation (1) for $m_1(t,x,\Gamma) = \mathsf{E}_x n(t,x,\Gamma)$ with the initial conditions $m_1(0,x,\Gamma) = \mathbf{I}_\Gamma(x)$. Then we have

$$m_1(t,x,\Gamma) = (\boldsymbol{I}_\Gamma, \psi_0)\psi_0(x) e^{\lambda_0(\beta)t} + \tilde{m}_1(t,x,\Gamma).$$

Here $\tilde{m}_1$ is the projection of m_1 on the invariant spectral subspace corresponding to the absolutely continuous part of the spectrum of $\mathcal{H}_\beta$. Due to scattering theory for the operator $\mathcal{H}_\beta$ (see Shaban and Vainberg[17]) we have that $\|\tilde{m}_1(t,x,\Gamma)\|_\infty = O(1)$ uniformly in Γ, i.e. main contribution to $m_1(t,x,\Gamma)$ for large sets Γ and not very large x give the first term:

$$m_1(t,x,\Gamma) = (\boldsymbol{I}_\Gamma, \psi_0)\psi_0(x) e^{\lambda_0(\beta)t}.$$

The asymptotics of $m_1(t,0,y)$ depends mainly on the structure of $\psi_0(y)$ when $|y| \to \infty$. It is not difficult to prove that

$$\psi_0(y) \asymp G_\lambda(0,y), \quad |y| \to \infty.$$

where we are writing $f(x) \asymp g(x)$ if $0 < c_1 \le \frac{f}{g} \le c_2 < \infty$ for some positive constants c_1, c_2. Moreover, in many cases there exists a constant $C > 0$ such that

$$\psi_0(y) \sim C \cdot G_\lambda(0,y), \quad |y| \to \infty.$$

3 Classification of the tails and asymptotic behavior of the Green functions

We consider four classes of the densities $a(x)$, $x \in \mathbb{R}^d$.

3.1 Very light tails

In this class the characteristic function

$$\widehat{a}(\kappa) = \int_{\mathbb{R}^d} e^{i(\kappa,x)} a(x) dx$$

is the entire function of d complex variables $\kappa_1, \dots, \kappa_d$. It is better to work with the moment generating function

$$\widehat{A}(\kappa) = \int_{\mathbb{R}^d} e^{(\kappa,x)} a(x) dx.$$

Put $H(\kappa) = \widehat{A}(\kappa) - 1$. This function is convex and one can define its Legendre transform

$$H_*(y) = \max_{\kappa \in \mathbb{R}^d} \{(y,\kappa) - H(\kappa)\}.$$

In terms of $H(\kappa)$ and $H_*(\kappa)$ by using the classical Cramer's approach one can prove the central limit theorem for $x(t)$, which covers the area of arbitrary large deviations. Applying the Laplace transform to the transition probabilities of $x(t)$ one can prove that for any fixed $\lambda > 0$

$$\ln G_\lambda(0,y) \sim -|y| \nu\left(\lambda, \frac{y}{|y|}\right), \quad |y| \to \infty.$$

Here the factor $\nu\left(\lambda, \frac{y}{|y|}\right)$ is strictly positive and can be explicitly expressed in terms of $H(\kappa)$ and $H_*(\kappa)$, see Molchanov and Yarovaya[16]. For small λ

$$\nu\left(\lambda, \frac{y}{|y|}\right) = O(\sqrt{\lambda}).$$

Let us recall that for a Brownian motion $b(t)$ with the generator Δ

$$G_\lambda(0,y) \sim \frac{e^{-\sqrt{\lambda}|y|}}{|y|^{\frac{d-1}{2}}},$$

i.e.,

$$\ln G_\lambda(0,y) \sim -\sqrt{\lambda}|y|.$$

Situation of very light tails is similar to the case of the Brownian motion treated in Carmona and Molchanov[3].

3.2 Subexponential tails

This is the most difficult case. The monograph by Borovkov and Borovkov[2] contains analysis of only ten cases. For the isotropic distribution with the density

$$a(x) \sim e^{-|x|^d L(|x|)}, \quad |x| \to \infty, \quad 0 < \alpha < 1,$$

where L is a smooth slowly varying function one can prove that for fixed $\lambda > 0$ and $|y| \to \infty$

$$\ln G_\lambda(0,y) \sim e^{-|y|^\alpha L(x)}.$$

The asymptotics is independent of λ, but, of course, it is not uniform in λ for $\lambda \to 0$.

3.3 Moderate power tails

Here the density $a(x)$ has regular behavior at intensity:

$$a(x) \sim \frac{h\left(\frac{x}{|x|}\right)}{|x|^{d+\gamma}}, \quad |x| \to \infty, \quad \gamma > 2,$$

where $h\left(\frac{x}{|x|}\right) \in C(S^{d-1})$, $h > 0$ (the last condition is very important). Since $\int_{\mathbb{R}^d} |x|^2 a(x)dx < \infty$ the random walk $x(t)$ after normalization is asymptotically Gaussian and converges in law to the Brownian motion. But this is true only in region $|x| = o(\sqrt{t})$. The large deviations are essentially non Gaussian. The detailed analysis of $p(t,x,y)$ see in Borovkov and Borovkov[2]. From this analysis it is not difficult to derive that

$$G_\lambda(0,y) \sim c(\lambda)a(y) \sim c(\lambda)\frac{h\left(\frac{y}{|y|}\right)}{|y|^{d+\gamma}}.$$

3.4 Heavy tails

Here

$$a(x) \sim \frac{h\left(\frac{x}{|x|}\right)}{|x|^{d+\gamma}}, \quad |x| \to \infty,$$

but $\gamma < 2$ (for details of the model see Yarovaya[22]). The process $x(t)$ non belongs to the domain of attraction of the stable law in $\mathbb{R}^d$ with the parameter γ and the function $\tilde{h}\left(\frac{\kappa}{|\kappa|}\right)$ on S^{d-1} which play the same role as parameter β in the case of $d = 1$. The function $\tilde{h}(\cdot)$ can be expressed in terms of $h(\cdot)$. The limit

theorems for $p(t,x,y)$ in this case see again in Borovkov and Borovkov[2]. The asymptotic of the Green function for $|y| \to \infty$ is the same as in the case 3.3:

$$G_\lambda(0,y) \sim c(\lambda) \frac{h\left(\frac{y}{|y|}\right)}{|y|^{d+\gamma}}.$$

Now we define the front $F(t)$ of the population in the spirit of the classical KPP model. Let us assume that $x = 0$, that is the population starts from the single particle at the origin. Then for the density $m_1(t,0,y)$ we have the asymptotics

$$m_1(t,0,y) \sim \psi_0(0)\psi_0(y)e^{-\lambda_0(\beta)t}$$

or, taking into account that $\psi_0(y) \asymp G_\lambda(0,y)$,

$$m_1(t,0,y) \asymp G_\lambda(0,y)e^{-\lambda_0(\beta)t}.$$

We already have mentioned the relation $\psi_0(y) \asymp G_\lambda(0,y)$. It takes place in all the cases 3.1-3.4, and for the cases 3.2-3.4 we even have asymptotics up to the constant factor.

Like in the case of the KPP model we define the front of particle propagation $F(t)$ by the relation $m_1(t,0,y) \asymp \text{const}$, i.e., with the log accuracy

$$\lambda_0(\beta)t - \ln G_\lambda(0,y) = O(1).$$

It gives the following answers for

- **very light tails**: the front propagates linearly in t and its shape depends on level lines of the functions H and H_*;
- **subexponential tails**: the front is spherical due to isotropy and it is given by relation

  $$|y| \sim \left(\frac{t}{L_1(t)}\right)^{1/\alpha},$$

  and polynomial propagation takes place since $\frac{1}{\alpha} > 2$;
- **moderate power tails and heavy tails**: now front propagates exponentially fast in time:

  $$\frac{h\left(\frac{y}{|y|}\right)}{|y|^{d+\gamma}} \sim e^{\lambda_0(\beta)t},$$

i.e.,

$$|y| \sim \frac{\lambda_0(\beta)t}{d+\gamma}.$$

Let us stress that in all three cases 3.2-3.4 we used assumption on the regular structure of the tails. Without regularity the concept of the front has no sense.

Our next goal is the analysis of the population inside the propagating front.

4 Non-intermittency of the population inside the propagating front

The concept of intermittency for the study of the Solar magnetic field on the temperature field of the Earth ocean was proposed by Ya. Zeldovich and introduced in mathematics in the semi-physical review Zeldovich *et al.*[23]. It was developed later in the numerous pure mathematical works (see, Molchanov and Cranston[3], Molchanov[12], Gartner and Molchanov[6,7], Albeverio *et al.*[1], Gartner *et al.*[8]).

At the physical level, say, the magnetic field is intermittent if almost all its energy is concentrated on the set of very low density, or, as in a population dynamic case, almost all particles are concentrated inside compactly supported clusters (patches, spots) and between the clusters we have small amount of particles.

Mathematically, definition of intermittency must include the passing to the limit: not simply very small ε, but $\varepsilon \to 0$. The formal definition: consider a family of non-negative homogeneous and continuous in space and time ergodic random fields $X(t,x)$, $t \geq 0$, $x \in \mathbb{R}^d$. We say that this family is *intermittent* asymptotically for $t \to \infty$ if

$$\mathsf{E}X^2(t,x) = m_2(t) \gg (\mathsf{E}X(t,x))^2 = m_1^2(t),$$

i.e.,

$$\frac{m_2(t)}{m_1^2(t)} \to \infty.$$

If $m_2(t) = o(m_1^2(t))$, but one can find integer $k \geq 3$ such that

$$\mathsf{E}X^k(t,x) = m_k(t) \gg (\mathsf{E}X(t,x))^k = m_1^k(t).$$

we say that the family $X(t,x)$ is *weakly intermittent*. In the case of the lattice population dynamics $X(t,y) = n(t,\cdot,y)$.

We will use the same definitions also in the case of non-homogeneous fields. In our model we will apply the concept of the intermittency deep enough inside the front of the propagation. The discussion of the phenomenon of intermittency including the explanation why the progressive growth of the moments implies the high irregularity of the field $n(t,x,y)$: clusterization, patches etc., can be found in the above mentioned publications Molchanov and Cranston [3], Gartner and Molchanov[6,7] and Zeldovich *et al.*[23].

Recently in Koralov and Molchanov[11] the intermittency of the point field $n(t,x,\Gamma)$ was proven for the classical KPP model in $\mathbb{R}^d$, which is based on the non-linear equation

$$\partial_t u_z = \Delta u_z + \beta(u_z^2 - u_z),$$

where

$$u_z(0,x,\Gamma) = \begin{cases} z, & x \in \Gamma, \\ 1, & x \neq \Gamma, \end{cases}$$

and $x \in \mathbb{R}^d$ is the location of the initial particle. Of course, we can not apply the definition of the intermittency directly to the generalized field $n(t,x,\Gamma)$,

but one can use the natural averaging: $\tilde{n}(t,x,B_1(x))$ is the number of particles at the moment t in the unite ball $B_1(x)$ centered at $x \in \mathbb{R}^d$. In the KPP model the front propagates linearly in t which is seen, for $x=0$, from the relation

$$\frac{e^{-y^2/4t}}{(4\pi t)^{d/2}} e^{\beta t} \approx 1.$$

It gives for $F(t)$ the equation

$$|y| = 2\sqrt{\beta}t = k_0 t, \quad k_0 = 2\sqrt{\beta}.$$

Speed of the front is equal to $2\sqrt{\beta}$. According to Koralov and Molchanov[11] there exists the constant $k_1 \in (0,k_0)$, such that for

$$k_1 t < |y| < k_0 t$$

the field $\tilde{n}(t,x) = n(t,x,B_1(x))$ is intermittent. If $|y| \geq k_0 t$ the field is also intermittent, but in the weak sense.

The fundamental difference between the KPP model, where $V(x) \equiv \beta > 0$, and our model with compactly supported potential $V(x) = \beta V_0(x)$ is related to the absence of intermittency in our model.

Theorem 2. *For any $\varepsilon > 0$ inside the ε-neighbourhood of the front, i.e., for*

$$|y| \leq (1-\varepsilon) F\left(t, \frac{y}{|y|}\right),$$

we have for $t \to \infty$

$$\mathsf{E}\tilde{n}^2(t,y,B_1(y)) = O(\mathsf{E}\tilde{n}(t,y,B_1(y))^2.$$

The proof is based on direct calculations. To solve the problem

$$\begin{cases} \partial_t m_2 & = \mathcal{H}_\beta m_2 + 2\beta m_1, \\ m_2(0,\cdot) = \boldsymbol{I}_{B_1(y)}. \end{cases}$$

one can project it on two invariant subspaces: $L_2^{(0)} = \{f : \mathrm{span}\{\psi_0\}\}$ and $L_2^{(0)\perp} = \{f : (\psi_0, f) = 0)\}$. In $L_2^{(0)}$ we get the differential equation which can be solved explicitly, the part of the solution in $L_2^{(0)\perp}$ is growing much slower. We are not presenting the pure analytical proof due to paper volume restriction. The same approach is working for the higher moments of the order more than or equal to 3 and leads to the following limit theorem.

Theorem 3. *Assume that $t \to \infty$, $|y| = |y(t)| \in (1-\varepsilon)F(t, y/|y|)$. Then for the random variables $n^* = \frac{n(t,0,y)}{\mathbf{E}_0 n(t,0,y)}$ there exists the limiting distribution. The moments of the distribution can be calculated successively, starting from the second moment.*

At the end of this section let us discuss another property of the random walk with the finite number of the generating sites. Consider the event: $A_\infty = \{n(t,x,\mathbb{Z}^d) \leq C\}$ for any $t < \infty$. It means, that the population is uniformly bounded for any $t > 0$. Since the model does not contain the mortality then $n(t,x,\mathbb{Z}^d) \geq n(0,x,\mathbb{Z}^d) = 1$.

Theorem 4. *If the underlying random walk $x(t)$ is recurrent then $\mathsf{P}(A_\infty) = 0$, i.e., the population exponentially increases P-almost sure for $t \to \infty$.*

The proof of this result is simple: the initial particle returns to the support of the function $V(x)$ infinitely many times, i.e., it produces infinitely many offspings since at any visit to the support of the function $V(x)$ it produces the offsprings with uniformly positive probability.

In other words it means that the condition $\lambda_0(\beta) > 0$ for any $\beta > 0$ implies $\mathsf{P}(A_\infty) = 0$, and the population is exponentially growing P-almost sure.

For the transient process $x(t)$ the situation is different. It is obvious that x does not belong to the support of the function $V(x)$ with positive probability because the random walk of the initial particle started from $x \in \mathbb{Z}^d$ never visits the support of the function $V(x)$, that is $n(t, x, \mathbb{Z}^d) \equiv 1$ for $t > 0$.

Let us introduce the event

$$A_1 = \{n(t, x, \mathbb{Z}^d) \equiv 1\}, \quad t \geq 0,$$

and the function

$$\pi_1(x) = \mathsf{E}_x \boldsymbol{I}_{A_1} = \mathsf{P}_x(A_1).$$

Similarly, for every $k \in \mathbb{N}$ and $t \to \infty$ we define

$$A_k = \{n(t, x, \mathbb{Z}^d) \to k\} = \{\exists \tau_k : n(t, x, \mathbb{Z}^d) \equiv k,\ t \geq \tau_k\},$$

and

$$\pi_k(x) = \mathsf{E}_x \boldsymbol{I}_{A_k} = \mathsf{P}_x(A_k),$$

and also

$$A_\infty = \{n(t, x, \mathbb{Z}^d) \to \mathbf{C} < \infty\}, \quad \mathbf{C} > 0,$$

and

$$\pi_\infty(x) = \mathsf{E}_x \boldsymbol{I}_{A_\infty} = \mathsf{P}_x(A_\infty).$$

All these events are the elements of the final σ-algebra of our branching random walk, see Molchanov and Yarovaya[15]. Clearly,

$$\pi_\infty(x) = \sum_{k=1}^{\infty} \pi_k(x).$$

All the functions $\pi_k(x)$, $k \geq 1$, can be calculated directly as solutions of appropriate equations, see Molchanov and Yarovaya[15]. However, for our purpose it is more convenient to use the generating functions like in the classical Galton-Watson theory. Let us point out the difference between our case and the Galton-Watson branching processes. In the latter case the population in the supercritical regime can degenerate if the rate of mortality b_0 is positive. In the situation of a branching random walk with $b_0 = 0$ the population remains bounded due to the fact that initial particle or its offsprings leave forever the support of the function V.

Put $u_z^*(x) = \lim_{t\to\infty} u_z(t,x,\mathbb{Z}^d) = \sum_{k=1}^{\infty} \pi_k(x) z^k$, $|z| < 1$. Note that $z^{n(t,x,\mathbb{Z}^d)} \to 0$ if $n(t,x,\mathbb{Z}^d) \to \infty$. The limit exists since $n(t,x,\mathbb{Z}^d)$ increases when $t \to \infty$. Passing to the limit in the initial equation we get

$$\mathcal{L}u_z^* + \beta V_0(\cdot)((u_z^*)^2 - u_z^*) = 0$$

with the constant boundary conditions at infinity. It is clear that $\pi_1(x) \to 1$ as $|x| \to \infty$, $\pi_k(x) \to 0$ as $|x| \to \infty$ and $k \geq 2$, i.e., $u_z^*(x) \to z$ as $|x| \to \infty$.

To find $u_z^*(x)$ let us introduce $v_z(x) = z - u_z^*(x)$ where $v_z(x) \to 0$ as $|x| \to \infty$. Then

$$\mathcal{L}v_z + \beta V_0(\cdot)((z - v_z)^2 - (z - v_z)) = 0,$$

that is

$$(\mathcal{L}v_z)(x) = -\beta V_0(x) \Phi_z(x),$$

where $\Phi_z = ((z - v_z)^2 - (z - v_z))$. For every $x = y_i$ belonging to the support of the function V this last equation can be treated as the quadratic system

$$v_z(y_i) = \beta \sum_{y_j \in \operatorname{supp} V} G_0(y_i, y_j) V_0(y_j) \Phi_z(y_j).$$

In some cases, e.g., for systems with a single generating centre, several centres with high level of symmetry and condition $V(x) \equiv C$ on $\operatorname{supp} V$ where C is a constant, and so on, this system can be solved explicitly, see Molchanov and Yarovaya[15] for additional information.

5 Acknowledgement

The research is supported by the RSF grant 14-21-00162.

References

1. S. Albeverio, L. Bogachev, S. Molchanov and E. Yarovaya. Annealed moment Lyapunov exponents for a branching random walk in a homogeneous random branching environment. *Markov Processes and Related Fields*, **6**, 4, 473–516, 2000.
2. A. Borovkov and K. Borovkov *Asymptotic Analysis of Random Walks. Heavy-Tailed Distributions*, Cambridge University Press, Cambridge, 2008.
3. R. Carmona and S. Molchanov. Parabolic Anderson model and intermittency. *Memoirs of American Math Soc.*, **518**, 1994.
4. M. Cranston, L. Koralov, S. Molchanov S. and B. Vainberg. Continuous model for homopolymers. *J. Funct. Anal.*, **256**, 8, 2656-2696, 2009.
5. F. Gantmacher. *The Theory of Matrices*, AMS Chelsea Publishing: Reprinted by American Mathematical Society, 2000.
6. J. Gartner and S. Molchanov. Parabolic problems for the Anderson model. I. Intermittency and related topics. *Comm. Math. Phys.*, **132**, 3, 613-655, 1990.
7. J. Gartner and S. Molchanov. Parabolic problems for the Anderson model. II. Second-order asymptotics and structure of high peaks. *Probab. Theory Related Fields*, **111**, 1, 17–55, 1998.

8. J. Gartner, W. Konig and S. Molchanov. Geometric characterization of intermittency in the parabolic Anderson model. *Ann. Probab.*, **35**, 2, 439–499, 2007.
9. T. Kato. *Perturbation Theory for Linear Operators*, Springer-Verlag, Heidelberg, 1966; Mir, Moscow, 1972.
10. A. Kolmogorov, I.Petrovskii and N. Piskunov. A study of the diffusion equation with increase in the amount of substance, and its application to a biological problem. *Byul. Mosk. Gos. Univ.*, Mat. Mekh. **1**, 6, 1-26, 1937.
11. L. Koralov and S. Molchanov. Structure of the population inside the propagating front. *J. Math. Sci.*, **189**, 4, 637–659, 2013.
12. S. Molchanov. Lectures on random media. *Lecture Notes in Math.*, Berlin: Springer, **1581**, 242–411, 1994.
13. S. Molchanov and E. Yarovaya. Branching processes with lattice spatial dynamics and a finite set of particle generation centers. *Dokl. Math.*, **86**, 2, 638-641, 2012.
14. S. Molchanov and E. Yarovaya. Limit theorems for the Green function of the lattice Laplacian under large deviations of the random walk. *Izv. Math.*, **76**, 1190-1217, 2012.
15. S. Molchanov and E. Yarovaya. Population structure inside the propagation front of a branching random walk with finitely many centers of particle generation. *Dokl. Math.*, **86**, 3, 787-790, 2012.
16. S. Molchanov and E. Yarovaya. Large Deviations for a Symmetric Branching Random Walk on a Multidimensional Lattice. *Proceedings of the Steklov Institute of Mathematics*, **282**, 186-201, 2013.
17. W. Shaban and B. Vainberg. Radiation conditions for the difference Schrödinger operators. *Appl. Anal.*, **80**, 3-4, 525–556, 2001.
18. E. Yarovaya. *Branching Random Walks in Nonhomogeneous Environment*, Tsentr Prikl. Issled. Mekh.Mat. Fak. MGU, Moscow, 2007. [in Russian].
19. E. Yarovaya. Criteria of exponential growth for the numbers of particles in models of branching random walks. *Theory Probab. Appl.*, **55**, 661-682, 2011.
20. E. Yarovaya. Spectral properties of evolutionary operators in branching random walk models. *Math. Notes*, **92**, 115-131, 2012.
21. E. Yarovaya. Branching Random Walks with Several Sources. *Mathematical Population Studies*, **20**, 14–26, 2013.
22. E. Yarovaya. Criteria for transient behavior of symmetric branching random walks on $\mathbb{Z}$ and $\mathbb{Z}^2$. *New Perspectives on Stochastic Modeling and Data Analysis*, ISAST: Athens, Greece, 283-294, 2014.
23. Y. Zeldovich, S. Molchanov, A. Ruzmakin and D. Sokoloff. Intermittency, diffusion and generation in a nonstationary random medium. *Mathematical physics reviews*, Chur: Harwood Academic Publ., **7**, 3–110, 1988.

2 CHAPTER

Markov and semi-Markov models

The Coxian Phase-type distribution with a Hidden Node

Hannah Mitchell[1], Adele H. Marshall[1], and Mariangela Zenga[2]

[1] Queen's University Belfast Department of Mathematics and Physics, Belfast, United Kingdom
(E-mail: hmitchell03@qub.ac.uk a.h.marshall@qub.ac.uk)
[2] University of Milan-Bicocca, Department of Statistics and Quantitative Methods, Milan, Italy
(E-mail: mariangela.zenga@unimib.it)

Abstract. Healthcare providers are under increased pressure to ensure that the quality of care delivered to patients are off the highest standard. Modelling quality of care is difficult due to the many ways of defining it. This paper introduces a potential model which could be used to take quality of care into account when modelling length of stay. The Coxian phase-type distribution is used to model length of stay and quality of care incorporated into this using a Hidden Markov model. This model is then applied to a simulation dataset as well as patient data from the Lombardy region of Italy
Keywords: Coxian phase-type distribution, Hidden Markov model, Quality of Care.

1 Introduction

Healthcare systems across Europe and further afield have come under increased scrutiny in recent years. Many European countries are encountering a growing older population and this comes with many problems for not only governments but also healthcare providers. Elderly individuals tend to spend longer in care than the rest of the population due to complex and time consuming medical conditions and rehabilitation. This in turn puts a strain on the hospitals budget, with healthcare managers coming under increased pressure to make sure that the hospitals deliver the best quality of care available but at the same time effectively and efficiently managing an already stretched budget [1].

Quality of care can be defined in many ways making it difficult to measure and use within a scientific study. The purpose of this paper is to develop a model which incorporates the concept of quality of care within it. An outline of how the Hidden Markov model (HMM) could potentially incorporate quality of care into a model is given. The Hidden Markov model has an underlying hidden stochastic process which potentially could represent quality of care. Initially developed as extensions for measurement errors of the standard Markov chain

New Trends in Stochastic Modeling and Data Analysis (pp. 77-90)
Raimondo Manca - Sally McClean - Christos H Skiadas (Eds)

model, the HMM but have been used in many areas of research including signal processing, in particular speech processing, medical applications and economics [4], [2], [6].

Modelling patient flow in healthcare systems is considered vital in understanding the system's activity. The Coxian phase-type distribution has successfully managed to achieve this where the distribution describes the time to absorption of a finite Markov chain in continuous time where there is a single absorbing state and the stochastic process starts in the first transient state [8]. Using the Coxian phase-type distribution has proved to be not only useful in healthcare modelling [22] but also in modelling the length of stay in Italian and Greek Universities [3] and the length of time taken for a component to fail [11].

The aim of this paper is to combine the Hidden Markov Model and the Coxian phase-type distribution with the intention of encapsulating quality of care. The Coxian phase-type distribution with a hidden node will attempt to model patient flow in healthcare with the quality of care delivered by the hospital incorporated into it via the hidden layer. The quality of care delivered by hospitals has previously been modelled using measures such as the nurse-staffing levels and the number of deaths [19], number of readmissions [13], and patient length of stay in hospital [18].

The Coxian pahse-type distribution with a hidden node will be applied to healthcare data from the Lombardy region of Italy between 2008-2011. The model will also be applied to a simulated dataset from a known Coxian phase-type distribution as a means of demonstrating the hidden node representing quality of care and how it can affect the length of stay of individuals. This model will subsequently highlight when the quality of care delivered by the hospital has changed and how quality of care affects a patients length of stay.

2 Hidden Markov Models

Hidden Markov models were developed by Baum in 1960 [2]. They are used extensively in signal progressing particularity in speech recognition, but their application has since been expanded upon and they have now been used in healthcare [4], financial [5] and economic applications [6].

The Hidden Markov model (HMM) is used to describe a stochastic system and is made up of a finite set of states. Each state generates an observation as well as being associated with a probability distribution. The state of the underlying Markov process cannot be observed directly but can be inferred from observations. The HMM was first developed with discrete outcomes with the Poisson distribution proving to be a popular probability distribution for this. Some applications however have observations that have continuous signals or outputs and so it would be advantageous to develop the model so that continuous densities can be used. The model has since then been developed further to allow for continuous outcomes with the mixed Gaussian/Gaussian distribution

being used for those applications [23].

Figure [1] shows the HMM which is a doubly embedded stochastic process,

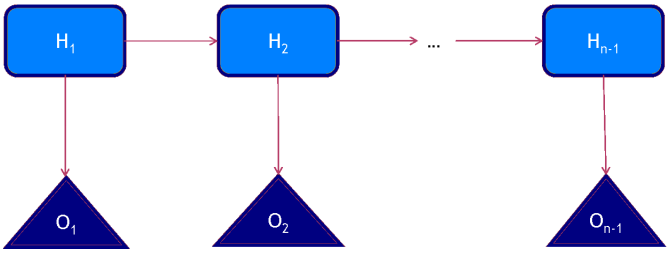

Fig. 1. The Hidden Markov Model

where the outcome (probability distribution) is observed with an underlying hidden stochastic process.

The formal definition of a Hidden Markov Model is as follows [2],

$$\lambda = (A, B, \pi) \tag{1}$$

A is a transition array, storing the probability of state j following state i.

$$A = [a_{ij}], \quad a_{ij} = P(q_t = s_j |\ q_{t-1} = s_i)$$

where $1 \leq i,\ j \leq N$

B is the observation array, storing the probability of observation k being produced from the state j, independent of t:

$$B = [b_i(k)], \quad b_i(k) = P(x_t = v_k | q_t = s_i)$$

S is the state alphabet set, and V is the observation alphabet set:

$$S = (s_1, s_2, ..., s_N)$$

Where N is the number of states in the model with the individual sates s

$$V = (v_1, v_2, ..., v_M)$$

M is the number of distinct observation symbols per state. The observation symbols correspond to the physical output of the system being modelled. The individual symbols are denoted by v.

π is the initial probability array:

$$\pi = [\pi_i], \quad \pi_i = P(q_1 = s_i)$$

The model makes two assumptions. The first is that the current state is dependent only on the previous state, which is known as the Markov property. The second is that the output observation at time t is dependent only on the current state, it is independent of previous observations and states.

The Baum-Welch algorithm which incorporates the EM-algorithm is used to estimate the parameters of the HMM. It is an iterative procedure which adjusts the HMM parameters to obtain the maximum probability of obtaining the observation sequence. Details of this algorithm can be seen in Rabiner [2].

3 Coxian Phase-type Distribution

Past investigations of modelling length of stay led to the discovery that a two-term mixed exponential model produces a good representation of patient survival [24]. Since then further research has endeavoured to improve the mixed exponential models with the incorporation of more complex compartmental systems and more sophisticated stochastic models such as the Coxian phase-type distribution.

The Coxian phase-type distribution is a special type of stochastic model that represents the time to absorption of a finite Markov chain in continuous time where there is a single absorbing state and the stochastic process starts in a transient state. They are a subset of the phase-type distributions introduced by Neuts in 1975 [8], having the benefit of overcoming the problem of generality within phase-type distributions.

A Coxian phase-type distribution $(X(T); t \geq 0)$ may be defined as a (latent) Markov chain in continuous time with states 1,2,...,n,n+1, $X(0)$=1,

and for i=1,2,...,n-1,

$$\text{prob}\{X(t+\delta t) = i+1 | X(t) = i\} = \lambda_i \delta t + 0(\delta t) \tag{2}$$

and for i=1,2,...,n

$$\text{prob}\{X(t+\delta t) = n+1 | X(t) = i\} = \mu_i \delta t + 0(\delta t). \tag{3}$$

here states 1,2,...,n are latent (transient) states of the process and state n+1 is the absorbing state. λ_i represents the transition from state i to state (i+1) and μ_i the transition from state i to the absorbing state (n+1). The Coxian phase-type distribution is defined as having a transition matrix $\mathbf{T}$ of the following form.

$$T = \begin{pmatrix} -(\lambda_1+\mu_1) & \lambda_1 & 0 & ... & 0 & 0 \\ 0 & -(\lambda_2+\mu_2) & \lambda_2 & ... & 0 & ... \\ ... & ... & ... & ... & ... & ... \\ 0 & 0 & 0 & ... & -(\lambda_{n-1}+\mu_{n-1}) & \lambda_{n-1} \\ 0 & 0 & 0 & ... & 0 & -\mu_n \end{pmatrix} \tag{4}$$

The survival probability that $X(t)$=1,2,...,n is given by

$$S(x) = \alpha \exp(\mathbf{T}x)\mathbf{e} \tag{5}$$

where α=(1, 0, 0, ..., 0, 0), $\mathbf{e}$ is a column vector of 1's and $\mathbf{T}$ is the transition matrix.

The probability density function of X is

$$f(x) = \mathbf{p} \exp(\mathbf{T}x)\mathbf{q} \tag{6}$$

where $\mathbf{q} = -\mathbf{T}\mathbf{e} = (\mu_1, \mu_2, ..., \mu_n)^T$ and p=α=(1, 0, 0, ..., 0, 0). An illustration

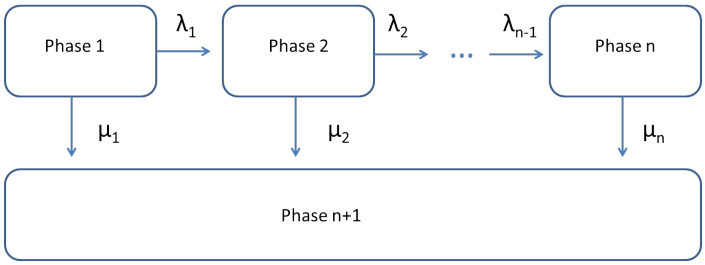

Fig. 2. Phase diagram of the Coxian Distribution

of the Coxian phase-type distribution can be seen in Figure (2). From this figure it can be seen that the process starts in the first phase and sequentially moves either through each transient state or into the absorbing state at any stage, because of this the Coxian phase-type distribution can be thought of as having some real world meaning. For example the distribution could be thought of in a hospital scenario with each phase seen as some progression of treatment. The first phase could be admittance followed by treatment and rehabilitation, with the individual being able to leave the hospital during any phase due to discharge, transfer or death.

Coxian phase-type distributions have been used in a variety of settings from component failure data [14] to prisoner remand times [15]. Marshall et al. [3] used the Coxian phase-type distribution to model career progression of students at university. Most applications of the Coxian phase-type distribution have been in modelling the length of time spent in hospital in particular McClean et al. [22] showed that the distribution was appropriate for describing

the length of time of geriatric patients in hospital.

The parameters of the Coxian phase-type distribution can be estimated in a variety of ways using a range of computer programmes or packages. Payne et al. [9] investigated the efficiency of fitting the Coxian phase-type distribution to healthcare data using SAS, R, Matlab and EMpht. EMpht which is a programme written in C uses the EM algorithm as its optimisation function and it was shown to have consistently high rates of convergence. This approach to fitting the Coxian phase-type distribution has been coded in Matlab.

4 Quality of Care

Quality of Care is a multifaceted concept, whose incorporation into scientific study as a result is deemed difficult but one of great importance and interest [16]. In 1855 (during the Crimean War), Florence Nightingale noticed that soldiers operated in large hospitals were more likely to die than those operated on in smaller hospitals. She identified that poor sanitation and the rapid spread of infection from patient to patient in large hospitals was the cause, so she set about doing something to improve the sanitary conditions in English field hospitals. More than a century later, there is still great interest in characterising hospitals that provide better or worse care with the aim of improving the quality delivered [17].

Until recently, to ensure that patients are receiving high-quality medical care, professional judgement was relied upon [21]. Hospitals routinely monitored poor outcomes, such as deaths or infections to identify ways to improve the quality of care. In general the monitoring of and improvement of quality was left to the clinician.

Quality of care can be defined in many ways and is not amenable to a single performance measure. In general it is defined as having the following six key domains [20]:

1) **Effectiveness**: This refers to the extent to which an intervention produces its intended result, and the concept of appropriateness; concentrating on whether interventions or services are provided to those who would benefit from them and withheld from those who would not.

2) **Access**: Access monitors waiting times, with lower waiting times for patient procedures being more beneficial.

3) **Capacity**: This takes into account the number of medical staff, bed numbers, along with how well equipped the hospitals and or surgeries are as well as the budget allocated/available to each provider.

4)**Safety**: Safety is concerned with infection control while the patient is in hospital and the elimination of unnecessary risk of harm to patients.

5) **Patient Centredness**: This measures how patients rate the quality that they are receiving whilst in hospital.

6) **Equity**: Equity is concerned with significant inequalities in life expectancy and mortality from major diseases between the least and most deprived groups.

Quality of Care has previously been incorporated into studies using the number of deaths [19], readmission [13] and length of stay of patients [18] as common proxies for the measurement of it.

Each of these proxies do have limitations when using them as a measurement for quality of care. Using death rate might not be the best measure of quality of care as it is not necessarily the quality that the hospital offers that causes the outcome but rather the disease or injury endured by the patient. Given that it is a geriatric ward that this paper will look at, death is more likely amongst this group of individuals than any other due to old age or the lowered ability to recover from disease and infection. Readmissions also could have the limitation that the data is not available for use (as is this case with the data used here) or indeed the individual could be readmitted into the same hospital but with a different complaint. Elderly patients tend to be admitted into hospital due to one condition but in fact they may be suffering from several other aliments. This also has an effect on length of stay. Elderly individuals tend to spend longer in hospital due to the multitude and variety of illness that many of them suffer from at any one time. Therefore to use length of stay data as a proxy, very long length of stays as well as short length of stays (which are mainly attributed to patients who die) could serve as flagging up potentially poorer quality of care delivered to these patients [10]. Due to length of stay being related to the outcome of patients, and that the data used does not have readmission information, length of stay was used and quality of care inferred from it.

Quality of care is difficult to measure due to its many factors, internal and external. One potential way of measuring quality is by treating it as a hidden layer. Length of stay has been seen as an indicator of quality of care and it has been shown that the Coxian phase-type distribution gives a good representation of length of stay. In this paper the Coxian phase-type distribution has been combined with the HMM, thus giving the effect of a hidden node (representing quality) being incorporated into the Coxian phase-type distribution.

4.1 Coxian phase-type distribution with a hidden node

The Hidden Markov model with continuous outcomes has only ever used the Gaussian or the mixed Gaussian distribution as its probability density function. The model was expanded upon so that the outcomes which are best represented using a Coxian phase-type distribution could be used, by letting this distribution be the probability density function.

The Coxian phase-type distribution with a hidden node was developed, with the hidden node representing quality. This model has the Markov property within the hidden layer and the probability density function. Given quality of care is being represented as the hidden layer the Markov property could infer that the quality of care delivered by the hospital for example does not depend on the past but from the previous quality delivered. This assumes that if poor quality of care was obtained during a measurement that the hospital would rectify the problem immediately so that the next patient or time measured would receive the newly modified care system. Figure [3] shows a representation of

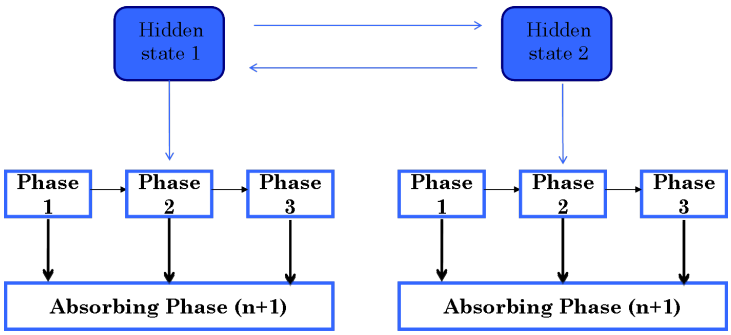

Fig. 3. Phase diagram of the Coxian phase-type distribution with a hidden node

the Coxian phase-type distribution with the hidden node. The hidden Markov model was given two hidden states, to represent good and poor quality of care, and from these two states a Coxian phase-type distribution produced. The formal definition of the HMM is given by equation (1), where λ is the parameter estimates of the model.

For the HMM the general Q function for the complete-data log-likelihood is given as

$$Q(\lambda, \lambda') = \Sigma_{q \epsilon Q} \log P(O, q|\lambda) P(O, q|\lambda') \tag{7}$$

where λ' is the initial/previous parameter estimates, O=$(o_1, ..., o_T)$ are the observed data and q=$(q_1, ..., q_T)$ is the underlying hidden state sequence.

Given a particular state sequence q, representing $P(O, q|\lambda')$ that is,

$$P(O, q|\lambda') = \pi_{q0} \Pi_{t=1}^{T} a_{q_{t-1} q_t} b_{q_t}(o_t) \tag{8}$$

where π_{q0} is the probability of initially being in state q, $a_{q_{t-1} q_t}$ is the probability of moving between the hidden states and $b_{q_t}(o_t)$ is the probability of a particular observation vector at a particular time t for state q_t. The Q function then becomes:

$$Q(\lambda, \lambda') = \Sigma_{q \epsilon Q} \log \pi_{q0} P(O, q|\lambda') + \Sigma_{q \epsilon Q} \{\Sigma_{t=1}^{T} \log a_{q_{t-1} q_t}\} p(O, q|\lambda') + \tag{9}$$

$$\Sigma_{q\epsilon Q}\{\Sigma_{t+1}^{T}\log b_{q_t}(o_t)\}P(O,q|\lambda')$$

The parameters that require optimisation are in three independent terms and can thus be optimised individually. The Coxian phase-type distribution being the output of the Hidden Markov model, $b_{q_t}(o_t)$ in equation [9] can be replaced by the probability density function of the Coxian phase-type distribution, equation [6]. The model is implemented in Matlab with the EM and Runge-kutta algorithms used to for fitting the Coxian phase-type distribution and the Baum-Welch used to fit the HMM.

The Viterbi algorithm [2] finds the best state sequence for the observations of the hidden states. It is also coded in Matlab so that the state which best represents the quality of care at each time point can be produced. This will also highlight when a change of state is most likely to occur.

5 Simulation Study

The actuar package in R was used to simulate length of stay data from a three phase Coxian phase-type distribution.The simulated dataset consists of 100 data points ranging from 0.19 to 84.65 days with an average of 23 days. Table [1] displays the three phase Coxian distribution parameters used to simulate the data. The proposed Coxian HMM was applied to the dataset using Matlab.

Table 1. Coxian phase-type distribution for simulated data

Phase	Transition Rates
3	$\mu_1 = 0.0462$, $\mu_2 = 0.0011$, $\mu_3 = 0.0779$, $\lambda_1 = 0.0589$, $\lambda_2 = 0.0779$

The model probability of initially being in either state is

$$\pi = (\,0.2367\ 0.7633\,) \tag{10}$$

The initial probability suggests that the hospital quality of care is initially in state 2. The transition matrix for the Hidden Markov model was given as

$$A = \begin{pmatrix} 0.5091 & 0.4909 \\ 0.5107 & 0.4893 \end{pmatrix} \tag{11}$$

The hidden transition matrix and initial probabilities of the model suggest that the hospital starts in state 2 with a probability of 0.7633. The hidden transition matrix shows that the probability of being in state 1 and moving to state 2 at the next time point is 0.4904 and the probability of being in state 2 and moving to state 1 is 0.5107. This suggests that although the hospital care is initially in state 2 there is a slightly higher probability that the hospital quality of care will transition to state 1 and a slightly higher probability of staying in state 1 than transitioning back to state 2.

The parameters for the Coxian phase-type distributions given by each state are provided below. Table [2] shows the parameters for state 1 and state 2. The Coxian phase-type distribution for state 1 and state 2 both suggest that

Table 2. State 1 and 2 Coxian Phase-type distribution parameter estimates

State	Parameter Estimates
1	$\mu_1 = 0.0000$, $\mu_2 = 3.3570$, $\mu_3 = 0.0608$ $\lambda_1 = 0.0608$, $\lambda_2 = 2.0900$
2	$\mu_1 = 0.0000$, $\mu_2 = 2.7302$, $\mu_3 = 0.0609$ $\lambda_1 = 0.0583$, $\lambda_2 = 2.2430$

no patients left the system in the first phase but all transitioned through to the next stage of treatment. In state 1 the patients left the second phase of the Coxian phase-type distribution at a faster rate than in state 2. They exited into the absorbing state at a transition rate of 3.357 in comparison to state 2 which had a transition rate of 2.7302. The original Coxian phase-type distribution showed that no one left at the second phase and the transition through to the second phase for the original distribution was similar to that of the two Coxian phase-type distributions with hidden nodes. The Coxian phase-type distributions between the two states after phase 2 are very similar with state 2 showing larger transition rates. State 2 suggests that patients go through the system slightly quicker in the final part of the Coxian phase-type distribution than in state 1.

The interpretation of the states are difficult. In this context they are thought of as quality of care. In general the interpretation of the states are taken by the average of the outcomes of the HMM. The Viterbi algorithm gives the best state that each observation belongs to, from this the average length of stay of each state was found. The outcome of the Viterbi algorithm also gives how the states change over time, with lower length of stays changing the state from state 1 to state 2. Those observations which the Viterbi algorithm showed to be in state 1 had an average length of stay of 42.62 days, whereas the average length of stay for the observations in state 2 was 9.15 days. This would suggest that given the individuals are in the system longer that state 1 shows a better quality of care than state 2.

In general patients who leave the system at the start tend to leave due to death in-comparison to those individuals who are transferred to another hospital or home. This suggests given the average length of stay of each of the states that state 1 suggests better quality than state 2. However state 1 shows that individuals leave phase 2 at a faster rate than state 2.

The phases in the 3 phase Coxian distribution could be thought of as acute care for the first phase, further treatment for the second and rehabilitation for the final phase. Given both outcomes suggest that no one left the first

phase through the absorbing state, patients left at a slightly faster rate in state 1 and along with the average length of stay being a lot greater than state 2 would suggest possibly that the hospital is potentially ill equipped to cope with certain individuals aliments and are waiting for them to be transferred to a different hospital or care-home. This may fall under the quality of care domain of Capacity if the hospital is not well equipped, and hence the quality of care delivered to some individuals is of a poorer standard.

From previous research small and long length of stays both are possibly highlighting decreased quality of care [10]. However with this dataset the model has partitioned the small and large length of stays as two different quality of care states. If more detail is available, for example the outcome of the patients along with the aliments/problems of the patients, this may also help with the interpretation of the states.

6 Italian dataset

The proposed Coxian HMM is applied to a large Italian administrative dataset, which contains all of the geriatric wards in the Lombardy Region. There were no day hospital cases with all patients being ordinary admission. The data consists of length of stay information for 2174 patients aged 65 years of age or older that were admitted into a geriatric ward between 2008-2011. The hospital considered for this illustration is a public hospital with an average length of stay of 17.83 days.

A Coxian phase-type distribution was fitted to the data resulting in a four Coxian as the best fit, determined so by comparing the AIC values. The parameter estimates of this Coxian phase-type distribution can be seen in table (3) The Coxian phase-type distribution with a hidden node was then applied

Table 3. State 1

Phases	Transition rates
4	$\mu_1 = 0.0000$, $\mu_2 = 0.0000$, $\mu_3 = 0.0000$, $\mu_4 = 0.220772$ $\lambda_1 = 0.220772$, $\lambda_2 = 0.220772$, $\lambda_3 = 0.220772$

to this data. The results show that the initial probability of being in each state is

$$\pi = (\,0.4984\ 0.5016\,) \tag{12}$$

The transition matrix is

$$A = \begin{pmatrix} 0.4986 & 0.5014 \\ 0.4986 & 0.5014 \end{pmatrix} \tag{13}$$

The initial probabilities show that the hospital is initially in state 2 with a probability of 0.5016. The A matrix shows that the hospitals hidden state has a small probability of changing if it is in state 1. The probability of it transitioning to state 2 is 0.5014 and the probability of remaining in state 2 if it is

in state 2 already is also 0.5014. Given the probabilities for the hidden states show that the observations are equally as likely to be in state 1 as in state 2 this potentially shows that the observations each month have not changed significantly to warrant a change in hidden state and therefore quality of care.

The Coxian phase-type distribution for each of the hidden states is displayed in table [4]. From table [4] the transition rates for the two states of the Coxian

Table 4. Coxian phase-type distributions for state 1 and state 2

States	Parameter Estimates
1	$\mu_1 = 0.000000$, $\mu_2 = 0.000000$, $\mu_3 = 0.000000$, $\mu_4 = 0.220756$ $\lambda_1 = 0.220756$, $\lambda_2 = 0.220756$, $\lambda_3 = 0.220756$
2	$\mu_1 = 0.000000$, $\mu_2 = 0.000000$, $\mu_3 = 0.000000$, $\mu_4 = 0.220774$ $\lambda_1 = 0.220774$, $\lambda_2 = 0.220774$, $\lambda_3 = 0.220774$

phase-type distribution with a hidden node are very similar. They are also similar to the original Coxian phase-type distribution parameters table [3]. This could suggest that there is barely any difference between the two states suggesting that the quality of care has not changed dramatically over time. Given that the Hidden Markov model with the Coxian phase-type distribution has given parameters very similar to the Coxian phase-type distribution perhaps this model "fine tunes" the Coxian phase-type distribution in allowing a hidden layer of unobserved factors to be taken into account.

When the Viterbi algorithm is applied, it shows that the best state for each of the data points were the same. This suggests that the quality of care delivered has remained the same throughout the months. Looking at the average length of stay for each month the range is small suggesting no real difference in length of stay over the years.

The hidden transition matrix, the Coxian phase-type distributions for the two hidden states and the Viterbi algorithm all suggest that the quality if care in Hospital A has remained the same over the 4 year period.

A more in-depth approach could be suggested by looking at the length of stay data over each week or to use data manipulation so it could be used for each day if there is missing time points. This would then go into more detail if there had been any changes of quality of care on a day to day basis. To get a better picture of quality of care within this hospital, covariates could be incorporated into the model. If the hospital is a public or private hospital, if its small or large, the number of staff that they have working each day and the number of beds that are available each day may give a better picture as to the quality delivered by the hospital.

7 Conclusions/Further Work

This paper introduces the Coxian phase-type distribution with a hidden node. It expanded the Hidden Markov model to allow the Coxian phase-type distribution as the probability density function to represent the observations. This model was then applied to a simulated dataset and a real hospital dataset from the Lombardy region of Italy. The model was used to measure quality of care and how it affects the Coxian phase-type distribution as well as giving how the quality of care changes over time and the probabilities of a change of quality of care happening. The results show how interpreting the states of the hidden Markov model is difficult, and that taking the average outcome of each state requires further refinement.

Further work includes incorporating covariates into the transition matrix of the Hidden Markov model with the Coxian phase-type distribution as the output. This will show how quality of care changes or effects the length of stay of patients when for example the number of beds, staff levels etc change. This has the potential to be used therefore by hospital managers for planning and efficiently running the healthcare system. Other future work includes incorporating covariates into the Coxian phase-type distribution to show how certain they affect patient length of stay. This has previously been incorporated into a Coxian (without the HMM). Cost is factor in the running of the hospital and the quality of care delivered. Quality of care and cost potentially go hand in hand thus further work will investigate the inclusion of cost into the model. The Coxian phase-type distribution has been previously developed to estimate costs therefore there is potential to incorporate this theory into the Hidden model. Having Cost in this model will also benefit the healthcare managers so they can plan and evaluate the possible benefits or problems associated with reducing the amount of money, staff, beds etc when trying to run a hospital which delivers high quality of care to all patients within a tight and stringent budget.

References

1. Janssen. Economist Intelligence Unit, The future of healthcare in Europe. *The Economist*, Janssen, 2011
2. L. R. Rabiner. A Tutorial on Hidden Markov Models and Selected Applications in Speech Recognition. *Proceedings of the IEEE*, 77, **2**, 257-286, 1989.
3. A.H.Marshall, M. Zenga, S. Giordano. Modelling Students' Length of Stay at University Using Coxian Phase-type Distributions. *International Journal of Statistics.* 73-89, 2013
4. B. Cooper and M. Lipsitch. The analysis of hospital infection data using hidden Markov models. *Biostatistics.* 2, **2**, 223-237, 2004.
5. A. Gupta and B. Dhingra. Stock Market Prediction Using Hidden Markov models. *IEEE.* 2012.
6. R. Bhar and S. Hamori. Hidden Markov Models: Applications to Financial Economics. *Advanced Studies in Theoretical and Applied Econometrics.* Springer, 2004.

7. S. Asmussen, O. Nerman and M. Olsson. Fitting Phase-type Distributions via the EM Algorithm. *Scandinavian Journal of Statistics*, 23, **4**,419-441, 1996.
8. M.F. Neuts, Matrix-Geometric Solutions in Stochastic Models. *John Hopkins University Press*, 1981.
9. K. Payne, A.H. Marshall and K.J. Cairns. Investigating the efficiency of fitting Coxian phase-type distributions to health care data. *IMA Journal of Management Mathematics*, 2011.
10. J.W. Thomas, K. E. Guire, G.G. Horvat. Is patient length of stay related to quality of care. *Hospital Health Service.* 42, **4**, 489-507, 1997.
11. M.J. Faddy. Phase-type distributions for Failure Time. *Mathematical computer Modelling*, 22, **10-12**, 63-70, 1995
12. S.I. McClean, P. Millard. Modelling In-Patient Bed Usage Behaviour in a Department of Geriatric Medicine *Methods of Information in Medicine*, 32, 79-81, 1993.
13. A. Clarke. Readmission to Hospital: a measure of quality or outcome? *The international journal of healthcare improvement.* 13, 10-11,2004.
14. M. J. Faddy. Phase-type distributions for Failure Time. *Mathematical computer Modelling*, 22, 247-255,1994.
15. M. J. Faddy. Examples of fitting structured phase-type distributions. *Applied Stochastic models and data analysis.*247-255, 1994.
16. L. Fallowfield. What is quality of life? *Health economics*,2009.
17. E. B. Keeler, L. V. Rubenstein, K.L.Kahn, D. Draper, E.R. Harrison, M.J. McGinty, W.H. Rogers, R.H. Brook. Hospital Characteristics and Quality of Care. *The Journal of the American Medical Associatio.* 268,**13**, 1709-1714, 1992.
18. T. P. Meehan, M.J. Fine, H.M. Krumholz, J.D. Scinto, D.H. Galusha, J.T. Mockalis, G.F. Weber, M.K. petrillo, P.M. Houck, J.M. Fine. Quality of care, Process, and Outcomes in Elderly Patients With Pneumonia. *The Journal of the American Medical Association.* 278, **23**, 2080-2084,1997.
19. J. Needleman, P. Buerhaus, S. Mattke, M. Stewart. Nurse-Staffing levels and the Quality of Care in Hospitals. *The New England Journal of Medicine.* 346, **22**, 2002.
20. K. Sutherland, N. Coyle. Quality in Healthcare in England, Wales, Scotland, Northern Ireland: an intra-UK chartbook. *The Health Foundation*, 2008.
21. D. Blumenthal. Quality of Health Care, Part 2: Measuring Quality of Care. *The New England Journal of Medicine.*, 1996.
22. S.I. McClean, P. Millard. Patterns of Length of Stay after Admission in Geriatric Medicine: An Event History Approach. *The Statistician*, 263-274, 1993.
23. J.A. Bilmes. A Gentle Tutorial of the EM Algorithm and its Applications to Parameter Estimation for Gaussian Mixture and Hidden Markov Models. *International Computer Science Institute.* Berkeley, 1998.
24. P.H. Millard. Throughput in a department of geriatric medicine: a problem of time, space and behaviour. *Health trends.* 24, 20-24, 1991.

Discrete observation of a continuous time semi Markov model for HIV control

Zacharias Kyritsis[1] and Aleka Papadopoulou[2]

1.Department of Mathematics, Aristotle University of Thessaloniki, Greece (Email: zkyritsi@math.auth.gr)
2.Department of Mathematics, Aristotle University of Thessaloniki, Greece (Email: apapado@math.auth.gr)

The aim of the present paper is to review a continuous time semi Markov model for HIV control and to apply an algorithm for data simulation analysis which we run to provide the data for transitions and the sojourn times of the corresponding visited states. After the simulation process three different models are developed and validated for the discrete observation of the simulated continuous process and an estimation method is applied to get the respective distributions. Finally, the above results are illustrated numerically with synthesized data.
Keywords: health care, semi Markov process, HIV

1 Introduction

The definition of the non homogeneous semi Markov process is provided in Iosifescu-Manu [10] for the continuous time case, in Janssen and De Dominics [12] for the discrete case and in De Dominics and Manca [7]. Later on the definition of a non homogeneous semi Markov system in discrete time is provided in Vassiliou and Papadopoulou [27] and the asymptotic behavior of the same model is studied in Papadopoulou and Vassiliou [24]. Important theoretical results and applications for semi Markov models can be found in work of Cinlar [4], [5], [6], Teugels [26], Keilson [13], [14], McLean and Neuts [21], Howard [9], McClean [17], [18], [19], [20], Limnios et al [15] and in Janssen [11].

In the present, we study the discrete observation of a continuous time semi Markov model for HIV control. In section 2, first we describe the semi Markov model for HIV control, review the continuous time case and then we provide the technique for the discrete observation of the reviewed model. In section 3, the technique described in Section 2 is illustrated with synthesized data derived by a simulation process. Last, conclusions from the previous results are provided.

2 Discrete observation of a continuous time semi Markov model for HIV control

The process of infection by HIV is characterized by two fundamental markers. The first is the viral load (VL) and the second CD4 lymphocyte. Hence, the history of the disease can be considered as a series of stages through which a patient progresses. The first stage is called primary infection. And the corresponding symptoms vary to duration that is twenty eight days in average

New Trends in Stochastic Modeling and Data Analysis (*pp.* 91-101)
Raimondo Manca – Sally McClean – Christos H Skiadas (Eds)

and at least one week. At this stage there are no specific symptoms and often they are not recognized as signs of HIV infection. Even if a patient goes to a doctor or a hospital, he might be misdiagnosed. The second stage is called clinically asymptomatic stage lasts for an average of ten years and, as its name suggests, that is free from major symptoms. The HIV antibodies are detectable in the blood, so antibody tests will show a positive result. On the third stage called symptomatic HIV the lymph nodes and tissues are damaged because of the years of activity, HIV mutates and becomes more pathogenic, leading to more T helper cell destruction and the body fails to keep up with replacing the lost T helper cells. Antiretroviral treatment is usually started once an individual's CD4 index falls to a low level which is an indication that the immune system is deteriorating. Finally, on the fourth stage called progression for AIDS as the immune system becomes more and more damaged the individual may develop increasingly severe opportunistic infections and cancers, leading eventually to an AIDS diagnosis.

Using these markers and the above mentioned four stages we can describe the progress of HIV by a semi Markov model considering four health states (Tan [25]) as follows:

Primary infection → First stage: VL≤400 and CD4≤200
Asymptomatic stage → Second stage: VL≤400 and CD4>200
Symptomatic HIV → Third stage: VL>400 and CD4>200
Progression for AIDS → Fourth stage: VL>400 and CD4≤200

From the above, we can consider a non homogeneous semi Markov process with discrete and finite state space symbolized by S={1, 2, 3, 4}. The continuous time case for non homogeneous semi Markov systems is studied in Papadopoulou and Vassiliou [23]. The transition probability matrix of the embedded Markov chain is defined by $\mathbf{P}(s,t)=\{p_{ij}(s,t)\}_{i,j\in S}$, where $p_{ij}(s,t)$=prob{a patient selects state j for its next transition during (s,t) / entered state i at time s}and the holding time mass function matrix for the semi Markov process is defined by $\mathbf{H}(m)=\{h_{ij}(m)\}_{i,j\in S}$ where $h_{ij}(m)$=prob{a patient which entered state i at its last transition to hold for m time in state i before making its next transition given that state j has been selected}.

Also, we define by :

$$^{\leq}w_i(s,t) = \text{prob}\{\text{ a patient which entered state i at time s holds for time } \leq t \text{ in i before making its next transition }\} = \sum_{k=1}^{4}\int_0^t p_{ik}(s,s+x)\,h_{ik}(x)dx$$

Also, we can define:

$$\varphi_{ij}(s,t) = \text{prob}\{\text{a patient which entered state i at time s is in state j at time } s+t\} = \delta_{ij}\,{}^{>}w_i(s,t) + \sum_{k=1}^{4}\int_0^t p_{ik}(s,s+x)\,h_{ik}(x)\varphi_{kj}(s+x,t-x)dx \quad (1)$$

and if we define $c_{ij}(s,x)=p_{ij}(s,s+x)h_{ij}(x)$

$$\varphi_{ij}(s,t) = \delta_{ij} {}^{>}w_i(s,t) + \sum_{k=1}^{4} \int_0^t c_{ik}(s,x)\varphi_{kj}(s+x, t-x)\, dx \qquad (2)$$

where:

$$\delta_{\iota j} = \begin{cases} 1, & if\ i = j \\ 0, & otherwise \end{cases}$$

The above equation can be written in matrices form as follows:

$$\mathbf{\Phi}(s,t) = {}^{>}\mathbf{W}(s,t) + \int_0^t \mathbf{C}(s,x)\, \mathbf{\Phi}(s+x, t-x)dx \qquad (3)$$

where $\mathbf{C}(s, x)=\mathbf{P}(s, s+x)\Diamond\mathbf{H}(x)$ is the Hadamard product of the two matrices. The initial condition for equation (3) is $\mathbf{\Phi}(s,0)=\mathbf{I}$.

The matrix $\mathbf{\Phi}(s,t)$ defines the interval transition probabilities for the patients of the non homogeneous semi Markov chain which is imbedded in our system. This semi Markov chain is fully described by the probability $p_{ij}(s,t)$ and the probability density functions of the holding times $h_{ij}(x)$ as it is shown by equation (1). So, we have a non homogeneous semi Markov system in which the individual transitions take place according to a non homogeneous semi Marko chain. Using probabilistic argument it can be proved that the closed analytic form of probabilities $\varphi_{ij}(s,t)$ is:

$$\mathbf{\Phi}(s,t) = {}^{>}\mathbf{W}(s,t) + \int_0^t \mathbf{C}(s,x_1)\{{}^{>}\mathbf{W}(s+x_1, t-x_1) + \mathbf{C}(s+x_1, t-x_1)\}dx_1$$
$$+ \sum_{k\geq 2} \int_0^t \int_0^{t-x_1} \int_0^{t-x_1-x_2} \dots \int_0^{t-x_1-\cdots-x_{k-1}} \mathbf{C}(s,x_1)\mathbf{C}(s+x_1,x_2) \dots \mathbf{C}(s+\cdots+$$
$$x_{k-1}, x_k)\{{}^{>}\mathbf{W}(s+\cdots+x_k, t-x_1-\cdots x_k) + \mathbf{C}(s+\cdots+x_k, t-x_1-\cdots-x_k)\}$$
$$dx_k dx_{k-1} \dots dx_2 dx_1 \qquad (4)$$

We assume that our system is a closed one i.e. the total patients' population is constant at any time. The previous hypothesis is not in conflict with real systems because the patients' population under treatment, in that kind of chronic diseases, is usually constant. Thus, the states sizes of the system at any time is described by the vector $\mathbf{N}(t)=[N_1(t), N_2(t), N_3(t), N_4(t)]$ where $N_i(t)$ is the expected number of patients in the i-th state at time t. It can be proved that:

$$N_i(t) = \sum_{j=1}^{4} N_j(0)\varphi_{ij}(0,t). \qquad (5)$$

Equation (5) in matrix form is as follows:

$$\mathbf{N}(t)=\mathbf{N}(0)\mathbf{\Phi}(0,t) \qquad (6)$$

where $\mathbf{N}(0)$ is the initial population structure.

Relations (5) and (6) provide the expected population structure as a function of the basic sequences of the system.

The corresponding discrete non homogeneous semi Markov model was defined in Vassiliou and Papadopoulou [27]. The transition probability matrix of the embedded Markov chain is defined by $\mathbf{P}(t)=\{p_{ij}(t)\}_{i,j\in S}$, where $p_{ij}(t)$=prob{a patient which entered in state i at time t to move in the state j at its next transition} and the holding time mass function matrix for the semi Markov chain is defined by $\mathbf{H}(m)=\{h_{ij}(m)\}_{i,j\in S}$ where $h_{ij}(m)$=prob{a patient which entered state i at its last transition to hold for m time in state i before making its next transition given that state j has been selected}.
Also, we define as:

$$w_i(t,m) = \text{prob\{a patient which entered state i at time t to stay m time units in state i before its next transition\}.}$$

It's also proved that:

$$w_i(t,m) = \sum_{j=1}^{4} p_{ij}(t)h_{ij}(m) \quad \text{for } i = 1,2,3,4 \text{ and } t, m = 0, 1, 2, \ldots$$

and $w_i(0,t)=0$ for every i, t.
Moreover, let us define:

$$\varphi_{ij}(t,m) = \text{prob \{ a patient which entered state i at time t to be in state j after m steps\}.}$$

It's also proved that:

$$\varphi_{ij}(t,m) = \delta_{ij} \sum_{s=m+1}^{\infty} w_i(s,t) + \sum_{k=1}^{4}\sum_{s=1}^{m} p_{ik}(t)h_{ik}(s)\varphi_{kj}(t+s,m-s) \qquad (7)$$

for i, j=1, 2, 3, 4 and t, m =0, 1, 2, ...
Also, we define by $^{>}\mathbf{W}(t,m)$ the 4×4 matrix which has zeros everywhere apart from the diagonal which has in position i the element:

$$\sum_{s=m+1}^{\infty} w_i(t,s) = 1 - \sum_{s=1}^{m} w_i(t,s).$$

Then the equation (7) can be written in matrices as follows:

$$\mathbf{\Phi}(t,s) = {}^{>}\mathbf{W}(t,s) + \sum_{s=1}^{m} [\mathbf{P}(t) \lozenge \mathbf{H}(s)]\mathbf{\Phi}(t+s, m-s). \qquad (8)$$

Obviously $\mathbf{\Phi}(t,0)=\mathbf{I}$.

The corresponding states' sizes description in the discrete time case is given by the vector $\mathbf{N}(t)=[N_1(t), N_2(t), N_3(t), N_4(t)]$ where $N_i(t)$ is the expected number of patients in the i-th state at time t, where

$$N_i(t) = \sum_{j=1}^{4} N_j(0)\varphi_{ij}(0,t). \qquad (9)$$

The respective matrix form is:

$$\mathbf{N}(t)=\mathbf{N}(0)\mathbf{\Phi}(0,t) \qquad (10)$$

where $\mathbf{N}(0)$is the initial population structure.

The choice, in practice, between the discrete and continuous time versions of a model is partly a matter of realism and partly one of convenience. On grounds

of realism, for example one would usually want to model the movement of people between occupations or regions in continuous time, but in practice the computational advantages of treating time as discrete have often led to the choice of a discrete time model (Bartholomew [2], page 85).

There are two main reasons that we can observe a continuous process in two or more specified intervals. The first reason is the observed computational advance when we treat the time as a discrete variable. The second is that practical difficulties often occur in considering continuous time models, which arise from the fact that is rarely possible to observe continuous data (Bartholomew [2]).

In what follows, we will describe the technique applied for the discrete observation of the continuous time model presented at first. A discrete model can be developed by discretization per unit time of the transition probability and the holding time mass function matrix. The discretization per unit time of the transition probability matrix is based on the relationship :

$$\mathbf{P}(t) =) \int_{bt}^{b(t+1)} \mathbf{P_j}(u)du \qquad (11)$$

where b is the defined unit and $\mathbf{P_j}(u)$ is the transition probability matrix of the corresponding jump process.

In the following the above relationship is applied to the data of Mathieu et al [16] where $\mathbf{P_j}(u)$ is of linear form and for the cases i) b=1 and ii) b=0.5. The corresponding graphs are presented in Figures 2.1 and 2.2.

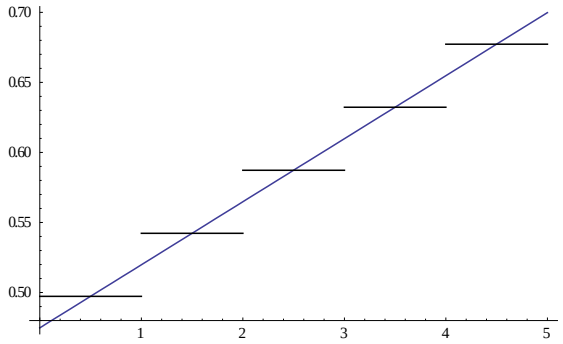

Figure 2.1: b=1

Concerning the holding time distributions, there are several ways to derive the corresponding discrete lifetime distribution from a continuous one. Two of the most usually applied are: a) consider a characteristic property of a continuous distribution and then build the similar property in discrete time and b) consider the discrete holding time as the integer part of the continuous holding time (Bracquemond and Gaudoin [3]).

By applying the second technique and if we consider the continuous time random variable T which describes the holding time in a state we can define the corresponding discrete random variable K and for time unit b=1 as:

$$K=[T]+1. \qquad (12)$$

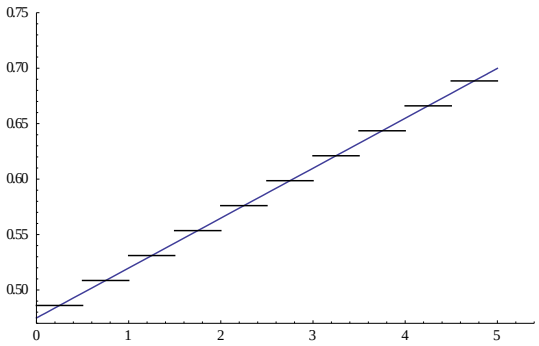

Figure 2.2: b=0.5

Also, the equivalent random variable L for time unit b=0.5 is :

$$L=[2T]+1 . \quad (13)$$

Let that F_K, R_K and F_T, R_T denote the cumulative distribution and reliability functions of the random variables K and T respectively. Then, the relationship between the probability function of K and the cummulative distribution function of T is:

$$\begin{aligned} p(k) &= Pr\{K = k\} = Pr\{k-1 \le T < k\} \\ &= F_T(k) - F_T(k-1), \quad \forall k \in N \end{aligned} \quad (14)$$

Furthermore:

$$F_K(k) = Pr\{K \le k\} = Pr\{[T]+1 \le k\} = Pr\{T < k\} = F_T(k) \quad (15)$$

and

$$R_K(k) = R_T(k) \quad (16)$$

Finally and according to the previous, we discretize the holding times using the variables K and L and then, we can estimate the parameters of the holding time distributions to the states.

3 Illustration

In the present section, the discrete observation technique of a continuous semi Markov model is illustrated numerically with data from an HIV patients' population.

Firstly, a Monte Carlo simulation method is performed by using the data concerning the transition probabilities and the conditional distributions of the holding times as assessed by Mathieu et al [18]. The purpose of the simulation is to obtain the basic characteristics of the process in continuous time. The simulation is performed in ARENA 13.5 environment.

So, we consider a sampling path of a Semi-Markov chain over a period of time [0,C] where are observed M patients. Each patient starts the immunological and virological trajectory in any state, which is revealed by the first measurement at time t=0 and we assume that the k-th patient changes state n_k times in the instants $s_{k,1}<s_{k,2,}<\ldots<s_{k,n}<\ldots$ and occupies states $J_{k,1}<J_{k,2}<\ldots<J_{k,n}<\ldots$ and $J_{p,n} \neq J_{p,n+1}$ for every $n \in N$. In fact, such a path is a sequence H(C) of visited states and sojourn times :

$$H(C) = \{X_0, J_0, X_1, \ldots, J_{N(C)-1}, X_{N(C)}, J_{N(C)}\}$$

The above process is simulated by an algorithm of five steps as follows:

1. Set k=0, S_o=0 and sample J_0 from the initial distribution
2. Sample the random variable J~ $p(J_k,.)$ and set J_{k+1}=J
3. Sample the random variable X~ $H_{J_kJ_{k+1}}(.)$
4. Set S_{k+1}= S_k + X
5. If S_{k+1}>M then end else set k=k+1 and continue to step 2

Thus, we can get the trajectory of a patient and if we do the same repeatedly for 1000 times we can get the trajectories of 1000 patients. The results of the simulation are presented in Table 1.

Table 1: Results of Simulation

Transitions	Number of transitions	Mean sojourn time (years)
1→2	934	1,59
1→3	195	1,77
1→4	473	1,69
2→1	807	0,15
2→3	2842	0,87
3→2	2759	1,08
3→4	506	0,8
4→1	358	1,16
4→2	164	1,58
4→3	469	1,74
Total	9507	

Using the results derived from the simulation we developed three discrete time models for HIV and we compared them with the continuous model. The transition probabilities and the holding times are derived by applying equations (11)-(14). We then estimated the parameters of the holding time distributions for the health states. For the holding times we used the type I discrete Weibull distribution (Nakagawa and Osaki [22]) and the geometric distribution. In the first and second model, the method of proportions (Ali Khan et al [1]) was used in order to estimate the parameters of the type I discrete Weibull distribution. In the third model we used the method of maximum likelihood to estimate the parameters of the geometric distribution. Finally, we evaluated the numerical results for the survival functions of every state and the population structures derived from the three models in comparison to the continuous one. The results are presented in Figures 3.1, 3.2, 3.3, 3.4, 3.5, 3.6, 3.7 and 3.8.

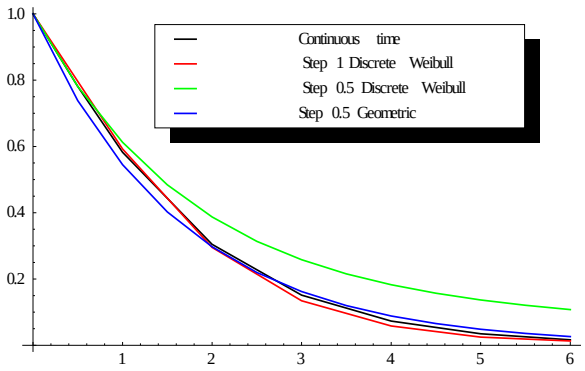

Figure 3.1 Survival function for state 1

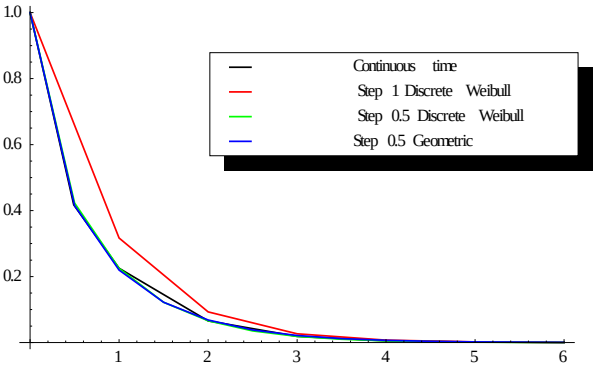

Figure 3.2 Survival function for state 2

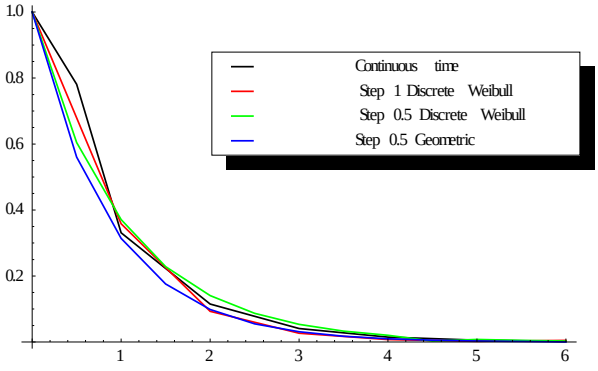

Figure 3.3. Survival function for state 3

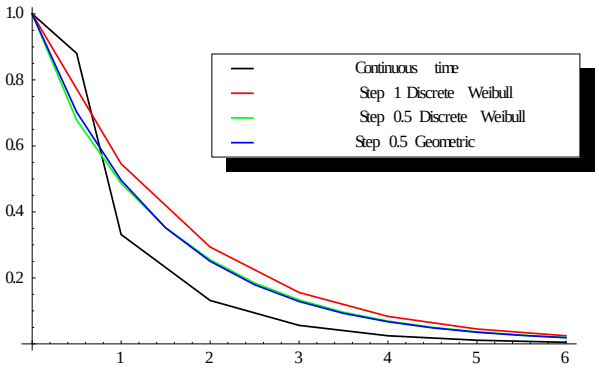

Figure 3.4 Survival function for state 4

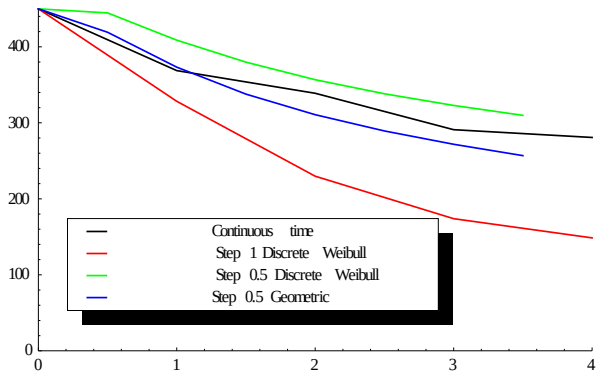

Figure 3.5 Population of state 1

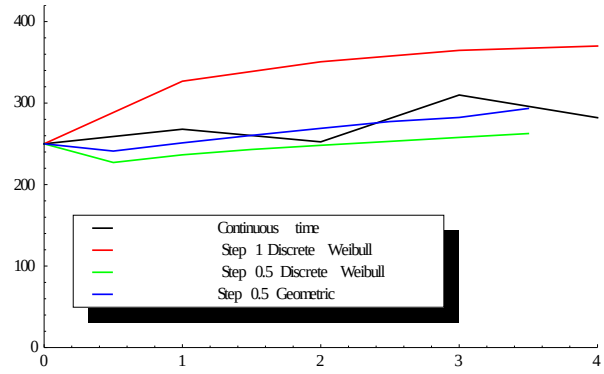

Figure 3.6 Population of state 2

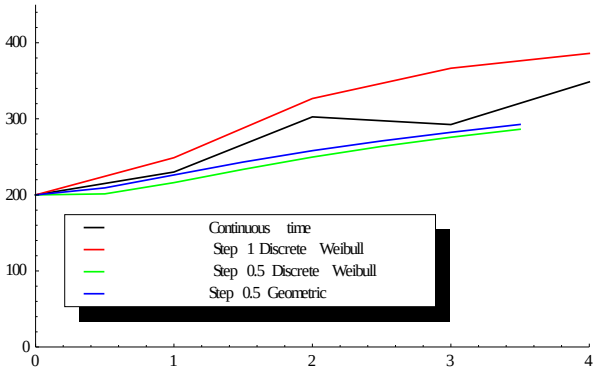

Figure 3.7 Population of state 3

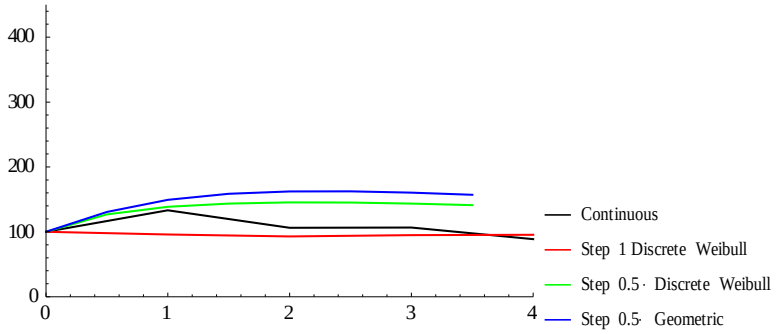

Figure 3.8 Population of state 4

Conclusions

In the present paper we reviewed a continuous time semi Markov model for HIV control and we provided a technique for the discrete observation of the continuous model. This technique was applied to the reviewed model. For this purpose, we used a simulation process to illustrate the discrete observation technique with synthesized data. Finally, we developed three discrete time models for HIV and we compared them with the continuous model. The derived results demonstrate the potential of the applied technique to provide a tool for discrete observation of continuous models.

References

1. Ali Khan, M., Khalique, A., & Abouammoh, A. (1989). On estimating parameters in a discrete Weibull distribution. *IEEE Transactions on Reliability, Vol. 38, No. 3*, 348 -350.
2. Bartholomew, D.J. (1982). Stochastic Models for Social Process, 3rd edition, Wiley. Chichester.
3. Bracquemond, C., & Gaudoin, O. (2003). A survey on discrete lifetime distributions. *International Journal of Reliability, Quality and Safety Engineering ,10(1)*, 69-98.

4. Cinlar, E. (1969). Markov renewal theory. Adv. Appl. Prob. 1:123-187.
5. Cinlar, E. (1975a). Markov renewal theory: A survey. Manage. Sci, 21:727-752
6. Cinlar, E. (1975b). Introduction to Stochastic Processes. Englewood Cliffs, NJ: Prentice Hall.
7. De Dominics, R., Manca, R. (1985). Some new results on the transient behavior of semi Markov reward processes. Methods Oper. Res. Comput. 13:823-838.
8. Foucher, Y., Mathieu, E., Sain-Pierre, P., Durand, J., & Daures, J. (2005). A Semi-Markov Model Based on Generalized Weibull Distribution with an illustration for HIV Disease. Biometrical Journal,vol.47 , pages 825-833.
9. Howard, R. (1972). Dynamic Probabilistic Systems, vol. II. D Wiley.
10. Iosifescu-Manu, A. (1972). Non homogeneous semi Markov processes Studiisi Cercetuari Mathematice 24:529-533.
11. Janssen, J. (1986), Semi Markov Models: Theory and Applications. Janssen, J., ed. New York: Plenum Press.
12. Janssen, J., De Dominics, R. (1984). Finite non homogeneous semi Markov processes: Theoretical and computational aspects. Insurance: Math. Econ. 3:157- 165.
13. Keilson, J. (1969). On the matrix renewal function for Markov renewal processes. Ann. Math. Statist., 40:1901-107.
14. Keilson, J. (1971). A process with chain dependent growth rate. Markov Part II: The ruin and ergodic problems. Adv. Appl. Prob. 3:315-338.
15. Limnios, N., & Oprisan, G. (1999). *'Semi Markov Processes and Reliability.* Boston: Birkhauser.
16. Mathieu, E., Loup, P., Dellamonica, P., & Duares, J. (2006). 'Markov modeling of immunogical and virological states in HIV-1 infected patients. *Biometrical Journal,vol.48* , pages. 834-846.
17. McCLean, S.I. (1976). The two stage model for personnel behavior. J.R.S.S. A1399:205-217
18. McCLean, S.I. (1978). Continuous time stochastic models for a multigrade population. J. Appl. Prob. 15: 26-32
19. McCLean, S.I. (1980). A semi-Markovian model for a multigrade population . J. Appl. Prob. 17:846-852
20. McCLean, S.I. (1986). Semi-Markov models for manpower planning. In: Semi-Markov Models: Theory and applications. New York: Plenum Press, 283-300.
21. McLean, R.A., Neuts, M.F. (1967). The integral of a step function defined on a semi Markov process. Siam. J. Appl. Math. 15:726-737.
22. Nakagawa, T., & Osaki, S. (1975). The discrete Weibull distribution. *IEEE* Transactions on Reliability, Vol. 24, No.5 , pages 300-301.
23. Papadopoulou, A., & Vassiliou, P.-C. (1999). Continuous time non homogenous Semi Markov systems. Semi Markov Models and Applications, J.Janssen & N.Limnios (Eds), Kluwer Academic Publishers, Dordrecht , 15 , pages 241-251.
24. Papadopoulou, A. A., Vassiliou, P.-C. G. (1994). Asymptotic behavior of non homogeneous semi-Markov systems. Linear Algebra Appl. 210:153–198.
25. Tan, W.Y. (2000) Stochastic modeling of AIDS Epidemiology and HIV Pathogenesis. World Scientific: Singapore
26. Teugels, J.L. (1976). A bibliography on semi-Markov processes. J. Comp. Appl. Math. 2:125-144
27. Vassiliou. P.-C., Papadopoulou A. (1992). Non homogeneous semi Markov systems and maintainability of the state sizes. Journal of Applied Probability, 29, pages 519-534.

Detecting regime changes in Markov models

Jesús E. García[1] and V. A. González-López[2]

[1] Department of Statistics, University of Campinas, Brazil
(e-mail: jg@ime.unicamp.br)
[2] Department of Statistics, University of Campinas, Brazil
(e-mail: veronica@ime.unicamp.br)

Abstract. Let C be a data collection, indexed by time. $C = \{D(t_1), ..., D(t_n)\}$, where $D(t_i)$ was collected at time $t_i, t_i \leq t_j$ if $i \leq j$. Also, each $D(t_i)$ follows a Markovian model with finite alphabet A, denoted by $M(t_i)$. We device a consistent procedure to detect changes in the model at time t_{i_0} that allows to decide if $D(t_{i_0})$ and $D(t_{i_0-1})$ are coming from the same Markovian source. The procedure is based on the equivalence relationship introduced by the Minimal Markov Models that enable to associate to each Markovian model a minimal number of parameters enough to describe a Markovian source. Under the possibility of regime change, we can have situations in which $D(t_1), ..., D(t_{i_0-1})$ are coming from a Markovian model $M(t_{i_0-1})$ different to the Markovian model $M(t_{i_0})$ appropriated for $D(t_{i_0})$. We apply the procedure to detect prosodic changes from classical to modern European Portuguese In this context, each $D(t_i)$ is a written text in European Portuguese and t_i is the author's date of birth from 16th century to the 19th century. We detect two main change points, the first one at the turn of the 16th century to the 17th century. The second one, in the second half of the 18th century that spreads to the end of the century.
Keywords: Minimal Markov models, Model selection, Bayesian information criterion, Historical linguistics.

1 Introduction

Our goal in practical terms is to explore whether using Markov structures can be extracted rhythmic properties of texts written in European Portuguese. Taking in consideration that rhythm is a consequence of several characteristics, like number of syllables in the words, position in the word of the stressed syllable, simple and complex syllabic structure, etc., it is possible to look for temporal changes in the rhythm, using written texts (see Frota *et al.* [1], Galves *et al.* [2], Galves and Faria [3]). We also want to demonstrate that such models may be useful for the study of the prosodic changes in texts sorted by chronological time.
In Frota *et al.* [1] it is proved that in fact the European Portuguese has undergone a significant alteration, perceived from the 16th century to the 17th. This finding is consistent with the conjecture that the Portuguese is losing some of its features of "romance language" with the passing of the centuries. In Frota

New Trends in Stochastic Modeling and Data Analysis (pp. 103-109)
Raimondo Manca - Sally McClean - Christos H Skiadas (Eds)

et al. [1] significant changes are verified on two phonological features, the size of the words and the position of the stress. Thus, from the 16th century to the centuries 17th, 18th and 19th, Frota *et al.* [1] shows: (a) a pattern of increase in the proportion of monosyllables (in the universe defined by words of at most two syllables) and (b) a pattern of increase in the proportion of words with stress on the last syllable (in the universe defined by words with stress positioned in the penultimate or in the last syllable).
This paper aims to investigate the problem by incorporating the Markovian structure inherent to written texts. Supported by a model of this nature we can leverage all the available information about the data. Given that the model used in Frota *et al.* [1], based on the beta-binomial distribution, requires preprocessing of the data to obtain the independence between the realizations (words in that case), interfering with the maintenance of the rhythm and at the same time produces a reduction of the sample size of the written texts. So, (i) the number of syllables in each word and (ii) the placement of stress, will be investigated under a richest model that allows to incorporate a dependence structure between words through each text and enables consider jointly, the features (i) and (ii). To achieve a more comprehensive view of linguistic phenomena studied at present, it should be noted that linguistic structures can be studied in their formats "spoken language" and "written language". The processing and types of statistical models are completely defined by the differentiated nature of the data. For example, for acoustic signal processing see García *et al.* [5] and for recent research about the statistical modeling see García *et al.* [7], García *et al.* [8] and García *et al.* [9].
Using the linguistic problem as a motivating basis, we introduce in this paper a consistent method for to find changes of regime in Markov processes. The method takes advantage of the conception of minimal Markov models by García and González-López [6] and the decision rule was formulated using the Bayesian Information Criterion (BIC). The minimal Markov model's estimation can be consistently performed through the BIC, see for details García and González-López [6]. Also for related topics about those models, see García *et al.* [7], García *et al.* [9] and Galves *et al.* [4]. In this paper, the minimal Markov models estimated through the BIC allow to define the rule for deciding whether or not there is a change of regime in the Markov process.

2 Historical data

Tycho Brahe corpus is an annotated historical corpus, freely accessible at Galves and Faria [3]. This corpus uses the chronological criterion of the author's birthdate to assign a time for written text. The subset of historical written texts included in this study, listed in Table 1 is composed by 17 texts from 15 authors, coming from four genres. In Table 1 we report also the number of orthographic words (ow) by text.

The data collection $C = \{D_{t_1}, ..., D_{t_n}\}$ is now given by the written texts listed in Table 1.

D_t	Gândavo	Pinto	Sousa	Brandão	Vieira	Vieira
t	1502	1510	1556	1584	1608	1608
Type	N	N	N	N	L	S
ow	22850	39941	50218	43192	47888	49275
D_t	Chagas	Bernardes	Oliveira	Aires	Costa	Alorna
t	1631	1644	1702	1705	1714	1750
Type	P	P	L	P	L	L
ow	48670	49479	16629	56055	24538	43318
D_t	Garrett	Garrett	Fronteira	Camilo	Ortigão	
t	1799	1799	1802	1826	1836	
Type	L	N	N	N	L	
ow	30070	45800	54826	20142	27420	

Table 1. Subset of Tycho Brahe corpus used in this study, coming from four genres: narrative (N), letters (L), philosophical (P) and sermons (S).

2.1 Encoding texts

Each written text was processed with a slightly modified version of the perl-code "silaba" that can be freely downloaded for academic purposes at `www.ime.usp.br/ tycho/prosody/vlmc/tools/sil4.pl` . The software was used to extract two components of each orthographic word, denoted by (i, j), where i is the total number of syllables that make up the word, $i = 1, 2, ..., 8$ and j indicates the syllable in which is registered the stress in the word, $j = 0, 1, 2, .., 8$. Where, $j = 0$ means no stress in the word and this just happens in orthographic words with one syllable. The period (final of sentence) was codified as $(0, 0)$.
The alphabet was defined as exposed in Table 2. Note that the set of words represented by $(i, 0), i \geq 2$ corresponds to the empty set.

orthographic word	element alphabet
$(0, 0)$	a
$(1, 0)$	b
$(1, 1)$	c
$(2, 1)$	d
$(2, 2)$	e
$(i, 1)$, $i \geq 3$	f
$(i, 2)$, $i \geq 3$	g
(i, j), $i, j \geq 3$	h

Table 2. Definition of the alphabet A.

3 The Markovian model

The minimal Markov models applied in this paper, were introduced in García and González-López [6]. Those models are generalizations of Variable Length Markov Chains models, used to discover the differences between branches of the Portuguese in Galves *et al.* [4].
Let (X_t) be a discrete time (order $M < \infty$) Markov chain on a finite alphabet A. Let us call $\mathcal{S} = A^M$ the state space. Denote the string $a_m a_{m+1} \dots a_n$ by a_m^n, where $a_i \in A$, $m \leq i \leq n$.
For each $a \in A$ and $s \in \mathcal{S}$, $P(a|s) = \text{Prob}(X_t = a | X_{t-M}^{t-1} = s)$.
Let $\mathcal{L} = \{L_1, L_2, \dots, L_K\}$ be a partition of $\mathcal{S}$, for $a \in A$, $L \in \mathcal{L}$, $P(L, a) = \sum_{s \in L} \text{Prob}(X_{t-M}^{t-1} = s, X_t = a)$, $P(L) = \sum_{s \in L} \text{Prob}(X_{t-M}^{t-1} = s)$ and $P(a|L) = \frac{P(L,a)}{P(L)}$ with $P(L) > 0$.

Definition 1. Let (X_t) be a discrete time order M Markov chain on a finite alphabet A. We will say that $s, r \in \mathcal{S}$ are equivalent (denoted by $s \sim_p r$) if $P(a|s) = P(a|r)$ $\forall a \in A$. For any $s \in \mathcal{S}$, the equivalence class of s is given by $[s] = \{r \in \mathcal{S} | r \sim_p s\}$.

The previous definition allows to define a Markov chain with a "minimal partition", that is the one which respects the equivalence relationship.

Definition 2. let (X_t) be a discrete time, order M Markov chain on A and let $\mathcal{L} = \{L_1, L_2, \dots, L_K\}$ be a partition of $\mathcal{S}$. We will say that (X_t) is a Markov chain with partition $\mathcal{L}$, if this partition is the one defined by the equivalence relationship $\sim_p$ introduced by definition 1.

In a given sample x_1^n, coming from the stochastic process, we denote the number of occurrences of elements into L followed by a for,

$$N_n^{\mathcal{L}}(L, a) = \sum_{s \in L} N_n(s, a), \ L \in \mathcal{L},$$

where the number of occurrences of s in the sample x_1^n is denoted by $N_n(s)$ and the number of occurrences of s followed by a in the sample x_1^n is denoted by $N_n(s, a)$. The accumulated number of $N_n(s)$ for s in L is denoted by,

$$N_n^{\mathcal{L}}(L) = \sum_{s \in L} N_n(s), \ L \in \mathcal{L}.$$

The model, in this context given by the "minimal partition $\mathcal{L}$", can be selected consistently, using the Bayesian Information Criterion. This means, the best partition is the one that maximizes

$$\text{BIC}(x_1^n, \mathcal{L}) = \sum_{a \in A, L \in \mathcal{L}} N_n^{\mathcal{L}}(L, a) \ln \Big(\frac{N_n^{\mathcal{L}}(L, a)}{N_n^{\mathcal{L}}(L)} \Big) - \frac{(|A| - 1)|\mathcal{L}|}{2} \ln(n),$$

over the space of partitions.

3.1 Criterion of remoteness between processes

The BIC allows to compare datasets as we will show in the next result. If two variables X and Y have the same distribution we will assume the next notation $X =^d Y$. Also, if $(x)_{i=1}^n$ and $(y)_{i=1}^m$ are samples of X and Y respectively, we will denote by $(x)_{i=1}^n \perp (y)_{i=1}^m$ the independence between the samples.

Theorem 1. *Given the stochastic process X_{t_i} of order $M < \infty$ with sample $(x_{t_i})_1^{n_i}$ of size $n_i, i = 1, 2$, such that $(x_{t_1})_1^{n_1} \perp (x_{t_2})_1^{n_2}$. $X_{t_1} \neq^d X_{t_2}$ if, and only if*

$$BIC\Big((x_{t_1})_1^{n_1}, (x_{t_2})_1^{n_2}, \mathcal{L}\Big) < \sum_{k=1,2} BIC((x_{t_k})_1^{n_k}, \mathcal{L}^k)$$

with

$$BIC\Big((x_{t_1})_1^{n_1}, (x_{t_2})_1^{n_2}, \mathcal{L}\Big) = \sum_{a\in A, L\in\mathcal{L}} N^{\mathcal{L}}_{n_1+n_2}(L,a) \ln\Big(\frac{N^{\mathcal{L}}_{n_1+n_2}(L,a)}{N^{\mathcal{L}}_{n_1+n_2}(L)}\Big) - \frac{(|A|-1)}{2}|\mathcal{L}| \ln(n_1+n_2).$$

Corollary 1. *Under the assumptions of Theorem 1, $d_{1,2} > 1$, with*

$$d_{1,2} = \frac{2\sum_{a\in A} B(\mathcal{L}^1, n_1, a) + B(\mathcal{L}^2, n_2, a) - B(\mathcal{L}, n_1+n_2, a)}{(|A|-1)\left\{|\mathcal{L}^1| \ln(n_1) + |\mathcal{L}^2| \ln(n_2) - |\mathcal{L}| \ln(n_1+n_2)\right\}}$$

and $B(\mathcal{L}, n, a) = \sum_{L\in\mathcal{L}} N_n^{\mathcal{L}}(L,a) \ln\Big(\frac{N_n^{\mathcal{L}}(L,a)}{N_n^{\mathcal{L}}(L)}\Big)$.

Given the dataset D_{t_i} consider the stochastic process X_{t_i} of order $M < \infty$ generator of D_{t_i}, with sample $(x_{t_i})_1^{n_i}$ of size n_i.
Following the codification given by Table 2, each sample will be composed by the concatenation of symbols from $A = \{a, b, c, d, e, f, g, h\}$. Based on previous works, that investigate similar data (see, for example Galves *et al.* [4]) the value of M considered here was 4.
Assuming that the data collection is made up of independent texts (which is the case treated here, as each text is a complete work in itself), under the assumption:

$$X_{t_i} =^d X_{t_j} \text{ and } (x_{t_i})_1^{n_i} \perp (x_{t_j})_1^{n_j}, i \neq j$$

$$\text{BIC}\Big((x_{t_i})_1^{n_i}, (x_{t_j})_1^{n_j}, \mathcal{L}\Big) > \sum_{k=i,j} \text{BIC}((x_{t_k})_1^{n_k}, \mathcal{L}^k)$$

and

$$d_{i,j} < 1.$$

That means that both: D_{t_i} and D_{t_j} come from the same model, given by the minimal partition $\mathcal{L}$. In another case D_{t_i} and D_{t_j} come from different models, $\mathcal{L}^i$ and $\mathcal{L}^j$ respectively.
In the next section we use the values of $d_{i,j}$ to measure the distance between the models associated with written texts. Thus, texts that are identified with the same model show no change points in the timeline. When $d_{i,j}$ exceeds the value 1, a change point is identified.

4 Results and Conclusions

Each horizontal line drawn in Figure 1 represents the text written by a particular author. On the line of each text is shown the value of d computed for two consecutive texts in time. Thus, for example, the text titled as "Gândavo (1502)" was compared with the author's text immediately following, that is the text titled as "Pinto (1510)" and the value of d displayed in Gândavo (1502)'s line. Now, when the line shows two points (two values of d), such as the case of the Brandão (1584)'s line, is because there are two texts in the sample of the same year. For instance, those texts are from Vieira (1608):(a) letters and (b) sermons.

In this analysis we detect two main change points, the first one at the turn

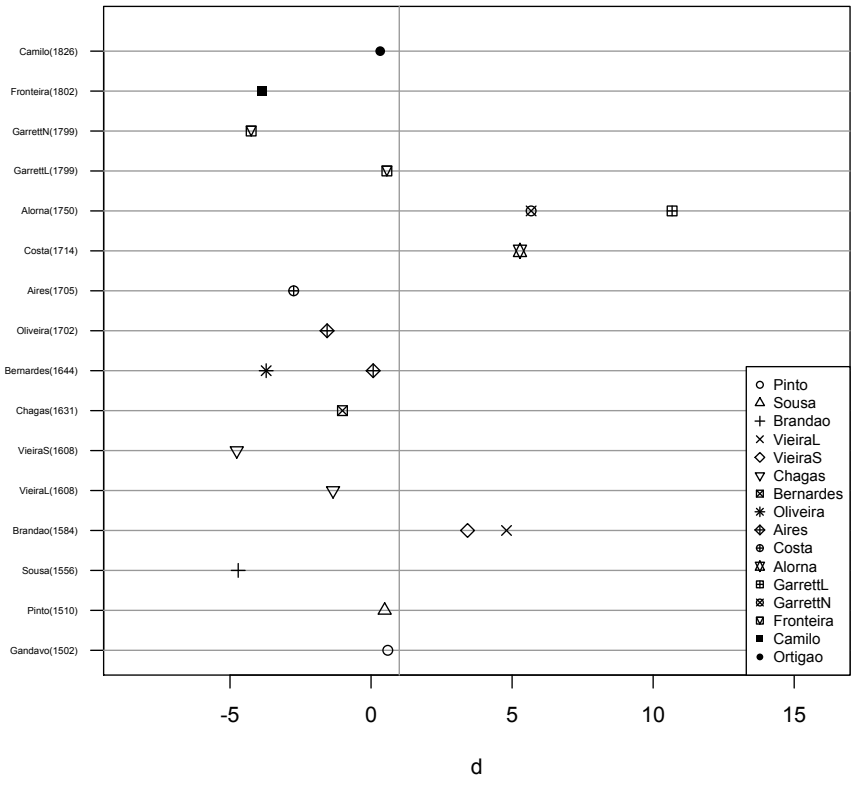

Fig. 1. Each horizontal line represents a written text from European Portuguese, those were ordered by time from down to top. The vertical line represents $d = 1$, greater values of d indicates the presence of a change point.

of the 16th century to the 17th century. The second one, in the second half of the 18th century that spreads to the end of the century. Our findings complement the results attained in Galves *et al.* [2], which study the changes of the European Portuguese in the same period of time, through the analysis of clitic placement.

5 ACKNOWLEDGMENTS

The authors gratefully acknowledge the support for this research provided by (a) FAEPEX-Unicamp, (b) USP's project "Mathematics, computation, language and the brain", FAPESP's projects (c)"Portuguese in time and space: linguistic contact, grammars in competition and parametric change" 2012/06078-9 and (d)"Research, Innovation and Dissemination Center for Neuromathematics" 2013/ 07699-0, (S. Paulo Research Foundation).

References

1. Frota, S., Galves, C., Vigário, M., Gonzalez-Lopez, V., and Abaurre, B., "The phonology of rhythm from Classical to Modern Portuguese", *Journal of Historical Linguistics*, 2(2), 173-207 (2012).
2. Galves, C., Britto, H. and de Sousa, M. C. P., "The Change in Clitic Placement from Classical to Modern European Portuguese", *Journal of Portuguese Linguistics*, 4(1), 39-67 (2005).
3. Galves, C. and Faria, P., *Tycho Brahe Parsed Corpus of Historical Portuguese.* `http://www.tycho.iel.unicamp.br/ tycho/corpus/en/index.html` (2010).
4. Galves, A., Galves, C., García, J. E., Garcia, N. L., and Leonardi, F. "Context tree selection and linguistic rhythm retrieval from written texts", *The Annals of Applied Statistics*, 6(1), 186-209 (2012).
5. García, J., Gut, U., and Galves, A. "Vocale-a semi-automatic annotation tool for prosodic research". In *Speech Prosody 2002, International Conference.* (2002).
6. García, J., and González-López, V. A. "Minimal markov models", arXiv preprint arXiv:1002.0729 (2010).
7. García, J. E., González-López, V. A., and Viola, M. L. L., "Robust model selection and the statistical classification of languages", in *XI BRAZILIAN MEETING ON BAYESIAN STATISTICS: EBEB 2012 (Vol. 1490, No. 1, pp. 160-170). AIP Publishing,* (2012).
8. García, J. E., González-López, V. A., and Nelsen, R. B. "A new index to measure positive dependence in trivariate distributions", *Journal of Multivariate Analysis*, 115, 481-495 (2013).
9. García, J. E., González-López, V. A., and Viola, M. L. L., "Robust Model Selection for Stochastic Processes", *Communications in Statistics - Theory and Methods*, 43 (10-12) 2516-2526 (2014).

3 CHAPTER

Clustering and Partitioning

Probabilistic Approach for Comparing Partitions

Osvaldo Silva[1], H. Bacelar-Nicolau[2], Fernando C. Nicolau[3], and Áurea Sousa[4]

[1] Dep. of Math., CES-UA, University of Azores, Ponta Delgada, Azores, Portugal
(Email: osilva@uac.pt)
[2] Faculty of Psychology, LEAD; ISAMB, CEA; University of Lisbon, Lisboa, Portugal
(Email: hbacelar@fp.ul.pt)
[3]FCT, Department of Mathematics, New University of Lisbon, Monte da Caparica, Portugal
(Email: fernandonicolau@netcabo.pt)
[4] Dep. of Math., CEEAplA, University of Azores, Ponta Delgada, Azores, Portugal
(Email: aurea@uac.pt)

Abstract: The comparison of two partitions in Cluster Analysis can be performed using various classical coefficients (or indexes) in the context of three approaches (based, respectively, on the count of pairs, on the pairing of the classes and on the variation of information). However, different indexes usually highlight different peculiarities of the partitions to compare. Moreover, these coefficients may have different variation ranges or they do not vary in the predicted interval, but rather only in one of their subintervals. Furthermore, there is a great diversity of validation techniques capable of assisting in the choice of the best partitioning of the elements to be classified, but in general each one tends to favour a certain kind of algorithm. Thus, it is useful to find ways to compare the results obtained using different approaches. In order to assist this assessment, a probabilistic approach to comparing partitions is presented and exemplified. This approach, based on the *VL (Validity Linkage) Similarity*, has the advantage, among others, of standardizing the measurement scales in a unique probabilistic scale. In this work, the partitions obtained from the agglomerative hierarchical cluster analysis of a dataset in the field of teaching are evaluated using classical and probabilistic (of *VL* type) indexes, and the obtained results are compared.

Keywords: Hierarchical cluster analysis, comparing partitions, affinity coefficient, *VL* methodology

1 Introduction

Cluster Analysis aims to identify groups (classes or clusters) of entities (individuals, objects, etc.), that are relatively homogeneous and well separated, based on similarities or dissimilarities between them.

There are multiple indexes for comparing partitions, which complicates the decision-making, given that different indexes generally evaluate different peculiarities of the partitions to compare. Moreover, there is a great diversity of validation techniques capable of assisting in the choice of the best partitioning of the elements to be classified, but in general each one of them tends to favour a certain kind of algorithm.

New Trends in Stochastic Modeling and Data Analysis (pp. 113-122)
Raimondo Manca – Sally McClean – Christos H Skiadas (Eds)

Thus, it is imperative to find ways to compare the results obtained using different approaches.
In Section 2 the indexes for the comparison of partitions are introduced using classical coefficients. Section 3 is dedicated to the comparison of partitions using probabilistic coefficients of the *VL* type. In Section 4, we compare the results obtained with the implementation of the two approaches, classical and probabilistic, to a real data set, under a wider validation work in Cluster Analysis, using resampling methods. Finally, Section 5 presents the main conclusions.

2 Coefficients for comparison of partitions pairs

The comparison of two partitions in Cluster Analysis can be performed using various indexes or classical coefficients in the context of three approaches (based respectively on the count of pairs, on the pairing of the classes and on the variation of information). However, each of these coefficients assumes a certain value, depending on its analytic expression, and some have different variation ranges or they do not vary in the predicted interval, but rather only in one of its subintervals. In order for these coefficients to be more easily comparable, one should keep in mind their intrinsic characteristics, categorizing them into groups with similar characteristics.
To compare two partitions, *P* and *P'*, of one same dataset of *n* cardinal based on the count of pairs, one can begin by constructing an associated 2 × 2 contingency table, as Table 1.

Table 1. Contingency table based on the count of pairs

	Partition *P'*	
Partition *P*	*a*	*b*
	c	*d*

Table 1 mentions the pairs of elements that exist in the two partitions, where "*a*" is the number of pairs of elements that are in the same classes in both partitions, "*b*" is the number of pairs of elements that belong to the same classes in a partition *P* but to different classes in the other partition (*P'*), "*c*" is the number of pairs belonging to different classes in the *P* partition and to the same classes in the *P'* partition and "*d*" is the number of pairs of elements belonging to different classes in both partitions. The total number of pairs of objects is $a + b + c + d = n \times (n-1) / 2$.
Silva (2012) contains a list of indexes for the comparison of binary data, which are functions of the four values of Table 1 and are also used for comparing partitions. In this list, the indexes are subdivided into similarity coefficients that consider the joint absence "*d*", similarity coefficients that do not take into account the joint absence "*d*" and other coefficients of association. For each of the coefficients the respective formula

is shown, as well as the symbol with which it is usually designated, its variation range and its author(s).

These indexes should be evaluated relatively to common properties, and can be sensitive to the number of classes in the partitions. Some of the indexes (for example, Hubbert and Rand) tend to have high values in the case of partitions with more classes, others in the case of partitions with a small number of classes (e.g. Jaccard). The adjusted Rand index has none of these undesirable characteristics (Milligan and Cooper, 1985; Jain and Dubes, 1988), which is why this is one of the indexes pertaining to the methodology used in this work. The standardized Ochiai index (a particular case of the affinity coefficient, e. g., Bacelar-Nicolau, 1985), has also been used with good results in the context of partitions comparison (Silva, 2004; Silva, 2012).

As noted above, the evaluation of the partitions comparison indexes based on the count of pairs must take into account the scale of variation and the relation that can be established between the various indexes from their mathematical expressions. Several studies of classification and comparison of these coefficients have been proposed by many authors since Sneath and Sokal (1963). Sibson (1972) made the grouping of coefficients into monotonic classes, establishing an equivalence relation in the set of comparison coefficients for binary data. Bacelar-Nicolau (1980, 1987) determined "*distributionally equivalent*" classes of coefficients, a concept that we will use in this work, as mentioned in the next section.

3 Comparison of pairs of partitions using probabilistic coefficients

Lerman (1970) proposed the use of a similarity coefficient of probabilistic nature between binary variables, which he then expanded to proximity coefficients between structures of the same type (Lerman, 1973, 1981). Bacelar-Nicolau (e.g., 1980, 1987) conducted a distributional study of the comparison coefficients for binary data, having verified and proved the distributional equivalence of a broad class of coefficients, under the assumption of fixed margins of the 2 × 2 contingency table associated with each pair of elements of the set to be classified. For other coefficients as well as in the hypothesis of free margins, although distributional exact equivalence does not occur, we can find classes of equivalent coefficients with respect to their asymptotic distribution, and take always, as information associated with a coefficient, its limit function of distribution (Bacelar-Nicolau, 1980, 1987; Lerman, 1981), which is a probabilistic similarity coefficient γ on the scope of *VL* methodology. Thus, we have for a similarity coefficient, S:

$$\gamma = F_S(s) = Prob_{H_0}\left(S \le s\right) \cong Prob_{H_0}\left(S^* \le s^*\right) \cong \phi\left(s^*\right)$$

where H_0 is an adequate reference hypothesis, F_S is the distribution function of S, $S^* = (S - E(S))/\sigma_S$, s^* is a realization of S^*, ϕ is the distribution function of the standard normal distribution and $E(S)$ and σ_S are respectively the mean value and the standard deviation, usually asymptotic. The probabilistic coefficient takes values in [0,1] (follows the Uniform distribution (0, 1)), and is generally calculated asymptotically because the exact distribution function may not be known. The *VL* coefficient was later extended to other types of data and to mixtures of different types of data (e.g. Bacelar-Nicolau, 1988, Nicolau, 1983; Nicolau and Bacelar-Nicolau, 1998; Bacelar-Nicolau *et al*, 2009, 2010).

The approach to comparing partitions, using probabilistic coefficients of the *VL* type, is based on studies of the comparison coefficients for binary data by Bacelar-Nicolau and proceeds as follows:

i) We start with a similarity index, S, for comparing two partitions, *P* and *P'*, based on the count of pairs of elements that exist in the two partitions.

ii) We calculate the value of $\gamma_{PP'}$ of the distribution function of the similarity index *S* used in point *s*, under the assumption of the considered reference:

$$\gamma_{PP'} = F_S(s) = Prob_{H_0}(S \le s) \cong Prob_{H_0}(S^* \le s^*) \cong \phi(s^*)$$

Two partitions, *P* and *P'*, will be considered the more consistent the larger is the value of $F_S(s)$, that is, the more unlikely is overcoming the *s* realization of *S* under the reference hypothesis.

As it has been pointed out by several authors (e.g., Lerman, 1973, 1981; Bacelar-Nicolau, 1980, 1987; Dubes and Jain, 1988), the different indexes do not show all values in [0, 1] and a proportion of the similarity between both partitions is assigned randomly. However, it is shown that the most used indexes are equivalent from the distributional point of view (Bacelar-Nicolau, 1980, 1987). The application of the *VL* methodology to these coefficients allows us to obtain comparison indexes of partitions that can be interpreted on a probabilistic scale. Thus, using a probabilistic coefficient we can choose only one classical coefficient in each (asymptotically) distributionally equivalent class of coefficients, in order to compare partitions.

4 Comparison of results obtained by classical and probabilistic approaches on a set of real data

The data (from a sample of 164 students) was obtained through a questionnaire containing twenty-two questions concerning attitudes/beliefs of students in the area of Social and Human Sciences regarding the subject of Statistics (Silva *et al*., 2007). Each

student selected one and only one of seven possible answers to each question (1 - *strongly disagree*, ..., 4 - *neither agree nor disagree*, ..., 7 - *strongly agree*).

An Agglomerative Hierarchical Cluster Analysis (*AHCA*), using the affinity coefficient (e.g., Bacelar-Nicolau, 1985) between variables and the probabilistic aggregation criteria *AVL*, *AV1* and *AVB* (e.g., Nicolau, 1983; Bacelar-Nicolau, 1985; Nicolau and Bacelar-Nicolau, 1998), was applied in order to obtain a typology of variables under study. The tables with the values of validation indexes to select the most significant partition, obtained from the initial data matrix, and the interpretation of the classes corresponding to this partition, in four classes, can be found in Silva et al. (2007). It has been noted that the most significant partition is the same for all three aggregation criteria.

The results were obtained for the case of evaluation and comparison of partitions using resampling methods. In the present study, we evaluate the most significant partition provided by the AHCA of the data, based on the affinity coefficient and on the aggregation criteria mentioned above. The procedure can briefly be described as follows: 1) from the original data 50 subsamples were generated, with a sampling rate defined *a priori* (80%), using simple random sampling; 2) the same model of AHCA was applied to data matrixes (subsamples) randomly generated by the Monte Carlo simulation method, to determine the partitions with the same number of classes presented by the most significant partition obtained from the original data; 3) this partition was compared to each of the partitions obtained in 2), based on the count of pairs, using each of the classical coefficients from the list in Silva (2012) or the associated *VL* probabilistic coefficient; statistics were also calculated regarding location and dispersion associated with each index, in order to analyze the respective behaviour.

Table 2 shows the values of summary statistics (measures of central tendency, dispersion and quantiles) for classical coefficients (Table 2-a) and probabilistic coefficients (Table 2-b) in the situation where joint absence "*d*" is not considered.

Silva (2012) also contains similar tables for the coefficients where the joint absence "*d*" is considered, as well as for other association coefficients.

It can be seen in Table 2-a) and in Silva (2012) that the most part of the classical comparison coefficients takes values in the interval [0,1]. However, the interval between the minimum and maximum values of the sampling distribution is very variable. The maximum value of the distribution reaches the upper limit 1 of the range in many of the coefficients, reaching a minimum often above 0.5 for the first two considered coefficients classes (similarity coefficients that consider the joint absence "d" and similarity coefficients that do not consider the joint absence "d"), but not for other association coefficients (Silva, 2012).

Table 2-a). Values of summary statistics related to classical coefficients that do not consider joint absence "*d*"

	S	J	O	CZ	K1	DW1	DW2	SS2	BB1	BB2	SO	JO	K2	FMG1
Min	.609	.432	.607	.603	.609	.547	.609	.276	.547	354	.299	1.219	.761	.544
Max	1.000	1.000	1.000	1.000	1.000	1.000	1.000	1.000	1.000	500	1.000	2.000	10.333	.938
Mean	.955	.908	.941	.941	.942	.934	.950	.870	.929	479	.891	1.884	2.491	.879
SD	.095	.177	.117	.119	.116	.138	.097	.238	.139	043	.222	.233	3.769	.118
Center	.804	.716	.803	.801	.804	.773	.804	.638	.773	427	.650	1.609	5.505	.741
.005	.609	.432	.607	.603	.609	.547	.609	.276	.547	354	.299	1.219	.761	.544
.01	.609	.432	.607	.603	.609	.547	.609	.276	.547	000	.299	1.219	.761	.544
.025	.673	.438	.609	.609	.610	.609	.673	.281	.609	379	.371	1.220	.761	.547
.05	.765	.513	.683	.678	.687	.609	.765	.345	.609	379	.371	1.374	.761	.620
.1	.765	.513	.683	.678	.687	.609	.765	.345	.609	379	.371	1.374	.770	.620
.25	.969	.912	.954	.954	.954	.969	.939	.838	.939	484	.938	1.908	1.054	.891
.5	1.000	1.000	1.000	1.000	1.000	1.000	1.000	1.000	1.000	500	1.000	2.000	2.491	.938
.75	1.000	1.000	1.000	1.000	1.000	1.000	1.000	1.000	1.000	500	1.000	2.000	5.798	.938
.9	1.000	1.000	1.000	1.000	1.000	1.000	1.000	1.000	1.000	500	1.000	2.000	10.333	.938
.95	1.000	1.000	1.000	1.000	1.000	1.000	1.000	1.000	1.000	500	1.000	2.000	10.333	.938
.975	1.000	1.000	1.000	1.000	1.000	1.000	1.000	1.000	1.000	500	1.000	2.000	10.333	.938
.990	1.000	1.000	1.000	1.000	1.000	1.000	1.000	1.000	1.000	500	1.000	2.000	10.333	.938
.995	1.000	1.000	1.000	1.000	1.000	1.000	1.000	1.000	1.000	500	1.000	2.000	10.333	.938

Similarly, measurements of location and dispersion of various classical coefficients show high variation. However, the sampling distributions of the associated probabilistic coefficients described in Table 2-b) feature ranges of similar magnitude with approximate minimum and maximum values.

Table 2-b). Values of summary statistics related to probabilistic coefficients that do not consider joint absence "d"

	S	J	O	CZ	K1	DW1	DW2	SS2	BB1	BB2	SO	JO	K2	FMG1
Min	.000	.004	.002	.002	.002	.003	.000	.006	.003	.002	.004	.374	.194	.002
Max	.682	.698	.691	.691	.691	.683	.697	.707	.696	.691	.688	1.000	.962	.691
Mean	.559	.557	.559	.559	.559	.561	.555	.554	.558	.560	.560	.438	.463	.559
SD	.233	.249	.242	.242	.242	.238	.249	.261	.247	.241	.242	.152	.305	.242
Center	.341	.351	.347	.347	.347	.343	.349	.357	.349	.346	.346	.687	.779	.347
.005	.000	.004	.002	.002	.002	.003	.000	.006	.003	.002	.004	.374	.194	.002
.01	.000	.004	.002	.002	.002	.003	.000	.006	.003	.000	.004	.374	.194	.002
.025	.002	.004	.002	.003	.002	.009	.002	.007	.011	.010	.009	.374	.194	.002
.05	.023	.013	.014	.013	.014	.009	.029	.014	.011	.010	.009	.374	.194	.014
.1	.023	.013	.014	.013	.014	.009	.029	.014	.011	.010	.009	.374	.195	.014
.25	.559	.509	.543	.544	.541	.600	.456	.447	.529	.550	.583	.374	.217	.540
.5	.682	.698	.691	.691	.691	.683	.697	.707	.696	.691	.688	.374	.360	.691
.75	.682	.698	.691	.691	.691	.683	.697	.707	.696	.691	.688	.479	.365	.691
.9	.682	.698	.691	.691	.691	.683	.697	.707	.696	.691	.688	.530	.702	.691
.95	.682	.698	.691	.691	.691	.683	.697	.707	.696	.691	.688	1.000	.962	.691
.975	.682	.698	.691	.691	.691	.683	.697	.707	.696	.691	.688	1.000	.962	.691
.990	.682	.698	.691	.691	.691	.683	.697	.707	.696	.691	.688	1.000	.962	.691
.995	.682	.698	.691	.691	.691	.683	.697	.707	.696	.691	.688	1.000	.962	.691

Figure 1 illustrates the variation of mean values of some coefficients, both classic (taking values in the range [0,1]) and probabilistic. As it can be seen, the mean values of the classical indexes, considering the values obtained in 50 resamplings, vary greatly from index to index.

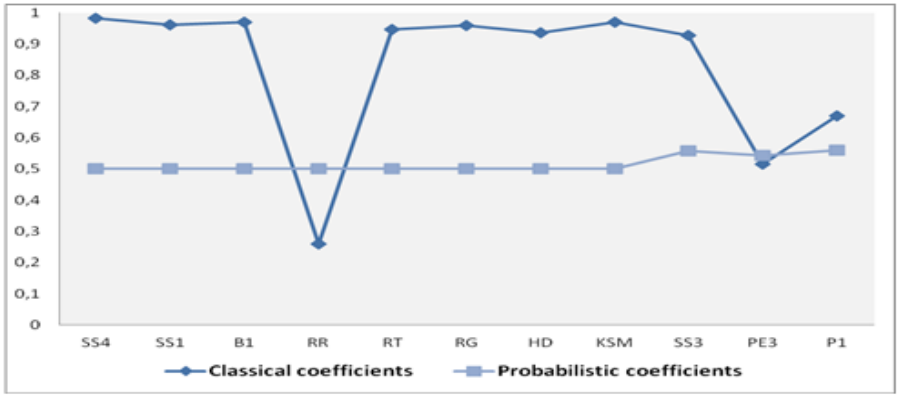

Fig. 1. Variation of means obtained for some classical and probabilistic coefficients

In the context of the *VL* approach it is found that, contrary to the respective basic indexes, the values obtained for means and other location measures of the sampling distribution of the probabilistic coefficient have been very close, as can be seen in Figures 1 and 2, as well as in Silva (2012).

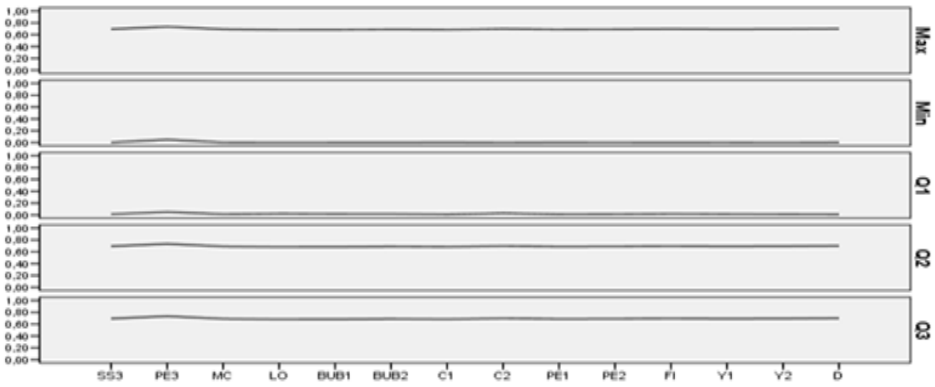

Fig. 2. Variation of the values of some summary statistics for the probabilistic *VL* coefficients associated with classical association coefficients.

These results are consistent with the theory that shows the property of (exact or asymptotic) distributional equivalence between comparison coefficients for binary data (Bacelar-Nicolau, 1980, 1987), mentioned in Section 3. The comparison of partitions using probabilistic coefficients of *VL* type is therefore a simpler and more robust approach than the comparison based on classical coefficients: instead of determining several of these indexes, we will choose a single index in each of the (exact or asymptotically) distributionally equivalent classes and use the *VL* probabilistic coefficient associated to it, which also has the advantage of standardizing the measurement scale on the same probabilistic scale. Finally, the variation ranges and other statistics provided by the *VL* coefficient tables allow us evaluate the quality of the most significant partition provided by the three models of probabilistic classification. This conclusion is supported by an appropriate set of validation coefficients, which are not presented in this work.

5 Conclusions

In this work, we compare the performances of classical indexes with an associated probabilistic approach for the comparison of pairs of partitions. The described resampling methodology is part of a work on the evaluation of the stability of the obtained classifications in a AHCA.

Usual classical indexes show not to be a convenient choice since they may have distinct display ranges as well as quite different values for other statistics of location and dispersion or they do not take values in the entire variation interval but only in part of that interval. The probabilistic approach to the comparison of partitions using probabilistic coefficients of *VL* type has, among others, the advantage that all classical indexes used lead, exactly or asymptotically, to very close values of the probabilistic index (theoretically conduct to the same value, in the case of the reference hypothesis considered here) and in a probabilistic scale (0, 1). Thus, instead of determining various indexes the *VL* approach can be applied to any of the indexes belonging to a given class of distributionally equivalent indexes to carry out the comparison of partitions pairs with the same number of classes.

References

1. Bacelar-Nicolau, H., Contributions to the Study of Comparison Coefficients in Cluster Analysis, PhD Thesis (in Portuguese), Universidade de Lisboa (1980).
2. Bacelar-Nicolau, H., The Affinity Coefficient in Cluster Analysis, Methods of Operations Research, vol. 53, Martin J. Bekmann et al (ed.), Verlag Anton Hain, Munchen, pp. 507-512 (1985).

3. Bacelar-Nicolau, H., On the Distribution equivalence in Cluster Analysis, In Proceedings of the NATO ASI on Pattern Recognition Theory and Applications, Springer - Verlag, New York, pp. 73-79 (1987).
4. Bacelar-Nicolau, H., Two Probabilistic Models for Classification of Variables in Frequency Tables, In: Bock, H.-H. (Eds.), Classification and Related Methods of Data Analysis, North Holland, pp. 181-186 (1988).
5. Bacelar-Nicolau, H.; Nicolau, F.C.; Sousa, Á.; Bacelar-Nicolau, L., Measuring Similarity of Complex and Heterogeneous Data in Clustering of Large Data Sets, Biocybernetics and Biomedical Engineering, vol. 29, no. 2, pp. 9-18 (2009).
6. Bacelar-Nicolau, H.; Nicolau, F.C.; Sousa, Á.; Bacelar-Nicolau, L., Clustering Complex Heterogeneous Data Using a Probabilistic Approach, In *Proceedings of Stochastic Modeling Techniques and Data Analysis International Conference* (SMTDA2010), 85-93 (2010) (electronic publication) .
7. Jain, A. K.; Dubes, R. C., *Algorithms for Clustering Data*. Prentice Hall, Englewood Cliffs, NJ (1988).
8. Lerman, I. C., *Les Bases de la Classification Automatique*. Paris, Gauth.-Villars (1970).
9. Lerman, I. C., Étude Distributionnelle de Statistiques de Proximité entre Structures Algébriques Finies de Même Type – application à la Classification Automatique. In: *Cahiers du B.U.R.O.*, N^{o}. 19, Paris (1973).
10. Lerman, I. C., Classification et Analyse Ordinale des Données, Dunod, Paris (1981).
11. Milligan, G. W.; Cooper, M. C., An Examination of Procedures for Determining the Number of Clusters in a Data Set. Psychometrika, 50, 159-179, (1985).
12. Nicolau, F.C., Cluster Analysis and Distribution Function, Methods of Operations Research, vol. 45, 431-433 (1983).
13. Nicolau, F.C. and Bacelar-Nicolau, H., Some Trends in the Classification of Variables, In: Hayashi, C., Ohsumi, N., Yajima, K., Tanaka, Y., Bock, H.-H., Baba, Y. (Eds.), Data Science, Classification, and Related Methods. Springer-Verlag, pp. 89-98 (1998).
14. Sibson, R., Multidimensional Scalling in Theory and Pratice. In: *Les Méthodes Mathématiques de l`Archéologie*, Centre d`Analyse Documentaire pour l`Archéologie, Marseille, 43-73 (1972).
15. Silva, A., Saporta, G. e Bacelar-Nicolau, H., *Missing Data and Imputation Methods in Partition of Variables*. Classification, Clustering and Data Mining Applications, Springer, 631-637 (2004).
16. Silva O.; Bacelar-Nicolau, H. e Nicolau, F., Utilização da Análise Classificatória para Avaliar as Atitudes/Crenças em relação à Estatística de Alunos da Área de

Ciências Sociais e Humanas. In: *Actas do XIV Congresso Anual da Sociedade Portuguesa de Estatística*, (Ferrão, M. et al. Eds.) Edições S.P.E, 751-759 (2007).

17. Silva, O., Contributions to the Evaluation and Comparison of Partitions in Cluster Analysis, PhD Thesis (in Portuguese), Universidade dos Açores, Ponta Delgada (2012).
18. Sneath, P. H.; Sokal, R. R., *Principles of Numerical Taxonomy*. Freeman, San Francisco (1963).

On Cluster Analysis of Complex and Heterogeneous Data

Helena Bacelar-Nicolau[1], Fernando C. Nicolau[2], Áurea Sousa[3] and Leonor Bacelar-Nicolau[4]

[1]University of Lisbon, Faculty of Psychology, LEAD; ISAMB; Lisbon, Portugal
Email: hbacelar@psicologia.ulisboa.pt
[2]University of Lisbon, FCT, Department of Mathematics, Caparica, Portugal
Email: fernandonicolau@netcabo.pt
[3]University of Azores, Dep. of Math., CEEAplA, Ponta Delgada, Azores, Portugal
Email: aurea@uac.pt
[4]University of Lisbon, Faculty of Medicine, Institute of Preventive Medicine, ISAMB, Lisbon, Portugal
Email: lnicolau@fm.ul.pt

Abstract: Cluster analysis or "unsupervised" classification (from "unsupervised learning", in pattern recognition literature) usually concerns a set of exploratory multivariate data analysis methods and techniques for grouping either statistical data units or variables into groups of similar elements, that is finding a clustering structure in the data. Classical clustering methods usually work with a set of objects as statistical data units described by a set of homogeneous (that is, of the same type) variables in a *two-way* framework. This paradigm can be extended in such way that data units may be either simple / *first-order* elements (e.g., objects, subjects, cases) or groups of / *second-order or more* elements from a population (e.g., subsets, samples, classes of a partition) and/or descriptive variables may simultaneously be of different (e.g., binary, multi-valued, histogram or interval) types. Therefore, one has a complex and/or heterogeneous data set under analysis. In that case classification will often be carried out by using a *three-way* or a *symbolic/complex* approach. The present work synthesizes previous methodological results and shows several developments mostly regarding hierarchical cluster analysis of complex data, where statistical data units are described by either a homogeneous or a heterogeneous set of variables. We will illustrate that approach on a case study issued from the statistical literature. The methodology has been applied with success in a data mining context,

New Trends in Stochastic Modeling and Data Analysis (*pp.* 123-134)
Raimondo Manca – Sally McClean – Christos H Skiadas (Eds)

concerning multivariate analysis of real-life data bases from economy, management, medicine, education and social sciences.

Keywords: Three-way data, Symbolic data, Interval data, Cluster analysis, Similarity coefficient, Hierarchical clustering model.

1 Introduction

In complex and large data bases, we are very often concerned with matrices where data units are described by some heterogeneous set of variables. Therefore, the question arises of how we should measure the similarity between statistical data units in a coherent way, if different types of variables are involved. Traditionally, partial similarity coefficients for each type of variables are computed, and then a convex linear combination of those similarities gives a global similarity between data units. Such procedures should be performed in a consistent way, combining comparable similarity coefficients in a valid / robust global similarity. Clustering data sets where mixed variables types are involved has interested many researchers. In two-way data matrices a well known coefficient for comparing subjects described by different types of variables was already proposed in 1971 by Gower. Cluster analysis of *symbolic* data described by mixed variables types may be found, for instance, in Bacelar-Nicolau *et al.* (2009, 2010) and in De Carvalho and Souza (2010), while Chavent *et al*. (2003) and Bacelar-Nicolau *et al.* (2014) concern clustering of interval data, which plays a special role in this paper. A number of dissimilarity coefficients, like adaptive squared Euclidean, city-block, Hausdorff distances or generalized Minkowski metrics, among others, may be found in those papers, either in a hierarchical or in a non hierarchical clustering context. In this paper, we deal with a consistent global affinity coefficient as the basis of hierarchical clustering methods (Bacelar-Nicolau, 2002; Bacelar-Nicolau *et al*., 2009, 2010). The next section gives a brief description of our approach to clustering statistical data units described by three different types of variables commonly found in real databases. The third section illustrates a case study with mixed data that partially applies the methodology and the last section concerns conclusions and some developments.

2 Complex and Heterogeneous Data

Let $D = \{1,...,n\}$ be a set of n statistical data units which are described by a set of p variables, $Y = \{Y_1, ...,Y_p\}$. Cluster analysis usually aims to obtain a classification of one of the two data sets, either D or Y, given the other one. Here we will be concerned with clustering models on the set of data units D. The data units can be either simple elements (e.g., subjects, individuals, cases) or subsets of objects in some population (e.g., subsamples of a sample, classes of a partition, subgroups of the population). Such kind of data might be represented in a generalized three-way data matrix where the *k-th* row, ($k=1,... ,n$), gives the description of the k-th data unit by the p variables, and the (k,j)-*th* entry, ($k=1,... ,n$; $j=1,...,p$), may contain

for instance a finite number of real values, a frequency distribution, a probability distribution or an interval of the real data set *R*, instead of one single value.
In most mixed or heterogeneous data sets we have been studying, those values concern discrete, binary or interval types of variables, either conjointly or in two by two type combinations. Hence in the set $Y = \{Y_1,...,Y_j,..., Y_{j'},..., Y_{j''},...,Y_p\}$ of p variables, we will assume that Y_j represents a *discrete* or a *categorical (modal)* variable with m_j ($\lambda=1,...,m_j$) modalities, also called a *histogram* variable, $Y_{j'}$ is a $m_{j'}$ *–dimensional binary vector* and $Y_{j''}$ is an *interval* variable, where j, j' and j'' belong to $\{1,...,p\}$ (e.g., Bacelar-Nicolau, 2000; Bacelar-Nicolau *et al*., 2009, 2010). Thus the corresponding *generalized columns* have n rows, and the k-*th* row ($k=1,... ,n$) contains: for Y_j , a frequency distribution $\left(n_{kj1},...,n_{kjm_j}\right)$, where $n_{kj\lambda}$ is the number of subjects in the k-*th* data unit who share the λ-*th* category of the j-*th* variable; for $Y_{j'}$, an element $\{0,1\}_k^{m_{j'}}$ of the power set $\{0,1\}^{m_{j'}}$, the whole binary sub-table being an element of $\{0,1\}^{n\times m_{j'}}$; for $Y_{j''}$, an interval $I_{kj''}$ of the real axis. Hence the data set may be represented by the following generalized table:

Table 1. Generalized three-way data matrix with heterogeneous variables

$D\backslash V$	…	Y_j	…	$Y_{j'}$	…	$Y_{j''}$	…
M	…	…	…		…		…
k	…	$\left(n_{kj1},..., n_{kjm_j}\right)$		$\{0,1\}_k^{m_{j'}}$	…	$I_{kj''}$	…
M	…	…	…	…	…	…	…
k'	…	$\left(n_{k'j1},..., n_{k'jm_j}\right)$	…	$\{0,1\}_{k'}^{m_{j'}}$	…	$I_{k'j''}$	…
M	…	…	…	…	…	…	…

Therefore, a consistent global similarity (or dissimilarity) coefficient should be used for such mixed types of data.

2.1. Discrete and categorical variable

Let Y_j be a *discrete* or a *categorical* (*modal*) variable with m_j ($\lambda=1,...,m_j$) modalities. Then, its general k-term ($k=1,...,n$) may be obtained by simply replacing $x_{kj\lambda}$ by the frequency $n_{kj\lambda}$ of the λ-*th* category or modality ($\lambda=1,...,m_j$). The relative frequencies $p_{kj} = n_{kj\lambda}/n_{kj\bullet}$, $\lambda=1,...,m_j$, generate a discrete probability distribution, that is a *profile*, or else a histogram, $((m_1, p_{kj1}), \ldots, (m_j, p_{kjm_j}))$.
Therefore, in order to measure partial/local similarity between each pair (k, k') of data units, over a modal variable, one may choose a similarity (or a dissimilarity)

coefficient for probability distributions (e.g., Bacelar-Nicolau, 1988; Bock and Diday, 2000; Bacelar-Nicolau, 2000).

2.2. Binary vector

Let us now take variable $Y_{j'}$, a $m_{j'}$ – dimensional binary vector (see *Table 1*). Given the data units k and k', let us represent by $s_{j'}$ the cardinal of positive agreements ($x_{kj'\lambda}=x_{k'j'\lambda}=1$), $t_{j'}$ the cardinal of negative agreements ($x_{kj'\lambda}=x_{k'j'\lambda}=0$), and $u_{j'}$ and $v_{j'}$ the cardinals of disagreements (respectively, $x_{kj'\lambda}=1$, $x_{k'j'\lambda}=0$ and $x_{kj'\lambda}=0$, $x_{k'j'\lambda}=1$). Then, we also have: $s_{j'}=\sum_{\lambda=1}^{m_{j'}} x_{kj'\lambda}x_{k'j'\lambda}$, $t_{j'}=\sum_{\lambda=1}^{m_{j'}}(1-x_{kj'\lambda})(1-x_{k'j'\lambda})$, $u_{j'}=\sum_{\lambda=1}^{m_{j'}} x_{kj'\lambda}(1-x_{k'j'\lambda})$ and $v_{j'}=\sum_{\lambda=1}^{m_{j'}}(1-x_{kj'\lambda})x_{k'j'\lambda}$.

One can find quite a large list of coefficients for binary data in the statistical literature, computed from those cardinals. Thus, a local similarity coefficient for a pair of rows (*k, k'*), *k, k'=1,...,n,* over a binary vector, may be computed from the 2×2 contingency table associated with the pair (*k, k'*) in the *j'-th* binary sub-table, as follows:

Table 2. Table of agreements and disagreements for a binary vector

$k \setminus k'$	**Agreement (1)**	**Disagreement (0)**	**Total**
1	$s_{j'}=\sum_{\lambda=1}^{m_{j'}} x_{kj'\lambda}x_{k'j'\lambda}$	$u_{j'}=\sum_{\lambda=1}^{m_{j'}} x_{kj'\lambda}(1-x_{k'j'\lambda})$	$s_{j'}+u_{j'}=m_{kj'}$
0	$v_{j'}=\sum_{\lambda=1}^{m_{j'}}(1-x_{kj'\lambda})x_{k'j'\lambda}$	$t_{j'}=\sum_{\lambda=1}^{m_{j'}}(1-x_{kj'\lambda})(1-x_{k'j'\lambda})$	$v_{j'}+t_{j'}=m_{j'}-m_{kj'}$
Total	$s_{j'}+v_{j'}=m_{k'j'}$	$u_{j'}+t_{j'}=m_{j'}-m_{k'j'}$	$m_{j'}$

where $m_{kj'}$ ($m_{k'j'}$) denotes the cardinal of presences in the data unit k (respectively, k') for the binary vector $Y_{j'}$.

2.3. Interval-type variable

A variable $Y_{j''}$ defined on the set D of statistical data units is an interval variable if for all $k \in D$ the subset $Y_{j''}(k)$ is an interval of the real data set $\mathbb{R}$. Let $Y_{j''}$ be an interval variable associated with a generalized column j'' (see *Table 1*), where each cell *(k, j'')* contains an interval $I_{kj''}$ ($k=1,...,n$).

Let $I_{j''}$ be the union of the intervals $I_{kj''} : I_{j''} = \cup I_{kj''}$ ($k = 1,...,n$). Thus, $I_{j''}$ is the domain of $Y_{j''}$. Let $\{I_{j''\lambda} : \lambda = 1,..., m_{j''}\}$ be a set of $m_{j''}$ elementary intervals, such that the following properties hold, for $\lambda, \lambda' = 1,...., m_{j''}$, $\lambda \neq \lambda'$; $k = 1,..., n$:

i) $I_{j''} = \cup I_{j''\lambda}$; ii) $I_{j''\lambda} \cap I_{j''\lambda'} = \phi$; iii) $I_{kj''} \cap I_{j''\lambda} = I_{j''\lambda}$, if $I_{kj''} \cap I_{j''\lambda} \neq \phi$, and $I_{kj''} \cap I_{j''\lambda} = \phi$, otherwise.

Let $x_{kj''\lambda}$ be $x_{kj''\lambda} = |I_{kj''} \cap I_{j''\lambda}|$, where $|\ |$ represents the interval range. Then, $x_{kj''\lambda} = |I_{j''\lambda}|$ if $I_{kj''} \cap I_{j''\lambda} = I_{j''\lambda}$, and $x_{kj''\lambda} = 0$, otherwise.

Therefore, one has for each pair ($I_{kj''}$, $I_{k'j''}$) of intervals: $x_{kj''\bullet} = |I_{kj''}|$, $x_{k'j''\bullet} = |I_{k'j''}|$ and $\sum_{\lambda=1}^{m_{j''}} \sqrt{x_{kj''\lambda} x_{k'j''\lambda}} = |I_{kj''} \cap I_{k'j''}|$. Consequently, the ($k,k'$)-*th* pair of intervals in the *j''-th* generalized column of *Table 1*, can be associated to a *generalized 2×2 contingency table* as follows:

Table 3. Table of agreements and disagreements for interval variables

k \ k'	**Agreement**	**Disagreement**	**Total**
Agreement	$s_{j''} = \|I_{kj''} \cap I_{k'j''}\|$	$u_{j''} = \|I_{kj''} \cap I^c_{k'j''}\|$	$s_{j''} + u_{j''} = \|I_{kj''}\|$
Disagreement	$v_{j''} = \|I^c_{kj''} \cap I_{k'j''}\|$	$t_{j''} = \|I^c_{kj''} \cap I^c_{k'j''}\|$	$v_{j''} + t_{j''} = \|I^c_{kj''}\|$
Total	$s_{j''} + v_{j''} = \|I_{k'j''}\|$	$u_{j''} + t_{j''} = \|I^c_{k'j''}\|$	$\|I_{j''}\|$

Into the cells of *Table 3*, agreements or disagreements are measured by the respective interval ranges, instead of the cardinals computed for a binary vector. Note that $I^c_{kj''}$ represents the complementary interval of $I_{kj''}$ in the domain $I_{j''}$.

2.4. Global affinity coefficient

The three approaches above for representing binary, modal and interval valued variables lead to a comprehensive approach for measuring global proximity between complex data units (*k, k'*) described by those heterogeneous kinds of variables. A special interesting case arises when only binary and interval valued variables are present in a database, since then all (the large list of) association coefficients for binary data defined from the 2×2 related contingency table can also be used in exactly the same way for interval data, from the corresponding *generalized 2×2 contingency table*. If modal variables are also present in the database, a global proximity coefficient between (*k, k'*) has to consistently take in

account proximity between histograms as well. The *affinity coefficient* responds to those requirements.

The *affinity coefficient* was formerly introduced by the pioneer work of K. Matusita, started with Matusita (1951) for measuring proximity between two probability distribution functions. It is related to a special case of the Hellinger (or Bhattacharyya) distance.

We have extensively studied the affinity coefficient and its properties, several affinity generalizations and some particular cases in cluster analysis context (e.g., Bacelar-Nicolau, 1988, 2000, 2002; Bacelar-Nicolau *et al*., 2009, 2010). The weighted generalized affinity coefficient $a(k,k')$, between a pair of statistical data units *k, k' ∈ D* (*k, k'=1,...,n*), may be defined in a three-way context, as the weighted mean of local / partial affinities between *k* and *k'* over the *j-th* variable *(j=1,...,p)*, as follows:

$$a(k,k') = \sum_{j=1}^{p} \pi_j \cdot aff(k,k';j) = \sum_{j=1}^{p} \pi_j \cdot \sum_{\lambda=1}^{m_j} \sqrt{\frac{x_{kj\lambda}}{x_{kj\bullet}} \cdot \frac{x_{k'j\lambda}}{x_{k'j\bullet}}} \qquad (1)$$

where the sum named *aff* (*k,k';j*) is the generalized local affinity between *k* and *k'* over the *j-th* variable, m_j representing the number of "modalities" of this variable; $x_{kj\lambda}$ is a real non-negative value (a suitable adaptation of the formula above may be considered if real or frequency negative values appear) whose meaning depends on the type of *j-th* variable or equivalently on the nature of the *j-th* corresponding sub-table and π_j are weights such that $0 \le \pi_j \le 1$, $\Sigma \pi_j = 1$.

Either the local affinities, or the whole weighted generalized affinity coefficient, take values in the interval [0,1] and satisfy the set of main proprieties of a similarity coefficient.

A probabilistic affinity coefficient may very often be associated with $a(k,k')$, giving place to a probabilistic clustering approach. In this work, some hierarchical clustering models used such approach (e.g., Lerman, 1970, 1981, 2000; Bacelar-Nicolau, 1987, 2000; Bacelar-Nicolau *et al*., 2010; Nicolau and Bacelar-Nicolau, 1982, 1998).

It is easy to prove that the generalized local affinity coefficient *aff* (*k,k';j*) in the mathematical expression (1) applies for each of the three types of variables described above (see Sections 2.1, 2.2 and 2.3).

For a histogram, the local affinity between *k* and *k'* is given by:

$$aff(k,k';j) = \sum_{\lambda=1}^{m_j} \sqrt{\frac{x_{kj\lambda}}{x_{kj\bullet}} \cdot \frac{x_{k'j\lambda}}{x_{k'j\bullet}}} = \sum_{\lambda=1}^{m_j} \sqrt{\frac{n_{kj\lambda}}{n_{kj\bullet}} \cdot \frac{n_{k'j\lambda}}{n_{k'j\bullet}}}$$

In the cases of a binary vector and an interval variable, we respectively obtain:

$$aff(k,k';j') = \sum_{\lambda=1}^{m_{j'}} \sqrt{\frac{x_{kj'\lambda}}{x_{kj'\bullet}} \cdot \frac{x_{k'j'\lambda}}{x_{k'j'\bullet}}} = \frac{s_{j'}}{\sqrt{m_{kj'} m_{k'j'}}}$$

and

$$aff(k,k';j'') = \sum_{\lambda=1}^{m_{j''}} \sqrt{\frac{x_{kj''\lambda}}{x_{kj''\bullet}} \cdot \frac{x_{k'j''\lambda}}{x_{k'j''\bullet}}} = \frac{\left|I_{kj''} \cap I_{k'j''}\right|}{\sqrt{\left|I_{kj''}\right| \cdot \left|I_{k'j''}\right|}} = aff\left(I_{kj''}, I_{k'j''}\right)$$

Thus, we find the well known Ochiai coefficient for binary data, and a *generalized Ochiai coefficient*, for interval data. In both cases local affinities might consequently be computed through two different ways, either by using *aff* (*k,k';j'*) and *aff* (*k,k';j''*), respectively (see expression (1)), or alternatively by using (see Tables 2 and 3) the *2×2 contingency* and the *2×2 generalized contingency tables* (Bacelar-Nicolau *et al*., 2009, 2010).

In conclusion, the global weighted generalized affinity coefficient (1) holds for mixed data where histogram, binary and interval variables are simultaneously present.

3. Application to a Case Study: Horse data set

Here, we briefly illustrate how the extended generalized affinity coefficient works over a real data set where histogram and interval variables are present.

The horse data set is issued from the literature of multivariate and symbolic data analysis. The data set (http://www.ceremade.dauphine.fr/~touati) consists of twelve (second order) statistical data units which represent groups of horse races from a sample of 60 races. The groups are described by three histogram and seven interval valued variables.

The twelve data units are named as follows: *ES/R*, *MA/R*, *EN/R*, *AM/R*, *EN/L*, *AM/L*, *ES/L*, *ES/D, EN/D*, *EN/P*, *ES/P* and *AM/P,* where labels *ES*, *EN*, *AM* and *MA* refer to *Southern Europe*, *Northern Europe*, *America* and *Arab World*, respectively, while *R*, *L*, *D* and *P* refer to *Racehorse*, *Leisure Horse*, *Draft Horse and Poney*, respectively (De Carvalho and Souza, 2010).

The histogram variables are *Country* (15 countries), *Robe* (10 categories) and *Aptitude* (9 categories) and the interval variables are *Height at the withers / Size (min)*, *Height at the withers / Size (max)*, *Weight (min), Weight (max), Mares, Stallions* and *Birth.*

A brief description of the variables, by type, partial description over the set of statistical data units and number of modalities of each histogram variable or number of computed elementary intervals of each interval variable may be seen in the following table:

Table 4. Short description of Horse data set variables

Variables	*Type*	*Transposed matrix*				*Number of modalities or of elementary intervals*
		ES/R	*MA/R*	...	*AM/P*	
Country	*Histogram*	(0.33,…,0)	(0,…,0)	…	(0, …,0)	*15 modalities*
Robe	*Histogram*	(0.33,…,0)	(0,…,0)	…	(0, …,0)	*10 modalities*
Aptitude	*Histogram*	(0.33,…,0)	(0,…,0)	…	(0, …,0)	*9 modalities*
Size (min)	*Interval*	[145,155]	[130,155]	…	[120,120]	*17 elementary intervals*
Size (max)	*Interval*	[158,175]	[150,167]	…	[147,147]	*13 elementary intervals*
Weight (min)	*Interval*	[410,460]	[390,430]	…	[170,170]	*17 elementary intervals*
Weight (max)	*Interval*	[550,630]	[570,580]	…	[290,290]	*18 elementary intervals*
Mares	*Interval*	[150,480]	[0,200]	…	[230,230]	*19 elementary intervals*
Stallions	*Interval*	[40,130]	[0,50]	…	[60, 60]	*16 elementary intervals*
Birth	*Interval*	[60,180]	[0, 70]	…	[80, 80]	*16 elementary intervals*

Thus each variable (generalized column) gave place to a sub-table with a suitable number of columns corresponding to a set of modalities (for the first three modal variables) or a set of elementary intervals (for the seven last interval valued variables).
According to the previous table, the generalized data matrix describing the statistical data units (*groups* of horses), was split into ten sub-tables with twelve rows and a different number of columns. *Table 5* partially illustrates the first and last sub-tables of the resulting generalized data matrix.

Table 5. Partial representation of the transformed data matrix for Horse data set

	Country							***Birth***					
	Saudi Arabia	G. Britain	France	...	Canada	Russia	...	[0, 19.5[	[19.5, 20.5[	[20.5, 29.5 [	...	[140.5, 180.5[	[180.5, 220.5[
ES/R	0	0	0.33	...	0	0	...	0	0	0	...	40	0
MA/R	0.33	0	0	...	0	0	...	19.5	1	9	...	0	0
EN/P	0	0.5	0	...	0	0.13	...	19.5	1	9	...	0	0
ES/D	0	0	1	...	0	0	...	0	0	0	...	0	0
EN/L	0	0.6	0	...	0	0	...	19.5	1	9	...	0	0
EN/R	0.22	0.22	0	...	0	0	...	0	0	0	...	40	40
AM/R	0	0	0	...	0	0	...	0	1	9	...	0	0
AM/L	0	0	0	...	0.33	0	...	19.5	1	0	...	0	0
ES/L	0	0	0.5	...	0	0	...	19.5	1	9	...	0	0
EN/D	0	0	0.5	...	0	0	...	0	0	0	...	0	0
ES/P	0	0	1	...	0	0	...	0	0	0	...	0	0
AM/P	0	0	0	...	0	0	...	0	0	0	...	0	0

The two sub-tables represent, respectively, the first histogram variable *Country* (where the data units are described by their corresponding profiles, as they were displayed at the site) and the last interval variable *Birth*.

For the interval variable, *Birth*, each row of its sub-table contains the 16 ranges of the intersection intervals between each elementary interval and the interval assumed by *Birth* in the group of horses described by that row.
In practice, for continuous variables (see variable *Birth*) we assume that the data were rounded to the nearest whole number, as it is usually done in classical statistics. Thus we represent each elementary interval by their so-called true limits (e.g. [20.5, 29.5] instead of [21, 29]). This is interesting particularly in case of elementary intervals that originally have equal lower and upper limits (e.g. [19.5, 20.5]).

The hierarchical clustering models we used for classifying the twelve complex data units were based on either the weighted generalized affinity coefficient $a(k,k')$ with equal weights, $\pi_j = 1/p$, or an associated coefficient related to the probabilistic approach referred to above (see Section 2). Both coefficients were combined with several classical (single linkage-SL, complete linkage-CL, etc.) and probabilistic *VL* (*V* for Validity, *L* for Linkage) aggregation criteria in order to obtain hierarchical clustering models. Note that the *VL* methodology is a probabilistic clustering approach based on the cumulative distribution function of similarity coefficients under suitable reference hypothesis (e.g. Bacelar-Nicolau, 1987; Bacelar-Nicolau *et al.*, 2009; Lerman, 1970, 1981, 2000), which may be combined either with classical or *VL* aggregation criteria.
Two kinds of clustering typologies arise, one into four clusters and the other one into three clusters and a few singletons (from the corresponding numerical tables of similarities and aggregation criteria, as well as from appropriate quality/validity indexes to choose de most significant partitions). The dendrograms are represented in the following figure, where probabilistic and empirical hierarchical clustering approaches were respectively used:

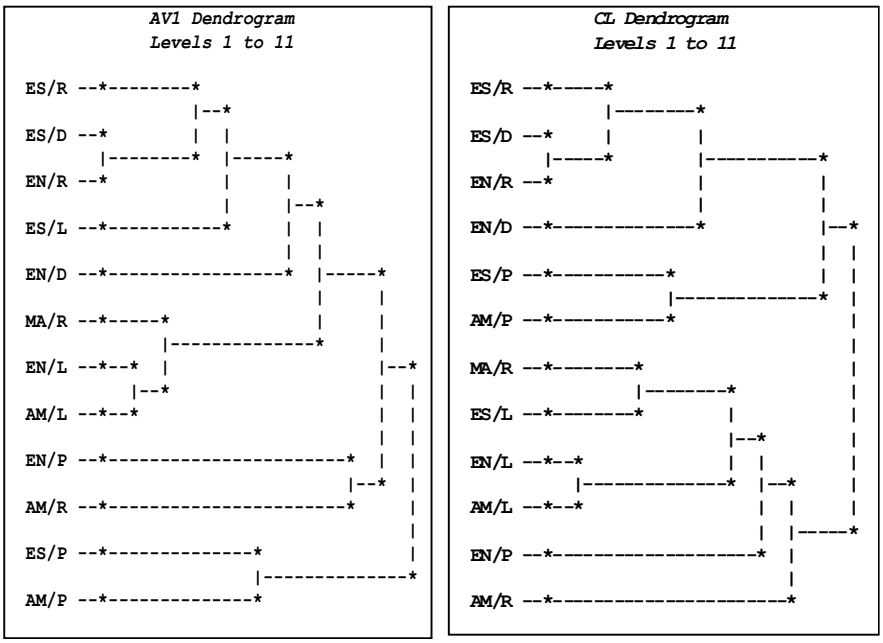

Fig. 1. Dendrograms for hierarchical clustering models based on the global generalized affinity coefficient

The main four clusters, obtained with the hierarchical clustering models associated with the dendrogram shown on the left side of Figure 1, are {*ES/R*, *ES/D, EN/R*, *ES/L*, *EN/D*}, {*MA/R*, *EN/L*, *AM/L*}, {*EN/P*, *AM/R*}, and {*ES/P*, *AM/P*}. Alternatively, three main clusters emerge from the models giving the dendrogram on the right side, {*ES/R*, *ES/D, EN/R*, *EN/D*}, {*ES/P*, *AM/P*} and {*MA/R*, *ES/L*, *EN/L*, *AM/L*}; then *EN/P* and *AM/R* join, one after the other, the third cluster, instead of merging together.

The clusters {*ES/R*, *ES/D, EN/R*, *EN/D*}, {*EN/L*, *AM/L*} and {*ES/P*, *AM/P*} show to be consistent in the way they are built into the hierarchical clustering models we have analyzed.

The following *a priori* classification into four classes was proposed for this data set: *Racehorse (R)*={*ES/R*, *MA/R*, *EN/R*, *AM/R*}, *Leisure Horse (L)*= {*EN/L*, *AM/L*, *ES/L*}, *Draft horse (D)*={*ES/D*, *EN/D*} and *Poney (P)*={*EN/P*, *ES/P*, *AM/P*}. Therefore, looking at the consistent clusters indicated above, the first one merges together the *a priori* draft horse and half racehorse classes. The second one is the *a priori* leisure horse class, without *ES/L.* The third one is the *a priori* poney class, without *EN/P.*

The horse data set was analyzed, among others, by De Carvalho and Souza (2010), with three non-hierarchical different algorithms. In their study, the clustering results also do not replicate the *a priori* classification. Besides, the authors obtain different partitions with different methods but they also find some consistent

clusters, which in fact are the same consistent clusters we have listed above. Note that a hierarchical clustering model brings additional information on the way partitions are built.

4. Conclusions. Future developments

The three approaches described above for representing histograms, binary and interval valued variables lead to a comprehensive approach for measuring global proximity between complex data units (*k, k'*). The weighted generalized affinity coefficient holds for mixed data where those kinds of heterogeneous variables are present. In fact, it is a similarity coefficient defined for comparing distribution laws, gives the Ochiai and the generalized Ochiai coefficients for binary and interval variables, respectively, and may be represented by the same mathematical expression for all three types of variables. Consequently, a unique algorithm works for those variable types.
Future developments include analyzing adaptive families of probabilistic clustering models and computational upgrading. Applications to real databases have mainly been developed in health and social sciences, education, economy and management.

Main References

1. Bacelar-Nicolau, H., On the distribution equivalence in cluster analysis, In *Proceedings of the NATO ASI on Pattern Recognition Theory and Applications*, Springer -Verlag, New York, pp. 73-79 (1987).
2. Bacelar-Nicolau, H., Two probabilistic models for classification of variables in frequency tables, In: Classification and Related Methods of Data Analysis, H.-H. Bock (Eds.) North Holland, Elsevier Sciences Publishers B.V., pp. 181-186 (1988).
3. Bacelar-Nicolau, H., The Affinity Coefficient, In: Analysis of Symbolic Data: Exploratory Methods for Extracting Statistical Information from Complex Data, H.-H. Bock and E. Diday (Eds.), Series: Studies in Classification, Data Analysis, and Knowledge Organization, Springer-Verlag, Berlin, pp. 160-165 (2000).
4. Bacelar-Nicolau, H., On the Generalised Affinity Coefficient for Complex Data, *Biocybernetics and Biomedical Engineering*, vol. 22, n^{o}. 1, pp. 31-42 (2002).
5. Bacelar-Nicolau, H.; Nicolau, F.C.; Sousa, Á.; Bacelar-Nicolau, L., Measuring Similarity of Complex and Heterogeneous Data in Clustering of Large Data Sets, *Biocybernetics and Biomedical Engineering*, vol. 29, n^{o}. 2, pp. 9-18 (2009).
6. Bacelar-Nicolau, H.; Nicolau, F.C.; Sousa, Á.; Bacelar-Nicolau, L., Clustering Complex Heterogeneous Data Using a Probabilistic Approach, *Proceedings of*

Stochastic Modeling Techniques and Data Analysis International Conference (SMTDA2010), pp. 85-93 (2010) (electronic publication).

7. Bacelar-Nicolau, H.; Nicolau, F.C.; Sousa, Á.; Bacelar-Nicolau, L., Clustering of Variables with a Three-Way Approach for Health Sciences, *Testing, Psychometrics, Methodology in Applied Psychology (TPM)*, Vol. 21, n^{o}. 4, pp. 435-447 (2014).
8. Bock, H.-H. and Diday, E., Analysis of Symbolic Data: Exploratory Methods for Extracting Statistical Information from Complex Data, Series: Studies in Classification, Data Analysis, and Knowledge Organization, Springer-Verlag, Berlin (2000).
9. Chavent, M., De Carvalho, F.A.T., Lechevallier Y. and Verde, R., Trois nouvelles méthodes de classification automatique de données symboliques de type intervalle, *Revue de Statistique Appliquée, vol. LI, n^{o}. 4*, pp. 5-29 (2003)
10. De Carvalho, F. A. T. and Souza, R. M. C. R., Unsupervised pattern recognition models for mixed feature-type symbolic data, *Pattern Recognition Letters* 31, pp. 430-443 (2010).
11. Lerman, I. C., Sur l`Analyse des Données Préalable à une Classification Automatique (Proposition d'une Nouvelle Mesure de Similarité), *Rev. Mathématiques et Sciences Humaines, vol. 32, n^{o}. 8,* pp. 5-15 (1970).
12. Lerman, I. C., Classification et Analyse Ordinale des Données, Dunod, Paris (1981).
13. Lerman, I. C., Comparing Taxonomy Data, *Rev. Mathématiques et Sciences Humaines, 38^{e} année, n^{o} 150*, pp. 37-51 (2000).
14. Matusita, K., On the Theory of Statistical Decision Functions, *Ann. Instit. Stat. Math, vol. III*, pp. 1-30 (1951).
15. Nicolau, F. C. and Bacelar-Nicolau, H., Nouvelles Méthodes d'Agrégation Basées sur la Fonction de Répartition, *Collection Séminaires INRIA 1981, Classification Automatique et Perception par Ordinateur*, Rocquencourt, pp. 45-60 (1982).
16. Nicolau, F.C. and Bacelar-Nicolau, H., Some Trends in the Classification of Variables, In: Hayashi, C., Ohsumi, N., Yajima, K., Tanaka, Y., Bock, H.-H., Baba, Y. (Eds.), Data Science, Classification, and Related Methods. Springer-Verlag, pp. 89-98 (1998).

Address for correspondence
Helena Bacelar-Nicolau
Faculdade de Psicologia, LEAD; Universidade de Lisboa
Alameda da Universidade 1649-013 Lisboa, Portugal
Email: hbacelar@psicologia.ulisboa.pt

Non-normalized PageRank and random walks on N-partite graphs

Christopher Engström and Sergei Silvestrov

Division of Applied Mathematics, School of Education, Culture and Communication, Mälardalen University, Box 883, 721 23 Västerås, Sweden
(e-mail: christopher.engstrom@mdh.se, sergei.silvestrov@mdh.se)

Abstract. In this article we will look at a variation of the PageRank algorithm originally used by L. Page and S. Brin to rank home pages on the Web. We will look at a non-normalized variation of PageRank and show how this version of PageRank relates to a random walk on a graph. The article has its main focus in understanding the behavior of the ranking depending on the structure of the graph and how the ranking changes as the graph change. More specific we will look at N-partite graphs and see that by considering a random walk on the graph we can find explicit formulas for PageRank of the vertices in the graph. Both the case with uniform and non-uniform personalization vector are considered.
Keywords: PageRank, N-partite graph, random walk.

1 Introduction

Originally PageRank was introduced by L. Page and S. Brin 1996 in order to rank homepages in order of relevance Brin and Page[4]. PageRank can be computed as the stationary distribution of a random walk on a directed graph using a slightly modified adjacency matrix and a low probability to move to a new random vertex of the graph not depending on the outgoing edges of the current vertex.

While PageRank was originally used to rank homepages, similar methods have been used in other areas such as Eigentrust to combat malicious peers in P2P networks Kamvar *et al.*[10] or evaluating the importance of certain actors in financial networks Battiston *et al.*[2].

Much of the theory behind PageRank is well known from the results in linear algebra and the study of non-negative matrices and Markov chains Berman and Plemmons[3] Gantmacher[7] Rydén and Lindgren[11]. Apart from that some more properties of PageRank have been studied such as the convergence speed and its dependence on choice of damping factor c Haveliwala and Kamvar [8] and condition number Kamvar and Haveliwala [9].

In this article we will see that using a non-normalized version of PageRank using it is possible to find explicit expressions for PageRank for certain simple graphs. Some types of graphs have been previously studied such as a line of

New Trends in Stochastic Modeling and Data Analysis (*pp.* 135-144)
Raimondo Manca - Sally McClean - Christos H Skiadas (Eds)

vertices, complete graph or a combination of both Engström and Silvestrov [6], here we will take a look at another common type of graph, namely N-partite graphs. We will also consider both the case where the initial weight of vertices can differ and see how that influences the rank.

2 Notation and definitions

Traditionally PageRank is defined as in Def. 1.

Definition 1. PageRank $\boldsymbol{R}^{(1)}$ for vertices in system S consisting of n vertices is defined as the (right) eigenvector with eigenvalue one to the matrix:

$$M = c(\mathbf{A} + \boldsymbol{g}\boldsymbol{u}^\top)^\top + (1-c)\boldsymbol{u}\boldsymbol{e}^\top \tag{1}$$

where $\mathbf{A}$ is the adjacency matrix weighted such that the sum over every non-zero row is equal to one (size $n \times n$), $\boldsymbol{g}$ is a $n \times 1$ vector with zeros for vertices with outgoing edges and 1 for all vertices with no outgoing edges (dangling nodes), $\boldsymbol{u}$ is a $n \times 1$ non-negative vector with $||\boldsymbol{u}||_1 = 1$, $\boldsymbol{e}$ is a one-vector with size $n \times 1$ and $0 < c < 1$ is a scalar.

Usually $\boldsymbol{R}^{(1)}$ is also normalized such that $||\boldsymbol{R}^{(1)}||_1 = 1$ in which case PageRank can be seen as the stationary distribution of the Markov chain described by $\mathbf{M}^\top$ However we will use a slightly different version of PageRank (denoted $\boldsymbol{R}^{(3)}$ to keep consistent with previous work) as seen in Def. 2.

Definition 2. Consider a random walk on a graph with n vertices described by $\mathbf{A}$. We walk to a new vertex from our current with probability $0 < c < 1$ and stop the random walk with probability $1 - c$. Then PageRank $\boldsymbol{R}^{(3)}$ for a single vertex can be written as:

$$\boldsymbol{R}^{(3)}_j = \left(v_j + \sum_{e_i \in S, e_i \neq e_j} v_i P(e_i \to e_j) \right) \left(\sum_{k=0}^{\infty} (P(e_j \to e_j))^k \right) \quad . \tag{2}$$

where $P(e_i \to e_j)$ is the probability to hit node e_j in a random walk starting in node e_i. This can be seen as the expected number of visits to e_j if we do multiple random walks, starting in every vertex a number of times desribed by $\boldsymbol{V} = [v_1 \ v_2 \ \ldots v_n]^\top$.

We note that $\boldsymbol{V}$ corresponds to $\boldsymbol{u}$ in the original definition, except that it does not need to have a unit norm. While the definition might look very different it is worth to note that the two versions of PageRank are proportional ($\boldsymbol{R}^{(3)} \propto \boldsymbol{R}^{(1)}$), as can be seen for a very similar definition used in Engström *et al.*[5] and in a similar proof here for $\boldsymbol{R}^{(3)}$.

Theorem 1. *PageRank as defined in Definition 2 is equivalent to:*

$$\boldsymbol{R}^{(3)} = \frac{\boldsymbol{R}^{(1)}||\boldsymbol{v}||_1}{d}, \ d = 1 - \sum c\mathbf{A}^\top \boldsymbol{R}^{(1)} \tag{3}$$

where $\boldsymbol{v}$ is a non-negative weight vector such that $\boldsymbol{u} \propto \boldsymbol{v}$. Hence $\boldsymbol{R}^{(3)} \propto \boldsymbol{R}^{(1)}$ since they only differ by some scaling factor.

Proof. Starting with Def. 2:

$$\boldsymbol{R}_j^{(3)} = \left(\sum_{e_i \in S, e_i \neq e_j} v_i P(e_i \to e_j) + v_j \right) \left(\sum_{k=0}^{\infty} (P(e_j \to e_j))^k \right) \quad . \tag{4}$$

$(c\mathbf{A}^\top)^k_{ij}$ is the probability to be in vertex e_i starting in vertex e_j after k steps. Multiplying with the vector $\boldsymbol{v}$ therefore gives the sum of all the probabilities to be in node e_i after k steps starting in every node once weighted by $\boldsymbol{v}$. The expected total number of visits is the sum of all probabilities to be in node e_i for every step starting in every node:

$$\boldsymbol{R}_j^{(3)} = \left(\left(\sum_{k=0}^{\infty} (c\mathbf{A}^\top)^k \right) \boldsymbol{v} \right)_j \quad .$$

$\sum_{k=0}^{\infty} (c\mathbf{A}^\top)^k$ is the Neumann series of $(\mathbf{I} - c\mathbf{A}^\top)^{-1}$ which is guaranteed to converge since $c\mathbf{A}^\top$ is non-negative and have column sum < 1. This gives:

$$\boldsymbol{R}^{(3)} = \left(\left(\sum_{k=0}^{\infty} (c\mathbf{A}^\top)^k \right) \boldsymbol{v} \right) = (\mathbf{I} - c\mathbf{A}^\top)^{-1} \boldsymbol{v} \quad .$$

We continue by rewriting $\boldsymbol{R}^{(1)}$:

$$\boldsymbol{R}^{(1)} = \mathbf{M}\boldsymbol{R}^{(1)} \Leftrightarrow (\mathbf{I} - c\mathbf{A}^\top)\boldsymbol{R}^{(1)} = (c\boldsymbol{u}\boldsymbol{g}^\top + (1-c)\boldsymbol{u}\boldsymbol{e}^\top)\boldsymbol{R}^{(1)} \quad .$$

Looking at the right hand side we get:

$$(c\boldsymbol{u}\boldsymbol{g}^\top + (1-c)\boldsymbol{u}\boldsymbol{e}^\top)\boldsymbol{R}^{(1)} = \left(1 - c + c\sum \boldsymbol{R}_a^{(1)}\right)\boldsymbol{u} = \left(1 - c\sum \mathbf{A}^\top \boldsymbol{R}^{(1)}\right)\boldsymbol{u}$$

where $\boldsymbol{R}_a^{(1)}$ is the PageRank of all vertices with no outgoing edges. This gives:

$$\boldsymbol{R}^{(1)} = (\mathbf{I} - c\mathbf{A}^\top)^{-1} \left(1 - c\sum \mathbf{A}^\top \boldsymbol{R}^{(1)}\right)\boldsymbol{u} \quad . \tag{5}$$

From (3) we have

$$\boldsymbol{R}^{(3)} = \frac{\boldsymbol{R}^{(1)}||\boldsymbol{v}||_1}{d} \Rightarrow \boldsymbol{R}^{(1)} = \frac{\boldsymbol{R}^{(3)} d}{||\boldsymbol{v}||_1} \quad . \tag{6}$$

Substituting (6) into (5) gives:

$$\boldsymbol{R}^{(3)} = (\mathbf{I} - c\mathbf{A}^\top)^{-1} \frac{||\boldsymbol{v}||_1}{d} \left(1 - c\sum \mathbf{A}^\top \boldsymbol{R}^{(1)}\right)\boldsymbol{u} \quad .$$

Since $d = 1 - \sum c\mathbf{A}^\top \boldsymbol{R}^{(1)}$ and $\boldsymbol{v} = ||\boldsymbol{v}||_1 \boldsymbol{u}$ we end up with

$$\boldsymbol{R}^{(3)} = (\mathbf{I} - c\mathbf{A}^\top)^{-1} \boldsymbol{v} \quad .$$

Which is the same as what we got using Def. 2. □

By considering PageRank as defined in Def. 2 we can quite easily find the rank for some different simple types of graph structures we would not as easily be able to using Def. 1. This comes mainly from the fact that using PageRank $\boldsymbol{R}^{(3)}$ as defined in 2, it is obvious that a vertex can only influence the rank of other vertices to which there is a path and that the number of vertices does not have any influence on the rank of individual vertices. Neither of which is true for $\boldsymbol{R}^{(1)}$.

3 Bipartite graph

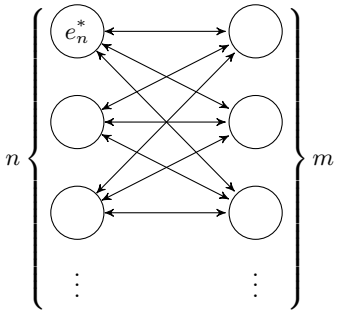

Fig. 1. Bipartite graph with n vertices on one side and m vertices on the other.

Theorem 2. *Consider a Bipartite graph with n vertices G_n on one side and m vertices G_m on the other. Let weight vector $\boldsymbol{V}$ be the one vector, then PageRank for one vertex $e_n^* \in G_n$ on the side with n vertices $R_{e_n^*}^{(3)}$ can be written:*

$$R_{e_n^*}^{(3)} = \frac{n + mc}{n - nc^2} \ . \tag{7}$$

To get the rank of a vertex on the other side, simply swap n and m with eachother.

Proof. We will use the definition of PageRank as defined in Def. 2. Let $e_n \in G_n$ and $e_m \in G_m$. We then have

$$P(e_m \to e_n^*) = \frac{c}{n} + \frac{(n-1)c}{n} cP(e_m \to e_n^*) \ . \tag{8}$$

Where the probability to reach e_n^* is written recursively as the probability to reach e_n^* in one step plus the probability that we reach e_n^* times the probability that we are back in any other state in G_n than the one we want to reach. Using this to rewrite (8) we get:

$$\left(1 - \frac{(n-1)c^2}{n}\right) P(e_m \to e_n^*) = \frac{c}{n} \ .$$

$$\Leftrightarrow P(e_m \to e_n^*) = \frac{c}{n}\frac{1}{\left(\frac{n-(n-1)c^2}{n}\right)} = \frac{c}{(n-(n-1)c^2)} \ . \tag{9}$$

If we instead start on the same side as the target vertex we get the probability as by first stepping once to the other side and use the previous results.

$$P(e_n \to e_n^*) = cP(e_m \to e_n^*) = \frac{c^2}{(n-(n-1)c^2)} \ . \tag{10}$$

The probability to get to e_n^* starting in e_n^* is the same as if we start in any other vertex on the same side.

$$P(e_n^* \to e_n^*) = P(e_n \to e_n^*) \ . \tag{11}$$

From 2 we can write the pageRank as:

$$R_{e_n^*}^{(3)} = (1 + mP(e_m \to e_n^*) + (n-1)P(e_n \to e_n^*)) \left(\sum_{k=0}^{\infty} P(e_n^* \to e_n^*)\right) \ .$$

Using (9) (10) and (11) we get:

$$\begin{aligned} R_{e_n^*}^{(3)} &= \left(1 + \frac{mc}{(n-(n-1)c^2)} + \frac{(n-1)c^2}{(n-(n-1)c^2)}\right)\left(\frac{n-(n-1)c^2}{n-(n-1)c^2-c^2}\right) \\ &= \frac{n-(n-1)c^2+mc+(n-1)c^2}{n-(n-1)c^2-c^2} = \frac{n+mc}{n-nc^2} \ . \end{aligned}$$

□

It is obvious that increasing the number of vertices on one side, decreases the rank of all the vertices on that side, while at the same time it increases the rank of those on the other side. We also note that in the symmetric case $n = m$, then this can be simplified to

$$\frac{n+nc}{n-nc^2} = \frac{1+c}{1-c^2} = \frac{1+c}{(1+c)(1-c)} = \frac{1}{1-c} \ .$$

This is the same as for a complete graph, and what we would expect for any strongly connected symmetric graph with no edges leading out of the graph.

3.1 Weighted bipartite graph

Theorem 3. *Consider a Bipartite graph with n vertices G_n on one side and m vertices G_m on the other. Then PageRank for one vertex $e_n^* \in G_n$ vertices $R_{e_n^*}^{(3)}$ can be written:*

$$R_{e_n^*}^{(3)} = \left(v_{e_n^*}\left(n-(n-1)c^2\right) + \sum_{e_m^i \in G_m} v_{e_m^i}\, c + \sum_{\substack{e_n^i \in e_n \\ e_n^i \neq e_n^*}} v_{e_n^i} c^2\right) \frac{1}{n-nc^2} \tag{12}$$

To get the rank of a vertex e_m^* on the other side, simply swap n and m with eachother.

Proof. Using (2) and taking the sum of the weights over vertices in G_n and G_m separately we get:

$$R^{(3)}_{e^*_n} = \left(v_{e^*_n} + \sum_{e^i_m \in G_m} v_{e^i_m} P(e_m \to e^*_n) + \right) \left(\sum_{k=0}^{\infty} P(e^*_n \to e^*_n) \right) + \left(\sum_{\substack{e^i_n \in G_n \\ e^i_n \neq e^*_n}} v_{e^i_n} P(e_n \to e^*_n) \right) \left(\sum_{k=0}^{\infty} P(e^*_n \to e^*_n) \right) \ .$$

Adding different weights obviously does not change the probabilities $P(e^*_n \to e^*_n)$, $P(u^*_n \to e^*_n)$. Using (9), (10) and (11) we get:

$$R^{(3)}_{e^*_n} = \left(v_{e^*_n} + \sum_{e^i_m \in G_m} \frac{v_{e^i_m} c}{(n-(n-1)c^2)} \right) \left(\frac{n-(n-1)c^2}{n-(n-1)c^2-c^2} \right) + \left(\sum_{\substack{e^i_n \in G_n \\ e^i_n \neq e^*_n}} \frac{v_{e^i_n} c^2}{(n-(n-1)c^2)} \right) \left(\frac{n-(n-1)c^2}{n-(n-1)c^2-c^2} \right) \ .$$

$$= \left(v_{e^*_n} \left(n-(n-1)c^2\right) + \sum_{e^i_m \in G_m} v_{e^i_m} c + \sum_{\substack{e^i_n \in G_n \\ e^i_n \neq e^*_n}} v_{e^i_n} c^2 \right) \frac{1}{n-nc^2} \ .$$

□

We note that Theorem 3 can also be used to find the rank of the vertices in a bipartite graph even if it is part of a larger graph with potentially some other edges from vertices outside the N-partite graph pointing at some of the vertices in the N-partite graph. This since assuming the bipartite graph itself does not have any edges to the outside, the return probability $\sum_{k=0}^{\infty} P(e_i \to e_i)^k$ will remain unchanged for vertices within the bipartite graph. If we know $R^{(3)}$ for the vertices outside the bipartite graph we can find new weights $\boldsymbol{v}_{e_i}$ by calculating

$$\boldsymbol{v}_{e_i} = \boldsymbol{v}_{e_i} + \sum_{\substack{j \to i \\ j \notin G_P}} \frac{c}{n_j} \boldsymbol{R}^{(3)}_{e_j} \ .$$

Here $j \to i$ denotes that there is an edge from vertex e_j to vertex e_i and n_j is the number of edges from e_j. This is similar to how it is done when removing 'dangling nodes' in the usual PageRank algorithm as in for example Andersson and Silvestrov[1] and how we can find formulas for many other types of graphs made up of more than one component Engström and Silvestrov[6].

Using Theorem 3 we notice a couple of things, first of all increasing one's own weight (through links from the outside or by itself) will always give a more or less linear increase in rank (more if n is small). Apart from that, we can also see that increasing the weight of said vertex gives a higher increase in rank for those on the other side than those on the same side (assuming $n \approx m$). We can also see that the number of vertices on the other side have no influence on the rank, only their combined weight. On the other hand the number of vertices on the same side is very important for the rank, the fewer vertices on the same side the higher the rank.

3.2 N-partite graph

Theorem 4. *Consider a N-partite graph with n vertices in every group of vertices and N groups of vertices $G_1, G_2, \ldots, G_N$. Let $\boldsymbol{V}$ be the one vector, then PageRank $R^{(3)}_{e^*_n}$ for one vertex $e^*_n \in G_n$ can be written:*

$$R^{(3)}_{e^*_n} = \frac{1}{1-c} \ . \tag{13}$$

For $N \geq 2$ and $n \geq 1$.

Proof. First we note that if $N = 1$ there would be no edges between any pair of vertices, hence we require $N \geq 2$. We let $e^i_j \in G_j$ and let

$$e^i_u \in G_u = \bigcup_{\substack{r=1,..N \\ r \neq j}} G_r \ .$$

Using the definition in Def. 2 we find the probability to reach e^*_j by writing it recursively.

$$P(e_u \to e^*_j) = \frac{c}{(N-1)n} + \frac{c(N-2)}{N-1} P(e_u \to e^*_j) + \frac{c(n-1)}{(N-1)n} cP(e_u \to e^*_j) \ . \tag{14}$$

Here the first term is the probability to end up in e^*_j in one step, the second is found by first going to any other vertex in G_u and the last by first going to any other vertex except e^*_j in G_j and back to G_u. Rewriting (14) we get:

$$\left(1 - \frac{c(N-2)}{N-1} - \frac{c^2(n-1)}{(N-1)n}\right) P(e_u \to e^*_j) = \frac{c}{(N-1)n}$$

$$\Leftrightarrow P(e_u \to e^*_j) = \frac{c}{(N-1)n - c(N-2)n - c^2(n-1)} \ . \tag{15}$$

The probability to reach e^*_j is obviously the same regardless of which vertex in G_j we start in. This probability can easily be found as the first step from there alwys takes us to G_u:

$$\begin{aligned} P(e^*_j \to e^*_j) &= P(e_j \to e^*_j) = cP(e_u \to e^*_j) \\ &= \frac{c^2}{(N-1)n - c(N-2)n - c^2(n-1)} \ . \end{aligned} \tag{16}$$

We assign

$$k = (N-1)n - (N-2)nc - c^2(n-1) \ . \tag{17}$$

We write the PageRank $R^{(3)}_{e^*_j}$ using (2) grouping the vertices in G_j and G_u separately giving:

$$R^{(3)}_{e^*_j} = \left(1 + (n-1)P(e_j \to e^*_j) + (N-1)nP(e_u \to e^*_j)\right)\left(\sum_{k=0}^{\infty} P(e^*_j \to e^*_j)^k\right) \ .$$

Using (15), (16) and (17) we end up with:

$$\begin{aligned} R^{(3)}_{e^*_j} &= \left(\frac{k}{k} + \frac{(n-1)c^2}{k} + \frac{(N-1)nc}{k}\right)\left(\frac{k}{k-c^2}\right) \\ &= \frac{k + (n-1)c^2 + (N-1)nc}{k-c^2} \ . \end{aligned}$$

Replacing k according to (15) once again and simplifying yields:

$$\begin{aligned} R^{(3)}_{e^*_j} &= \frac{(N-1)n - c(N-2)n - c^2(n-1) + (n-1)c^2 + (N-1)nc}{(N-1)n - c(N-2)n - c^2(n-1) - c^2} \ . \\ &= \frac{(N-1)n + nc}{(N-1)n - (N-2)nc - nc^2} = \frac{(N-1)+c}{(N-1) - (N-2)c - c^2} \ . \\ R^{(3)}_{e^*_j} &= \frac{(N-1)+c}{((N-1)+c)\,(1-c)} = \frac{1}{1-c} \ . \end{aligned}$$

Where we in the last step factorize and simplify since the nominator is a factor of the denominator. □

3.3 Weighted N-partite graph

Theorem 5. *Consider a N-partite graph with n vertices in every group of vertices and $N > 1$ groups of vertices $G_1, G_2, \ldots, G_N$ and weight vector $\boldsymbol{V}$ then PageRank $R^{(3)}_{e^*_n}$ for one vertex $e^*_j \in G_j$ can be written:*

$$\begin{aligned} R^{(3)}_{e^*_j} = \frac{v_{e^*_j}\left((N-1)n - (N-2)nc - c^2(n-1)\right)}{(N-1)n - (N-2)nc - nc^2} \\ + \frac{\sum_{e^i_j \in G_j,\, e^i_j \neq e^*_j} v_{e^i_j} c^2 + \sum_{e^i_u \in G_u} v_{e^i_u} c}{(N-1)n - (N-2)nc - nc^2} \ , \end{aligned} \tag{18}$$

where $e^i_j \in G_j$ and

$$e^i_u \in G_u = \bigcup_{\substack{r=1,\ldots N \\ r \neq j}} G_r \ .$$

For $N \geq 2$ and $n \geq 1$.

Proof. Like for the bipartite case changing the weights does not change any of $P(e_j \to e_j^*)$, $P(e_u \to e_j^*)$. From (2) and using the results in (15) and (16) gives:

$$\begin{aligned} R_{e_j^*}^{(3)} &= \left(v_{e_j^*} + \sum_{\substack{e_j^i \in G_j \\ e_j^i \neq e_j^*}} v_{e_j^i} P(e_j \to e_j^*) \right) \left(\sum_{k=0}^{\infty} P(e_j^* \to e_j^*)^k \right) \\ &\quad + \left(\sum_{e_u^i \in G_u} v_{e_u^i} P(e_u \to e_j^*) \right) \left(\sum_{k=0}^{\infty} P(e_j^* \to e_j^*)^k \right) \\ &= \left(\frac{v_{e_j^*} k}{k} + \sum_{\substack{e_j^i \in G_j \\ e_n^i \neq e_j^*}} v_{e_j^i} \frac{c^2}{k} + \sum_{e_u^i \in G_u} v_{e_u^i} \frac{c}{k} \right) \left(\frac{k}{k - c^2} \right) , \end{aligned}$$

where k is as defined in (17). After some simple rewriting we end up with:

$$\begin{aligned} R_{e_j^*}^{(3)} = \frac{v_{e_j^*} \left((N-1)n - (N-2)nc - c^2(n-1) \right)}{(N-1)n - (N-2)nc - nc^2} \\ + \frac{\sum_{\substack{e_j^i \in G_j \\ e_j^i \neq e_j^*}} v_{e_j^i} c^2 + \sum_{e_u^i \in G_u} v_{e_u^i} c}{(N-1)n - (N-2)nc - nc^2} , \end{aligned}$$

□

Similar to the weighted bipartite graph, Theorem 5 can also be used to find the rank of vertices not only for different weight configurations $\boldsymbol{V}$ but also if there are some other outside vertices linking to the N-partite graph. We can see that with an increased weight v_{e_i} we get more or less a constant increase in rank of vertex e_i. As before the weight of vertices in other groups give a higher increase in rank to vertices in other groups than the other vertices in the same group.

We note that this also gives the PageRank of vertices in a complete graph (graph where every vertex link to every other) with weighted vertices. By setting $n = 1$ we get the complete graph with PageRank:

$$R_{e_j^*}^{(3)} = \frac{v_{e_j^*} \left((N-1) - (N-2)c \right) + \sum_{e_u^i \in G_u} v_{e_u^i} c}{(N-1) - (N-2)c - c^2} . \tag{19}$$

It is worth to note that if we assume $\boldsymbol{V}$ is the one vector we end up with:

$$R_{e_j^*}^{(3)} = \frac{((N-1) - (N-2)c) + (N-1)c}{(N-1) - (N-2)c - c^2} = \frac{(N-1) + c}{((N-1) + c)(1-c)} = \frac{1}{1-c} .$$

We note that while N does not affect PageRank in the unweighted complete graph, if we allow weights for vertices to be different it does. We see that increasing ones own initial weight $\boldsymbol{v_i}$ with w increases rank by a factor $w/(1-c)$ while it increases the rank of everyone else by a lower amount $wc/((N-1) - (N-2)c - c^2)$, typically much lower unless N is very small.

4 Conclusions

We have seen that using a non-normalized version of PageRank and a probabilistic view we can find explicit expressions for some simple type of graphs such as N-partite graphs. This could be done in both the case with unweighted vertices as well as when they have different weights v_i. For the unweighted case we get very simple expressions, while for the weighted case we need to include a couple of sums of weights over different types of vertices.

Using the found expressions for the rank in our examples we could also see that it is easy to make some conclusions about the rate of change in rank if for example the number of vertices or their weights change as well as the influence of an outside vertex linking to one of the vertices in the N-partite graph.

Acknowledgments

This research was supported in part by the Swedish Research Council (621-2007-6338), Swedish Foundation for International Cooperation in Research and Higher Education (STINT), Royal Swedish Academy of Sciences, Royal Physiographic Society in Lund and Crafoord Foundation.

References

1. Andersson, F., and Silvestrov, S., "The Mathematics of Internet Search Engines", *Acta Appl. Math.* (2008) 104:211-242
2. Battiston, S., and Puliga, M., and Kaushik, R., and Tasca, P., and Calderelli, G., DeptRank: Too Central to Fail? Financial Networks, the FED and Systemic RiskMacmillan Publishers Limited (2012).
3. Berman, A. and Plemmons, R.J.*Nonnegative Matrices in the Mathematical Sciences*, Number del 11 in Classics in Applied Mathematics.
4. Brin, S., and Page, L. "The Anatomy of a Large-Scale Hypertextual Web Search Engine" *Computer Networks and ISDN Systems*, 30(1-7):107, 1998 Proceedings of the Seventh International World Wide Web Conference
5. Engström, C., and Silvestrov, S., and Hamon, T. "Variations of PageRank with application to linguistic data" in *Applied Stochastic Models and Data Analysis (ASMDA 2013). The 15th Conference of the ASMDA International Society* pages E-I, 9-18, 2013.
6. Engström, C., and Silvestrov, S. "PageRank for evolving link structures", *preprint*, CoRR. abs/1401.6092, http://arxiv.org/abs/1401.6092
7. Gantmacher, F.R. *The Theory of matrices. Gantmacher*, (1959).
8. Haveliwala, T., and Kamvar, S. "The Second Eigenvalue of the Google Matrix" Technical Report 2003-20, Stanford InfoLab (2003).
9. Kamvar, S., and Haveliwala, T. "The Condition Number of the PageRank Problem" Technical Report 2003-36, Stanford InfoLab (2003).
10. Kamvar, S. D., and Schlosser, M. T., and Garcia-Molina, H. "The Eigentrust algorithm for reputation management in P2P networks" in *Proceedings of the 12th international conference on World Wide Web*, WWW '03, pages 640-651 (2003).
11. Rydén, T., and Lindgren, G. *Markovprocesser*(in swedish), Univ. Lund (2000).

4 CHAPTER

Survival Analysis and Branching Processes

Stochastic Modelings in Software Reliability

Nuria Torrado[1]

Centre for Mathematics
University of Coimbra, Coimbra, Portugal
(e-mail: nuria.torrado@gmail.com)

Abstract. The reliability of software systems has become a major concern for our modern society because the demand for complex software systems has increased within the first decade of the 21st century. A software reliability model (SRM) is a mathematical tool to evaluate the software quantitatively. A large number of models have been proposed in the literature to predict software failures (see, e.g. Singpurwalla and Wilson[18]), but a few incorporate some significant metrics data observed in software testing. In this work, we present a new procedure to predict numbers of software failures using metrics information, from a Bayesian perspective. This new Bayesian software reliability model has been developed in collaboration with R.E. Lillo and M.P. Wiper (see Torrado *et al.*[19]).
Keywords: nonhomogeneous Poisson process, software failures, Bayesian statistical methods.

1 Introduction

Software reliability is defined as the probability that the software will function without failure under given environmental conditions during a specified period of time. Most software reliability models (SRMs) are based on the assumption that the software is possibly imperfectly corrected after each failure or after various fixed time periods. Often, it will be the case that information in the form of software metrics such as code length or complexity will be generated each time the software is corrected. See Fenton and Pfleeger[4] for a review of the main ideas.

From a statistical point of view, the random variables that characterize software reliability are the epoch times in which a failure of software takes place or the times between failures. Most of the well known models for software reliability are centered around the interfailure times or the point processes that they generate. A software reliability model specifies the general form of the dependence of the failure process on the principal factors that affect it: fault introduction, fault removal, and the operational environment.

A number of analytical models have been proposed for software reliability assessment. For good recent reviews till 2007 see e.g. the book by Pham[12].

Most of the works in the literature are devoted to estimate model parameters. Some important early references are Jelinski and Moranda[6], Moranda[10],

New Trends in Stochastic Modeling and Data Analysis (pp. 147-157)
Raimondo Manca - Sally McClean - Christos H Skiadas (Eds)

Goel and Okumoto[5], Littlewood and Verrall[7], Mazzuchi and Soyer[9], Musa and Okumoto[11], among others.

Some interesting software reliability modelling developed in the last two decades can be found in Boland and Singh[1], Rinsaka *et al.*[15], Shibata *et al.*[17], Wiper[20], Pievatolo *et al.*[13] and Torrado *et al.*[19].

In this paper, we shall develop an alternative approach to both Type I and Type II software reliability models based on exponential interfailure times or Poisson failure counts where the rates are modeled as Gaussian processes where software metrics data are used as inputs. This approach may be thought of as an extension of the work of Ray *et al.*[14] which generalizes this earlier, parametric regression based method to a nonparametric regression model.

Rather than use classical statistical inference techniques we shall here adopt a Bayesian approach, which has the advantages of being able to take into account any prior information available and also of taking parameter uncertainty into account when prediction of reliability is undertaken. Starting from Littlewood and Verrall[7], Bayesian approaches to many software reliability models have been considered.

In the article and in the presentation a short overview on the wide field of Bayesian inference in software reliability model is given, showing some results given by Torrado *et al.*[19] and also some of the current research the author is doing currently.

2 Short review on software reliability modeling

The use of statistical methods in software engineering has been increasing in the last decades. In the context of this discipline, as we defined above, software reliability measures the probability that a piece of software runs without failing under certain operational conditions for a given time. In software testing, software is run under an operational profile, that is certain conditions simulating real usage and after a given test period, the software is modified in order to correct any observed faults. Testing then proceeds until the software is judged sufficiently reliable for release.

A software reliability model (SRM) is a mathematical tool to evaluate the software quantitatively. The SRM's have been extensively developed in the literature. Most SRM's are based on stochastic counting processes, such as binomial process, pure birth process and nonhomogeneous Poisson process (NHPP). One may refer to two excellent books by Singpurwalla and Wilson[18] and Pham[12] on this topic. These stochastic models attempt to model either the times between successive failures of a piece of software or the number of failures in fixed time periods. Our classification scheme (see Figure 1) follows that of Singpurwalla and Wilson[18], and divides models into two types: Type I and Type II.

Type I models are those that model the times between successive failures. Under these types of models, the random variables $T_1, T_2, \ldots$, are modeled directly. This is often done by specifying the failure rate function for each random variable, h_i, $i = 1, 2, \ldots$, an then invoking the exponentiation formula to obtain their survival function, $\bar{F}_i$. Typically, each h_i is a nondecreasing

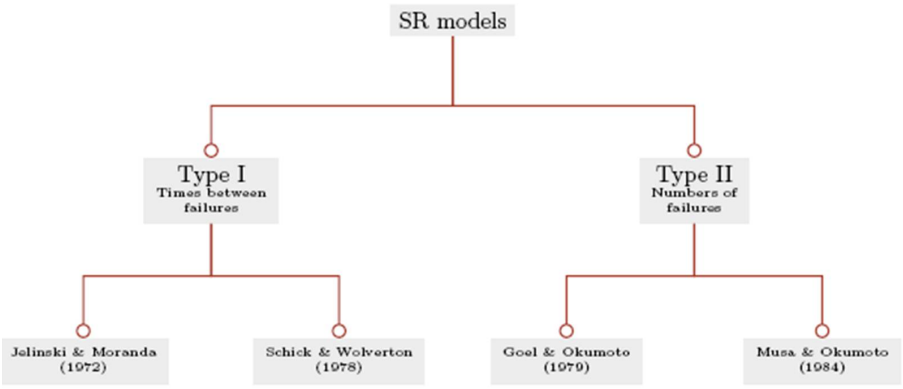

Fig. 1. Classification of software reliability (SR) models

function on t, for $t \geq 0$ to reflect the fact that between failures the reliability of the software increases.

Type II models are those that model the number of failures up to a given time. These models are based on stochastic counting processes for $N(t)$, the number of times the software fails in an interval $[0, t]$. The earliest and best known Type II models are those which assume that $N(t)$ is described by a Poisson process whose mean value function is based on assumptions about how the software experiences failure.

It is remarkable that a model of either type defines a model of the other. Specifically, for a sequence of interfailure times $T_1, T_2, \ldots$, for which a Type I model has been proposed, there is an implicit Type II model (cf. Singpurwalla and Wilson[18]), because

$$N(t) = \max \left\{ n \mid \sum_{i=1}^{n} T_i \leq t \right\},$$

and conversely, for a Type II model there is a Type I model, because with $T_0 = 0$, and $i = 2, 3, \ldots$,

$$T_i = \inf \{t \mid N(t) = i\} - T_{i-1}.$$

It is noteworthy two differences between Type I and Type II models. First, the total number of potential failures of Type II models is assumed to be infinite, so that the number of observed failures is a random variable having a Poisson distribution, as opposed to a fixed number of faults N that is assumed by Type I models. Second, in the Type II models the interfailure times are dependent whereas in the Type I models they were typically assumed independent.

2.1 Type I models

The Type I group of models is used to study the program hazard rate per fault at the failure intervals. The hazard rate function of the i'th interfailure time of some of these models are reported in Table 1.

Table 1. Some Type I software reliability models

$h_i(t) = \phi\,(N - i + 1)$	$h_i(t) = D\,k^{i-1}$
$h_i(t) = \phi\,(N - p(i-1))$	$h_i(t) = \phi\,(N - i - 1)\,t$

The first model to be widely known and used is the model by Jelinski and Moranda[6] (hereafter JM). They assume that the software contains an unknown number, say N, of faults and that each time the software fails, a bug is detected and perfectly corrected. Furthermore, the failure rate of T_i is proportional to $N - i + 1$, the number of faults remaining in the code, that is, for some constant $\phi > 0$, the hazard rate at the i'th failure interval is given by

$$h_i(t) = \phi\,(N - i + 1)\,, \quad i = 1, \ldots, N.$$

The survival function is

$$\bar{F}_i(t) = e^{-\phi(N-i+1)t}, \quad i = 1, \ldots, N.$$

The property of this model is that the failure rate is constant and the software during the testing stage is unchanged or frozen.

A modification to the JM model is the *Geometric Model* developed by Moranda[10]. He proposed a new model in which the program failure rate function is initially a constant D and decreases geometrically at failure times. In this case, the hazard rate function of the i'th interfailure times is

$$h_i(t) = D\,k^i,$$

and its survival function is

$$\bar{F}_i(t) = e^{-t\,D\,k^i},$$

where $D > 0$ is the initial program failure rate and k is the parameter of a geometric function ($0 < k < 1$).

Goel and Okumoto[5] extend the JM model by assuming that a fault is removed with probability p whenever a failure occurs. This model is called the *JM model with imperfect debugging* and the hazard rate function of time between failures when the imperfect debugging is at the i'th failure interval becomes

$$h_i(t) = \phi\,(N - p(i-1))\,.$$

The survival function is

$$\bar{F}_i(t) = e^{-\phi(N-p(i-1))\,t}, \quad i = 1, \ldots, N.$$

The model by Jelinski and Moranda is a special case of the preceding when $p = 1$.

The model by Schick and Wolverton[16] (hereafter SW) is another modification of the JM model. They assumed that the hazard rate of T_i is proportional to both the number of remaining faults in the software and the elapsed time since last failure. Thus, the hazard rate function between the $(i-1)$'th and the i'th failure can be expressed as

$$h_i(t) = \phi\,(N - i - 1)\,t,$$

where ϕ and N are the same as that defined in the JM model.

2.2 Type II models

In this subsection we shall describe briefly some Type II software reliability models. The models described here are only a small subset of those which appear in the literature.

The Type II models provide another analytical framework for describing the software failure phenomenon during testing. Recall that in this case, we look at $N(t)$ as the number of failures to time t. Then, $N(t)$ is modeled by a Poisson distribution with mean $\Lambda(t)$, that is, $\mathbb{E}\,[N(t)] = \Lambda(t)$. Under such models the reliability of the software for a mission of duration t is simply $\Pr(N(t) = 0)$.

The Goel-Okumoto model [5], referred to hereafter as GO, is a NHPP variant of the JM model. The GO model assumes that the cumulative number of failures detected by time t is a NHPP and its expectation could be described by the mean value function

$$\Lambda(t) = a(1 - e^{-bt}). \tag{1}$$

The intensity function is

$$\lambda(t) = \frac{d\Lambda(t)}{dt} = abe^{-bt}.$$

Observe that $\Delta(t) < \infty$ as $t \to \infty$. Therefore, this model cannot be applied to situations where new faults might be introduced in the process of debugging. Some NHPP models can incorporate the situation where new faults may be added during repairs, these models are the infinite failures models. It means that $\Delta(t) \to \infty$ as $t \to \infty$.

The Duane model [3], referred to hereafter as DU, originally devised for hardware reliability model, is an infinite failures model. This model is a NHPP with the expected number of failures

$$\Lambda(t) = at^b, \tag{2}$$

and the intensity function

$$\lambda(t) = abt^{b-1}.$$

This function is increasing for $b > 1$, decreasing for $b < 1$ and constant for $b = 1$. The DU model could be stochastically represented as a Weibull process, allowing for statistical procedures to be used in the application of this model

in reliability growth. In particular, this model is the counting process of the record values from a Weibull distribution.

In these NHPP models, usually parameter a represents the mean number of software failures that will eventually be detected, and parameter b represents the probability that a failure is detected in a constant period.

Musa and Okumoto[11] proposed another model for infinite failures. This NHPP is also called the *logarithm Poisson model*, referred to hereafter as MO. The mean value function is

$$\Lambda(t) = a\,\ln(1+bt), \quad t > 0,$$

and the intensity function is derived as

$$\lambda(t) = \frac{ab}{1+bt}.$$

Let us mention an homogeneous pure birth process, referred to hereafter as HPBP, for software reliability which is another variation of the JM model. This model, proposed by Boland and Singh[1], is a birth process approach to the geometric SRM. In this case, the cumulative number of failures detected by time t is a HPBP with birth rates

$$\lambda_i = D \cdot k^i, \quad i = 0, 1, \ldots.$$

Boland and Singh[1] showed that the mean value function is

$$\Lambda(t) = Dt + \sum_{i=1}^{\infty}(-1)^i \frac{(Dt)^{i+1}}{(i+1)!}\prod_{j=1}^{i}(1-k^j),$$

and the intensity function

$$\lambda(t) = D\left(1 + \sum_{i=1}^{\infty}(-1)^i \frac{(Dt)^i}{i!}\prod_{j=1}^{i}(1-k^j)\right).$$

Other types of mean value functions suggested by Yamada and Osaki[21], are the hyperexponential growth model and the Yamada-Osaki exponential growth model, respectively. Some of these models are reported in Table 2. For more details on software reliability models, see e.g. Pham [12] and Singpurwalla and Wilson[18].

3 A new software reliability model

In this subsection we present a new approach to both Type I and Type II software reliability models (see Section 2). Our model is a hierarchical non-parametric regression model based on exponential interfailure times or Poisson failure counts where the rates are modeled as Gaussian processes where software metrics data are used as inputs.

Table 2. Some Type II software reliability models

$\Lambda(t) = a\big(1 - \exp(-bt)\big)$	$\Lambda(t) = a\,\ln(1+bt)$
$\Lambda(t) = a\,t^b$	$\Lambda(t) = D\,t + \sum_{i=1}^{\infty}(-1)^i\,\frac{(D\,t)^{i+1}}{(i+1)!}\,\prod_{j=1}^{i}(1-k^j)$
$\Lambda(t) = \sum_{i=1}^{n} a_i\big(1 - \exp(-b_i t)\big)$	$\Lambda(t) = a\sum_{i=1}^{n} p_i\big(1 - \exp(-b_i t)\big)$

Gaussian process models have recently been used in Bayesian approaches to regression, classification and other areas. Formally, a Gaussian process is defined as following: A *Gaussian process* (hereafter GP) is a collection of random variables, any finite number of which have a joint Gaussian distribution.

It is well known that a GP is a generalization of the Gaussian probability distribution. Just as a Gaussian distribution is fully specified by its mean and covariance matrix, a GP is specified by a mean and a covariance function. We define the mean function $m(\boldsymbol{x})$ and the covariance function $C(f(\boldsymbol{x}), f(\boldsymbol{x}'))$ of a real process $f(\boldsymbol{x})$ as

$$\begin{aligned} m(\boldsymbol{x}) &= \mathbb{E}\left[f(\boldsymbol{x})\right], \\ C(f(\boldsymbol{x}), f(\boldsymbol{x}')) &= \mathbb{E}\left[\left(f(\boldsymbol{x}) - m(\boldsymbol{x})\right)\left(f(\boldsymbol{x}') - m(\boldsymbol{x}')\right)\right]. \end{aligned}$$

GPs are used in regression and classification problems. Here, we consider a regression problem where we have a data set $\mathcal{D}$ of M scalar observations with an arbitrary distribution with parameter λ_i and that the software being analyzed is possibly imperfectly corrected after each period. If we assume that we observe the times between successive M failures, say $T_1 = t_1, \ldots, T_M = t_M$, then, in this case, $\mathcal{D} = \{t_i : i = 1, \ldots, M\}$. We might also assume that interfailure times are exponentially distributed, that is,

$$T_i \mid \lambda_i \sim \mathcal{E}(\lambda_i).$$

When we assume that we observe the numbers of failures, say $N_1 = n_1, \ldots, N_M = n_M$ in M time periods of length $L_1, \ldots, L_M$ respectively, then $\mathcal{D} = \{n_i : i = 1, \ldots, M\}$. We also assume that the numbers of failures follows a Poisson distribution, that is, for $i = 1, \ldots, M$, we have

$$N_i \mid \lambda_i \sim \mathcal{P}(L_i\lambda_i)\,.$$

As part of the correction procedure, we shall suppose that after the $(i-1)$'th failure the software is possibly imperfectly corrected and software metrics, say $\boldsymbol{x}_i = (x_{i1}, \ldots, x_{ik})$ are generated for $i = 1, \ldots, M$. Such metrics may reflect both characteristics of the code such as number of lines or also measures of the amount of work undertaken on correction such as many hours or costs. Thus, it

is reasonable to suppose that changes in the quality of the code will be reflected in changes in the values of the software metrics.

In both cases, the rate, λ_i can be modeled as a function of the software metrics, $\boldsymbol{x}_i$, available after the last correction as

$$\ln \lambda_i \mid f_i = f(\boldsymbol{x}_i) + \epsilon_i, \tag{3}$$

where $\epsilon_i \sim N(0, \sigma^2)$ and $f : \Re^k \to \Re$ can take different forms. The most important problem to consider is how to model the unknown function, f. One possibility is to assume that f is a linear function of the software metrics, say

$$f(\boldsymbol{x}_i) = \beta_0 + \sum_{j=1}^{k} \beta_j \, x_{ij} \, ,$$

but there is quite a lot of evidence to illustrate that the relationship between software quality and software metrics is often highly non-linear and therefore, it seems preferable to use a more general, fully nonparametric model as for instance a GP model. Therefore, we have an approach to both Type I and Type II SR models which can be summarize, respectively, as following:

$$\begin{aligned} T_i \mid \lambda_i &\sim \mathcal{E}(\lambda_i), \\ \ln \lambda_i \mid f_i &= f(\boldsymbol{x}_i) + \epsilon_i, \\ \boldsymbol{f} \mid \boldsymbol{\theta} &\sim \mathcal{GP}(0, C(\boldsymbol{\theta})). \end{aligned} \qquad \begin{aligned} N_i \mid \lambda_i &\sim \mathcal{P}(L_i \lambda_i), \\ \ln \lambda_i \mid f_i &= f(\boldsymbol{x}_i) + \epsilon_i, \\ \boldsymbol{f} \mid \boldsymbol{\theta} &\sim \mathcal{GP}(0, C(\boldsymbol{\theta})). \end{aligned}$$

One possibility would be to use classical, nonparametric regression techniques, but here we prefer to use a Bayesian approach, as outlined in the next section.

4 A Bayesian approach to failure rate modeling

In this Section, we explain a Bayesian approach to software reliability modeling using Gaussian process prior distributions for the functional form, f. In our context, we propose using the Gaussian process as a prior distribution for the function f of (3). This, so called Gaussian process prior distribution is characterized by the form of the mean and covariance functions. Firstly, we assume that the mean function is $\mathbb{E}[f(\boldsymbol{x})] = 0$ and as covariance function we shall assume the *squared exponential covariance function* defined as

$$\mathbb{C}(f(\boldsymbol{x}_i), f(\boldsymbol{x}_j) \mid \boldsymbol{\theta}) = \eta^2 \exp\left\{ -\frac{1}{2} \sum_{\ell=1}^{k} \rho_\ell^{-2} \left(x_{i\ell} - x_{j\ell}\right)^2 \right\}, \tag{4}$$

where $\boldsymbol{\theta} = \left(\rho_1^2, \ldots, \rho_k^2, \eta^2\right)$ is the unknown parameter set, i.e., the *hyperparameter* set.

One advantage of the Gaussian process prior structure is that it leads to straightforward inference and prediction in the presence of normal noise. From (3), set $\zeta_i = \log \lambda_i$, when $\zeta_i = f(\boldsymbol{x}_i) + \epsilon_i$, for $i = 1, 2, \ldots$.

Assume now that for $i = 1, 2, \ldots$, the number of failures in a fixed time period of length T_i for the i'th release of the software follows a Poisson distribution and that the logged failure rate, ζ_i, is modeled as described above.

The basic Bayesian model is completed by defining prior distributions for the error variance, σ^2 and for the GP parameters, $\boldsymbol{\theta}$. Here, we assume inverse gamma priors, $\sigma^2 \sim \mathcal{IG}(\alpha_s, \beta_s)$, $\eta^2 \sim \mathcal{IG}(\alpha_e, \beta_e)$ and $\rho_j^2 \sim \mathcal{IG}(\alpha_{rj}, \beta_{rj})$, for $j = 1, \ldots, k$.

In Torrado *et al.*[19], we present an explicit and detailed Bayesian posterior inference for the failure rate model and applied this new model to three real data sets.

Our proposed model class includes many simpler models such as the JM model (see Section 2) which are independent of covariate information and also simpler regression functions. Furthermore, in many problems we may often have large numbers of metrics available and therefore, which model or which metrics to choose is an important problem. The standard approach to model selection in the classical context is to use selection criteria such as the Akaike or Bayesian information criterion. The most popular Bayesian selection criterion is the deviance information criterion (hereafter DIC). However, this criterion is highly dependent on the stability of the posterior (mean) parameter estimates and in the Gaussian process context, we have found that it is unstable. Therefore, we prefer to use a variant of the DIC, denoted DIC_3. This criterion is defined, for the Type II model with data $\boldsymbol{n} = (n_1, \ldots, n_M)$ and model $\mathcal{M}$ as

$$-4\,\mathbb{E}\left[\ln p(\boldsymbol{n}\boldsymbol{\theta}) \mid \boldsymbol{n}, \mathcal{M}\right] + 2\ln \widehat{p}(\boldsymbol{n} \mid \boldsymbol{n}, \mathcal{M}),$$

where

$$\widehat{p}(\boldsymbol{n} \mid \boldsymbol{n}, \mathcal{M}) = \prod_{i=1}^{M} \widehat{p}(n_i \mid \boldsymbol{n}, \mathcal{M}),$$

and

$$\widehat{p}(n_i \mid \boldsymbol{n}, \mathcal{M}) = \frac{1}{J}\sum_{j=1}^{J} p(n_i \mid \boldsymbol{n}, \lambda_{i,j}, \mathcal{M}) = \frac{1}{J}\sum_{j=1}^{J} \frac{\lambda_{i,j}^{n_i}\, e^{-\lambda_{i,j}}}{n_i!}.$$

This criterion is straightforward to calculate from the Markov Chain Monte Carlo (MCMC) output and, in our experience, gives much more satisfactory results than the DIC. As with the AIC and BIC, lower values of this criterion imply better fitting models.

5 Applications to a real data set

Finally, we present the analysis of a real data set, see Torrado *et al.*[19] for the analysis of two other real data sets.

The data set, referred to hereafter as DS, was presented by Dalal and McIntosh[2]. This data set consists of number of failures in given time periods and therefore can be analyzed using Type II models. DS contains approximately 400000 new or changed non-commentary source lines (hereafter NCNCSL), the staff time spent testing and the number of faults found. In order to undertake

Bayesian inference for the models described before, prior distributions for the GP parameter σ^2 and hyperparameters $\boldsymbol{\theta} = (\rho_1^2, \ldots, \rho_k^2, \eta^2)$ must be defined. As is typical in such problems, we shall assume independent, proper but relatively uninformative inverse gamma, $\mathcal{IG}(\alpha, \beta)$, priors, where $\alpha = \beta = 0.001$.

We shall consider three training sets for DS consisting of 99 (50%), 149 (75%) and 178 (90%) data, and three test sets consist of 99, 49 and 20 data, respectively. We then compute the estimated values of the deviance information criterion of our model using the new or changed noncommentary source lines (NCNCSL) as covariate. In order to study whether software metrics provide information to the model, we compare the GP model with two classical NHPP-SR models defined in Subsection 3. In particular, we shall consider a Bayesian approach to the GO model and the DU model as follows,

$$\begin{aligned} N_i \mid a, b &\sim \mathcal{P}(\Lambda(t_i)) \\ a &\sim \mathcal{G}(\alpha_a, \beta_a) \\ b &\sim \mathcal{G}(\alpha_b, \beta_b), \end{aligned}$$

where $\Lambda(t)$ is defined in (1) for the GO model and in (2) for the DU model.

Table 3. DIC_3 criterion for DS

75%	90%		
GP(NCNCSL)	299.80	517.90	625.73
GO-SRM	690.81	$1.0786e+003$	$1.2929e+003$
DU-SRM	694.12	$1.0744e+003$	$1.3161e+003$

From Table 3, it can be seen that our model can give the smallest DIC_3 value, i.e., in the estimation of software failure data is appropriate to use software metrics information.

Acknowledgements

This work is supported by the Centro de Matemática da Universidade de Coimbra (CMUC), funded by the European Regional Development Fund through the program COMPETE and by the Portuguese Government through the FCT - Fundação para a Ciência e a Tecnologia, under the project PEst-C/MAT/UI0324/2013.

References

1. P.J. Boland and H. Singh. A Birth-Process Approach to Moranda's Geometric Software Reliability Model, *IEEE Transactions on Reliability*, 52, 168–174, 2003.
2. S.R. Dalal and A.A. McIntosh. When to stop testing for large software systems with changing code, *IEEE Trans. Software Engineering*, 20, 318–323, 1994.

3. J.T. Duane. Learning curve approach to reliability monitoring, *IEEE Trans. Aerospace*, 2, 563–566, 1964.
4. N.E. Fenton and S.L. Pfleeger. *Software Metrics: A Rigorous & Practical Approach*, second ed. Boston: PWS Publishing, 1998.
5. A.L. Goel and K. Okumoto. Time-dependent error detection rate model for software reliability and other performance measures, *IEEE Trans. Rel.*, R-28, 206–211, 1979.
6. Z. Jelinski and P. Moranda. Software reliability research, in W. Freiberger (Ed.), *Statistical Computer Performance Evaluation*, New York: Academic Press, 465–484, 1972.
7. B. Littlewood and J.L. Verrall. A Bayesian reliability growth model for computer software, *Appl. Stat.*, 22, 332–346, 1973.
8. M.R. Lyu. *Handbook of Software Reliability Engineering*, IEEE Computer Society Press, McGraw-Hill, 1996.
9. T.A. Mazzuchi and R. Soyer. A Bayes empirical-Bayes model for software reliability, *IEEE Trans. Rel.*, R-37, 248–254, 1988.
10. P.B. Moranda. Prediction of software reliability and its applications, in *Proceedings of the Annual Reliability and Maintainability Symposium*, Washington DC, 327–332, 1975.
11. J.D Musa and K. Okumoto. A logarithmic Poisson execution time model for software reliability measurement, in Proc. of the seventh International Conference on Software Engineering, 230–237, 1984.
12. H. Pham. *System Software Reliability*, Springer, 2007.
13. A. Pievatolo, F. Ruggeri and R. Soyer. A bayesian hidden markov model for imperfect debugging, *Reliability Engineering and System Safety*, 103, 12–21, 2012.
14. B.K. Ray, Z. Liu and N. Ravishankar. Dynamic reliability models for software using time-dependent covariates, *Technometrics*, 48, 1–10, 2006.
15. K. Rinsaka, K. Shibata and T. Dohi. Proportional intensity-based software reliability modeling with time-dependent metrics, in Proceedings of the 30th Annual International Computer Software and Applications Conference, IEEE ,2006.
16. G.J. Schick and R.W. Wolverton. Assessment of software reliability, in Proc. in Operations Research, 395–422, 1978.
17. K. Shibata, K. Rinsaka and T. Dohi. PISRAT: Proportional intensity-based software reliability assessment tool, in Proceedings of the 13th International Symposium on Pacific Rim Dependable Computing, IEEE, 2007.
18. N.D. Singpurwalla and S. Wilson. *Statistical Methods in Software Engineering*, Springer: New York, 1999.
19. N. Torrado, M.P. Wiper and R.E. Lillo. Software reliability modeling with software metrics data via Gaussian processes, *IEEE Transactions on Software Engineering*, 39, 8, 1179–1186, 2013.
20. M.P. Wiper. Software reliability: Bayesian analysis, in F. Ruggeri, R. Kennet and W. Faltin (editors) Encyclopedia of Statistics in Quality and Reliability. Wiley, New York, 2007.
21. S. Yamada and S. Osaki, Software Reliability Growth Modeling: Models and Applications, *IEEE Trans. Software Engineering*, 11, 1431–1437, 1985.

Mathematical study of mortality dynamics in heterogeneous population composed of subpopulations following the exponential law

Demetris Avraam[1], Joao Pedro de Magalhaes[2], Séverine Arnold (-Gaille)[3] and Bakhtier Vasiev[1]

[1] Department of Mathematical Sciences, University of Liverpool, Liverpool, UK
(E-mail: davraam@liverpool.ac.uk and bnvasiev@liverpool.ac.uk)

[2] Integrative Genomics of Ageing Group, Institute of Integrative Biology, University of Liverpool, Liverpool, UK
(E-mail: aging@liverpool.ac.uk)

[3] Department of Actuarial Science, Faculty of Business and Economics (HEC Lausanne), University of Lausanne, Lausanne, Switzerland
(E-mail: severine.arnold@unil.ch)

Abstract. Many features of biological populations can be described in terms of their heterogeneity by taking into account variations among individuals and cohorts in the population. In demography, the heterogeneity of populations can explain various features of age-dependent demographic observations including those related to mortality dynamics. Mortality dynamics is underlined by the Gompertz law stating that the mortality rate increases exponentially between sexual maturity and considerably old ages (i.e. between 20 and 80 years old). Deviations from the exponential increase are observed at early- and late-life intervals. Different models (i.e Heligman-Pollard model) were developed over the past decades to describe and explain these deviations. These models postulate that a few different processes take place in the population and affect its mortality dynamics. In this study we present a model based on an assumption that mortality dynamics is indeed underlined by the exponential law and the irregularities at young and very old ages are due to the heterogeneity of human population. We demonstrate that the model is capable of reproducing the entire pattern of mortality and explaining the deviations from the exponential growth. The model fitted to Swedish age-dependent mortality rates indicates that the population should be composed of four subpopulations each following the exponential law of mortality increase over age. We also expand the idea of heterogeneity to probability density and survival functions, that is we adjust the model to the number of Swedish deaths and survivors instead of mortality rates.

Keywords: Gompertz law, Heterogeneity, Mathematical model, Model fitting, Probability density, Survival function.

New Trends in Stochastic Modeling and Data Analysis (*pp.* 159-171)
Raimondo Manca – Sally McClean – Christos H Skiadas (Eds)

1 Introduction

Analysis of the human mortality dynamics over the life-course is of great importance for many reasons including understanding the mechanisms of ageing and developing ways to control and extend the duration of lifespan. The mathematical modelling of the dynamics of human mortality makes a significant contribution to these studies. A number of studies have been performed to model (Makeham[21]; Siler[20]; Heligman and Pollard[12]; Lee and Carter[15]) and analyse (Gavrilov and Gavrilova[13]; de Magalhaes *et al.*[7]) mortality data as a function of age. Age-dependent mortality data are tabulated in life tables that contain essential information for the age-structure of a population (Preston *et al.*[17]).

Two of the basic quantities of interest tabulated in a human life table are the probability of death and the mortality rate. Probability of death, q_i, is the probability for an individual aged i to die before reaching age $i+1$ and is expressed as the ratio of the number of deaths of people aged i, ΔN_i, divided by the number of individuals alive at exact age i, N_i. Death (or mortality) rate m_i is defined as the number of deaths of people of age i divided by the average number of individuals of age i:

$$m_i = \frac{\Delta N_i}{0.5(N_i + N_{i+1})} \tag{1}$$

where the number of deaths of people aged i is represented as:

$$\Delta N_i = N_i - N_{i+1}. \tag{2}$$

The average number of survivors within one-year age interval approximately coincides with the number of survivors at the centre of the interval and therefore the mortality rate is commonly referred as central death rate.

Data on mortality rates can be found in two different formats depending on the way the data are recorded. Data recording deaths of individuals born the same year and growing up together (in the sense that they will celebrate their *i*-th birthday exactly i years after their birth) form the cohort data. Data recording deaths occurring during a specific year form the period data. In order to illustrate the difference between the period and cohort data, we briefly introduce the Lexis diagram. The Lexis diagram (Lexis[19]) outlines the stocks and flows of a population and the occurrence of demographic events (such as deaths) over age and time. It is a two-dimension graph (Fig. 1) in which the vertical axis represents the age and the horizontal axis the time, both measured in same units (e.g. years). Deaths occurring in a parallelogram formed by two diagonal lines in Fig. 1 contribute to cohort mortality, while the deaths occurring in a rectangle outlined by two vertical lines in Fig. 1 - to period mortality.

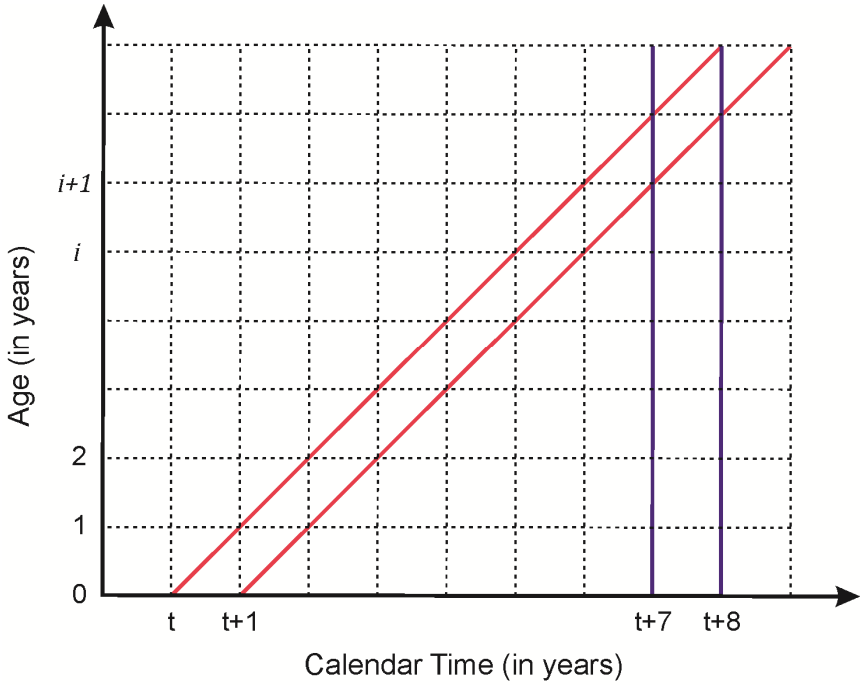

Fig. 1. Lexis diagram

The diagram illustrates demographic events as distributed over age and time. Cohort mortality rates refer to the deaths of a cohort that are occurring in a parallelogram formed by two diagonal lines. Period mortality rates refer to deaths occurring within a period outlined by two vertical lines.

The mortality rate of human populations (and other species as well) advances exponentially with age (i.e. follows the Gompertz law of mortality (Gompertz[1])) for a significant part of the age range starting from the period of reproductive maturity (age ~35) up to extreme old ages (age ~100). Mathematically, the Gompertzian dynamics of mortality is expressed as

$$m_i = m_0 e^{\beta i}, \tag{3}$$

where m_0 is the initial mortality at age $i = 0$ and parameter β defines the rate of change of mortality with age (usually called rate of ageing or Gompertz slope).

Graphically, mortality data are most frequently plotted in semi-logarithmic graphs (logarithm of mortality versus age) and therefore their exponential increase with age, as expressed by the Gompertz law of mortality (equation (3)), is represented with a straight line. Fig. 2 presents data (dots) on period mortality rates for the Swedish 2010 population together with the solid line representing the Gompertz function fitting the presented data. Even if the exponential growth accurately represents most of the ages, some peculiarities are observed in young (before 35) and extremely old (after 100) ages.

A number of mathematical models have been developed and used to analyse the human mortality dynamics and to clarify the deviations from the exponential growth. Various explanations have been given to the peculiarities of mortality at young and old ages. For example, the proposed explanations for the late-life mortality plateau include an assumption that the Gompertz law (exponential function) is not valid at those ages and that the mortality dynamics should be described by logistic, quadratic or some other mathematical functions (Gavrilov and Gavrilova[14]; Kannisto *et al.*[18]; Pham[5]). Other explanations take into account the heterogeneity of a population and its impact on the dynamics of mortality (Vaupel *et al.*[11]; Vaupel and Yashin[8]). The heterogeneity can be explained in different ways and can be described by different models (Lebreton[6]; Steinsaltz and Wachter[3]).

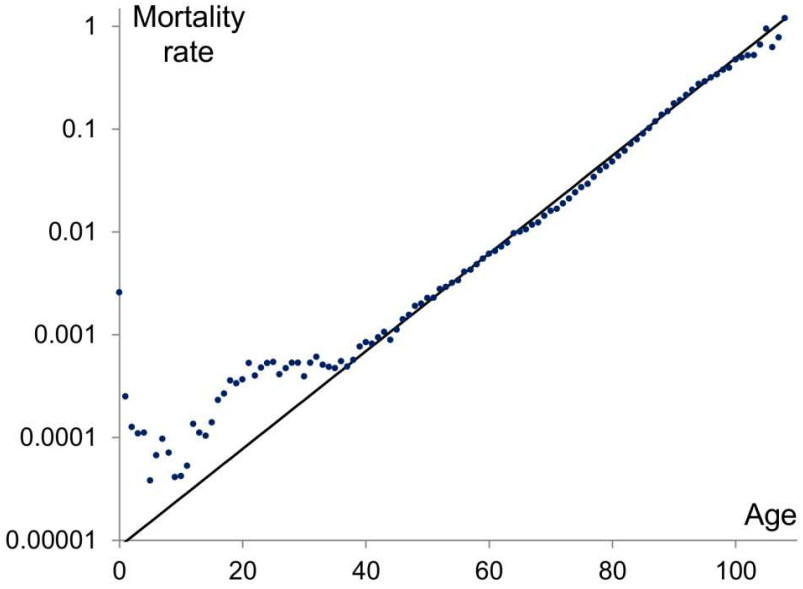

Fig. 2. Mortality rates of the 2010-period Swedish population set in a semi-logarithmic scale

The data are taken from the Human Mortality Database (http://www.mortality.org). The Gompertz function with parameters $m_0 = 8.7 \cdot 10^{-6}$ and $\beta = 0.109$ fits the data very well after the age of 35. Deviations from the exponential growth are observed at young (before 35) and considerably old (after 100) ages.

In this work, we aim to analyse the dynamics of mortality in human populations using the mathematical model that associates the exponential law for mortality dynamics with the heterogeneity of populations. We also develop the model for continuous age, which complements the discrete model developed in Avraam *et al.*[2]. Both, the discrete and continuous models, can reproduce and explain the pattern formed by period or cohort mortality rates across the

entire lifespan and are able to explain the deviations from the exponential growth. The model is fitted to Swedish period data and it is shown that a theoretical heterogeneous population composed by four subpopulations can reproduce the actual data fairly well. The model proposed in Avraam *et al.*[2], is then reformulated for the analysis of the probability density and survival functions of the population.

The remainder of this paper is structured as follows. In Section 2, the theoretical models in discrete and continuous age are introduced and their probability density and survival function for heterogeneous populations developed. Section 3 presents the fitting procedure we used. The models presented in Section 2 are applied to Swedish mortality rates in 2010 in Section 4 and obtained results are discussed in Section 5.

2 Mathematical model

2.1. Discrete model of mortality in heterogeneous populations

The main assumption of the model is that human populations are heterogeneous and composed of a number of subpopulations or individuals, which differ genetically and/or by life style factors (Vaupel *et al.*[10]; Vaupel[9]). The model that combines the heterogeneity with the Gompertz law of mortality (Avraam *et al.*[2]) has a further assumption that the mortality rate in each subpopulation grows exponentially (i.e. in the same way as in Gompertz law) with different mortality parameters (m_0, β) for each subpopulation, reflecting the variations in the genotype and life style. The notations N_{j0}, m_{j0} and β_j are used for the initial size, initial mortality rate and rate of ageing of the *j*-th subpopulation respectively. The mortality or the central death rate of the *j*-th subpopulation at age i is then expressed by the exponential function:

$$m_{ji} = m_{j0} e^{\beta_j i}. \tag{4}$$

Using the definition of mortality rate (equation (1)), the mortality of the entire heterogeneous population composed by n subpopulations is given by:

$$m_i = \frac{\sum_{j=1}^{n} \Delta N_{ji}}{0.5\left(\sum_{j=1}^{n} N_{ji} + \sum_{j=1}^{n} N_{j,i+1}\right)}, \tag{5}$$

with N_{ji} and ΔN_{ji} representing the number and the number of death of persons of age i in subpopulation j. By taking into account equations (1) and (4), equation (5) is rewritten as:

$$m_i = \frac{\sum_{j=1}^{n} \frac{N_{ji} m_{j0} e^{\beta_j i}}{1 + 0.5 m_{j0} e^{\beta_j i}}}{\sum_{j=1}^{n} N_{ji} - 0.5 \sum_{j=1}^{n} \frac{N_{ji} m_{j0} e^{\beta_j i}}{1 + 0.5 m_{j0} e^{\beta_j i}}}. \quad (6)$$

When dealing with period data the number of individuals aged i is constant for a stationary population and therefore the mortality rate is defined as the number of deaths ΔN_i divided by the actual size N_i. Thus, the model of mortality (equation (6)) for period data is simplified and can be expressed as a sum of weighted exponential terms:

$$m_i = \frac{\sum_{j=1}^{n} \Delta N_{ji}}{\sum_{j=1}^{n} N_{ji}} = \sum_{j=1}^{n} \rho_{ji} m_{ji} = \sum_{j=1}^{n} \rho_{ji} m_{j0} e^{\beta_j i}, \quad (7)$$

where each weight ρ_{ji} represents the proportion of the j-th subpopulation in the whole population at age i:

$$\rho_{ji} = \frac{N_{ji}}{N_i} \text{ with } \sum_{j=1}^{n} \rho_{ji} = 1.$$

2.2. Continuous model of mortality in heterogeneous populations

In the continuous model the age is defined by a real number x (continuous age) rather than by the integer number i. For continuous age, the instantaneous mortality, μ_x at age x (force of mortality) of a homogeneous population is defined as:

$$\mu(x) = \lim_{\Delta x \to 0} \frac{-\Delta N}{N(x) \Delta x} = \frac{-1}{N(x)} \frac{dN}{dx}. \quad (8)$$

Substituting the Gompertz law in the LHS of equation (8) and solving the differential equation results in:

$$N(x) = A e^{-\frac{\mu_0}{\beta} e^{\beta x}}, \quad (9)$$

where the constant of integration A is equal to $N_0 e^{\mu_0 / \beta}$ as estimated by the initial condition $N(x = 0) = N_0$. This means that the expression for the population size N at age x depends on the initial mortality, μ_0, and the mortality coefficient β:

$$N(x) = N_0 e^{\frac{\mu_0}{\beta}\left(1 - e^{\beta x}\right)}. \quad (10)$$

With heterogeneous populations, formula (10) is used to describe the size of each subpopulation at age x. Therefore, the subscript j is added in each parameter. As a result, the mortality of the entire population in continuous age is formulated by:

$$\mu(x) = \frac{\sum_{j=1}^{n} \mu_j(x) N_j(x)}{\sum_{j=1}^{n} N_j(x)} = \frac{\sum_{j=1}^{n} \mu_{j0} e^{\beta_j x} N_{j0} e^{(\mu_{j0}/\beta_j)(1-e^{\beta_j x})}}{\sum_{j=1}^{n} N_{j0} e^{(\mu_{j0}/\beta_j)(1-e^{\beta_j x})}}. \tag{11}$$

By solving equation (11) at integer values of age ($x = i$), equation (6) is found, providing then a link between the dynamics of mortality in the continuous and discrete models.

2.3. Probability density and survival function in heterogeneous populations

The consideration of heterogeneity in human population can be used for the derivation of models for other mortality-related variables that exist in human life tables. Such variables are the number of survivors and the number of deaths at age x. In this section, the models of probability density and survival function for heterogeneous populations are developed in continuous time.

In a homogeneous population, $S(x+\Delta x)$ denotes the probability of an individual to survive at age $x+\Delta x$ (usually called survival function) and is calculated as the difference between the probability to survive at age x and the probability to die between x and $x+\Delta x$:

$$S(x+\Delta x) = S(x) - S(x)\mu(x)\Delta x \tag{12}$$

$$\Rightarrow \frac{S(x+\Delta x) - S(x)}{\Delta x} = -\mu(x)S(x). \tag{13}$$

The limit of LHS of equation (13) when Δx tends to 0, is the derivative of $S(x)$ with respect to x :

$$\lim_{\Delta x \to 0} \frac{S(x+\Delta x) - S(x)}{\Delta x} = \frac{dS(x)}{dx}, \tag{14}$$

and therefore equation (13) can be written as the differential equation

$$\frac{dS(x)}{dx} = -\mu(x)S(x). \tag{15}$$

The solution of the differential equation (15) when the force of mortality $\mu(x)$ follows the Gompertz law, is

$$S(x) = A \exp\left(-\frac{\mu_0}{\beta} e^{\beta x} \right), \tag{16}$$

where the constant of integration A, is given by the initial condition $S(x=0) = 1$ and is equal to $A = e^{\mu_0/\beta}$.

By multiplying the survival function with the initial size of the population N_0, we find the number of individuals alive at age x. Therefore, for the heterogeneous population, the theoretical number of survivors at age x is given by:

$$N(x) = N_0 S(x) = N_0 \sum_{j=1}^{n} \rho_{j0} \exp\left(\frac{\mu_{j0}}{\beta_j} \left(1 - e^{\beta_j x} \right) \right). \tag{17}$$

The probability density function $f(x)$, of a heterogeneous population is obtained similarly. The probability $q(x)$ of an individual to die by age x is the complement of the probability to survive at the same age (i.e $q(x) = 1 - S(x)$) and therefore the probability density function is obtained by differentiating the cumulative distribution function $q(x)$ with respect to x:

$$f(x) = q'(x) = \mu_0 \exp\left(\beta x - \frac{\mu_0}{\beta} \left(e^{\beta x} - 1 \right) \right). \tag{18}$$

By multiplying the probability density function with the size of the initial population, we have the theoretical distribution of deaths across the lifespan, $\Delta N(x) = N_0 f(x)$.

For the case of a heterogeneous population composed by n subpopulations, the distribution of deaths is given by the sum of the number of deaths of individuals from each subpopulation:

$$\Delta N(x) = \sum_{j=1}^{n} N_{j0} f_j(x) = N_0 \sum_{j=1}^{n} \rho_{j0} \mu_{j0} \exp\left(\beta_j x - \frac{\mu_{j0}}{\beta_j} \left(e^{\beta_j x} - 1 \right) \right). \tag{19}$$

3 Fitting Procedure

The practical and commonly-used Least Squares Method was performed for the estimation of the model parameters that minimize the sum of the squared residuals between the theoretical and observed values. Log-Linear regression was used for the comparison between the logarithm of actual mortality rates and the logarithm of the theoretical mortality rates (logarithm of equation (6) or (11)), while Linear-regression was used to compare the actual number of deaths and survivors with the theoretical number of deaths given by equation (19) and theoretical number of survivors given by equation (17) respectively. In order to select the model with the optimal number of subpopulations, we used the Bayesian Information Criterion (BIC) (Schwarz[4]) which is given by the formula

$$BIC = n_d \ln\left(\hat{\sigma}_e^2 \right) + k \ln\left(n_d \right), \tag{20}$$

where n_d is the number of data points, $\hat{\sigma}_e^2$ is the sum of squared residuals divided by the number of data points and k is the number of free parameters. The model with the lowest BIC value represents the optimum. Note that each subpopulation is characterised by three parameters (initial mortality, rate of

ageing and its size or proportion with respect to the whole population) and also the sum of the subpopulations fractions is equal to unity. Therefore, the model of heterogeneous population composed by n subpopulations contains $k = 3n - 1$ unknown parameters.

4 Results

The theoretical heterogeneous population model is fitted to three different sets of mortality-related data (mortality rates, number of deaths and number of survivors) for the 2010 period Swedish data for the entire population including males and females. The data come from the website of Human Mortality Database, (http://www.mortality.org). We first fit the model to the mortality rates introduced in Fig. 2.

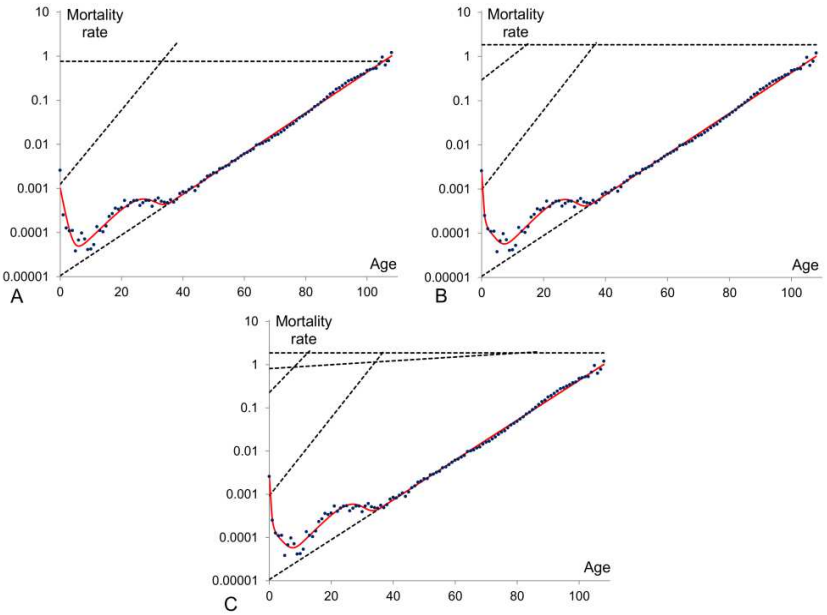

Fig. 3. The model of heterogeneous population fitted to the 2010 Swedish mortality rates

The heterogeneous population composed by three (panel A), four (panel B) and five (panel C) subpopulations are presented. The observed mortality rates are denoted by the dot points, the mortality dynamics of the subpopulations are given by the dashed lines and the total mortality of the whole population by the solid curve.

Fig. 3 presents the data and the fitted model composed by three (Fig. 3A), four (Fig. 3B) and five (Fig. 3C) subpopulations. The BIC values reveal that the population composed by four subpopulations ($BIC = -334.07$) fits the 2010 period Swedish data better than the model of three ($BIC = -302.06$) subpopulations and slightly better than the five-subpopulation model

($BIC = -315.73$). In the four-subpopulation model (Fig. 3B), the first subpopulation considered as the frailest (the subpopulation with the highest initial mortality) explains the sharp decline of mortality pattern at infant ages. The second subpopulation (with initial mortality closed to 0.3) mainly forms the left part of the local minimum that is observed at young ages (ages 2-7). The third subpopulation with initial mortality around 0.001 forms the local hump that appears over the reproductive period (ages 20-30). This hump is frequently called the accidental hump since it reflects external death factors such as accidents (for both sexes) and maternal mortality (for females). The fourth subpopulation is the most robust (having the lowest initial mortality) and has the biggest initial fraction. It explains the exponential growth of mortality at the period of ageing.

The fitting procedure is then applied to the numbers of deaths and survivors taken for the 2010 Swedish population, with equation (19) and equation (17) respectively. The BIC values indicate that the best fit to the observed numbers of deaths and survivors is obtained in both cases with a model composed by four subpopulations (Fig. 4).

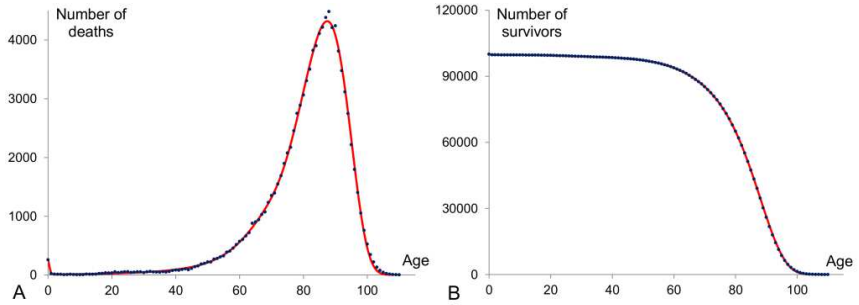

Fig. 4. The model of heterogeneous population fitted to the 2010 Swedish number of deaths and number of survivors

A: The density function of heterogeneous population composed by four subpopulations is fitted to the actual numbers of deaths and B: The survival function of heterogeneous population composed by four subpopulations is fitted to the actual numbers of survivors.

Consequently, the analysis shows that the assumption of population heterogeneity provides mathematical models that fit the mortality-related data (Fig. 3 and 4) better than a model of homogeneous population. On the other hand, the three attempts of fitting mortality-related data for the same population do not give the same values for the mortality parameters. The model for mortality rates of heterogeneous population provides the parameters that shape the mortality pattern of the entire lifespan, since by using the logarithm of mortality rates during the fitting procedure we increase the weight of young ages. The other two models (equations (17) and (19)) provide parameters that minimize the residuals mainly at adulthood span, since the differences between theoretical values and observations at young and extreme old ages are negligible. Besides, the theoretical relationships between equations (6), (11), (17) and (19) developed in Section 2 are valid only for cohort data with no

migration where the number of persons alive at age $i+1$ (N_{i+1}) in year t are equivalent to the number of persons alive at age i in year $t-1$ minus the number of persons who died at age i in year $t-1$, $N_i - \Delta N_i$. However, since we do not fit cohort data but period data and since the Swedish population is subject to migration flows, this relation does not hold, explaining partly the observed differences between the values of the parameters of the three fitted models. The mortality rates of the entire population resulting from the model applied to the three different sets of Swedish data are shown in Fig. 5. The dotted and dashed curves indicate that the parameters obtained by fitting the numbers of deaths and survivors, fail to accurately model the peculiarities of mortality pattern at early and extreme old ages. However they both create a smooth dip at around age 75 and thus better capture the mortality pattern at adult age than the curve of mortality obtained by fitting mortality rates (solid curve in Fig. 5).

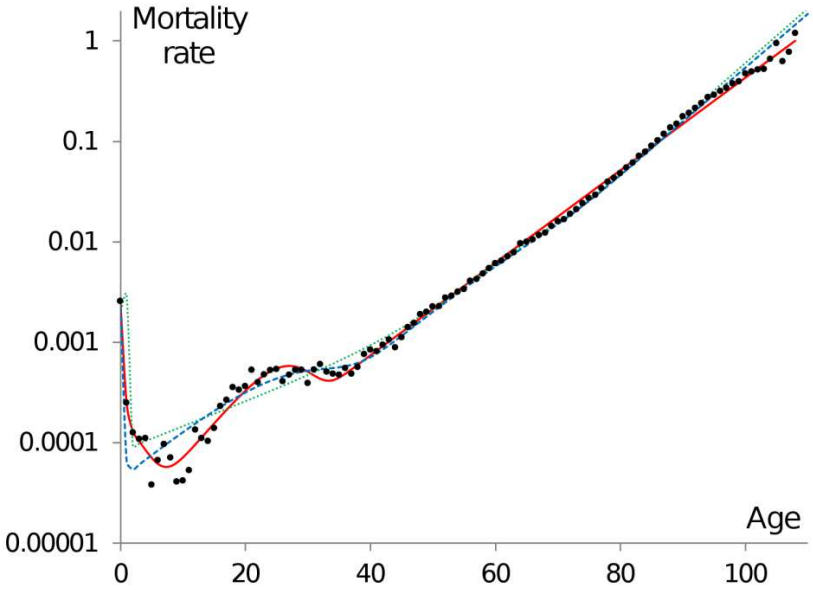

Fig. 5. Different fits of four-subpopulation heterogeneous model to 2010 Swedish mortality data

The solid (red) curve represents the mortality pattern resulting from the heterogeneous model fitted to the mortality rates (same pattern as in Fig. 3B) while the dotted (green) and dashed (blue) curves show the mortality pattern resulting from the model fitted to the numbers of deaths and the numbers of survivors respectively. (For interpretation of the references to colour in this figure legend, the reader is referred to the electronic version of this book.)

Conclusions

Modelling the dynamics of human mortality has long been the focus of various studies aiming an understanding the ageing processes and the causes of mortality at different ages. A number of studies have assessed the impact of heterogeneity on the dynamics of mortality, in particular at young and extremely old ages. The assumption that the population is heterogeneous combined with the assumption that the mortality dynamics of each subpopulation follows the exponential law, have been used to model the observed mortality dynamics and particularly to explain the deviations of mortality dynamics from the exponential growth (Avraam *et al.*[2]). In this work, we extended the model developed in Avraam *et al.*[2], from discrete to continuous time and we use it to reproduce and analyse the mortality dynamics across the entire human lifespan. The model contains meaningful demographic parameters and is capable of reproducing the actual data of a human population fairly well. The heterogeneity of a population is also used to derive models reproducing the patterns formed by the numbers of deaths and survivors.

The model reveals that we need to consider only four subpopulations to reproduce with sufficient accuracy the Swedish period mortality-related data (Fig. 3B and 4). The four-subpopulation model appears to be the optimum in all three fitted models we developed, that are 1) fitted model to mortality rates, 2) fitted model to the number of deaths and 3) fitted model to the number of survivors. Even though it probably underestimates the real heterogeneity of human populations, it shows how a simple mathematical model can well represent actual human mortality dynamics. Our analysis indicates that the contribution of heterogeneity differs across ages. The mortality model suggests that a small subpopulation with high initial mortality explains the decline in mortality at young ages as this subpopulation gradually disappears. Generally, the faster-ageing subpopulations are eliminated with increasing age and the entire population starts to act more-and-more homogeneously, as if it was composed by a single (with the lowest mortality) subpopulation.

The model presented in this study allows many future developments, such as an analysis of the time evolution of the Gompertz parameters. Indeed, such study could help to better understand past mortality evolutions, such as the ageing process, and could provide a new approach to forecast mortality trends of human populations. By comparing these projections with traditional forecasting techniques currently used in practice, such as the Lee-Carter and the Heligman-Pollard models (see for example Gaille[16]), the analysis of potential future mortality developments will be enhanced.

References

1. B. Gompertz, On the Nature of the Function Expressive of the Law of Human Mortality, and on a New Mode of Determining the Value of Life Contingencies, Philosophical Transactions of the Royal Society of London, 115, 513–585, 1825.
2. D. Avraam, J.P. de Magalhaes and B. Vasiev, A mathematical model of mortality dynamics across the lifespan combining heterogeneity and stochastic effects, Experimental Gerontology, 48, 801-811, 2013.
3. D.R. Steinsaltz and K.W. Wachter, Understanding mortality rate deceleration and heterogeneity, Mathematical Population Studies, 13, 19-37, 2006.
4. G. Schwarz, Estimating dimension of a model, Annals of Statistics, 6, 461-464, 1978.
5. H. Pham, Modeling US Mortality and Risk-Cost Optimization on Life Expectancy, IEEE Transactions on Reliability, 60, 125-133, 2011.
6. J.D. Lebreton, Demographic models for subdivided populations: The renewal equation approach, Theoretical Population Biology, 49, 291-313, 1996.
7. J.P. de Magalhaes, J.A.S. Cabral and D. Magalhaes, The influence of genes on the aging process of mice: A statistical assessment of the genetics of aging, Genetics, 169, 265-274, 2005.
8. J.W. Vaupel and A.I. Yashin, The deviant dynamics of death in heterogeneous populations, Sociological Methodology, 15, 179-211, 1985.
9. J.W. Vaupel, Biodemography of human ageing, Nature, 464, 536-542, 2010.
10. J.W. Vaupel, J.R. Carey, K. Christensen, T.E. Johnson, A.I. Yashin, N.V. Holm, I.A. Iachine, V. Kannisto, A.A. Khazaeli, P. Liedo, V.D. Longo, Y. Zeng, K.G. Manton and J.W. Curtsinger, Biodemographic trajectories of longevity, Science, 280, 855-860, 1998.
11. J.W. Vaupel, K.G. Manton and E. Stallard, Impact of heterogeneity in individual frailty on the dynamics of mortality, Demography, 16, 439-454, 1979.
12. L. Heligman and J.H. Pollard, The age pattern of mortality, Journal of the Institute of Actuaries, 107, 49-80, 1980.
13. L.A. Gavrilov and N.S. Gavrilova, The quest for a general theory of aging and longevity, Science of aging knowledge environment: SAGE KE 2003: RE5, 2003.
14. L.A. Gavrilov and N.S. Gavrilova, The reliability theory of aging and longevity, Journal of Theoretical Biology, 213, 527-545, 2001.
15. R.D. Lee and L.R. Carter, Modelling and forecasting U.S. mortality, Journal of the American Statistical Association, 87(419), 659-671, 1992.
16. S. Gaille, Forecasting mortality: when academia meets practise, European Actuarial Journal, 2(1), 49-76, 2012.
17. S. Preston, P. Heuveline and M. Guillot, Demography: Measuring and Modeling Population Processes, Blackwell, Oxford, 2000.
18. V. Kannisto, J. Lauritsen, A.R. Thatcher and J.W. Vaupel, Reductions in mortality at advanced ages – several decades of evidence from 27 countries, Population and Development Review, 20, 793-810, 1994.
19. W. Lexis, Einleitung in die Theorie der Bevölkerungs-Statistik, Strassburg: Karl J. Trübner, 1875.
20. W. Siler, Parameters of mortality in human populations with widely varying lifespans, Statistics in Medicine, 2, 373-380, 1983.
21. W.M. Makeham, On the Law of Mortality and the Construction of Annuity Tables, J. Inst. Actuaries and Assur. Mag., 8, 301-310, 1860.

Robust estimators for the bivariate power series offspring distributions

Dimitar Atanasov[1], Ana Staneva[2], and Vessela Stoimenova[3]

[1] New Bulgarian University, Sofia 1618, 21, Montevideo Street
(E-mail: datanasov@nbu.bg)
[2] Technical University of Sofia, Bulgaria, Sofia 1000, blvd Kliment Ohridski 8
and
Department of Probability, Operations Research and Statistics, Faculty of Mathematics and Informatics, Sofia University, 5 James Bourchier blvd., 1164, Sofia, Bulgaria
(E-mail: anastaneva@gmail.com)
[3] Department of Probability, Operations Research and Statistics, Faculty of Mathematics and Informatics, Sofia University, 5 James Bourchier blvd., 1164, Sofia, Bulgaria
and
Bulgarian Academy of Sciences, Institute of Mathematics and Informatics, Acad. Georgi Bonchev Str., Block 8, 1113 Sofia, Bulgaria
(E-mail: stoimenova@fmi.uni-sofia.bg)

Abstract. We consider the family of bivariate power series distributions. It is well studied that the maximum likelihood estimator of its parameters is not robust to outliers in the data. We consider the trimmed likelihood as a robust modification of the classical maximum likelihood and find a lower bound of its breakdown point. The distributions of this family serve well as offspring distributions in the two-type discrete time branching processes. We construct the maximum likelihood estimators of the process and show their relationship to the Harris type estimators of the mean vector. On the basis of different sampling schemes we show construction methods for the trimmed likelihood estimators.
Keywords: Bivariate power series distributions, Trimmed likelihood, Multitype branching processes.

1 Introduction

Branching processes form an important class of stochastic processes with numerous applications in different scientific and practical areas, many of them involving multitype modeling. Generally speaking, there is a number of objects, often called particles, cells, individuals, which, according to some probabilistic law, reproduce (or "branch") and die out. They can be of multiple types and may have different locations in space. Their evolution and generation may be independent or according to certain probabilistic laws.

New Trends in Stochastic Modeling and Data Analysis (pp. 173-1)
Raimondo Manca - Sally McClean - Christos H Skiadas (Eds)

One of the pioneering works on the formulation and handling of branching processes with several types of particles are the papers from 1947 by Kolmogorov and Dmitriev[12] and Kolmogorov and Sevastyanov[13] in the Markov case. Since then there is an impressive number of work in the area of branching processes theory and applications (see for example the books of Asmussen and Herring[1], Athreya and Ney[3], Harris[9], Jagers[11], Sevastyanov[14], Yakovlev and Yanev[27] and others).

Statistical estimation of the process' characteristics like the mean number of offspring, the criticality of the process, the offspring distribution and others, is an important issue in their study. Some of the most recent approaches devoted to the statistical inference for branching processes can be found in González et al.[7]. The work of Jacob[10] gives a comprehensive overview of the theoretical and statistical methods used in epidemiology. The importance of simulation, computing and more flexible statistical procedures can also be traced in González et al.[6].

As in other fields of statistics, there are different approaches for estimation - parametric, nonparametric and semiparametric settings. One possible approach for estimation in a contaminated sample is to combine the asymptotic distributions of the estimators with the method for constructing robust estimators, based on the trimmed likelihood. Robust estimation of the offspring distribution on the basis of the asymptotic behaviour of the (relative) frequencies in a multitype Bienayme-Galton-Watson branching process with a random number of ancestors are studied in Stoimenova and Atanasov[21],[4]. These works are based on the papers on the asymptotics and applications in cell biology in Yakovlev and Yanev[28],[29] and Yakovlev et al.[26]. The other approach is to use the exact offspring distribution in a specified parametric family like the multivariate power series. The robust estimation in the multivariate power series family is of inerest in itself. We consider numerical results for simulated data samples of different types - samples over family trees and over generation sizes - and compare estimators and their robust versions. In the class of the univariate power series offspring distributions some topics of the parametric estimation are considered in Stoimenova and Yanev[22] and of the robust parametric estimation - in Stoimenova[20].

2 Multivariate power series estimation

Let us suppose that the discrete real-valued random variables X and Y have the joint probability mass function of the form:

$$p_{ij} = \frac{a(i,j)\theta_1^i \theta_2^j}{A(\theta_1, \theta_2)}, \tag{1}$$

where $(i,j) \in \Im$ is the set of possible values of the random vector (X,Y), $(\theta_1, \theta_2) \in \Theta \subset R_2^+$ is the vector of positive parameters from the parameter space Θ, $a_k(i,j) > 0$ is nonnegative real-valued function of the random vector values, which may depend on some parameters, but does not depend on θ_1 and

θ_2, and

$$A(\theta_1, \theta_2) = \sum_{i=0}^{\infty} \sum_{j=0}^{\infty} a(i,j) \theta_1^i \theta_2^j. \tag{2}$$

We recall that the family of distributions having probability mass functions of the form (1) is called bivariate power series distribution family. The function $A(\theta_1, \theta_2)$ is called the defining function of the distribution. Note that the form (2) is the second-order Taylor expansion of the scalar-valued function of more than one variable $A(\theta_1, \theta_2)$ in a bivariate power series form. The coefficient $a(i,j)$ in the expansion is called the coefficient function.

The bivariate power series distribution family in (1) is a natural generalization of the univariate power series distribution family and a subclass of the multivariate power series distribution family. There are many sources concerning the properties and applications of the multivariate power series distributions. Among them we mention the pioneering papers of Katri[16], Patil[18], Gerstenkorn[5] and the thorough books on discrete multivariate distributions of Johnson et.al.[15] and discrete bivariate distributions of Kocherlakota[17]

The multivariate power series distributions form a subclass of the multivariate discrete exponential family, hence inheriting its properties for the moments, cumulants, covarances, additiveness and so on.

We recall that in the special cases when:

1. $A(\theta_1, \theta_2) = (1+\theta_1+\theta_2)^n$, $\theta_i > 0$, one has the trinomial distribution (positive multinomial) in a reparametrized form with parameters $p_i = \frac{\theta_i}{1+\theta_1+\theta_2} \in (0,1)$:

$$p_{ij} = \frac{a(ij)\theta_1^i \theta_2^j}{(1+\theta_1+\theta_2)^n} = \frac{n!}{i!j!(n-i-j)!} \left(\frac{\theta_1}{1+\theta_1+\theta_2}\right)^i \left(\frac{\theta_2}{1+\theta_1+\theta_2}\right)^j \cdot$$

$$\cdot \left(1 - \frac{\theta_1}{1+\theta_1+\theta_2} - \frac{\theta_2}{1+\theta_1+\theta_2}\right)^{n-i-j} = \frac{n!}{i!j!(n-i-j)!} p_1^i p_2^j (1-p_1-p_2)^{n-i-j}$$

   Note that the multinomial distribution without reparametrization is not a multivariate power series distribution in this sense since cannot be written in the form (1).
2. $A(\theta_1, \theta_2) = (1-\theta_1-\theta_2)^{-n}$, then one has the negative binomial distribution (negative multinomial in the bivarate case) with the same parameter $p_i = \theta_i \in (0,1)$, $p_1 + p_2 < 1$ and

$$p_{ij} = \frac{a(ij)\theta_1^i \theta_2^j}{(1-\theta_1-\theta_2)^{-n}} = \frac{(n+i+j-1)!}{i!j!(n-1)!} p_1^i p_2^j (1-p_1-p_2)^n$$

3. $A(\theta_1, \theta_2) = \exp\{\theta_1+\theta_2\}$, $\theta_i > 0$, then one has the bivarate Poisson (double Poisson) with $p_i = \theta_i > 0$ and

$$p_{ij} = \frac{a(ij)\theta_1^i \theta_2^j}{\exp\{\theta_1+\theta_2\}} = \frac{\theta_1^i e^{-\theta_1}}{i!} \frac{\theta_2^j e^{-\theta_2}}{j!}$$

4. $A(\theta_1, \theta_2) = -\log(1 - \theta_1 - \theta_2)$, $\theta_i > 0$, $\theta_1 + \theta_2 < 1$, one has the bivariate logarithmic series distribution

$$p_{ij} = -\frac{(i+j-1)!}{i!j!\log(1-\theta_1-\theta_2)}\theta_1^i\theta_2^j$$

Given n independent bivariate random variables $N_h = (X_h, Y_h)$, $h = 1, 2, \ldots, n$, each having the same multivariate power series distribution with probability mass function (1), the maximum likelihood estimators of the expected values EX, EY are simply the arithmetic means of the coordinates of the sample values:

$$\widehat{EX} = \frac{1}{n}(X_1 + \cdots + X_n) = \overline{X}_n \text{ and } \widehat{EY} = \frac{1}{n}(Y_1 + \cdots + Y_n) = \overline{Y}_n. \quad (3)$$

The likelihood function has the form

$$L(N_1, \ldots, N_n; \theta_1, \theta_2) = A(\theta_1, \theta_2)^{-n} \left\{ \prod_{h=1}^{n} a(X_h, Y_h) \right\} \theta_1^{\sum_{h=1}^{n} X_h} \theta_2^{\sum_{h=1}^{n} Y_h}. \quad (4)$$

Using the well known property of the multivariate power series

$$EX = \frac{\theta_1}{A(\theta_1, \theta_2)} \frac{\partial A(\theta_1, \theta_2)}{\partial \theta_1} \text{ and } EY = \frac{\theta_2}{A(\theta_1, \theta_2)} \frac{\partial A(\theta_1, \theta_2)}{\partial \theta_2} \quad (5)$$

and equating $\frac{\partial L}{\partial \theta_1} = 0$, $i = 1, 2$, one has (3). Hence the maximum likelihood estimators of the parameters θ_1 and θ_2 can be obtained as solutions of the equations

$$\overline{X}_n = \frac{\theta_1}{A(\theta_1, \theta_2)} \frac{\partial A(\theta_1, \theta_2)}{\partial \theta_1} \text{ and } \overline{Y}_n = \frac{\theta_2}{A(\theta_1, \theta_2)} \frac{\partial A(\theta_1, \theta_2)}{\partial \theta_2}. \quad (6)$$

Note that the sample mean is not robust to outliers in the data.

Example 1. Let us consider a simulated sample of 120 observations with double Poisson distibution. Let 100 of them be "true" observations with parameters $\theta_1 = 15$, $\theta_2 = 20$. Let 20 observations be outliers in the sample, again bivariate poisson distributied, but with different parameters: $\theta_1 = 5$, $\theta_2 = 15$. A graph of the sample can be seen in Figure 1 below:

Figure 1: Simulated data sample from bivariate Poisson distribution with 100 "true" observations (black) and 20 outliers (red).

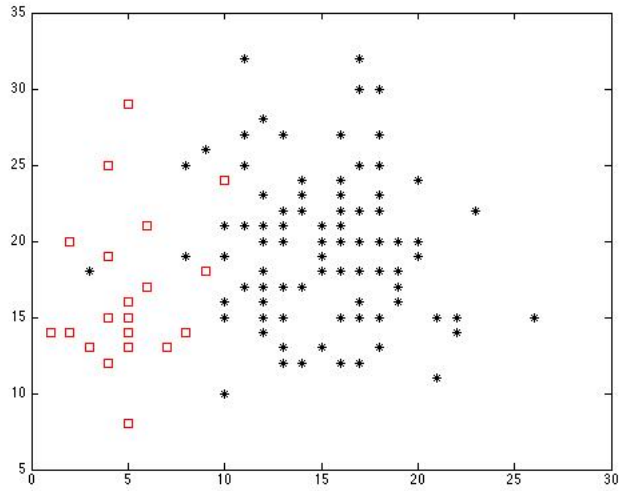

We recall that in this case the maximum likelihood estimators (MLE) of the parameters are the sample means itself. We obtain the following estimates:

MLE over the entire sample (120 observations): $\widehat{\theta}_1 = 13.5167$, $\widehat{\theta}_2 = 19.3417$

MLE for the "true" observations (100 observations): $\widehat{\theta}_1$ =15.2200 $\widehat{\theta}_2$ =19.8700

MLE of the outliers (20 observations): $\widehat{\theta}_1$ =5.0000 $\widehat{\theta}_2$ =16.7000

2.1 Trimmed likelihood estimation

Example 1 shows that an estimator is needed, which allows for:

- a certain (high) percent of 'contaminated' data: outliers
- an easy calculation of the breakdown point
- inheriting the consistency property of the maximum likelihood
- a direct application of the asymptotic and statistical theory for different classes of branching processes

For the reasons above in our work we consider the trimmed likelihood estimators of order k ($LTE(k)$), a generalization of the maximum likelihood estimators (MLE) and a subclass of the wighted and trimmed likelihood estimators of order k ($WLTE(k)$), which are introduced and studied by Vandev and Neykov[24],[25].

The $WLTE(k)$ may be considered as a robust extension of the MLE that possesses a high breakdown point. This modification considers the likelihood of individual observations as residuals and applies the basic idea of the least trimmed squares estimators (LTS) of Rousseeuw[19] using appropriate weights.

Vandev and Neykov[25] defined the $WLTE(k)$ estimators $\widehat{\theta}$, for the unknown parameter $\theta \in \Theta$ (θ may be a multivariate parameter, the only requirement imposed on Θ is to be a topological space) as

$$\widehat{\theta} = \underset{\theta \in \Theta}{argmin} \sum_{h=1}^{k} w_h f_{\nu(h)}(\theta), \tag{7}$$

where $f_{\nu(1)}(\theta) \leq f_{\nu(2)}(\theta) \leq \cdots \leq f_{\nu(n)}(\theta)$ are the ordered values of $f_h = -\log \varphi(x_h, \theta)$ at θ, $\varphi(x_h, \theta)$ is the probability density (probability mass function) of the observation x_h, θ is an unknown parameter and $\nu = (\nu(1), \cdots, \nu(n))$ is a corresponding permutation of the indices, which may depend on θ.

The nonnegative weights $w_h \geq 0$, $h = 1, \cdots, k$, are such that at least one positive exists, or equivalently, an index $k = \max\{h : w_h > 0\}$ exists. If all weights $w_h = 1$, $h = 1, \ldots, n$, then one has the least trimmed estimator LTE.

The idea behind formula (7) is that in the likelihood function are included only the k "most probable" observations (those with the largest value of the probability density function) from the sample of sample size n. The other $n-k$ observations are regarded as outliers. The number k, $[n/2] < k \leq n$, is called trimming factor and is used to calculate the breakdown point of the robust estimator. If $k = n$ and $w_i = 1$, $i = 1, \ldots, n$, one has the classical MLE.

Vandev and Neykov[25] proved that the finite sample breakdown point of the $WLTE(k)$ estimators is not less than $(n-k)/n$ if $n \geq 3d$, $(n+d)/2 \leq k \leq n-d$, when Θ is a topological space and the set $F = \{f_h(\theta),\ h = 1, \ldots, n\}$ is d-full.

A finite set F of n functions is called d-full, according to Vandev[23], if for each subset of cardinality d of F, the supremum of this subset is a subcompact function.

A real valued function $g(\theta)$ is called subcompact, if its Lesbegue sets $L_g(C) = \{\theta : g(\theta) \leq C\}$ are compact for any constant C (Vandev and Neykov [24]).

A simpler and easier to apply criterion for subcompactness is given in Atanasov[2], stating that a real valued continuous function $g(\theta)$, defined on an open subset of $\Theta \in R^n$, is subcompact if and only if for any sequence of points $\theta_s \to \theta_0$ where θ_0 belongs to the boundary of Θ, $g(\theta_s) \to \infty$ when $s \to \infty$. On the figure below one can see the form of the subcompact function:

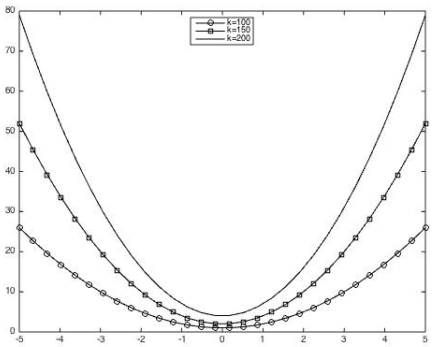

Figure 2. The likelihood function over 200 observations for different values of the trimming factor k based on subcompact likelihood curves.

We use the definition in Hampel et al.[8] of the finite sample breakdown point of an estimator T, at the finite sample $X = \{x_i; i = 1, \cdots, n\}$, is defined as the largest fraction m/n for which $\sup_{\tilde{X}} \left\| T(X) - T\left(\tilde{X}\right) \right\| < \infty$, where $\tilde{X}$ is

a sample obtained from X by replacing any m of the points in X by arbitrary values.

Thus, if one wants to study the breakdown point of the $WLTE(k)$ estimates for a particular distribution, one has to find out the index d of fullness of the corresponding set of log-density functions.

2.2 The breakdownpoint of the trimmed estimator of the power series parameters

In the case of independent bivariate power series distributed observations $N_h = (X_h, Y_h)$, $h = 1, 2, \ldots, n$, trimming factor k and equal weights $w_h = 1$, $h = 1, \ldots, n$ formula (7) for the $LTE(k)$ has the form

$$\widehat{(\theta_1, \theta_2)} = \underset{(\theta_1,\theta_2)\in\Theta}{argmin} \sum_{h=1}^{k} log \left\{ \frac{A(\theta_1, \theta_2)}{a(X_{\nu(h)}, Y_{\nu(h)})\theta_1^{X_{\nu(h)}}\theta_2^{Y_{\nu(h)}}} \right\}, \tag{8}$$

where $(\nu(1), \cdots, \nu(n))$ is the permutation of the indices, for which

$$\left\{ \frac{A(\theta_1, \theta_2)}{a(X_{\nu(1)}, Y_{\nu(1)})\theta_1^{X_{\nu(1)}}\theta_2^{Y_{\nu(1)}}} \right\} \leq \cdots \leq \left\{ \frac{A(\theta_1, \theta_2)}{a(X_{\nu(n)}, Y_{\nu(n)})\theta_1^{X_{\nu(n)}}\theta_2^{Y_{\nu(n)}}} \right\}.$$

Let us introduce the notations:

- $\Im$ is the set of all posible values of the random vector (X, Y);
- $\Im^1$ the set of all possible values of the random variable X, while $\Im^2$ is the set of all possible values of the random variable Y;
- Υ is the convergence region of the series $A(\theta_1, \theta_1)$, and $\partial\Upsilon$ is its boundary;
- $MinVX \in \Im^1$ is the minimal value of the random variable X, and $MinVY \in \Im^2$ - the minimal value of the random variable Y;
- $MaxVX \in \Im^1$ is the maximal value of the random variable X (which may be finite or infinity), and $MaxVY \in \Im^2$ - the maximal value of the random variable Y;
- If $(MinVX, MinVY) \in \Im$, then $N_{MinVX,MinVY}$ is the observed number vectors in the sample with minimal values of the coordinates;
- If $MaxVX < \infty$, $MaxVY < \infty$ and $(MaxVX, MaxVY) \in \Im$, then $N_{MaxVX,MaxVY}$ is the observed number vectors in the sample with maximal values of the coordinates;

Lemma 1. *Let us consider a sample of n independent bivariate power series distributed observations. For the breakdown point of the $LTE(k)$ estimator* (8) *the following statements hold:*

1. *If $|\Im| = \infty$, $(\theta_1, \theta_2) \in \Upsilon$, $\lim_{\theta_1,\theta_2\to\partial\Upsilon} \frac{A(\theta_1,\theta_2)}{\theta_1^i\theta_2^j} = \infty$ $\forall (i, j) \in \Im$ except for $(i, j) = (MinVX, MinVY)$, then the $WLT(K)$ estimator exists and its breakdownpoint is not less than $[n - k]/n$ if $n \geq 3(N_{MinVX,MinVY} + 1)$, $[n + N_{MinVX,MinVY} + 1]/2 \leq k \leq n - N_{MinVX,MinVY} - 1$.*

2. *If* $|\Im| < \infty$*;* $\theta_1 \in (0,\infty)$*,* $\theta_2 \in (0,\infty)$*, then the* $WLT(K)$ *estimator exists and its breakdownpoint is not less than* $[n-k]/n$*, if* $n \geq 3(max\{N_{MinVX,MinVY}, N_{MaxVX,MaxVY}\} + 1)$*, and* $[n + max\{N_{MinVX,MinVY}, N_{MaxVX,MaxVY}\} + 1]/2 \leq K \leq n - max\{N_{MinVX,MinVY}, N_{MaxVX,MaxVY}\} - 1$*.*
   If $(MaxVX, MaxVY) \notin \Im$*, then the statement in 1. hold.*
3. *If* $(\theta_1, \theta_2) \in \Phi \subset \Upsilon_1$*, where* Φ *is a compact set, then the* $WLT(k)$ *estimator exists and its breakdownpoint is not less than* $[n-k]/n$ *if* $n \geq 3$*,* $[n+1]/2 \leq k \leq n-1$*.*

Proof. The proof is analogous to the proof in the case of univariate power series (see Stoimenova[20]).

What we need to prove is that the function

$$F_{ij}(\theta_1, \theta_2) = \frac{A(\theta_1, \theta_2)}{\theta_1^i \theta_2^j}$$

is subcompact or equivalently, that

$$\lim_{\theta_1, \theta_2 \to \partial\Upsilon} \frac{A(\theta_1, \theta_2)}{\theta_1^i \theta_2^j} = \infty$$

for all $(i,j) \in \Im$. This is true under the conditions of Cases 1 and 2, except for the values $(MinVX, MinVY)$ and $(MaxVX, MaxVY)$, when the limit equals a constant. But the supremum of m functions F_{ij} is always bigger than their average and a continuous function, bigger than a subcompact function, is subcompact, which completes the proof.

Case 3 follows from the fact that any continous function defined on a compact set is subcompact.

Example 2. For the negative binomial, double Poisson and bivariate logarithmic series the conditions 1 hold. The value of the trimming factor and therefore - the breakdown point depends on the number of (0,0) observations.

Example 3. The trimmed estimates with trimming factor $120 - 25 = 95$ for the data from *Example 1* are θ_1 =15.1569, θ_2 =19.8529. In the simulated example due to the large values of the parameters there are no (0,0) observations and the trimming factor may be an integer in the region [61,119]. The breakdown point for the trimming factor of 95 is not less than 0.208.

3 Multitype discrete time branching processes with MPSOD

Let us suppose that our model describes the evolution of a population with two types of particles, which reproduce independently of each other. Each particle of, say, type 1 may have a number of offspring of type 1 and of type 2 according to some bivariate probabilistic law.

Let us denote by $T = \{1,2\}$ the set of particle types. Let $Z_i(t)$, $i = 1,2$, $t = 0,1,2,\ldots$, be the number of particles of type i in generation t. Let $\xi_k^j(t,l)$ be

a r.v., representing the number of offspring of type j, $j \in T$, in the generation $t+1$, produced from the l-th particle of type k in the generation t. Each particle, say the l-th particle of type $k \in T$ living in the $t-$th generation (t= 0,1,2,...), is associated with a random vector $\overrightarrow{\xi}_k(t,l) = (\xi_k^1(t,l), \xi_k^2(t,l))$. The distribution of the random vector $\overrightarrow{\xi}_k(t,l)$ does not depend on the generation, where the parent particle lives, and on the index l. The offspring of the particles in the generation t forms the next generation $t+1$. We denote by $\{p_{ij}^k\}$,

$$p_{ij}^k = P(\overrightarrow{\xi}_k(t,l) = (i,j)) = P(\xi_k^1(t,l) = i, \xi_k^2(t,l) = j),$$

$k = 1,2;\ t = 0,1,\ldots,\ l = 1,2,\ldots,Z(t-1)$, the bivariate joint distribution (offspring distribution, offspring law) of the vector $\overrightarrow{\xi}_k(t,l)$.

A two-type disctere time branching process (MBP) $\mathbf{Z}(t)$ is defined as a sequence of random vectors

$$\{\mathbf{Z}(t) = (Z_1(t), Z_2(t))\},$$

$t \in N_0 = \{0,1,2,\ldots\}$, where $Z_k(t)$, the number of particles of type $k \in T$ in generation t, satisfies the following recursive equations (the branching property):

$$Z_k(t+1) = \sum_{j=1}^{2} \sum_{l=1}^{Z_l(t)} \xi_j^k(t,l).$$

The main properties of the MBP processes have been thoroughly studied in many sources (see f.e. [1], [3], [9],[11] and others). One of the main problems considered in the study of a given type of a branching process is to determine the asymptotic behaviour of the process - whetheter it goes extinct or has an unlimited growth. The MBP processes are divided in three classes: subcritical, critical or supercritical, according to the magnitude of their real maximum-modulus eigenvalue ρ of the mean matrix $M = \{m_{ij}\}$, whose elemens m_{ij} are the mean numbers of offspring of type j of a descendant of type i. The extinction occurs with probability 1 iff the process is subcritical ($\rho < 1$) or critical ($\rho = 1$). Otherwise (in the supercritical case, when $\rho > 1$) it grows exponentially. The estimation of the subcritical or critical MBP faces many difficulties because of the limited (small) amount of data which may be observed especially in cases of a rapid extinction.

Example 4. Note that when one wants to simulate a two-type MBP, one has to specify the probability of a couple of offsping for the two types of particles. The third row of the matrix P in the table below states that the particle of type 1 (first column) has 2 children of type 1 (third column) and no children of type 2 (fourth column) with probability 0.4 (second column). The second column gives the probabilities p_{ij}^k that a particle of type k has i children of type 1 and j children of type 2. A simulation of the process with the probability matrix P, starting with two particles of type 1 and two particles of type 2 can be seen on the figure on the right hand side.

```
P = [1 0.2 1 0
     1 0.2 0 1
     1 0.4 2 0
     1 0.1 1 2
     1 0.1 2 1
     2 0.2 1 0
     2 0.2 0 1
     2 0.3 2 0
     2 0.3 0 2]
```

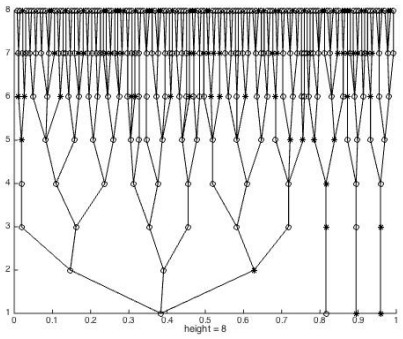

Figure 3. Generation of a MBP process given the distribution in matrix P.

3.1 Likelihood functions and robustness

As we have already noted, usually three sampling schemes are used for the estimation of the MBP. Let us denote by

$$\widetilde{\widetilde{\Im}}(n) = \{\xi_j^k(t,l),\ k,j = 1,2,\ t = 0,1,\ldots,n-1,\ l = 1,2,\ldots,Z_i(t)\},$$

the observations over the entire family tree (one can observe the number of offspring of each particle);

$$\widetilde{\Im}(n) = \{Z_k(s,(i,j)), s = 0,1,\ldots,n-1,\ k = 1,2,\ (i,j) \in \Im_k\},$$

where

$$Z_k(s,(i,j)) = \sum_{h=1}^{Z_1(s)} \sum_{l=1}^{Z_2(s)} I\{(\xi_1^k(s,l), \xi_2^k(s,l)) = (i,j)\}$$

is the number of particles of type k in generation s with i offspring of type 1 and j offspring of type 2, $\Im_k$ is the set of all possible values of the random vector $\overrightarrow{\xi}_k(s,l) = (\xi_1^k(s,l), \xi_2^k(s,l))$, I is the indicator variable; and

$$\Im(n) = \{\mathbf{Z}(0),\ldots,\mathbf{Z}(n)\}$$

is the sample over the generation sizes.

Let us suppose that the offspring distributions of the particles of type 1 and 2 are of the power series distribution family (1), (2), but with different parameters which have to be estimated:

$$p_{ij}^k = \frac{a_k(i,j)\theta_{1k}^i \theta_{2k}^j}{A_k(\theta_{1k},\theta_{2k})}, \tag{9}$$

where $k = 1,2$ is the particle type, $(i,j) \in \Im_k$ is in the set of possible number of offspring of type 1 and 2, $\theta_{1k}, \theta_{2k} \in \Theta_k \subset R^+$ are unknown parameters,

$a_k(i,j) > 0$ is the coefficient function of the series and

$$A_k(\theta_{1k}, \theta_{2k}) = \sum_{i=0}^{\infty} \sum_{j=0}^{\infty} a_k(i,j) \theta_{1k}^i \theta_{2k}^j \tag{10}$$

is the defining function. In (1) and (2) we have added the additional index k for the type of the descendant, hence obtaining (9) and (10).

When the entire family tree is observed, the likelihood function has the form

$$L(\widetilde{\widetilde{\Im}}(n)|\theta_{1k}, \theta_{2k}, k = 1,2) = L(\widetilde{\Im}(n)|\theta_{1k}, \theta_{2k}, k = 1,2) =$$
$$= \prod_{k=1}^{2} \prod_{s=1}^{n-1} \prod_{(i,j)\in\Im_k} p_{ij}^k = \prod_{k=1}^{2} \prod_{s=1}^{n-1} \prod_{(i,j)\in\Im_k} \left[\frac{a_k(i,j)}{A_k(\theta_{1k}, \theta_{2k})} \theta_{1k}^i \theta_{2k}^j \right]^{Z_k(s,(i,j))}$$

Due to the properties of the power series moments (5), in the branching context

$$E\xi_k^i(s,l) = m_{ik} = \frac{\theta_{ik}}{A_k(\theta_{1k}, \theta_{2k})} \frac{\partial A_k(\theta_{1k}, \theta_{2k})}{\partial \theta_{ik}},$$

one derives the following Harris type estimators for the mean number of offspring of a given type i from a father of type k:

$$\widehat{m}_{ik} = E\xi_k^i(t,l) = \frac{\sum\limits_{s=1}^{n} Z_i^k(s)}{\sum\limits_{n=0}^{n-1} Z_k(n)},$$

where $Z_i^k(s)$ is the number of children of type i in generation $s+1$, whose father is of type k. Simulational results have shown, that this type of estimator is not robust to outliers in the family tree.

Due to the independence of evolutions one can consider the likelihood function $L(\widetilde{\widetilde{\Im}}(n)|\theta_{1k}, \theta_{2k}, k = 1,2)$ as a product of two likelihood functions, depending on different parameters:

$$L(\widetilde{\widetilde{\Im}}(n)|\theta_{1k}, \theta_{2k}, k = 1,2) = L(\widetilde{\widetilde{\Im}}(n)|\theta_{11}, \theta_{11}) L(\widetilde{\widetilde{\Im}}(n)|\theta_{12}, \theta_{22}) \tag{11}$$

and study the breakdownpoints for each of them separately.

For each part of the likelihood (11) *Lemma 1* holds, except for the interpretation of the notation. Let us consider the distribution of the, say, type 1 particles. Then $\Im \equiv \Im_1$ is the set of all posible values of the vectors of offspring numbers; $\Upsilon \equiv \Upsilon_1$ is the convergence region of the series $A_1(\theta_{11}, \theta_{21})$, and $\partial\Upsilon_1$ is its boundary; $(MinV11, MinV12) \in \Im_1$ is the minimal numbers of offspring of type 1 and 2 respectively; $(MaxV11, MaxV12) \in \Im_1$ is the maximal numbers of offspring of type 1 and 2 respectively; $N_{MinV11,MinV12} \in \Im_1$ - the observed number of type 1 particles with minimal numbers of offspring of type 1 and 2, and $N_{MaxV11,MaxV12} \in \Im_1$ - the observed number of type 1 particles with maximal numbers of offspring of type 1 and 2.

Example 5. In the case of double Poisson offspring distribution for the particle of, say, type 1, the value of the breakdownpoint of the $WLT(K)$ estimator depends on the observed number particles which do not give any offspring.

3.2 The generation sizes scheme

Let us suppose, that we are able to observe the generation sizes only. The observations form the set

$$\Im(n) = \{\mathbf{Z}(0), \ldots, \mathbf{Z}(n)\}$$

The following statements are valid (see González et al.[6]):

$$P(\widetilde{\widetilde{\Im}}(n)|\Im(n), \theta_{11}, \theta_{21}) = \prod_{s=0}^{n-1} P(\widetilde{\widetilde{\Im}}(s)|\mathbf{Z}(s), \mathbf{Z}(s+1), \theta_{11}, \theta_{21})$$

and

$$P(\widetilde{\Im}(n)|\Im(n), \theta_{11}, \theta_{21}) = \prod_{s=0}^{n-1} P(\widetilde{\Im}(s)|\mathbf{Z}(s), \mathbf{Z}(s+1), \theta_{11}, \theta_{21}).$$

Therefore in the situation of power series with finite support $|\Im_1|, |\Im_2| < \infty$ one can use the multinomial distribution ([6]) to reconstruct the family tree:

$$P(\widetilde{\Im}(s)|\mathbf{Z}(s), \mathbf{Z}(s+1), \theta_{11}, \theta_{21}) = \frac{\prod\limits_{k=1,2} \frac{[Z_k(s)]!}{\prod\limits_{(i,j)} [Z_k(n,(i,j))]!} \prod\limits_{(i,j)} [p_{ij}^k]^{Z_k(s,(i,j))}}{P(\mathbf{Z}(s+1)|\mathbf{Z}(s))}$$

When the support $|\Im_1|, |\Im_2| = \infty$, for some distributions (f.e. double Poisson) one can compute directly from the expression

$$P(\widetilde{\widetilde{\Im}}(s)|\mathbf{Z}(s), \mathbf{Z}(s+1), \theta_{11}, \theta_{21}) = \frac{\prod\limits_{k=1,2} \prod\limits_{l=1}^{Z_k(s)} p^k_{\xi_1^k(s,l), \xi_2^k(s,l)}}{P(\mathbf{Z}(s+1)|\mathbf{Z}(s))}.$$

We may sumarize the procedure for the $WLT(k)$ estimation on the basis of the generation sizes in the following way:

1. Estimating the vector θ, for example using the Harris estimators on an available subset of the family tree, free of outliers.

2. Generating a family tree, using the observed generation sizes and the parameter value from 1.

3. Estimating the vector θ, using the $WLT(K)$ estimator over the entire family tree, and detecting the 'errors'.

This procedure gives good results if there are a few "impulse" outliers in the generation sizes on the basis of a process with a sufficiently large number of generations.

4 Acknowledgements

This work is supported by the European Social Fund through the Human Resource Development Operational Programme under contract BG051PO001-3.3.06-0052 (2012/2014) and is partially supported by the National Fund for Scientific Research at the Ministry of Education and Science of Bulgaria, grant NFSI I02/17 and by the financial funds allocated to the Sofia University St. Kl. Ohridski, grant No 012/2014.

References

1. Asmussen, S., H. Herring, *Branching Processes*, Birkhauser, Boston, 1983.
2. Atanasov D., Neykov N. On the Finite Sample Breakdown Point of the WLTE(k) and d-fullness of a Set of Continuous Functions. *Proceedings of the VI International Conference Computer Data Analysis And Modeling*,Minsk, Belarus, 2002.
3. Athreya, K.B., Ney, P.E. *Branching Processes.* Springer-Verlag, Berlin 1972.
4. Atanasov D., Stoimenova V. Simulation, Estimation and Robustification against Outliers in Branching Processes - a Computational Approach *Proceedings COMPSTAT*, 53–65, 2012.
5. Gerstenkorn, T. On multivariate power series distributions, *Revue Roumaine de Mathématiques Pures et Appliquées*, 26, 247–266, 1981.
6. González, M., Martín, J., Martínez, R., Mota, M. Non-parametric Bayesian estimation for multitype branching processes through simulation-based methods *Computational statistics & data analysis*, 52, 1281–1291, 2008.
7. González, M., del Puerto I. M., Martínez, R., Mota, M. *Workshop on Branching Processes and Their Applications.* Lecture Notes in Statistics, 197, Springer Verlag, 2010.
8. Hampel, F. R., Ronchetti, E.M., Rousseeuw, P. J., Sta- hel W. A. *Robust Statistics: The Approach Based on Influence Functions.* John Wiley and Sons, New York, 1986.
9. Harris, T.E. *The Theory of Branching Processes.* Springer-Verlag, Berlin, 1963.
10. Jacob, C. Branching processes: their role in epidemiology. *Int. J. Environ. Res. Public Health* 7, 11861204, 2010.
11. Jagers, P. *Branching Processes with Biological Applications.* Wiley, London, 1975.
12. Kolmogorov, A.N., Dmitriev, N.A. Branching random processes *Dokl. Akad. Nauk (Proc. Acad. Sci. USSR)*, **56**, 7–10, 1947 (in Russian).
13. Kolmogorov, A.N., Sevastyanov, B.A. Calculation of final probabilities of branching random processes. *Dokl. Akad. Nauk (Proc. Acad. Sci. USSR)*, **56**, 783–786, 1947 (in Russian).
14. Sevastyanov, B.A. *Branching Processes*, Nauka, Moscow, 1971 (in Russian).
15. Johnson, N., Kotz, S., Balakrishtnan, N, *Discrete multivariate distributions*, Wiley,
16. Khatri, C. G. On multivariate contagious distributions, *Sankhyia*, Series B, 33, 197–216, 1971.
17. Kocherlakota, S., Kocherlakota, K. *Bivariate discrete distributions*, Marcel Dekker Inc., New York, 1992
18. Patil, G. P. On multivariate generalized power series distribution and its applications to the multinomial and negative multinomial, *Clussical und Contugious Discrete Distributions* (Ed. G. P. Patil), Proceedings of International Symposium at McGill University on August 15-20, 183–194, Calcutta: Statistical Publishing Society; Oxford: Pergamon Press, 1965.

19. Rousseeuw P., Leroy A.,*Robust Regression and Outlier Detection*. John Wiley and Sons, New York, 1981
20. Stoimenova, V. Robust Parametric Estimation of Branching Processes with Random Number of Ancestors. *Serdica Math. J.* **31(3)**, 243–262, 2005.
21. Stoimenova V., Atanasov D. Robust estimation in multitype branching processes based on their asymptotic properties. *Pliska Stud. Math. Bulgar.***21**, 203–220, 2011.
22. Stoimenova, V., Yanev N. Parametric Estimation in Branching Processes with an Increasing Random Number of Ancestors. *Pliska Stud. Math. Bulgar.* **17**, 295–312, 2005.
23. Vandev D.L. A Note on Breakdown Point of the Least Median of Squares and Least Trimmed Estimators. *Statistics and Probability Letters* **16**, 117–119, 1993.
24. Vandev, D. L. and Neykov, N. M. Robust Maximum Likelihood in the Gaussian Case. *In: New Directions in Statistical Data Analysis and Robustness*, S. Morgenthaler, E. Ronchetti, and W. A. Stahel (eds.), (Basel: Birkhauser Verlag), 257–264, 1993.
25. Vandev D.L. and Neykov, N.M. About Regression Estimators with High Breakdown Point *Statistics*, **32**, 111–129, 1998.
26. Yakovlev, A.Y., Stoimenova, V.K., Yanev, N.M. Branching Processes as Models of Progenitor Cell Populations and Estimation of the Offspring Distributions. *J. American Statistical Assoc*, **103**, 1357–1366, 1998.
27. Yakovlev, A. Yu., Yanev, N. M. *Transient Processes in Cell Proliferation Kinetics*. Springer Verlag, Berlin, 1989.
28. Yakovlev A. Yu. , N. M. Yanev. Relative frequencies in multitype branching processes. *Ann. Appl. Probab.*,**19**, No.1, 1–14, 2009.
29. Yakovlev A. Yu., N. M. Yanev . Limiting distributions in multitype branching processes. *Stochastic Analysis and Applications*,**28**, No.6, 1040–1060, 2010.

5 CHAPTER

Stochastics

Are credit ratings time-homogeneous and Markov?

Pedro Lencastre[1,2], Frank Raischel[3], Pedro G. Lind[4], Tim Rogers[5]

[1] ISCTE-IUL, Av. Forças Armadas, 1649-026 Lisboa, Portugal
(e-mail: pedro.lencastre.silva@gmail.com)
[2] Mathematical Department, FCUL, University of Lisbon, 1749-016 Lisbon, Portugal
[3] Instituto Dom Luiz, University of Lisbon, 1749-016 Lisbon, Portugal
(e-mail: raischel@cii.fc.ul.pt)
[4] ForWind and Institute of Physics, University of Oldenburg, Ammerländer Heerstrasse 136, DE-26111 Oldenburg, Germany
(e-mail: pedro.g.lind@forwind.de)
[5] Centre for Networks and Collective Behaviour, Department of Mathematical Sciences, University of Bath, Claverton Down, BA2 7AY, Bath, UK

Abstract. We introduce a simple approach for testing the reliability of homogeneous generators and the Markov property of the stochastic processes underlying empirical time series of credit ratings. We analyze open access data provided by Moody's and show that the validity of these assumptions - existence of a homogeneous generator and Markovianity - is not always guaranteed. Our analysis is based on a comparison between empirical transition matrices aggregated over fixed time windows and candidate transition matrices generated from measurements taken over shorter periods. Ratings are widely used in credit risk, and are a key element in risk assessment; our results provide a tool for quantifying confidence in predictions extrapolated from rating time series.
Keywords: Generator matrices,Continuous Markov processes,Rating matrices,Credit Risk.

1 Motivation and Scope

After the Basel II accord in 2004 [1], ratings became an increasingly important instrument in Credit Risk, as they allow banks to base their capital requirements on internal as well as external rating systems. These ratings became instrumental in evaluating the risk of a bond or loan and in the calculation of the Value at Risk. As such, it is often desirable to quantify the uncertainty in these ratings, and predict the likelihood that an institution will be upgraded or downgraded in the near future. A common technique is to aggregate credit rating transition data over yearly or quarterly periods, and to model future transitions using these data. However, to be reliable the ratings' evolution

New Trends in Stochastic Modeling and Data Analysis (pp. 189-198)
Raimondo Manca - Sally McClean - Christos H Skiadas (Eds)

must obey particular features which we show below can be evaluated through analysis of the data published by rating agencies. Two sufficient properties for accepting the empirical data as a reliable indicator of future rating evolution are the existence of a generator and Markovianity[2].

There is a wide literature about non-Markovianity of rating evaluations, see e.g. Ref. [3] and references therein. To stress a test for the Markovianity of a transition processes, introduced in 2006[4] and more recently developed by D'Amico et al[5].

The representation of the evolution of a time-continuous process by an aggregated transition matrix will not be adequate if the underlying process is not Markov. Moreover, if there is no generator associated to the transition matrix, the process underlying the ratings is not continuous. Different techniques to estimate a transition matrix from a finite sample of data should be employed depending on whether the process is time-homogeneous or not[6,7]. Theoretically, both the Markov and the time-homogeneous assumptions simplify considerably the models in question[8], but typically only the latter is at times dropped in order to build a more general theoretical framework.

In this paper we test how well both conditions are met in different periods of time for a rating class in Moody's database. We compare transition matrices calculated under different assumptions and show that the Markov assumptions change considerably in time. Moreover, by computing a generator for each one of such different periods of time, assuming that homogeneity holds, i.e. the generator is constant we show that the generator changes considerably in time. Therefore we provide evidence that the rating series are not always Markovian and time-homogeneous. Finally, we argue that these deviations from the assumptions may, on the one hand, provide evidence for detecting discontinuities in the rating process, e.g. when establishing new evaluation criteria for a bank rating, and, on the other hand, can be taken as a tool for ascertaining how complete and trustful such rating criteria are.

We start in Sec. 2 by describing the empirical data collected from Moody's and in Sec. 3 we describe how to test the validity of both the homogeneity and Markovianity assumptions. Section 4 concludes the paper and presents some discussion of our results in the light of finance rating procedures.

2 Data: Six Years of Rating Transitions

The data analyzed in this paper is publicly available data that Moody's needs to disclose and keep publicly available in compliance with Rule 17g-2(d)(3) of US. SEC regulations [9].

The rating time series of each bank has a sample frequency of one day, starting in August of 2007 and ending in January 1st of 2013. The data sample is the set of rating histories from the banks around the world, that had a rating at the final date. Each value indicates the rating class of *Senior unsecured*[10] debt issues, at which the issuer is evaluated at that particular day.

One first important feature of this rating database is the growing number of rated entities, as can be seen in Fig. 1. The number of banks N_R included in the data set increased almost monotonically during the total time-span analyzed

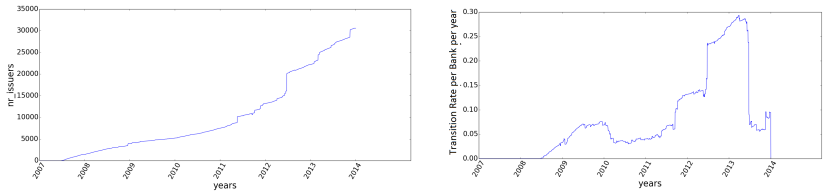

Fig. 1. (a) Number of bank entities in Moody's data sample as a function of time and **(b)** the transition probability, computed as moving averages during one-year periods.

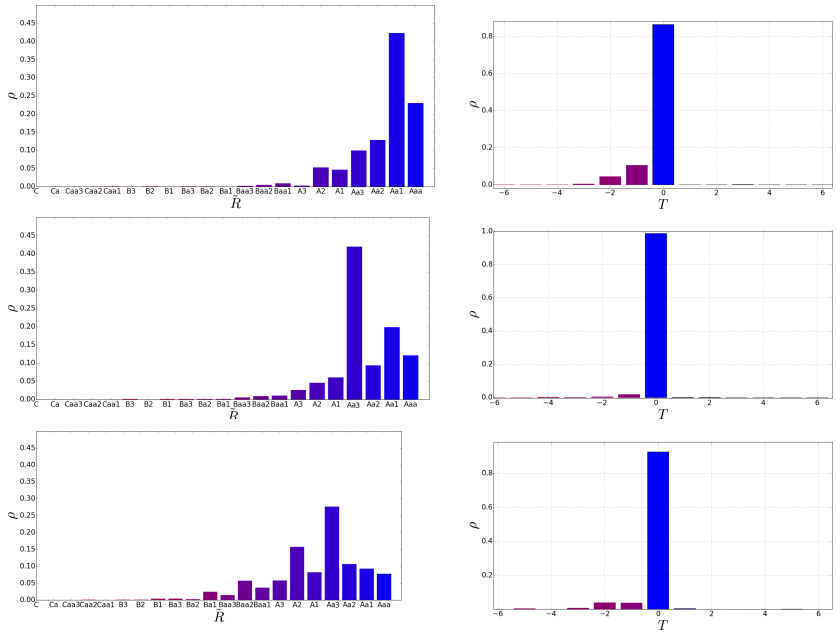

Fig. 2. Illustration of rating histograms for the rating state $\tilde{R}$ (left) and the corresponding rating variations $T = \Delta R$ (right), where R is an integer encoding the rating state, ranging from 0 (C) to 20 (Aaa). Three different days are selected: first day of 2009 (first row), 2011(second row) and 2013 (third row); cf. Fig. 3.

by us (see Fig. 1a). The first ratings in our database are from August of 2007. Until middle 2012 the number of ratings in our database grows steadily at a rate of about 3000 new ratings per year. In middle 2012 there is a great influx of classifications in our database, and until 2014 the number of ratings grows more irregularly and at an higher rate. Due to the increasing number of ratings in our database, we will often use measures where the normalization by the number of bank's debt ratings in the database is accounted for.

We count in Moody's database a total of $N_T = 3623$ rating transitions, that distribute heterogeneously in time. Indeed, the mean transition rate N_T per bank and per year also changes significantly, with a peaked activity during the year of 2012 and 2013 (see Fig. 1b). This will be of importance when

analyzing the evolution of the generator homogeneity and Markovianity of the corresponding transition matrices.

The rating category is a measure of the capacity of the institution to meet its financial obligations and to avoid default or government bailout. We have $n_s = 21$ rating states, using the usual Moody's classification [10].

Figure 2 shows three plots (left) illustrating the histogram of rating states at three different time, namely in January 2009, January of 2011 and January of 2013.

Henceforth, we define $\tilde{R}_i(t)$ as the rating of the bank number i at the instant t, and we map the rating states to a number series ordered by decreasing credit risk: state $\tilde{R} = C$ corresponding to label $R = 0$, and state $\tilde{R} = Aaa$ to label $R = 20$. With such a labelling it is possible to compute rating increments as

$$T_i(t, \tau) = R_i(t) - R_i(t - \tau). \tag{1}$$

When $T_i(t) > 0$ (resp. < 0) it means that bank i saw its rating increased (resp. decreased) during the last τ period of time. Unless stated otherwise we will use always $\tau = 365$ days. The plots in the right column of Fig. 2 show the histograms of the corresponding rating increments evaluated in January of 2009, January of 2011 and January of 2013, respectively.

We call henceforth $R(t)$ and $T(t)$ the aggregated processes of the ratings and rating increments, respectively, over all N_R companies observed at time t. Figure 3 shows the evolution of the first four moments for both rating distributions (left) and transition distributions (right), with $\tau = 365$ days.

The average rating $\langle R \rangle$ (Fig. 3a) decreased during most of the six year period records. We should note, however, that this is partially due to the new entries in the database whose initial rating is typically low, since $\langle T \rangle$ has positive periods during the first five years of the recorded set.

As for the rating variance σ_R (Fig. 3e), it steadily increases due to the concentration, in earlier times, of rating states in the better rating classes ($\langle T \rangle < 0$). The transition process T however exhibit two periods of increased variance σ_T (Fig. 3f), which reflect probably the respective increase in the number of transitions (compare with Fig. 1b).

The rating skewness μ_R (Fig. 3c) is positive across the years analysed due to the concentration of issuers in higher ratings.

The rating distribution is also typically leptokurtic (see Fig. 3d), as its kurtosis is always above three (Gaussian kurtosis), indicating a more pronounced flatness around the average of rating distributions. Concerning the third and fourth moments of transition distributions, Figs. 3g and 3h respectively, we see large fluctuations during the periods with fewer transitions. One can clearly sees a very high kurtosis and skewness, although the skewness maintains its negative value for most of the interval considered.

3 What is the Underlying Continuous Process?

In the following we assume that the set of rating transitions has a continuous processes underlying it, an assumption which has been the subject of previous

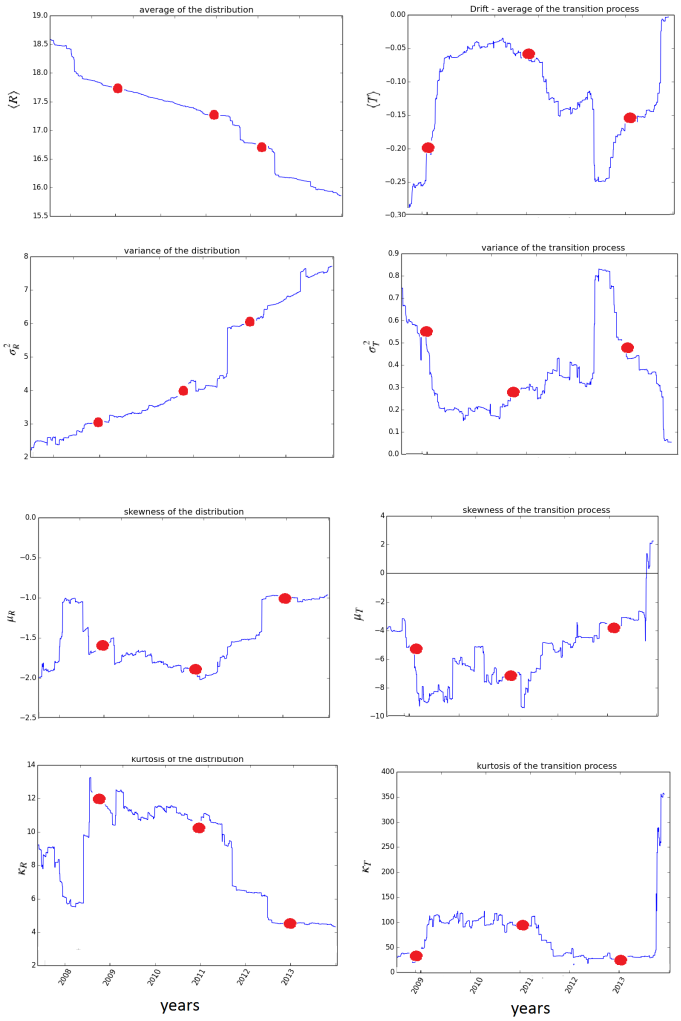

Fig. 3. Evolution of the first statistical moments of **(a-d)** the rating state R distribution and **(e-h)** its one-year-increment T distribution. From top to bottom: averages $\langle R \rangle$ and $\langle T \rangle$, variances σ_R^2 and σ_T^2, skewnesses μ_R and μ_T, and kurtosis κ_R and κ_T. Bullets indicate the days when the histograms in Fig. 2 were taken.

investigations without a clear result, see e.g. Ref. [11]. Even in case that there is a continuous process, the corresponding generator may be constant (homogeneous generator) or vary in time (non-homogeneous).

The non-homogeneity is important in the finance context since it limits the range of models that can be used. In particular, it has been argued [6] that a better method of estimating a transition matrix than the usual one exists, if we consider time-homogeneity. I think that the world is, in general, non-homogeneous! The main advantage of this method is the possibility to capture very small transition probabilities between two states, even when no

transitions occurred between those two states. The time-homogeneity condition is also important to check if the through the cycle rating philosophies [12,13] allegedly used, which imply that that the ratings must not follow external cycles, are being correctly followed or note. These methodologies do not hold if criteria by which ratings are ascribed to banks are not constant in time, but vary according to artificial or externally imposed factors[14].

Furthermore, another important feature of continuous transition processes is their Markovianity. The Markov property is important if the current rating of a bank is to be considered a complete indicator of its future risk. In this section we will address both these conditions separately.

3.1 Testing Time-Homogeneity

Mathematically, if a time-continuous Markov process is time-homogeneous then there is a constant matrix $\mathbf{Q}$, called a generator, solution of

$$\frac{d\mathbf{M}(t)}{dt} = \mathbf{Q}\mathbf{M}(t), \tag{2}$$

where $\mathbf{M}$ is the transition matrix, with entries M_{ij} giving the probability for observing a transition from state i to state j $(i, j = 1, \ldots, n_s)$. In other words, a time-continuous process is time-homogeneous if, being Markov, its transition matrix can be expressed as $\mathbf{M}(t) = e^{\mathbf{Q}t}$, and therefore it has a well-defined logarithm. We take the analogue from ordinary differential equations and loosely call $\mathbf{Q}$ the logarithm of $\mathbf{M}$.

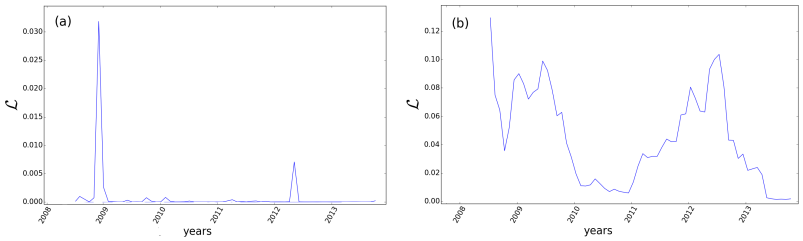

Fig. 4. Testing for temporal homogeneity: difference between the log-likelihood $\mathcal{L}$ of the transition matrix $\mathbf{M}^{(e)}$ and the transition matrix $\mathbf{M}$ calculated assuming time-homogeneity. Both matrices are calculated over a time interval $t_f - t_0$ **(a)** one month and **(b)** one year. The log-likelihood was calculated using Eq. (4) at the first day of each month from August 2008 to December 2013.

The mathematical conditions for the existence of a homogeneous generator give a bivalent result[11,15] that does not take into consideration neither noise generated from finite samples nor how distant an empirical process is from being time-continuous. Therefore, we neglect several mathematical results that determine if a generator exists or not, and assume that the process is Markov and time-continuous. Being Markov and time-continuous means that there is a generator satisfying Eq. (2) and that it either is constant or varies in time.

Next, we estimate the closest constant generator $\mathbf{Q}$ directly from the empirical data, compute the associated matrix $\mathbf{M} = e^{\mathbf{Q}t}$, and compare it with the empirical transition matrix $\mathbf{M}^{(e)}$. For estimating the generator matrix $\mathbf{Q}$ we follow the approach described in Ref. [7], calculating its off-diagonal elements as

$$Q_{ij} = \frac{N_T^{(ij)}}{\int_{t_0}^{t_f} N_R^{(i)}(t)dt}, \tag{3}$$

where $N_T^{(ij)}$ represents the number of transitions from i to j between the times t_0 and t_f, and $N_R^{(i)}(t)$ stands for the number of banks in state i at time t. The diagonal elements Q_{ii} follow from the condition $\sum_j Q_{ij} = 0$.

To compute the distance between a time-homogeneous process and the empirical process we compare $\mathbf{M}$ with $\mathbf{M}^{(e)}$, and plot the statistic:

$$\mathcal{L} = \frac{\sum_{i,j} N_T^{(ij)} \left(\log M_{ij} - \log M_{ij}^{(e)} \right)}{\sum_{i,j} N_T^{(ij)}} \,. \tag{4}$$

This is a log-likelihood ratio; loosely speaking it quantifies the error introduced by making the assumption of time homogeneity. The results are shown in Fig. 4: in panel (a) we aggregate the data in periods of one month while in panel (b) the aggregation period is one year.

It can be seen that there are two periods when the time-homogeneity condition becomes an insufficient approximation to the dynamics of the process marked by significant increases in $\mathcal{L}$. The first period starts in the latest half 2009, the second period around the middle of 2012.

These two periods can be better analysed taking also observations from Fig. 3.

In late 2009 and early 2010 the mean of the transition process $\langle T \rangle$ is relatively close to zero, which contrasts to period of late 2008 and early 2009. The high values of the variance σ_T is consistent with the relative high rate of transition in this period. The strongly negative values of the skewness μ_T indicate that there is some extreme transitions to lower rating states, which is also consistent with the high values of the kurtosis κ_T. The relatively high values of κ_T and the absolute value of μ_T tells us that the transitions did not follow a general trend, but were composed by some very drastic movement by just a few rated banks.

In 2012 the scenario is similar to 2010. Again there are more downgrades, but now the influence of extreme events is less pronounced. The companies are now much less clustered, i.e. with large dispersion in their ratings, as one can see by the high values in σ_R.

3.2 Testing the Markov Hypothesis

Mathematically, a Markov process x_t obeys the following condition:

$$\Pr(x_{t_1} | x_{t_2}, x_{t_3}, \dots) = \Pr(x_{t_1} | x_{t_2}) \tag{5}$$

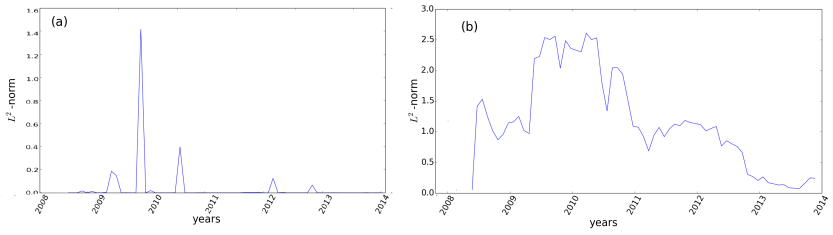

Fig. 5. Testing Markovianity: difference between the empirical transition matrix $\mathbf{M}^{(e)}_{0\tau}$ calculated over a time-interval $[0, \tau]$ and the product of the half-period matrices, $\mathbf{M}^{(e)}_{0\frac{\tau}{2}}$ and $\mathbf{M}^{(e)}_{\frac{\tau}{2}\tau}$, using the L^2-norm defined in Eqs. (7) and (8). Both matrices are calculated over a time interval of **(a)** one month and **(b)** one year. The difference was calculated at the first day of each month between August 2008 and December 2013.

with $t_1 > t_2 > t_3 > \ldots$. The conditional probability in the right hand-side of Eq. (5), $\Pr(x_{t_1}|x_{t_2})$, is exactly specified by the transition matrix $\mathbf{M}$.

The rating process should be assumed to be Markov, otherwise a rating would not represent a uniform risk class, as its elements could be distinguished according to their previous series of rating states.

From the definition of a Markov process in Eq. (5) it is straightforward to show that a Markov process also obeys

$$\mathbf{M}_{t_0 t_f} = \prod_{n=1}^{N} \mathbf{M}_{t_{n-1} t_n}, \tag{6}$$

where N is the number of subintervals in $[t_0, t_f]$ and labels $t_i t_j$ denote the time interval $[t_i, t_j]$ considered when determining $\mathbf{M}_{t_i t_j}$. Here we fix $N = 2$ and consider two equally spaced intervals with $\tau \equiv t_f - t_0 = 1$ month and $\tau = 1$ year. Equation (6) is known as the Chapman-Kolmogorov equation[16] and it does not hold in general either when the process is non-Markov or when we have an insufficiently short sample of data.

We will use the Chapman-Kolmogorov equation as a test indicating whether the rating database of Moody's is Markov. To that end, we consider empirical matrices $\mathbf{M}^{(e)}_{0\tau}$ computed for one month and one year intervals, and compare it with the associated product of the two corresponding half-periods, $\overline{\mathbf{M}^{(e)}}_{0\tau} = \mathbf{M}^{(e)}_{0\frac{\tau}{2}} \mathbf{M}^{(e)}_{\frac{\tau}{2}\tau}$. For the comparison we now use the L_2-norm instead of the the $\mathcal{L}$ log-likelihood, since the latter creates singularities when dealing with zero entries in the matrices, which now occur more frequently. The L_2-norm of the transition matrix is the maximum singular value of $\mathbf{A}$,

$$\|\mathbf{A}\| = \sigma_{\max}(\mathbf{A}), \tag{7}$$

and we compute it for the difference

$$\mathbf{A} = \mathbf{M}^{(e)}_{0\tau} - \overline{\mathbf{M}^{(e)}}_{0\tau}\,, \tag{8}$$

where $\|\cdot\|$ represents the usual Euclidean norm.

Results are shown in Fig. 5. Clearly, there is one periods when the Markov assumption seems less valid, namely in mid 2009. As said before, this coincides with an abrupt change in the statistics of T and R.

4 Discussion and conclusions

We have addressed time series of credit ratings publicly available at Moody's online site and studied simple ways to compute the validity of the time-homogeneous and Markov assumptions. We have shown how the accuracy of these assumptions varies with time. Naturally, when the Markov assumption fails, so does the time-homogeneous assumption, in particular during 2009 and beginning of 2010. In these periods the statistics of the process changed considerably. In the end of the year of 2012 the accuracy of the time-homogeneous assumption is low but the Markov approximation is within the usual fluctuation range.

One must stress that when the Markov assumption does not hold, the ratings are not a complete measure of the risk of a given entity, since further information besides the actual rating needs to be specified.

In fact, compared with homogeneous generators, non-homogeneity is by far a more realistic assumption, but its modelling approach requires better and higher sampled data. Such argument agrees with our findings that the present assumptions used for deriving rating matrices are not the best ones either because they deviate from more realistic assumptions, such as non-homogeneity, or because they can not be derived from the present empirical knowledge of the economical and financial environment.

Moreover, we can argue that even if well estimated, rating evaluations are of poor significance for practical purposes: they are a well-derived metric, at most, during expansive periods. We have shown how they fail during crisis and during the transition between crisis and economical expansion, precisely the periods where ratings are of used for decision-making and strategy adaptation in the markets.

Our approach can be improved by introducing for instance a more sophisticated procedure for extracting the histograms for the ratings and their increments, namely using the kernel based density, which is known to converge faster to the real distribution than the usual binning procedure. From this first approach to investigate Moody's rating database one can now approach the embedding problem for the series of transition matrices, where different generators estimates can be compared. These and other issues will be addressed elsewhere.

Acknowledgments

The authors thank Fundação para a Ciência e a Tecnologia for financial support under PEst-OE/FIS/UI0618/2011, PEst-OE/MAT/UI0152/2011, SFRH-/BPD/65427/2009 (FR). This work is part of a bilateral cooperation DRI/-DAAD/1208/2013 supported by FCT and Deutscher Akademischer Auslands-

dienst (DAAD). PL thanks Global Association of Risks Professionals (GARP) for the "Spring 2014 GARP Research Fellowship".

References

1. Basel Committee on Banking Supervision. Overview of the new baselcapital accord. *consultative document*, 2003.
2. Truek and Rachev. *Rating Based Modeling of Credit Risk: Theory and Application of Migration Matrices*. Academic Press, 2009.
3. G. d'Amico, J. Janssen, and R. Manca. Homogeneous semi-markov reliability models for credit risk management. *Decision in Economic and Finance*, 28:79–93, 2005.
4. Stenberg, Manca, and Silvestrov. Semi-markov reward models for disability insurance". rating based modeling of credit risk: Theory and application of migration matrices. In *Theory of Stochastic Processes*, volume 12, pages 239–254, 2006.
5. G. DAmico and F. Petroni. A semi-markov model for price returns. *Physica A*, 391:4867–4876, 2012.
6. Theodore Charitos, Peter R de Waal, and Linda C van der Gaag. Computing short-interval transition matrices of a discrete-time markov chain from partially observed data. *Statistics in medicine*, 27(6):905–921, 2008.
7. David Lando and Torben M Skødeberg. Analyzing rating transitions and rating drift with continuous observations. *journal of banking & finance*, 26(2):423–444, 2002.
8. Rafael Weißbach, Patrick Tschiersch, and Claudia Lawrenz. Testing time-homogeneity of rating transitions after origination of debt. *Empirical Economics*, 36(3):575–596, 2009.
9. https://www.moodys.com/pages/reg001004.aspx.
10. S Moody. moodys rating symbols & definitions. *Moodys Investors Service, Report*, 79004(08):1–52, 2004.
11. R.B. Israel, J.S. Rosenthal, and J.Z. Wei. Finding generators for markov chains via empirical transition matrices, with applications to credit ratings. *Mathematical Finance*, 11(2):245–265, 2001.
12. John Kiff, Michael Kisser, and Miss Liliana Schumacher. *Rating Through-the-Cycle: What does the Concept Imply for Rating Stability and Accuracy?* Number 13-64. International Monetary Fund, 2013.
13. Z. Varsanyi. Rating philosophies: some clarifications. 2007.
14. Jerome Mathis, James McAndrews, and Jean-Charles Rochet. Rating the raters: are reputation concerns powerful enough to discipline rating agencies? *Journal of Monetary Economics*, 56(5):657–674, 2009.
15. EB Davies. Embeddable markov matrices. *Electronic Journal of Probability*, 15:1474–1486, 2010.
16. Hannes Risken. *Fokker-Planck Equation*. Springer, Berlin, 1984.

Perturbation Methods for Pricing European Options in a Model with Two Stochastic Volatilities

Betuel Canhanga[1], Anatoliy Malyarenko[2], Ying Ni[2], and Sergei Silvestrov[2]

[1] Faculty of Sciences, Department of Mathematics and Computer Sciences, Eduardo Mondlane University, Box 257, Maputo, Mozambique (e-mail: betuel.canhanga@mdh.se)

[2] Division of Applied Mathematics, School of Education, Culture and Communication, Mälardalen University, Box 883, SE-721 23 Västerås, Sweden (e-mail: anatoliy.malyarenko@mdh.se, ying.ni@mdh.se, sergei.silvestrov@mdh.se)

Abstract. Financial models have to reflect the characteristics of markets in which they are developed to be able to predict the future behaviour of a financial system. The nature of most trading environments is characterised by uncertainty that is expressed in mathematical models in terms of volatilities. In contrast to the classical Black–Scholes model with constant volatility, our model of mean-reversion type includes two stochastic volatilities, a fast-changing and a slow-changing, which can be interpreted as the effects of weekends and the effects of seasons of the year (summer and winter) on the asset price.

We perform explicitly the transition from the real-world probability measure to the risk-neutral one by introducing two market prices of risk and applying Girsanov Theorem. To solve the boundary value problem for the partial differential equation that corresponds to the case of a European option, we perform both regular and singular multi-scale expansions in fractional powers of the speed of mean-reversion factors. We then construct an approximate solution given by the classical two-dimensional Black–Scholes model plus some terms that expand the results obtained by Black and Scholes. Concrete examples are presented.

Keywords: Financial market, Mean reversion volatility, Risk-neutral measure, Partial differential equation, Regular perturbation, Singular perturbation, European option.

1 Introduction

European options are financial instruments that are signed today to be executed at a predetermined future time, i.e the maturity, and at a predefined price, i.e. the strike price. Divided in two types, call (put) option is a contract that gives the buyer of the contract the right but not obligation to buy (sell) an asset at the strike price at maturity. One has to pay to get rights without obligations,

New Trends in Stochastic Modeling and Data Analysis (pp. 199-210)
Raimondo Manca - Sally McClean - Christos H Skiadas (Eds)

the question is how much will be paid to buy such type of contract. The answer to this question is addressed in various mathematical options pricing models. This type of models gives the relation between parameters involved in the price evolution of an asset and the value of its contingent claims, for example, a call option on the asset. Since the price process is not deterministic, one has to consider stochastic changes of prices that will impose the presence of volatility terms on mathematic modelling. Black and Scholes [1] has presented the celebrated option pricing model considering volatility as constant. To overcome the limitations of constant volatility many researchers have considered models that incorporates stochastic volatility (Heston [2], Christoffersen et al [11], Hull [9], Grzelak and Oosterlee [10], Chiarella and Ziveyi [3], among others).

Our model was considered by Christoffersen et al [11]. They write down without proof the characteristic function of the log-spot price, and value the European call option by Fourier inversion. In the present paper we apply the approach by Fouque et al [7] instead. This approach gives us possibility to analyse the structure of the approximate solution as a sum of the Black–Scholes price and several correction terms, see formula (26).

A companion paper containing numerical calculations that illustrate the accuracy of the approximation and comparison with the Fourier inversion approach, is in preparation.

2 The model

Consider the price evolution of an asset (for example an equity stock) that is governed by the following stochastic differential equation

$$\mathrm{d}S_t = \mu S_t\,\mathrm{d}t + \sqrt{V_{1,t}}S_t\,\mathrm{d}W_1 + \sqrt{V_{2,t}}S_t\,\mathrm{d}W_2, \tag{1}$$

where μ is the mean return of the asset, $V_{1,t}$ and $V_{2,t}$ are two uncorrelated and finite variance processes described by Heston [2] that also change stochastically according to the following equations

$$\begin{aligned}
\mathrm{d}V_{1,t} &= \frac{1}{\varepsilon}(\theta_1 - V_{1,t})\,\mathrm{d}t + \rho_{13}\sqrt{\frac{1}{\varepsilon}V_{1,t}}\,\mathrm{d}W_1 + \sqrt{\frac{1}{\varepsilon}(1-\rho_{13}^2)V_{1,t}}\,\mathrm{d}W_3,\\
\mathrm{d}V_{2,t} &= \delta(\theta_2 - V_{2,t})dt + \rho_{24}\sqrt{\delta V_{2,t}}\,\mathrm{d}W_2 + \sqrt{\delta(1-\rho_{24}^2)V_{2,t}}\,\mathrm{d}W_4.
\end{aligned} \tag{2}$$

Here $\dfrac{1}{\varepsilon}$ and δ are the speeds of mean reversion; θ_1 and θ_2 are the long run means; $\sqrt{\dfrac{1}{\varepsilon}}$ and $\sqrt{\delta}$ the instantaneous volatilities of $V_{1,t}$ and $V_{2,t}$ respectively and $W_i,\ i = \{1,2,3,4\}$ are Wiener processes. The correlations between the asset price S_t and the variance processes $V_{1,t}$ and $V_{2,t}$ are given respectively by $\rho_{13}\sqrt{\dfrac{V_{1,t}}{\varepsilon}}$ and $\rho_{24}\sqrt{V_{2,t}\delta}$ which are chosen as in Chiarella and Ziveyi [3] to avoid the product term $\sqrt{V_{1,t}V_{2,t}}$.

In equation (2) choosing ε and δ to be small and to follow Feller [4] conditions, we have a fast mean reversion speed for $V_{1,t}$ and a slow mean reversion

speed for $V_{2,t}$. Therefore in our model the underlying asset price S_t is influenced by two volatility terms that behave completely differently. For example, one may change each month whereas the other one may change twice a day.

The finiteness of the two variances gives guarantee that equation (1) has a solution under the real-world probability measure. In addition it ensures that there exists an equivalent risk neutral measure under which the same equation has a solution and the discounted stock price process under this measure is a martingale.

2.1 Change of measure — application of Girsanov Theorem

According to Girsanov theorem (see for example Kijima [5]), under the equivalent risk neutral measure the processes $W_i^*,\ i = 1, \ldots, 4$, defined by $dW_i^* = \lambda_i dt + dW_i$, where λ_i are the market prices of risk. Making use of this result, we can write

$$\mathrm{d}W_i = -\lambda_i \,\mathrm{d}t + \mathrm{d}W_i^*, \qquad i = 1, 2, 3, 4, \tag{3}$$

where $\lambda_1 = \frac{\mu-(r-q)}{2\sqrt{V_{1,t}}}$; $\lambda_2 = \frac{\mu-(r-q)}{2\sqrt{V_{2,t}}}$; $\lambda_3 = \frac{\lambda_1\sqrt{V_{1,t}\varepsilon}}{\sqrt{1-\rho_{13}^2}}$ and $\lambda_4 = \frac{\lambda_2\sqrt{V_{2,t}\varepsilon}}{\sqrt{1-\rho_{24}^2}}$. Substituting equation (3) in equations (1) and (2), collecting similar terms and considering that under risk neutral measure μ is equal to $r - q$, we obtain the following system of stochastic differential equations

$$\begin{aligned}
\mathrm{d}S_t &= (r-q)S_t\,\mathrm{d}t + \sqrt{V_{1,t}}S_t\,\mathrm{d}W_1^* + \sqrt{V_{2,t}}S_t\,\mathrm{d}W_2^*,\\
\mathrm{d}V_{1,t} &= \left(\frac{1}{\varepsilon}(\theta_1 - V_{1,t}) - \frac{1}{\sqrt{\varepsilon}}\lambda_3\sqrt{V_{1,t}(1-\rho_{13}^2)}\right)\mathrm{d}t + \frac{1}{\sqrt{\varepsilon}}\sqrt{V_{1,t}}\rho_{13}\,\mathrm{d}W_1^*\\
&\quad + \frac{1}{\sqrt{\varepsilon}}\sqrt{V_{1,t}(1-\rho_{13}^2)}\,\mathrm{d}W_3^*,\\
\mathrm{d}V_{2,t} &= \left(\delta(\theta_2 - V_{2,t}) - \sqrt{\delta}\lambda_4\sqrt{V_{2,t}(1-\rho_{24}^2)}\right)\mathrm{d}t + \sqrt{\delta}\sqrt{V_{2,t}}\rho_{24}\,\mathrm{d}W_2^*\\
&\quad + \sqrt{\delta}\sqrt{V_{2,t}(1-\rho_{24}^2)}\,\mathrm{d}W_4^*.
\end{aligned} \tag{4}$$

Having our system given under risk neutral measure, the next step is to find the option price U of the underlying asset. To do this we need to construct the correlation matrix and perform some calculations.

$$\sigma = \begin{pmatrix} S_t\sqrt{V_{1,t}} & S_t\sqrt{V_{2,t}} & 0 & 0\\ \sqrt{\frac{V_{1,t}}{\varepsilon}}\rho_{13} & 0 & \sqrt{\frac{(1-\rho_{13}^2)V_{1,t}}{\varepsilon}} & 0\\ 0 & \rho_{24}\sqrt{\delta V_{2,t}} & 0 & \sqrt{\delta(1-\rho_{24}^2)V_{2,t}} \end{pmatrix},$$

and

$$\sigma\sigma^\top = \begin{pmatrix} S_t^2(V_{1,t}+V_{2,t}) & \frac{\rho_{13}S_tV_{1,t}}{\sqrt{\varepsilon}} & \rho_{24}S_tV_{2,t}\sqrt{\delta}\\ \frac{\rho_{13}S_tV_{1,t}}{\sqrt{\varepsilon}} & \frac{V_{1,t}}{\varepsilon} & 0\\ \rho_{24}S_tV_{2,t}\sqrt{\delta} & 0 & \delta V_{2,t} \end{pmatrix}.$$

Let us now consider $U = U(t, S_t, V_{1,t}, V_{2,t})$ as a function that has continuous second derivatives with respect to variables S_t, $V_{1,t}$, and $V_{2,t}$ and first derivative with respect to time. Using Feynman–Kac theorem (see for example Kijima [5]), Andersen and Piterbarg [12] have proved that the solution of system of differential equations (4) can also be expressed as the unique solution of the following parabolic partial differential equation

$$\begin{aligned}(r-q)S_t\frac{\partial U}{\partial S_t} &+ \left[\frac{1}{\varepsilon}(\theta_1 - V_{1,t}) - \lambda_1 V_{1,t}\right]\frac{\partial U}{\partial V_{1,t}} + [\delta(\theta_2 - V_{2,t}) - \lambda_2 V_{2,t}]\frac{\partial U}{\partial V_{2,t}} \\ &+ \frac{1}{2}\left[(V_{1,t}+V_{2,t})S_t^2\frac{\partial^2 U}{\partial S_t^2} + \frac{1}{\varepsilon}V_{1,t}\frac{\partial^2 U}{\partial V_{1,t}^2} + \delta V_{2,t}\frac{\partial^2 U}{\partial V_{2,t}^2}\right] \\ &+ \frac{1}{\sqrt{\varepsilon}}\rho_{13}S_t V_{1,t}\frac{\partial^2 U}{\partial S_t \partial V_{1,t}} + \sqrt{\delta}\rho_{24}S_t V_{2,t}\frac{\partial^2 U}{\partial S_t \partial V_{2,t}} = rU - \frac{\partial U}{\partial t},\end{aligned}$$

subject to the terminal value condition $U(T, S_t, V_{1,t}, V_{2,t}) = h(S_t)$. Here the coefficients of first order derivatives are coefficients of the $\mathrm{d}t$ terms in the stochastic differential equations in (4) and the coefficients of second order derivatives come from $\sigma\sigma^\top$. Collecting terms with the same powers of ε and δ gives

$$\begin{aligned}\frac{1}{\varepsilon}&\left[(\theta_1 - V_{1,t})\frac{\partial U}{\partial V_{1,t}} + \frac{1}{2}V_{1,t}\frac{\partial^2 U}{\partial V_{1,t}^2}\right] + \frac{1}{\sqrt{\varepsilon}}\rho_{13}S_t V_{1,t}\frac{\partial^2 U}{\partial S_t \partial V_{1,t}} \\ &+ \frac{\partial U}{\partial t} + (r-q)S_t\frac{\partial U}{\partial S_t} - \lambda_1 V_{1,t}\frac{\partial U}{\partial V_{1,t}} - \lambda_2 V_{2,t}\frac{\partial U}{\partial V_{2,t}} + \frac{1}{2}(V_{1,t}+V_{2,t})S_t^2\frac{\partial^2 U}{\partial S_t^2} - rU \\ &+ \sqrt{\delta}\rho_{24}S_t V_{2,t}\frac{\partial^2 U}{\partial S_t \partial V_{2,t}} + \delta\left[(\theta_2 - V_{2,t})\frac{\partial U}{\partial V_{2,t}} + \frac{1}{2}V_{2,t}\frac{\partial^2 U}{\partial V_{2,t}^2}\right] = 0\end{aligned}$$

or

$$\left(\frac{1}{\varepsilon}\mathcal{L}_0 + \frac{1}{\sqrt{\varepsilon}}\mathcal{L}_1 + \mathcal{L}_2 + \sqrt{\delta}\mathcal{M}_1 + \delta\mathcal{M}_2\right)U = 0 \tag{5}$$

for

$$\mathcal{L}_0 = (\theta_1 - V_{1,t})\frac{\partial}{\partial V_{1,t}} + \frac{1}{2}V_{1,t}\frac{\partial^2}{\partial V_{1,t}^2}, \tag{6}$$

$$\mathcal{L}_1 = \rho_{13}S_t V_{1,t}\frac{\partial^2}{\partial S_t \partial V_{1,t}},$$

$$\mathcal{L}_2 = \frac{\partial}{\partial t} + (r-q)S_t\frac{\partial}{\partial S_t} + \frac{1}{2}(V_{1,t}+V_{2,t})S_t^2\frac{\partial^2}{\partial S_t^2} - r - \lambda_1 V_{1,t}\frac{\partial}{\partial V_{1,t}} - \lambda_2 V_{2,t}\frac{\partial}{\partial V_{2,t}},$$

$$\mathcal{M}_1 = \rho_{24}S_t V_{2,t}\frac{\partial^2}{\partial S_t \partial V_{2,t}},$$

$$\mathcal{M}_2 = (\theta_2 - V_{2,t})\frac{\partial}{\partial V_{2,t}} + \frac{1}{2}V_{2,t}\frac{\partial^2}{\partial V_{2,t}^2}.$$

Our aim is to find the price of a European option with payoff function $h(S_t)$ at maturity T. Taking into account the Markov property and the fact that our

system is considered under the risk neutral probability measure, we can apply Feynman–Kac theorem to obtain the option price as

$$U(t, S_t, V_{1,t}, V_{2,t}) = e^{-(T-t)}\mathsf{E}^* \left[h(S_t) \mid S_t = s, V_{1,t} = v_1, V_{2,t} = v_2 \right].$$

Calculation of this expectation is very complicated because it involves many parameters that have to be clearly measured and applied. To avoid this complication, we present a perturbation method that approximates the option price by a quantity that depends on much less parameters than those imposed by Feynman–Kac theorem. From our system and also our partial differential equation, it is clear that $U(t, s, v_1, v_2)$ depends on ε and δ. From now on, to make this dependence clear, we write $U^{\varepsilon;\delta}(t, s, v_1, v_2)$ instead of $U(t, s, v_1, v_2)$. Our assumption is that if ε and δ are small, the associated operators will diverge and be small respectively. Therefore we use the approach of singular and regular perturbations.

3 Regular and singular perturbation

We now make a formal asymptotical expansion as presented in Fouque et al [6] and Fouque et al [7]. We start by performing a regular perturbation with respect to δ, followed by a singular perturbation with respect to ε.

Assume that our solution can be expressed in the following form

$$U^{\varepsilon,\delta} = U_0^\varepsilon + \sqrt{\delta} U_1^\varepsilon + \delta U_2^\varepsilon + \delta\sqrt{\delta} U_3^\varepsilon + \cdots \tag{7}$$

and use this expansion in (5) we have

$$\left(\frac{1}{\varepsilon}\mathcal{L}_0 + \frac{1}{\sqrt{\varepsilon}}\mathcal{L}_1 + \mathcal{L}_2 + \sqrt{\delta}\mathcal{M}_1 + \delta\mathcal{M}_2 \right) (U_0^\varepsilon + \sqrt{\delta} U_1^\varepsilon + \delta U_2^\varepsilon + \delta\sqrt{\delta} U_3^\varepsilon + \cdots) = 0.$$

Collecting terms with the same power of $\sqrt{\delta}$, the above equation can be rearranged into

$$\begin{aligned}
&\left(\frac{1}{\varepsilon}\mathcal{L}_0 + \frac{1}{\sqrt{\varepsilon}}\mathcal{L}_1 + \mathcal{L}_2 \right) U_0^\varepsilon \\
&+ \sqrt{\delta} \left[\left(\frac{1}{\varepsilon}\mathcal{L}_0 + \frac{1}{\sqrt{\varepsilon}}\mathcal{L}_1 + \mathcal{L}_2 \right) U_1^\varepsilon + \mathcal{M}_1 U_0^\varepsilon \right] \\
&+ \delta \left[\left(\frac{1}{\varepsilon}\mathcal{L}_0 + \frac{1}{\sqrt{\varepsilon}}\mathcal{L}_1 + \mathcal{L}_2 \right) U_2^\varepsilon + \mathcal{M}_1 U_1^\varepsilon + \mathcal{M}_2 U_0^\varepsilon \right] \\
&+ \delta\sqrt{\delta} \left[\left(\frac{1}{\varepsilon}\mathcal{L}_0 + \frac{1}{\sqrt{\varepsilon}}\mathcal{L}_1 + \mathcal{L}_2 \right) U_3^\varepsilon + \mathcal{M}_2 U_1^\varepsilon + \mathcal{M}_1 U_2^\varepsilon \right] \\
&+ \delta^2 \left[\left(\frac{1}{\varepsilon}\mathcal{L}_0 + \frac{1}{\sqrt{\varepsilon}}\mathcal{L}_1 + \mathcal{L}_2 \right) U_4^\varepsilon + \mathcal{M}_1 U_3^\varepsilon + \mathcal{M}_2 U_2^\varepsilon \right] + \cdots = 0.
\end{aligned} \tag{8}$$

Since $\delta > 0$, the asymptotic equality (8) holds only if all coefficients of δ are equal to zero under some appropriate final conditions. In particular we have

$$\left(\frac{1}{\varepsilon}\mathcal{L}_0 + \frac{1}{\sqrt{\varepsilon}}\mathcal{L}_1 + \mathcal{L}_2 \right) U_0^\varepsilon = 0, \qquad U_0^\varepsilon(T, s, v_1, v_2) \quad = h(s). \tag{9}$$

Solving the above partial differential equation with terminal condition $h(s)$ gives U_0^ε. To obtain U_1^ε we solve the following nonhomogeneous partial differential equation with terminal condition equal to zero, which follows also from the asymptotic equality (8),

$$\left(\frac{1}{\varepsilon}\mathcal{L}_0 + \frac{1}{\sqrt{\varepsilon}}\mathcal{L}_1 + \mathcal{L}_2\right) U_1^\varepsilon + \mathcal{M}_1 U_0^\varepsilon = 0, \qquad U_1^\varepsilon(T, s, v_1, v_2) = 0. \tag{10}$$

3.1 First order approximation

Expanding each $U_i^\varepsilon, i = 0, 1, 2, \ldots$ in terms of ε gives

$$U^{\varepsilon,\delta} = \sum_{i\geq 0}\sum_{j\geq 0} (\sqrt{\delta})^i (\sqrt{\varepsilon})^j U_{j,i}.$$

In particular

$$U_0^\varepsilon = U_{0,0} + \sqrt{\varepsilon}U_{1,0} + \varepsilon U_{2,0} + \varepsilon\sqrt{\varepsilon}U_{3,0} + \cdots. \tag{11}$$

Therefore the first order approximation is given by

$$U^{\varepsilon,\delta} = U_{0,0} + U_{1,0}^\varepsilon + U_{0,1}^\delta, \text{ where } U_{1,0}^\varepsilon = \sqrt{\varepsilon}U_{1,0} \text{ and } U_{0,1}^\delta = \sqrt{\delta}U_{0,1}. \tag{12}$$

Let us start by computing $U_{0,0} = U_0$. Equation (9) and (11) implies

$$\begin{aligned}\frac{1}{\varepsilon}\mathcal{L}_0 U_0 + \frac{1}{\sqrt{\varepsilon}}\left(\mathcal{L}_0 U_{1,0} + \mathcal{L}_1 U_0\right) + \left(\mathcal{L}_0 U_{2,0} + \mathcal{L}_1 U_{1,0} + \mathcal{L}_2 U_0\right)\\ + \sqrt{\varepsilon}\left(\mathcal{L}_0 U_{3,0} + \mathcal{L}_1 U_{2,0} + \mathcal{L}_2 U_{1,0}\right) + \cdots = 0.\end{aligned}$$

Since $\varepsilon > 0$ all coefficients of ε in the above equation should be equal to zero, which yields

$$\begin{aligned}\mathcal{L}_0 U_0 &= 0,\\ \mathcal{L}_0 U_{1,0} + \mathcal{L}_1 U_0 &= 0,\\ \mathcal{L}_0 U_{2,0} + \mathcal{L}_1 U_{1,0} + \mathcal{L}_2 U_0 &= 0,\\ \mathcal{L}_0 U_{3,0} + \mathcal{L}_1 U_{2,0} + \mathcal{L}_2 U_{1,0} &= 0.\end{aligned} \tag{13}$$

The first equation in (13) has exponential form solutions and can also have a constant with respect to v_1 as its solution, which suggests that we can write U_0 as $U_0 = U_0(t,\ s,\ v_2)$. The motivation of this choice is given in Fouque et al [7] by the fact that we want to have the leading-order price independent of the current value of the fast factor. Note that U_0 in this form does not depend on v_1 and the operator $\mathcal{L}_1$ contains only the mixed partial derivative with respect to the cross term of s and v_1. Taking consideration of this fact we obtain from the second equation in (13) $\mathcal{L}_1 U_0 = 0$ and hence $\mathcal{L}_0 U_{1,0} = 0$. This implies that

$$U_{1,0} = U_{1,0}(t,\ s,\ v_2)$$

for the same reasons as in the first equation of (13). It follows that

$$\mathcal{L}_1 U_{1,0} = 0. \tag{14}$$

The third equation in (13), together with equation (14), gives

$$\mathcal{L}_0 U_{2,0} + \mathcal{L}_2 U_0 = 0, \tag{15}$$

which is a Poisson equation for $U_{2,0}$ with $\mathcal{L}_2 U_0$ as a source. The solvability condition of Poisson equation (Fouque et al [7]) implies that

$$\langle \mathcal{L}_2 U_0 \rangle = 0, \tag{16}$$

where

$$\langle f \rangle = \int f(s)\pi(s)ds$$

denotes averaging over the invariant distribution Π.

Since U_0 does not depend on either v_1 or on the terms in the differential equation defined by operator $\mathcal{L}_2$, it follows that

$$\left\langle \frac{\partial U_0}{\partial t} + (r-q)s\frac{\partial U_0}{\partial s} - \lambda_2 v_2 \frac{\partial U_0}{\partial v_2} + \frac{1}{2}(v_1+v_2)s^2\frac{\partial^2 U_0}{\partial s^2} - rU_0 \right\rangle = 0.$$

Thus we have the following partial differential equation

$$\frac{\partial U_0}{\partial t} + (r-q)s\frac{\partial U_0}{\partial s} + \frac{1}{2}\sigma_1^2(v_2)s^2\frac{\partial^2 U_0}{\partial s^2} - rU_0 - \lambda_2 v_2 \frac{\partial U_0}{\partial v_2} = 0,$$

where $\sigma_1^2(v_2) = \int (v_1 + v_2)\Pi(dv_1)$.

The above partial differential equation is the Black–Scholes two-dimensional partial differential equation (Conze et al [8]) with volatility given by averaged effective volatility. Therefore we can rewrite it as

$$\mathcal{L}_{BS}(\sigma_1(v_2))U_{BS} = 0,$$

with the payoff function

$$U_{BS}(T, s, \sigma_1(v_2)) = h(s),$$

where the notation U_{BS} stands for the solution to the corresponding two-dimensional Black–Scholes model. Therefore we have

$$U_0 = U_{BS}. \tag{17}$$

3.2 Fast time scale correction

After having described U_0 as the price given by the two-dimensional Black–Scholes model, we proceed to calculate the price value given by $U_{1,0}$. The last equality in equation (13) is also the Poisson equation on $U_{3,0}$ and to be solvable it must also follow the central condition, specifically the average of source term must be in the null set of the operator $\mathcal{L}_0$, or

$$\langle \mathcal{L}_1 U_{2,0} + \mathcal{L}_2 U_{1,0} \rangle = 0. \tag{18}$$

Since $U_{1,0}$ does not depend no v_1 the equation (18) can be written as

$$\langle \mathcal{L}_1 U_{2,0} \rangle + \langle \mathcal{L}_2 \rangle U_{1,0} = 0.$$

From (15) and (16)

$$U_{2,0} = -\mathcal{L}_0^{-1} \left(\mathcal{L}_2 U_0 \right) = -\mathcal{L}_0^{-1} \left[\mathcal{L}_2 - \langle \mathcal{L}_2 \rangle \right] U_0 + C(t, s, v_2).$$

The term $C(t, s, v_2)$ does not have any impact on the solution of our equation, since, for differential operator $\mathcal{L}_1$ it is constant. It follows therefore that

$$\langle \mathcal{L}_1 U_{2,0} \rangle = -\langle \mathcal{L}_1 \mathcal{L}_0^{-1} \left(\mathcal{L}_2 - \langle \mathcal{L}_2 \rangle \right) \rangle U_0.$$

Making

$$\sqrt{\varepsilon} \langle \mathcal{L}_1 \mathcal{L}_0^{-1} \left(\mathcal{L}_2 - \langle \mathcal{L}_2 \rangle \right) \rangle = \mathcal{B}^{\varepsilon}$$

our problem can be expressed as

$$\sqrt{\varepsilon} \langle \mathcal{L}_2 \rangle U_{1,0} = \langle \mathcal{L}_2 \rangle U_{1,0}^{\varepsilon} = \mathcal{B}^{\varepsilon} U_0$$

with final condition equal to zero.

3.3 Formula for $U_{1,0}^{\varepsilon}$ with European Options

To be able to compute $U_{1,0}^{\varepsilon}$ we need to compute the operator $\mathcal{B}^{\varepsilon}$. We start by defining

$$D_k = x_i^k \frac{\partial^k}{\partial x_i^k}; \quad i = 1, 2, \tag{19}$$

so that

$$\mathcal{L}_2 - \langle \mathcal{L}_2 \rangle = \frac{1}{2} \left(f(v_1, v_2) - \sigma^2(v_2) \right) s^2 \frac{\partial^2}{\partial s^2} = \frac{1}{2} \left(f(v_1, v_2) - \sigma^2(v_2) \right) D_2.$$

Now, suppose that $\phi(v_1, v_2)$ is the solution of

$$\mathcal{L}_0 \phi(v_1, v_2) = f^2(v_1, v_2) - \sigma^2(v_2).$$

Then

$$\mathcal{L}_2 - \langle \mathcal{L}_2 \rangle = \frac{1}{2} \mathcal{L}_0 \phi(v_1, v_2) D_2$$

which implies that

$$\mathcal{L}_0^{-1} \left(\mathcal{L}_2 - \langle \mathcal{L}_2 \rangle \right) = \frac{1}{2} \phi(v_1, v_2) D_2;$$

$$\mathcal{L}_1 \mathcal{L}_0^{-1} \left(\mathcal{L}_2 - \langle \mathcal{L}_2 \rangle \right) = \mathcal{L}_1 \frac{1}{2} \phi(v_1, v_2) D_2$$

and

$$\begin{aligned} \langle \mathcal{L}_1 \mathcal{L}_0^{-1} \left(\mathcal{L}_2 - \langle \mathcal{L}_2 \rangle \right) \rangle &= \left\langle \rho_{13} s v_1 \frac{\partial^2}{\partial s \partial v_1} \right\rangle \frac{1}{2} \phi(v_1, v_2) D_2 \\ &= \left\langle \frac{1}{2} \rho_{13} v_1 \frac{\partial \phi(v_1, v_2)}{\partial v_1} D_1 D_2 \right\rangle. \end{aligned}$$

Due to the results above, the operator $\mathcal{B}^\varepsilon$ can be written as

$$\mathcal{B}^\varepsilon = \sqrt{\varepsilon}\left\langle \frac{1}{2}\rho_{13} v_1 \frac{\partial \phi(v_1, v_2)}{\partial v_1} D_1 D_2 \right\rangle = \frac{\sqrt{\varepsilon}\rho_{13}}{2}\left\langle v_1 \frac{\partial \phi(v_1, v_2)}{\partial v_1} \right\rangle D_1 D_2$$

or

$$\mathcal{B}^\varepsilon = -\Upsilon_2^\varepsilon(v_2) D_1 D_2$$

where $\Upsilon_2^\varepsilon(v_2) = -\frac{\sqrt{\varepsilon}\rho_{13}}{2}\left\langle v_1 \frac{\partial \phi(v_1, v_2)}{\partial v_1} \right\rangle$.

Considering European options, our equation can be expressed as

$$\mathcal{L}_{BS}(\sigma(v_2)) U_{1,0}(t, s, v_2)^\varepsilon = \mathcal{B}^\varepsilon U_{BS}; \quad U_{1,0}^\varepsilon(T, s, v_2) = 0 \tag{20}$$

and $U_{1,0}^\varepsilon$ will be equal to $-(T-t)\mathcal{B}^\varepsilon U_{BS}(t, s, \sigma(v_2))$. To prove this, we need to show that it solves (20). Taking the left side of (20) and applying $U_{1,0}^\varepsilon$ gives

$$\mathcal{L}_{BS}(\sigma(v_2)) U_{1,0}^\varepsilon = \mathcal{L}_{BS}(\sigma(v_2)) - (T-t)\mathcal{B}^\varepsilon U_{BS}(t, s, \sigma(v_2))$$

$$\mathcal{L}_{BS}(\sigma(v_2)) U_{1,0}^\varepsilon = \mathcal{B}^\varepsilon U_{BS} - (T-t)\mathcal{L}_{BS}(\sigma(v_2))\mathcal{B}^\varepsilon U_{BS}$$

$$\mathcal{L}_{BS}(\sigma(v_2)) U_{1,0}^\varepsilon = \mathcal{B}^\varepsilon U_{BS},$$

which proves that

$$U_{1,0}^\varepsilon = -(T-t)\mathcal{B}^\varepsilon U_{BS}. \tag{21}$$

3.4 Slow time scale correction for $U_{0,1}^\delta$

We consider now the second term in expansion (7) and perform expansion as we did in (11) to construct the $U_{0,1}$ term, as follows

$$U_1^\varepsilon = U_{0,1} + \sqrt{\varepsilon} U_{1,1} + \varepsilon U_{2,1} + \varepsilon\sqrt{\varepsilon} U_{3,1} + \cdots .$$

Using this expansion of U_1 in (10) gives

$$\begin{aligned}\left(\frac{1}{\varepsilon}\mathcal{L}_0 + \frac{1}{\sqrt{\varepsilon}}\mathcal{L}_1 + \mathcal{L}_2\right)(U_{0,1} + \sqrt{\varepsilon} U_{1,1} + \varepsilon U_{2,1} + \varepsilon\sqrt{\varepsilon} U_{3,1} + \cdots) \\ = -\mathcal{M}_1(U_0 + \sqrt{\varepsilon} U_{1,0} + \varepsilon U_{2,0} + \varepsilon\sqrt{\varepsilon} U_{3,0} + \cdots).\end{aligned}$$

Collecting terms with the same power of $\frac{1}{\sqrt{\varepsilon}}$ in the above equation yields

$$\begin{aligned}&\frac{1}{\varepsilon}\mathcal{L}_0 U_{0,1} + \frac{1}{\sqrt{\varepsilon}}(\mathcal{L}_0 U_{1,1} + \mathcal{L}_1 U_{0,1}) + (\mathcal{L}_0 U_{2,1} + \mathcal{M}_1 U_0 + \mathcal{L}_1 U_{1,1} + \mathcal{L}_2 U_{0,1}) \\ &\quad + \sqrt{\varepsilon}(\mathcal{L}_0 U_{3,1} + \mathcal{L}_1 U_{2,1} + \mathcal{L}_2 U_{1,1} + \mathcal{M}_1 U_{1,0}) + \cdots = 0,\end{aligned}$$

which implies that

$$\begin{aligned}\mathcal{L}_0 U_{0,1} &= 0, \\ \mathcal{L}_0 U_{1,1} + \mathcal{L}_1 U_{0,1} &= 0, \\ \mathcal{L}_0 U_{2,1} + \mathcal{M}_1 U_0 + \mathcal{L}_1 U_{1,1} + \mathcal{L}_2 U_{0,1} &= 0, \\ \mathcal{L}_0 U_{3,1} + \mathcal{L}_1 U_{2,1} + \mathcal{L}_2 U_{1,1} + \mathcal{M}_1 U_{1,0} &= 0.\end{aligned} \tag{22}$$

From equations (22) with the same reasons as in equations (13) and (14) we consider $U_{0,1}$ to be constant with respect to fast factor v_1. Therefore $U_{0,1} = U_{0,1}(t, s, v_2)$. As an immediate consequence of the above choice and the fact that operator $\mathcal{L}_1$ contains only the mixed derivative with respect to the cross term sv_1, we have $\mathcal{L}_0 U_{1,1} = 0$. It follows then $U_{1,1} = U_{1,1}(t, s, v_2)$ implying that $\mathcal{L}_1 U_{1,1} = 0$ and the third equality in equation (22) can be transformed into

$$\mathcal{L}_0 U_{2,1} + \mathcal{M}_1 U_0 + \mathcal{L}_2 U_{0,1} = 0.$$

The above is the Poisson equation in v_1 and the solvability condition of the Poisson equation implies that

$$\langle \mathcal{L}_2 U_{0,1} + \mathcal{M}_1 U_0 \rangle = 0.$$

Since the averaging procedure is done with respect to v_1 and the fact that $U_{0,1}, U_0$ do not depend on v_1,, we can multiply both sides of the above equation by $\sqrt{\delta}$ and obtain

$$\langle \mathcal{L}_2 \rangle U^{\delta}_{0,1} = -\sqrt{\delta} \langle \mathcal{M}_1 \rangle U_0$$

with $\langle \mathcal{L}_2 \rangle$ defined in the same way as in (16). This means that we have a non-homogeneous two-dimensional Black–Scholes partial differential equation for $U^{\delta}_{0,1}$. We need now to compute the right hand side of our equation and we do it by averaging $\mathcal{M}_1$ with respect to invariant distribution Π, i.e;

$$\begin{aligned}\sqrt{\delta}\langle \mathcal{M}_1 \rangle U_0 &= \sqrt{\delta} \left\langle \rho_{24} s v_2 \frac{\partial^2}{\partial s \partial v_2} \right\rangle U_0 \\ &= \sqrt{\delta}\rho_{24} \langle v_2 \rangle \frac{\partial}{\partial \sigma(v_2)} \frac{\partial \sigma(v_2)}{\partial v_2} D_1 U_0 = 2\mathcal{A}^{\delta} U_{BS};\end{aligned}$$

where

$$\mathcal{A}^{\delta} = \Theta^{\delta}_1(v_2) D_1 \frac{\partial}{\partial \sigma(v_2)}, \quad \Theta^{\delta}_1(v_2) = \frac{1}{2}\sqrt{\delta}\rho_{24}\langle v_2 \rangle \frac{\partial \sigma(v_2)}{\partial v_2}. \tag{23}$$

It follows then

$$\mathcal{L}_{BS} U^{\delta}_{0,1} = -2\mathcal{A}^{\delta} U_{BS}; \quad U^{\delta}_{0,1}(T, s, v_2) = 0. \tag{24}$$

3.5 Formula for $U^{\delta}_{0,1}$ with European Options

For European options, if U satisfies the partial differential equation from the two-dimensional Black-Scholes model with given terminal condition, using the Greeks (sensitivities of the option price to a single-unit change in the value of a state variable or a parameter), the relation $\frac{\partial U}{\partial \sigma} = (T-t)\sigma x^2 \frac{\partial^2 U}{\partial x^2}$ holds (see Fouque et al [7]). Making use of this property the operator $\mathcal{A}^{\delta}$ defined in (23) can be expressed as

$$\mathcal{A}^{\delta} = \Theta^{\delta}_1(v_2) D_1 (T-t)\sigma(v_2) v_2^2 \frac{\partial^2}{\partial v_2^2} = \sigma(v_2)(T-t)(\Theta^{\delta}_1(v_2) D_1 D_2).$$

Using the above formula, problem (24) can be solved by

$$U^{\delta}_{0,1} = (T-t)\mathcal{A}^{\delta} U_{BS}, \tag{25}$$

which can also be proved similarly as we did with $U^{\varepsilon}_{1,0}$.

3.6 First Order Approximation

From formulas (12), (17), (21) and (25) the first order approximation is given by

$$U^{\varepsilon,\delta} = U_{BS} + (T-t)\left(\mathcal{A}^{\delta} + \mathcal{B}^{\varepsilon}\right) U_{BS}. \tag{26}$$

4 Conclusions

In this paper we transformed the Chiarella and Ziveyi [3] model to a model with two volatility parameters that influence the asset price with different frequencies with one being fast-changing and the other slow-changing. Girsanov theorem is applied to construct risk-neutral measures and Feynman–Kac theorem is used to produce a partial differential equation that gives the option price for the underlying asset. We introduce singular and regular perturbation in our method. The obtained solution $U^{\varepsilon,\delta}$ involves Greeks of the two-dimensional Black–Scholes model evaluated at the average effective volatility. The contribution of the fast-changing parameter and the slow-changing parameter to the option price is contained in the average effective volatility and in the effects of correlations factors ρ_{13} and ρ_{24} between Wiener processes that govern the asset price, the fast variance process and the slow variance process. The presented results generalise the corresponding results in Fouque et al. [9] to the setting with two stochastic volatilities. In short, our solution gives the approximation of European option price in a model with two stochastic volatilities. Specifically our approximation contains a leading term which is the Black–Scholes two-dimensional option price, in addition it contains influences of the fast-changing and the slow-changing parameters that acts differently on the asset price evolution.

5 Acknowledgements

This work was partially supported by Swedish SIDA Foundation International Science Program. Betuel Canhanga thanks Division of Applied Mathematics, School of Education, Culture and Communication, Mälardalen University for creating excellent research and educational environment.

References

1. Black, F., and Scholes, M. "The pricing of options and corporate liabilities". *J. Political Economy* 81:637–654 (1973).
2. Heston, S.L. "A closed-form solution for options with stochastic volatility with applications to bonds and currency options". *Rev. Finan. Stud.* 6:327–343 (1993).
3. Chiarella, C, and Ziveyi, J. "American option pricing under two stochastic volatility processes". *J. Appl. Math. Comput.* 224:283–310 (2013).
4. Feller, W. "Two singular diffusion problems". *Ann. Math.* 54:173–182 (1951).
5. Kijima, M. "Stochastic Processes with Applications to Finance", Second Edition, Capman and Hall/CRC, (2013).

6. Fouque, J.-P., Papanicolaou, G., Sircar, R., and Solna, K. "Singular Perturbation in Option Pricing" (2011).
7. Fouque, J.-P., Papanicolaou, G., Sircar, R., and Solna, K. "Multiscale stochastic volatility for equity, interest rate and credit derivatives", Cambridge University Press, Cambridge (2011).
8. Conze, A., Lantos, N., and Pironneau, O. "The forward Kolmogorov equation for two dimenssional options"; University Pierre et Marie Curie; 2010.
9. John C. Hull "Options, Futures, and Other Derivatives (5th Edition)"; Pearson; 2009.
10. Grzelak, L. A; Oosterlee, C.W "On the Heston Model with stochastic interest rate" SIAM J. Fin.Math.2: 255286; 2011.
11. Christoffersen, P.; Heston, S.; Jacobs, K. "The shape and term structure of the index option smirk: why multifactor stochastic volatility models work so well" Manage.Sci.55(2) 1914-1932; 2009.
12. L. Andersen and V. Piterbarg. "Interest rate modeling Volume 1 - foundations and vanilla models"; Atlantic Financial Press, 2010.

Construction of moment-matching multinomial lattices for pricing of Asian options under a jump-diffusion process

Karl Lundengård[1], Carolyne Ogutu[2], Sergei Silvestrov[1], and Patrick Weke[2]

[1] Division of Applied Mathematics, School of Education, Culture and Communication, Mälardalen University, Box 883, SE-721 23 Västerås, Sweden (e-mail: karl.lundengard@mdh.se, sergei.silvestrov@mdh.se)
[2] School of Mathematics, University of Nairobi, Box 30197 - 00100, Nairobi, Kenya (e-mail: cogutu@uonbi.ac.ke, pweke@uonbi.ac.ke)

Abstract. Asian options are options whose value depends on the average asset price during its lifetime. They are useful because they are less subject to price manipulations. We consider Asian option pricing on a lattice where the underlying asset follows Merton-Bates jump-diffusion model as given in Cont and Tankov[2]. We describe the construction of the lattice using the moment matching technique which results in an equation system described by a Vandermonde matrix. Using some properties of Vandermonde matrices we calculate the jump probabilities of the resulting system. Some conditions on the possible jump sizes in the lattice are also given.
Keywords: Jump-diffusion process, lattices, Vandermonde matrix, Asian options, option pricing.

1 Pricing of Asian options and jump-diffusion option pricing

Asian options are path dependent options whose payoffs depend on the average price during a specific period of time before maturity. The averages are considered to be either geometric or arithmetic averages. Assuming the geometric average results in a closed-form formula for the European option price within the classical Black–Scholes model. This is because the geometric average of log-normally distributed random variables also has a lognormal distribution and this simplifies the mathematics involved in the pricing problem. In contrast, the arithmetic average of lognormal random variables is not log-normally distributed, thus there exists no closed-form formula for European Asian options based on the arithmetic average of the underlying asset prices. There are, however, approximation methods that have been developed to aid in pricing Asian options, here we will consider lattice methods. Lattice methods are based on a discrete approximation of the process such that the time span is divided into n time steps and specifies asset price at each time step. At each time step the process can jump to L different asset prices, henceforth referred to as nodes.

New Trends in Stochastic Modeling and Data Analysis (pp. 211-220)
Raimondo Manca - Sally McClean - Christos H Skiadas (Eds)

We will model the options underlying asset using a Merton-Bates jump-diffusion process. Popular methods for pricing (primarily American and European) options of jump-diffusion processes include binomial methods ($L = 2$, see Cox *et al.*[3], Amin[1], Hilliard and Schwartz[5] among others) and trinomial methods ($L = 3$, see Dai *et al.*[4] among others). For any of these methods it is required that the first L moments match the asset return and that the probabilities of moving to any given node is between zero and one.

Asian options can be priced on the lattice just like European and American options. However, the pricing algorithm is more complex as the value of Asian options is influenced by historical average prices of the underlying asset. For most nodes, there is more than one possible option value at a node since there is more than one price path reaching this node and most of these price paths carry distinct historical average prices. Let $S_0, S_1, ..., S_n$ denote the prices for the underlying asset over the life of the option and K be the exercise price. The arithmetic Asian call has a terminal value given by (c.f. Lyuu[7])

$$\max\left(\frac{1}{n+1}\sum_{i=0}^{n} S_i - K, 0\right) .$$

The value of the put has a terminal value of

$$\max\left(K - \frac{1}{n+1}\sum_{i=0}^{n} S_i, 0\right) .$$

At initiation, Asian options cannot be more expensive than the standard European options under the Black–Scholes Option Pricing Model. Asian options are generally hard to price since there are usually many price paths that end in the same node. As an example, suppose we wish to price an Asian option on a binomial lattice and let us denote a change in asset price upwards with $S_{k+1} = S_k u$ and a downward change with $S_{k+1} = S_k d$. Given a node S_0u^2d, there are three different paths that lead to it. That is, $\big(S_0, S_0u, S_0u^2, S_0u^2d\big)$, $\big(S_0, S_0u, S_0du, S_0u^2d\big)$ and $\big(S_0, S_0d, S_0ud, S_0u^2d\big)$. This leads to different averages. In the binomial tree the averages for the tree do not combine and thus, a straightforward algorithm is to enumerate the 2^n price paths for an n-period binomial tree and the average payoffs. This is generally not possible but there are approximation methods such as the one described in Hull and White[6].

Here we will consider multinomial methods with higher L. In Lundengård *et al.*[8] it was shown that for the type of multinomial method described in section 2 it will not always be possible to find a distance between the nodes (jump-size) in the lattice such that the first L moments are matched. Here some of the results from Lundengård *et al.*[8] will be further simplified and some conditions for the existence of jump-sizes for quadrinomial ($L = 4$) and pentanomial ($L = 5$) methods that ensures matching of the moments will be shown. These conditions will not guarantee that the probability of moving from one node to another is always between zero and one.

2 Moment-matching multinomial lattice methods

We want to match the moments of a random variable X with a discrete random variable Z. Let Z denote a discrete random variable as given below (Primbs *et al.*[11]):

$$Z = m_1 + (2i - L - 1)\,\alpha \;\text{ with probability } p_i,\; i = 1, 2, ..., L,$$

where α is the jump size (distance between two outcomes), m_1 is the mean of X and L is the number of lattice nodes. Here α must be real and positive.

The requirement that the k:th moment matches the asset return on an L-node lattice can be written:

$$\sum_{i=1}^{L} p_i (2i - L - 1)^k \alpha^k = \mu_k$$

where μ_k is the k:th moment. We will also use the notation $\mu_0 = 1$ which means that matching to μ_0 is equivalent to the sum of all probabilities being equal to one.

Matching the first L moments can be written $A\boldsymbol{p} = \boldsymbol{\mu}$ where $\boldsymbol{p}$ is a column vector containing the jump probabilities, $\boldsymbol{\mu}$ is a column vector containing the moments and A is the general lattice matrix for the jump diffusion process that takes the following form:

$$A = \begin{bmatrix} 1 & \cdots & 1 & \cdots & 1 \\ (1-L)\alpha & \cdots & (2n-L-1)\alpha & \cdots & (L-1)\alpha \\ \vdots & \ddots & \vdots & \ddots & \vdots \\ ((1-L)\alpha)^k & \cdots & ((2n-L-1)\alpha)^k & \cdots & ((L-1)\alpha)^k \\ \vdots & \ddots & \vdots & \ddots & \vdots \\ ((1-L)\alpha)^L & \cdots & ((2n-L-1)\alpha)^L & \cdots & ((L-1)\alpha)^L \end{bmatrix}.$$

Note that the general lattice matrix A is a non-square *Vandermonde matrix*, c.f. definition 1.

Definition 1. A *Vandermonde matrix* is a square matrix of the form

$$V_L = \begin{bmatrix} 1 & 1 & \dots & 1 \\ x_1 & x_2 & \dots & x_L \\ x_1^2 & x_2^2 & \dots & x_L^2 \\ \vdots & \vdots & \vdots & \vdots \\ x_1^{L-1} & x_2^{L-1} & \dots & x_L^{L-1} \end{bmatrix}, \tag{1}$$

where all x_i are distinct numbers.

Note that the requirement that all x_i are distinct is usually not included in the definition. Here it has been added since two x_i being equal would indicate two overlapping nodes which can be combined to a single node. If all x_i are distinct the matrix is also guaranteed to be invertible.

Choosing elements

$$x_i = (2i - L - 1)\alpha \ , \ 1 \leq i \leq L \tag{2}$$

will give the general lattice matrix with the final row missing.

The inverse of the Vandermonde matrix is known, see Macon and Spitzbart[9], and can be used to calculate the transition probabilities.

Theorem 1. *The elements of the inverse of an L-dimensional Vandermonde matrix V_L can be calculated by*

$$\left(V_L^{-1}\right)_{ij} = \frac{(-1)^{j-1}\sigma_{L-j,i}}{\prod\limits_{\substack{k=1 \\ k\neq i}}^{L}(x_k - x_i)},$$

where $\sigma_{j,i}$ is the jth elementary symmetric polynomial with variable x_i set to zero:

$$\sigma_{j,i} = \sum_{1\leq m_1<m_2<\ldots\ <m_j\leq L} \prod_{n=1}^{j} x_{m_n}(1-\delta_{m_n,i}) \ , \ \delta_{a,b} = \begin{cases} 1 \ , \ a = b, \\ 0 \ , \ a \neq b. \end{cases}$$

For a Vandermonde matrix, V_L, with x_i of the form (2) the expression for the elements of the inverse matrix can be simplified.

$$\left(V_L^{-1}\right)_{ij} = \frac{(-1)^{j-i}}{2^{L-2}\alpha^{j-1}} \cdot \frac{\tilde{\sigma}_{L-j,i}}{(i-1)!(L-i)!} \tag{3}$$

and the $\sigma_{j,i}$ terms can be simplified as follows

$$\begin{aligned} j = 2k+1 \quad &: \quad \tilde{\sigma}_{j,i} = x_{L-i+1} \sum_{\substack{s\in\tilde{B}_k \\ x_i\notin s}} \tilde{\pi}_k(s), \\ j = 2k \quad &: \quad \tilde{\sigma}_{j,i} = \sum_{\substack{s\in\tilde{B}_k \\ x_i\notin s}} \tilde{\pi}_k(s). \end{aligned}$$

From this it is also clear that $\tilde{\sigma}_{j,i} = (-1)^j\tilde{\sigma}_{j,L-i+1}$.

Proving theorem 1 does not require sophisticated arguments but takes some work. We will prepare with proving the following lemma.

Lemma 1. *Let B be a set of n distinct real values evenly distributed around zero. Denote the set of combinations of k elements from B with B_k. Let $\pi : B_k \mapsto \mathbb{R}$ be the product of all elements in a given combination.*
If k is odd

$$\sum_{s\in B_k} \pi_k(s) = 0 \tag{4}$$

and if k is even

$$\sum_{s\in B_k}\pi_k(s)=\sum_{s\in\tilde{A}_{\frac{k}{2}}}\tilde{\pi}_{\frac{k}{2}}(s) \tag{5}$$

where $\tilde{B}=\{b\in B|b>0\}$, $\tilde{B}_k$ is the set of combinations of k elements from $\tilde{B}$ and $\tilde{\pi}:\tilde{B}_k\mapsto\mathbb{R}$ is the product of the square of the elements in a combination multiplied by $(-1)^k$.

Proof. When k is odd it is possible for all $s\in B_k$ to rewrite the product $\pi_k(s)=b_l\pi_{k-1}(r)$ such that b_l is not a factor in $\pi_{k-1}(r)$ for some $b_l\in B$, $r\in B_{k-1}$. If $b_l=0$ it is obvious that $\pi_k(s)=0$ and for any other $a_l\in B$ there is another combination $t\neq s$ such that $\pi_k(t)=-b_l\pi_{k-1}(r)=-\pi_k(s)$ and thus

$$\sum_{s\in B_k}\pi_k(s)=0+\sum_{r\in B_{k-1}}(b_r-b_r)\pi_k(s)=0.$$

When k is even we can use an argument analogous to the odd case and conclude that for each combination $s\in B_k$ that can be rewritten such that $\pi_k(s)=b_l\pi_{k-1}(r)$ where b_l is not a factor in $\pi_{k-1}(r)$ for some $b_l\in B$, $r\in B_{k-1}$ there is also a combination that generate an annihilating term in the sum over all the products. Thus the only remaining terms in the sum over the products will contain both b_l and $-b_l$ as factors and thus any term can be written on the form

$$\pi_k(s)=\prod_{b\in s}b\cdot(-b)=(-1)^{\frac{k}{2}}\prod_{b\in s}b^2.$$

Proof (Theorem 1). Showing that expression 3 is valid is a straightforward simplification of the general expression of the inverse of the Vandermonde matrix given in Macon and Spitzbart[9]. For more details, see Lundengård *et al.*[8]. Following this argument will give another expression for $\sigma_{j,i}$:

$$\sigma_{j,i}=\sum_{1\leq m_1<m_2<\ldots\ <m_j\leq L}\prod_{n=1}^{j}x_{m_n}(1-\delta_{m_n,i})\ ,\ \delta_{a,b}=\begin{cases}1\ ,\ a=b,\\0\ ,\ a\neq b.\end{cases}$$

With the notation used in Lemma 1 this expression can be rewritten as a sum of products of combinations of the elements in $\boldsymbol{x}$,

$$\begin{aligned}\tilde{\sigma}_{j,i}&=\sum_{1\leq m_1<\ldots\ <m_j\leq L}\prod_{n=1}^{j}(2n-L-1)(1-\delta_{m_n,i})=\sum_{\substack{s\in B_j\\ i\notin s}}\pi_j(s)\\&=\sum_{\substack{s\in B_{j-1}\\ x_i\notin s\\ -x_i\notin s}}-x_i\pi_{j-1}(s)+\sum_{\substack{s\in B_j\\ x_i\notin s\\ -x_i\notin s}}\pi_j(s),\end{aligned}$$

where B is the set formed by the values of the elements in $\boldsymbol{x}$. Now the simplified expression for $\sigma_{j,i}$ in 1 follows by directly applying Lemma 1.

Matching the lattice to the first $L-1$ moments gives the equation

$$\boldsymbol{p} = V_L^{-1}\boldsymbol{\mu}, \tag{6}$$

where $\boldsymbol{p}$ and $\boldsymbol{\mu}$ are vectors containing the probabilities and moments respectively. Using formulas (1) and (6) gives

$$p_i = \sum_{j=1}^{L} \left(V^{-1}\right)_{ij} \mu_{j-1} = \sum_{j=1}^{L} \frac{(-1)^{j-i}}{2^{L-1}\alpha^{j-1}} \cdot \frac{\tilde{\sigma}_{L-j,i}}{(i-1)!(L-i)!}\mu_{j-1}\,. \tag{7}$$

The lattice models also require that the L:th moment is matched:

$$\sum_{i=1}^{L} p_i x_i^L = \mu_L.$$

Using equation (7) this requirement can be rewritten as a polynomial equation $P_L(\alpha) = 0$ where

$$P_L(\alpha) = -\mu_L + \sum_{j=1}^{L} \alpha^{L-j+1}\mu_{j-1}\left(\sum_{i=1}^{L} \frac{(-1)^{j-i}(2i-L-1)^L\tilde{\sigma}_{L-j,i}}{2^{L-1}(i-1)!(L-i)!}\right) \tag{8}$$

and α is a real, positive number. For further details, see Lundengård *et al.*[8]. Next we will show that expression (8) can be simplified further.

Lemma 2. *Let*

$$c(j) = \sum_{i=1}^{L} \frac{(-1)^{L-j}(2i-L-1)^L\tilde{\sigma}_{L-j,i}}{2^{L-1}(i-1)!(L-i)!}. \tag{9}$$

Then $c(j) = 0$ if $L-j$ is even and if $L-j$ is odd

$$c(j) = \sum_{i=1}^{\lfloor \frac{L}{2} \rfloor} \frac{(-1)^{j-i}(2i-L-1)^L\tilde{\sigma}_{L-j,i}}{2^{L-2}(i-1)!(L-i)!}.$$

Proof. Split the sum into two parts:

$$\begin{aligned} c(j) = &\sum_{i=1}^{\lfloor \frac{L}{2} \rfloor} \frac{(-1)^{j-i}(2i-L-1)^L\tilde{\sigma}_{L-j,i}}{2^{L-1}(i-1)!(L-i)!} \\ &+ \sum_{i=\lfloor \frac{L}{2} \rfloor+1}^{L} \frac{(-1)^{j-i}(2i-L-1)^L\tilde{\sigma}_{L-j,i}}{2^{L-1}(i-1)!(L-i)!}. \end{aligned}$$

Changing index in the second sum according to $k = L-i+1$ gives:

$$\begin{aligned} c(j) = &\sum_{i=1}^{\lfloor \frac{L}{2} \rfloor} \frac{(-1)^{j-i}(2i-L-1)^L\tilde{\sigma}_{L-j,i}}{2^{L-1}(i-1)!(L-i)!} \\ &+ \sum_{k=1}^{\lfloor \frac{L}{2} \rfloor+a} \frac{(-1)^{j-k-L+1}(2k-L+1)^L\tilde{\sigma}_{L-j,L-k+1}}{2^{L-1}(n-k)!(k-1)!}. \end{aligned}$$

where $a = 1$ when L is odd and $a = 0$ when L is even.

The final remark in Theorem 1 gives $\tilde{\sigma}_{L-j,i} = (-1)^{L-j}\tilde{\sigma}_{L-j,L-i+1}$ and thus recombining the two sums gives:

$$c(j) = \left(1 - (-1)^{L-j}\right) \sum_{i=1}^{\lfloor \frac{L}{2} \rfloor} \frac{(2i - L - 1)^L \tilde{\sigma}_{L-j,i}}{2^{L-1}(i-1)!(L-i)!}.$$

Since the factor in front of the sum is zero when j is odd and two otherwise this concludes the proof.

Lemma 3. *The polynomial given by* (8) *can be written on the form*

$$P(\alpha) = \begin{cases} \mu_L - \sum_{j=1}^{\lfloor \frac{L}{2} \rfloor} c(2j-1)\ \mu_{L-2j}\ \alpha^{L-2j} & \text{if } L \text{ even.} \\ \mu_L - \sum_{j=1}^{\lfloor \frac{L}{2} \rfloor} c(2j)\ \mu_{L-2j+1}\ \alpha^{L-2j+1} & \text{if } L \text{ odd.} \end{cases} \tag{10}$$

where $c(j)$ is defined by (9).

Proof. This lemma follows from substituting the $c(j)$ in Lemma 2 in the polynomial defined by (8).

3 On the existence of suitable jump sizes

There are conditions that must be satisfied for the moment matching lattice methods to work. The distance between the lattice nodes, α, must be a positive real root to the polynomial given by (10). For this α the probabilities to move to node i, given by (7), must be between zero and one.

To examine whether there are any positive real roots for (10) Sturm's theorem, formulated as in Prasolov[10], will be used.

Theorem 2 (Sturm's theorem).
Let $p_0(x)$ be a polynomial and $p_1(x) = p_0'(x)$. Using polynomial division we can find $p_2(x), \ldots, p_n(x)$ such that

$$\begin{aligned} p_{k-2}(x) &= q_{k-1}(x)p_{k-1}(x) - p_k(x), \\ p_{n-1}(x) &= q_n(x)p_n(x). \end{aligned}$$

The sequence $S_L(x) = \{p_0(x),\ p_1(x), \ldots,\ p_n(x)\}$ is called the canonical Sturm chain. The number of real roots of $p_0(x)$, m, confined between a and b, $a < b$, $p(a) \neq 0$, $p(b) \neq 0$, is given by $m = v_L(a) - v_L(b)$ where $v_L(x)$ is the number of sign variations in $S(x)$ ignoring zeros.

There are many sources for proofs of Sturm's theorem, e.g. Prasolov[10].

For the quadrinomial ($L = 4$) and pentanomial ($L = 5$) lattices the following canonical Sturm chains correspond to the polynomial $P(\alpha)$ given by (10):

$$S_4(\alpha) = \left\{ -9\alpha^4 + 10\mu_2\alpha^2 - \mu_4,\ \ -36\alpha^3 + 20\mu_2\alpha, \right. \\ \left. \left(\frac{36}{5}\frac{\mu_4}{\mu_2} - 20\mu_2\right)\alpha,\ \ -\mu_4 \right\}, \tag{11}$$

$$S_5(\alpha) = \left\{ -64\mu_1\alpha^4 + 20\mu_3\alpha^2 - \mu_5,\ \ -256\mu_1\alpha^3 + 40\mu_3\alpha, \right. \\ \left. -10\mu_3\alpha^2 + \mu_5,\ \ \left(\frac{256}{10}\frac{\mu_1}{\mu_3}\mu_5 - 40\mu_3\right)\alpha,\ \ \mu_5 \right\}. \tag{12}$$

To find all the positive roots of $P(\alpha)$ we only need to consider the interval confined between 0 and some r large enough that the highest order term will dominate each expression in the Sturm chain. For this interval the sign of the elements in $S_L(0)$ will be determined by the constant term in each polynomial and the signs of the elements in $S_L(r)$ will be determined by the coefficients of the highest order term. Since, by definition, increasing r will not change the sign of any element the total number of real positive roots will be given by $q = v_L(0) - v_L(r)$.

Lemma 4. *For $L = 4$ the polynomial $P(\alpha)$ given by* (10) *will have* 2 *positive real roots if $36\mu_4 > 100\mu_2^2$ else there will be no positive real roots. With an underlying asset described by a Merton–Bates jump-diffusion process with Lévy measure*

$$l(dx) = \frac{\lambda}{\sqrt{2\pi\delta^2}} \exp\left(-\frac{(dx-\eta)^2}{2\delta^2}\right), \tag{13}$$

see Cont and Tankov [2], this corresponds to $\lambda < \dfrac{36}{100}\dfrac{3+6\eta^2+\eta^4}{(1+\eta^2)^2}$.

Proof. Since all even-numbered moments are positive expression (11) gives $v_4(0) = 0$ and $v_4(r) = 0$ unless $\dfrac{36}{5}\dfrac{\mu_4}{\mu_2} - 20\mu_2 > 0$ which will give $v_4(r) = 2$. Thus $36\mu_4 > 100\mu_2^2$ will give $q = v_4(r) - v_4(0) = 2$ positive real roots if $36\mu_4 > 100\mu_2^2$. With an underlying asset described by a Merton–Bates jump-diffusion process given by (13) the second and fourth moments will be

$$\mu_2 = \frac{\lambda\delta^2(1+\eta^2)}{\sigma^2 + \lambda\delta^2 + \lambda\eta^2}, \tag{14}$$

$$\mu_4 = \frac{\lambda\delta^4(3+6\eta^2+\eta^4)}{(\sigma^2 + \lambda\delta^2 + \lambda\eta^2)^2}, \tag{15}$$

for derivations of these expressions see Lundengård *et al.*[8]. Substituting (14) and (15) into the condition $36\mu_4 > 100\mu_2^2$ and simplifying the expression gives the result

$$\lambda < \frac{36}{100}\frac{3+6\eta^2+\eta^4}{(1+\eta^2)^2}.$$

Conditions on moments	Number of real positive roots
$\mu_1 > 0\ ,\ \mu_3 > 0\ ,\ \mu_5 < 0:$	$q = \begin{cases} 1 & \text{if } 16\mu_1\mu_5 > 25\mu_3^2, \\ 0 & \text{otherwise.} \end{cases}$
$\mu_1 > 0\ ,\ \mu_3 < 0\ ,\ \mu_5 > 0:$	$q = \begin{cases} 1 & \text{if } 16\mu_1\mu_5 < 25\mu_3^2, \\ 0 & \text{otherwise.} \end{cases}$
$\mu_1 < 0\ ,\ \mu_3 > 0\ ,\ \mu_5 < 0:$	$q = \begin{cases} 1 & \text{if } 16\mu_1\mu_5 > 25\mu_3^2, \\ 0 & \text{otherwise.} \end{cases}$
$\mu_1 > 0\ ,\ \mu_3 < 0\ ,\ \mu_5 < 0:$	$q = 1$
$\mu_1 < 0\ ,\ \mu_3 > 0\ ,\ \mu_5 > 0:$	$q = 1$
$\mu_1 = 0\ ,\ \mu_3 > 0\ ,\ \mu_5 > 0:$	$q = 1$
$\mu_1 = 0\ ,\ \mu_3 < 0\ ,\ \mu_5 < 0:$	$q = 1$
otherwise :	$q = 0$

Table 1. The number of real positive roots, q, of the polynomial $P(\alpha)$ given by (10) for $L = 5$ depending on the signs μ_1, μ_3 and μ_5.

Lemma 5. *For $L = 5$ the number of positive real roots, q, of the polynomial $P(\alpha)$ given by* (10) *will vary according to the table below.*

Proof. For the Sturm chain S_5 given by (12) we have $S_5(0) = \{-\mu_5,\ \mu_5,\ 0,\ \mu_5\}$ and thus the number of sign changes is $v_5(0) = 1$ unless $\mu_5 = 0$ which gives $v_5(0) = 0$. If none of the moments are equal to 0 then the signs of the elements $S_5(r)$ is determined by the signs of μ_1, μ_3, μ_5 and the expression $\frac{256}{10}\frac{\mu_1}{\mu_3}\mu_5 - 40\mu_3$. Examining all 16 possible combinations of signs of these elements gives the result that is shown in table 1 apart from the last three rows. If any moment is allowed to be 0 then the elements whose sign needs to be considered changes. For instance if $\mu_1 = 0$ then the signs of the elements $S_5(r)$ is determined by the signs of μ_3 and μ_5. Examining all the cases when one or more of the relevant parameters are equal to zero gives the remaining results shown in table 1.

Note that the existence of real positive roots does not guarantee that the probabilities given by (7) will be between zero and one.

Acknowledgements This work was partially supported by The International Science Program, SIDA foundation and by Mälardalen University. Carolyne Ogutu

is grateful to the research environment in Mathematics and Applied Mathematics at the Division of Applied Mathematics of the School of Education, Culture and Communication (UKK) at Mälardalen University for their hospitality and creating excellent conditions for research, research education and cooperation. She is also grateful for the support of the International Science Program, Uppsala University, Sweden, through collaboration with The Eastern African Universities Mathematics Programme.

References

1. Amin, K. L. "Jump diffusion option valuation in discrete time", *The Journal of Finance* **48**(5), 1833–1863 (1993)
2. Cont, R. and Tankov, P. *Financial Modelling with Jump Processes*. Financial Mathematics Series. CRC Press (2004)
3. Cox, J. C., Ross, S. A., and Rubinstein, M., "Option pricing. A simplified approach", *Journal of Financial Economics* **7**(3), 229–263 (1979)
4. Dai, T.-S., Wang, C.-J., Lyuu, Y.-D., and Liu, Y.-C., "An efficient and accurate lattice for pricing derivatives under jump-diffusion process", *Applied Mathematics and Computation* **217**, 3174–3189 (2010)
5. Hilliard, J. E., and Schwartz, A., "Pricing European and American derivatives under a jump-diffusion process: A bivariate tree approach", *Journal of Financial and Quantitative Analysis* **40**(3), 671–691 (2005)
6. Hull, J. and White, A. "Efficient procedures for valuing European and American path-dependent options", *Journal of Derivatives* **1**(1), 21–31 (1993)
7. Lyuu, Y. *Financial Engineering and Computation: Principles, Mathematics and Algorithms*. Cambrige University Press (2002)
8. Lundengård, K., Ogutu, C., Silvestrov S., and Weke, P., "Asian Options, Jump-Diffusion Processes on a Lattice, and Vandermonde Matrices", in *Modern Problems in Insurance Mathematics*, Silvestrov, Dmitrii, Martin-Löf, Anders, Eds., Springer-Verlag, Berlin, 337–364 (2014)
9. Macon, N. and Spitzbart, A., "Inverses of Vandermonde matrices", *The American Mathematical Monthly* **65**(2), 95–100 (1958)
10. Prasolov, V. V., *Polynomials*, *Algorithms and Computation in Mathematics* **11**, Springer-Verlag, Berlin (2004)
11. Primbs, J. A., Rathinam, M., and Yamada, Y., "Option pricing with a pentanomial lattice model that incorporates skewness and kurtosis", *Applied Mathematical Finance* **14**(1), 1–17, February (2007)

Modeling and analysis of cyclic inhomogeneous Markov processes: a wind turbine case study

Teresa Scholz[1,2], Vitor V. Lopes[3,4], Pedro G. Lind[5], and Frank Raischel[6,7]

[1] Center for Theoretical and Computational Physics, University of Lisbon, Portugal
[2] Energy Analysis and Networks Unit, National Laboratory of Energy and Geology, Lisbon, Portugal
(e-mail: tascholz@fc.ul.pt)
[3] DEIO-CIO, Science faculty, University of Lisbon, Portugal
[4] Universidad de las Fuerzas Armadas-ESPE, Latacunga, Ecuador
[5] ForWind-Center for Wind Energy Research, Institute of Physics, Carl-von-Ossietzky University of Oldenburg, Oldenburg, Germany
[6] Department of Theoretical Physics, University of Debrecen, Debrecen, Hungary
[7] Center for Geophysics, IDL, University of Lisbon, Portugal

Abstract. A method is proposed to reconstruct a cyclic time-inhomogeneous Markov process from measured data. First, a time-inhomogeneous Markov model is fit to the data, taken here from measurements on a wind turbine. From the time-dependent transition matrices, the time-dependent Kramers-Moyal coefficients of the corresponding stochastic process are computed. Further applications of this method are discussed.
Keywords: time-inhomogeneous Markov process; cyclic Markov process; Kramers-Moyal coefficients.

1 Introduction

Many complex systems can be described, within a certain level of modelization, as stochastic processes. A general stochastic process can be characterized in the linear noise approximation through a Fokker-Planck equation, in continuous variables. For dealing with discrete variables in discrete time steps, often Markov Chains are the models of choice. Although in many cases both approaches converge in the limit of small time steps and increments of the stochastic variables, this correspondence is in general non-trivial[11]. In the Fokker-Planck picture, the so-called Kramers-Moyal (KM) coefficients provide a complete description of a given stochastic process[2].

In the past decades, numerical procedures have been established to estimate the KM coefficients from measured stochastic data, which are applicable for any stationary, i.e. time-homogeneous, Markov process. These methods require large sequences of data, but they are robust[1], have well-known errors and limitations[3], require little intervention and are typically parameter-free[1,5].

However, for non-stationary Markov processes, much fewer methods and results are available to our knowledge. In this case, estimations of the time-dependent KM coefficients can be obtained by two approaches: either the data from the inhomogeneous

New Trends in Stochastic Modeling and Data Analysis (pp. 221-232)
Raimondo Manca - Sally McClean - Christos H Skiadas (Eds)

process is split into shorter, homogeneous sequences, on which then an estimate of the KM coefficients can be performed through the aforementioned methods[13]. Or, if the inhomogeneous process is also cyclic, a parametrized time-dependent *ansatz* for the KM coefficients can be fit to the data[14]. Compared to the stationary processes, both approaches for the inhomogeneous case require a much higher level of pre-analysis, guesswork and iterative improvement.

In this paper, we present a method that allows to estimate the transition matrices of a time-inhomogeneous Markov model from data. As reported in a previous publication[6], this method provides results with a considerable level of accuracy. Under well-known limitations, the discrete Markov model corresponds to a continuous stochastic process in the form of a Fokker-Planck equation, which is completely characterized, in this case, through its time-dependent KM coefficients. From the transition matrices, we can immediately calculate these KM coefficients, and therefore characterize the dynamical features underlying the time-dependent stochastic process.

We apply this methodology to data from a turbine in a wind park, where measurements of the wind velocity and direction, and the electric power output of the turbine are taken in 10 minute intervals. The results presented from this analysis show the general applicability of our method and are in agreement with previous findings.

This paper is organized as follows. We start in Sec. 2 by introducing both the cyclic time-dependent Markov model and the procedure for extracting stochastic evolution equations directly from data series. In Sec. 3 we describe the data and in Sec. 4 we present the time-dependent functions that define the stochastic evolution of the state of the wind turbine. Section 5 concludes the paper.

2 Methodology

This section describes the methodology used for the data analysis. In Sec. 2.1 the cyclic inhomogeneous Markov model to represent the daily patterns in the data is described and in Sec. 2.2 we explain how stochastic evolution equations are derived directly from the Markov process transition matrices.

2.1 Modelling cyclic time-dependent Markov processes

The goal of this time-inhomogeneous Markov process is to get a model that accurately reproduces the long-term behavior while considering the daily patterns observed in the data. Thus, the proposed objective function combines two maximum likelihood estimators: the first term maximizes the likelihood of the cycle-average probability; and, the second term maximizes the likelihood of the time-dependent probability. The final optimization problem is transformed into a convex one using the negative logarithm of the objective function. This section gives a brief overview over the final optimization problem. A detailed description of the objective function, the parametrization of the time-variant probability functions, and the constraints that must be added to the optimization problem to ensure its Markov properties is provided in [6].

A discrete finite Markov process $\{X_t \in S, t \geq 0\}$ is a stochastic process on a discrete finite state space $S = \{s_1, ..., s_n\}$, $n \in \mathbb{N}$, whose future evolution depends only on its current state [8]. It can be fully described by the conditional probability

$Pr\{X_{t+1} = s_j \mid X_t = s_i\}$ of the Markov process moving to state s_j at time step $t+1$ given that it is in state s_i at time t. It is called the t-th step transition probability, denoted as $p_{i,j}(t)$.

Being time-dependent, the Markov process has associated transition probability matrices P_t that change with time. Considering n possible states, the matrices P_t have dimension $n \times n$ with entries $[P_t]_{i,j} = p_{i,j}(t)$ for all $i, j = 1, \ldots, n$, satisfying $p_{i,j}(t) \geq 0$ and $\sum_j p_{i,j}(t) = 1$.

Markov process is called cyclic with period $T \in \mathbb{R}$, if T is the smallest number, such that $p_{i,j}(mT + r) = p_{i,j}(r)$ for all $m \in \mathbb{N}$ and $0 \leq r < T$. See Ref. [9]. Since this paper deals with discrete data, T and r can considered to be multiples of the time step Δt between successive data points and therefore integers. One can describe the cyclic Markov process by T transition matrices P_r, $r = 0, ..., T-1$. The remainder of time step t modulo T will be denoted as r_t and consequently $r_t = r_{t+mT}$. We fix $T = 1$ day and use $\Delta t = 1$.

In this paper, the transition probabilities $p_{i,j}(z)$ are modeled by Bernstein polynomials, namely

$$p_{i,j}(z) = \sum_{\mu=0}^{k} \beta_\mu^{i,j} b_{\mu,k}(z), \tag{1}$$

where $z = r/T$ indicates the time of the day ($T = 1$ day), $b_{\mu,k}(z)$ is the μ-th Bernstein basis polynomial of order k, and $\beta_\mu^{i,j} \in \mathbb{R}$. The choice of these polynomials has several advantages properly described in [6].

To maximize the likelihood of the time-dependent transition probabilities given the data, the objective function must consider the time of the day z when the transition happens. The corresponding term of the objective function is thus given by $\sum_{(i,j)_z \in \mathcal{S}_z} \log(p_{i,j}(z))$, where $\mathcal{S}_z$ is the set of observed transitions together with the time z when they happen. This estimator allows to compute the intra-cycle transition probability functions, and thus to represent the daily patterns present in the data.

A second term is added to this function, namely $\sum_{(i,j)\in\mathcal{S}} \log(p_{i,j}^{avg})$, where $\mathcal{S}$ is the set of transitions observed in the data and $p_{i,j}^{avg}$ is the cycle-average (daily) probability of transition from state s_i to s_j. It is given by $p_{i,j}^{avg} = \frac{1}{k+1} \sum_{\mu=0}^{k} \beta_k^{i,j}$. This second term is the maximum likelihood estimator for the daily average probability and its addition to the objective function increases the consistency of the long-term behavior of the Markov process with the data.

Using the resulting overall objective function the optimization problem to be solved for the transition probability coefficients $\beta_\mu^{i,j}$ is translated into the minimization of

$$\mathcal{L} = -\sum_{(i,j)\in\mathcal{S}} \log\left(\frac{1}{k+1} \sum_{\mu=0}^{k} \beta_\mu^{i,j}\right) - \sum_{(i,j)_z \in \mathcal{S}_z} \log\left(\sum_{\mu=0}^{k} \beta_\mu^{i,j} b_{\mu,k}(z)\right) \tag{2}$$

subject to

$$\sum_j \beta_\mu^{i,j} = 1 \tag{3a}$$

$$\beta_0^{i,j} = \beta_k^{i,j} = \tfrac{1}{2}(\beta_1^{i,j} + \beta_{k-1}^{i,j}) \tag{3b}$$

$$0 \leq \beta_k^{i,j} \leq 1 \tag{3c}$$

with $i, j = 1, \ldots, n$ and $\mu = 0, \ldots, k$, k being the order of the Bernstein polynomials. Constraint (3a) assures the row-stochasticity of the transition matrices, while the constraint (3b) imposes $\mathcal{C}^0$- and $\mathcal{C}^1$-continuity at $z = 0$. Constraint (3c) bound the transition probabilities between 0 and 1. This constraint is derived using a property of the Bernstein polynomials to always lie in the convex hull defined by their control points $(\frac{k}{\mu}, \beta_\mu)$, $\mu = 0, ..., k$. This convex hull bound can be tightened by subdivision using the de Casteljau algorithm, as described in [6].

2.2 Extracting the stochastic evolution equation

In this section we characterize general stochastic processes through a Fokker-Planck equation. We consider a N-dimensional stochastic process $\mathbf{X} = (X_1(t), \ldots, X_N(t))$ whose probability density function (PDF) $f(\mathbf{X}, t)$ evolves according to the Fokker-Planck equation (FPE) [2]

$$\begin{aligned}\frac{\partial f(\mathbf{X}, t)}{\partial t} = &- \sum_{i=1}^{N} \frac{\partial}{\partial x_i} \left[D_i^{(1)}(\mathbf{X}) f(\mathbf{X}, \mathbf{t}) \right] \\ &+ \sum_{i=1}^{N} \sum_{j=1}^{N} \frac{\partial^2}{\partial x_i \partial x_j} \left[D_{ij}^{(2)}(\mathbf{X}) f(\mathbf{X}, t) \right] \quad . \end{aligned} \tag{4}$$

The functions $D_i^{(1)}$ and $D_{ij}^{(2)}$ are the first and second Kramers-Moyal coefficients respectively, more commonly called the drift and diffusion coefficients.

These coefficients provide a complete description of a given stochastic process and are defined as

$$\mathbf{D}^{(k)}(\mathbf{X}) = \lim_{\Delta t \to 0} \frac{1}{\Delta t} \frac{\mathbf{M}^{(k)}(\mathbf{X}, \Delta t)}{k!} \quad , \tag{5}$$

where $\mathbf{M}^{(k)}$ are the first ($k = 1$) and second ($k = 2$) conditional moments. $\mathbf{D}^{(1)}$ is the drift vector and $\mathbf{D}^{(2)}$ the diffusion matrix.

If the underlying process is stationary and therefore both drift and diffusion coefficients do not explicitly depend on time t, the conditional moments can be directly derived from the measured data as [1,5]:

$$\begin{aligned} &M_i^{(1)}(\mathbf{X}, \Delta t) = \langle Y_i(t + \Delta t) - Y_i(t) | \mathbf{Y}(t) = \mathbf{X} \rangle \\ &M_{ij}^{(2)}(\mathbf{X}, \Delta t) = \\ &\langle (Y_i(t + \Delta t) - Y_i(t))(Y_j(t + \Delta t) - Y_j(t)) | \mathbf{Y}(t) = \mathbf{X} \rangle \, , \end{aligned} \tag{6}$$

where $\mathbf{Y}(t) = (Y_1(t), \ldots, Y_N(t))$ exhibits the N-dimensional vector of measured variables at time t and $\langle \cdot | \mathbf{Y}(t) = \mathbf{X} \rangle$ symbolizes a conditional averaging over the entire measurement period, where only measurements with $\mathbf{Y}(t) = \mathbf{X}$ are taken into account. In practice binning or kernel based approaches with a certain threshold are applied in order to evaluate the condition $\mathbf{Y}(t) = \mathbf{X}$. See e.g. Ref. [1] for details. If the process is non-stationary and time-inhomogeneous, we must consider an explicit time-dependence of the KM coefficients, which translates into time-dependent conditional moments that can be calculated using a short-time propagator[1]. In our case, this

short-time propagator corresponds to the transition probabilities $p_{i,j}(t)$, yielding for the first conditional moment

$$M^{(1)}(P_k, v_k, \theta_k, t + \Delta t) = \begin{pmatrix} \sum_j p_{k,j}(t)\,(v_j - v_k) \\ \sum_j p_{k,j}(t)\,(P_j - P_k) \\ \sum_j p_{k,j}(t)\,(\theta_j - \theta_k) \end{pmatrix} . \tag{7}$$

The expressions for higher conditional moments are straightforward and follow directly from Eq.(5).

3 Data description and accuracy of the model representation

The data for this study was obtained from a wind power turbine in a wind park located in a mountainous region in Portugal. The time series consists of a three-year period (2009-2011) of historical data gotten from the turbine data logger. The sampling time of 10 minutes leads to 144 samples each day. The data-set comprises three variables, wind power, speed and direction (nacelle orientation). The wind speed information was collected from the anemometer placed in the wind turbine hub.

For this Markov model, each state is defined by the values of all three variables, namely the wind speed, wind direction and power output. Figure 1 shows the data observations and the state partitions projected into the wind direction and speed plane (right) and the wind power and speed plane (left).

As expected, the observations projected into the wind power and speed plane define the characteristic power curve of the wind turbine.

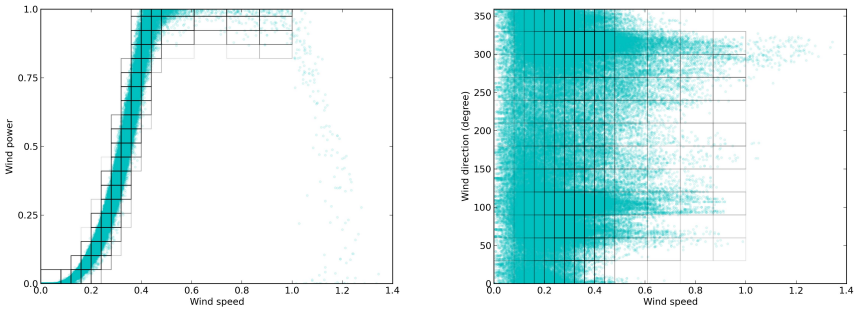

Fig. 1. Representation of all data points projected into the: a) wind direction and speed plane (left); and, b) wind power and speed plane (right). Each rectangle is the projection of a state polyhedron into the two planes. Overall, they define the final state partition for the three-dimensional variable space.

The data space is discretized unevenly to get a good resolution of the high-slope region of the power curve. In a previous work [7], this partition was used in a time-homogeneous Markov chain and proved to lead to an accurate representation of the original data. The wind direction and power are divided by an equally spaced grid leading to 12 and 20 classes with binwidth of 0.05 times the maximum power output

and 30 degrees, respectively. The wind speed is divided as follows: values below the cut-in speed (0.08) define one class; between the cut-in and rated wind speed (0.48) the discretization is narrowed by selecting 10 classes with a binwidth of 0.04 times the cut-out wind speed; and between the rated and cut-out wind speed (1) discretization is widened and 4 classes are defined with a binwidth of 0.13 times the cut-out wind speed. Data points with wind speed above the cut-out wind speed are discarded. The complete state set is constructed by listing all possible combinations of the classes of each variable. Due to physical constraints between the variables, most of the states are empty and can are therefore discarded. This reduces the number of states from 3840 to 778, for this turbine.

To compare the model with the original data, wind power, speed and direction time series were simulated adapting the method described by Sahin and Sen [10] to the cyclic time-inhomogeneous Markov model as follows. First, we compute the cumulative probability transition matrices P_r^{cum} with entries $[P_r^{\text{cum}}]_{i,j} = \sum_{j'=0}^{j} p_{i,j'}(r)$. Then an initial state s_i, i.e. $X_0 = s_i$, is randomly selected. A new datapoint X_{t+1} is generated by uniformly selecting a random number ϵ between zero and one and choosing for X_{t+1} the corresponding state $s_{i'}$ such that the probability of reaching it from the current state s_i fullfils $[P_{r_t}^{\text{cum}}]_{i,i'} \geq \epsilon$.Based on this discrete state sequence, a real value for the wind power/speed/direction variables is generated by sampling each state partition uniformly.

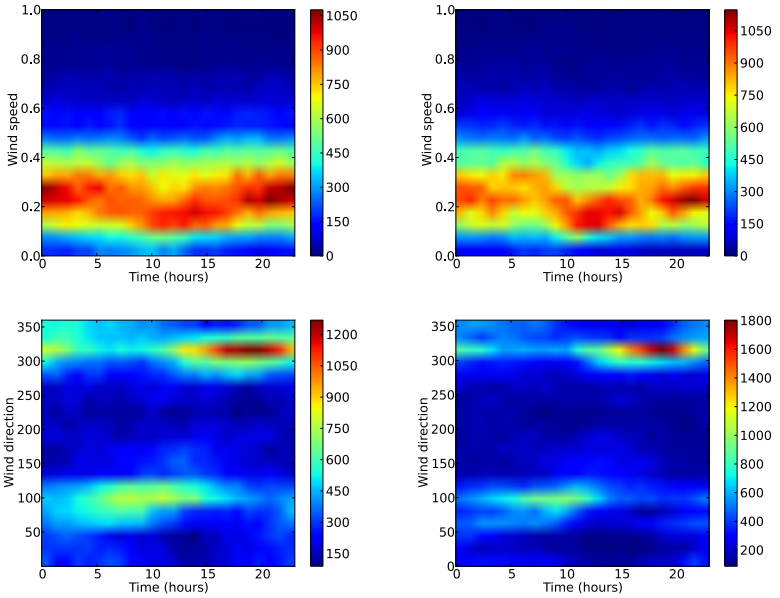

Fig. 2. Two dimensional histograms of the synthetic time-series data, generated with the time-variant Markov model (left) and the original data (right): speed-time (top) and direction-time (bottom). Due to confidentiality, wind speed data values are reported as a fraction of the cut-out speed, respectively.

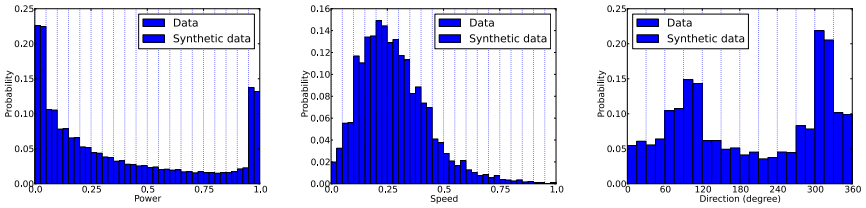

Fig. 3. Comparison of the probability distribution of wind power (left), wind speed (middle) and wind direction (right) of the original with the synthesized data. Due to confidentiality, wind power and speed data values are reported as a fraction of the rated power and the cut-out speed, respectively.

From the synthetic as well as the original data, histograms are computed and compared to demonstrate the models capability to reproduce the original data. Figure 2 shows the two dimensional histograms of wind speed-time and wind direction-time for both the synthetic (left) and original time-series data (right). The comparison of the histograms shows, that the model can capture the data's daily patterns. Figure 3 shows the probability distribution of the wind power, speed and direction states, computed from the original (dark blue) and the synthetic data (light blue). Comparison shows, that the model is capable of reproducing the long-term statistics of the original data.

4 The evolution of drift and diffusion in wind power output

With the procedure outlined in Sec. 2 and having the 144 transition matrices generated as described in Sec. 3 and 2.1, we can now reconstruct the time-dependent stochastic process by calculating the KM coefficients $\mathbf{D}^{(i)}(\hat{\mathbf{X}}, t)$ at each time step $t = 1, \ldots, 144$. Although we obtain the KM coefficients as a function of all three stochastic variables, $[P, v, \theta]$, we here consider only their dependency on the velocity and power production, $\hat{\mathbf{X}} = [\mathbf{P}, \mathbf{v}]$, averaging over the contributions from θ.

The results of this process are presented in Fig.4, where the reconstructed KM coefficients are plotted for three time steps, namely at 6, 12 and 18 hours. The support of the coefficients is limited to the available data which follows the power curves in the v-P plane. From the inspection of Figs. 4, changes in time seem not significative. This means, that even though both the Markov and the stochastic evolution model contain additional degrees of freedom due to their time-dependent formulation, they are capable of capturing the v-P-dependency, which is invariant. This is expected since the wind turbine operation characteristics should not change through the daily cycle. However, it can be seen in fig. 5 that the procedure is capable of detecting even subtle temporal changes in the transition matrix, which lead to strong daily changes in the KM coefficients.

For all plotted times, the drift coefficients $D^{(1)}$ indicate a restoring force towards the power curve, in accordance with previous results[12]. The diffusion coefficients—only the diagonal components are shown here—show an order of magnitude weaker diffusion in the velocity than in the power, where the latter shows a strong component for diffusion in the $P-$ direction for the high slope region of the power curve. These

results again are consistent with our previous analysis of a time-homogeneous model [12]. Remarkably, the out-of the $v, P-$ plane diffusion of the direction component $D_{\theta\theta}^{(2)}$ is strongest for both very high and very low velocities, and for intermediate velocities off the power curve.

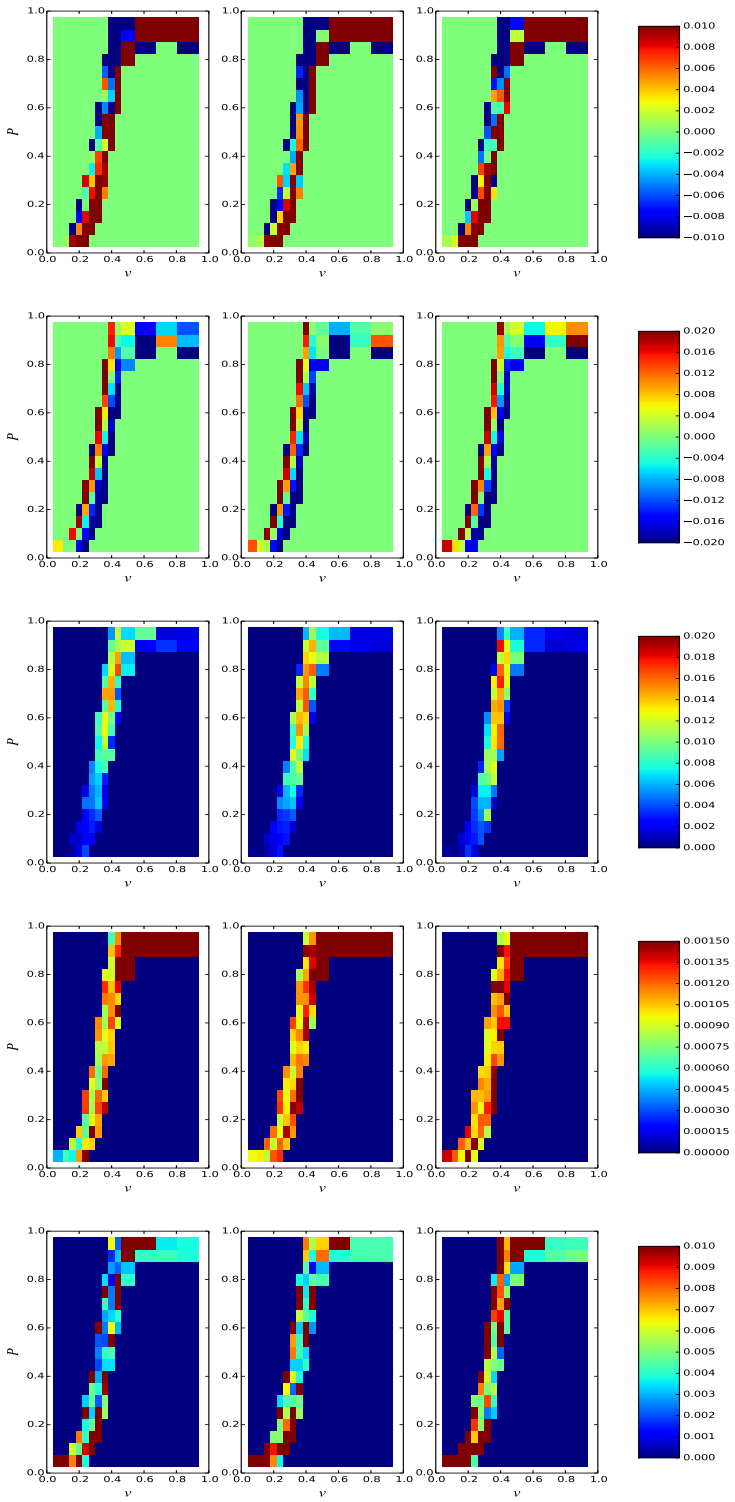

Fig. 4. The first (top two rows: power and speed) and second (bottom three rows: power, speed and direction) Kramers-Moyal coefficients for various times (left: 6hours, middle: 12hours, right: 18hours).

Next, we present a closer inspection of the time-dependence of both drift and diffusion, by considering their temporal evolution at a specific point, namely at $(v, P) = (0.34, 0.53)$, which is close to the center of the power curve. Apparently, our method creates smooth curves for the temporal evolution. This is expected since, as a consequence of the parametrization of the Markov model, it can be shown that the conditional moments used to derive the Drift and Diffusion coefficients also can be expressed by Bernstein polynomials in time. Most strikingly, it can be seen that the temporal evolution of both the drift and diffusion coefficient is decoupled between the components. Furthermore, for the same component the evolution of the diffusion coefficient seems to be delayed with respect to the drift. The dominant component is always the power production P, whose drift changes from a positive maximum at 6 h to a negative minimum at 17 h, i.e. the restoring force oscillates from a tendency to higher P values in the morning to a tendency to lower P values in the evening.

It should be noted that the chosen point (v, P) is not necessarily characteristic of the wind field or of the turbine's power production. Other points along the power curve, specifically for low velocities and near the rated wind speed are either more frequent or more characteristic, and their analysis should give increased insight into the temporal evolution of wind speed and power production.

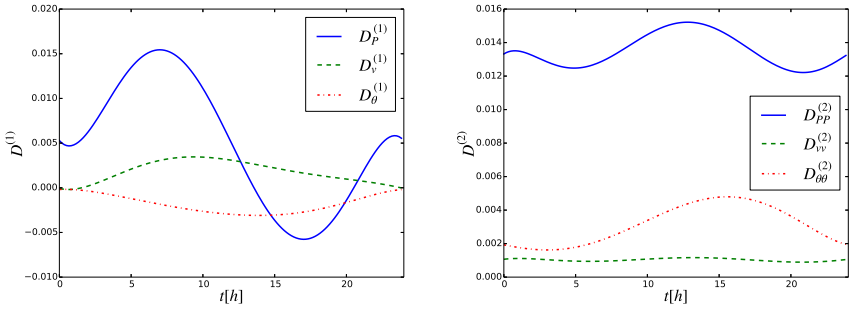

Fig. 5. The first (left) and second (right) Kramers-Moyal coefficient, by components, near the center of the power curve, $(v, P) = (0.34, 0.53)$,as a function of time.

5 Conclusions

We have shown in this paper how a time-dependent multi-dimensional stochastic process can be reconstructed from experimental data. Our method provides results in terms of the time-dependent transition matrix of a Markov model, from which the time-dependent Kramers-Moyal coefficients for a corresponding continuous process can be calculated. Application of this method to data from a turbine in a wind park gives results consistent with a previous time-independent method, and adds surprising new insight into the temporal dynamics of the wind field and the machine power production. Preliminary results have shown that the dependence with time observed in Fig. 5 changes depending which region of the power curve we choose. A more systematic study for the full power-velocity range will be carried out in an extended study.

Future research will also address the question of applicability of our method to more general cases, dealing also with the reliability and relative errors of this approach.

The aforementioned equivalence of the transition Matrix and the KM coefficients is valid if two requirements are fulfilled. First, the transition amplitudes need to have Gaussian shape, which corresponds to the existence of Gaussian noise in the stochastic process. The validity of this assumption has been checked previously for a similar system and can be reasonably assumed in this case. Secondly, the binning of the stochastic variables for determining the Markov process transition matrix must be small enough[11]. We will investigate the validity of this assumption and the corresponding errors in a forthcoming publication.

Acknowledgements

The authors acknowledge helpful discussions with David Kleinhans, who provided the basic idea to calculate the Kramers-Moyal coefficients directly. The authors thank Fundação para a Ciência e a Tecnologia for financial support under PEst-OE/FIS/-UI0618/2011, PEst-OE/MAT/UI0152/2011, FCOMP-01-0124-FEDER-016080 and SFRH/-BD/86934/2012 (TS). VVL thanks the Prometeo Project of SENESCYT (Ecuador) for financial support. PGL thanks the German Environment Ministry for financial support (0325577B). This work is part of a bilateral cooperation DRI/DAAD/1208/-2013 supported by FCT and Deutscher Akademischer Auslandsdienst (DAAD). FR assisted in fundamental research in the frame of TÁMOP 4.2.4. A/2-11-1-2012-0001 National Excellence Program, elaborating and operating an inland student and researcher personal support system. The project was subsidized by the European Union and co-financed by the European Social Fund. FR would like to thank F.Kun, Univ. Debrecen, for his hospitality.

References

1. R. Friedrich, J. Peinke, M. Sahimi and M.R.R. Tabar, "Approaching complexity by stochastic methods: From biological systems to turbulence", Phys. Rep. **506** 87 (2011).
2. H. Risken, *The Fokker-Planck Equation* (Springer, Heidelberg,1984).
3. D. Kleinhans, "Estimation of drift and diffusion functions from time series data: A maximum likelihood framework", Phys. Rev. E **85** 026705 (2012).
4. F. Boettcher, J. Peinke, D. Kleinhans, R. Friedrich, P.G. Lind, M. Haase, "Reconstruction of complex dynamical systems affected by strong measurement noise", Phys. Rev. Lett. **97** 090603 (2006).
5. P.G. Lind, M. Haase, F. Boettcher, J. Peinke, D. Kleinhans and R. Friedrich, "Extracting strong measurement noise from stochastic time series: applications to empirical data", Physical Review E 81 041125 (2010).
6. T. Scholz, V.V. Lopes, A. Estanqueiro, "A cyclic time-dependent markov process to model daily patterns in wind turbine power production", Energy **67**(0), 557-568, 2014.
7. V.V. Lopes, T. Scholz, A. Estanqueiro, and A.Q. Novais, "On the use of Markov chain models for the analysis of wind power time series", Environment and Electrical Engineering (EEEIC), 2012 11th International Conference on, 770-775, 2012.
8. J.G. Kemeny and J.L. Snell, "Finite Markov Chains", New York : Springer-Verlag, 1976.

9. A. Platis and N. Limnios and M. Le Du, "Dependability analysis of systems modeled by non-homogeneous Markov chains", Reliability Engineering and System Safety, **61**(3), 235-249, 1998.
10. A.D. Sahin and Z. Sen, "First-order Markov chain approach to wind speed modelling", Journal of Wind Engineering and Industrial Aerodynamics, **89**(3-4), 263-269, 2001.
11. N.G. van Kampen, *Stochastic Processes in Physics and Chemistry* (North Holland, 2007).
12. F.Raischel, T.Scholz, V.V.Lopes and P.G.Lind, "Uncovering wind turbine properties through two-dimensional stochastic modeling of wind dynamics", Phys. Rev. E **88** 042146 (2013).
13. A.M.van Mourik, A.Daffertshofer, P.J.Beek, "Estimating Kramers Moyal coefficients in short and non-stationary data sets", Physics Letters A **351**, Issue 1-2, 13-17, 2006.
14. C.Micheletti, G.Bussi, A.Laio, "Optimal Langevin Modeling of out-of-Equilibrium Molecular Dynamics Simulations", The Journal of Chemical Physics **129**, 7, 2008.

6 CHAPTER

Data Analysis

Modeling errors in temperature forecasts

Rui Gonçalves[1]

LIAAD - INESC TEC
and Faculty of Engineering of the University of Porto, Portugal
(e-mail: rjasg@fe.up.pt)

Abstract. In this work, we consider the modeling of forecasting temperature errors in meteorology. In particular we do so for daily maximum and minimum temperatures in the city of Porto and during the year 2011. Like in Lefebvre[6] we use pdfs of the power normal family of pdfs that are obtained from the Gaussian pdf by raising the Gaussian random variable to an exponent c where $c = \{(2k+1)/(2j+1)\}$ and $k, j = \{0, 1, \ldots\}$. We compare the fit to the data of the power normal model pdf to the fit of different non Gaussian models such as the Laplace and the Pearson type IV. We conclude that the power normal model gives the best fitting results with exponents close to those obtained by Lefebvre[6]. For the case of errors in minimum temperature forecasts we found that the data is already approximately Gaussian.
Keywords: Nearly Gaussian random variable, kurtosis, power transformation.

1 Introduction

Forecasting in temperature and precipitation is important to agriculture, to estimate the demand of certain goods on over coming days. On daily basis, people use weather forecasts to determine what clothe to wear, to plan outdoors activities and for the protection of life and goods. The problem of modeling forecasts errors of temperatures has been addressed in Lefebvre[6] and Wilks[8] among others. In temperature forecasts, common sense tell us that we should expect a rather symmetrical error distribution with small deviation. For instance, on a forecast of 15 degrees Celsius it is not expected to occur a temperature of 35 degrees.
Lefebvre[6] considered power transformations as a way to find a pdf for NG variables. The power transform gives rise to the power normal pdf's family. The data that we use in application of this theory is the daily forecast errors in maximum and minimum temperature in the city of Porto (one observation and respective forecast per day) and for the year 2011. On section (2) we present the nearly Gaussian random variable. We calculate the ordinary central moment and the kurtosis coefficient of a Gaussian variable X with zero mean raised to a power c. We also describe a method to find the specific pdf of the power normal family that models data. In section (3) we apply the

New Trends in Stochastic Modeling and Data Analysis (pp. 235-242)
Raimondo Manca - Sally McClean - Christos H Skiadas (Eds)

The data was collected by Instituto Português do Mar e da Atmosfera (IPMA)

method described on section (2) to the data. Firstly, we consider the errors in maximum temperatures. Using the Lilliefors and the Shapiro-Wilk test we conclude that normality is rejected. Using the sample kurtosis and a table of the theoretical kurtosis of a power normal random variable we found the exponents 9/11 and 7/9 to be appropriated to transform the original data in a sample with Gaussian distribution. This means that the original data can be well fitted by a Gaussian distribution raised to the power 11/9 or 9/7. In the case of the one day ahead forecast of minimum temperature errors we found that normality is not rejected. In section (4), we compare the fit of the power normal distribution to other distributions such as the Laplace and the Pearson type IV and we compare the results of the Qui-square goodness-of-fit test to conclude that all pvalues observed are greater than the usual significance levels but the pvalue associated with the power normal is significantly greater than the others.

2 Power transformation and the power normal

In this section we will follow Lefebvre[6]. The pdf of a random variable resulting form the power transformation of a normal random variable is given in the following proposition.

Proposition 1. *If $Y = X^c$ is gaussian, $Y \sim N(\mu, \sigma^2)$, then the pdf of the power transformation of a Gaussian variable, $X = Y^{1/c}$ is,*

$$f_X(x) = \frac{1}{\sqrt{2\pi}\sigma} c|x^{c-1}| \exp\left[-\frac{1}{2}\left(\frac{x^c-\mu}{\sigma}\right)^2\right].$$

This transformation is related to the Box-Cox transformation. We will call it the power normal pdf. The more interesting case for applications is when μ is zero and $c \in]0,1[$ that is the range of c values for which Y is a nearly Gaussian random variable. An example pdf is given in figure (2). In order to identify the exponent c from experimental data we must relate c with some statistical measure. If X is a Gaussian random variable with parameters $\mu = 0$ and variance σ^2, then for $c > 0$

$$E(X^c) = \int_{-\infty}^{\infty} \frac{x^c}{\sqrt{2\pi}\sigma} e^{-\frac{x^2}{2\sigma^2}} dx = \frac{2^{c/2}}{2\sqrt{\pi}} \sigma^c [1 + (-1)^c] \Gamma\left(\frac{c}{2} + \frac{1}{2}\right),$$

where Γ is the gamma function. Hence, the following proposition (see Lefebvre[6]) may be stated

Proposition 2. *The kurtosis coefficient of the random variable $Y = X^c$ when $X \sim N(0, \sigma^2)$ is given by*

$$\beta_2(c) = \frac{\int_{-\infty}^{\infty} \frac{1}{\sqrt{2\pi}} x^{4c} e^{-x^2/2} dx}{\left(\int_{-\infty}^{\infty} \frac{1}{\sqrt{2\pi}} x^{2c} e^{-x^2/2} dx\right)^2} = \sqrt{\pi} \frac{\Gamma(2c + \frac{1}{2})}{\Gamma^2(c + \frac{1}{2})}.$$

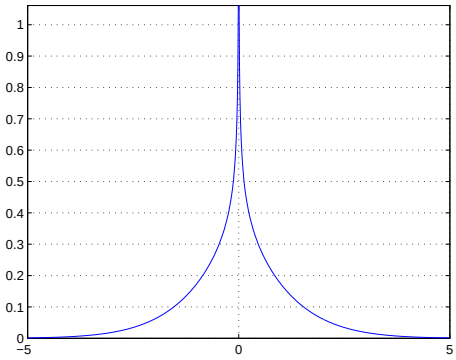

Fig. 1. Pdf of a Gaussian variable raised to the power 0.7.

c	$\beta_2(c)$	c	$\beta_2(c)$
7/9	2.237	17/15	3.58
9/11	2.358	15/13	3.08
11/13	2.447	11/15	2.11
13/15	2.514	19/21	2.643
15/17	2.566	23/25	2.697
17/19	2.6	29/31	2.753
13/11	3.828	31/33	2.767
23/19	3.979	21/23	2.672
11/9	4.042	35/37	2.79
9/7	4.404	37/39	2.8

Table 1. Kurtosis of the random variable $Y = X^c$ where $X \sim N(0,1)$ for a few values of c.

We present the table (1) that shows $\beta_2(c)$ for some values of c. This table will be used to select an exponent c, close to 1, so that, raising the values of the nearly Gaussian sample to $1/c$ one obtains an approximately Gaussian sample. Note that the identification of the exponent c requires that the variable should have mean and skewness close to zero. To estimate the power normal parameter for a given a sample $x_1, \ldots, x_n$ we center the data defining

$$z_i = x_i - \bar{x},$$

so that the mean of the z_i is 0. Assuming that the skewness coefficient is close to zero and the kurtosis is not close to 3 to be Gaussian then, by selecting an appropriate c from table (1), we find the transformation $W = Z^{1/c}$ that is likely to transform the data into a an approximately Gaussian.

3 Application to temperature forecasts

In this section we apply the method described in the last section. Our goal is to find statistical models for the forecasting errors of minimum and maximum

temperatures. The size of our data set is 347 (there is a few missing data). We define X as $X = T_F - T_O$ where T_F is the forecast and T_O the observed temperatures. Firstly, we consider the one day ahead maximum temperature forecasts during the year 2011.

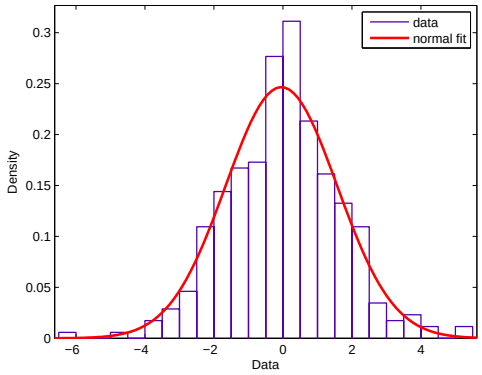

Fig. 2. Histogram and Gaussian fit to the errors X in maximum temperature forecasts.

The figure (2) is an histogram for the maximum temperature forecast errors data with the Gaussian fit on top. We note that there are more observations in the center when comparing to the Gaussian density. This feature is typical of the nearly Gaussian random variables. Hence, we will try to fit an appropriate member of the power normal family of distributions. But, before applying any statistical test we must make sure that there is none or very little temporal correlation among the data. A way of measuring temporal correlation is by computing the sample autocorrelation function (ACF). The data with small temporal correlation has an ACF within the 95% confidence bounds for white noise. Since we've found 3 out of 20 values outside the bounds then we decided to take a subset of the data. We kept only one in each pair of forecasting errors. This procedure reduces the data size to an half (173). Using the software SPSS we performed the Lilliefors and Shapiro-Wilk tests and we obtained pvalues of 0.023 and 0.1 respectively. The pvalue of Lilliefors test is less that the usual significance levels (0.05 to 0.1) used in statistical tests. So, we conclude that the Gaussian distribution is not a good model for X. Next, we tried classic models for the forecast errors such as the Laplacian and the Student's T and in both cases it turned out that the models were not acceptable. Now, we turn our attention to the power normal family. To find the right transformation we must compute some statistics of the data first. Let us define the mean of X by

$$\bar{x} = \sum_{i=1}^{n} \frac{x_i}{n},$$

and

$$\hat{\mu}_k = \sum_{i=1}^{n} \frac{(x_i - \bar{x})^k}{n-1},$$

for $k = 1, 2, ...,$ is the estimated k-th order central moment. The sample standard deviation $s_x = \sqrt{\hat{\mu}_2}$. The sample skewness coefficient is

$$b_1 = \frac{\hat{\mu}_3}{s_x^3},$$

and the sample kurtosis is

$$b_2 = \frac{\hat{\mu}_4}{s_x^4}.$$

The observed statistics for the error in the maximum temperature are:

$$\bar{x} = -0.0458;\ s_x = 1.616\ b_1 = 0.035;\ b_2 = 3.567.$$

The mean is close to zero so there is no need to center the data. The kurtosis of the reduced data set is 4.0583. Based on the kurtosis in table (1), we tried the transformation

$$w_k = x_k^{9/11}.$$

We found that the gaussian distribution is an acceptable model to the w_k's. Applying the Lilliefors test (with Matlab) the p-value increased from 0.023 before the transformation to at least 0.2 and the p-value of the Shapiro-Wilk p-value test is 0.439. Because the values of the sample kurtosis are not exactly equal to those of the table we also tried another exponent close to 9/11. In fact, trying

$$w_k = x_k^{7/9},$$

and applying the Lilliefors and Shapiro-Wilks tests (with SPSS) we obtain the p-values 0.2 and 0.439 which are equal to those obtained for the former exponent. Hence, we can use a Gaussian distribution raised to the power 11/9 to model the data. Raising the original data to the power 9/11 we obtain an approximately Gaussian distribution with mean -0.027 and standard deviation 1.311

$$X^{(9/11)} \approx N(-0.027, 1.311^2).$$

4 Fitting results

In this section, we will compare the power normal family fitting results to those of the symmetric Laplace and the Pearson IV distributions. Firstly, we consider the Laplace distribution

$$f(x|\mu, b) = \frac{1}{2b} \exp\left(-\frac{|x-\mu|}{b}\right).$$

The estimate for μ is zero and the maximum likelihood estimate for b is $b = \sum_{i=1}^{n} |X_i - \hat{\mu}|$. Secondly, we considered the Pearson type IV distribution, its pdf is

$$f_X(x) = k\left[1 + \left(\frac{x-\lambda}{a}\right)^{-m}\right] \exp\left\{-\nu \arctan\left(\frac{x-\lambda}{a}\right)\right\},$$

for $x \in \mathbb{R}$ and the parameters m, $m > 1/2$, ν, a and λ are real constants. The normalizing constant k is given by,

$$k = \frac{2^{2m-2}|\Gamma[m + (i\nu/2)]|^2}{\pi a \Gamma(2m-1)}.$$

Using the estimators given by the method of moments (see Stuart and Ord[7]) we obtained

$$\hat{m} = 5.5666, \hat{\nu} = -1.6843, \hat{a} = 4.2831, \hat{\lambda} = -0.8211.$$

The results of the chi-square tests are presented in table (2). We see that the

interval	n_j	X	Lap	Pearson IV
$(-\infty$, -2.5)	8	10.6870	9.4782	4.4115
(-2.5, -2)	11	7.01236	5.2715	7.9234
(-2, -1.5)	12	10.4451	8.20341	12.8885
(-1.5, -1,0)	11	14.8661	12.7660	18.4764
(-1, -0.5)	16	20.4931	19.8660	22.9571
(-0.5, 0)	31	32.2387	30.9149	24.566
(0,0.5)	31	25.1018	30.9149	22.7495
(0.5, 1)	21	17.5664	19.8659	18.4937
(1,1.5)	10	12.4670	12.7659	13.4767
(1.5,2)	9	8.50495	8.20342	8.996
(2, 2.5)	7	5.54012	5.27154	5.6398
(2.5, ∞)	6	7.92306	9.47825	3.3908
d^2		8.63832	14.0892	13.1724
p-value		0.47131	0.11919	0.15496

Table 2. Chi-Square goodness of fit test to determine whether a Gaussian $N(-0.027, 1.311^2)$ distribution raised to the power 11/9 is a good model for the raw data. The five columns give the chosen subintervals, the number n_j of observations in each subinterval and the expected e_j number of observations for each subinterval and for the Gauss, Laplace and Pearson IV distributions in this order.

p-value of the observed statistic for the power transformation of the normal is considerably better than the others. Next, we turn our attention to the forecasts errors of minimum temperatures. Like in the case of the maximum temperature when computing the ACF there are 2 values outside the 95% confidence bounds therefore we decided to eliminate one value in each two. The observed statistics for the error in the minimum temperature for the reduced data set are:

$$\bar{x} = 0.099;\ s_x = 1.52\ b_1 = -0.04;\ b_2 = 2.67.$$

Applying the Lilliefors and the Shapiro-Wilk tests (again with SPSS) we found a pvalue of at least 0.2 for the Lilliefors test and a pvalue of 0.439 for the Shapiro-Wilk test. This means that the data is already approximately Gaussian and there is no need for transformations.

5 Concluding remarks

In this paper, we show that a using an appropriate exponent of the form $(2k+1)/(2j+1)$, $k, j = 0, 1, ...$ the power transformation of a nearly Gaussian random variable can be Gaussian. The transformation is bijective so it may be used in both positive and negative data. We applied the method described in section (2) to data consisting of the one day ahead forecast errors in daily maximum and minimum temperatures. In the case of errors in maximum temperatures we used both Lilliefors and Shapiro-Wilk tests and we concluded that normality was rejected. Afterwards, using the sample kurtosis and the table (1) we found the appropriate exponents 9/11 and 7/9 that transform the original data in a sample with Gaussian distribution. Fitting results of the power normal, Laplace and Pearson IV distributions were compared and the pvalue of the power normal was found to be significantly greater than the other two. Surprisingly, in the case of the one day ahead forecast for daily minimum temperature errors, normality was not rejected.

6 Acknowledgments

This work is financed by the ERDF - European Regional Development Fund through the COMPETE Programme (operational programme for competitiveness) and by National Funds through the FCT - Fundação para a Ciência e a Tecnologia (Portuguese Foundation for Science and Technology) within project "FCOMP-01-0124-FEDER-037281".

References

1. Box, G.E.P and Cox.D. R. "An analysis of transformations", *J. Roy. Statist. Soc. Ser. B*, 26, pp. 211-243, 1964.
2. Gonçalves, R., Pinto, A. and Stollenwerk, N. "Cycles and universality in sunspot numbers fluctuations", *The Astrophysical Journal*, 691, pp.1583-1586, 2009.
3. Gonçalves, R., Ferreira, H.,Pinto, A. and Stollenwerk, N. " Universality in nonlinear prediction of complex systems" *Journal of Difference Equations and Applications*, 15, 11-12, pp.1067-1076, 2009.
4. Gonçalves, R., Ferreira, H. and Pinto, A. " Universality in the stock exchange market", *Journal of Difference Equations and Applications*, 17,7 pp. 1049-1063, 2010.
5. Gonçalves, R., Ferreira, H., Stollenwerk, N. and Pinto, A. " Universal fluctuations of the AEX index" *Physica A: Statistical Mechanics and its Applications*, 389,21, pp. 4776-4784, 2010.

6. Lefebvre, M. " Nearly Gaussian Distributions and Application" *Communications is Statistics - Theory and Methods*, 39, pp 823-836, 2010.
7. Stuart, A. and Ord, K. *Kendall's Advanced Theory of Statistics*, vol 1, 6th, ed. Oxford University Press, 2010.
8. Wilks, D. *Statistical Methods in the atmospheric Sciences* vol. 59, Academic Press, 1995.

Assessment of Classical and Bayesian approach for Estimation of Structural changes in Panel Data

Ishita Basak[1], and Ashis Kumar Chakraborty[2]

[1] Statistical Quality Control & Operations Research (SQC & OR) Unit, Indian Statistical Institute, Kolkata, India
(E-mail: ishita.basak@gmail.com)

[2] Statistical Quality Control & Operations Research (SQC & OR) Unit, Indian Statistical Institute, Kolkata, India
(E-mail: akchakraborty123@rediffmail.com)

Abstract: The current research focuses on different general modeling approaches to determine the presence or absence of multiple change points in each row of the 2-D data congregated at numerous time points on different subjects. Two approaches, Classical and Bayesian were implemented to estimate the change points in the per capita income change of 50 US states observed from 1948 to 2013. The Classical approach was applied following Random effects model with three terms in consideration *viz.*, common term for all subjects, subject specific error term and individual error term. Estimation of change points were done by least square theory. The Bayesian approach was employed concerning three assumptions: (a) subjects follow normal distribution having a change in parameters after the change points, (b) a correlation exists among the parameters before and after the change point for each subject, (c) change points of different series follow a common distribution. In this approach, estimation was performed by Markov Chain Monte Carlo (MCMC) method. A comparison amid the two estimates was executed by determining the standard error. In conclusion, two change points were observed in many of the states, generally, in 1984 and 1988. Some of the states exhibited no evidence of structural changes implying diminished effect of Great Moderation. The Bayesian approach displayed better estimate over the Classical one.

Keywords: Panel data, Change point, Classical approach, Least square theory, Bayesian approach, Markov Chain Monte Carlo method.

1 Introduction

In various applications, the data obtained during an extensive time period has to be investigated representing that probable statistical model may alter once or several times during the period of surveillance. The alteration in statistical model signifies a change and the point of alteration occurrence is the change point. In a series of random variables $X_1, X_2, \ldots\ldots X_n$ if $X_1, X_2, \ldots\ldots X_\eta$ follows a common distribution F and $X_{\eta+1}, X_{\eta+2}, \ldots\ldots X_n$ have distribution G with F ≠ G, then, the index 'η' is called the change point. The change-point problem was first introduced in the quality control context by Page [1]. The application of change point problems is found in statistical quality control theory, reliability, stochastic process, testing and estimation of change in the patterns of a regression models in statistics as well as in subjects like genetics, medicine, finance, stock market data and various others fields. Statistical exploration of change-point problems depend on the type of data to be examined. Time series data is usually of two types: one-dimensional and multi-dimensional or panel data. A 2-D data quite often, may be a panel data gathered at several time points on numeral subjects. Introduction of a shared involvement for all the themes (subjects) may lead to single or multiple change points occasionally called structural changes, in each row of panel data.

Some prominent instances are evidence of structural breaks in volatility due to Great Moderation in each of the 50 US states, change in blood pressure of patients in data recorded weekly before and after application of a certain drug, monthly number of traffic deaths on rural interstate roads for all US states from the time period of April, 1985 to April,1989 including the year in which the 55 miles per hour speed limit was lifted, etc.

New Trends in Stochastic Modeling and Data Analysis (*pp.* 243-255)
Raimondo Manca – Sally McClean – Christos H Skiadas (Eds)

Several literature have been reported on change point analysis of panel data. A common break model with breaks occurring at the same time point for all the subjects was developed by Joseph [2]. The assumption was that the pre-break data was sampled from a common single distribution and post break data from a common distribution. Joseph and Berger [3] have taken into account the fact that time of break may not be same for all the subjects and developed a model with the assumption that change points are not identical; rather they are samples from a common distribution function with parameter**.** Model with common break for all subjects and the break point being estimated by the theory of least squares was suggested by Bai and Perron [4] along with the consistency and asymptotic distribution of the estimate. The method was also extended for partial structural change model where not all the parameters but only a few are subject to shifts due to structural change. An efficient dynamic programming algorithm was proposed by Bai and Perron [5] to obtain global minimizers of the sum of squared residuals for both pure and partial structural change model. A simulation analysis was carried out by Bai and Perron [6] to access the adequacy of the previously proposed methods and compare between their relative merits, size and power of tests for structural change. Bai [7] studied the problem of common breaks in heterogeneous means and variances in panel data i.e., magnitude of change for the series depend on index, but assumed that breaks for all the subjects occur at the same time.

However a more realistic model is that the break points in the panel data occur at different time points for each of the subjects and common break points would be a special case of the more realistic model. More practical assumptions are (i) the change points of different subjects do not occur at the same time and (ii) the magnitude of break depends on the subjects i.e., the amount of change may not be same for all the subjects. A model for US data on quarterly personal income in million dollars of states from 1st quarter of the year 1948 to the third quarter of the year 2012 during Great Moderation has been proposed by taking into account the above mentioned assumptions. But this model has an intrinsic assumption that observations are independent in each row of the data i.e., the observations taken over regular time interval for the same subject are independent of each other. This assumption is not at all true, as the internal characteristic of the subject is the common internal aspect that is existent among all the observations recorded over time on a particular subject. The elimination of this common internal factor will end in independent observations along each row of the panel data. Analyzing these independent observations acquired after removal of the internal shared factor for each subject to estimate their change point will result in an improved and more precise estimation of change point for the panel data.

In the present research article, a methodology to eliminate internal communal factor for each subject have been proposed and the change point analysis of the resulting independent data have been accomplished under the assumption of heterogeneity in the timings of structural changes. Assessment of change point is done in both Classical and Bayesian approach. The Classical method was applied following one way Random effects model with three terms in consideration *viz.*, common term for all subjects signifying the common effect of the whole panel data, subject specific error term symbolizing the common internal effect of each subject and individual error term. Change points were calculated using the theory of least squares. The Bayesian tactic was hired concerning three assumptions: (a) subjects follow normal distribution having a change in parameters after the change points, (b) a correlation exists among the parameters before and after the change point for each subject which represents the internal common effect of each subject before and after the change point, (c) change points of different series follow a common distribution signifying common effect of the whole panel data. In this method, assessment was executed by Markov Chain Monte Carlo (MCMC) method. Comparison amid the two methods is also exhibited.

The rest of the research article is organised as follows: Section 2 discusses the general structure of panel data in detail particularly that of the US state level data from 1948 first quarter to 2012 third quarter on which the model of interest is based. Section 3 defines our model and Section 4 describes the methodology to eradicate internal

communal factor for each subject of the panel data, whereas Section 5 and Section 6 demonstrates the analysis by Classical methodology and Bayesian methodology respectively. Section 7 explains the results and the comparisons and section 8 concludes the paper.

2 Panel data

The structure of the panel data has the form of an $\boldsymbol{N}$ **x** $\boldsymbol{T}$ matrix $\boldsymbol{X}$ as follows. Each sequence $X_{i1}, X_{i2}, \ldots\ldots, X_{iT}$ represents observations over time from the i^{th} subject, $i = 1, \ldots, N$**.** A change is said to have occurred at τ_i in sequence or row i , $i = 1, \ldots., N$, and $1 \leq \tau_i \leq N - 1$, if $X_{i1}, X_{i2}, \ldots., X_{i\tau_i}$ are identically distributed with common distribution function F_{i1} and $X_{i\tau_i+1}, X_{i\tau_i+2}, \ldots., X_{iN}$ are identically distributed with common distribution function F_{i2} with $F_{i1} \neq F_{i2}$. If $\tau_i = T$, then there is no change in row 'i'. Thus $\tau_1, \tau_2, \ldots. \tau_N$ gives the change points which are generally unknown. The distributions of the points of change, 'τ_i', and the unknown parameters of the distributions F_{ik}, $i = 1, \ldots., N; k = 1,2$ are to be estimated from the data matrix (1).

$$\boldsymbol{X} = \begin{pmatrix} X_{11} & X_{12} & \ldots. & X_{1\tau_1} & X_{1\tau_1+1} & \ldots. & X_{IT} \\ X_{21} & X_{22} & \ldots. & X_{2\tau_2} & X_{2\tau_2+1} & \ldots. & X_{2T} \\ \ldots & \ldots & \ldots. & \ldots & \ldots & \ldots. & \ldots \\ \ldots & \ldots & \ldots. & \ldots & \ldots & \ldots. & \ldots \\ \ldots & \ldots & \ldots. & \ldots & \ldots & \ldots. & \ldots \\ \ldots & \ldots & \ldots. & \ldots & \ldots & \ldots. & \ldots \\ \ldots & \ldots & \ldots. & \ldots & \ldots & \ldots. & \ldots \\ X_{N1} & X_{N2} & \ldots. & X_{N\tau_N} & X_{N\tau_N+1} & \ldots. & X_{NT} \end{pmatrix} \quad \ldots\ldots. (1)$$

Instance: During 1980s, the major United States macroeconomic time series of output growth and inflation have experienced a considerable decrease in volatility. This is generally talked about to as Great Moderation. The origin behind this reduction may be that better monetary policy steadied the economy or may be upgraded inventory control facilitated the stabilization. The data is published by the Bureau of Economic Analysis, USA. A structure of the data on 50 US state level quarterly personal incomes from 1st quarter of the year 1948 to 3rd quarter of the year 2012 is given in Table 1.

Table 1. Structure of the data on US state level quarterly total personal income in US million dollars from 1st quarter of 1948 to 3rd quarter of 2012

	1948 Q1	**1948 Q2**	**1948 Q3**	**1948 Q4**	**1949 Q1**	**……..**	**2012 Q2**	**2012 Q3**
Alabama	2459	2582	2638	2681	2551	……	171631	172835
Alaska	297	311	333	356	388	……	33918	34050
Arizona	862	892	945	922	918	……	235331	236833
Colorado	1752	1807	1858	1852	1804	……	233400	234776
…..	…….	……	……	……	……	……	……	…….
….	……..	……	……	……	……	……	……	…….
West Virginia	2033	1969	2200	2188	2092	……	64126	64271

Observing Table 1, it can be straightforwardly understood that each cell value signifies quarterly income of each state of US, each row of the table represents each state of US and each of the time interval is denoted by each column of the panel data matrix.

One way to track down the source of the Great Moderation is to analyze the data at state level. States are subjected to conjoint nation-wide and global shocks. A recent work by Owyang *et al.* [8] described the state-level facts of Great Moderation in growth rate of unemployment. However, the researchers conducted the structural change analysis by univariate method i.e., they estimated the change point series by series without taking into account the similarity among different states. Liao [9] in his unpublished manuscript fitted a multivariate model for change point detection at the state level for data on per capita income of the states. But the assumption of normal distribution for income was not quite reasonable.

In the present research article, we at first, modelled the data on 50 US state level quarterly total personal incomes supposing the data to follow Pareto distribution. The reason behind using Pareto distribution is that it is generally taken as the typical income distribution. We assumed that per capita incomes of each state follow Pareto distribution and there is change in the parameter values of the distribution after the change point which requires to be estimated. Later on, we eliminated the common influence of a state from observations over time in each row of the panel data matrix and remodelled the data and estimated the data using Classical as well as Bayesian approach. The following Sections describe the detailed accomplishment of the work done.

3 The model

Considering the data on per capita quarterly income of 50 US states from 1st quarter of the year 1948 to 3rd quarter of the year 2012 we have, $N = 50$ and $T = 259$.

The growth in log of income is computed for state i, $i = 1,2, \ldots 50$ and time point t, $t = 1,2, \ldots .259$ as,

$$X_{it} = log(personal\ income_{it}) - log(personal\ income_{it-1})$$

We made the following assumptions for our model:

i. Series i experiences a single structural break at time τ_i, $i=1,2..\ N$
ii. $\tau_i \neq \tau_j$, for some $i \neq j$, that is, structural break does not occur at the same time for all the N series.
iii. Magnitude of change occurred may vary for each series.
iv. For series i,

$$X_{it} \sim Pareto(\alpha_{i1}) \quad for\ t \leq \tau_i$$
$$X_{it} \sim Pareto(\alpha_{i2}) \quad for\ \tau_i + 1 < t \leq T - 1 \qquad \ldots\ldots (2)$$

Therefore, $\theta = \{\alpha_{ij}\}, = 1,2\ ;\ = 1,2 \ldots . . N\ ;\ t = 1,2 \ldots . T$ are the unknown model parameters along with $\tau = (\tau_1, \tau_2, \ldots . . \tau_N)$, vector of change points assumed to follow normal distribution i.e.,

$$\tau_i \sim N\ (\mu_i, \sigma_i^2)\ ;\ i = 1,2, \ldots . N$$

The model parameters $\{\vec{\theta}, \vec{\mu}, \overrightarrow{\sigma^2}\}$ need to be estimated.

Initial values of τ_i*'s* are chosen from growth rate graph of the states. As for example, for the state Colorado, the graph in Fig. 1 is as follows:

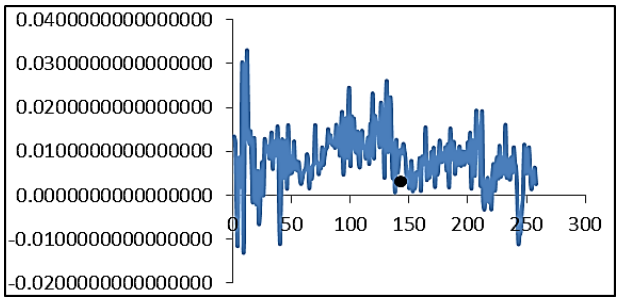

Fig. 1. Income growth in terms of difference in logarithm for the state Colorado

Hence, from the above graph, the initial estimate of τ_i is taken to be 145 *i.e.*, 3rd quarter of 1980. The model parameters were estimated by Gibbs Sampling and Markov Chain Monte Carlo technique. The steps of estimation are as follows:

Step 1: Given initial values $\left(\alpha_{ij}^{(0)}, \tau_i^{(0)}, \mu_i^{(0)}, \sigma_i^{(0)}\right)$, $i = 1,2, \ldots .50$; $j = 1,2$.

Step 2: Update parameters α_{ij} , $j = 1,2$.

Given initial values $\left(\alpha_{ij}^{(0)}, \tau_i^{(0)}, \mu_i^{(0)}, \sigma_i^{(0)}\right)$, $i = 1,2, \ldots .50$; $j = 1,2$ and data matrix $\boldsymbol{X}$, the posterior conditional distribution of $\alpha_{i1}^{(1)}$ is,

$$\alpha_{i1}^{(1)} \mid \tau_i^{(0)}, \mu_i^{(0)}, \sigma_i^{(0)} \sim Gamma\ (\alpha_{ij}^{(0)} + \tau_i^{(0)}, \quad \beta_0 + \sum_{i=1}^{\tau_i^{(0)}} \frac{X_i}{X_m})$$

and that of $\alpha_{i2}^{(1)}$ is,

$$\alpha_{i2}^{(1)} \mid \tau_i^{(0)}, \mu_i^{(0)}, \sigma_i^{(0)} \sim Gamma\ (\alpha_{ij}^{(0)} + M - \tau_i^{(0)}, \quad \beta_0 + \sum_{i=\tau_i^{(0)}}^{M} \frac{X_i}{X_m})$$

Step 3: Update parameters τ_i , $i = 1,2, \ldots M$

$\tau \sim f(\tau \mid \alpha, \mu, \sigma, X) \propto f\ (X \mid \alpha, \tau).f(\ \tau \mid \mu, \sigma\ )$

Draw $\tau_i^{(1)}$ given $\alpha_{ij}^{(1)}, \mu_i^{(0)}, \sigma_i^{(0)}$.

Step 4: Update parameters μ_i and σ_i , $i = 1,2, \ldots .50$

Draw ($\mu_i^{(1)}, \sigma_i^{(1)}$) given ($\alpha_{ij}^{(1)}, \tau_i^{(1)}, X$).

$$(\mu_i^{(1)}, \sigma_i^{(1)} \mid \tau_i^{(1)}) \sim Normal - Inverse\ Gamma\ (\frac{(\lambda_0\mu_0 + N\tau_{mean})}{\lambda_0} + N, \lambda_0 + N, \gamma_0 + \frac{N}{2}, \delta_0 + \frac{1}{2}\sum_{i=1}^{M}(\tau_i - \tau_{mean})^2 + \frac{N\lambda_0(\tau_{mean} - \mu_0)^2}{2(\lambda_0 + N)})$$

But the dependence between α_{i1} and α_{i2} in (2) for each $i = 1, 2 \ldots . . N$ is not taken into account in this model. Hence we go for the next model which is a more generalized one.

A generalised panel data model is given by,

$$y_{it} = \alpha + X_{it}'\beta + u_{it} \quad i = 1,2, \ldots . N, \quad t = 1,2, \ldots . . T \qquad \ldots\ldots . (3)$$

where, i denote subjects present in each row of the panel data e.g., households, individuals, countries, etc.; t denotes the time intervals at which observations are realised; α denotes the scalar that symbolises the common effect of panel data which is present in all observations, $\beta_{k\times 1}$ denotes the vector of parameters are may have altered after the change point, X_{it} denotes the i^{th} observation on k explanatory variables (covariates) at time t and u_{it} denotes the error term corresponding to i^{th} observation on k explanatory variables at time *t*.

Now as observations for each subject over time are interdependent, so the error term u_{it} can be splitted as,

$$u_{it} = \mu_i + v_{it} \quad i = 1,2,\ldots.N, \quad t = 1,2,\ldots..T \qquad \ldots\ldots.. (4)$$

where, μ_i denotes unobservable individual specific effect for each of the subjects that leads to correlation among observations in each row and v_{it} denotes the purely random disturbance term.

Our problem is to eliminate the unknown μ_i term which will result in independent observations across each row of the panel data.

4 Elimination of Communal effect

As μ_i's are unknown and random quantities, it is reasonable to assume that $\mu_i's$ are independent and identically distributed with $\mu_i \sim (0, \sigma_\mu^2)$ and also the random disturbance term v_{it} 's are independent and identically distributed with $v_{it} \sim Normal(0, \sigma_v^2)$. Another practical assumption is that μ_i's are independent of v_{it}'s and the covariate matrix X_{it} is independent of μ_i and v_{it}. Hence the model is a **one way random effects model.** Inference pertains to large population from which the sample is drawn. Writing equation (3) as,

$$y = \alpha l_{NT} + X\beta + u = Z\delta + u \qquad \ldots\ldots\ldots\ldots (5)$$

where, y is the $NT \times 1$ response vector, X is $NT \times k$ covariate matrix, $Z_{NT\times k}$ is the augmented matrix of the form $Z = [l_{NT}\ X]$, δ' denotes the set of unknown parameters $(\alpha'\beta')$ and l_{NT} is vector of ones of dimension NT.

Therefore $u = (u_{11}, u_{12}, \ldots.u_{1T}, u_{21}, u_{22}, \ldots.u_{2T}, \ldots\ldots\ldots u_{N1}, u_{N2}, \ldots.u_{NT})$ in (4) can be written in the form ,

$$u = Z_\mu \mu + v \ldots\ldots\ldots\ldots\ldots (6)$$

where, $v = (v_{11}, v_{12}, \ldots.v_{1T}, v_{21}, v_{22}, \ldots.v_{2T}, \ldots\ldots\ldots v_{N1}, v_{N2}, \ldots.v_{NT})$ and $\mu' = (\mu_1, \mu_2, \ldots., \mu_N)$ and $Z_\mu = I_N \otimes l_T$, I_N being the identity matrix of order $N \times N$ and l_T is a vector of ones of dimension T.

Thus we have the final equation as,

$$y = Z\delta + Z_\mu \mu + v \ldots\ldots\ldots\ldots (7)$$

Now $Z_\mu{}'Z_\mu = I_N \otimes J_T$ where J_T is a matrix of ones of dimension $T \times T$.

Denoting Ω as variance-covariance matrix of u we have,

$$\Omega = E(uu') = Z_\mu E(\mu\mu') + \sigma_v^2 I_{NT}$$

With

$$Var(u_{it}) = \sigma_\mu^2 + \sigma_v^2 \ for\ all\ i,t$$
$$Cov(u_{it}, u_{js}) = \sigma_\mu^2 + \sigma_v^2 \ for\ i = t, j = s$$
$$= \sigma_\mu^2 \ for\ i = t, j \neq s$$
$$= 0 \ otherwise$$

In order to obtain the generalized least squares estimator of the regression coefficients, Ω is required. But Ω is a huge matrix of dimension $NT \times NT$.

A suitable technique is replacing J_T by $T\overline{J_T}$, I_T by $E_T + \overline{J_T}$. Hence $E_T =, I_T - \overline{J_T}$.

So, $\Omega = \mathrm{T}\sigma_\mu^2(I_N \otimes \overline{J_T}) + \sigma_v^2(I_N \otimes E_T) + \sigma_v^2(I_N \otimes \overline{J_T})$

Collecting terms with same matrices, $\Omega = \left(\mathrm{T}\sigma_\mu^2 + \sigma_v^2\right)(I_N \otimes \overline{J_T}) + \sigma_v^2(I_N \otimes E_T)$

$$= \sigma_1^2 P + \sigma_v^2 Q$$

where, $\sigma_1^2 = \mathrm{T}\sigma_\mu^2 + \sigma_v^2 = 1^{st}\ unit\ characteristic\ root\ of\ \Omega$ of multiplicity N and $\sigma_v^2 = 2^{nd}\ unit\ characteristic\ root\ of\ \Omega$ of multiplicity $N(T-1)$

Now, $\Omega^{-1} = \frac{1}{\sigma_1^2}P + \frac{1}{\sigma_v^2}Q$ implying $\Omega^{-\frac{1}{2}} = \frac{1}{\sigma_1}P + \frac{1}{\sigma_v}Q$ implying $\sigma_v\Omega^{-\frac{1}{2}} = \frac{\sigma_v}{\sigma_1}P + Q$

Taking the transformation, $y^* = \sigma_v\Omega^{-\frac{1}{2}}y$, $Z^* = \sigma_v\Omega^{-\frac{1}{2}}Z$, following equation is obtained,

$$\boldsymbol{y_{it}^* = Z^*\delta_{it} + v_{it}^*\ for\ i = 1, 2, \ldots . N\ ; t = 1, 2, \ldots . T} \quad \text{…….(8)}$$

Hence the observations within each row are independent of each other as after the transformation the term μ_i is removed from the model. But, there may be dependency among the rows (as there may be some common factor affecting all the subjects in the panel) e.g., how different patients suffering from the same disease respond to a new treatment; when the same treatment being given to all the patients. This dependency is taken care off during estimation of change points.

5 Classical method of estimation

In Classical strategy, change points were computed applying the theory of least squares. The dependency among the subjects was taken care off by the following two ways:

i. Assuming common break for all the rows of the panel
ii. Assuming each row has break points at different times.

Under the assumption of common break and considering two breaks present in the data for each row, we have the model for each of the N subject, $i = 1,2, \ldots . . N$ as,

$$\begin{aligned} y_{it}^* &= Z^*\delta_{it_1} + v_{it}^* \quad t = 1,2, \ldots . . k_1 \\ y_{it}^* &= Z^*\delta_{it_2} + v_{it}^* \quad t = k_1 + 1, k_1 + 2, \ldots . . k_2 \\ y_{it}^* &= Z^*\delta_{it_3} + v_{it}^* \quad t = k_2 + 1, k_2 + 2, \ldots . . T \end{aligned}$$

Then the sum of squared residuals for the equation in the i^{th} row is given by,

$$S_{iT}(k_1, k_2) = \sum_{t=1}^{k_1}\left(y_{it}^* - Z^*\delta_{it_1}\right)^2 + \sum_{t=k_1+1}^{k_2}\left(y_{it}^* - Z^*\delta_{it_2}\right)^2 + \sum_{t=k_2+1}^{T}\left(y_{it}^* - Z^*\delta_{it_3}\right)^2$$

where, $k_1 = 2,3, \ldots \ldots T-1; k_2 = k_1 + 1, \ldots \ldots . T-1\ ; i = 1,2, \ldots \ldots . N$

Total sum of squared residuals for all the N equations is as follows,

$$SSR(k_1, k_2) = \sum_{i=1}^{N} S_{iT}(k_1, k_2)$$

Thus the least square estimator for the break points in the common break model for the panel data is obtained as,

$$\left(\widehat{k_1}, \widehat{k_2}\right) = argmin_{2 \le k_1 \le T-1; k_1 < k_2 \le T-1}\ SSR(k_1, k_2) \quad \text{…….(9)}$$

Under the assumption of break points at different times and considering two breaks present in the data for each row, we have the model for each of the N subject, $i = 1, 2, \ldots . . N$ as,

$$y_{it}^{*} = Z^{*}\delta_{it_1} + v_{it}^{*} \quad t = 1,2,\ldots..k_{i_1}$$
$$y_{it}^{*} = Z^{*}\delta_{it_2} + v_{it}^{*} \quad t = k_{i_1}+1, k_{i_1}+2,\ldots..k_{i_2}$$
$$y_{it}^{*} = Z^{*}\delta_{it_3} + v_{it}^{*} \quad t = k_{i_2}+1, k_{i_2}+2,\ldots..T$$

Then the sum of squared residuals for the equation in the i^{th} row is given by,

$$S_{iT}(k_{i_1}, k_{i_2}) = \sum_{t=1}^{k_{i_1}} \left(y_{it}^{*} - Z^{*}\delta_{it_1}\right)^2 + \sum_{t=k_{i_1}+1}^{k_{i_2}} \left(y_{it}^{*} - Z^{*}\delta_{it_2}\right)^2 + \sum_{t=k_{i_2}+1}^{T} \left(y_{it}^{*} - Z^{*}\delta_{it_3}\right)^2$$

where, $k_{i_1} = 2,3,\ldots\ldots T-1; k_{i_2} = k_1+1,\ldots\ldots.T-1\,; i = 1,2,\ldots\ldots N$

Thus the least square estimator for the break points in the i^{th} row for the panel data model is acquired as,

$$(\widehat{k_{i_1}}, \widehat{k_{i_2}}) = argmin_{2\le k_{i_1}\le T-1; k_1<k_{i_2}\le T-1} S_{iT}(k_{i_1}, k_{i_2}) \qquad \ldots\ldots\ldots\ldots(10)$$

6 Bayesian method of estimation

In Bayesian strategy, change points were figured applying the Markov Chain Monte Carlo (MCMC) technique. The dependency among the subjects was taken care off by the following two ways:

i. Assuming common break for all the rows of the panel
ii. Assuming each row has break points at different times.

Under the assumption of common break and considering two breaks present in the data for each row, we have the model for each of the *N* subject, $i = 1,2,\ldots..N$ as,

$$y_{it}^{*} \sim iid\ Normal\left(Z^{*}\delta_{it_1}, \sigma_v^2\right) for\ t \le k_1$$
$$y_{it}^{*} \sim iid\ Normal\left(Z^{*}\delta_{it_2}, \sigma_v^2\right) for\ k_1+1 < t \le k_2$$
$$y_{it}^{*} \sim iid\ Normal\left(Z^{*}\delta_{it_3}, \sigma_v^2\right) for\ k_2+1 < t < T$$

Likelihood for the series i is given by,

$$f(y_i^{*}; \delta_{it_1}, \delta_{it_2}, \delta_{it_3}, \sigma_v^2, k_1, k_2)$$
$$\propto \prod_{t=1}^{k_1} e^{-\frac{1}{2\pi\sigma_v}\left(y_{it}^{*} - Z^{*}\delta_{it_1}\right)^2} \prod_{t=k_1+1}^{k_2} e^{-\frac{1}{2\pi\sigma_v}\left(y_{it}^{*} - Z^{*}\delta_{it_2}\right)^2} \prod_{t=k_2+1}^{T} e^{-\frac{1}{2\pi\sigma_v}\left(y_{it}^{*} - Z^{*}\delta_{it_3}\right)^2}$$

Hence, likelihood for the panel data is given by,

$$f(y^{*}; \delta_{it_1}, \delta_{it_2}, \delta_{it_3}, \sigma_v^2, k_1, k_2)$$
$$\propto \prod_{i=1}^{N} \left\{ \prod_{t=1}^{k_1} e^{-\frac{1}{2\pi\sigma_v}\left(y_{it}^{*} - Z^{*}\delta_{it_1}\right)^2} \prod_{t=k_1+1}^{k_2} e^{-\frac{1}{2\pi\sigma_v}\left(y_{it}^{*} - Z^{*}\delta_{it_2}\right)^2} \prod_{t=k_2+1}^{T} e^{-\frac{1}{2\pi\sigma_v}\left(y_{it}^{*} - Z^{*}\delta_{it_3}\right)^2} \right\}$$

…… (11)

From this likelihood, the common change points k_1 and k_2 and other unknown parameters were estimated by the MCMC technique.

Under the assumption of break points at different times and considering two breaks present in the data for each row, we have the model for each of the *N* subject, $i = 1,2,\ldots..N$ as,

$$y_{it}^{*} \sim iid\ Normal\left(Z^{*}\delta_{it_1}, \sigma_v^2\right) for\ t \le k_{i_1}$$

$$y_{it}^{*} \sim iid\ Normal\left(Z^{*}\delta_{it_2}, \sigma_v^2\right) for\ k_{i_1} + 1 < t \leq k_{i_2}$$
$$y_{it}^{*} \sim iid\ Normal\left(Z^{*}\delta_{it_3}, \sigma_v^2\right) for\ k_{i_2} + 1 < t < T$$

Likelihood for the row i is given by,

$$f\left(y_i^{*}; \delta_{it_1}, \delta_{it_2}, \delta_{it_3}, \sigma_v^2, k_{i_1}, k_{i_2}\right)$$
$$\propto \prod_{t=1}^{k_{i_1}} e^{-\frac{1}{2\pi\sigma_v}\left(y_{it}^{*} - Z^{*}\delta_{it_1}\right)^2} \prod_{t=k_{i_1}+1}^{k_{i_2}} e^{-\frac{1}{2\pi\sigma_v}\left(y_{it}^{*} - Z^{*}\delta_{it_2}\right)^2} \prod_{t=k_{i_2}+1}^{T} e^{-\frac{1}{2\pi\sigma_v}\left(y_{it}^{*} - Z^{*}\delta_{it_3}\right)^2} \quad \ldots\ldots\ldots (12)$$

From the above likelihood, the common change points k_{i_1} and k_{i_2} and other unknown parameters for each row were estimated by the MCMC technique as before.

7 Results and Discussion

7.1 Estimation of parameters by Gibbs sampling method for the model in equation (2)

The estimated values of the change points for each of the 50 states along with the standard errors are given in Table 2.

From Table 2, it was observed that the panel data method resulted in concentrated pattern of breaks around 1984 and 1988. The standard errors of the estimates of change points for our model were significantly less than that of single series model for each state proposed by Owyang *et al.* [8]. Our model also comparatively gave better estimates than panel data model fitted by Liao [9]. The change point estimates of some states like Delaware, Minnesota and Tennessee had large standard errors. This indicated that they had no effect of Great Moderation. The states which had small standard errors like Arizona, Arkansas, Colorado, District of Columbia, Idaho, Kansas, Kentucky, Maine, Maryland, Massachusetts, Missouri, Montana, Nebraska, Nevada, New Hampshire, New York, North Carolina, North Dakota, Vermont, West Virginia etc, had very high effect in their income due to Great Moderation. Pennsylvania was an exception whose standard error of the estimated change point increased from 3.214 (single series model) to 27.768 in our model. It was 38.626 in the model by Liao [9]. This may be due to the fact that there is more than one structural break present in these states. This necessitates the extension of our model for the investigation of multiple structural breaks.

Table 2: Estimated change points and the standard errors for each state

Alabama	**Alaska**	**Arizona**	**Arkanas**	**California**	**Colorado**	**Connecticut**
1984Q3	1988Q2	1985Q1	1984Q1	1988Q4	1982Q3	1988Q4
9.8765	9.1293	2.6754	3.8321	6.4532	4.3215	5.6219
Delaware	**District of Columbia**	**Florida**	**Georgia**	**Hawaii**	**Idaho**	**Illinois**
1983Q1	1969Q3	1988Q3	1985Q3	1991Q3	1983Q1	1987Q2
40.4532	2.5648	5.4278	5.1762	8.3651	4.8327	17.6432
Indiana	**Iowa**	**Kansas**	**Kentucky**	**Louisiana**	**Maine**	**Maryland**
1984Q4	2000Q3	1984Q1	1984Q3	1986Q4	1989Q2	1989Q1
8.7634	25.4265	2.3567	1.9456	1.9274	2.6345	2.7362
Massachusetts	**Michigan**	**Minnesota**	**Mississippi**	**Missouri**	**Montana**	**Nebraska**
1989Q1	1983Q2	1994Q1	1957Q1	1984Q4	1983Q3	1984Q2
2.8654	8.7369	14.7861	5.9327	2.8387	2.1758	1.5046
Nevada	**New Hampshire**	**New Jersey**	**New Mexico**	**New York**	**North Carolina**	**North Dakota**
1981Q3	1989Q1	1989Q1	1984Q2	1987Q3	1984Q4	1989Q1
2.5476	3.3277	4.2163	5.1456	3.8605	1.4677	0.5659
Ohio	**Oklahoma**	**Oregon**	**Pennsylvania**	**Rhode Island**	**South Carolina**	**South Dakota**
1984Q4	1982Q3	1982Q1	1966Q4	1989Q1	1984Q3	1983Q3
5.9457	3.397	3.2177	27.768	3.6058	4.1285	4.9626
Tennessee	**Texas**	**Utah**	**Vermont**	**Virginia**	**Washington**	**West Virginia**
1985Q4	1983Q2	1983Q1	1989Q2	1986Q2	2003Q4	1981Q4
13.226	6.9788	5.3124	2.2341	7.6773	4.6378	1.6541

As an illustration, we have again exhibited the estimated change point of Colorado graphically in Fig. 2.

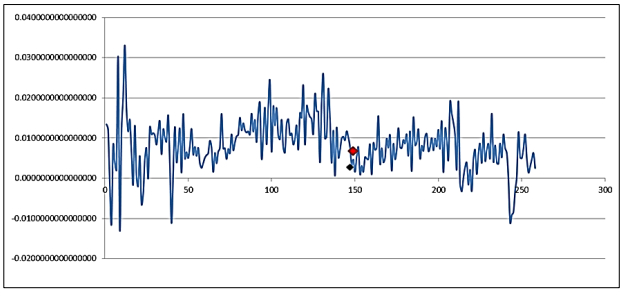

Fig. 2. Total Income (million US dollars) graph of Colorado showing the estimated change point (red dot) and the initial value taken for Gibbs Sampling (black dot)

7.2 Estimation of parameters for the model in equation (9) and (11)

Estimated common structural break for all the states by Classical and Bayesian method and the standard errors are given in the following Table 3.

Table 3. Estimated common change points and the standard errors

	Common break for all states	
	1st break	**2nd break**
Classical method	1984Q4 9.8765	1988Q3 8.7865
Bayesian method	1984Q4 6.2564	1988Q3 5.7234

From the Table 3, it is clear that most of the states of the panel data have two breaks, first break around the 4th quarter of 1984 and the second break around 3rd quarter of the year 1988. Bayesian estimators of the break points have lower standard errors than the Classical one, hence, Bayesian strategy gave better estimate than the classical one.

7.3 Estimation of parameters for the model in equation (10) and (12)

The histogram in Fig. 3 of the estimated break points for all the states exhibit two peaks, one peak around 1984 and another around 1988 and is in accordance with the conclusion drawn from the common breaks model.

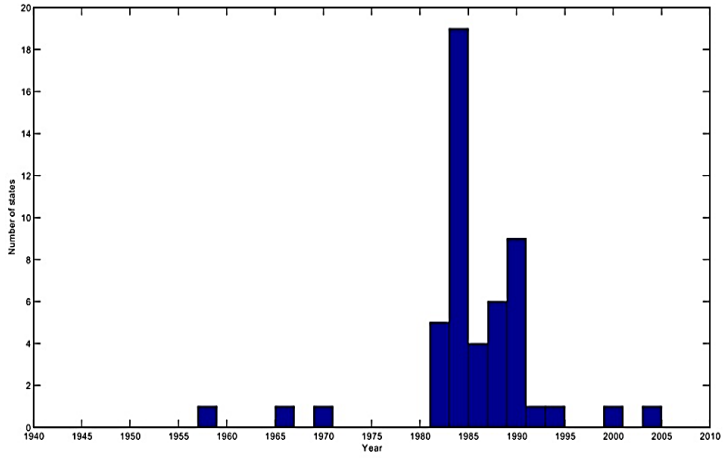

Fig. 3. Histogram of the estimated break points for all the states

Estimated structural breaks for each of the states by Classical and Bayesian method for each of the states is given in Table 4. The upper value for each state gave the Classical estimate while the lower value depicted the Bayesian estimate. From Table 4, it is clear that Bayesian method gives better estimates as the standard errors are low.

Table 4. Estimated change points for different states

Alabama		**Alaska**		**Arizona**		**Arkanas**		**California**		**Colorado**		**Connecticut**	
1981 Q2	1984 Q3	1970 Q3	1988 Q2	1964 Q3	1985 Q1	1984 Q1		1966 Q4	1987 Q1	1982 Q2	1997 Q2	1967 Q2	1985 Q1
1981 Q2	1984 Q3	1970 Q3	1988 Q2	1964 Q3	1985 Q1	1984 Q1		1966 Q4	1987 Q1	1982 Q2	1997 Q2	1967 Q2	1985 Q1
Delaware		**District of Columbia**		**Florida**		**Georgia**		**Hawaii**		**Idaho**		**Illinois**	
1953 Q3	1988 Q1	1965 Q1	1988 Q3	1971 Q1	1988 Q1	1957 Q4	1983 Q1	1984Q3		1984Q4		1959 Q1	1984 Q3
1953 Q3	1988 Q1	1965 Q1	1988 Q3	1971 Q1	1988 Q1	1957 Q4	1983 Q1	1984Q3		1984Q4		1959 Q1	1984 Q3
Indiana		**Iowa**		**Kansas**		**Kentucky**		**Louisiana**		**Maine**		**Maryland**	
1957Q4		1967 Q2	1984 Q3	1959 Q1	1984 Q1	1960 Q4	1984 Q1	1956 Q1	1978 Q3	1966 Q2	1988 Q1	1960 Q3	1988 Q1
1957Q4		1967 Q2	1984 Q3	1959 Q1	1984 Q1	1960 Q4	1984 Q1	1956 Q1	1978 Q3	1966 Q2	1988 Q1	1960 Q3	1988 Q1
Massachusetts		**Michigan**		**Minnesota**		**Mississippi**		**Missouri**		**Montana**		**Nebraska**	
1959 Q1	1983 Q1	1957 Q4	1979 Q1	1968 Q1	1983 Q1	1956Q3		1960 Q1	1981 Q3	1955 Q2	1981 Q3	1967 Q1	1981 Q2
1959 Q1	1983 Q1	1957 Q4	1979 Q1	1968 Q1	1983 Q1	1956Q3		1960 Q1	1981 Q3	1955 Q2	1981 Q3	1967 Q1	1981 Q2
Nevada		**New Hampshire**		**New Jersey**		**New Mexico**		**New York**		**North Carolina**		**North Dakota**	
1962 Q1	1983 Q1	1959 Q1	1985 Q4	1959 Q1	1985 Q4	1963 Q2	1982 Q1	1963 Q2	1982 Q2	1958 Q3	1981 Q4	1962 Q4	1981 Q1
1962 Q1	1983 Q1	1959 Q1	1985 Q4	1959 Q1	1985 Q4	1963 Q2	1982 Q1	1963 Q2	1982 Q2	1958 Q3	1981 Q4	1962 Q4	1981 Q1
Ohio		**Oklahoma**		**Oregon**		**Pennsylvania**		**Rhode Island**		**South Carolina**		**South Dakota**	
1959 Q1	1984 Q4	1972 Q2	1981 Q3	1975Q4		1958 Q3	1982 Q2	1958 Q1	1984 Q4	1959 Q1	1981 Q2	1960 Q4	1981 Q3
1959 Q1	1984 Q4	1972 Q2	1981 Q3	1975Q4		1958 Q3	1982 Q2	1958 Q1	1984 Q4	1959 Q1	1981 Q2	1960 Q4	1981 Q3
Tennessee		**Texas**		**Utah**		**Vermont**		**Virginia**		**Washington**		**West Virginia**	
1957 Q3	1981 Q2	1958 Q1	1978 Q3	1959 Q2	1981 Q4	1959 Q1	1984 Q3	1963 Q3	1984 Q4	1959 Q1	1977 Q3	1958 Q2	1978 Q3
1957 Q3	1981 Q2	1958 Q1	1978 Q3	1959 Q2	1981 Q4	1959 Q1	1984 Q3	1963 Q3	1984 Q4	1959 Q1	1977 Q3	1958 Q2	1978 Q3

As an illustration we again observe the graph of Colorado in Fig. 4, which shows that the graph stabilises after the first change point (red dot) and it has a structural shift during the second change point (green dot).

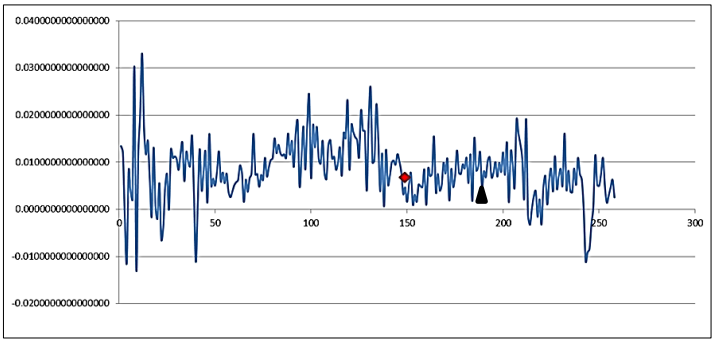

Fig. 4. Graph of state Colorado with two break points

The graphs of posterior distribution of break dates for each of the states as shown in Fig. 5 shows the location of change points for each of the 50 states of US over the years.

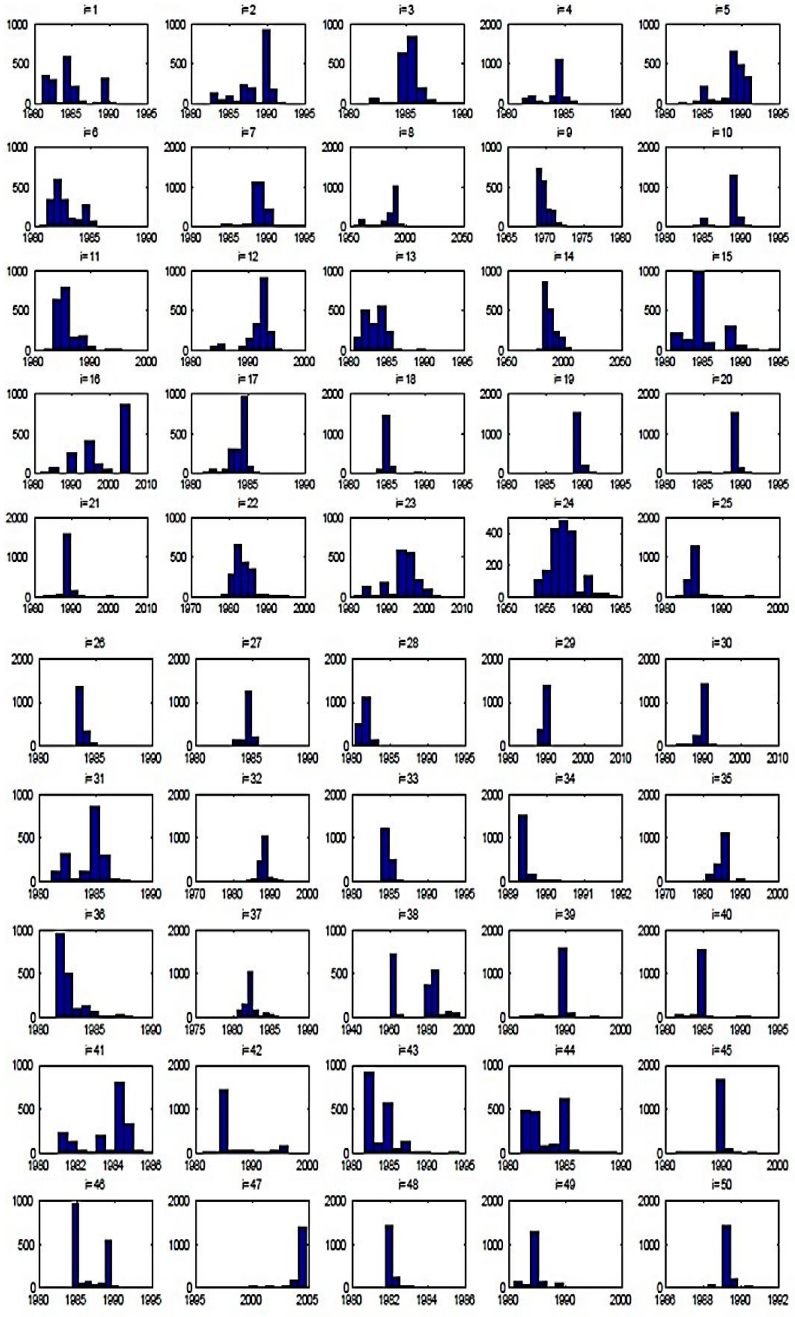

Fig. 5. Histogram of the posterior distribution of the estimated break points for individual states

Conclusions

Most of the states have two change points with some exceptions. The graph of Colorado clearly depicted that structural breaks are more efficiently captured by our present model. The model takes into account the inter-dependency among the subjects i.e., interdependency among the data of each state which is a practical intrinsic assumption of every panel data. Bayesian model has low standard errors than the Classical model. States having single or no change points or change points much before 1984 or change points much after 1989 can be analyzed individually to inspect the fact whether changes were due to Great moderation or due to any other reason.

A two way random effects model can be implemented to eliminate the common factor present for all the subjects.

References

1. E. S. Page. Continuous Inspection Schemes, Biometrika, 41, 100{115, 1954.
2. W. Joseph. Maximum likelihood estimation in the multi-path change point problem, Annals of Institute of Statistical Mathematics, 45, 3, 511{530, 1993.
3. W. Joseph and L. Berger. Analysis of Panel Data with change points, Statistica Sinica, 7, 687{703, 1997.
4. J. Bai and P. Perron. Estimating and testing linear models with multiple structural changes, Econometrica, 66, 1, 47{78, 1998.
5. J. Bai and P. Perron. Critical values for multiple structural change tests, Econometrics, 6, 1, 72{78, 2003.
6. J. Bai and P. Perron. Multiple Structural Change Models: A simulation analysis, Econometric Theory and Practice: Frontiers of Analysis and Applied Research, Cambridge University Press, 212{237, 2004.
7. J. Bai. Common Breaks in means and variances for panel data, Journal of Econometrics, 157, 78{92, 2010.
8. M. T. Owyang, J. Piger and H. J. Wall. A state level analysis of Great Moderation, Regional Science and Urban Economics, 38,578{589, 2008.
9. W. Liao. Structural breaks in panel data models: A new approach, Unpublished manuscript, 2008.

Genetic algorithm-based tuning of the *C-Value* for term ranking

Christopher Engström[1], Thierry Hamon[2,3], and Sergei Silvestrov[1]

[1] Division of Applied Mathematics, School of Education, Culture and Communication, Mälardalen University, Box 883, 72123 Västerås, Sweden (e-mail: Christopher.engstrom@mdh.se, Sergei.silvestrov@mdh.se)
[2] LIMSI-CNRS, BP133, Orsay, France (e-mail: thierry.hamon@limsi.fr)
[3] University Paris 13, Sorbonne Paris Cité, France

Abstract. Text mining in scientific and technical fields requires terminological resources to access the knowledge of the domain, but such resources suffer of low coverage. Approaches based on linguistic rules have been proposed to automatically extract terms to help the terminology building from corpora. However, the quality of the term extraction results is not sufficient and existing term ranking metrics fail to offer convicting results. We propose to improve the *C-Value* ranking metrics by considering the syntactic role of the nested terms and by optimising the parameters with a genetic algorithm. Evaluation performed on a biomedical text collection demonstrates the *C-Value* parametrisation better rank the extracted terms: the average precision increases by 9% when compared to the frequency based ranking and by 12% when compared to the *C-Value* based ranking.
Keywords: C-Value, Genetic algorithm, Terminology, Text Mining, Natural language processing.

1 Introduction

Text mining in scientific and technical fields such as medicine, legal domain, energy production, requires terminological resources to access the vocabulary and the knowledge of the domain Meystre *et al.* [19]. While this knowledge is usually recorded in terminologies, such resources suffer of low coverage when they identify terms in corpora Bodenreider *et al.* [2], McCray *et al.* [18].

Approaches mainly based on linguistic rules, have been proposed to automatically identify noun phrases which are potential terminological entities, i.e. candidate terms Cabré *et al.* [5]. But it remains difficult to catch the specialisation level of the extracted noun phrases, and to recognise terms of the domain. In a text mining perspective, candidate terms have to be first ranked according to their termhood and then the term list is cut off to reduce the number of irrelevant noun phrases with linguistic characteristics similar to terms. Several term ranking metrics as the *C-Value* used the frequency or the length of the

New Trends in Stochastic Modeling and Data Analysis (pp. 257-268)
Raimondo Manca - Sally McClean - Christos H Skiadas (Eds)

terms Frantzi *et al.* [11], but also lexical or contextual information Drouin [9]. However, these metrics fail to offer corpus-independent methods for filtering or ranking the extracted terms. We assume this is due to the lack of use of syntactic information in the ranking metrics and also that the termhood requires to take into account terminological practice of each domain. Thus, we propose to improve the integration of information as term length, nestedness and frequency, by (i) parametrising the *C-Value* according to the syntactic role of the terms and (ii) by optimising the parameter values with a genetic algorithm to reflect the terminological practice.

We first present related work (section 2). Then we describe the corpus and the term extraction method we used (section 3) and the parametrised *C-Value* and the optimisation method (section 4). The section 5 discusses the results and the impact of the proposed measure on the term ranking.

2 Background

The identification of the termhood usually takes place after the candidate term extraction. It can be helped by using statistical information and metrics or the contexts of the noun phrase. Frequency of the noun phrase has been commonly used as ranking metric Daille [6], Justeson and Katz [14], Drouin [9]. But such statistical information is not sufficient to fully capture the termhood Velardi *et al.* [21] and especially decreases either the recall as many candidate terms occur only once in the corpus Justeson and Katz [14], Drouin [8], Dowdall *et al.* [7] or the precision Frantzi *et al.* [11]. The length of the noun phrases, i.e. the number of words, may also be a clue to distinguish terms among the noun phrases extracted from texts. Thus, Drouin [8] proposes to consider that the inverted length of the terms: longer is a term, less important is the term. Such information combined to the frequency slightly increases the precision: single word candidate terms or short noun phrases are preferred. On the contrary, *C-Value* Frantzi *et al.* [10] intends to promote the longer candidate terms. Even if its impact has not been clearly evaluated, the increase of the precision seems to remain low. Given these results, the contribution of the term length seems corpus-dependent.

But the main contribution of the *C-Value* is to take into account the nestedness of the candidate terms, i.e. the string inclusion of a term in another, and thus their independence compared to the other terms. The *C-Value* assumes the frequency and the length of the noun phrase reflect its termhood. However, when the candidate term is nested in longer candidate terms, the termhood negatively depends on the frequency of the longer candidate terms, which is positively moderated by the number of candidate terms including the current noun phrase (equation 1). The measure takes into account statistical information associates to the terms and leads to measure the independence of terms Frantzi *et al.* [10], Maynard and Ananiadou [17]. Long multi-word terms which are not components of other terms are favoured. In order to considered the single word term in the same manner than the multi-words terms, Drouin [8] adds 1 to the length of the terms $|t|$.

$$C-Value(t) = \begin{cases} log_2(|t|+1) \cdot f(t) \; if \; t \; is \; not \; nested \; in \; a \; term \\ log_2(|t|+1) \cdot (f(t) - \frac{1}{P(T_t)} \sum_{t' \in T_t} f(t')) \; otherwise \end{cases} \quad (1)$$

where $f(t)$ is the frequency of the term t in the document collection, $|t|$ is the number of words of the term t, $f(t')$ is the frequency of the term t as component of a longest term, T_t is the set of terms that nest the term t, $P(T_t)$ is the number of longer terms that nest the term t. The logarithm of the term length aims at attenuating the effect of the length of the candidate term. When compared to the frequency, the impact of the *C-Value* has been demonstrated, especially on nested terms. The precision increases by about 31% for the candidate terms only appearing as nested, but only by 1% for all the candidate term Frantzi *et al.* [11]; Drouin [8] also observes that the *C-Value* concentrates the relevant candidate terms at the top of the list.

The context of the candidate terms may be also helpful to identify the termhood of the extracted noun phrases. The *NC-Value* attempts to combine contextual information with the *C-Value* Frantzi *et al.* [11]. It assumes the top-ranked candidate terms are relevant and their context may reflect the termhood. The list of candidate terms ranked by the *C-Value* is re-ranked according to the frequency of the words in the context of the top-ranked candidate terms. While Frantzi *et al.* [11] reports improvements, the impact of the context is variable or may depend on the corpora: Korkontzelos *et al.* [16] observes that the *C-Value* and the *NC-value* give equivalent results on two biomedical corpora. Termhood can also be defined as the semantic relatedness to a domain, represented as a vector of generic words occurring in the corpus Bordea *et al.* [3]. Such a model outperform the *NC-Value* on a biomedical corpus while the both are equivalent for a keyphrase extraction.

While a specialised lexicon defined by contrast with a non-technical corpus can be used as starting point for focusing the term extraction on noun phrases containing specific words Drouin [9], ranking and filtering the candidate term list may also rely on the lexicon. Velardi *et al.* [21] proposes a combination of contrastive and consensus metrics to model the relevance and the lexical cohesion of the candidate terms in regard to the domain. The evaluation of the metrics on a tourism corpus, after the pruning of the term list, and comparison with frequency, show a increase of the precision but at the expense of the recall. However, the same approach used on three other corpora underperforms the NC-value in most of the case Bordea *et al.* [3].

These works show that identifying the termhood remains difficult and results depend on the corpus. The *C-Value* appears to outperform frequency and, in most of the case, is equivalent to metrics using the context of candidate terms. However we argue that there is still room for improvement as the *C-Value* equally considers all the candidate terms without taking into account the syntactic role of the candidate terms in the longer terms.

3 Corpus and term extraction

3.1 Corpus description and pre-processing

In the following experiments, we use the Genia corpus Kim *et al.* [15]. The topic of this collection of 1,999 Medline abstracts is the transcription factors in human bloods cells. The corpus contains 18,545 sentences and 436,967 words. Each abstract is annotated with terms (mostly noun phrases) referring to physical biological entities (organisms, proteins, cells, genes) and biologically meaningful terms (e.g. molecular functions). We consider the 36,607 annotated terms (97,829 occurrences) as our reference on this corpus.

The corpus has been pre-processed in the Ogmios platform Hamon *et al.* [12]. The platform has been configured to perform a word and sentence segmentation, and then associates to each word its part-of-speech category and its lemma with the Genia Tagger Tsuruoka *et al.* [20]. 49,249 candidate terms have been extracted by YaTeA (section 3.2).

3.2 Term extraction

The extraction of the candidate terms is performed by the term extractor YaTeA Aubin and Hamon [1]. Each noun phrase which seems to be relevant in the targeted domain, is represented by a syntactic binary tree describing the syntactic role of the two term component. For instance the head component of the candidate term *full maturation of erythrocytes* is *full maturation* and the modifier component is *erythrocytes*. Recursively, *maturation* is the head component of *full maturation* and *full* its modifier component. At this step, each component can be a multi-word or a single-word term and is considered as a candidate term. The parsing of the terms provides the syntactic role of the terms but also the information on their nestedness. Statistical measures as the frequency or the *C-Value* are also associated to each term.

4 Parametrised *C-Value* and optimisation method

In this section, we describe the parametrisation of the *C-Value* in order to better take into account the terminological practice, the syntactic role and the distribution of the nested terms.

4.1 *C-Value* parametrisation

The original *C-Value* gives strong influence to the length of the terms ($|t|$): *C-Value* ranks a very long term found only once above a shorter term. However, this choice may depend on the terminological practice of each domain. The ranking metrics has to be more flexible instead of always preferring long

version 3.02, `http://www.nactem.ac.uk/genia/genia-corpus/event-corpus`
`http://www.ncbi.nlm.nih.gov/pubmed`
`http://search.cpan.org/~thhamon/Lingua-YaTeA/`

high frequency terms and the weight of the candidate term length may be parametrised. To keep the effect of the term length on the frequencies ($log_2(|t|)$) and to give more effect to the shorter terms if required, we change the length weight as the $log_2\left(\frac{|t|+1}{|t|}\right)$. We also consider the exponential parameter $\alpha \geq 0$ on the term length for taking into account the terminological practice which would prefer short or long terms: $log_2(\frac{|t|+1}{|t|^\alpha})$. A large α will give a penalty to long terms, while a low $\alpha < 1$ will instead penalise short terms. The figure 1 illustrates the variation of $log_2(|t|+1) - \alpha log_2(|t|)$ on the Genia corpus when $\alpha = 0.5$, 1 or 1.5.

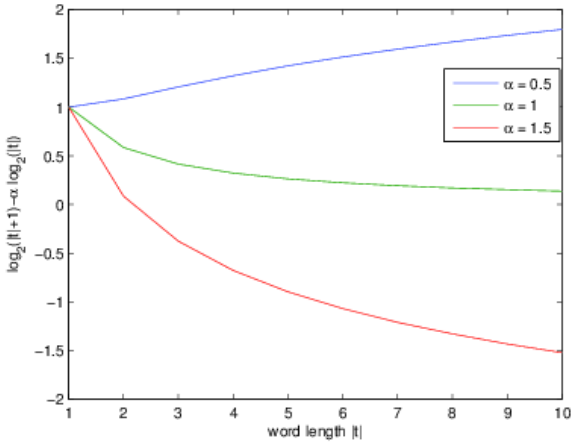

Fig. 1. Example of $log_2(|t|+1) - \alpha log_2(|t|)$ variation for several α values.

$$C - Value'(t) = \begin{cases} log_2\left(\frac{|t|+1}{|t|^{\alpha_R}}\right) \cdot f(t), \text{ if } t \text{ is not nested in a term (Root)} \\ log_2\left(\frac{|t|+1}{|t|^{\alpha_H}}\right) \cdot (f(t) - \frac{1}{P(T_t)} \sum_{t' \in T_t} f(t')), \\ \qquad\qquad \text{if } t \text{ is a Head term} \\ log_2\left(\frac{|t|+1}{|t|^{\alpha_M}}\right) \cdot (f(t) - \frac{1}{P(T_t)} \sum_{t' \in T_t} f(t')), \\ \qquad\qquad \text{if } t \text{ is a Modifier term} \end{cases} \quad (2)$$

This modification of the modified length weight do not take into the syntactic role of the terms and their nestedness. However, we have three different types of terms: (i) root terms which are not nested in any other term, (ii) head terms which have been defined as the head of another term and (iii) modifier terms which have been defined as the modifier of another term. To reflect these three syntactic role, we defined three distinct parameters α: α_R for the root terms, α_H for the head terms, α_M for the modifier terms (equation (2). We do note that a term can be both a Head term and Modifier term, but if it is a Root term it can not be any other type as well. Moreover, if a term is both Head

and Modifier we will calculate both metrics and take the average of the values. With this modified *C-Value*, candidate terms appearing in modifier position are differently ranked from those appearing in head position.

The longer candidate terms including a nested term are equally considered in the *C-Value*. The nested term is then penalised with mean of the nesting term frequencies independently of their distribution. For instance, it gives the same penalty to a term included in three terms with frequencies 10, 1 and 1, as a term included in three terms with the equal frequencies 4, 4, and 4. In that respect, instead of using the mean of the frequency, we use a β-norm to give more penalty to a term nested in several terms with unbalanced distribution of the frequencies (see equation (3)). Indeed, when $\beta > 1$, the more equally distributed the term is among the including terms, lower is penalty given by the $C - Value^*(t)$. While when $\beta < 1$, it gives a higher penalty the more equally distributed the term is. If β is close to 1 the distribution is not taken into account. If $\beta \geq 1$ the largest possible penalty to a term is equal to $\sum_{t' \in T_t} f(t')$ and occurs when the term is only included in another ($|T_t| = 1$).

Moreover keeping either the nested terms or the nesting terms, or even both may be influenced by the terminological practice. We add a parameter c to define the influence of nesting terms: higher c gives a higher penalty if the term is included in other terms. As it can not be assumed the parameters β and c have the same values with the Head terms and Modifier terms, we distinguish them: β_H and c_H for the Head terms, and β_M and c_M for the Modifier terms. The equation 3 summarises our proposition of improvement on the *C-Value*, namely the *C-Value**.

$$C - Value^* = \begin{cases} log_2\left(\frac{|t|+1}{|t|^{\alpha_R}}\right) \cdot f(t), \text{ if } t \text{ is not nested in a term (Root)} \\ log_2\left(\frac{|t|+1}{|t|^{\alpha_H}}\right) \cdot \left(f(t) - c_H \left(\sum_{t' \in T_t} f(t')^{\beta_H}\right)^{1/\beta_H}\right), \\ \qquad\qquad \text{if } t \text{ is a Head term} \\ log_2\left(\frac{|t|+1}{|t|^{\alpha_M}}\right) \cdot \left(f(t) - c_M \left(\sum_{t' \in T_t} f(t')^{\beta_M}\right)^{1/\beta_M}\right), \\ \qquad\qquad \text{if } t \text{ is a Modifier term} \end{cases} \quad (3)$$

4.2 Genetic algorithm-based optimisation model

In order to better reflect the terminological practice, we use a genetic algorithm to optimise the parameters (α_R, α_H, α_M, β and c) according to the corpus. The parameters are estimated using a real-coded genetic algorithm Wright [22] with fitness function: $f = \sum_{i \in I} r(i)$ where $I = \{N/6,\ 2N/6,\ 3N/6,\ 4N/6,\ 5N/6\}$, N is the total number of terms, and $r(i)$ is the number of annotated terms among the i highest ranked terms. For the genetic algorithm we use a population of 200 individuals. Parents are selected using a tournament selection scheme and a BLX-0.5 blend crossover scheme to create new samples Herrera *et al.* [13]. We use a 20% mutation rate where we replace an old parameter with a new randomly generated one.

We define several model configurations to increasingly evaluate the impact of the parameters and the role of the genetic algorithm (table 1). The model

M_1 does not use the genetic algorithm and the parameters are set to 1. Each parameter is then set to 1, the genetic algorithm has to estimate the optimal value of the others (models $M_{\beta c}$, $M_{\alpha^3 c}$, $M_{\alpha^3 \beta}$) given examples issued from the corpus. We then estimate three parameters α equally and β and c separately (model $M_{\alpha\beta c}$). The syntactic role of the terms is also distinguished by estimating separately the three parameters α only (model $M_{\alpha^3\beta c}$) and then also the two parameters β and c (model $M_{\alpha^3\beta^2 c^2}$).

Model	Parameters	Model	Parameters
M_1	$\alpha = \beta = c = 1$	$M_{\alpha\beta c}$	$\alpha_R = \alpha_H = \alpha_M, \beta_H = \beta_M, c_H = c_M$
$M_{\beta c}$	$\alpha = 1, \beta_H = \beta_M, c_H = c_M$	$M_{\alpha^3\beta c}$	$\alpha_R, \alpha_H, \alpha_M, \beta_H = \beta_M, c_H = c_M$
$M_{\alpha^3 c}$	$\alpha_R, \alpha_H, \alpha_M, \beta = 1, c_H = c_M$	$M_{\alpha^3\beta^2 c^2}$	$\alpha_R, \alpha_H, \alpha_M, \beta_H, \beta_M, c_H, c_M$
$M_{\alpha^3\beta}$	$\alpha_R, \alpha_H, \alpha_M, \beta_H = \beta_M, c = 1$		

Table 1. Model definition and parameter settings

5 Results and discussion

We performed experiments on the Genia corpus (section 3.1) to evaluate the behaviour of the parameters and identify the best configurations. We use several measures to evaluate the results against the reference: precision, recall, F-measure and the average precision Buckley and Voorhees [4]. We also consider the R-precision Buckley and Voorhees [4], i.e. the precision at the rank R corresponding to the number of terms to recognise in the given corpus. This evaluation measure can also be viewed as the point where the precision and the recall are equals, and in that respect, as the rank for which the precision should be optimal and more suitable for terminology building. The obtained results are compared to two baselines: the ranking with the frequency and with the *C-Value* (equation (1)).

Model	R-prec$_{train}$	R-prec$_{test}$	avg Prec$_{train}$	avg Prec$_{test}$
frequency	0.4590	0.4671	0.4338	0.4441
C-Value	0.3344	0.3594	0.3935	0.4147
M_1	0.5091	0.5090	0.5088	0.5124
$M_{\beta c}$	0.4974	0.5084	0.4910	0.5002
$M_{\alpha^3 c}$	0.5259	0.5285	0.5416	0.5407
$M_{\alpha^3\beta}$	0.5293	0.5272	0.5387	0.5363
$M_{\alpha\beta c}$	0.5144	0.5139	0.5266	0.5269
$M_{\alpha^3\beta c}$	0.5197	0.5207	0.5386	0.5360
$M_{\alpha^3\beta^2 c^2}$	0.5222	0.5233	0.5330	0.5262

Table 2. R-precision and average precision on the Genia corpus (60% for training, 40% for test).

First, the corpus has been randomly split in two parts: 60% for the training, 40% for the test. The genetic algorithm estimates the parameter values on the

training part and we evaluate the defined values on the test part. Parameters estimation are stopped after 50 iterations using a population size of 200 (as described at the section 4.2). Although the result is likely to get a little better with more time, we observed in preliminary experiments the improvement is expected to be very small. The table 2 presents the R-precision and the average precision on the training and test set. We observe that the training and test sets give very similar results. Also regarding the baselines, the ranking based on the original *C-Value* has lower R-precision and average precision than the ranking using the frequency. However, all the models based on the *C-Value** outperform the baselines: when comparing results with frequency on the test set, the average precision increases from 4,5 to 9% depending on the models, and between 8.5% and 12% regarding the *C-Value*; similar improvements are observed with the R-precision.

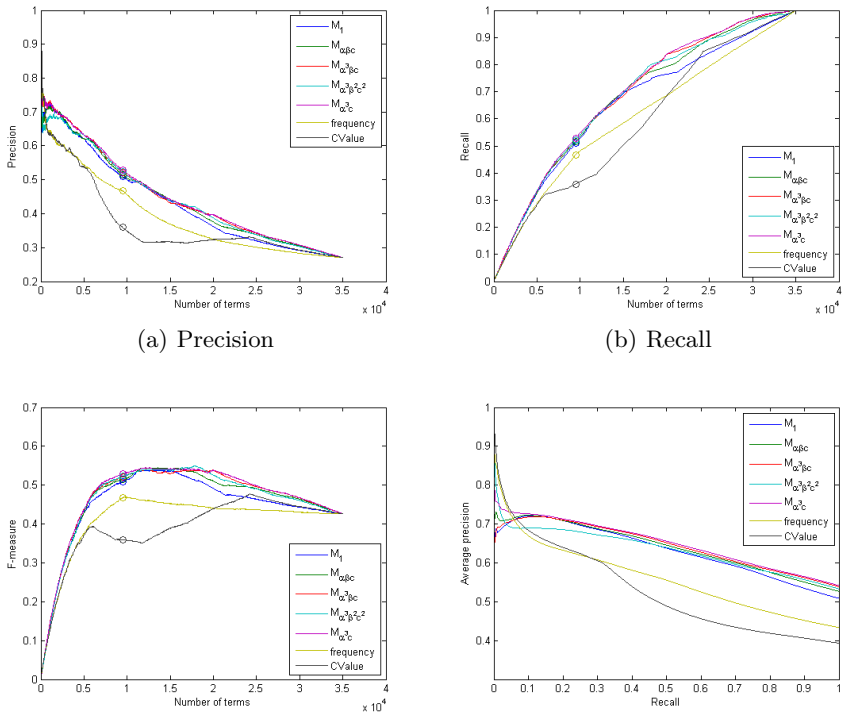

(a) Precision (b) Recall

(c) F-measure (d) Average Precision

Fig. 2. Evolution of the precision, the recall, the F-measure and the average precision on the ranked list of candidate terms extracted from the test part of Genia.

The evolution of the precision, the recall, the F-measure and the average precision according to the ranking of the terms extracted from the test set can be seen in figure 2. We only present the models M_1, the best model regarding the average precision ($M_{\alpha^3 c}$) and the models where all the parameters are

defined by the genetic algorithm. For the very first terms, the precision and the average precision are better with frequency and the *C-Value* while the recall and the F-measure are similar for all the ranking models. In particular, the evolution of the average precision (figure 2(d)) shows that the model $M_{\alpha^3\beta^2c^2}$ approaches the curve shape of the frequency and the *C-Value* ranking, and then tend to be similar for the first ranked terms. But we can observe that the models based on the *C-Value** improved the ranking after one hundred terms and until 70% of the list of candidate terms, regarding the precision as well as the recall. Moreover, the average precision of these models remains higher than results obtained with the frequency and the *C-Value*. The models based on the *C-Value** rank similarly the candidate terms even if the results obtained with the model M_1 appears to be a little lower than the others mainly with the recall and the F-measure. We also perform a 10-fold cross-validation on the corpus to study how the model can adapt the parameters of the *C-Value** and evaluate the stability of the parameter values. Table 4 presents the results of the cross-validation. As previously, *C-Value** based models consistently give better R-precision and average precision than using only the frequency or the *C-Value*. The variation of the results on the ten sets is very low and demonstrates the stability of the evaluation measure.

Model	α_R	α_H	α_M	β_H	β_M	c_H	c_M
M_1	1	1	1	1	1	1	1
$M_{\beta c}$	1	1	1	0.997	0.997	0.7095	0.7095
$M_{\alpha^3 c}$	1.1014	1.0344	0	1	1	0.91	0.91
$M_{\alpha^3\beta}$	1.1622	1.1445	0.075	1.0132	1.0132	1	1
$M_{\alpha\beta c}$	1.1604	1.1604	1.1604	1.0140	1.014	0.9953	0.9953
$M_{\alpha^3\beta c}$	1.1067	1.0961	0.0857	0.9538	0.9538	0.8316	0.8316
$M_{\alpha^3\beta^2c^2}$	1.3005	0.6093	0.7381	1.5085	1.1307	1.5224	1.17

Table 3. Values of the parameters estimated by the genetic algorithm on the Genia training part.

Model	R-prec	R-prec variation	Mean avg Prec
Frequency	0.3882	$6.7096 \cdot 10^{-5}$	0.3589
C-Value	0.3055	$9.9977 \cdot 10^{-5}$	0.3509
M_1	0.4208	$9.4632 \cdot 10^{-5}$	0.3956
$M_{\alpha^3 c}$	0.4318	$1.5695 \cdot 10^{-4}$	0.4212
$M_{\alpha^3\beta}$	0.4324	$1.3770 \cdot 10^{-4}$	0.4098
$M_{\alpha^3\beta c}$	0.4317	$1.5274 \cdot 10^{-4}$	0.4165
$M_{\alpha^3\beta^2c^2}$	0.4337	$1.4017 \cdot 10^{-4}$	0.4191

Table 4. Evaluation with a 10-fold cross-validation on the models.

Table 3 presents the parameter values estimated by the genetic algorithm on the 60% training part of the Genia corpus. The mean value and the variance of the parameters estimated for the 10-fold cross validation is given in table 5.

The low variances of the values for the 10-fold cross-validation shows that the random definition of the sub-corpus has no influence on the ranking. Comparison of models and the parameters values lead to several observations. Even if the genetic algorithm has a positive impact on the results, the M_1 is useful for ranking the terms when there are no annotated terms for training. The parameters α strongly influence the results: equally setting them has a negative effect (model $M_{\alpha\beta c}$) and leads to the worst model ($M_{\beta c}$) when they are set to 1. The weight of the Modifier terms is significantly smaller than the other two α, with a value close to 0. It means that the shorter Modifier candidate terms are penalised. On the contrary, as α_R and α_H have values higher than 1, we can note that shorter Head or Root candidate terms are preferred. The parameter β is usually very close to 1, which means the distribution among included terms is not taken into account, and more, when we set it to 1, we obtain the best R-precision and average precision (model $M_{\alpha^3 c}$). The value of the parameter c varies between 0 and 1 and we also observed that setting it to 1 does not have a large impact on the average precision and the term ranking even if the R-precision is a little bit lower (model $M_{\alpha^3\beta}$ compared to $M_{\alpha^3\beta c}$). Unsurprisingly, more parameters generally leads to better results. But defining all the parameters thanks to the genetic algorithm (model $M_{\alpha^3\beta^2 c^2}$) does not lead to the best results. We can also observe that the values set in this model are rather different from the others models. We assume that the genetic algorithm sets local optimal values for the parameters without being able to find global ones.

Model		α_R	α_H	α_M	β_H	β_M	c_H	c_M
$M_{\alpha^3 c}$	mean	1.1040	1.0743	0		(1)		0.9115
	variance	$5.2 \cdot 10^{-6}$	0.0015	0		(0)		$1.3 \cdot 10^{-5}$
$M_{\alpha^3\beta}$	mean	1.2058	1.1262	0.3400		1.0078		(1)
	variance	0.0011	0.0005	0.0116		$2.2 \cdot 10^{-5}$		(0)
$M_{\alpha^3\beta c}$	mean	1.1389	1.0905	0.1216		0.9891		0.9255
	variance	0.0002	0.0022	0.0102		0.0003		0.0035
$M_{\alpha^3\beta^2 c^2}$	mean	1.1661	0.9059	0.3046	1.2843	1.0581	1.0705	0.8991
	variance	0.0042	0.0452	0.0405	0.2780	0.0024	0.0481	0.0154

Table 5. Parameter estimation with a 10-fold cross-validation on the models.

6 Conclusion

We work on the ranking of candidate terms extracted from specialised corpora. We propose an improved and parametrised *C-Value*, the *C-Value**, to better take into account the syntactic role of the nested terms when considering the length of the term to rank, but also the distribution of the terms including it. Parameters are optimised with a standard genetic algorithm. With this new ranking measure, R-precision and average precision increase respectively by 9 and by 12% on the text collection used for the evaluation. Study of the evolution of the precision, the recall and the F-measure shows a notable

improvement on 70% of the ranked list of candidate terms. As future works, we plan to study the behaviour of the *C-Value** and the parameter estimation method on smaller training set. This point is crucial as it is unusual to have corpora with annotated terms. Besides, we would like to evaluate how the method may depend on the corpora and the used term extractor.

References

1. S. Aubin and T. Hamon. Improving term extraction with terminological resources. In T. Salakoski, F. Ginter, S. Pyysalo, and T. Pahikkala, editors, *Advances in Natural Language Processing (5th International Conference on NLP, FinTAL 2006)*, number 4139 in LNAI, pages 380–387. Springer, August 2006.
2. O. Bodenreider, T. C. Rindflesch, and A. Burgun. Unsupervised, corpus-based method for extending a biomedical terminology. In *Workshop on Natural Language Processing in the Biomedical Domain (ACL2002)*, pages 53–60, 2002.
3. G. Bordea, P. Buitelaar, and T. Polajnar. Domain-independent term extraction through domain modelling. In *Proceedings of the 10th International Conference on Terminology and Artificial Intelligence (TIA 2013)*, France, 2013.
4. C. Buckley and E. Voorhees. Retrieval system evaluation. In E. Voorhees and D. Harman, editors, *TREC: Experiment and Evaluation in Information Retrieval*, chapter 3. MIT Press, 2005.
5. M. T. Cabré, R. Estopà, and J. Vivaldi. Automatic term detection: a review of current systems. In *Recent Advances in Computational Terminology*. John Benjamins, Amsterdam, Philadelphia, 2001.
6. B. Daille. Study and implementation of combined techniques for automatic extraction of terminology. In *Proceedings of the The Balancing Act : Combining Symbolic and Statistical Approaches to Language, Workshop at the 32nd Annual Meeting of the Association for Computational Linguistics*, pages 29–36, Las Cruces, NM, 1994.
7. J. Dowdall, MichaelHess, N. Kahusk, K. Kaljurand, M. Koit, F. Rinaldi, and KadriVider. Technical terminology as a critical resource. In *Proceedings of LREC'2002*, 2002.
8. P. Drouin. *Acquisition automatique des termes : l'utilisation des pivots lexicaux spécialisés*. PhD thesis, Université de Montréal, 2002.
9. P. Drouin. Term extraction using non-technical corpora as a point of leverage. *Terminology*, 9(1):99–117, 2003.
10. K. T. Frantzi, S. Ananiadou, and J. Tsujii. Automatic term recognition using contextual clues. In *Proceedings of the Second Workshop on Multilingality in software Industry: The AI Contribution (MULSAIC'97), , 15th International Joint Conference on Artificial Intelligence, IJCAI'97*, pages 73–79, Nagoya, Japan, August 1997.
11. K. T. Frantzi, S. Ananiadou, and H. Mima. Automatic recognition of multi-word terms: the C-Value/NC-Value method. *International Journal on Digital Libraries*, 3(2):115–130, 2000.

12. T. Hamon, A. Nazarenko, T. Poibeau, S. Aubin, and J. Derivière. A robust linguistic platform for efficient and domain specific web content analysis. In *Proceedings of RIAO 2007*, Pittsburgh, USA, 2007. URL `\url{http://riao.free.fr/papers/64.pdf}`. 15 pages.
13. F. Herrera, M. Lozano, and A. M. Sánchez. A taxonomy for the crossover operator for real-coded genetic algorithms: An experimental study. *International Journal of Intelligent Systems*, 18(3):309–338, 2003. ISSN 1098-111X. doi: 10.1002/int.10091. URL `http://dx.doi.org/10.1002/int.10091`.
14. J. S. Justeson and S. M. Katz. Technical terminology: some linguistic properties and an algorithm for identification in text. *Natural Language Engineering*, 1(1):9–27, 1995.
15. J.-D. Kim, T. Ohta, Y. Teteisi, and J. Tsujii. Genia corpus - a semantically annotated corpus for bio-textmining. *Bioinformatics*, 19(1):180–182, 2003. Oxford University Press.
16. I. Korkontzelos, I. P. Klapaftis, and S. Manandhar. Reviewing and evaluating automatic term recognition techniques. In B. Nordström and A. Ranta, editors, *Advances in Natural Language Processing (6th International Conference on NLP, GoTAL 2008)*, number 5221 in LNAI, pages 248–259. Springer, August 2008.
17. D. Maynard and S. Ananiadou. Identifying terms by their family and friends. In *Proceedings of COLING 2000*, pages 530–536, Saarbrucken, Germany, 2000.
18. A. T. McCray, A. C. Browne, and O. Bodenreider. The lexical properties of the gene ontology (GO). In *Proceedings of the AMIA 2002 Annual Symposium*, pages 504–508, 2002.
19. S. M. Meystre, G. K. Savova, K. C. Kipper-Schuler, and J. F. Hurdle. Extracting information from textual documents in the electronic health record: a review of recent research. *IMIA Yearbook of Medical Informatics*, 42(5):923–936, 2008.
20. Y. Tsuruoka, Y. Tateishi, J.-D. Kim, T. Ohta, J. McNaught, S. Ananiadou, and J. Tsujii. Developing a robust part-of-speech tagger for biomedical text. In *Proceedings of Advances in Informatics - 10th Panhellenic Conference on Informatics*, LNCS 3746, pages 382–392, 2005.
21. P. Velardi, M. Missikoff, and R. Basili. Identification of relevant terms to support the construction of domain. In *Proceedings of the ACL-EACL Workshop on Human Language Technologies*. Kluwer Academic Publisher, 2001.
22. A. H. Wright. Genetic algorithms for real parameter optimization. *Foundations of genetic algorithms*, 1:205–218, 1991.

Employment and Fertility – A Comparison of the Family Survey 2000 and the Pairfam Panel

Andreas Groll[1] and Jasmin Abedieh[2]

[1] Ludwig-Maximilians-University
Department of Mathematics, Munich, Germany
(E-mail: groll@math.lmu.de)
[2] Ludwig-Maximilians-University
Institute of Statistics, Munich, Germany
(E-mail: jasmin.abedieh@hotmail.de)

Abstract. The major objective of this work is the analysis of the relationship of employment and fertility in Germany, also regarding causality. Based on Germany's current panel analysis of intimate relationships and family dynamics (pairfam), Cox's proportional hazards model is used to investigate the influence of labor force participation of women on the transition into motherhood. The obtained results serve as validation of an earlier study presented in Schröder and Brüderl [25], where the effect of employment on the fertility is analyzed for women based on the data of the West-German Family Survey 2000, using a proportional hazards model with a piecewise constant baseline hazard. In general, the estimated effects for the Cox model based on the pairfam data are surprisingly consistent with the results from Schröder and Brüderl [25], whereas indirect causality test results disagree.
Keywords: Pairfam, Employment, Fertility, Event data analysis, Cox's proportional hazards model.

1 Introduction

Today, there exist already several empirical studies in the literature, which clearly indicate that there is evidence for an influence of female labor force participation on the fertility. In this context, Schröder and Brüderl [25] mention several works which use event data analysis for different western industrial nations to show that employed women have a lower transition rate for delivering a (further) child than non-working women, see e.g. Felmlee [11] and Budig [6] for the US or Liefbroer and Corijn [23] for Flanders and the Netherlands. Apart from a few studies such as Kohlmann and Kopp [17], Kreyenfeld [18], Dornseiff and Sackmann [10], Lauer and Weber [20] or Kreyenfeld [19], which partly have a different analytical focus or exhibit some methodical problems, the work of Schröder and Brüderl [25] is the first study that explicitly analyzes if and to what extent there is a relationship between the labor force participation of women and their fertility in Germany, based on the West-German Family

New Trends in Stochastic Modeling and Data Analysis (pp. 269-285)
Raimondo Manca - Sally McClean - Christos H Skiadas (Eds)

Survey 2000. This study is replicated and validated here for the territory of the reunified Germany based on Germany's current panel analysis of intimate relationships and family dynamics (pairfam), release 4.0 (Nauck et al. [24]). A detailed description of the study can be found in Huinink et al. [16]. So the main focus in this work is the analysis of the influence of labor force participation of women on the transition into motherhood. Besides, like Schröder and Brüderl [25] we also investigate the causality of a possible (negative) effect of employment on the fertility, using a similar indirect causality test as proposed there. Note that our analyses are also restricted on transitions of childless women into motherhood, i.e. women delivering their first child.

The rest of the article is structured as follows. The most important sociological theories concerning employment and fertility are shortly summarized in Section 2. In Section 3 we discuss some theoretical aspects concerning the causality of a potential negative effect of female labor force participation on the fertility and propose a suitable indirect causality test. The data, the used methods and the results are presented in Section 4, before we finally conclude in Section 5.

2 Sociological theories concerning employment and fertility

Though lively discussed in media and social sciences, according to Schröder and Brüderl [25] only few theoretical approaches concerning the explicit mechanisms of employment and fertility exist. Schröder and Brüderl [25] provide a compact summary of the existing sociological theories and hypothesis in this context. Among the most important and relevant theories are the following two:

The hypothesis of incompatibility of roles: the roles of a woman as mother on the one hand and as employee on the other hand are generally incompatible, as simultaneous childcare and labor force participation would either reduce the productivity of the job performance or the quality of childcare.

The hypothesis of substitution: both of these roles are linked with certain rewards or incentives of e.g. emotional, social or financial kind; furthermore, the rewards that go along with one role can partially be substituted by those of the other role.

However, the gist of both theories does not directly explain why labor force participation thus necessarily has a negative effect on the fertility, because according to Schröder and Brüderl [25] employed women could simply give up their role as employee by the time they want to have children. At this point another theory has to be mentioned, which plays a major role in this context.

The economic theory of fertility: this theory is embedded in the well-known rational choice framework for understanding and modeling social and economic behavior. Here, the main idea is that couples are regarded as consumers, who take their decision with regard to the number of children they want to have after an extensive cost-benefit-assessment. Among the most famous protectionists of the economic theory of fertility are Leibenstein and Becker.

Leibenstein [21] considers children to implicate three different types of benefit: a consume benefit, as children are a general enrichment for parents, bringing affection and personal gratification to them; an income benefit, arising from the productive activities of the children; and finally, an insurance benefit, as children care and assist their parents in their old ages. At the same time, children cause direct (food, clothes, education etc.) and indirect costs (the raising of children goes along with a huge expenditure of time, strongly limiting the engagement of the parents in other activities) for their parents. While nowadays the last two types of benefit became more or less obsolete, at least in western industrial nations, where child labor is illegal since many decades and the requirement of insurance is transferred as far as possible to responsible institutions (compare Huinink and Konietzka [15]), the consume benefit has remained rather consistent and can already be achieved by a small number of children, according to Leibenstein [21]. At the same time, with increasing economic wealth, the costs of children have generally increased. Consequently, by the theory of Leibenstein the number of children is decreasing with increasing economic wealth.

A similar approach is presented in Becker [3], where children are regarded as consumer products, offering psychological benefit to their parents. Both the quantity and quality of children are included, the quality of children covering several characteristics such as education, health or future income. For Becker quantity and quality of children can (at least partly) be substituted, creating an incentive for parents to invest into the quality of their children, i.e. to spend more efforts on care and education, rather than to realize a higher number of children. On the other hand, similar to Leibenstein's indirect costs of children, Becker associates the costs that arise by the time spent for children. The idea is that child education is highly time-consuming and hence competes with other activities, e.g. employment. The time used for education could instead be used for employment, and the corresponding loss of earnings generates the so-called opportunity costs. This aspect is especially relevant for an employed woman. As soon as she stops working, even if only temporarily, her opportunity costs increase. Besides, the higher the wage rate the higher the opportunity costs (see Huinink and Konietzka [15]). Finally, as for Becker quantity and quality of children are more or less exchangeable, an employed women can realize her psychological benefit by investing in the quality of a child instead of deciding to get another child. Accordingly, with more and more women being employed and increasing income levels, also Becker's theory indicates a general decline in the number of children in developed nations. For more information about the economic theory of fertility, see also Hotz et al. [14]. A useful introduction and summary regarding important highlights of the attempts to develop an "economic" theory of human fertility are found in Leibenstein [22].

Several models exist, which consider the connection between the decision of women with respect to labor force participation and a demand for children, see e.g. Willis [28]. In most of these models the decisions relating to fertility and time allocation depend on basic economic variables such as man's income and woman's wage rate. As in these models the decisions relating to the number of

children and to the time that a woman spends for labor force participation are usually ultimately determined at the beginning of the marriage, these models are called *static life time models*.

As pointed out by Schröder and Brüderl [25], so-called *dynamic life cycle models* are more realistic, where the whole life time is divided into periods and then for each period the time is determined that a woman spends for child education and employment (or leisure time, depending on the model) together with the corresponding fertility decision. The major assumption in these models is that the previous employment history and the current work effort have an influence on the income. Consequently, employed women are able to achieve higher wage rates than non-working women and hence, these models expect a causal negative effect of employment on the fertility.

As already stated in the introduction, in fact several studies exist that confirm this hypothesis. In particular, Schröder and Brüderl [25] have found that practically all studies that base on event data analysis and investigate the influence of female labor force participation and fertility in western industrial nations have found such a negative effect, which is independent from the country and from the parity of the child. Apparently, the existing empirical studies confirm the theoretical considerations presented in this section. However, in spite of the results of existing studies, following Schröder and Brüderl [25] one has to be careful when making statements with regard to causality of this negative effect and a more sophisticated analysis seems necessary, see next section.

3 Causality

In this section we discuss some theoretical aspects concerning the causality of the negative effect of female labor force participation on the fertility. According to Schröder and Brüderl [25], one cannot directly conclude from the results of the presented existing studies that the effect is causal, i.e. the reason for the probability of birth being lower for employed women than for non-working women is in fact their labor force participation. If so, reversely, this would require that the decisions related to the labor force participation are made independent from the fertility decisions. But Schröder and Brüderl [25] point out that it is also conceivable that fertility decisions may have an influence on the labor force participation. Some studies have tried to account for this problem by considering suitable control indicators for the fertility and employment intentions, see e.g. Budig [6] or Cramer [9], but unfortunately the operationalization of these variables is quite imprecise. However, in most analyses the fertility intentions are not controlled at all. Otherwise, the results of two studies for Sweden (Hoem and Hoem [13]) and Great-Britain (Wright et al. [29]) indicate that fertility decisions also influence the labor force participation. Hence, Schröder and Brüderl [25] conclude that the relationship between employment and labor force participation is in fact quite complex. In this context they also graphically illustrate how, beside the employment status, also attitudes, moral concepts and long-term plans on the one hand, but

also opportunities and restrictions on the other hand could have effects on the fertility.

But for the present analysis the relationship between fertility decisions and the preceding employment status is of most interest. In this context, one problem is that the exact time of a fertility decision cannot be observed and usually birth is used as a simple indicator. Hence, neither the influence of the preceding employment status on the fertility decision nor a possible influence of a fertility decision on the subsequent employment period can be analyzed in a reasonable way. For this reason, Schröder and Brüderl [25] also mention that it is possible that the effect of the current labor force participation on the fertility, to which most of the studies mentioned in Section 1 refer, in fact is an effect of the anticipated fertility on the employment status. Furthermore, they point out that for an optimal analysis of the influence of the employment status on the fertility a data set would be required, which contains the fertility intentions as a time-dependent covariate with the same temporal preciseness as the employment variable. For this purpose a panel with rather short interview intervals would be required. Unfortunately, such data are currently not available, neither for our analysis nor in Schröder and Brüderl [25].

Another important aspect in this context is the problem of so-called *unobserved heterogeneity*, also known as self-selection or spurious correlation. Even if the fertility intentions could be observed at any time and an effect of the preceding employment status on the fertility would be discovered, statements concerning the causality of this effect can only be made, if one can control for all factors which may have an influence on both the employment status and the fertility decision. If instead some of these factors are unobservable, then the relationship between fertility and labor force participation is (at least partly) a spurious correlation, i.e. non-working women would possibly be more likely to get children than employed women anyway (also without a causal effect of the employment status on the fertility), simply because they differ with respect to some unobserved factors relevant for the fertility decision. Hence, the effect of the employment status on the fertility would (at least partly) reflect this unobserved heterogeneity[1], compare Schröder and Brüderl [25].

Regarding these theoretical considerations, a major task is now to find a suitable method, which allows to empirically test the causality of the employment effect. Ideally, panel data containing the fertility intentions as a time-dependent covariate with the same temporal preciseness as the employment variable would be available, but as mentioned above such data are not (yet) on hand. Hence, Schröder and Brüderl [25] propose two indirect[2] causality tests.

---

[1]Possible candidates for such unobserved factors are the family, employment and career orientation or the fertility intentions. In this context Schröder and Brüderl [25] mention several research results, which indicate that such unobserved factors might be relevant. For example, Stolzenberg and Waite [26] found a negative relationship between (long-term) fertility intentions and employment plans and Cramer [9] and Budig [6] show that fertility intentions actually have an effect on the fertility.

[2]Schröder and Brüderl [25] call these tests *indirect*, because they base on additional assumptions, which cannot be checked on the basis of their data. Nevertheless, the

The first test assumes that women have different family orientations and can be divided into different (observable) groups according to their family orientation. It analyzes the progress of the effect of employment on the fertility over the cohorts and is based on the assumption that the differences with regard to family orientation between employed on non-working women have increased over the cohorts[3]. However, in the following analysis we abstain from performing this test for two reasons. First, pairfam's youngest cohort covers people born in the years 1971-1973, so even women from the youngest cohort already benefit from modern opportunities and working time organization models increasing the compatibility of family and work, such as e.g. public financial support, part-time work, trust-based working etc., when they reach their reproductive age. Second, in total pairfam contains only three different cohorts and people from the third cohort (1991-1993) are still in their teens at the time of the third interview wave (2010/2011). So, our data basis contains basically women belonging to only two different cohorts and hence, the corresponding indirect causality test would not be very meaningful.

With their second indirect causality test Schröder and Brüderl [25] want to check if the effect of the current employment status on the fertility in fact results from a reverse effect of an anticipated fertility decision on the employment status. The idea is that if some women would determine their employment status due to a preceding fertility decision, then one could expect among the group of women, who change from employment to unemployment and vice versa, a high percentage of such women. For this reason women are divided into the following four different groups: (a) mainly employed, (b) mainly non-working, (c) changers from employment to unemployment and (d) changers from unemployment to employment. For women belonging to group (c) one would expect very high transition rates for the transition into motherhood, while on the contrary for women belonging to group (d), very low transition rates are expected. Finally, for the other two groups (a) and (b) one would expect moderate transition rates lying in between. If instead only the current employment status causally affects the transition rate into motherhood, one would expect that the transition rate of currently employed women is much lower than the one of currently non-working women, independent of the former employment history. Following Schröder and Brüderl [25], we hope that if we regard a survival model with a single categorical covariate for these four groups, this allows us some conclusions about the causality of the effect of employment on the fertility or whether the effect in fact results from a reverse effect of an

---

tests are quite transparent, compare e.g. Brüderl et al. [5] or Beck and Hartmann [2] for similar test applications.

[3]The idea behind this assumption is that while in the 1950s and 1960s the bigger part of the female population was extensively restricting their labor force participation when getting their children, nowadays women have many possibilities and alternatives to combine their professional career with their family life, with the consequence that today only women with a very strong child-orientation are supposed to decide themselves against labor force participation. Hence, an increasing effect of employment over the cohorts would indicate self-selection as described in Section 3.

anticipated fertility decision on the employment status. We present the results of the corresponding indirect causality test in Section 4.

4 Data, methods and results

In this section we first illustrate the data and shortly comment on operationalization. Furthermore, we explain the used methods and finally present the results.

4.1 Data

Germany's current panel analysis of intimate relationships and family dynamics (pairfam, release 4.0; Nauck et al. [24]), started in 2008 and contains about 12,000 randomly chosen respondents, belonging to the birth cohorts 1971-73, 1981-83 and 1991-93. Pairfam follows the cohort approach, i.e. the main focus is on anchor persons of certain birth cohorts, who provide in yearly conducted interviews detailed information, orientations and attitudes (mainly concerning the family situation) of themselves and their partners. A detailed description of the study is found in Huinink et al. [16].

Here, for a subsample of 2,289 women the retention time (in days) until the birth of the first child is considered as the dependent variable, starting at their 14th birthdays. In order to ensure that the independent time-varying covariates are temporally preceding the events, the duration until conception (and not birth) is considered, i.e. the time of event is determined by subtracting 7.5 months from the date of birth, which is when women usually notice pregnancy. For each woman the employment status is given as a time-varying categorical covariate with eight categories, compare Table 3. Note that due to gaps in the women's employment histories a category called "no info" is introduced. As in the study of Schröder and Brüderl [25], for women who belong to this category for longer than 24 months it is set to "unemployed". Besides, several other time-varying and time-constant control variables are considered. Tables 2-4 give an overview of all considered variables together with their proportions in the sample. An extraction of the data set is shown in Table 1.

Id	start	stop	birth	employment	education level	relationship status	cohort	# siblings	education level of parents
111000	0	730	0	school	apprenticeship	single	1	1	traineeship
111000	730	1434	0	no info	apprenticeship	single	1	1	traineeship
111000	1434	1891	0	no info	apprenticeship	cohab	1	1	traineeship
111000	1891	1939	1	full-time	apprenticeship	cohab	1	1	traineeship
907000	0	365	0	school	secondary educ.	single	2	0	traineeship
907000	365	2438	0	no info	secondary educ.	single	2	0	traineeship
⋮	⋮	⋮	⋮	⋮	⋮	⋮	⋮	⋮	⋮

Table 1: Structure of the data

For the indirect causality test we extract a second, smaller data set, called *event.data.test*, with the employment status as the only covariate of interest. Observations in the categories "school", "education" or "no info" are dropped. As in Schröder and Brüderl [25], we construct the time-varying covariate *employ.test* with four categories: (a) mainly employed, (b) mainly non-working,

(c) changers from employment to unemployment, (d) changers from unemployment to employment. Each category is computed proportionally on the preceding intervals (threshold: $> 50\%$) and also accounts for the current employment status. E.g., if a woman has been employed for more than 50 % of her employment biography and is currently unemployed, then she is currently in status (c).

One can observe that most of the variables have similar proportions compared to the West-German Family Survey 2000 , with the major difference that for the variable *employment status* we found higher proportions in the categories "school" and "no info" and consequently lower proportions in the categories "full-time employed", "part-time employed" and "education", see Table 3.

4.2 Methods

In the following we use a semi-parametric approach, which is suitable for the estimation of the influence of specific covariates on the survival time of certain statistical objects. The most common class of models used in the literature is the class of hazard rate models, in particular the so-called proportional hazards rate (PH-)model. This model belongs to the class of semi-parametric regression models, as for the baseline hazard function no specific form needs to be assumed.

	proportion
Birth cohort	
1971-1973	0.49
1981-1983	0.41
1991-1993	0.10
# siblings	
no siblings	0.20
one sibling	0.44
two siblings	0.21
three or more siblings	0.14
Education level of parents	
university with PhD	0.015
university without PhD	0.095
A levels	0.003
college of higher education	0.138
apprenticeship	0.103
traineeship	0.440
general secondary education	0.005
secondary education	0.024
no graduation	0.007
other graduation	0.001
no info	0.169
Number of women	2,289
Number of events	1,371

Table 2: Distribution of the time-constant covariates in the sample

	# days	proportion
Employment status		
full-time employed	3,089,174	0.274
self-employed	85,560	0.007
part-time employed	252,396	0.022
marginally employed	107,087	0.009
education	165,165	0.015
school	2,634,246	0.233
unempl./job-seeking/housewife	216,639	0.019
no info	4,737,190	0.420
Education level		
university with PhD	483,529	0.043
university without PhD	1,669,741	0.148
A levels	396,253	0.035
college of higher education	1,764,788	0.156
apprenticeship	2,226,048	0.197
traineeship	4,004,395	0.355
general secondary education	298,837	0.026
secondary education	299,438	0.027
no graduation	45,206	0.004
no info	99,222	0.009
Relationship status		
single	5,471,726	0.485
partner	3,310,963	0.293
cohabitation	1,904,906	0.169
married	599,862	0.053
Number of women	2,289	
Number of events	1,371	
Number of days	11,287,457	

Table 3: Distribution of the time-varying covariates in the sample

	# days	proportion
Combination employment history/ current employment status		
continuously unemployed	150,340	0.040 (0.013)
change from employed to unemployed	66,299	0.018 (0.006)
change from unemployed to employed	85,717	0.023 (0.008)
continuously employed	3,448,500	0.919 (0.306)
Number of women	1,705	
Number of events	863	
Number of days	3,750,856	

Table 4: Distribution of the four groups that are considered in the indirect causality test; in brackets: proportion with respect to the main data set

The influence of explanatory variables is modeled parametrically, assuming that these covariates directly influence an individual's hazard rate. The hazard

rate has the following well-known form:

$$\lambda(t, \mathbf{x}) = \lambda_0(t) \exp(\mathbf{x}^t \boldsymbol{\beta}) = \lambda_0(t) \exp(x_1 \beta_1) \cdot \ldots \cdot \exp(x_p \beta_p),$$

with baseline-hazard $\lambda_0(t)$ and linear predictor $\mathbf{x}^t \boldsymbol{\beta}$ (usually containing no intercept β_0, as it is already covered by $\lambda_0(t)$). The hazard rate is defined as follows:

$$\lambda(t, \mathbf{x}) = \lim_{\Delta t \to 0} \frac{P(t \leq T < t + \Delta t | T \geq t, \mathbf{x})}{\Delta t},$$

representing the instantaneous risk of a transition at time t (here: a transition into motherhood), given that the transition did not yet occur. Characteristic property is the proportionality of the hazard rates: for two arbitrary individuals with corresponding vectors of covariates $\mathbf{x}_i, \mathbf{x}_j$ we get

$$\frac{\lambda(t, \mathbf{x}_i)}{\lambda(t, \mathbf{x}_j)} = \frac{\lambda_0(t) \exp(\mathbf{x}_i^t \boldsymbol{\beta})}{\lambda_0(t) \exp(\mathbf{x}_j^t \boldsymbol{\beta})} = \exp((\mathbf{x}_i - \mathbf{x}_j)^t \boldsymbol{\beta}),$$

i.e. the proportion of the hazard rates of woman i and j at time t is not depending on time, but solely on their covariate realizations; major objective is the estimation of the covariate effects $\boldsymbol{\beta}$.

4.3 Results

In the following we consider two rather similar PH-models, the famous Cox-model (Cox [7]) and the so-called piece-wise constant (PWC-)model (e.g. Blossfeld et al. [4]). In the PWC-model the basic assumption is that the baseline hazard can change on predefined intervals, but remains constant within these intervals. In contrast, the Cox-model uses the so-called Nelson-Aalen estimator (Aalen [1]) for the baseline hazard. The corresponding cumulative baseline hazard functions are illustrated in Figure 1, showing that the PWC cumulative hazard is coarser, but has the same general course as the Cox estimate. Exemplarily, a Cox model incorporating all covariates from Section 4.1 can be fitted in R using the package `survival` (Therneau and Grambsch [27]) by the call:

```
>cox.obj <- coxph(Surv(start,stop,birth) ~ employment + education
+ relationship + siblings + edu.parents + cohort + cluster(id),
data=event.data, method="breslow"),
```

presuming that all categorical covariates are already transformed into factors[4]. Similarly, a PWC-model can be fitted using the `phreg` function from the R package `eha`. Figure 1 also shows the effect of the *employment status* on the cumulative baseline hazard functions for both approaches: women, who are still at school (blue), have the lowest transition rate into motherhood, whereas women in the reference category (represented by the baseline hazard; black), i.e. who are unemployed, job-seeking or housewives have the highest transition rate. As the Cox estimates are smoother, exhibit no big jumps and hence

[4]The `cluster(id)` term in the formula implies that robust variance estimators are used. The `method` argument specifies the method for tie handling.

more adequately model the data structure, in the following we focus on the Cox model when comparing our results with those obtained in Schröder and Brüderl [25].

Figure 2 shows the estimated fixed effects and 95%-confidence intervals corresponding to the German Family Survey 2000 (Schröder and Brüderl [25]; dashed lines) and the pairfam data (solid lines). As not all covariates exhibit

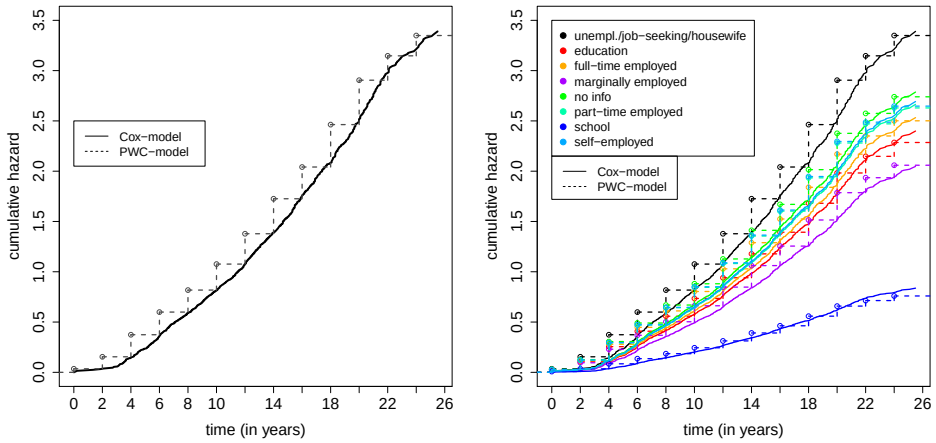

Fig. 1: Left: comparison of the cumulative baseline hazard functions, PWC- and Cox-model; right: effect of the *employment status* on the cumulative baseline hazard functions, PWC- and Cox-model

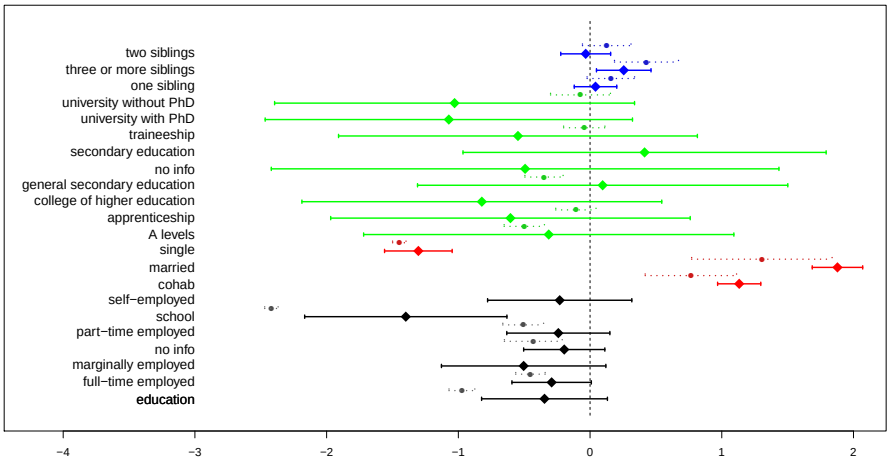

Fig. 2: Comparison of the fixed effects corresponding to the German Family Survey 2000 data (Schröder and Brüderl [25]; dashed lines) and the pairfam data (solid lines)

exactly the same categories for both studies, only the effects of those covariates are shown where a comparison is (at least approximately) possible. Note that

the effects of the *parents' education level* are not shown here, as in the pairfam study it is measured in more detailed levels compared to the German family survey. First, it turns out that the estimated effects for the Cox model based on pairfam are surprisingly consistent with those from Schröder and Brüderl [25]. Second, standard errors and confidence intervals are larger for the pairfam data, which is partly due to the used special variance-robustness method. All estimated (exponential) regression coefficients together with standard errors are presented in Table 6 in the Appendix.

In detail, we get the following results. Similar to Schröder and Brüderl [25], we find a strong negative, significant effect when women still go to school. Besides, the categories "part-time employed" and especially "full-time employed" have negative effects on the transition into motherhood compared to unemployed women, the first effect being close to significance and the latter being significant. Hence, our results confirm a negative effect of female labor force participation on the fertility for whole Germany. Later, we focus on the investigation of the causality of this effect.

With respect to the other control variables we find that the degree of institutionalization of the relationship shows the expected effects: married women have the highest transition rate into motherhood, followed by (unmarried) women who live together with their partner and women who live (apart) together with a partner; single women have the lowest transition rates. While the birth cohort has no influence on the hazard rate, women who grow up with many siblings have significantly higher transition rates. Besides, it is seen that in comparison to the reference category "no graduation" higher educational levels, except for the two types of secondary education, have negative effects, with similar trends as in Schröder and Brüderl [25], though without being significant. Similar tendencies, but with significance, are observed for the *parents' level of education* see Table 6. Next, we consider several goodness-of-fit criteria for the fitted model.

Goodness-of-fit

First, we check the proportional hazards (PH-)assumption for the hazard function. Grambsch and Therneau [12] propose a test on the validity of the PH-assumption against the alternative of time-varying coefficients. While Table 6 in the Appendix shows that the global test rejects the PH-assumption, also tests for single covariates should be considered, in particular those corresponding to key variables. A closer examination of the single tests shows that for the variables *education level* and *relationship status* the PH-assumption is generally violated ($\alpha = 0.05$), as for at least one category the null hypothesis is significantly rejected. In contrast, for the variables *employment status*, *cohort*, *number of siblings* and *parents' education level* the PH-assumption is not rejected.

The model's overall performance can be graphically assessed by investigating the Cox-Snell residuals (Cox and Snell [8]), i.e. by comparing empirical and theoretical cumulative hazard functions of the residuals. If the true underlying model is close to the specified one, the estimated cumulative hazard rate of the Cox-Snell residuals is close to the bisecting line, which is generally fulfilled here, see Figure 3 in the Appendix. Besides, similar to the residuals of an or-

dinary least-squares-estimator in linear regression, the Cox-deviance residuals can be regarded, separately for each covariate. They should vary symmetrically around zero and are also suitable to detect outliers. Figure 4 in the Appendix shows the Cox-deviance residuals, exemplarily for the covariates *employment status* and *relationship status*, which manifest a slight negative trend, i.e. survival times are slightly over-estimated by the model. Consequently, some model assumptions might be violated. Nevertheless, all in all the fitted model seems appropriate and provides an adequate fit.

Indirect causality test
To check if the effect of the current employment status on the fertility in fact results from a reverse effect of an anticipated fertility decision on the employment status, we fit the following model:

```
>cox.obj2 <- coxph(Surv(start,stop,birth) ~ employ.test + cluster(id),
 data=event.data.test, method="breslow"),
```

which is based on the smaller data set *event.data.test* and on the constructed time-varying covariate *employ.test*, introduced in Section 4.1. Even though the fitted effects in Table 5 show the same trend as in Schröder and Brüderl [25], they are far from significance. Hence, our test does not directly indicate that the estimated negative effect of female labor force participation is not causal.

	$exp(\beta)_{SB}$	$exp(\beta)_{pairfam}$
Combination employment history/ current employment status		
continuously unemployed	1	1
change from employment to unemployment	$1.822***$	1.014
changers from unemployment to employment	$0.449*$	0.653
continuously employed	0.862	0.776
individuals	2,093	1,705
number of events	1,447	863

Table 5: Comparison of the indirect causality test results for the German Family Survey 2000 data (Schröder and Brüderl [25]; $exp(\beta)_{SB}$) and the pairfam data ($exp(\beta)_{pairfam}$); $^{\bullet}p < 0.1;^{*}p < 0.05;^{**}p < 0.01;^{***}p < 0.001$.

5 Conclusion

In this work the relationship of employment and fertility in reunified Germany is analyzed on basis of the pairfam data, also regarding causality. We find that the estimated effects for a Cox proportional hazards model based on the pairfam data are surprisingly consistent with the results of an earlier study from Schröder and Brüderl [25], which is based on the West-German Family Survey 2000. However, a corresponding indirect causality test cannot confirm the opposite direction, namely that self-selection in terms of anticipated fertility decisions also affects employment. We conclude that with respect to causality a more sophisticated analysis seems necessary.

Acknowledgment: This article uses data from the German family panel pairfam, coordinated by Josef Brüderl, Johannes Huinink, Bernhard Nauck, and Sabine Walper. Pairfam is funded as long-term project by the German Research Foundation (DFG).

Appendix: Estimation, goodness-of-fit and PH-test results

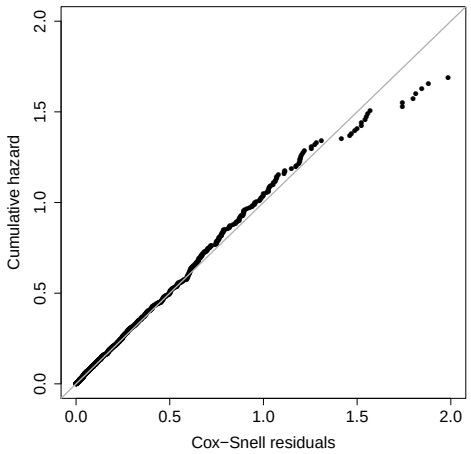

Fig. 3: Cox-Snell residuals for the Cox-model

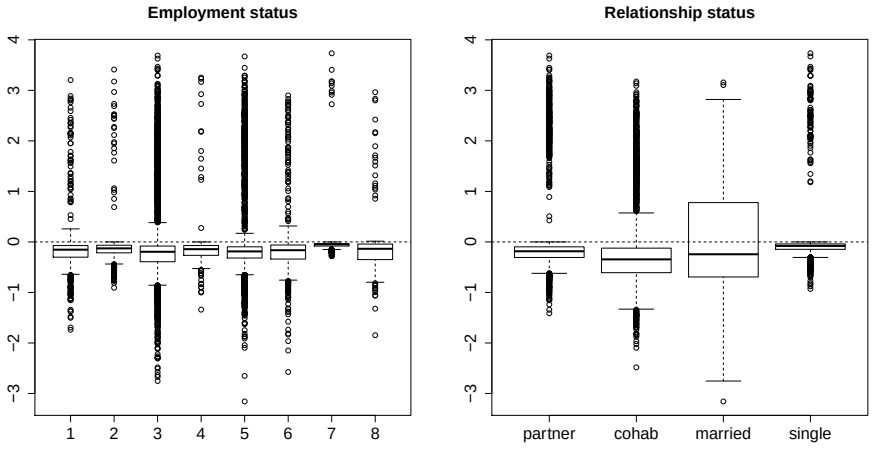

Fig. 4: Cox-deviance residuals for the Cox-model

	exp(β)	se(β)	ρ	χ^2	$P(\cdot > \chi^2)$
Employment status (Ref.: unempl./job-seeking/housewife)					
education	0.708	0.244	0.006	0.045	.832
full-time employed	0.747$^{\bullet}$	0.154	0.046	3.572	.059
marginally employed	0.604	0.318	0.006	0.051	.822
no info	0.882	0.157	0.037	2.444	.118
part-time employed	0.786	0.200	0.024	1.031	.310
school	0.247***	0.392	-0.014	0.292	.589
self-employed	0.794	0.279	0.048	3.679	.055
Cohort (Ref.: cohort 1)					
cohort 2	1.049	0.065	0.006	0.059	.809
cohort 3	0.884	0.348	0.016	0.392	.531
Relationship status (Ref.: partner)					
cohabitation	3.103***	0.084	0.008	0.125	.724
married	6.543***	0.098	-0.085	14.208	$<$ .001
single	0.272***	0.131	-0.042	3.027	.082
Education level (Ref.: no graduation)					
A levels	0.730	0.717	0.040	9.826	.002
apprenticeship	0.546	0.696	0.040	10.362	.001
college of higher education	0.440	0.697	0.045	13.069	$<$ .001
general secondary education	1.100	0.717	0.034	7.321	.007
no info	0.611	0.983	0.014	0.802	.370
secondary education	1.513	0.703	0.034	7.425	.006
traineeship	0.579	0.695	0.038	9.284	.002
university with PhD	0.342	0.711	0.046	13.158	$<$ .001
university without PhD	0.358	0.697	0.049	15.783	$<$ .001
# siblings (Ref.: no siblings)					
one sibling	1.042	0.082	0.045	0.09	7.68e-01
two siblings	0.967	0.097	0.036	2.59	1.08e-01
three or more siblings	1.291*	0.106	-0.004	0.03	8.54e-01
Education level parents (Ref.: no graduation)					
A levels	0.430	0.516	-0.018	0.345	.557
apprenticeship	0.492*	0.296	-0.056	3.557	.059
college of higher education	0.526*	0.293	-0.052	3.084	.079
general secondary education	1.156	0.553	-0.007	0.068	.795
no info	0.725	0.291	-0.076	6.448	.112
secondary education	0.578	0.343	-0.045	3.104	.078
traineeship	0.573$^{\bullet}$	0.286	-0.070	5.385	.020
other	0.134***	0.330	0.013	0.185	.667
university with PhD	0.429*	0.395	-0.043	2.347	.125
university without PhD	0.603$^{\bullet}$	0.298	-0.054	3.202	.074
Global test				158.451	$<$ .001

Table 6: Estimated (exponential) regression coefficients together with robust standard errors (left) and test on the PH-assumption (right) for the Cox-model on the pairfam-data; $^{\bullet}p < 0.1$;* $p < 0.05$;** $p < 0.01$;*** $p < 0.001$.

References

[1] O. O. Aalen. A linear regression model for the analysis of life-times. *Statistics in Medicine*, 8:907–925, 1989.

[2] N. Beck and J. Hartmann. Die Wechselwirkung zwischen Erwerbstätigkeit der Ehefrau und Ehestabilität unter der Berücksichtigung des sozialen

Wandels. *Kölner Zeitschrift für Soziologie und Sozialpsychologie*, 51:655–680, 1999.

[3] Gary S. Becker. An economic analysis of fertility. In National Bureau of Economic Research, editor, *Demographic and economic change in developed countries: a conference on the Universities-National Bureau Committee for Economic Research*, pages 209–231. Princton University Press, Princton, 1960.

[4] H.P. Blossfeld, G. Rower, and K. Golsch. *Event history analysis with Stata*. NJ: Erlbaum, Mahwa, 2007.

[5] J. Brüderl, A. Diekmann, and H. Engelhardt. Erhöht eine Probeehe das Scheidungsrisiko? Eine empirische Untersuchung mit dem Familiensurvey. *Kölner Zeitschrift für Soziologie und Sozialpsychologie*, 49:205–222, 1997.

[6] M. J. Budig. Are women's employment and fertility histories independent?an examination of causal order using event history analysis. *Social Science Research*, 32:376–401, 2003.

[7] D. R. Cox. Regression models and life tables (with discussion). *Journal of the Royal Statistical Society*, B 34:187–220, 1972.

[8] D. R. Cox and E. J. Snell. A general definition of residuals (with discussion). *Journal of the Royal Statistical Society series B*, 30:248–275, 1968.

[9] J. C. Cramer. Fertility and female employment - problems of causal direction. *American Sociological Review*, 45:167–190, 1980.

[10] J.-M. Dornseiff and R. Sackmann. Familien-, Erwerbs- und Fertilitätsdynamiken in Ost- und Westdeutschland. In W. Bien and J. H. Marbach, editors, *Partnerschaft und Familiengründung, Ergebnisse der dritten Welle des Familien-Survey*. Leske+Budrich, Opladen, 2003.

[11] D. H. Felmlee. The dynamic interdependence of women's employment and fertility. *Social Science Research*, 22:333–360, 1993.

[12] P. Grambsch and T. Therneau. Proportional hazards tests and diagnostics based on weighted residuals. *Biometrika*, 81:515–526, 1994.

[13] B. Hoem and J. M. Hoem. The impact of women's employment on 2nd and 3rd births in modern Sweden. *Population Studies*, 43:47–67, 1989.

[14] V.J. Hotz, J. A. Klerman, and R. J. Willis. The economics of fertility in developed countries. In M. Rosenzweig and O. Stark, editors, *Handbook of Popoulation and Family Economics*, pages 275–347. 1997.

[15] J. Huinink and D. Konietzka. *Familiensoziologie. Eine Einführung*. Campus Verlag GmbH, Frankfurt am Main, 2007.

[16] J. Huinink, J. Brüderl, B. Nauck, S. Walper, L. Castiglioni, and M. Feldhaus. Panel analysis of intimate relationships and family dynamics (pairfam): Conceptual framework and design. *Journal of Family Research*, 23: 77–101, 2011.

[17] A. Kohlmann and J. Kopp. Verhandlungstheoretische modellierung des Übergangs zu verschiedenen Kinderzahlen. *Zeitschrift für Soziologie*, 26: 258–274, 1997.

[18] M. Kreyenfeld. *Employmend and Fertility - East Germany in the 1990s*. University Rostock, Rostock, 2001.

[19] M. Kreyenfeld. Fertility decision in the FRG and GDR: An analysis with data from the German fertility and family survey. *Demographic Research Special Collection*, 3:275–318, 2004.

[20] C. Lauer and A. M. Weber. Employment and mothers after childbirth: a French-German comparison. *ZWE Discussion Paper*, 03-50, 2003.

[21] H. Leibenstein. *Economic Backwardness and Economic Growth.* John Wiley & Sons, New York, 1957.

[22] Harvey Leibenstein. An interpretation of the economic theory of fertility: Promising path or blind alley? *Journal of Economic Literature*, 12:457–479, 1974.

[23] A.C. Liefbroer and M. Corijn. Who, what, where, and when? Specifying the impact of educational attainment and labour force participation on family formation. *European Journal of Population*, 15:45–75, 1999.

[24] B. Nauck, J. Brüderl, J. Huinink, and S. Walper. The german family panel (pairfam). *GESIS Data Archive, Cologne*, 2013. ZA5678 Data file Version 4.0.0.

[25] J. Schröder and J. Brüderl. Der Effekt der Erwerbstätigkeit von Frauen auf die Fertilität: Kausalität oder Selbstselektion? *Zeitschrift für Soziologie*, 37:2:117–136, 2008.

[26] R. M. Stolzenberg and L. J. Waite. Age, fertility expectations and plans for employment. *American Sociological Review*, 42:769–783, 1977.

[27] T. Therneau and P. Grambsch. *Modeling Survival Data: Extending the Cox Model.* Springer-Verlag, 2000.

[28] R. J. Willis. New approach to economic theory of fertility behavior. *Journal of Political Economy*, 81:14–64, 1973.

[29] R. E. Wright, J. F. Ermisch, and P. R. A. Hinde. The 3rd birth in great-britain. *Journal of Biosocial Science*, 20:489–496, 1988.

Building-type classification and discrimination based on measurements of energy consumption data

Ying Ni[1], Christopher Engström[1], Anatoliy Malyarenko[1], and Fredrik Wallin[2]

[1] School of Education, Culture and Communication, Division of Applied Mathematics, Mälardalen University, Västerås, Sweden (e-mail: ying.ni@mdh.se, christopher.engstrom@mdh.se, anatoliy.malyarenko@mdh.se)

[2] Future Energy Center, Mälardalen University, Västerås, Sweden (e-mail: fredrik.wallin@mdh.se)

Abstract. In this paper we apply data-mining techniques to a classification and discrimination problem using hourly energy (electricity) consumption data from 350 Swedish households over the duration of one month.

There are two goals of the project, first we want to find a good classifier which could be used to classify households into either apartment or detached house given such energy consumption data, second we are interested in finding which feature variables of the energy consumption data would be useful for discriminating between the two classes.

To characterise each household, we compute selected statistical attributes of the data as well as the load profile throughout the day for that household. In order to select a good representative set of feature variables, we first rank the variable importance using technique of random forest. In an attempt to find a few "best" predictors as well as finding a good classifier, two classification techniques are used namely classification tree and linear discriminant analysis.

Both the classification tree and the linear discriminant analysis are shown to be plausible classification models on the given data under a 10-fold cross-validation procedure. Discriminating feature variables found by both classification methods give consistent and good results when used as predictors.

Keywords: data-mining, energy consumption data, classification of energy customers, discrimination of energy data, discrimination and classification.

1 Introduction

In this paper we consider a classification and discrimination problem on a large data set of actual energy (electricity) consumption measurements for 350 Swedish households. The goal is to classify the energy-using households into two classes with one being apartments and the other one being detached houses. We also attempt to find the "best" feature variables that can be used to discriminate the two classes. The motivation is to both discover knowledge from the

New Trends in Stochastic Modeling and Data Analysis (pp. 287-298)
Raimondo Manca - Sally McClean - Christos H Skiadas (Eds)

real-world data and also make predictions later when one needs to determine the source of a given time series of energy measurements. To solve this classification and discrimination problem, we apply data-mining techniques including random forests, classification tree and discriminant analysis. The technique of random forests is used for ranking the set of the candidate feature variables and the classification tree and discriminant analysis are used both as classification models and methods for finding discriminating feature variables.

There are several reviews summarizing the methods used when classifying and clustering different electric loads (Zhou et. al [13]) and consumption patterns (Chicco [3]). Both of these discuss the importance of load data preparation, pre-clustering, clustering implementation, cluster analysis and finally determine applications for the clusters. Some key methodologies used are: K-Means, hierarchical clustering, fuzzy clustering and self-organization mapping (López et al. [7]; Zhou et. al. [13]). Jota et al. [6] shows on the possibilities to use load curves to obtain a deeper understanding of the building energy usage in various types of commercial buildings and hospitals. In several papers clustering techniques are used in order to provide electric customer segmentation (López et al.[7]; Chicco [4]) and same principles are valid to distinguish different types of domestic consumers such as apartments and houses.

In the present work, the most crucial task for the classification problem is to find good predictors, i.e. to select a set of feature variables that can well explain the differences in terms of energy consumption between an apartment and a detached house. Some standard statistical attributes like mean, standard deviation, skewness, kurtosis and quantiles are used. In searching for the best predictors we also find it interesting to use some heuristic variables like the maximum/minimum hourly consumption during an average day (named as"dailyMaxMean"/"dailyMinMean"). Moreover the daily load profile, defined here as the hourly consumption at clock hour 00:00, 01:00, ... 23:00 averaged over all working days during the month, are included in the set of attributes. Daily load profiles are used to characterise the consumption patterns of households in for example Rodrigues et.al.[9].

2 The data

Our study is on a data set of electricity consumption measurements provided by the Swedish Energy Agency. The data set consists of 350 Swedish households with each household observed for one month during the period from year 2005 to 2008. The original data contains detailed electricity consumption measurements divided in ten-minute intervals for each electric component in the household, such as light sources, cold appliances, white goods, audiovisuals and their seasonally-adjusted counterparts. We work on the seasonally-adjusted measurements so we assume that the time of data collection for each household has limited impact on our classification/discrimination problem. For more details regarding to this data set we refer to the report from the Swedish end-use

The original data contains measurement for 389 households and we use a subset of the data here.

metering campaign (Zimmerman [14]) and the description of its project "Improved energy statistics in buildings and industry" (Swedish Energy Agency [10]). The present study uses one-hour data which is the total electricity consumption aggregated in two steps. The first step is to obtain electricity consumption for each ten-minute time interval by aggregating measurements from all sources, i.e. including all light sources and all appliance sources. The second step is to sum up all ten-minute intervals within a specific clock hour.

There are problems of missing values. Most often the problem is that the recorded consumption values exist for electrical appliances but not for the light sources. Such problems are treated in the ten-minute measurements level. The treatments are different for two different cases. The more frequent case is that those missing values for light sources appear at the beginning or the end of the observation time period, which is handled by simply removing the existing extra values for appliances before aggregation. In some cases the missing values occur in the middle of the observation period, these missing values are approximated by the average value at that point in time for the same weekdays.

3 Feature selection

The processed data contains information on building type, namely apartments or detached houses, and hourly electricity consumption values which we will use to perform the classification task. Take the hourly electricity consumption observations for a specific household as a sample. Since we have in total 350 households monitored for approximately one month, we have then 350 samples each contains approximately $30 \times 24 = 720$ observation values. To fit a classifier on this data, we need to select feature variables that are relevant for this classification. We start with building two separate histograms on all samples that have building type as apartment and detached house respectively, as shown in Figure 1 below.

The histograms suggest that the empirical distributions of apartments (called flats in Figure 1 for brevity) and houses differ obviously in mean and the tail behaviour of both left and right tails. Therefore we include into our set of candidate feature variables nine standard statistics: mean (of hourly consumption for each household), standard deviation, skewness, kurtosis, median, 25%/75% quantiles and "gMaxima"/"gMinima" (the maximum /minimum value over all observed hourly consumption values for that household). We shall also include two more heuristic variables, namely the average/mean of daily maximum (hourly) consumption values (hereafter shortened to "dailyMaxMean") and the average/mean of daily minimum (hourly) consumption values (hereafter shortened to "dailyMinMean"). The variable"dailyMinMean" is calculated in two steps. First we compute the minimum hourly consumption value for each day then in the second step we average over all 30 observation days. The intuition to "dailyMaxMean" is obvious, apartments should in general have lower hourly peak than houses. On the other hand, detached houses tend to have lower hourly minimum usage than apartments, hence "dailyMinMean" is included in our set. For each sample/household, we can compute a single value

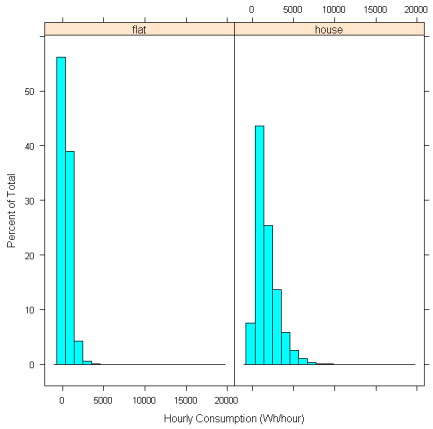

Fig. 1. Histograms of hourly energy consumption values for apartments (left) and houses (right)

of each of the above-mentioned 11 variables which are then used to characterise the corresponding sample/household.

We run a *Random Forest* in **R** to rank the importance of these variables. The random forest technique is an ensemble method formed by a large set of tree-based models each of which are grown with random subspace method (see Breiman [1] for details). As shown in Figure 2 (left), the random forest technique ranks the variable "25% quantile" as the most explanatory variable for predicting the building type, followed by "dailyMinMean", "mean" and so on. This is an interesting result since intuitively one might think the mean hourly consumption is the most useful variable in predicting whether the corresponding household is a detached house or an apartment.

Let us define the load profile of a household as the electricity consumption for each specific clock hour during an average working day. For instance, suppose that a household is observed for one month, then its load profile at 8 am is the hourly consumption occurred during 8:00 and 9:00 o'clock averaged over all working days (i.e. about 20 working days). It might be interesting to include the load profile into the set of feature variables since houses and apartments might have different patterns in terms of its load profile throughout the day. Figure 2 (right) gives the ranking by the random forest technique when we include the 24 load values at clock hour 00:00, 01:00, 02:00, ... 23:00, namely, "X0", ..., "X23", averaged over all working days during the month. It confirms that "25% quantile" and "dailyMinMean" are important variables, but also ranks the load values at 06:00 and 07:00 clock as highly relevant for classifying houses and apartments.

The horizontal axis in both parts of Figure 2 gives the "MeanDecreaseAccuracy" of each variable which is the percentage increase in the error of the forest if we remove that variable. This percentage increase in error is calculated as the average increase in the mean squared error of each classification tree grown in the forest. To select a subset of the feature variables, we decide on the thresh-

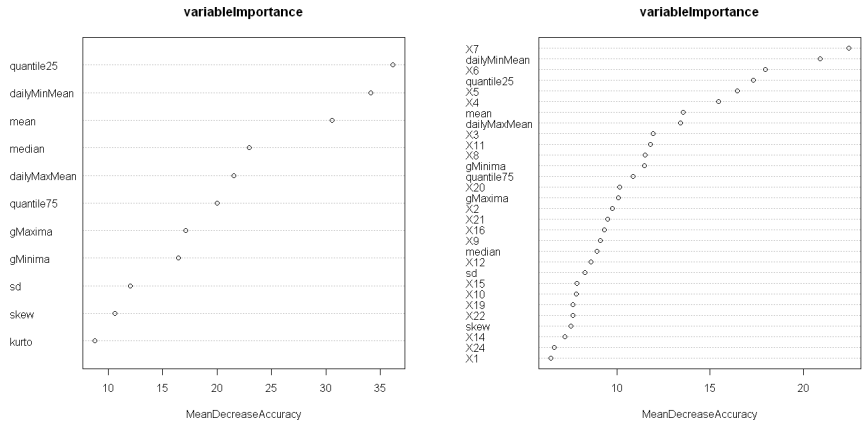

Fig. 2. Variable importance ranking on statistical feature variables (left) and on all feature variables (right)

old value of 10 for "MeanDecreaseAccuracy" in Figures 2 (right) which gives the following set of feature variables: "quantile25","dailyMinMean", "mean", "dailyMaxMean", "gMinima", "quantile75" , "gMaxima", and the load values Xi with $i = 3 - 8, 11, 20$. We will fit the data using a classification tree in the next section using both the whole set of 15 feature variables or some selected subsets of it.

4 A classification tree

We start with formulating the classification problem. Our training data consists $N = 350$ observations $(x_i, f(x_i)), i = 1, 2, \ldots, N$. Each observation contains $p = 15$ features variables as selected from the previous section, i.e. $x_i = (x_{i1}, x_{i2}, \ldots, x_{ip})$ and the target $f(x_i)$ which is the classification outcome k, $k = 1$, 2 (apartment or house).

A classification tree uses recursive binary splitting of feature variables $x = (x_1, x_2, \ldots, x_p)$ to partition the feature space into a set of regions, say M regions $R_1, R_2, \ldots, R_M$. The classification outcome for an observation in a specific region $R_m, m = 1, \ldots, M$ is modelled by the majority class in this region k_m, $k_m = 1$ or $= 2$, and hence

$$\hat{f}(x) = \sum_{m=1}^{M} k_m I(x \in R_m), \tag{1}$$

where I is the indicator function.

Some error minimization criterion, for instance minimizing the impurity measures the Gini index or the entropy, is adopted to decide on the splitting variables and splitting points and in general the shape of the tree. For a detailed discussion on the classification tree method we refer to Breiman *et al.*[2].

We use `rpart` package (Therneau and Atkinson [11]) in **R** to fit a classification tree to our training data. To make a graphical representation of the tree we use the `DMwR` package (Torgo [12]).

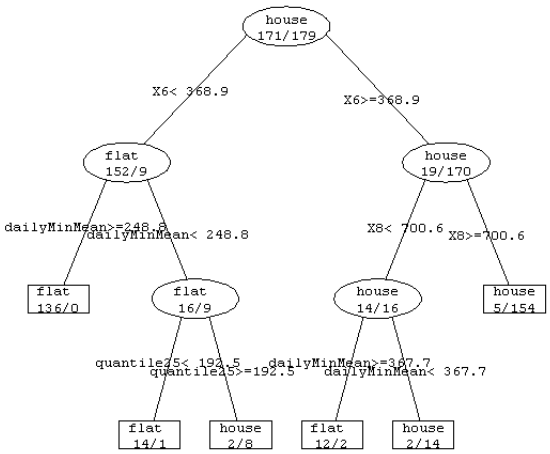

Fig. 3. The default classification tree (CP 0.01)

The tree in Figure 3 uses the whole set of the 15 feature variables. It partitions the feature space into six regions $R_i, i = 1, 2, \ldots$ corresponding to the six terminal nodes/leaves of the tree. For example region R_1 is determined if conditions $X6 < 368.9$ and "dailyMinMean" ≥ 248.8 are satisfied. There're 136 apartments (called flats in the tree) and 0 houses in this region hence $k_1 = 1$. Consider an observation $x_j \in R_1$, then by formula (1) the classification outcome $\hat{f}(x_j) = k_1 = 1$.

When we build a classification tree, we need to consider the trade-off between the benefit of an accurate prediction and the risk of an oversized and over-fitted tree. To reach the best balance between these two we can check the corresponding cost complexity parameter (cp) values and relative errors, i.e. to perform a so-called a *cost complexity pruning* (Breiman et. al.[2]) of the tree.

For each sub-tree of the default tree given in Figure 3, we have the following information on the corresponding cost complexity parameter (`CP`), number of splits (`Nsplit`), relative error (`Rel error`) on the training data itself, the ten-fold cross validation relative error (`Rel xerror`) and its standard deviation (`std`) with prefix "`x`" in `xerror` standing for "cross-validation", as presented in Table 1.

The most useful estimate on the predictive performance is `Rel xerror` which refers to the average relative error computed from ten-fold cross validation procedures. This validation procedure randomly partitions the data set into 10 subsets, use 9 of them as the training data to fit a classifier on, the remaining 1 subset is used for evaluating the classifier. Note that the relative

Table 1. Errors on the training set and 10-fold cross validation errors for sub-trees of the default tree (Root node error: 171/350 = 0.48857)

CP	Nsplit	Rel error	Rel xerror (std)	Abs error	Abs xerror (std)
1. 0.8363	0	1.0000	1.0000 (0.0547)	0.4886	0.4886 (0.0267)
2. 0.0292	1	0.1637	0.2047 (0.0328)	0.0800	0.1000 (0.0160)
3. 0.0175	3	0.1053	0.1754 (0.0306)	0.0514	0.0857 (0.0150)
4. 0.0100	5	0.0702	0.1637 (0.0297)	0.0343	0.0800 (0.0145)

error from a ten-fold cross validation procedure is a random variable with estimated mean `Rel xerror` and standard deviation `std` due to the randomness of this validation method.

It is worth mentioning that both `Rel error` and `Rel xerror` are errors relative to the root node error (0.48857). The root node error is simply the misclassification error if we use the majority class to predict all households before any splitting. Since we have 179 houses and 171 apartments in the data sets, by classifying all households as houses lead to a root node error of 171/350 = 0.48857. The corresponding absolute (misclassification) errors on the training data, denoted by `Abs error`, and the average absolute error for ten-fold cross validation method, denoted by `Abs xerror`, are smaller and equal to `Rel error` and `Rel xerror` multiplied with the root node error (0.48857) respectively. In Table 1 we also list `Abs error` and `Abs xerror` together with their standard deviations in order to be able to compare the results to those from the linear discriminant analysis conducted in the coming section.

The default tree in Figure 3 is tree number 4 with 5 tests and an average relative error of 0.16374 with standard deviation of 0.029681 using ten-fold cross validation. However the simpler tree number 3 has a value of 0.17544 which is within one standard deviation of `Rel xerror` for tree number 3, i.e. $0.17544 \in (0.16374 - 0.029681, 0.16374 + 0.029681)$. Using the so-called "1-SE" selection approach, we may choose tree number 3 as our classification model. We will call the sub-tree chosen in this way the "best tree" The corresponding absolute (misclassification) cross-validation error is 8.57%.

Experiments have been made by fitting a classification tree on various subsets of the predictors (hereafter phrases "feature variable" and "predictors" are used interchangeably), all 15 feature variables selected by *Random Forest* excluding load values (hereafter shortened to "all variables") or all load values selected by *Random Forest* (hereafter shortened to "all load values"), all variables + load values or a selection of only a few variables. The resulting absolute misclassification errors on the training set, for the best tree and from a 10-fold cross validation procedure can be found in Table 2.

Note that **(i)** the first row for "all variables + all load values" refers to best tree given in Table 1; **(ii)** the best tree for "all load values" can have `nsplit` of 3 at another experiment since it is chosen using the "1-SE" rule of the random variable `xerror` which is the cross-validation error; **(iii)** Other

Table 2. Error of the best tree on training set and 10-fold cross validation error for different predictor variables

Predictors	**Nsplit**	**Abs error**	**Abs xerror (std)**
all variables + all load values	3	0.0514	0.0857 (0.0150)
all variables	3	0.0629	0.0914 (0.0154)
all load values	1	0.0800	0.1029 (0.0162)
dailyMinMean + 25% quantile	5	0.0429	0.0771 (0.0143)
load values X6 +dailyMinMean	5	0.0371	0.0629 (0.0130)
load values X7 +dailyMinMean	3	0.0600	0.0800 (0.0145)

pairs of predictor have also been tested other than those given in Table 2, with no results better than 8.00% `Abs xerror`.

From Table 2, one can see that using a classification tree is very suitable for this problem since the cross validation errors `Abs xerror` are moderately low. The best performed tree, however, is obtained by using a pair of predictors namely "dailyMinMean" combined with "25% quantile" (`Abs xerror` of 7.71 %) or one of the morning load values for 6am (`Abs xerror` of 6.29 %) or 7am (`Abs xerror` of 8.00 %). These quantities are very easy to obtain given a time series of the energy consumption data. We note that the high ranking load values given by *Random Forest* as in Figure 2 and the 25% quantile all have a very high correlation with each other. For example 25% quantile and load value X7 have a correlation of 0.89. This explains why either the morning load values or "25% quantile" can be combined with "dailyMinMean" for a good result.

For illustration, two scatter plots of some of these "best predictors" are given below in Figure 4, with houses plotted in red plus signs and apartments in green circles.

5 Linear discriminant analysis

Looking at the scatter plots in Figure 4 we can clearly make out the two classes (houses and apartments). As an alternative to the tree classification method we also classify the data using linear discriminant analysis as described in Johnson and Wichern [5]. The analysis will be done using the original 11 feature variables and 24 load variables as well as a subset of the 15 "best" variables as indicated by the *Random Forest* ranking.

The same $N = 350$ observations $x_1, x_2, \ldots, x_N$ where each observation contains a number of variables $x_i = (x_{i1}, x_{i2}, \ldots, x_{ip})$ with p varying between 2 and 35 depending on choice of variables used. The goal is to classify each observation as either an apartment or a house.

First a multivariate Gaussian distribution is fitted to each class $k, k = 1, 2$ (apartment and house respectively) with mean μ_k, the mean is estimated from

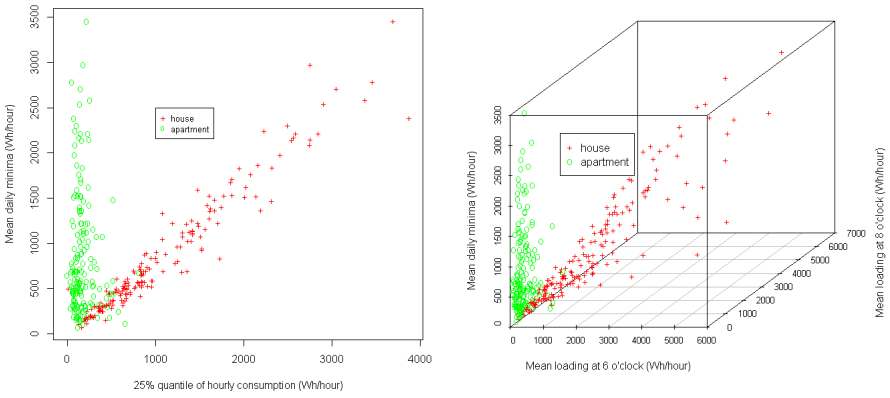

Fig. 4. A scatter plot (left) and a 3D scatter plot on selected variables (right)

the N observations using the sample mean:

$$\hat{\mu}_k = \frac{\sum_{n=1}^{N} M_{nk} x_n}{\sum_{n=1}^{N} M_{nk}},$$

where $M_{nk} = 1$, if obeservation n belongs to class k and $M_{nk} = 0$ otherwise.

Both classes are assumed to have the same covariance matrix which is estimated using the sample covariance where we first subtract corresponding sample mean from the observations of each class. The elements q_{nm} of the sample covariance matrix Q can be written as:

$$q_{nm} = \frac{1}{N-1} \sum_{i=1}^{N} (x_{in} - \hat{\mu}_{in})(x_{im} - \hat{\mu}_{im})$$

where $\hat{\mu}_{in} = \sum_{k=1}^{K} M_{ik} (\hat{\mu}_k)_n$, is the sample mean of variable n for the class of which observation i belongs, K is the number of classes ($K = 2$ in this case). To classify an observation we start by calculating the posterior probability that the observation belongs to every class and find the class it is most likely to come from. With 2 classes, using equal misclassification cost and prior probability (we have approximately the same number of houses as apartments in our data) we can classify an observation x_i by calculating:

$$\hat{y}_i = (\hat{\mu}_1 - \hat{\mu}_2) Q^{-1} x_i$$

$$\hat{m} = \frac{1}{2} (\hat{\mu}_1 - \hat{\mu}_2) Q^{-1} (\hat{\mu}_1 + \hat{\mu}_2).$$

If $\hat{y}_i > \hat{m}$ we assign x_i to class 1 (apartment) and if not we assign it to class 2 (house). $\hat{m}$ can be seen as the "midpoint" between the two classes where we simply check on which side an observation lies. This is also equal to

Fisher's discriminant function since we have equal misclassification and prior probabilities (Johnson and Wichern [5]).

To do the classification we use the "ClassificationDiscriminant" object and the related functions in MATLAB (Statistics Toolbox). We perform linear discriminant analysis for multiple sets of predictors: all original feature variables, all load values, all original feature variables and all load values or a selection of only a few variables. The resulting absolute misclassification errors on the training set and from a 10-fold cross validation procedure can be found in Table 3. The other pairs among those ranking high as indicated by the *Random*

Table 3. Error on training set and 10-fold cross validation error for different predictor variables

predictors	Abs error	Abs xerror (xstd)
all original variables + all load values	0.0971	0.1057 (0.0487)
all original variables	0.0857	0.0886 (0.0494)
all load values	0.1400	0.1600 (0.0715)
dailyMinMean + 25% quantile	0.0600	0.0686 (0.0335)
load values X6 +dailyMinMean	0.0800	0.0800 (0.0295)
load values X7 +dailyMinMean	0.1057	0.1057 (0.0674)

Forest feature selection have also been tried, as well as some combinations of $3-4$ variables in the cases where the first two gave a reasonable result. In most cases this gave an absolute cross-validation error around $0.08-0.1$ when dailyMinMean is used and around $0.12-0.16$ if not. It is worth repeating that the highly ranked load values suggested by *Random Forest* and the 25% quantile are all highly correlated with each other. In our experiments the "dailyMinMean" together with "25% quantile" give the best result, replacing "25% quantile" with one of the load values gave worse result even though they have a higher ranking from the *Random Forest*. Using the "dailyMinMean" together with "25% quantile" we obtain a very low error rate as seen in Table 3, both in terms of absolute error on the training data set as well as the absolute error from a 10-fold cross-validation procedure. A scatter plot of these two variables as well as the line separating the two classes made from our analysis can be seen in Fig. 5.

6 Conclusion and future work

We have observed different patterns in terms of energy consumption for different building types as house and apartments on a data set of energy consumption values for 350 Swedish households. Motivated by this observation, we have conducted a classification and discrimination task using techniques as random forest, classification tree and linear discriminant analysis method. We note that statistics like the mean of daily minimum (hourly) consumption values (shortened as "dailyMinMean") along with "25% quantile" or the morning

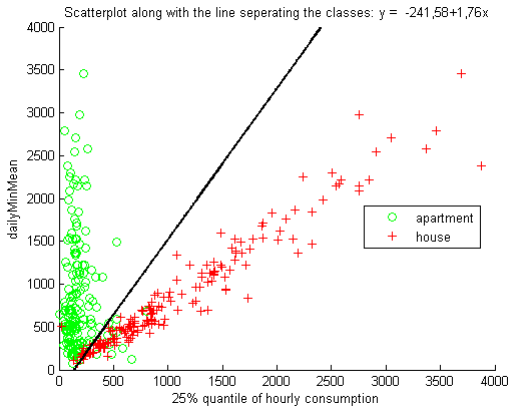

Fig. 5. A scatter plot of dailyMinMean and 25% quantile and a plot of the classification boundary. $y = -241.58 + 17.6x$

load values worked well as predictors when trying to discriminate between the two classes (house or apartment). This result is further confirmed by the fitted classification models, namely the classification tree and linear discriminant analysis method. In addition, load profile at certain morning clock hours can also be useful in the classifying task, given the fact that they are highly correlated to the feature variable "25% quantile". These quantities can be easily obtained given a time series of energy consumption data with unknown building type.

We have found that the classification tree method is a plausible classifier for our case. In particular, the best trees built using pairs of "X6"+ "dailyMinMean" and "25% quantile" + "dailyMinMean" have cross-validation (absolute) errors of 6.29% and 7.71% respectively, as shown in Table 2.

The linear discriminant analysis has also shown to give good results on our data set. When the best predictors such as "25% quantile" and "dailyMinMean" are used for the linear discriminant analysis, we obtain only 6.29% 10-fold cross validation (absolute) error.

The classification has been done with hourly energy consumption values aggregated from the original data of consumption values for each ten-minute interval. A natural question arises as to whether the high-frequency ten-minute data provides more information in the classification task or a customer clustering task than the lower-frequency data like one-hour data. We have addressed these questions in the follow-up work by Ni *et al.*[8].

7 Acknowledgements

The authors are very grateful to the Swedish Energy Agency for the financial support under research grant 33707-1. Special thanks also go to the article's anonymous reviewer, who provided thorough and in-depth feedback that improved this article in a substantial way. Appreciations also go to professor

Sergei Silvestrov who has been very helpful in facilitating the research project and company Revolution Analytics for providing the useful software Revolution R Enterprise 6.0 for academic users.

References

1. Breiman, L., Random forests. *Machine Learning*, 45,**1**, 5–32, 2001.
2. Breiman, L., Friedman, J. Olshen, R., and Stone, C.,*Classification and regression trees*. Statistics/Probability Series. Wadsworth & Brooks/Cole Advanced Books & Software, 1984.
3. Chicco, G. Overview and performance assessment of the clustering methods for electrical load pattern grouping. *Energy*, Vol. 42, **1**, pp. 68–80, 2012.
4. Chicco, G., Napoli, R., Piglione, F. Application of clustering algorithms and self organising maps to classify electricity customers. *Proc. of IEEE Power Tech Conference*, Bologna, 23–26 June, 2003.
5. Johnson, R. A. and Wichern, D. W. *Applied multivariate statistical analysis,* 5^{th}ed. Prentice Hall, 2002.
6. Jota, P.R.S., Silva, V.R.B., Jota, F.G. Building load management using cluster and statistical analyses. *International Journal of Electrical Power and Energy Systems*, Vol. 33, **8**, pp. 1498–1505, 2011.
7. López, J.J., Aguado, José A, Martín, F., Muñoz, F., Rodríguez, A., Ruiz, José E. Hopfield-K-Means clustering algorithm: A proposal for the segmentation of electricity customers. *Electric Power Systems Research*, Vol. 81, pp. 716–724, 2011.
8. Ni, Y., Engstrm, C., Malyarenko, A. and Wallin, F. Investigating the added values of high frequency energy consumption data using data mining techniques. *AIP Conference Proceedings 1637 (2014)*, Vol. 1637, S. Sivasundaram(ed.), AIP Publishing, pp. 734–743, 2014.
9. Rodrigues,F., Duarte, J.,Figueiredo, V., Vale, Z.and Cordeiro, M., A comparative Analysis of Clustering Algorithms Applied to Load Profiling, *Machine Learning and Data Mining in Pattern Recognition,* ser. Lecture Notes in Computer Science, P. Perner and A. Rosenfeld(Eds), Springer Berlin Heidelberg, vol. 2734, pp. 73–85, 2003.
10. Swedish Energy Agency, http://www.energimyndigheten.se/Statistik/FESTIS/ (Accessed 2014-03-20).
11. Therneau, T. M. and Atkinson, B. R port by Brian Ripley. *rpart: Recursive Partitioning*. R package version 3.1-46, 2010.
12. Torgo, L., *Data Mining with R, learning with case studies*, Chapman and Hall/CRC. URL: http://www.dcc.fc.up.pt/ ltorgo/DataMiningWithR, 2010.
13. Zhou, KL., Yang, SL., Shen, C. A review of electric load classification in smart grid environment. *Renewable and Sustainable Energy Reviews*, Vol. 24, pp. 103–110, 2013.
14. Zimmerman, J.P. End-use metering campaign in 400 households in Sweden. September 2009, http://www.energimyndigheten.se/Global/Statistik/F%C3%B6rb%C3%A4ttrad%20energistatistik/Festis/Final_report.pdf (Accessed 2014-03-20)

Vandermonde matrices, extreme points and orthogonal polynomials

J. Österberg[1], K. Lundengård[1], and S. Silvestrov[1]

Division of Applied Mathematics, School of Education, Culture and Communication, Mälardalen University, Box 883, SE-721 23 Västerås, Sweden (e-mail: jonas.osterberg@mdh.se, karl.lundengard@mdh.se, sergei.silvestrov@mdh.se)

Abstract. Vandermonde matrices and their determinant appear in many different problems, including interpolation of data, moment matching in stochastic processes with applications to computer-aided decision support and in various types of numerical analysis. Motivated by these and other applications the values of the determinant of Vandermonde matrices are analyzed both visually and analytically over the unit sphere in various dimensions and under various norms. The extreme points of the determinant over these surfaces are related to polynomials and classical orthogonal polynomials in particular. Some of the polynomials are identified and recursive definitions are provided.
Keywords: Vandermonde matrix, Determinant, Extreme points, Orthogonal polynomials, Moment matching.

1 The Vandermonde matrix

A rectangular Vandermonde matrix of size $m \times n$ is determined by n values $\boldsymbol{x}_n = (x_1, \cdots, x_n)$ and is defined by

$$V_{mn}(\boldsymbol{x}_n) = \left[x_j^{i-1}\right]_{mn} = \begin{bmatrix} 1 & 1 & \cdots & 1 \\ x_1 & x_2 & \cdots & x_n \\ \vdots & \vdots & \ddots & \vdots \\ x_1^{m-1} & x_2^{m-1} & \cdots & x_n^{m-1} \end{bmatrix}. \tag{1}$$

Note that some authors use the transpose of this as the definition and possibly also let indices run from 0. All entries in the first row of Vandermonde matrices are ones and by considering $0^0 = 1$ this is true even when some x_j is zero. We have the following well known theorem.

Theorem 1. *The determinant of (square) Vandermonde matrices has the well known form*

$$\det V_n(\boldsymbol{x}_n) \equiv v_n(\boldsymbol{x}_n) = \prod_{1 \le i < j \le n} (x_j - x_i). \tag{2}$$

New Trends in Stochastic Modeling and Data Analysis (pp. 299-308)
Raimondo Manca - Sally McClean - Christos H Skiadas (Eds)

This determinant is also simply referred to as the *Vandermonde determinant*.

Perhaps the most well known application of Vandermonde matrices is polynomial interpolation. Given a set of points $(x_i, y_i) \in \mathbb{C}^2$, $1 \leq i \leq n$, define the two row vectors $\boldsymbol{x}_n = (x_1, \cdots, x_n)$ and $\boldsymbol{y}_n = (y_1, \cdots, y_n)$ and let all x_i be pairwise distinct. Then the polynomial of minimal degree that interpolates these points has coefficients $\boldsymbol{c}_n$ where $\boldsymbol{c}_n V_n(\boldsymbol{x}_n) = \boldsymbol{y}_n$, that is $\boldsymbol{c}_n = \boldsymbol{y}_n V_n(\boldsymbol{x}_n)^{-1}$. Note that since the x_i are pairwise distinct the determinant $v_n(\boldsymbol{x}_n)$ is nonzero by Theorem 1 and so the solution is unique. More information and an expansion on this can be found in El-Mikkawy[1] and references therein.

There are other applications as well, for instance in Lundengård *et al.*[4] we find an application of the Vandermonde matrix to moment matching of random variables with a discrete random variable. This has applications in pricing of Asian options and other areas.

In the article Klein and Spreij[3] we find an application of Vandermonde matrices to the important area of time-series analysis.

The work done here recaptures the work presented in Szegő[7]. A more explicit treatment is provided together with some slight generalization of the ideas.

2 Optimizing the determinant

Consider the unit $(n-1)$-sphere under the p-norm ($p \in \mathbb{Z},\ p \geq 1$), we define

$$\mathcal{S}_p^{n-1} = \{\boldsymbol{x}_n \in \mathbb{R}^n \ : \ |x_1|^p + \cdots + |x_n|^p = 1\}\,.$$

When $p = 2$ we have the Euclidean norm and thus the usual $(n-1)$-sphere, when $p = \infty$ we have the cube defined by the boundary of $[-1, 1]^n$. The 2-sphere for some different norms are depicted in Figure 1.

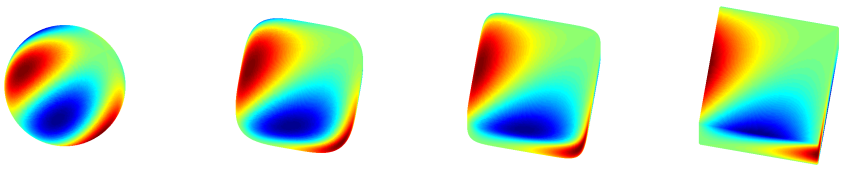

Fig. 1. Value of $v_3(\boldsymbol{x}_3)$ over: $\mathcal{S}_2^2$ (left), $\mathcal{S}_4^2$ (middle left), $\mathcal{S}_8^2$ (middle right) and $\mathcal{S}_\infty^2$ (right).

The four separate plots in Figure 1 are all rotated slightly by the same transformation for visual clarity and the mappings of color to value are slightly different between the figures. The positive maxima can be seen to lie in the dark red regions and the minima can be found in the dark blue regions. As we soon will see the extreme points on $\mathcal{S}_2^2$ are $(-1/\sqrt{2}, 0, 1/\sqrt{2})$ and the vectors constructed by permutating the coordinates of this vector, making a total of $6 = 3!$ extreme points. Similarily, for the cube we have the vectors formed by the six

permutations of the coordinates in $(-1, 0, 1)$. The two stated vectors are both maxima and are shown in the top left maxima in the figures, odd permutations of these vectors will give minima and even permutations will give again maxima. This follows directly from the anti-symmetry of the Vandermonde determinant, given a permutation $\sigma \in S_n$ we have $v_n(x_{\sigma_1}, \cdots, x_{\sigma_n}) = \operatorname{sgn}(\sigma) v_n(x_1, \cdots, x_n)$.

We are thus faced with the problem of maximizing $|v_n(\boldsymbol{x}_n)|$ over $\mathcal{S}_p^{n-1}$. By the symmetry of $|v_n|$ we do not loose any generality by assuming that the coordinates are ordered and pairwise distinct, $x_1 < \cdots < x_n$.

Theorem 2. *The coordinates $x_1 < \cdots < x_n$, $n \geq 2$, that maximize the absolute value of the Vandermonde determinant over the unit sphere in $\mathbb{R}^n$, under the p-norm, that is $\mathcal{S}_p^{n-1}$, are unique. Furthermore, the coordinates are symmetric so that $x_i = -x_{n-i+1}$ for $1 \leq i \leq n$ and the total number of maxima, counting permutations, are $n!$.*

This is an extension of a result presented by Szegő[7, p.140].

Proof. Suppose that we have two different sequences of coordinates $\boldsymbol{x}_n$ and $\boldsymbol{x}'_n$:

$$x_1 < \cdots < x_n,$$

$$x'_1 < \cdots < x'_n,$$

both maximizing $|v_n|$ on $\mathcal{S}_p^{n-1}$, so $|v_n(x_1, \cdots, x_n)| = |v_n(x'_1, \cdots, x'_n)| = v_n^{max}$ is the maximum value. Now define a new configuration $\boldsymbol{z}_n$ defined by,

$$z_i = \frac{x_i + x'_i}{2\sigma}, \quad 1 \leq i \leq n,$$

where $\sigma > 0$ is a normalization constant to assure that $\boldsymbol{z}_n$ lies on the sphere. It is easy to see that we have

$$z_1 < \cdots < z_n.$$

Note that $\sigma \leq 1$ by necessity since $\mathcal{S}_p^{n-1}$ is the boundary of a convex set. This follows directly from the absolute homogeneity and the triangle inequality associated with the p-norm:

$$\left\| \frac{\boldsymbol{x}_n + \boldsymbol{x}'_n}{2} \right\|_p \leq \left\| \frac{\boldsymbol{x}_n}{2} \right\|_p + \left\| \frac{\boldsymbol{x}'_n}{2} \right\|_p = 1.$$

We have established that $\boldsymbol{z}_n$ lies on $\mathcal{S}_p^{n-1}$. For each $1 \leq i < j \leq n$ we now have

$$\begin{aligned} |z_j - z_i| &= \frac{\left|x_j + x'_j - x_i - x'_i\right|}{2\sigma} = \frac{|x_j - x_i| + \left|x'_j - x'_i\right|}{2\sigma} \\ &\geq |x_j - x_i|^{\frac{1}{2}} \left|x'_j - x'_i\right|^{\frac{1}{2}}, \end{aligned}$$

where the last step follows from $\sigma < 1$ and the general relation

$$\left(\frac{a+b}{2}\right)^2 = \left(\frac{a-b}{2}\right)^2 + ab \geq ab.$$

It follows that

$$|v_n(\boldsymbol{z}_n)| \geq |v_n(\boldsymbol{x}_n)|^{\frac{1}{2}} \, |v_n(\boldsymbol{x}'_n)|^{\frac{1}{2}} = v_n^{max},$$

and to not have a contradiction, we must have that the equality holds, that is $\boldsymbol{x}_n = \boldsymbol{x}'_n$, and so the maximum is unique.

Now, consider

$$v_n(-\boldsymbol{x}_n) = (-1)^{\frac{n(n-1)}{2}} v_n(\boldsymbol{x}_n),$$

which follows easily from the degree of the expansion of v_n, where every term is of degree $\frac{n(n-1)}{2}$. If follows that if $\boldsymbol{x}_n$ is a maximum of $|v_n|$ on the sphere then $-\boldsymbol{x}_n$ is also a maximum. Now, since the maximum with ordered coordinates $x_1 < \cdots < x_n$ is unique we must have that $-x_n = x_1, \cdots, -x_1 = x_n$, that is $x_i = -x_{n-i+1}$ for $1 \leq i \leq n$ and so the maxima are symmetric.

From $x_i = -x_{n-i+1}$ and the pairwise distinctness of the coordinates (the determinant is non-zero at the maximum) we have that the $n!$ permutations $(x_{\sigma_1}, \cdots, x_{\sigma_n})$ are the distinct maxima. □

Remark 1. The condition $x_i = -x_{n-i+1}$ for the ordered maximum $x_1 < \cdots < x_n$ implies that the maxima all lie in the hyperplane $x_1 + \cdots + x_n = 0$. These facts can be used to visualize v_n on $\mathcal{S}_p^{n-1}$ for $n = 4, 5, 6, 7$, while we for $n \geq 8$ have more than three degrees of freedom.

As an interesting example we provide a plot of v_4 over all points on the Euclidean hypersphere that is constructed by selecting an orthonormal basis in $\mathbb{R}^4$ that is in turn orthogonal to $(1, 1, 1, 1)$. We do not miss any extrema by doing this since all extrema, considered as points in $\mathbb{R}^4$, must be orthogonal to this vector. We provide both a 3D plot and a plot in spherical coordinates by the following transformations.

$$\boldsymbol{x}_4 = \begin{bmatrix} -1 & -1 & 0 \\ -1 & 1 & 0 \\ 1 & 0 & -1 \\ 1 & 0 & 1 \end{bmatrix} \begin{bmatrix} 1/\sqrt{4} & 0 & 0 \\ 0 & 1/\sqrt{2} & 0 \\ 0 & 0 & 1/\sqrt{2} \end{bmatrix} \boldsymbol{t}. \tag{3}$$

$$\boldsymbol{t}(\theta, \phi) = \begin{bmatrix} \cos(\phi)\sin(\theta) \\ \sin(\phi) \\ \cos(\phi)\cos(\theta) \end{bmatrix}. \tag{4}$$

In Figure 2 the placement of the $4! = 24$ extreme points of v_n over $\mathcal{S}_2^3$ can be seen.

Motivated by the fact that there is only one set of coordinates and that the maxima are constructed from different orderings of these, it makes sense to instead consider the polynomial constructed from these coordinates. Our task now is to find the polynomials that define the optimizing coordinates for different $n \geq 2$ and $p \geq 1$,

$$P_p^n(x) = \prod_{i=1}^{n} (x - x_i),$$

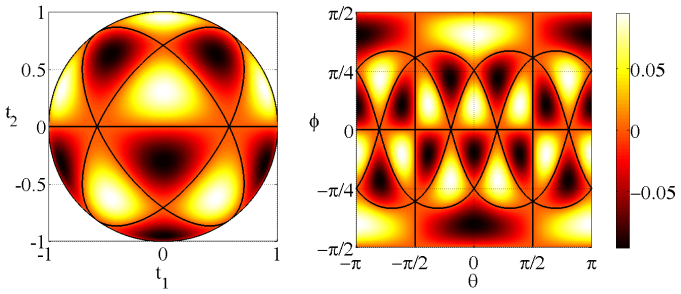

Fig. 2. The values of the Vandermonde determinant over $\mathcal{S}_2^3$.

where x_i are the distinct maximizing coordinates that depend on n and p. We have

$$\begin{aligned} P_p^{n\prime}(x_k) &= \sum_{j=1}^{n} \prod_{\substack{i=1 \\ i\neq j}}^{n} (x - x_i)\Big|_{x=x_k} = \prod_{\substack{i=1 \\ i\neq k}}^{n} (x_k - x_i), \\ P_p^{n\prime\prime}(x_k) &= \sum_{l=1}^{n} \sum_{\substack{j=1 \\ j\neq l}}^{n} \prod_{\substack{i=1 \\ i\neq j \\ i\neq l}}^{n} (x - x_i)\Big|_{x=x_k} = \sum_{\substack{j=1 \\ j\neq k}}^{n} \prod_{\substack{i=1 \\ i\neq j \\ i\neq k}}^{n} (x_k - x_i) + \sum_{\substack{l=1 \\ l\neq k}}^{n} \prod_{\substack{i=1 \\ i\neq l \\ i\neq k}}^{n} (x_k - x_i) \\ &= 2 \sum_{\substack{j=1 \\ j\neq k}}^{n} \prod_{\substack{i=1 \\ i\neq j \\ i\neq k}}^{n} (x_k - x_i), \end{aligned}$$

and it is easy to show that

$$\frac{P_p^{n\prime\prime}(x_k)}{P_p^{n\prime}(x_k)} = 2 \sum_{\substack{i=1 \\ i\neq k}}^{n} \frac{1}{x_k - x_i}. \tag{5}$$

Define

$$s_p^n(\boldsymbol{x}_n) = \left(\sum_{i=1}^{n} |x_i|^p \right) - 1,$$

so that s_p^n vanishes exactly on the unit sphere under the p-norm, that is $\mathcal{S}_p^{n-1} = \left\{ \boldsymbol{x}_n \in \mathbb{R}^n \ : \ s_p^n(\boldsymbol{x}_n) = 0 \right\}$. We have the partial derivatives

$$\frac{\partial s_p^n(\boldsymbol{x}_n)}{\partial x_k} = p\, |x_k|^{p-1} \operatorname{sgn}(x_k).$$

To maximize $|v_n(\boldsymbol{x}_n)|$ over the surface $s_p^n(\boldsymbol{x}_n) = 0$ we transform the objective function by applying a (strictly increasing) logarithm:

$$w_n(\boldsymbol{x}_n) = \log(|v_n(\boldsymbol{x}_n)|) = \sum_{1 \le i \le j} \log(|x_j - x_i|),$$

with partial derivatives

$$\frac{\partial w_n(\boldsymbol{x}_n)}{\partial x_k} = \sum_{\substack{i=1 \\ i\neq k}}^{n} \frac{1}{x_k - x_i} = \frac{1}{2}\frac{P_p^{n\prime\prime}(x_k)}{P_p^{n\prime}(x_k)}.$$

By the method of Lagrange multipliers we now have that the maxima of $|v_n(\boldsymbol{x}_n)|$ on $\mathcal{S}_p^{n-1}$ must be stationary points to the Lagrangian

$$\Lambda(\boldsymbol{x}_n, \lambda) = w_n(\boldsymbol{x}_n) - \lambda s_p^n(\boldsymbol{x}_n), \tag{6}$$

which explicitly means

$$\frac{\partial w_n(\boldsymbol{x}_n)}{\partial x_k} = \lambda \frac{\partial s_p^n(\boldsymbol{x}_n)}{\partial x_k},$$

for some multiplier $\lambda \in \mathbb{R}$. We then get

$$\frac{1}{2}\frac{P_p^{n\prime\prime}(x_k)}{P_p^{n\prime}(x_k)} = \lambda p\,|x_k|^{p-1}\operatorname{sgn}(x_k).$$

Letting $\rho = -2\lambda p$ we then get

$$P_p^{n\prime\prime}(x_k) + \rho\,|x_k|^{p-1}\operatorname{sgn}(x_k)P_p^{n\prime}(x_k) = 0. \tag{7}$$

This leads us to our first set of polynomials defining the solution to our maximization problem.

Theorem 3. *The polynomial P_2^n, of degree $n > 2$ and with a leading coefficient of 1, whose roots form the coordinates in the points $\boldsymbol{x}_n \in \mathbb{R}^n$ that maximize $|v_n(\boldsymbol{x}_n)|$ over the Euclidean hypersphere $\mathcal{S}^{n-1}$ satisfy the differential equation*

$$P_2^{n\prime\prime}(x) + n(1-n)xP_2^{n\prime}(x) + n^2(n-1)P_2^n(x) = 0. \tag{8}$$

Furthermore, the coefficients for the three terms of highest degree are

$$c_n = 1, c_{n-1} = 0, c_{n-2} = -\frac{1}{2}, \tag{9}$$

and the subsequent coefficients are defined recursively by

$$c_k = -\frac{(k+1)(k+2)}{n(n-1)(n-k)}c_{k+2}. \tag{10}$$

Proof. By Equation (7) we have

$$P_2^{n\prime\prime}(x) + \rho x P_2^{n\prime}(x)\Big|_{x=x_k} = 0, \quad 1 \leq k \leq n.$$

The left part of this equation represents n evaluations of a polynomial of degree n that vanishes on $x_1, \cdots, x_n$ and must thus be a constant multiple of P_2^n, that we defined as the polynomial that vanishes on $x_1, \cdots, x_n$, and so

$$P_2^{n\prime\prime}(x) + \rho x P_2^{n\prime}(x) + \sigma P_2^n(x) = 0.$$

Two find the coefficients σ and ρ we need to adapt this polynomial to the sphere. We require $\sum_{i=1}^{n} x_i^2 = 1$ and by the symmetry from Remark 1 we have $\sum_{i=1}^{n} x_i = 0$. The condition $c_n = 1$ is by choice. The condition $c_{n-1} = 0$ follows from the expansion of the coefficients in P_2^n.

$$P_n^p(x) = \prod_{i=1}^{n}(x - x_i) = \sum_{k=0}^{n}(-1)^{n-k} e_{n-k}(x_1, \cdots, x_n) x^k,$$

where e_k is the elementary symmetric polynomial defined by

$$e_k(x_1, \cdots, x_n) = \sum_{i_1 < \cdots < i_k} x_{i_1} x_{i_2} \cdots x_{i_k}.$$

We have $c_{n-1} = -e_1(x_1, \cdots, x_n) = -(x_1 + \cdots + x_n) = 0$. The condition $c_{n-2} = -\frac{1}{2}$ places us on the unit sphere

$$e_1(x_1, \cdots, x_n)^2 - 2e_2(x_1, \cdots, x_n) = x_1^2 + \cdots + x_n^2 = 1,$$

$$-2e_2(x_1, \cdots, x_n) = 1,$$

$$c_{n-2} = e_2(x_1, \cdots, x_n) = -\frac{1}{2}.$$

This establishes Equation (9) in the theorem.

Now, the coefficients $c_n, \cdots, c_0$ for any polynomial solution $p(x)$ of degree n to a differential equation on the form

$$p^{n\prime\prime}(x) + \rho x p^{n\prime}(x) + \sigma p^n(x) = 0,$$

must satisfy

$$\begin{aligned} \rho n c_n + \sigma c_n &= 0 \\ \rho(n-1)c_{n-1} + \sigma c_{n-1} &= 0 \\ n(n-1)c_n + \rho(n-2)c_{n-2} + \sigma c_{n-2} &= 0. \end{aligned}$$

The second of these equations is trivial since $c_{n-1} = 0$. The first and third equation simplifies to

$$\begin{aligned} \rho n + \sigma &= 0, \\ n(n-1) - \frac{1}{2}\rho(n-2) - \frac{1}{2}\sigma &= 0, \end{aligned}$$

and so

$$\begin{aligned} \rho &= \frac{-2n(n-1)}{n-(n-2)} = -n(n-1) \\ \sigma &= n^2(n-1), \end{aligned}$$

which establishes Equation (8) in the theorem.

For the recursive formula for the coefficients $c_{n-3}, \cdots, c_0$, Equation (10), we again look at the slightly more general case and retain ρ, σ. The coefficients for the polynomial p satisfying

$$p^{n\prime\prime}(x) + \rho x p^{n\prime}(x) + \sigma p^n(x) = 0,$$

must satisfy

$$c_{k+2}(k+1)(k+2) + \rho k c_k + \sigma c_k = 0,$$

that is

$$c_k = \frac{-(k+1)(k+2)}{\rho k + \sigma} c_{k+2}.$$

For P_2^n we then have

$$c_k = \frac{-(k+1)(k+2)}{-n(n-1)k + n^2(n-1)} c_{k+2}, \tag{11}$$

and Equation (10) follows. □

The case $p = \infty$ follows in a similar manner.

Theorem 4. *The polynomial P_∞^n, of degree $n > 2$ and with a leading coefficient of 1, whose roots form the coordinates in the points $\boldsymbol{x}_n \in \mathbb{R}^n$ that maximize $|v_n(\boldsymbol{x}_n)|$ over the cube $\mathcal{S}_\infty^{n-1}$ satisfy*

$$P_\infty^n(x) = (x-1)(x+1)p_\infty^n(x). \tag{12}$$

where p_∞^n is defined by the differential equation:

$$(1-x^2)p_\infty^{n\,\prime\prime}(x) - 4x p_\infty^{n\,\prime}(x) + m(m+3)p_\infty^n(x) = 0,$$

where $m = n-2$ is the degree of the polynomial p_∞^n. Furthermore, the first two coefficients for p_∞^n are $c_m = 1, c_{m-1} = 0$ and the subsequent coefficients satisfy

$$c_k = \frac{(k+1)(k+2)}{k(k+3) - m(m+3)} c_{k+2}. \tag{13}$$

Proof. It is easy to show that the coordinates -1 and $+1$ must be present in the maxima points, if they were not then we could rescale the point so that the value of $|v_n(\boldsymbol{x}_n)|$ is increased, which is not allowed. We may thus assume the ordered sequence of coordinates

$$-1 = x_1 < \cdots < x_n = +1.$$

The absolute value of the Vandermonde determinant then becomes

$$|v_n(\boldsymbol{x}_n)| = 2 \prod_{i=2}^{n-1} \left(|1+x_i|\,|1-x_i|\right) \prod_{1<i<j<n} |x_j - x_i|\,.$$

We now take the logarithm of this, differentiate and equate the partial derivatives to zero to find the stationary points (actually maxima), and arrive at

$$\frac{1}{x_k+1}+\frac{1}{x_k-1}+\sum_{\substack{i=2\\ i\neq k}}^{n-1}\frac{1}{x_k-x_i}=0, \quad 1<k<n,$$

which by the essence of Equation (5) can be written

$$\frac{1}{x_k+1}+\frac{1}{x_k-1}+\frac{1}{2}\frac{{p_\infty^n}''(x_k)}{{p_\infty^n}'(x_k)}=0, \quad 1<k<n, \tag{14}$$

for some polynomial p_∞^n constructed from the roots $x_2,\cdots,x_{n-1}$.

The left part of Equation (14) now identifies a differential expression on p_∞^n which we by the same method as for $p=2$ identify by a multiple of p_∞^n, that is

$$(1-x^2){p_\infty^n}''(x)-4x{p_\infty^n}'(x)+\sigma p_\infty^n(x)=0. \tag{15}$$

The constant σ is found by considering the coefficient for x^m:

$$-m(m-1)-4m+\sigma=0 \quad \Leftrightarrow \quad \sigma=m(m+3).$$

Finally

$$(1-x^2){p_\infty^n}''(x)-4x{p_\infty^n}'(x)+m(m+3)p_\infty^n(x)=0.$$

The polynomial that provide all coordinates for the maxima is then

$$P_\infty^n(x)=(x-1)(x+1)p_\infty^n. \tag{16}$$

Equation (13) follows by the same methods as for $p=2$, that is, by identifying all coefficients in the differential equation to be identically zero. □

We have provided the means to describe the coordinates of the extreme points of the Vandermonde determinant over the unit spheres under the Euclidean norm and under the infinity norm. The resulting polynomials can be identified by rescaled Hermite polynomials, $H_n(x\sqrt{n(n-1)/2})$, and Gegenbauer polynomials, $C_n^{(3/2)}(x)$, respectively. For norms other than $p=2$ and $p=\infty$ further analysis is warranted.

Acknowledgements This research was supported in part by the Swedish Research Council (621-2007-6338), Swedish Foundation for International Cooperation in Research and Higher Education (STINT), Royal Swedish Academy of Sciences, Royal Physiographic Society in Lund and Crafoord Foundation.

References

1. El-Mikkawy, M., "Vandermonde interpolation using special associated matrices", *Applied Mathematics and Computation* 141:589–595 (2003).
2. Goldwurm, M. and Lonati, V., "Pattern statistics and Vandermonde matrices", *Theoretical Computer Science* 356:153–169 (2006).

3. Klein, A. and Spreij, P., "Some results on Vandermonde matrices with an application to time series analysis", *Siam J. Matrix Anal. Appl.* 25:213–223 (2003).
4. Lundengård, K., Ogutu, C., Silvestrov, S. and Weke, P., "Asian Options, Jump-Diffusion Processes on a Lattice, and Vandermonde Matrices", *Modern Problems in Insurance Mathematics, Silvestrov, Dmitrii, Martin-Löf, Anders, Eds.* Springer-Verlag, Berlin, 337–364 (2014).
5. Lundengård, K., Österberg, J., Silvestrov, S., "Extreme points of the Vandermonde determinant on the sphere and some limits involving the generalized Vandermonde determinant", arXiv:1312.6193 (2013).
6. Serre, D., *Matrices: Theory and Applications*, Springer (2002).
7. Szegő, G., *Orthogonal polynomials*, American mathematics society (1939).

7 CHAPTER

Demography and Related Applications

Demographic and Health Indicators in the Pomaks of Rhodopi, Greece

Konstantinos N. Zafeiris[1], Christos H. Skiadas[2]
[1]Laboratory of Anthropology, Department of History and Ethnology, Democritus University of Thrace, Greece (E-mail: kzafiris@he.duth.gr)
[2]ManLab, Department of Production Engineering and Management, Technical University of Crete, Chania, Greece (E-mail: skiadas@cmsim.net)

Abstract: Based on the Health State Theory several demographic and health state indicators were calculated for the Pomaks of Organi and Kehros, a Slavic speaking population from Mountainous Rhodopi (Greece). Results indicate a rapid health transition and a general improvement of the health status of the population. Gradually, by the 1990s Pomaks converge to the total population of Thrace.
Keywords: Pomaks, Thrace, Health State Indicators

1 Introduction

Life table analysis has for long been (Graunt [3], Halley [4]) used to estimate probabilities of survival and life expectancy in different ages during the course of human life. However, if applied in its classical form - as a technique aimed to describe the patterns of mortality and survival - it fails to give an overall picture of the total health status of a population and its changes with age and time, especially, if health is positively defined not simply as the absence of a disease or infirmity but in a broader way as *"a state of complete physical, mental and social well being"* (WHO [20]). Several solutions have been given to this problem.

In order to mathematically describe the state of health of a population, Chiang [1] introduced the term *"Index of health H_x",* based on the probability distribution of the number and the duration of illness and the time lost due to death (time of death) calculated from data from the Canadian Sickness Survey, 1950-1951. Sanders [8] used life table techniques to construct tables of *"effective life years"*, as a measure of the current health of the population based on mortality and morbidity rates. In that case, morbidity was measured by the functional adequacy of an individual to fulfill the role which a healthy member of his age and sex is expected to fulfill in his society. Sullivan [9] criticized these approaches on grounds of the methodology used and its effectiveness in measuring the health status of a population and later [10] he used life table techniques to calculate two related indices: the expectation of life free of

New Trends in Stochastic Modeling and Data Analysis (*pp.* 311-324)
Raimondo Manca – Sally McClean – Christos H Skiadas (Eds)

disability and the expectation of disability, based on published data of the current abridge life tables and surveys conducted by the National Center for Health Statistics. Torrance [19] developed a health status index model for the determination of the amount of health improvement created by a health care program, calculating a point-in-time health index (H_t), a period-of-time health index ($H_{t1,t2}$) and a health life expectancy index (E_x). The first measures the instantaneous health of all individuals in the population at a single point in time and averages these to give a group's index. The second is similar but it refers to a period of time, i.e. a year. The third is calculated by a method that uses the actual mortality and morbidity experience of the population to determine a table of age and sex specific health expectancy figures.

Jansen and Skiadas [5] introduced the general theory of dynamic models for modeling human life using life table data from France and Belgium; this was the first effort to exclusively use published death and population statistics in order for the health status of the population to be evaluated. In their model, the main assumption regarding the state of human health is that it follows a stochastic process expressed by a variable named $S_{(t)}$ and that the end of life time is reached when this stochastic variable arrives at a minimum level of health state. However an important hypothesis was set: despite the fact that the health state of an individual is unpredictable the mortality curve of human populations can be modeled and because of that the health state form derived from these data can be modeled too (see Skiadas and Skiadas [17]. Then the Health State Function (H_x) of a population was introduced, elaborated later (Skiadas and Skiadas [11] [12] [13] [14] [15] [16] [18]) and evaluated with several methods (see Skiadas and Skiadas, [17]), with particular emphasis on the calculation of the Loss of Healthy years (see Skiadas and Skiadas [17] in comparison with Mathers et al. [6] [7]). The mathematical formula for the calculation of Health State H_x is:

$$H_x = \pm\left(-2xln\frac{d_{(x)}\sqrt{x^3}}{k}\right)^{\frac{1}{2}}$$

where k is a parameter given by $k=\max(d_{(x)}\sqrt{x^3})$ and $d_{(x)}$ is the number of deaths per 100.000 of population provided by the classical Life Tables, or preferably they may correspond to the probability density function. According to theory developed by Jansen and Skiadas [5], the Health State Function has an improvement stage of human health during the first years after birth, followed by a decreasing one during middle and old ages.

Based on the Health State Theory (HST) many Demographic and Human Development Indicators have been proposed and calculated efficiently for numerous national populations based on data published by National Statistical Services or found in other databases (see Skiadas and Skiadas [15] [14] [13]). This paper is a first attempt to apply the Health State Theory techniques to data

already used for the evaluation of the mortality transition in the Pomaks of Organi and Kehros (Zafeiris [22] [21]), i.e. it is a first effort to apply HST on small and isolated populations.

Map 1: the geographic location of the under study population

The data used here are from two former administrative communities, namely Organi and Kehros, located in the northeastern part of the Department of Rhodopi of Greek Thrace, over the Rhodopi Mountain (Map, 1; see Zafeiris, [22] [21]). These communities were comprised of 23 settlements and extended to an area of 346 Km^2. They are inhabited by the Pomaks; in general a Muslim population, speaking a Slavic idiom with many Greek and Turkish loan words, spread on both sides of the Greek-Bulgarian borders. Pomaks of Organi and Kehros constituted a geographically and culturally isolated population, struggling for their survival in quite a harsh environment. In the past they were small farmers, stockbreeders and woodcutters. Though field work evidence suggests that a time varying trend of migration from their mountainous dwellings to the plains of Greek Thrace was observed in the past, after the arsis of geographic isolation because of the construction of roads in the Rhodopi Mountain, this trend was magnified and a significant and continuous increasing number of them settled in small lowland villages and the city of Komotini. Thus, the aim of this study is the analysis of health characteristics of a population firstly at its original mountainous place and secondly in the place to which it has gradually dispersed through time.

2 Data and Methods

The methodology used for the preparation of the abridged life tables for males and females is described in Zafeiris [22]. On these tables, the calculations based on the Health State Theory (Skiadas & Skiadas [13] [14] [15]) were made. As it is said before, the Health State Function (H_x) aims to the quantification of the health state of a population and is based on the death probability function (g_x) and a parameter called k, which is calculated from the g_x distribution (see Skiadas & Skiadas [11], p. 97). However, because the studied population is small the H_x distributions were subjected to chance fluctuations by age. In order to smooth them two order polynomial trend lines were fitted, in which as intercept the H_0 values were set, i.e. the health state level of infants (the R^2 was at all times much greater than 0,90). Because the original life tables were "closing" by the age of 85, the H_x values beyond this age were estimated with the use of the fitted line.

According to this fitted line the following health state indicators were calculated and used in this paper: H_0, H_{max} - i.e. the maximum value of the H_x distribution which is a measure of the maximum health state achieved by the population - and Total Health state (THS), which corresponds to the sum of H_x values before the zero point of the health status of the population and is then a comprehensive assessment of the health levels of the population. Afterwards, the total health state from max to zero health was estimated as a sum of the H_x values from the maximum point of the Health State Function until its zero point and will be an overall measure of health during its progressive reduction phase in the human life cycle. Additionally, the "loss of Healthy Life Years" because of severe causes (LHLY1) as well as that because of moderate and severe causes (LHLY3) were calculated (see Skiadas and Skiadas [12], p. 18). Based on that, life expectancy at birth for moderate & severe disability causes (HLEB 3) as well as that only of the severe causes (HLEB 1) were calculated simply as the difference of life expectancy at birth (LEB) and LHYL3 or LHLY1 respectively (see Skiadas & Skiadas [11], p. 101).

Rotated factor loadings		
component	1	2
LEB	,977	-,213
H_{max}	,937	-,452
THS	,938	-,479
THS from max to zero health	,873	,128
LHLY1	-,215	,958
LHLY3	-,411	,903
HLEB3	,953	-,494
HLEB1	,958	-,415
H_o	,892	-,127

Table 1. Factor loadings of PCA

The results of the analysis were compared with those of the urban, rural and total populations (including semi-urban) of Thrace and the relevant ones of the entire country, for which, in order to be comparable, exactly the same method described above was used. Then, a principal component analysis was carried out in order to visualize the geometric relationships among the populations studied, in fact in order for these to be classified according to their survival and health characteristics and the similarities they exhibited. Several rotation methods of PCA were used, giving similar results. The one cited here is the Oblimin with Kaiser Normalization which is a method for oblique (non-orthogonal) rotation (see Field [2], pp. 702-703). The variables used are seen in Table 1, however because of the scaling differences existing among them their values were transformed to their z-scores before the method appliance. The PCA was performed with 2 factors, as suggested by the scree plot (not cited here) of the eigenvalues against factors and the Kaiser criterion for keeping in a PCA all factors with eigenvalue greater than 1 (see Field [2], pp. 677-678). The KMO test (Keiser-Meyer-Olkin measure of sampling adequacy) was 0.763, well above the value of 0.5 which is considered the minimum accepted value for which the factor analysis yield distinct and reliable factors (see Field [2], pp. 684-685). The Bartlett's test of sphericity was 1929,991 ($p<0.000$) and the determinant of the correlation matrix was 2,18E-15

which indicate the validity of the PCA (See Field [2], pp. 694-695). The two factors PCA explained 91.272% of the variance observed, 72,193% by the first component and 19,079% by the second one. The scatter diagram produced by the PCA was based on the relevant regression scores of the components extracted by the analysis.

3 Results

Mortality transition in the Pomaks of Organi and Kehros (Pomaks from now on) (Zafeiris [21] [22]) was accompanied, quite predictably, by a rapid transition of the health status of the population (Figure 1).

In that course, females' total health state level (THS) was increased by 54,3% between 1962 and 1992 (calculations based on the results cited in Figure 2). Similarly, males' THS increased by 36,8% between 1967 (when its minimum value was observed) and 1992. Between 1962 and 1967 males' THS seem to have declined. Females, on the contrary, at the same time had 18,3% gains in their THS.

It must be stressed out that despite the fact that THS levels prevailed significantly in the female population, in 1962 the opposite is observed. This is because of the elevated death probabilities of women mainly of reproductive age, because of the total absence of maternity homes and in general of the basic infrastructure for ensuring the health status of the mothers and their children. This absence was also imminent later on though it not easily recognized in the analysis results. In any case, a similar but insignificant reversal is found in 1982.

If these temporal trends are compared with the urban, rural and total populations of Thrace and then with those of the entire country, a rather complicated pattern of THS levels transition emerges. While male levels seem to be more or less stable between 1961 and 1971 in the entire country, in Thrace they decreased by about 2-2,5%; a trend that continued until 1981 in the rural and urban populations while in the total one THS levels remained stable. In contrast, between 1971 and 1981 the country's populations had significant gains. Consequently, a progressive divergence of the Thrace was observed until 1981. Eventually its populations would start to converge as a result of the acceleration of the health state transition between 1981 and 1991, but this convergence was not fully completed by 1991.

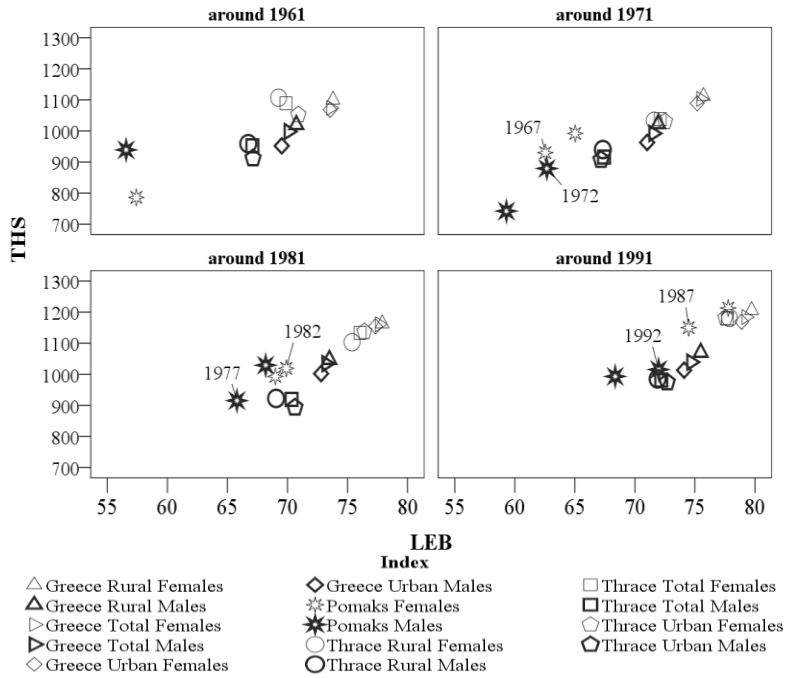

Fig. 1. Life expectance at birth (LEB) versus total health state levels (THS; fitted values).

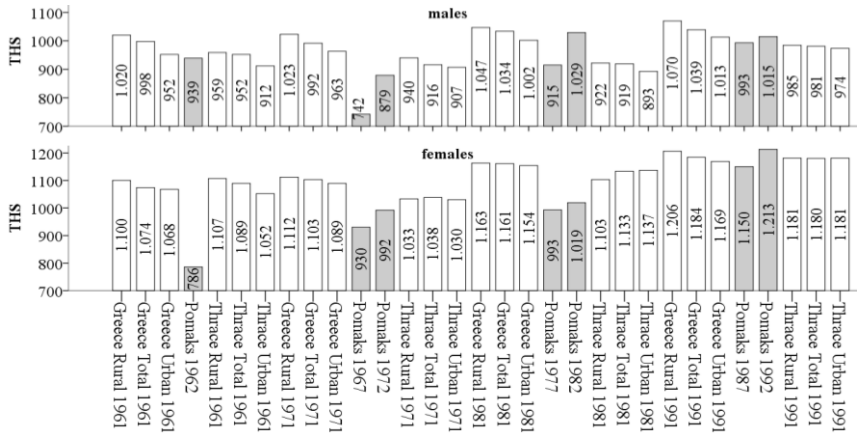

Fig. 2. Total health state levels (THS; fitted values).

Thracian females, like males, were also under held a “counter transition” of the THS levels, but in them this was more intense and finalized earlier; between 1961 and 1971 their “losses” were at the range of 2-7%, but between 1971 and

1981 their "gains" were high (~7-10%). The growth of THS levels continued later, even if it slowed significantly (~4% growth) apart from the rural population where it remained rather high (7,1%). Meanwhile, a continuous growth of THS levels was observed in the female populations of the entire country. This growth was originally minor, accelerated between 1971 and 1981 and then stalled, but still remained positive. Because of the different tempo of the THS transition, in the end the Thracian populations and those of the entire country converged significantly.

The different tempo of this transition is described by the relative growth of THS levels between 1961 and 1991. For the entire country THS gains were 4,9-6,4% for males and 9,5-10,2% for females. In Thrace they were about 2,7-6,8 and 6,7-12,3% respectively. But between 1971 and 1991 males had an increase of about 5% and females of 7,3-8,% for the entire country, while the respective figures for Thrace were 4,8-7,4% and 13,7-14,7%.

However, comparing these figures with those of the Pomaks it is obvious that THS transition was more rapid and intense in them. At the end - even if at the beginning their population was cited quite distantly - it followed the aforementioned trend of convergence with the others. Males, through a variable course, outpaced the Thracian populations in 1982, filling the "gap" observed between Thrace and the entire country. Female Pomaks followed a time variable but ultimately increasing course of their THS levels but these were consistently smaller than those of the Thracian populations until 1992. Then they prevailed in THS levels slightly and converged and even outpaced the population of the entire county.

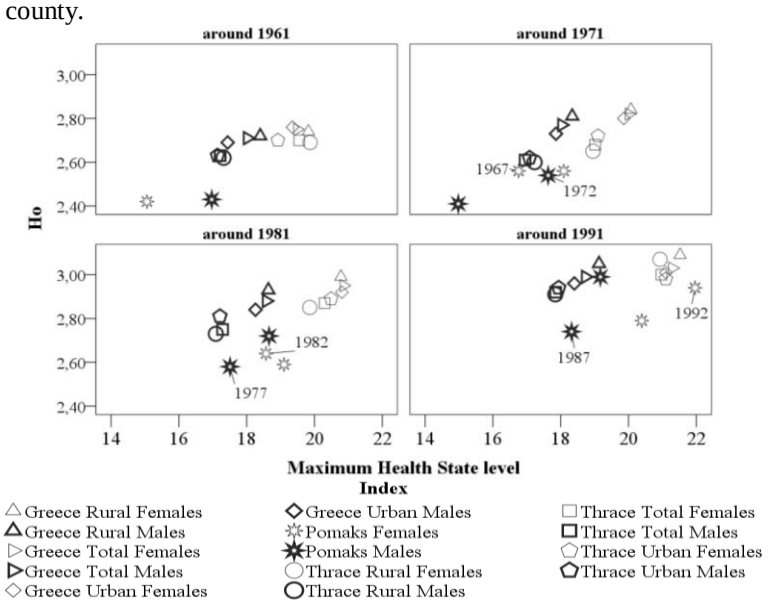

Fig. 3. H_0 versus maximum health state level.

Between 1961 and 1991 THS temporal changes were accompanied by a variable but ultimately increasing trend of the health state level of the infants (H_0) in all the populations studied (Figure 3). In males, three groups of populations were formed during that course. At the highest levels of H_0, i.e. at the best health state of the infants, the populations from the entire country were positioned, followed by the Thracian populations in the middle. Pomaks, for most of the time were located at the outskirts of this scheme, with lower H_0 levels and time-varying differences with the other populations and only in 1991 did they manage to converge with them. A similar pattern is observed for the female Pomaks, but there the differences with the other populations were greater at all times.

Meanwhile, maximum health state (H_{max}) levels of males increased significantly. While originally Pomaks were below them, in 1972 they outpaced the Thracian populations and, despite the observed discontinuities, they gradually converged with those of the entire country. Females of Pomak origin, in their turn, converged, and even outpaced, the other populations only in 1992. As a result, because of the differences observed at the starting point and the maximum level of the health state distribution by sex and age, Pomaks, either males or females, were mounted apart from the other populations studied as it is seen in Figure 3, and only after 1991 is a significant convergence.

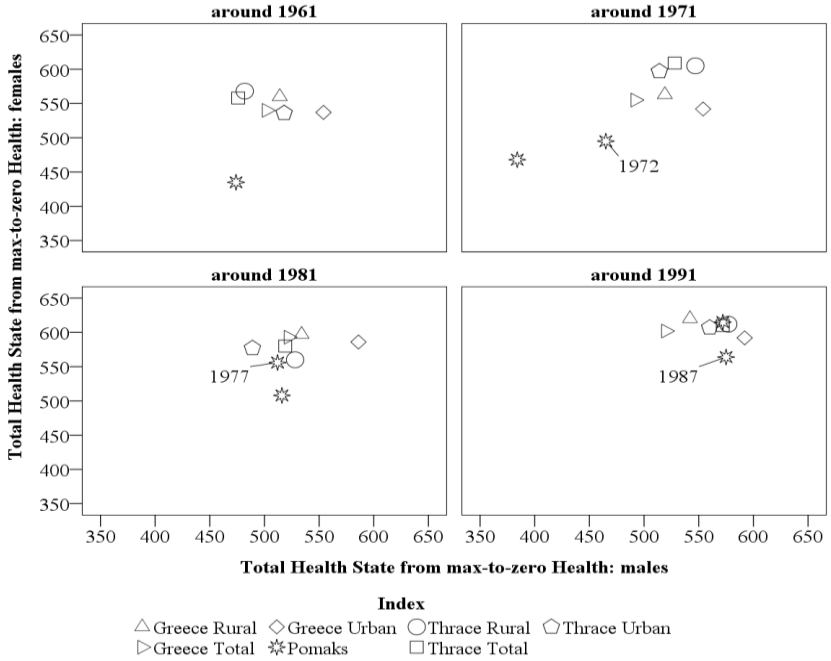

Fig. 4. Total Health State from max-to-zero Health.

The total health state from max to zero health is quite dissimilar among the populations studied (Figure 4). As an overall measure of health during its

progressive reduction phase in the human life cycle, it seems that the Pomak women, on one hand were in accordance with the general tendency of the with time improvement of their health status after middle age even if that took place in quite different tempos and followed different timetables among the populations studied. On the other hand, and for the majority of the times studied, Pomaks experienced larger burdens than those of the other women. The original convergence trend of Pomaks which was observed until 1977 was interrupted later and only in 1991 do they exhibit significant similarities with the other populations. A similar pattern of improvement of the total health status after middle age is observed in Pomak males, but their convergence was not interrupted in any way and after 1977 they exhibited major similarities with the other populations and in some cases they overtook them.

The Healthy life expectancy under severe and moderate causes (HLEB3) is in accordance with this trend of a significant lag of the health status of the Pomak population up to one time point and its convergence with the other populations later on (Figure 5). Obviously, women live longer than males - as evidenced by their LEB levels (Figure 1), and judging from the HLEB3 they are burdened by serious diseases later in their lives. However, an important exception is found for the Pomak women in 1962, as a result of their low health status in those days which was discussed previously.

Because of this, their losses of healthy years because of moderate and severe causes (LHLY3) were at their maximum values then. Afterwards, following a variable course their losses were gradually limited and at the end they were fully converged with the other populations. Pomak males followed a variable and eventually convergence course through time in both LHLY3 and HLEB3 levels. In total, Pomaks, both males and females, tended to cluster apart from the other populations until 1981, when their distances became smaller, as seen in their positions in the scatter diagrams of Figure 5. Later on, they exhibited many similarities with the other populations.

This distinction is apparent if the losses of healthy life years because of severe causes (LHLY1) and the relevant life expectancy (HLEB1) are taken into consideration (Figure 5). The temporal trends of both male and female populations are largely similar with those described above for LHLY3 and HLEB3, though more tight groupings are observed because in reality LHLY1 and HLEB1 (severe causes) is one of the components of LHLY1 and HLEB1; the other one is the component of the moderate causes.

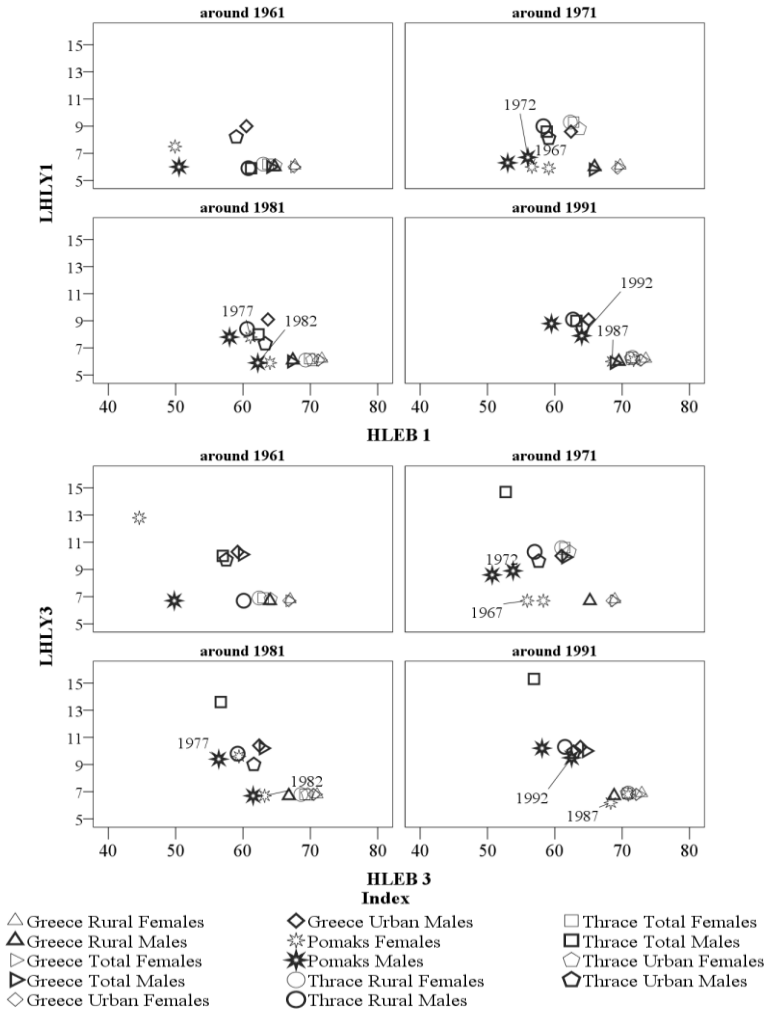

Fig. 5. LHLY1 versus HLEB1 and LHLY3 versus HLEB3.

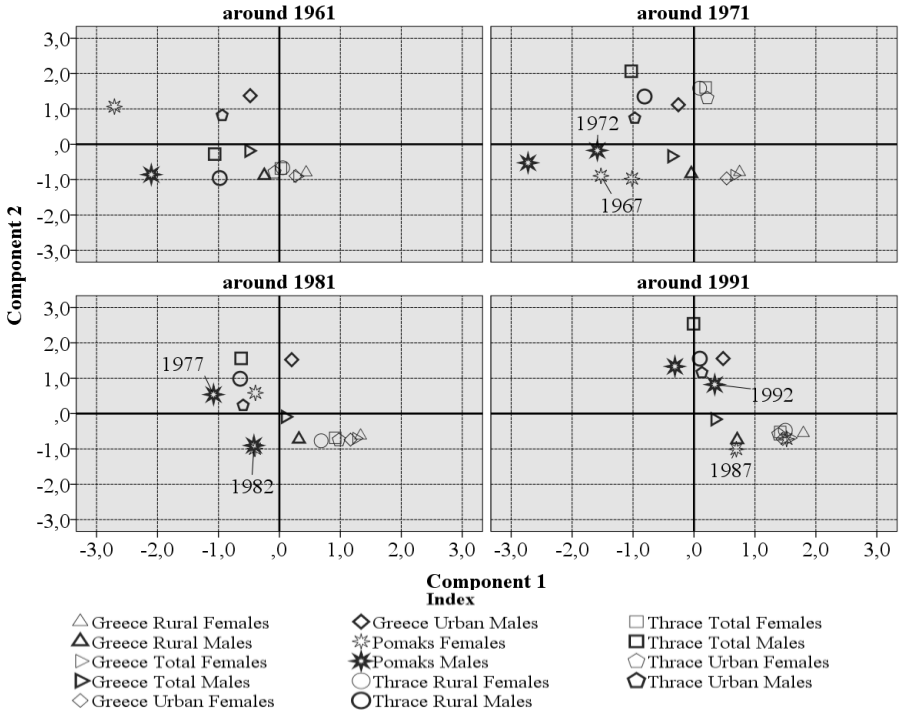

Fig. 6. PCA analysis results.

The principal components analysis (PCA) condenses the high variability observed among the populations studied (Figure 6). In general, a clear and predictable distinction of males and females is observed which is combined within the two sexes with a general tendency of convergence of all the populations studied. Around 1961, all the female populations, except the Pomaks which were placed distantly apart, clustered together according to a pattern in which those from the entire country had somewhat better health and survival characteristics. Ten years later because of the variations of component 2, which mainly summarizes the information for the years lost because of the moderate and severe causes, the Thracian women were differentiated significantly. However, their distances with the other women of the entire country because of component 1 were rather small. Pomak women in their turn reduced their distances from other populations but these remained large. From 1981 onwards, all the female populations started to exhibit more similarities and the Pomak one diminished its distances with the others even further. As a result by 1991 all the female populations had very similar health and survival characteristics.

The observed variability was higher in the male populations studied, where a tripartite pattern of differentiation in health and survival characteristics is more

visible. According to this pattern the populations from the entire country had better health and survival characteristics than the others, even if they were somewhat diverse concerning component 2 levels. They were followed by the Thracian populations and then by the Pomaks. As happened with the females, in all the populations a significant change in their health and survival characteristics was observed through time and the Pomaks, originally distantly apart, finally managed to converge with the others. However, even in 1991, a significant variability was observed for the male populations and their convergence was not as strong as that of the females.

Conclusions

Significant differences were found in the demographic and health state indicators among the populations per period of study. The mortality transition was accompanied by a health transition, which led to the gradual convergence of these populations, even if it had a different momentum and pace among the populations studied. Women benefited more during this transition.

The original differences found in the Pomak population must be attributed to the natural and manmade environment, social, economic and cultural, in which they struggled for their survival. The environmental conditions are adverse in Rhodopi, especially during wintertime, and agricultural production was limited. The population lived in conditions of underdevelopment and every day activities acted as rather aggravating factors concerning health and mortality. The geographic isolation of mountainous Rhodopi was accompanied by if not non-existent at least inadequate health infrastructure and provision of health. This situation was aggravated still further because of the low economic and educational status of the population. Originally, as field work evidence suggests, some women, giving excuses based on their perception about their religious beliefs, refused to be examined by medical doctors. This practice was eventually abandoned completely, and it is well known that the presence of medical doctors in the mountainous area has positively contributed to the decline of mortality since (and quite obviously) diseases and accidents could be addressed more easily. However, women's health and also child mortality were aggravated in the past because of the absence of qualified medical personnel, i.e. obstetricians and midwives, which caused the high divergence observed in the female population in the past. Later on, this problem diminished because Pomak women started to give birth to their children in obstetric clinics in Komotini and the nearby city of Alexandropoulis.

The convergence of the Pomak population with the Thracian ones and the populations of the entire country reflect the socio-economic transition under held by them after the arsis of the geographic isolation and gradual dispersion of part of the population in the lowlands. Gradually, either in the highlands or the lowlands, they were exposed to a different and less isolated socio-economic

environment into which they were fully integrated. Their exposure to the free economy with paid work status or because of their involvement mainly with technical occupations, accompanied by cultural diffusion processes caused several economic, social and cultural transformations in the Pomak micro society and led to a rise in living standards, health provision and consequently to the improvement of health status and a reduction in mortality (see Zafeiris [21] [22].

References

1. C. L Chiang. *An Index of Health: Mathematical Models*, U.S. Department of HEW, Public Health Service, Publication No. lCXK). Series 2, No. 5, 1965.
2. A. Field. *Discovering statistics using IBM SPSS statistics*. 4th edition. SAGE, London, 2013.
3. J. Graunt. *Natural and Political Observations Made upon the Bills of Mortality*, London, First Edition, 1662; Fifth Edition, 1676.
4. H. Halley, An Estimate of the Degrees of Mortality of Mankind, Drawn from the Curious Tables of the Births and Funerals at the City of Breslau, with an Attempt to Ascertain the Price of Annuities upon Lives, *Philosophical Transactions*, 17, 596-610, 1693.
5. J. Janssen and C. H. Skiadas. Dynamic modelling of life-table data, *Applied Stochastic Models and Data Analysis*, 11, 1, 35-49, 1995.
6. C. D. Mathers, R. Sadana, J. A. Salomon, C. JL. Murray and A. D. Lopez. Healthy life expectancy in 191 countries, 1999. *The Lancet*, 357, 1685–91, 2001.
7. C. D. Mathers, C. JL. Murray, A. D. Lopez, J. A. Salomon, R. Sadana, A. Tandon, B. L. Ustün and S. Chatterj. *Estimates of healthy life expectancy for 191 countries in the year 2000: methods and results*, Global Programme on Evidence for Health Policy Discussion Paper No. 38, World Health Organization, November 2001 (revised).
8. B. S. Sanders. Measuring Community Health Levels. *American Journal of Public Health*, 54, 1063-1070, 1964.
9. D. F. Sullivan. *Conceptual Problems in Developing an Index of Health*, U.S. Department of HEW, Public Health Service Publication No. 1000, Series 2, No. 17, 1966.
10. D. F. Sullivan. A single index of mortality and morbidity. *HSMHA Health Reports*, 86, 347-354, 1971.
11. C. H. Skiadas and C. Skiadas. Estimating the Healthy Life Expectancy from the Health State Function of a Population in Connection to the Life Expectancy at Birth. In *The Health State function of a population.* (Skiadas, C. H. and Skiadas, C., eds). 1st ed. Athens, 97-109, 2012.
12. C. H. Skiadas and Skiadas, C. *The Health State function of a Population. Supplement. Demographic and Human Development indicators. 35 countries studied.* ISAST, Athens, 2013.
13. C. H. Skiadas and C. Skiadas, *The Health State Function of a Population*.2nd edition. Athens, 2013.

14. C. H. Skiadas and C. Skiadas. *Supplement: The Health State Function of a Population*. ISAST, Athens, 2013.
15. C. H. Skiadas and C. Skiadas. *Demographic and Health indicators for 193 countries of the World Health Organization and the United Nations. Second supplement of the book The Health State Function of a Population.* Athens, 2014.
16. C. H. Skiadas and C. Skiadas. The First Exit Time Theory applied to Life Table Data: the Health State Function of a Population and other Characteristics, *Communications in Statistics-Theory and Methods*, 34, 1585-1600, 2014.
17. C. H. Skiadas and C. Skiadas. The Health State Curve and the Health State Life Table: Life Expectancy and Healthy Life Expectancy Estimates. Under review, 2014.
18. C. H. Skiadas and C. Skiadas. Exploring the State of a Stochastic System via Stochastic Simulations: An Interesting Inversion Problem and the Health State Function, *Methodology and Computing in Applied Probability*. To appear, 2014.
19. G. W. Torrance Health Status Index Models: A Unified Mathematical View. *Management Science*, 22, 9, 990-1001, 1976.
20. WHO, Preamble to the Constitution of the World Health Organization as adopted by the International Health Conference, New York, 19-22 June, 1946; signed on 22 July 1946 by the representatives of 61 States (*Official Records of the World Health Organization*, no. 2, p. 100) and entered into force on 7 April 1948.
21. K. N. Zafeiris. *Comparative analysis of the biological and demographic Structures of isolated populations in the Department of Rhodopi.* PhD Thesis. Democritus University of Thrace, Department of History and Ethnology. Komotini, Laboratory of Anthropology, 2006. [In Greek].
22. K. N. Zafeiris. A method for calculating life tables using archive data. An example from mountainous Rhodopi. Paper presented in the 3rd SMTDA Conference. 11-14 June 2014, Lisbon, Portugal. Under publication.

A method for calculating life tables using archive data. An example from mountainous Rhodopi

Konstantinos N. Zafeiris[1]

[1] Laboratory of Anthropology, Department of History and Ethnology, Democritus University of Thrace. Email: kzafiris@he.duth.gr

Abstract: Using archive data, the Pomaks of Organi and Kehros (Greek Thrace) were studied. In order for the mortality transition to be evaluated a life table analysis was carried out. Results suggest a rapid mortality transition. Finally, Pomaks have converged to the total Thracian population.
Keywords: Mortality, life tables, Pomaks, Thrace.

1 Introduction

While much has been done concerning the life table analysis of mortality and health of Greece (see for example Skiadas & Skiadas [16] [15] [14]), such techniques have rarely been used in order to estimate mortality levels and transitions in the anthropological populations of the country. This paper is an attempt to apply these techniques to isolated populations, using the available archive data for the Pomaks of two former municipalities of Rhodopi, Greece (Zafeiris [21]). In a subsequent paper the Health State Theory techniques will also be applied for the calculation of several health state and demographic indicators for this population.

Map 1: The major Pomak areas (in grey).

The Pomaks (Map 1) were originally a mountainous population mainly living on either side of the Greek – Bulgarian Borders (Bacharov [2]; Georgieva [4];

New Trends in Stochastic Modeling and Data Analysis (*pp.* 325-337)
Raimondo Manca – Sally McClean – Christos H Skiadas (Eds)

Zafeiris [21]). They use a Slavic dialect with numerous Turkish and Greek loans and they are Muslims, in fact Islamised ex-Christian populations (Georgieva [4]; Papachristodoulou [10]).

This study concerns the mortality transition of the Pomaks of Organi and Kehros, i.e of two former administrative communities (part nowadays of the municipality of Fillyra) which are located in the most north-eastern part of the Department of Rhodopi of Greek Thrace over Rhodopi Mountain. The community of Organi consisted of 11 settlements, and covered an area of 200 Km^2. That of Kehros covered an area of 146 Km^2 and consisted of 12 settlements (National Statistical Service of Greece [8]). Pomaks, while originally geographically or even culturally isolated, lived in a harsh environment, where forests of conifers and deciduous trees were interspersed among limited cultivations and moderately extensive pasture lands. In its traditional stage, the local economy was based on family production. People were small farmers, cultivating mainly tobacco and crops and other products for home use. Others were involved in stockbreeding or forestry. Through time many of them have permanently migrated to the lowland villages and to a lesser degree to the city of Komotini, adapting to new environments and activities. Thus, the aim of this study is the analysis of mortality of a population firstly at its original mountainous place and secondly in the place in which it has gradually dispersed through time.

2 Data and Methods

We have used the civil register archives of the former municipalities of Organi and Kehros in order to reconstruct the life lines of every person of the two populations. The main book used was the Registrar General of the two municipalities, along with birth, death and marriage books. The Registrar General book is comprised of numbered family registers, each one containing registries for every member of a nuclear family which consists in its typical form of the head of the family (the husband) and his wife (or wives in the case of remarriage(s)) and the children of the family. For each one of them surname, first name, father's and mother's names are known along with demographic information: birth date, death date, marriage, transcription to another municipality, loss of citizenship, divorce. When a child from a family gets married it is transcribed to another family registry as head (husband) if it is a male or as a wife if it is a female, and it is deleted from the paternal one. However, in a special column of the book the number of the family of destination is written during this process, while the number of the family of origin is written in another column in the new family registry. It must be noted that the divorced husbands remain as heads at their family registry. Women are transcribed to a new family registry as divorced, following the same procedure as above. So formally, a person's position in the archive can be identified by a series of reference numbers consisting of its paternal family number and the number of the family registries in which it has been transcribed. In that way a

person can be followed up until their death or deletion because of their transcription following migration to another municipality.

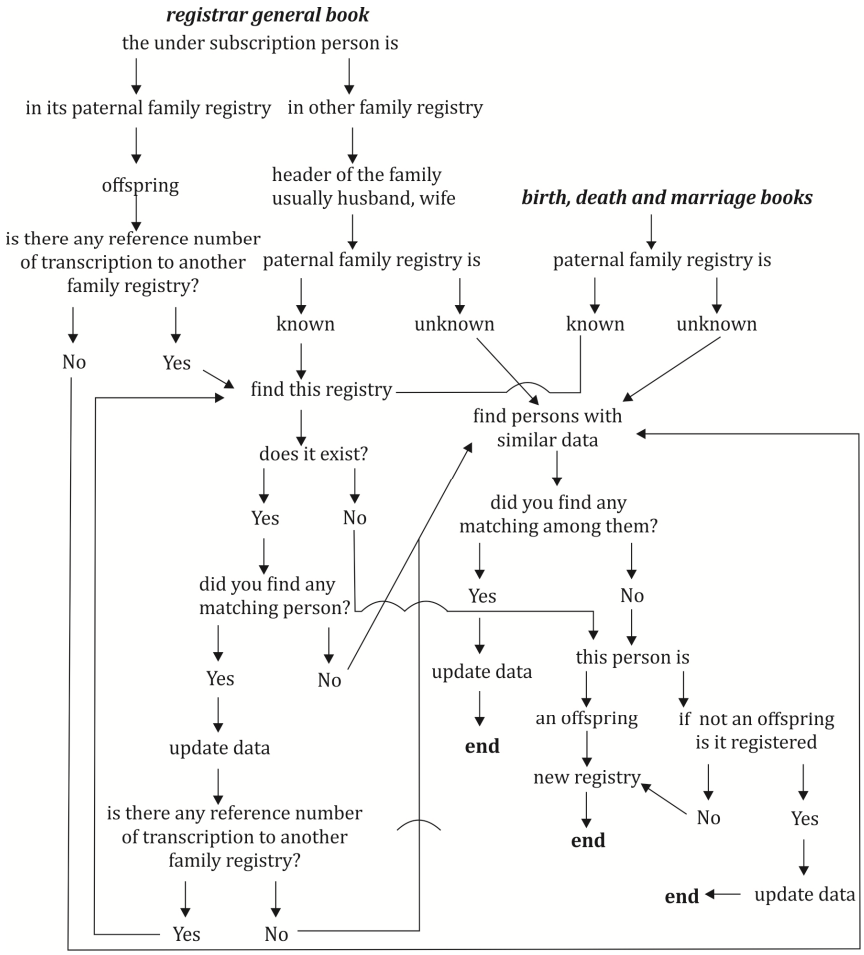

Fig. 1. An algorithm for data entry in the computer.

However, the Registrar General and the other available books were in hand written form and the data contained within should be stored in a database manually in order for the analysis to be carried out. As obvious in the previous paragraph the majority of the people were included in the Registrar General book more than once, in some cases 3, 4 or more times and no demographic analysis can be carried out, if this is not taken into consideration. In addition, the demographic data of the different sources or book registries had to be easily updated, as is also the case with the genealogical relationships of the members of the populations. Because none of the known available commercial software

was considered suitable for this purpose a new one was developed, named in this stage of development Demstat V2 (Demographic Statistics V2).

It was built in a Visual Fox Pro environment and it was based on the SQL language syntax (see http://msdn.microsoft.com/en-us/vfoxpro/default). It retains a four-fold process. Firstly, a relational database was constructed consisting of 18 tables, connected to each other by various keys and relational expressions. A special effort was made in order to find the most parsimonious solution during this process: on one hand personal time and effort along with computer and memory requirements should be taken into consideration and on the other hand every one of the archival books used should be able to be reproduced in its original, but digital form. The last was because data entry after its finalization had to be verified digitally once again. Secondly, a friendly user interface was constructed comprised of several forms, programs and routines. The basic characteristic of this interface was that data could be entered into the computer in a dynamic way according to the strategy that the user chose every time as the most suitable for each case. One of the algorithms used for this is described in Figure 1.

Additionally, in parallel to the original data entry for the persons, a digital library of all surnames and first names existing in the population was created for spelling errors to be checked. If such errors were identified, a new corrected form of the mistakenly written entry was entered in the library. Because the population is a Muslim one a variety of sources was used (Underhill [20]; Tuncay & Karatzas [18]; Pampoukis [9]; Tzemos [19]). Afterwards, a new corrected record from the library was added for every person's mistakenly written surname or name in the database. However, the original form of every surname and name was also kept.

The third aim of the software was the construction of the genealogical trees and pedigrees of the population in any possible form: patrilineal, matrilineal, bilateral etc. The fourth aim of the software was the demographic and genealogical analysis of the population which was based on the life lines of the persons of the population. The demographic analysis was based on the two dimensional form of Lexis diagram (see Feeney [3]), which as is known for every person contains information about its cohort, the date of occurrence of a demographic event and the age of that person in that demographic event. However, because persons' life lines were known, for the analysis of any demographic phenomenon either the average population or the relevant person years lived in the population in a time period could be used. Similarly, the analysis could be based by choice either on the "squares" or the "parallelograms" of the lexis diagram.

After entering the data, a validation of the records took place following three procedures. In order for the manually entered records to be validated for their precision concerning the people linkages the Registrar General Book was

restored digitally in both original and digital state of family and people registries. Then a routine was built in SQL in order for the different reference numbers to be followed up and the records corresponding to them to be compared using several criteria like surname, name, father's and mother's name (corrected forms), birth date, death date, marriage date. If these criteria were satisfied the relevant records were considered to refer to the same person and the manual linkage of the records done before was verified. Afterwards the opposite routine was used; people were firstly identified by the criteria described above and secondly their reference numbers were compared. In the third procedure a manual check of the results of the process took place, as happened with a few problematic records like those with mistaken reference numbers or mistaken father's names etc.

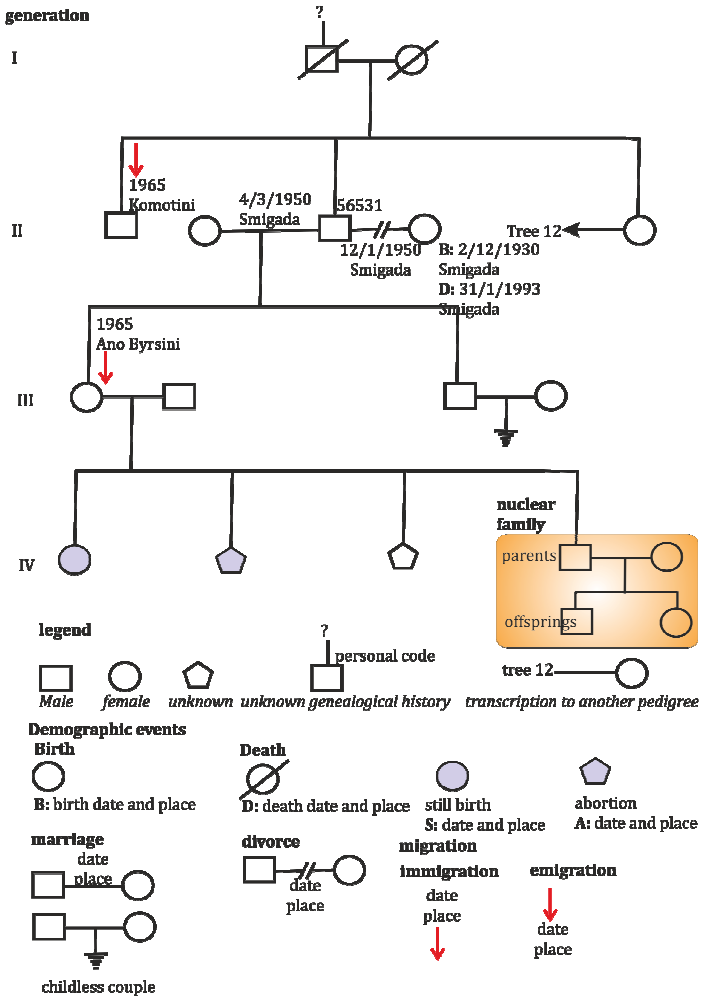

Fig. 2. A patrilineal genealogical tree or pedigree.

Then the patrilineal genealogies (Figure 2) of the population were constructed and used as a basic research tool in the field work carried out afterwards, when data were tested for their validity and completeness and the data base was once again updated if any omitted or false data were found. We have to note that inhabitants not registered in the Registrar General Book were not identified during the field work, because the population lives in a mountainous area and the only type of immigration which occurred there was the marital one which presupposes registration in the archives. However, through time many of the registered citizens of the two municipalities migrated to the Rhodopi plain, mainly to small villages of the area and to a lesser degree to the urban center of Komotini.

The life line for each of the members of the populations was constructed and used in the following analysis. By studying all these life lines at any given time period, i.e. by studying the population at risk of a specific demographic phenomenon, the person-years lived by the members of the population were calculated as well as its composition by sex and age and the demographic events which occurred (see Preston et al. [12], pp. 3-16). In this analysis, as the starting point of a person's life line was considered their birth, unless an immigrant where their date of migration is considered as the starting point, and as the terminal point of the life line were considered the death of a person, their transcription to another municipality and the end of the research. The average population for every year was calculated as the mean population between two subsequent New Year's days.

Then the age specific mortality rates per sex were calculated using standard procedures (see for example Preston et al. [12], p. 21-23) for five year periods because the population is small and subjected to chance fluctuations. For each of the 5-year periods the numerator of the age specific mortality rate formula was smoothed as the average annual number of deaths per age class during that period, while as denominator the average population in the middle year of that period was used. Subsequently a life table analysis (see Preston et al. [12], pp. 38-69) was carried out for both sexes based on one year age classes up to the age of five, and five years long age classes for the older ages. Life tables were considered to be closed by the age of 85 for both sexes.

The probability of death for life table analysis was calculated using the Chiang's method (Namboodiri [6], p. 85):

$$ {}_n q_x = \frac{n^*{}_n M_x}{1 + (n - {}_n a_x)^*{}_n M_x} , $$

where ${}_nM_x$ is the age specific mortality rate between age x and [x+n), n is the length of the age interval in an abridged life table and ${}_na_x$ is the fraction of the interval between x and [x+n) birthdays lived on average by those dying in that

interval. The values ${}_na_x$ were calculated directly from the data for the ages less than 5 years. For the older age classes, because the observed number of deaths was small, deaths were considered to be equally distributed in each age class.

In order for the results of the analysis to be compared with the population of Thrace and Greece published data concerning deaths per sex and age and the relevant age distributions were used (vital events statistics and population censuses results published by the National Statistic Service of Greece, nowadays National Statistical Authority, www.statistics.gr) and life tables for the census years between 1961 and 1991 were calculated. Infant mortality rate (IMR) and though q_0 was calculated following Pressat [11] as:

$$IMR = \frac{D_{(0,t)}}{1/3 * b_{t-1} + 2/3 * b_t},$$

where D stands for infant deaths and b for births, where t is the year. The number of infant deaths was smoothed as the mean number of infant deaths in the census year and its adjusting ones. For years 1 to 5 the Reed-Merrell formula ([13], cit. Naboodiri [6]) was used:

$${}_nq_x = 1 - \exp(-n\ *{}_nM_x - a * n^3 *{}_nM_x{}^2)$$

where n=1, a=0.008 and ${}_nM_x$ the age specific mortality rates. For the remaining age groups the Chiang's method was used.

The calculated death probabilities were applied to an abridged life table (closing at the age of 85) prepared by Skiadas and Skiadas ([14] [15] [16]), in order for the life expectancies at birth to be estimated.

3 Results

The Pomak population of Organi and Kehros (Pomaks from now on) underwent a rapid mortality transition between 1962 and 1992 (Figure 3). During that period, female life expectancy at birth (LEB) increased by 35,4%, from 57,4 to 77,8 years. Similarly, LEB of the male population increased by 15,4 years or by 27,3%. However, if Pomaks are compared with the total, the rural and the urban population of Thrace, as well as with the analogous populations of Greece, for most of the time a three zone pattern of classification is emerging. At the upper zone, that of the highest LEB, though the lower mortality, the population of Greece is located. The middle zone is formed by the Thracian population and the third one - that of the higher mortality – by the Pomaks.

This tripartite scheme results from the economic, social and political peripheral inequalities observed in the country. It is indicative of that situation that in Thrace, even in the 1980s, the local economy was based on the primary sector, especially agricultural production, which accounted for 70% of the income of the inhabitants (Stathakis [17]). Even more, in 2001 the whole region of Eastern Macedonia and Thrace was in the first position (i.e. the worst one) of the Human Poverty Index (HPI) ranking among the regions of Greece and in the last position according to its Human Development Index (HDI) (see Kalogirou et al. [5], pp. 50 and 57 respectively).

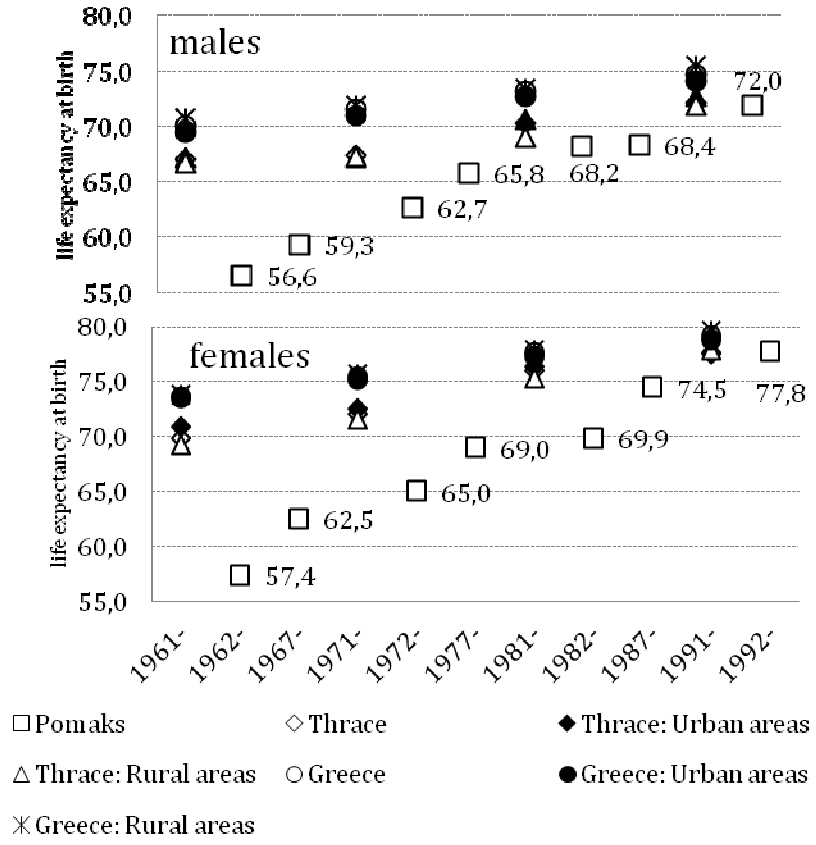

Fig. 3. Life expectancy at birth (LEB) in various populations

Table 1. Life expectancy in Thrace

	Males			Females		
	Total [(1)]	Urban	Rural	Total	Urban	Rural
1961-	67,1	67,1	66,7	69,9	70,9	69,3
1971-	67,4	67,2	67,3	72,1	72,5	71,6
1981-	70,3	70,6	69,1	76,1	76,4	75,4
1991-	72,2	72,7	71,9	77,7	77,5	77,7

(1) Including semi-urban population

Pomaks in their turn struggled for their survival in the past in adverse environmental conditions, especially during winter time. According to data of the Hellenic National Meteorological Service (http://www.hnms.gr/hnms/greek/index_html), the average temperature between years 1960 and 1982 in Komotini ranged between 4,62 and 6,9 ^{o}C in the winter months, while the respective lower ones ranged between -3,76 and -7,32 ^{o}C. Official data for mountainous Rhodopi is absent; however temperatures there are rather lower. According to the NGO "Arktouros" [1] in 1978-89 in Sidironero (Drama) they were less than -10 ^{o}C during winter and in Leivaditis (Xanthi) lower than -12 down to -20 ^{o}C.

More than that, the geographic isolation of the Pomak region in the past was another aggravating factor of mortality. Transportation and communication among the small settlements and the lowlands of Rhodopi was carried out mainly by mules and camels through the treacherous mountain paths. Started mainly after the 1960s, all efforts for the construction of roads were partially efficient; characteristically in the early 1990s the only paved road was the one connecting Komotini with Organi. Additionally, if not absent, electricity supply was gradually available for a few of the villages, as was the case with telephone connections and only much later did local infrastructures improve in an adequate way (Zafeiris [21]).

It is not surprising then that the local economy was rather a pre-industrial one, based on limited resources and with no real opportunities for economic development, which as a matter of fact was the problem with the mountainous

Greece as a whole and especially with the Department of Rhodopi in those days. Additionally the medical care of the population was largely inadequate and even in the 1990s it was administered by few small agrarian clinics. All that, along with the very high illiteracy rate of the population, can explain the high mortality rates of this epoch. Characteristically enough, even in 1981 in the highlands of the Department of Rhodopi, only 35% of the males and 33% of the females had finished the bilingual minority elementary schools existing in Greek Thrace, while the illiteracy rate was 37,4% and 45% respectively (National Statistical Service of Greece [7]).

However, through time a general arsis of the geographic isolation took place in mountainous Rhodopi. Meanwhile a significant portion of the population had migrated to the lowland villages or the city of Komotini, and several transformation processes occurred in the whole of the Muslim minority of the area, like the modernization of agricultural production, the involvement of the population in the open market economy etc. A progressive elevation of the living standards and Health Services was observed and as a result the mortality rates reduced (especially infant mortality) as did the "mortality gap" between the Pomaks and the other people of the area (Zafeiris [21]).

Despite the fact that Thrace is still one of the poorest areas of the Greek periphery all the populations benefited a lot from the developmental processes which occurred in the country between 1961 and 1991 (Table 1; Figure 1). During that time the LEB of the total population of Thrace increased, though at a lower rate than that of the Pomaks; 11,2% for the total female population, 9,4% for the urban and 12,4 for the rural one. The respective figures for the male population were between 7,6-8,3%. As a result by 1991 Pomaks had totally converged to the population of Thrace. In the mean time LEB in the total population of the country has increased somewhere near 6,6-8%, and both the Thracian population and the Pomaks have converged to the total population of Greece. However, important differences still existed in 1991, even though these became lesser in comparison to those which existed in the past.

In the Thracian population, females' improvements in LEB between 1961 and 1971 were more than 2 years for the total and the rural population and 1,6 for the urban one, while male gains were small. In 1981 mortality transition was accelerated and at the end, in 1991, the total, urban and rural populations per sex converged, when the observed differences among them were very small.

It is obvious that the observed LEB differences between the two sexes are positively correlated with LEB levels until 1981: the higher the LEB the greater the differences in LEB between males and females. In 1991, when LEB was at

its maximum levels the differences between the two sexes narrow, though they remain big enough. Overall, females have all the time longer lives and they benefited more than males during mortality transition in the area.

In Pomaks, LEB sex differences per studied period tended to be smaller in comparison to the population of Thrace until 1987. Field work evidence suggests that on the one hand everyday life and the general living conditions in mountainous Rhodopi in the past were aggravating factors for the chances for survival. On the other hand women of reproductive ages were additionally burdened by complications during pregnancy, delivery and the postpartum period. In the past, because of their geographic isolation and the absence of qualified medical personnel, these women used to give birth to their children at home aided by the older women of the village and some uneducated midwives. Nowadays, all the Pomak women benefit from the tertiary health system of Thrace, and especially the obstetric clinics of the General Hospital of Komotini and the University Hospital of Alexandroupolis. Probably this is one of the reasons that in 1987 the differences between the two sexes were maximized.

Conclusions

Through time a general trend of decrease in mortality levels in Thrace was observed. The most rapid mortality transition was that of the Pomak population of Organi and Kehros which had the greatest improvements in life expectancy at birth. As a result by the end of the study all the Thracian populations converge to lower mortality levels.

References

1. Arktouros. *Study for Rhodopi and its natural character*. ny [In Greek].
2. M. Bacharov. The current ethnic panorama in Bulgaria. *GeoJournal*, 43,3, 215-224, 1997.
3. G. Feeney. Lexis Diagram. In Demeny, P. and McNicoll, G. (eds.) *Encyclopedia of Population, Volume 2*, Macmillan Reference USA, 586-588, 2003.
4. T. Georgieva. Pomaks: Muslim Bulgarians, *Islam and Christian - Muslim Relations,* 12, 3: 303-316, 2001.
5. S. Kalogirou, A. Tragaki, C. Tsimpos and E. Moustaki E. *Spatial inequalities of income, development and poverty in Greece. Projects 2011*. John Latsis Benefit foundation. 2011. Available at:

   http://www.latsis-foundation.org/en/101/projects_2011.html
6. K. Namboodiri. *Demographic Analysis.* A Stochastic Approach. Academic Press Inc, San Diego, 1991.
7. National Statistical Service of Greece. *Résultats du recensement de la population et des habitations. Effectué le 5 Avril 1981. Volume V. Fascicule 9. Epire.* Imprimerie Nationale, Athènes, 1991.
8. National Statistical Service of Greece. Distribution of the area of the country according to its principal use. Athens, 1986.
9. I. T. Pampoukis. *The Turkish Vocabulary of the Modern Greek Language*. Papazisis, Athens, 1988. [In Greek]
10. P. Papachristodoulou. The Pomaks, *Arheion Thrakikou Laografikou kai Glossologikou Thisavrou*, 23, 3-25, 1958. [In Greek]
11. R. Pressat, R. *Demographic Analysis: Methods, Results, Applications.* Aldine publishing, New York, 1980.
12. H. Preston, P. Heuviline and M. Guillot, M. *Demography. Measuring and Modeling Population Processes*. Blackwell Publishers, Oxford, 2001.
13. L. J.Reed and M. Merrel, M., A short Method for constructing an abridged life table. *American Journal of Hygiene*, 30, 33-62, 1939.
14. C. H. Skiadas, and C. Skiadas. *The Health State Function of a Population*.2nd edition. Athens, 2013a.
15. C. H Skiadas and C. Skiadas. *Supplement: The Health State Function of a Population.* ISAST, Athens, 2013b.
16. C. H. Skiadas and C. Skiadas. The First Exit Time Theory applied to Life Table Data: the Health State Function of a Population and other Characteristics, *Communications in Statistics-Theory and Methods,* 34: 1585-1600, 2014.
17. D. Stathakis. Processing in Thrace, *Thrakiki Epetirida,* Δ, 1983. [In Greek]

18. F. Tuncay and L. Karatzas. *Turkish-Greek Dictionary.* Center for Eastern Languages and Culture, Athens, 2000.

19. G. Tzemos, *The of Turkish Origins Greek Surnames*. Kessopoulos, Thessaloniki, 2003. [In Greek]

20. R. Underhill. *Turk Dili Grameri, dil, Turk dili, Turkce Grameri. Turkish Grammar.* 7th edition. The MIT Press, Cambridge, 1993.

21. K. N. Zafeiris. *Comparative analysis of the biological and demographic Structures of isolated populations in the Department of Rhodopi*. PhD Thesis. Democritus University of Thrace, Department of History and Ethnology. Komotini, Laboratory of Anthropology, 2006. [In Greek].

Software Package for Calculating the Fractal and Cross Spectral Parameters of Cerebral Hemodynamic in a Real Time Mode

Valery Antonov[1] and Artem Zagaynov[2]

[1]Saint-Petrsburg State Polytechnical University, Saint-Petersburg, Russia
Email: antonovvi@mail.ru
[2]Military Space Academy Mozhaiskogo, Saint-Petersburg, Russia
Email: zagainov239@gmail.com

Abstract: The aim of the work is to create an automated system of calculating the cross spectral characteristics of the two time series. Among them there are cross amplitude, coherence spectral density, the phase shift, as well as correlation and fractal indexes computing in a real time mode. The complex processes the two time series, corresponding to values of blood flow velocity (BFV) and systemic arterial pressure (SAP), connected via Doppler graft or stored on the media in text format.

Keywords: automated system of calculating, two time series, cross spectral characteristics, fractal indexes.

1. Introduction. Regulation of cerebral circulation is a perfect physiological mechanism aimed to provide chemical and physical brain homeostasis. Clarification of the functional tasks of cerebral blood flow regulation in dependence with an input perturbation provides a conceptual framework for the development of methods for controlling the regulation of cerebral circulation. Study of cerebral regulation's features has important role in clinic. The state of regulatory mechanisms determines the laws of the pathogenic process in various lesions of the brain.

At the present time for the assessment of cerebral blood flow regulation mechanisms different types of functional test based on transcranial Doppler are used.

Anyway, these tests involves impact on the body of the subject, which inevitably leads to some distortion reactions. This led for further improvement of noninvasive assessment of cerebral blood flow regulation, which allow to

New Trends in Stochastic Modeling and Data Analysis (pp.339-345)
Raimondo Manca – Sally McClean – Christos H Skiadas (Eds)

monitor parameters of cerebral and systemic hemodynamic in the absence of any external influences.

Being a truly non-invasive, this method allows to evaluate the state of regulatory circuits of the cerebral blood flow circulation in situ, and that determines its value for the clinic.

Analysis of slow-wave processes for assessing cerebral autoregulation (CA) is inextricably linked with a Software Package, which is under consideration.

The currently known linear and fractal figures are necessary to calculate some nonlinear parameters. Thus, one method of processing is a linear frequency analysis . For a discrete signal, frequency sequence is searched by a conventional fast Fourier transform algorithm. The resulting array of frequencies has several indicators of low and high frequency components, and with its help we can calculate the power spectral density, and other characteristics.

Also, when using nonlinear analysis the delay option must be set to restore the attractor by Takens delay.

The main characteristics of the nonlinear signal in the work are: a two-dimensional reconstructed attractor and correlation dimension and its dynamic trend in the embedding space of dimension 3. Graphical objects score calculated in real time represented on the graphs as well as the changing trend component.

This paper considers the currently known linear and fractal figures. Such presentation is necessary to calculate some nonlinear parameters. Thus, one method of processing is a linear frequency analysis. For a discrete signal frequency sequence is searched by a conventional fast Fourier transform algorithm. The resulting array of frequencies has several indicators of low and high frequency components, and with its help we can calculate the power spectral density, and other characteristics [1,2] .

Also, when using nonlinear analysis the delay option must be set to restore the attractor by Takens delay. Usually it is made to look like the first zero of the autocorrelation function.

The main characteristics of the nonlinear signal in the work are: a two-dimensional reconstructed attractor and correlation dimension and its dynamic trend in the embedding space of dimension 3. Graphical objects score calculated in real time represented on the graphs as well as the changing trend component

.

2. The functionality of the interface. In the target present package contains 5 tabs - menu " FILE "," CROSS SPECTRAL ANALISYS "," FRACTAL ANALISYS "," PARAMETERS "," HELP ".

2.1. Menu. "File" - standard, with features:

- Open the file (data file with the extension *. Txt, package file with the extension *. Cdm, open). Recall that in practical calculations will need to open two different files.
- Get data from Doppler graft (retrieve data from the Doppler)

- Save package file (with the extension *. cdm, save)
- Save any image processed data (graphical extension, save image)
- Interrupt the program (exit)

2.2. Menu "CROSS SPECTRAL ANALYSIS" contains the maximum possible number of points in the array (150,000 for each time series):
- Spectral density LFV
- Spectral density SAP
- Joint spectral density LFV and SAP
- Coherency
- Cross amplitude
- Phase offset

2.3 . Menu " FRACTAL ANALYSIS ." The delay parameter is set statically and not change at all times when handling a single signal. The user decides how to ask - or kind of attractor , or by calculating the autocorrelation function . Separately, you can run the processing , pre- used settings in the menu settings (Functional properties :
- A two-dimensional image of the attractor of the system (2D phase space)
- Calculation of the correlation dimension (the dimension of the embedding space
3 , correlation dimension).

2.4 . " Menu "Options.
- Task tab weight window (background Hannah Bartlett, Hamming, Nutall, Gauss, Dolph-Chebyshev, weight window)
- Tab job processing parameters (window width, etc. processing parameters)
- Task tab delay parameter (delay time)
- Check for trends allocation (allocation trends)

3. Numerical algorithms

1. Menu "CROSS SPECTAL ANALYSIS":
To calculate the DFT applied by the algorithm of fast transformation. As the real part of the time series used LCS as imaginary - SAD. To obtain the transformation X_k constructed cumulative spectral density, their individual spectral density $\sqrt{(\mathrm{Re}\, X_k)^2 + (\mathrm{Im}\, X_k)^2}$, phase shift (as the arctangent of the ratio), coherence (as normalized amplitude). For more details see [3].

2. Menu "FRACTAL ANALYSIS":
At the initial stage, we propose to carry out a separate spectral analysis of time series BFV and separately for the time series of SAD.
To specify the method of two-dimensional attractor delays Takens:

$$\vec{x}(i) = (a(i), a(i+\tau), ..., a(i+\tau(n-1))) = (x_1, x_2, ..., x_n)$$

where a (i) - the original time series, n - the dimension of the embedding τ - time delay, and the resulting vector - coordinates of one point on the reconstructed attractor.

In this case *n* satisfies the conditions of Takens: $n \geq 2[d_A]+1,$
where d_A - the reduced dimension of the attractor.

Takens theorem asserts that the number of samples N → ∞ constructed by the delay map is smooth and reversible almost any delay τ. Properties built so attractor metrically (and probability) equivalent to the original attractor of a dynamical system.
The most acceptable method recommended in the literature [4,6,7, etc.], is to find the first zero of the autocorrelation function:

$$B(\tau) = \frac{1}{N-\tau}\sum_{k=1}^{N-\tau}(a_k - \bar{a})(a_{k+\tau} - \bar{a})$$

where the original time series, $a_k = a(k\Delta t)$, $\tau_{opt} = \min_{\tau_i}\{B(\tau_i) = 0\}$

Application of this method is associated with the hypothesis uncorrelated coordinate points of the attractor by the orthogonality of the basis vectors embedding space. However, these claims are not equivalent, and the choice of the delay parameter in this manner is not always optimal. An alternative method is to build a function of the average mutual information method AM Fraiser et al., Described in [6-9]. For this purpose, the interval $[\min_k a_k, \max_k a_k]$ is divided into L equal parts. Typically, [8] L is selected from the Stark formula:
$L = [\log_2 N]+1$

Event «a (t) belongs to the i-th interval " refers to Ai, event «a (t + τ) belongs to the j-th interval » - Bj. P - probability of the corresponding event. Function of the average mutual information is defined as :

$$I(\tau) = -\sum_{i=1}^{L}\sum_{j=1}^{L} P(A_i B_j)\cdot \log_2 \frac{P(A_i B_j)}{P(A_i)P(B_j)}$$

and as the optimal delay parameter selected first local minimum of the function constructed :

$$\tau_{opt} = \min_{\tau_i}\{I'(\tau_i) = 0, I'(\tau_i^-) < 0, I'(\tau_i^+) > 0\}$$

Function of the average mutual information is a more accurate measure of independence . [6] It is also shown that for some test data (attractor of the Lorenz equations) value of the optimal delay parameter obtained by this method is preferred over the first .

$$D_C = \lim_{\varepsilon \to 0} \frac{\ln(\sum_{i=1}^{M(\varepsilon)} p_i^2)}{\ln(\varepsilon)}$$

This equality conveniently represented in the following form :

$$\lim_{\varepsilon \to 0} \frac{\ln(C(\varepsilon))}{\ln(\varepsilon)}$$

where $C(r) = \lim_{m \to \infty} \frac{1}{m^2} \sum_{i,j=1}^{m} \theta(r - \rho(x_i, x_j))$ - - the correlation integral , $\theta(\alpha) = \begin{cases} 1, \alpha \geq 0 \\ 0, \alpha < 0 \end{cases}$ - the Heaviside function , ρ - distance in N- dimensional space. Attractors , consisting of a finite number of points , it is easy to understand that the following expression of the correlation integral :

$$C(r) = \sum_{i=0}^{m-2} \sum_{j=i+1}^{m-1} \frac{\theta(r - \rho(x_i, x_j))}{m(m-1)/2}$$

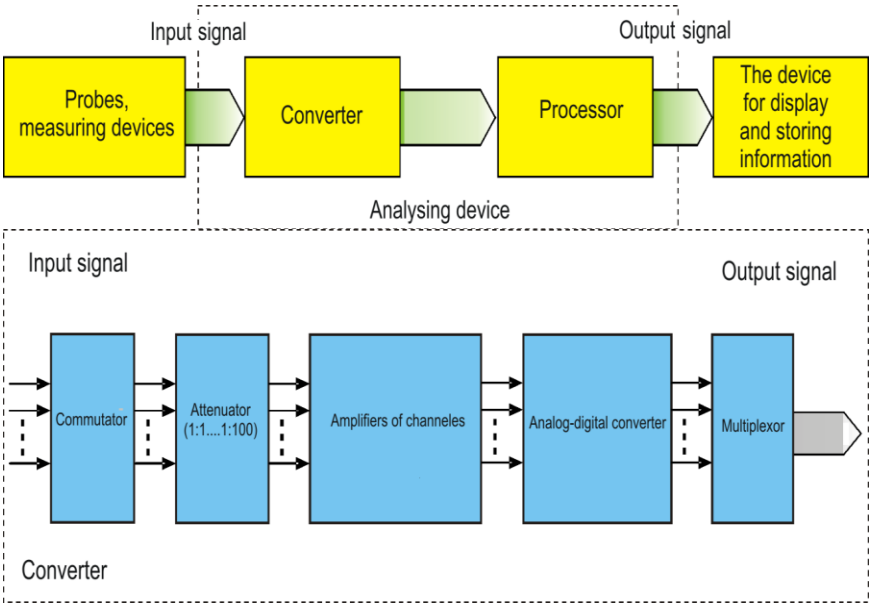

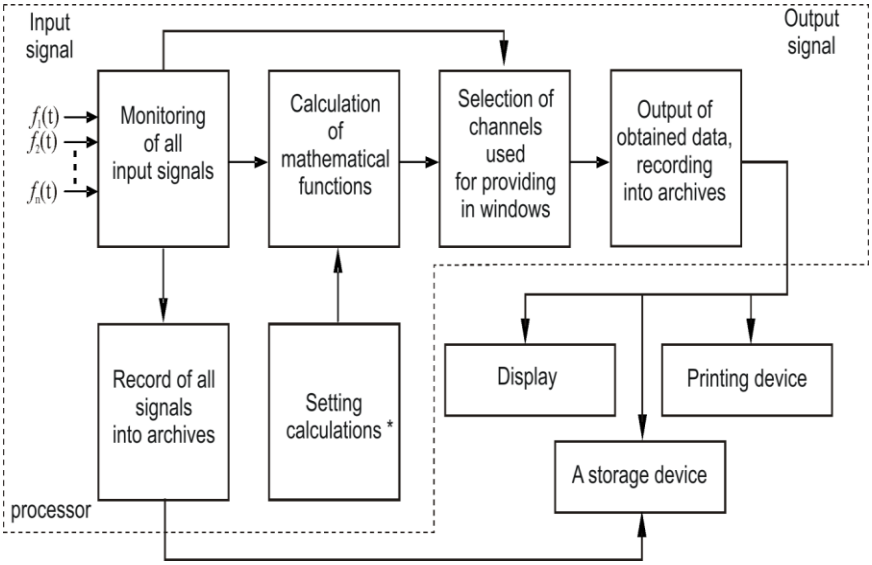

Fig.1. Bookkeeping scheme

Accepted that $C(r) \sim r^{D_2}$. Location $\ln C(r) \sim D_2 \ln r$ and correlation dimension can be evaluated to give the slope of the logarithm of the correlation integral . The easiest way to obtain a linear dependence on the sequence of pilot data , as is known , is a method of least squares. Despite its simplicity , in this case, it is quite suitable , since we can choose their own range of distances r and consider , say, a uniform grid. Based on the method of least squares , we obtain the following system for the estimation of the correlation dimension :

$$y(x) = D_2 x + b$$

$$\begin{cases} \sum_{i=1}^{M} \ln C(r_i) \ln r_i = D_2 \sum_{i=1}^{M} \ln^2 r_i + b \sum_{i=1}^{M} \ln r_i \\ \sum_{i=1}^{M} \ln C(r_i) = D_2 \sum_{i=1}^{M} \ln r_i + bM \end{cases}$$

where M - number of measurements of the correlation integral for different distances ri (calculated , in this case , on a uniform grid) .

The validity of the above law is limited to the values ri, quite small compared to the size of the attractor. Obviously, with increasing r to the size of the attractor C (r) → 1, and a decrease due to the finite points on the attractor C (r) → 0 and the specified power law is valid only in a limited range of r (the so-called scaling range) which can be used to determine the dimension of the attractor .

This range must be set to practice under consideration for biomedical signals and change depending on the type of signal (like attractor corresponding signal). In the case of experimental data, we do not know the dimension of the phase space of the system. But it is shown that for the considered it sufficient to calculate the signals in spaces with dimension N = 3 .
The bookkeeping scheme of the program represented in Fig.1.
The work performed under the auspices of cerebral pathology lab, St. Petersburg Neurosurgical Institute. Head of the laboratory - Professor V.Semenyutin**.**

References

[1] V.Antonov, A.Kovalenko, A. Zagaynov, V.V. Quang. The research of Fractal Characteristics of the Electrocardiogram in a Real Time Mode. Journal of Mathematics and System Science. V.2, N3, March 2012. P. 191-195

[2].Antonov V.I Zagaynov A.I, Wu Kuang Van. Automated software for numerical multifractal studies. Scientific and technical statements STU. 2 (169), 2013. P.71-77.

[3] G. Nussbaumer Fast Fourier transform and convolution algorithms for computing / / Per. with Engl. , Radio and communication, - M. : 1985 , P.248

[4] SL Marple, Digital spectral analysis and its applications . / / Per. with Engl. - Wiley , 1990, pp. 584

[5] R. K. Belyaev Methods of analysis of heart rate variability / / Tutorial Implementation of laboratory training course " Analysis and transformation of biomedical signals », http://konstb.newmail.ru / liter/hrv/UchPos2.htm, 2004 , p.14

[6] Makhortykh SA, VV Sychev Algorithms for calculating the characteristics of stochastic signals and its application to the analysis of electrophysiological data. / / Abstracts. Nonlinear Phenomena in Biology. Pushchino: 1998 . P.33- 34

[7] Meckler A. Application of the device nonlinear dynamical systems analysis for EEG signal processing , Actual problems of modern mathematics : the scientists note , T. 13 (2), 2004 , C. 112-140

[8] VA Golovko Neural processing methods chaotic processes / / Scientific session of the MiFi 2005 . VII All-Russian Scientific Conference " Neuroinformatics 2005" Lectures on Neuroinformatics . - M.: MiFi 2005 . pp. 43-91

[9] NB Janson , Anischenko VS Modeling of dynamic systems from experimental data / / Izvestija Vuzov " IPA " , v.3 , № 3, 1995 , C. 112-121

Life Expectancy and Modal Age at Death in Selected European Countries in the Years 1950-2012

Jana Langhamrová[1], Kornélia Cséfalvaiová[2] and Jitka Langhamrová[3]

[1]University of Economics, Prague, Czech Republic
Email: jana.langhamrova@vse.cz
[2]University of Economics, Prague, Czech Republic
Email: xcsek00@vse.cz
[3]University of Economics, Prague, Czech Republic
Email: langhamj@vse.cz

Abstract: At present, the majority of developed countries deal with the phenomenon of population ageing. This ongoing process is primarily caused by the increasing life expectancy at birth. Length of life is usually expressed by the indicator of life expectancy at age *x*. The values of life expectancy and modal age at death are different from the view of time evolution. This is particularly because life expectancy is the average age of deceased persons in the stationary population, whereas modal age at death is the most common age at death. The aim of this article is to analyse the trends in the development of the death rates in selected European countries using various methods for the death rates compensation. By means of data from the Human mortality database life expectancies and modal ages at death in selected countries will be calculated and compared. The purpose of this paper is to highlight the changes in the trend and dynamics of the life expectancy at birth and to compare its progress with the trend and dynamics of the modal age at death. By comparing the evolution of life expectancy at birth, life expectancy at age 65 and modal age at death, it is visible that modal age at death is not increasing as rapidly as life expectancy at age *x*. It is necessary to compensate the values of modal age at death or to use a more accurate calculation applying the Gompertz-Makeham function. Furthermore, there is a noticeable difference in the development of Western and Eastern Europe.

Keywords: Population ageing, Life expectancy at birth, Modal age at death

1 Introduction

21th century is from the demographic point of view mainly associated with the issue of population aging. This process is accompanied by an increasing rate of elderly persons, especially in economically developed countries. Mortality rates are improving and people live longer. The development of mortality in developed countries was neither linear nor logistic. Periods of faster or slower decline varied in time and some trends in mortality were unexpected. Currently,

New Trends in Stochastic Modeling and Data Analysis (*pp. 347*-357)
Raimondo Manca – Sally McClean – Christos H Skiadas (Eds)

decrease in mortality in older age groups is mentioned as a major factor in the aging population. Trend of continuous aging of the European population will continue in the next period. Demographic aging is defined as a shift of the age structure to older ages (Gavrilov - Heuveline, 2003).

The question of longevity - the individual's ability to survive and the average length of human life have always been the object of interest of human populations. Longevity is often incorrectly defined as the presence of a larger group of old aged people at some territory in a certain population. This term does not refer to the upper limit of human life, which we can reach. It reports that natural life expectancy is increasing for which we consider modal age at death (Pavlík, 2009). In studies of longevity the most often used indicators are life expectancy and modal age at death.

Life expectancy is an indicator like average. It represents the average age of deaths in a stationary population. Modal age at death is an indicator like mode. It is the age at which adults most frequently die and from this perspective it better captures the length of human life than the life expectancy (Demopædia). Modal age at death is kind of a typical age, which most people in the population are expected to live.

From a long-term view, life expectancy and modal age at death are extending in most of the selected countries. This ongoing growth has a different intensity for each country. In the Czech Republic, and even in the former socialist countries, growth in life expectancy was noticed only in the 1990s of the 20th century. In some of the Western European countries, for example in Austria, life expectancy has been growing steadily since the 1970s of the 20th century. This has created significant differences in life expectancy and modal age at death between countries. These differences are slowly decreasing as the differences in mortality between women and men are descending. However, male excess mortality remains in all selected countries.

Since the beginning of the 20th century we have been watching a significant improvement in the development of life expectancy and modal age at death. The increase of life expectancy is generally seen as a positive process. Primary impulse of the increase of life expectancy was caused by decline of infant mortality and consequently by decrease of mortality in older age groups. Due to the improvement of mortality ratios, modal age at death is increasing and life expectancy is gradually approaching. While examining trends in mortality, life expectancy and modal age at death should be followed synchronously. As long as mortality rates of different age groups will tend to improve, life expectancy and modal age at death will increase as well. The speed of development will depend on the ages that contribute to the improved mortality rates (Wilmoth, 2000).

Unlike life expectancy at birth, modal age at death is substantially affected by mortality of adults and therefore reacts more sensitive to changes that occur among older aged population (Horiuchi 2008; Kannisto 2001). In countries with low mortality rates, where most of the deaths are recorded in old age, the indicator modal age at death becomes primary for monitoring the changes in the age-at-death distribution (Ouellette - Bourbeau, 2011). After improved mortality

in the first years of life, the current answer for extending life expectancy and modal age at death is associated with reducing mortality rates in old ages.
Life expectancy is extending due to low child mortality and modal age at death is increasing due to the decline in mortality rates at high ages (Canudas-Romo, 2010). The differences in the trends over time of these indicators of longevity well reflect their orientation to various aspects of mortality (Cheung – Robine, 2009). Life expectancy is currently the most commonly used mortality indicator despite the fact that it includes disadvantages of mean. Modal age at death has no disadvantages of average, it is the modal age at death among adults. For the purpose of this article life tables were calculated for selected countries. Life expectancy was calculated by (Fiala, 2005) using the Gompertz-Makeham function. In this article we present only the method for calculating the modal age at death.

2 Calculating Modal Age at Death

Modal age at death can be estimated as a rough estimate (age at last birthday with the maximum number of deaths). We are looking for an age when the number of deaths in mortality tables is the highest.
However, as already mentioned, this is only a rough estimate and more accurate results are obtained when using parameters of Gompertz-Makeham function. Calculation of modal age at death was performed by Fiala (2005). For this calculation it is necessary to know some source data as total deaths is specified age group ($M_{t,x}$) and mid-year population in the same age group ($\overline{S_{t,x}}$) or total population at the beginning of one year ($S_{t,x}$) or total population at the end of one year ($S_{t+1,x}$). Primary characteristics of mortality are age-specific death rates. Age-specific death rate for one calendar year is calculated using the formula

$$m_{t,x} = \frac{M_{t,x}}{\overline{S}_{t,x}}.$$

When we don´t know the number of mid-year population, but we have the number of total population at the beginning of the year *t* and *t+1*, we use the following formula

$$m_{t,x} = \frac{M_{t,x}}{\frac{S_{t,x} + S_{t+1,x}}{2}},$$

Where $M_{t,x}$ is the number of total deaths in completed years *x* and in calendar year *t*, $S_{t,x}$ is the total population aged *x* at the beginning of the year *t*. Compensation of age-specific death rates at age 60 and above can be calculated by Gompertz-Makeham equation

$$\tilde{m}_x^{(GM)} = a + b \cdot c^{x+\frac{1}{2}}.$$

We select the beginning of the first $x_0 = 60$ and the length of intervals $k = 8$. We calculate the summation of empirical death rates by age in each interval and mark them as *G1, G2, G3*

$$G_1 = \sum_{x=60}^{67} m_x,$$
$$G_2 = \sum_{x=68}^{75} m_x,$$
$$G_3 = \sum_{x=76}^{83} m_x.$$

Now we can calculate the value of the parameter c of Gompertz-Makeham function whose eighth squared value can be expressed by using the sum of empirical death rates by age in each interval

$$c^8 = \frac{G_3 - G_2}{G_2 - G_1}.$$

Furthermore, it is necessary to calculate the value of the subexpression, by which we can express the remaining two parameters of the function

$$K_c = c^{60,5} \cdot (1 + c + ... + c^7) = c^{60,5} \cdot \frac{c^8 - 1}{c - 1}.$$

We can calculate the parameters b by using next expressions

$$b = \frac{G_2 - G_1}{K_c \cdot (c^8 - 1)},$$
$$a = \frac{G_1 - b \cdot K_c}{8}.$$

And according to these parameters of the Gompertz-Makeham function we can now calculate the modal age at death more precisely

$$\hat{y} = \frac{\ln \frac{\ln c - 2a + \sqrt{(\ln c - 4a) \cdot \ln c}}{2b}}{\ln c}.$$

3 Modal Age at Death and Life Expectancy in Selected European Countries

For reasons of comparison, countries representing the former socialist countries were selected (Bulgaria, Czech Republic, Slovakia, Ukraine) and the advanced Western countries (Austria, France, the Netherlands, Sweden). Choice of countries was also carried out according to the availability of required data. Not all countries are listed here because of the length of the article. Calculations are based on the data from "Human Mortality Database" for available years. Differences in modal age at death between women and men were smoothed by using the three-year moving average method to better reflect the trend over time. In this article this method was used only in case of differences in modal age at death between woman and men.

There are visible differences among the former socialist countries in the development of modal age at death, because modal age at death is developing more slowly compared to Western countries. At the beginning of the studied period differences in modal age at death between men and women were lower – 5 years for men and 3 years for women. Lowest values of modal age at death showed men in 1950 in the Czech Republic and Austria, women in the Czech Republic and Slovakia, highest values of modal age at death were for men and women in the Netherlands and Sweden. The highest values of modal age at death at the end of the studied period achieved France for both men and women. By contrast, the lowest values for both men and women were achieved by Ukraine (see figure 1 and figure 2). During the followed period differences between countries increased significantly, from a long-term view there is a divergence in the development of modal age at death. The difference between the countries at the end of the studied period was markedly higher – 14,5 years for men and 8,5 years for women.

From the perspective of the male excess mortality (see figure 1 and figure 2) it is visible how modal age at death for men and women differs in selected countries in different years. Again, differences between the former socialist countries and Western countries are noticeable. The smallest variance in modal age at death between men and women in 2010 was in Sweden and France and the highest variance was in Ukraine (see figure 3). According to figures 1 and 2 we can see that there was no growth in the decades at the beginning of the studied period, but rather a slight decrease of modal age at death. Only since 1970s there is an extending modal age at death in majority of the countries.

There was a considerable variability in the distribution of deaths by age in the previous period. At the present time, difference in the distribution of deaths by age has stabilized. What is more, the current model of mortality decrease where most of deaths are concentrated in a tight age range and where variability is low, could be kept for the future development (Wilmoth – Horiuchi, 1999).

Although mortality has been concentrated into shorter age intervals, it is impossible to tell for sure that it ever would be modified into one point in age. In human longevity, heterogeneity is a factor of individual variation (Vaupel 1979; Wilmoth – Horiuchi, 1998).

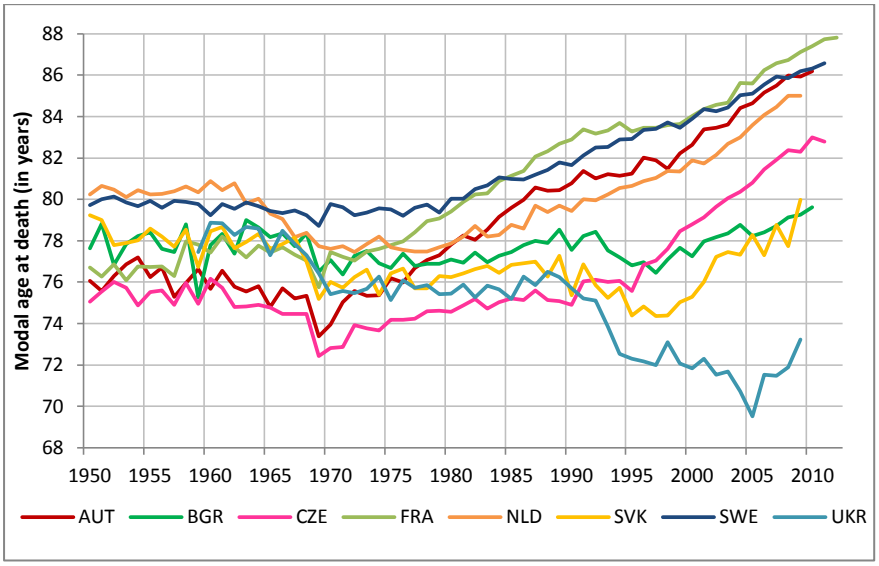

Fig. 1 Modal age at death for men in selected European countries in 1950-2012

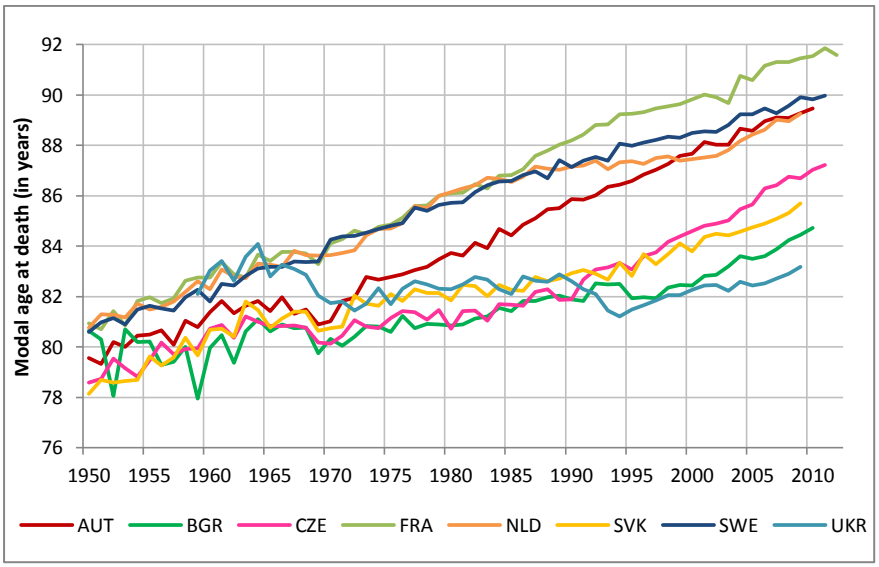

Fig. 2 Modal age at death for women in selected European countries in 1950-2012

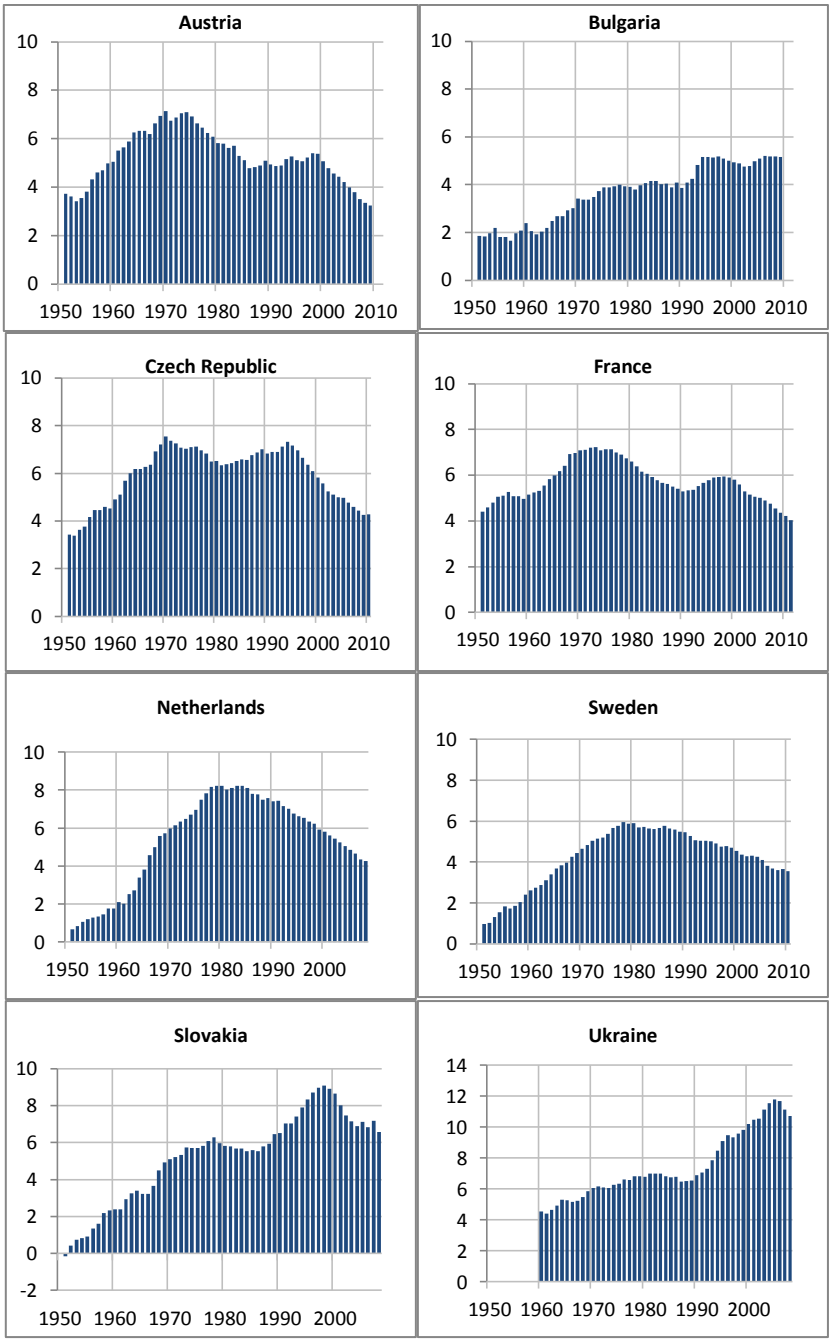

Fig. 3 Difference in modal age at death between women and men in selected European countries in 1950-2012

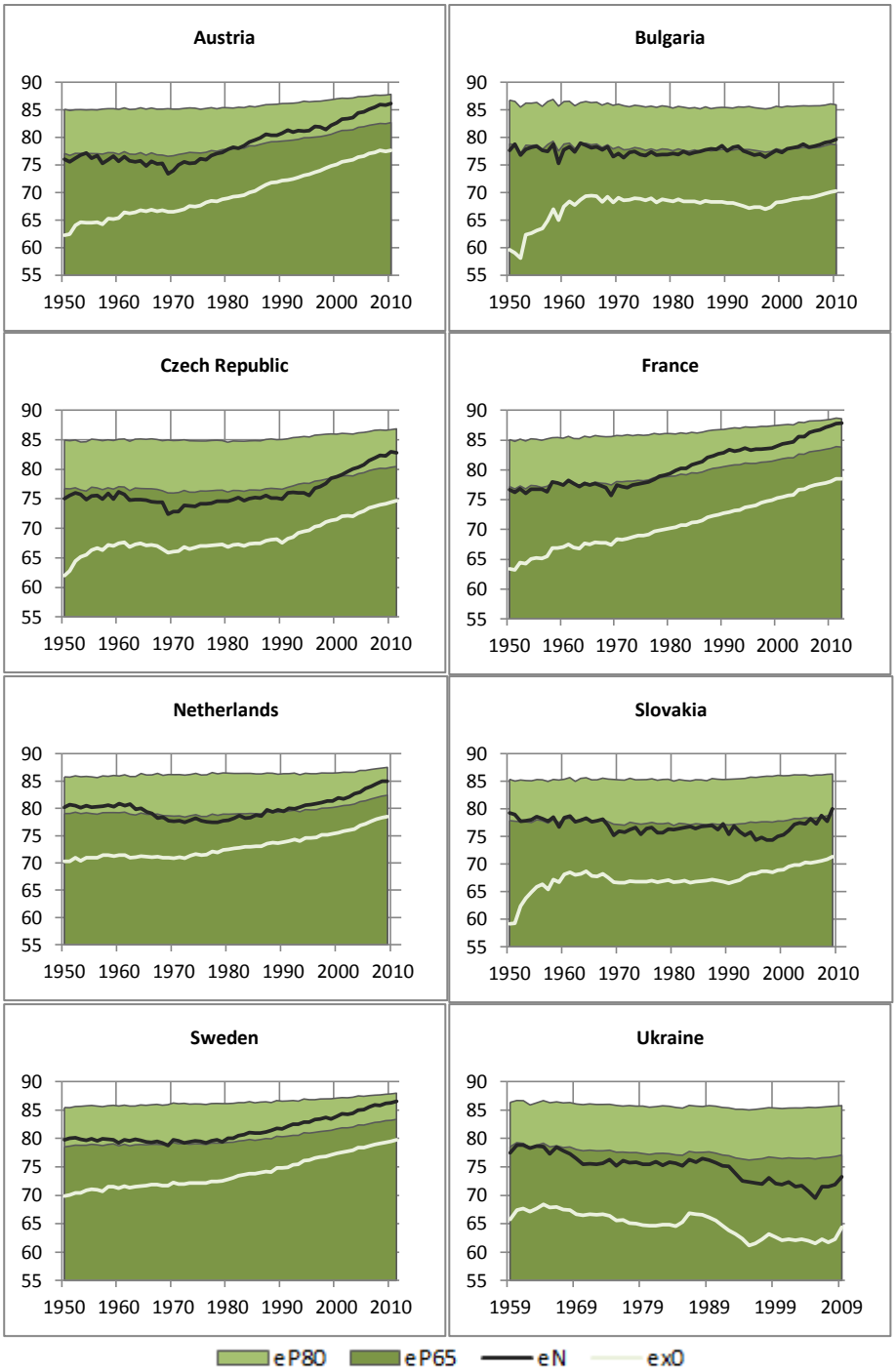

Fig. 4 Modal age at death, life expectancy at birth, probable age at death of 65-year-old and 80-year-old men in selected European countries in 1950-2012

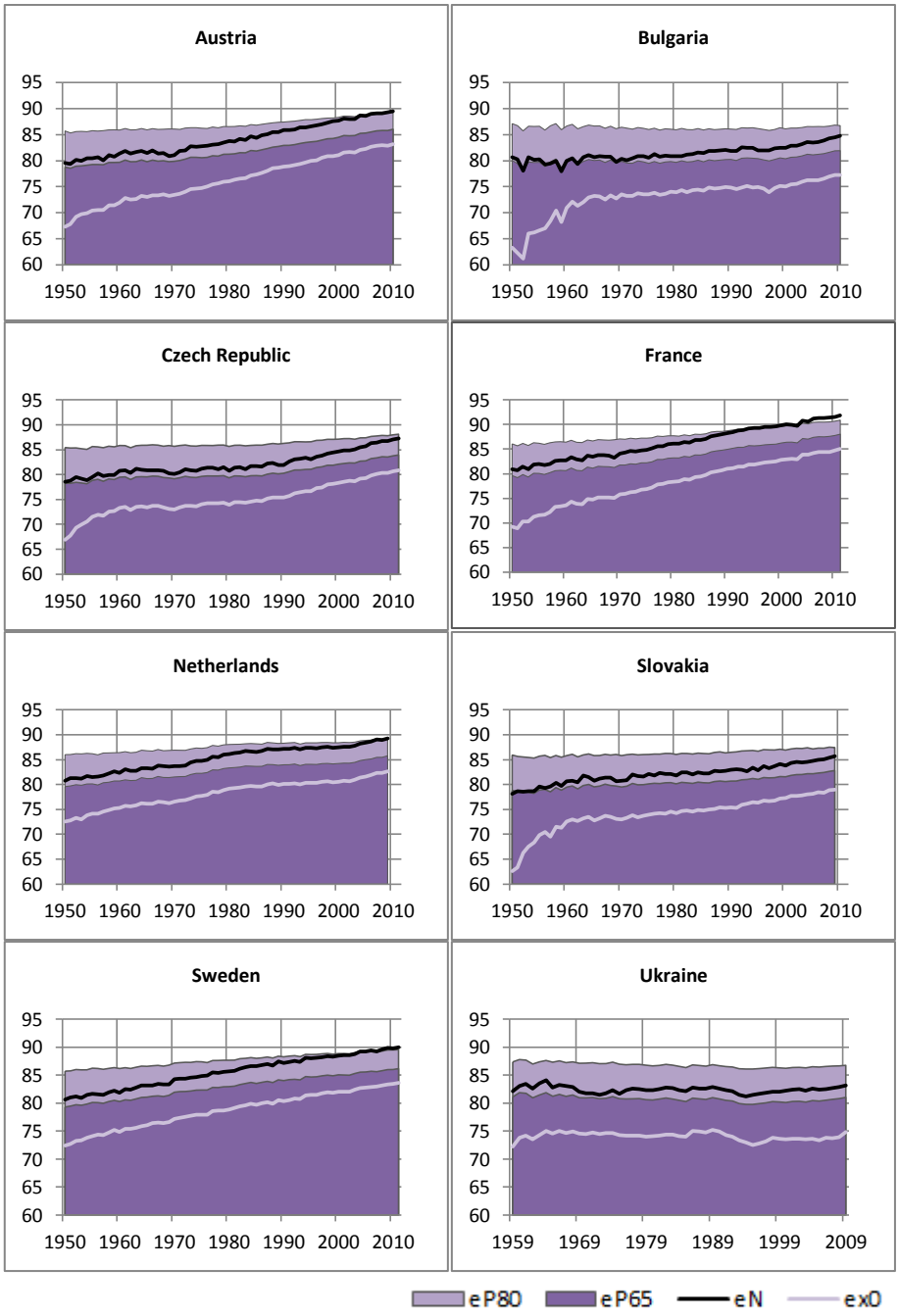

Fig. 5 Modal age at death, life expectancy at birth, probable age at death of 65-year-old and 80-year-old women in selected European countries in 1950-2012

Figure 4 and figure 5 compare the behaviour of modal age at death, life expectancy at birth and probable age at death for both men and women in monitored European countries in 1950-2012. The probable age of death we understand life expectancy for a *x*-year-old person plus age *x* years. Extending life expectancy and modal age at death for men and women are significant in Austria, Czech Republic, France, the Netherlands and Sweden. In Bulgaria, Slovakia and Ukraine the growth tendency of these indicators is not as high as in previous countries. From the figures 4 and 5 it is visible that modal age at death is copying the behaviour of probable age at death of 80-year-old men and women in the last decades and this trend is mainly in Western countries (Austria, France, the Netherlands, Sweden).

4 Conclusions

Life expectancy is influenced by infant mortality and by mortality at younger ages. Modal age at death is influenced by mortality in older ages. That is why it better reflects the typical life expectancy and longevity characteristics. Therefore, it is an appropriate complementary indicator for the evaluation of population aging. In terms of trends in life expectancy and modal age at death in the years 1950-2012 there is an increase of lifespan in most of the selected countries. Different trend is evident in the former socialist countries and in Western countries. In all countries male excess mortality is considerable. Expected future increase in life expectancy and modal age at death will considerably speed up the process of demographic aging. Population growth of Europe stagnates or is at very low levels. Acceleration of population aging means a burden for the productive part of the population and at this level we can not expect a significant improvement. According to projections, future working part of the population will be significantly formed by older people as well, due to improving mortality rates and longer lifespan. Evolution of mortality rates affects the process and intensity of population aging of developed countries. Mortality in the highest age groups in the next period may be affected by changes in the evolution of mortality. On the one hand, increase in the future longevity can be expected and modern technology will greatly help to reduce mortality at old ages (Illes et al., 2007). On the other hand, decrease of mortality can be slowed by epidemic of obesity and diabetes in developed countries (Olshansky et al., 2005). In the following period, these contradictory trends may influence the development of mortality and subsequently reflect on the process of demographic aging of populations of developed countries.

Acknowledgement

This article was supported by the Internal Grant Agency of University of Economics in Prague No. 68/2014 under the title “Economic and health connections of population ageing.”

References

1. Canudas-Romo, V. Three Measures of Longevity: Time Trends and Record Values. *Demography: The Population Association of America*. 2010, No. 2. http://www.ncbi.nlm.nih.gov/pmc/articles/PMC3000019/
2. Demopaedia [online]. 2012 [2014-03-25]. http://www.demopaedia.org/
3. Fiala, T. Výpočty aktuárské demografie v tabulkovém procesoru. Praha: Oeconomica, 2005. 177 s. ISBN 80-245-0821-4.
4. Gavrilov, L.A. and Heuveline, P. (2003). Aging of Population. In: Demeny, P. and McNicoll, G. (eds.). *The Encyclopedia of Population*. New York: Macmillan Reference USA: 32-37.
5. Horiuchi S, Wilmoth JR, Pletcher S. "A Decomposition Method Based on a Model of Continuous Change" Demography. 2008;45:785–801.
6. Cheung – Jean-Marie Robine. Dissecting the compression of mortality in Switzerland. Demographic Research [online]. 2009, No. 21 [cit. 2014-03-30]. DOI: 10.4054/DemRes.2009.21.19. http://www.demographic-research.org/volumes/vol21/19/21-19.pdf
7. Illes, J. – A. de Grey – M. Rae. 2007. "Ending aging: The rejuvenation breakthroughs that could reverse human aging in our lifetime." Nature, 450 (7168), 351–352.
8. Kannisto V. "Mode and Dispersion of the Length of Life" Population: An English Selection. 2001;13:159–71.
9. Olshansky, S. J. – D. J. Passaro – R. C. Hershow – J. Layden – B. A. Carnes – J. Brody – L. Hayflick – R. N. Butler – D. B. Allison – D. S. Ludwig. 2005. "A potential decline in life expectancy in the United States in the 21st century." New England Journal of Medicine, 352 (11), 1138–1145.
10. Ouellette, N. – R. Bourbeau. Changes in the age-at-death distribution in four low mortality countries: A nonparametric approach. *Demographic Research*. 2011, No. 25. DOI: 10.4054/DemRes.2011.25.19. http://www.demographic-research.org/volumes/vol25/19/25-19.pdf
11. Pavlík, Z. et al. *Demografie (nejen) pro demografy*. Praha: SLON, 2009, 241 s. ISBN 978-80-7419-012-4.
12. Vaupel, J. W. et al. The impact of heterogeneity in individual frailty on the dynamics of mortality. Demography [online]. 1979, No. 3, 439-454 [cit. 2014-03-30]. http://www.ressources-actuarielles.net/EXT/ISFA/1226.nsf/0/2d6493f9f0d93b50c125774b0045c00b/$FILE/Vaupel-Demography-16-1979-3.pdf
13. Wilmoth John R. "Demography of Longevity: Past, Present and Future Trends" Experimental Gerontology. 2000; 35:1111–29.
14. Wilmoth, John R. – S. Horiuchi. 1998. Do the oldest-old grow old more slowly? Paper presented at *Collogue médicine et recherche*, Paris
15. Wilmoth, John R. – S. Horiuchi. Rectangularization Revisited: Variability of Age at Death within Human Populations. Demography [online]. 1999, No. 36, 475-495 [cit. 2014-03-30]. http://www.jstor.org/stable/2648085

Youth mortality by violence in the semiarid region of Brazil

Neir Antunes Paes[1], and Everlane Suane de Araújo Silva[2]

[1] Postgraduate Programme in Decision Modelling and Health of the Department of Statistics of the Federal University of Paraíba, Cidade Universitária, João Pessoa, PB, Brazil.
(Email: antunes@de.ufpb.br)

[2] PhD Candidate in Postgraduate Programme in Decision Modelling and Health of the Department of Statistics of the Federal University of Paraíba, Brazil
(Email: everlanesuane@hotmail.com)

Abstract: The Brazilian semiarid region is the world's largest in terms of density population and extension with 22 million inhabitants in 2010. An ecological study addressing the mortality by aggression for 137 microregions of the Brazilian semiarid region to young males, in the year 2010, was performed. Two indicators were calculated for each microregion: standardized mortality rates by violence and an indicator named Reducible Gaps of Mortality. We investigated the correlation between standardized mortality rates and a set of 154 indicators that express living conditions. 18 of them were considered as significant. By means of the multivariate technique - Principal Component Analysis - the construction of a Synthetic Indicator was performed, which was categorized in four strata reflecting different living conditions and mortality rates. The results showed that microregions with high values of mortality rates by aggressions were present in all strata, thus contradicting some studies linking high rates of mortality due to aggression to low condition of life. This paradox allowed us to raise issues to identify the most vulnerable regions, and contribute to the decision making process to combat mortality by violence of the Brazilian semiarid population.
Keywords: Mortality by violence. Living conditions. Young.

1 Introduction

The semiarid region is divided into 137 microregions and, in turn, distributed in 1,135 municipalities in the geographic space of 9 (from 27) units of the federation. It is the world's largest in terms of population density and extent, with some 22.6 million people in 2010, and represent approximately 12% of the population. The indicators show that the level of development is considered as the most precarious of the country, and flattens to many African countries less developed, Brasil [1].

New Trends in Stochastic Modeling and Data Analysis (pp.359 -366)
Raimondo Manca – Sally McClean – Christos H Skiadas (Eds)

Currently, public security gains prominence among the issues that most concern the Brazilian society, and takes along with health and education, the priority for the attention of public authorities according to Waiselfisz [2]. Today the external causes in Brazil are the third most frequent cause of death, and predominate in the age group 10-24 years for males, Brasil [3]. Paradoxically, has occupied a limited place in the themes discussed by public administrators to implement policies to promote the common welfare in this region, UNICEF [4]. It is a problem to be overcome, the lack of a synthetic statistical indicator that expresses the association between living conditions and mortality from violence. In seeking to answer this question, we have as main objective the construction of a synthetic indicator for young men aged 10-24 years in the Brazilian semiarid region.

2 Methods

This is an ecological study of census basis that covers nine states. The geographical units of study are the 137 microregions that form the semiarid region in 2010. The following demographic and socioeconomic indicators were used: population, income, education and health. Data on deaths of residents were obtained from the website of the Ministry of Health through the Brazil Mortality Information System [5]. Indicators related to cause of death from aggression of the youths and indicators of living conditions were calculated: a) Standardized Mortality Rate (SMR); b) Reducible Gaps of Mortality (RGM), which means how much a region missed in preventing a particular cause of mortality compared with the SMR of a reference region (Here we considered the median of the microregions) c) 154 indicators on living conditions (health, education and income) were selected, which were obtained from Brazil Atlas of Human Development [6] produced by the United Nations Development Programme .

In order to measure the degree and direction of the linear association between the variables (living conditions and mortality rates by aggression) the Pearson correlation coefficient was calculated, and was built a correlation matrix on them, adopting a level of significance of $\alpha = 0.05$.

The multivariate technique Factor Analysis (FA) was used for the calculation of a Synthetic Indicator corresponding to each microregion (Hair et al., [7]. The number of factors extracted was obtained by the criterion of latent roots (eigenvalues) greater than one. The method of orthogonal Varimax rotation was used to facilitate the reading of the factors and simplify the columns of the matrix factors. The measures used were the adequacy of Kaiser-Meyer-Olkin (KMO) and Bartlett Sphericity Test, which indicate the degree of susceptibility or adjustment to the FA. Thus, one can evaluate that the confidence level of the data for the multivariate method of FA was successfully employed. Another measure of fitness used consisted of verifying the communality of the variables with values ≥ 0.50 as having a sufficient explanation. Thus, variables were identified and grouped into factors. A Synthetic Indicator was generated by the linear combination of the variables and coefficients generated by principal component. Therefore, the

Synthetic Indicator, which summarizes the living conditions and mortality by aggression for the semiarid microregions was given by:

$$Synthetic\ Indicator\ d_k = w_{1k}\, v_{1k} + w_{2k}\, v_{2k} + \ldots + w_{pk}\, v_{pk}$$

Where *k* represents the number of microregions (137), *p* is the number of variables (v) selected by the correlation test (18), and (*w*) the weights or coefficients generated by the main component.

After obtaining the values of the Synthetic Indicator, which represent living conditions together with mortality by aggressions, the microregions were sorted in descending order into quartiles, corresponding to four strata. As a way to show a correspondence of our indicator with a very known Synthetic Indicator (Human Development Index - HDI), to each stratum was assigned a combination that associates the degree of HDI with a degree of violence: (I) HDI medium with high degree of violence, (II) HDI medium with low degree of violence; (III) HDI low with high degree of violence (IV) HDI low with low degree of violence. This made it possible to identify the best and worst microregions in terms of living conditions associated with different degrees of deaths from violence.

3 Results and Discussion

The figures show that 53% of the municipalities in the semiarid region showed a degree of urbanization higher than 50%, much lower than the rest of the country, reaching up to about 85%. With a small urban predominance, the male mortality by aggressions exceeded significantly the female mortality in 2010. The mortality by aggressions on the total deaths for the young men was very high reaching a percentage of 62.1%. For women, this percentage reached a maximum value of 33.4%. Among men, 72 of the 37 microregions, ie, 52.2% of them had a percentage of deaths by aggressions higher than 25%. Similarly, high rates of standardized mortality were found. The rates for men ranged between 3.6 and 63.3 deaths/100.000 men, while for women the range was between 1.3 and 21.5 deaths/100.000 women.

The values of RGM suggest that the states of Ceará, Pernambuco and Alagoas stood out for having the majority of microregions in the most critical situation, with positive values, compared to the median value. This is indicative of a greater need for attention to reducing the incidence of these deaths. The States of Paraiba, Sergipe and Bahia presented the values of the microregions in two situations: below and higher in relation to the SMR of the microrregion considered as reference. The states of Rio Grande do Norte and Minas Gerais have had most of their microregions in a more favorable situation with negative values. The Piauí State, was the only one with SMR below (negative) the reference value.

The correlation matrix among the 154 variables used initially to express the conditions of life and SMR by aggression, revealed that only 18 of them were statistically significant ($p<0.05$). They correspond to the six dimensions of the

Brazil Atlas of Human Development [6]: demography, income, employment, housing, vulnerability and education, the latter being responsible for the largest number of indicators.

From the 18 selected variables, 6 factors were selected after applying the technique of factor analysis (FA). These factors explained 75.9% of the total variability in the data. They include the variables of living conditions correlated with SMR by aggression, which were used for the stratification of the microregions towards greater explicability of the multivariate analysis.

To confirm the hypothesis that the correlation matrix is an identity matrix (Table 1), Bartlett's test of sphericity produced a chi-square statistic equal to 1941.390 with degree of freedom (df) of 153, providing significant p-value = 0.000, whose decision was to reject the null hypothesis H_0: the correlation matrix is an identity matrix. Therefore, the correlation matrix is significantly different from the identity matrix. The KMO index - a measure of sampling adequacy showed a score of 0.730 indicating that the adequacy of the factor analysis method was "medium" for the treatment of the data. The communality for each variable presented a recommended value, ie, above 0.50.

The classification of variables in each factor was based on the value of the factorial loading. The six factors were selected for analysis using the latent root criterion, where the factor/component is selected if its eigenvalue is greater than one (1). The first factor explained most of the variability in the data (27.0%), and involved six indicators/variables with prevalent coefficients. This factor was formed by the dimension related to education indicators. The second factor was formed by two indicators related to the work and income. In the third factor appeared indicators of the dimension: housing, vulnerability and demography. Fourth, fifth and sixth factors included indicators related to income, work and vulnerability.

The correspondence from the Synthetic Indicator proposed in this work with the HDI indicator combined with different levels of violence is shown in Table 1, classified in four strata.

Table 1. Classification of stratum, according to the condition of life and the standardized mortality rates by aggression of the microregions of the semiarid for young males, Brazil 2010.

HDI/SMR	Stratum I	Stratum II	Stratum III	Stratum IV
	HDI medium with high degree of violence	HDI medium with low degree of violence	HDI low with high degree of violence	HDI low with low degree of violence
IDH Medium	0,611	0,601	0,586	0,578
SMR Medium	44,734	35,027	47,810	39,528

Sources of basic data: Brazil 2013 Human Development Atlas [6].
HDI - Human Development Index, SMR - Standardized Mortality Rate by aggression.

The values of the Synthetic Indicator for microregions according to the adopted classification are shown in Table 2. The microregions that comprise the stratum I, associates a standard of living expressed by an average of HDI of 0.611, classified

Table 2. Classification of microregions of the semiarid, according to the living conditions and mortality rates by aggression for males, Brazil 2010.

Stratum I-HDI medium with high degree of violence		Stratum II-HDI medium with low degree of violence		Stratum III-HDI low with high degree of violence		Stratum IV-HDI low with low degree of violence	
Microregions	*Scores*	*Microregions*	*Scores*	*Microregions*	*Scores*	*Microregions*	*Scores*
Mossoró (RN)	3667,9	Cajazeiras (PB)	487,6	Itaberaba (BA)	-42,0	Alto Médio Canindé (PI)	-511,1
Macaíba (RN)	2586,8	Santa Maria da Vitória (BA)	437,0	Serra de Santana (RN)	-86,5	Seridó Ocidental (RN)	-513,0
Cariri (CE)	2523,2	Janaúba (MG)	398,3	Campina Grande (PB)	-130,2	Traipu (AL)	-554,5
Sertão do São Francisco (AL)	2229,4	Euclides da Cunha (BA)	389,0	Cariri Oriental (PB)	-130,9	Montes Claros (MG)	-562,7
Pedra Azul (MG)	2134,8	Itapetinga (BA)	380,6	Curimataú Oriental (PB)	-165,2	Boquira (BA)	-564,0
Macau (RN)	2105,4	Guanambi (BA)	375,2	Barra (BA)	-185,0	Vale do Ipojuca (PE)	-572,7
Seridó Oriental (RN)	2086,7	Santa Quitéria (CE)	358,7	Juazeiro (BA)	-186,6	Chorozinho (CE)	-577,4
Propriá (SE)	2023,7	Médio Jaguaribe (CE)	316,7	Guarabira (PB)	-218,4	Pio IX (PI)	-613,4
Senhor do Bonfim (BA)	1995,6	Serrinha (BA)	315,9	Salinas (MG)	-220,5	Cotegipe (BA)	-619,9
Tobias Barreto (SE)	1956,5	Litoral Nordeste (RN)	315,4	Umbuzeiro (PB)	-236,2	Brejo Pernambucano (PE)	-620,2
Vale do Açu (RN)	1801,3	Pajeú (PE)	307,9	Esperança (PB)	-243,8	Sousa (PB)	-641,1
Nossa Senhora das Dores (SE)	1747,0	Almenara (MG)	298,1	Palmeira dos Índios (AL)	-245,9	Jeremoabo (BA)	-653,5
Itapipoca (CE)	1630,7	Agreste Potiguar (RN)	273,1	Batalha (AL)	-268,8	Patos (PB)	-684,0
Carira (SE)	1575,9	Chapada do Araripe (CE)	272,1	Alagoinhas (BA)	-297,8	Garanhuns (PE)	-697,8
Baixo Curu (CE)	1528,7	Sertão de Cratéus (CE)	255,3	Coreaú (CE)	-301,4	Baturité (CE)	-718,4
Chapada do Apodi (RN)	1496,0	Umarizal (RN)	250,8	Serra do Pereiro (CE)	-309,5	Itaporanga (PB)	-740,2
Bertolínia (PI)	1430,1	Seridó Ocidental Paraibano (PB)	223,8	Cariri Ocidental (PB)	-330,5	Borborema Potiguar (RN)	-743,8
Alto Médio Gurguéia (PI)	1273,2	Barro (CE)	197,4	Curimataú Ocidental (PB)	-349,8	Itabaiana (PB)	-858,6
Santo Antônio de Jesus (BA)	1248,2	Sertão de Quixeramobim (CE)	177,0	Catolé do Rocha (PB)	-354,9	Araçuaí (MG)	-900,1
Petrolina (PE)	1141,2	Valença do Piauí (PI)	171,7	Santana do Ipanema (AL)	-368,2	Arapiraca (AL)	-956,6
Pacajus (CE)	1106,2	Serra de São Miguel (RN)	169,8	Sertão de Inhamuns (CE)	-372,1	Picos (PI)	-962,5
Itaparica (PE)	1067,1	Caririaçu (CE)	145,5	Bom Jesus da Lapa (BA)	-372,6	Várzea Alegre (CE)	-982,4
Lavras da Mangabeira (CE)	1009,6	Pau dos Ferros (RN)	144,3	Seridó Oriental Paraibano (PB)	-375,1	Médio Capibaribe (PE)	-1029,3
Litoral de Aracati (CE)	928,0	Meruoca (CE)	132,4	Canindé (CE)	-383,7	Livramento do Brumado (BA)	-1110,7
Iguatu (CE)	873,6	Piancó (PB)	114,8	Brejo Santo (CE)	-414,1	Brumado (BA)	-1117,2
Baixo Jaguaribe (CE)	839,5	Jacobina (BA)	109,4	Feira de Santana (BA)	-424,0	Serrana do S. Alagoano (AL)	-1130,5
Seabra (BA)	782,9	Ipu (CE)	106,1	Serra do Teixeira (PB)	-435,2	Vale do Ipanema (PE)	-1146,5
Sertão do São Francisco (SE)	781,9	Floriano (PI)	104,8	Ribeira do Pombal (BA)	-442,4	Vitória da Conquista (BA)	-1371,7
Baixa Verde (RN)	715,7	Médio Oeste (RN)	92,2	Araripina (PE)	-449,5	Chapadas do Extremo Sul (PI)	-1452,6
Fortaleza (CE)	608,8	Capelinha (MG)	67,8	Sertão de S. Pompeu (CE)	-463,1	Brejo Paraibano (PB)	-1565,2
Salgueiro (PE)	606,4	Paulo Afonso (BA)	55,2	Alto Capibaribe (PE)	-466,9	São Raimundo Nonato (PI)	-1692,4
Sobral (CE)	570,7	Médio Curu (CE)	44,1	Campo Maior (PI)	-508,8	Sertão do Moxotó (PE)	-1742,4
Angicos (RN)	568,3	Jequié (BA)	2,1	Januária (MG)	-509,7	Agreste de Itabaiana (SE)	-1773,0
Ibiapaba (CE)	561,7	Uruburetama (CE)	-15,6	-	-	Litoral Piauiense (PI)	-2002,3
-	-	Irecê (BA)	-32,4	-	-	Grão Mogol (MG)	-2362,7

Sources of basic data: Brazil 2013 Human Development Atlas [6].
HDI: Human Development Index.

as medium degree of violence. The microregions were considered with high level of violence. In stratum II the average HDI with a score of 0.601, was also considered medium grade, and was associated with a low level of violence. Stratum III presented an average HDI of 0.586 and stratum IV with 0.578, both considered of low levels. The microregions were associated, respectively, to a high and low level of violence.

All strata included microregions with high and low values of SMR by agression, no matter the level of the HDI, medium or low. For instance, the microregion of Mossoró (RN) with the highest score (3667.9) in Stratum I was associated to a very high mortality rate. At the other extreme is the microregion of Irecê (BA) with the lowest score (-32.4) in the Stratum II, which was associated to a low mortality rate. Similarly, this fact was also observed when considering the Stratum III and IV. Strong positive association was found for microregions with a medium score of living conditions and a low mortality rate. On the other hand, microregions with low life conditions was associated with high mortality. This fact sugests a paradox for the Brazilian semiarid region.

In many cases it was possible to note the disparity between microregions belonging to the same State. The regions of almost all states were classified in all strata. It was unable to identify a unique pattern of relationship between level of living conditions and level of violence. These relationships occurred in various ways, independent of the level of development of the region.

4 Conclusions

The mortality rates by aggressions and reducible gaps of mortality revealed high magnitudes at several regions of the semiarid region. The results point to the need for development of more effective and explicit politics to prevent these deaths among youth. The link between high mortality rates by aggressions and low living condition is very usual. Nevertheless, it was found that the microregions of the Brazilian semiarid region in 2010 with high levels of mortality were present in all strata of living conditions (medium or low).

In the application of Factor Analysis, the first factor explained most of the variability in the data (27.0%), which was formed by indicators related to education dimension. Groot and Brink [8] in a study conducted in 1996 in the Netherlands, Duenhas and Gonçalves [9] in Spain, Soares [10] for a set of countries, support the idea that education is a means of crime prevention, especially violent crimes. These authors argue that education can contribute to reducing violence.

For Brazil, study carried out by Lobo and Fernandez [11] covering ten counties in the metropolitan region of Salvador for the period 1993-1999 indicated that if municipalities have access to education could contribute to reducing crime. Duenhas and Gonçalves [9] found that municipalities that spent more on education and public safety in the period 2000-2005 presented fewest number of homicides per hundred thousand inhabitants. Using longitudinal aggregate data regarding to Census 1991 and 2000, Oliveira [12] found association between crime to the size

of cities. This study raises the hypothesis that cities with larger populations have higher rates of homicide. Also argued that inequality, poverty and inefficiency of teaching contribute to increased violence in Brazil. França, Paes and Andrade [13] developed a study for Brazilian metropolitan and non-metropolitan areas for 2000. They found that the M-HDI (Municipal Human Development Index) acted in the opposite direction: a higher degree of development of these municipalities favored a lower rate of young homicide.

The conclusions drawn by the authors do not seem to express what we found for the semiarid region of Brazil. Violence is present both in very urbanized regions as in the less urbanized; in more developed regions or not; both in regions with higher educational level as the lower level. Thus, it appears that violence in the semiarid region presents multiple relationships difficult to capture. The coexistence of different living conditions associated with different levels of violence in these regions appears as a paradox, whose population coexists with an open insecurity. The existence of this paradox makes it difficult to identify any patterns of association between living conditions and violence.

Even considering limitations such as data quality for some microregions, and measurement errors in the construction of the indicators, the results suggest that one can not explain violence by a single variable, or by a short set of them. Despite the effort to capture the violence of young people, after a selection of 154 indicators/variables that resulted in 18 of them statistically significant, which represented various dimensions of living conditions, the theme does not end here.

References

1. BRAZIL. Instituto Nacional do Semiárido. Synopsis of the census for the Brazilian semiarid, http://www.insa.gov.br/censosab/publicacao/sinopse.pdf, 2013.
2. Waiselfisz, J. J., Map of Violence 2012: The New Pattern of Homicidal Violence in Brazil. São Paulo: Sangari Institut, 2011.
3. BRAZIL. Ministério da Saúde. Epidemiology of external causes in Brazil: mortality from accidents and violence in the period 2000-2009, http://portal.saude.gov.br/portal/arquivos/pdf/cap_11_saude_brasil_2010.pdf, 2010.
4. UNICEF. Fundo das Nações Unidas para a Infância - The Brazilian Semiarid, and Food Safety and Nutrition in Children and Adolescents, 2005.
5. BRAZIL. Mortality Information System . Deaths from external causes, http://tabnet.datasus.gov.br/cgi/deftohtm.exe?sim/cnv/ext10ba.def , 2013.
6. Brazil 2013 Human Development Atlas. http://atlasbrasil.org.br/2013/pt/home/, 2014.
7. Hair, J. F. et al., Multivariate Data Analysis, 7th edition, Pearson Prentice-Hall Publishing, 2009.
8. Groot, W. and Brink, H. M. V. D., The effects of Education on Crime. "Scholar" Research Center for Education and labor Market – Department of Economics, University of Amsterdam, Amsterdam, 2002.
9. Duenhas, R. A. and Gonçalves, F. O., Education, Public Safety and Violence in Brazilian Municipalities: An Analysis of Dynamic Panel Data. Paper presented at XVII National Meeting of Population Studies, Caxambú, Brazil, 21-23 September, 2010.
10. Soares, R. R., Development, crime and punishment: accounting for the international differences in crime rates, in Journal of Development Economics, **7**3, 1, 155-184, 2004.
11. Lobo, L. F. e Fernandez, J. C., Crime in the metropolitan city of Salvador**.** Paper

presented at XXXI National Meeting of Economy, Porto Seguro, Brazil, 09-12, December, 2003.
12.Oliveira, C. A., Crime and the size of the Brazilian cities: focus of the criminal economy. Paper presented at XXXIII National Meeting of Economy, Natal, Brazil, 06 – 09 December, 2005.
13. França, M. C. and Paes, N. A. and Andrade, R. C. C., Determinants of mortality by homicide among young people in urban areas of Brazil. Paper presented at International Seminar on "Violence in Adolescence and Youth in Developing Countries". Organized by: IUSSP Scientific Panel on Young People's Life Course in Developing Countries. New Delhi, India, 09-11 October, 2012.

Smoothing of probabilities of death for older people in life expectancy tables

Gustaf Strandell[1], Tomas Johansson[2]

[1] Statistics Sweden, SCB, 701 89 Örebro, Sweden
(E-mail: Gustaf.Strandell@scb.se)
[2] Statistics Sweden, SCB, 701 89 Örebro, Sweden
(E-mail: Tomas.Johansson@scb.se)

Abstract. This paper focuses on the smoothing procedure used at Statistics Sweden for handling of probabilities of death for persons in the highest ages, where the population is small and mortality is high. The paper also demonstrates how the smoothing affects the estimated average life expectancies at the national and regional levels.
Keywords: Life table, Probabilities of death, Smoothing, Life expectancy.

1 Introduction

Life expectancy tables in Sweden are based on data on population size and deaths during either a one-year or a five-year period. The tables are produced annually for the whole country, for its 21 counties and 290 municipalities (the table based on one year of data is only produced for the whole country). In addition to the remaining average life expectancies, the publication of the life expectancy table includes sex-specific probabilities of death for all ages.
In 2012, Statistics Sweden conducted a review of the calculations for the periodic life expectancy tables. The project had two main objectives, of which the second is addressed in this paper:

1. A quality assured production system, and
2. Review of the handling of probabilities of death for very old persons at the national and regional levels.

Usable estimates of probabilities of death q_x can be difficult to obtain for the highest ages in a population. Since there might be few survivors and hence few deaths in higher ages the observed probabilities of death can often be seen to fluctuate significantly between ages or between time periods.

New Trends in Stochastic Modeling and Data Analysis (pp. 367-376)
Raimondo Manca – Sally McClean – Christos H Skiadas (Eds)

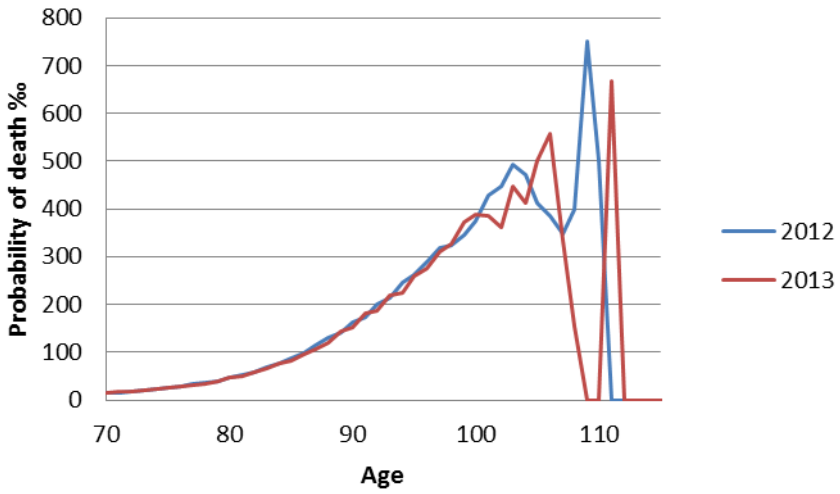

Fig.1. Non smoothed probabilities of death (‰) for the population of Sweden 2012 and 2013

To address this problem Statistics Sweden applies a smoothing procedure to the probabilities of death for the highest ages and over the years various methods to do this has been tried. Until 1986 Wittstein's method was used, which overestimated the probabilities of death for the oldest persons. Therefore in 1987, Sten Martinelle at Statistics Sweden constructed a new smoothing procedure which was used successfully for many years. However, this method, where by Martinelles modeled probabilities of death replaced the observed probabilities for ages 90 and above, relied heavily on mortality data for Sweden and some other countries up to 1987 and did not fully take into account the observed probabilities to be smoothed. Therefore, over time, the smoothing process deteriorated, resulting in a systematic underestimation of probabilities of death and an overestimation of the remaining life expectancy for newborns, e_0. Thus, in 2012, when the calculations for the life expectancy table were up for review it was decided that Martinelles method was to be evaluated, resulting in an updated method which provides smoothed probabilities of death with a better fit to the observed data.
This report focuses on the updated method used since 2012 by Statistics Sweden. It also demonstrates how the updated smoothing affects estimated average life expectancies at the national and regional levels.

2 The model for smoothing probabilities of death

The updated method used by Statistics Sweden for smoothing of the probabilities of death in high ages is based on the model chosen by Sten Martinelle for old-age mortality, Martinelle[3].

The basic assumption underlying the model states that age specific adult mortality for a single individual in a population, in terms of the force of mortality $\mu(x)$ where x denotes age, is well approximated by the Gompertz-Makeham formula

$$\mu(x) = A + Be^{kx} \qquad A \geq 0,\ B > 0, k > 0.$$

The constant B is called the 'frailty' of the individual and measures his or her inability to withstand destruction.

In the past many authors has pointed out that it is medically well established that frailty is different for different individuals in a population. It is hence customary to assume that frailty follows a probability distribution over a population rather than being the same number for all individuals. This line of thought has given rise to the study of so called frailty models within the theory of survival analysis, see for example Wienke[5]. It was proved by Beard[1] that if the frailty B is gamma distributed then the mean of the force of mortality taken over the population follows the Perks formula, as suggested by Perks already in 1932, Perks (1932):

$$\mu(x) = \frac{A + Be^{kx}}{1 + De^{kx}} \qquad A \geq 0, B > 0, D > 0, k > 0.$$

Martinelles main objection towards using Perks formula is that it implies that the force of mortality approaches a constant limit value B/D in high ages. He argues that there is no empirical evidence for a plateau in the mortality for centenarians. Therefore he modifies the assumption leading to Perks formula, and replaces the assumption of a gamma distributed frailty with an assumption of a frailty with a generalized gamma distribution which has been shifted to the right, thus assuming that it is impossible for the frailty to assume values very close to zero.

In the case where the constant A in the Gompertz-Makeham formula is assumed to be zero, which seems reasonable in Sweden in modern times, Martinelles model of the frangible man states the following:

If the force of mortality for individuals with frailty z follow the Gompertz-Makeham law $\mu(x \mid z) = ze^{kx}$ and the frailty variable z has a shifted gamma distribution with density

$$g(t) = \begin{cases} \dfrac{b^a (t-c)^{a-1}}{\Gamma(a)} e^{-b(t-c)} & \text{for } t > c \\ 0 & \text{for } t \leq c \end{cases}$$

$(a, b, c > 0)$, then the mean force of mortality over the population, $\mu(x)$, is given by

$$\mu(x) = \left(c + \frac{\eta}{1 + \eta\alpha^2 \int_{x_0}^{x} e^{kt} dt} \right) e^{kx}$$

Where η and α are the mean and the relative standard deviation of the variable $z-c$.

As usual the probabilities of death q_x is (with good approximation) associated with the force of mortality by

$$q_x = 1 - e^{-\mu(x)}.$$

Substituting the expression above for the modelled mean force of mortality into this expression for q_x, we end up with the formula we use for smoothing of the probabilities of death for high ages

$$q_x = 1 - e^{\left(c + \frac{\eta}{1+\eta\alpha^2 \int_{x_0}^{x} e^{kt} dt} \right) e^{kx}}.$$

This far, the new updated procedure used by Statistics Sweden since 2012 follows Martinelles suggestions in Martinelle[3]. The fitting of the model to mortality data is however new and improved. Martinelle used a large set of historical mortality data for a number of countries to produce a more or less universal smoothing curve which was used for all regions and all time periods. Instead of using a large set of historical data the model is now, whenever possible, fitted using only probabilities of death observed for the region and the time period for which the life expectancy table is to be produced. Thus the smoothed probabilities now more explicitly take into account the observed difference in mortality between regions and between time periods.

The model for the age specific probabilities of death contains 4 parameters: α, k, c and η. The modeled probabilities dependence on α and k is indicated in the diagram below where $c = 1{,}363 \cdot 10^{-7}$ and $\eta = 5{,}535 \cdot 10^{-7}$.

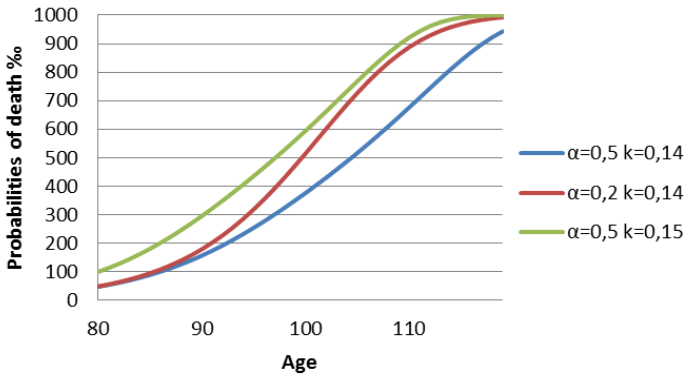

Fig.2. Modeled probabilities of death

For the very high ages a decrease in α leads to a steeper increase of the probabilities of death between ages, an increase in k leads to an almost constant increase of the probabilities for a broad interval of high ages.
It is technically cumbersome to fit this model to mortality data without first fixing two of the parameters. After testing numerous different parameter settings against data we decided to fix the parameters $\alpha \equiv 0{,}5$ and $k \equiv 0{,}14$. Our experimentation also showed that it is not recommended to use probabilities of death for all available ages to fit the model. We got much better results when we restricted the mortality data used as input to the fitting procedure to ages in a span between m and n, to be specified below, then when we used all ages or even all higher ages. Finally we decided it preferable to use age specific weights in the fitting of the model. The reason for this is that especially for smaller populations, the probabilities of death for certain ages can be zero (if no one dies) or one (if everybody dies) and these extreme values has a tendency to gain an unjustified influence on the modeled probabilities of death for the other ages. Therefore we decided to use the number of deaths per age as weights in the fitting of the model.
To fit the model to observed probabilities of death we use a weighted least square method: If the model $q_x = q_x(c,\eta)$, where α and k has been fixed as above, is to be fitted to the observed probabilities of death $\tilde{q}_m,...,\tilde{q}_n$ over the age interval from age m to age n, we try to find c and η which minimizes the expression

$$\frac{1}{n-m+1}\sum_{x=m}^{n} v_x{}^2(\tilde{q}_x - q_x(c,\eta))^2$$

where v_x are the nonnegative weights. To do this in practice we use the *model procedure* in SAS.

3 Results

At the national level, the model is fitted using probabilities of death observed in the age interval between $m = 90$ and $n = 100$ years. Since the number of individuals in the higher ages, and hence the number of deaths among them, has increased over the years the age at which the smoothing start to take place was also increased from 91 to 95 years.

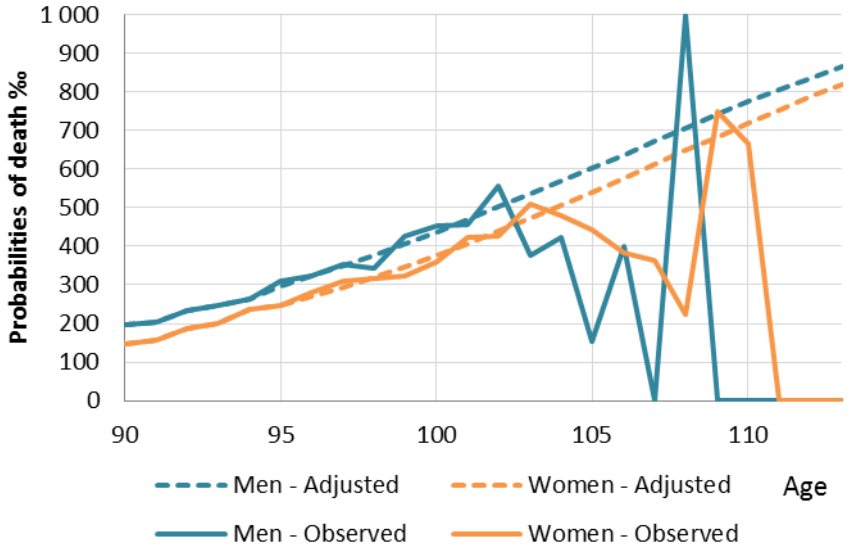

Fig.3. Observed and adjusted probabilities of death by sex and age (90 to 113) for Sweden 2012

The effect of the update of the smoothing method on the probabilities of death can be seen in the diagram below. For example the probability of death for women age 100 in 2011 was raised by over 10% with the updated method compared with the old method.

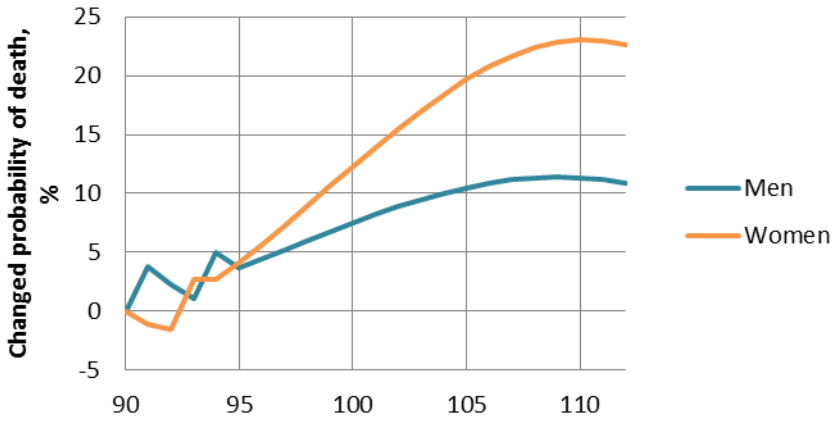

Fig.4. Difference in probability of death between new and old smoothing method 2011

Although the probabilities of death for ages 95 and over have clearly changed with the new method compared with the old one, the update of the smoothing method did not bring about particularly large changes in average life expectancies for the whole of Sweden. As suspected, the updated method gives life expectancies which are very close to those gained if the life expectancy table were to be produced without any smoothing. For the whole country the smoothing has thus more of a cosmetic effect on the mortality data (which is a good thing and can be very important for the presentation of the data).

Sex	Age	No smoothing	Old smoothing method	Updated smoothing method
Male	**e0**	79.8	79.81	79.79
	e85	5.51	5.54	5.5
Female	**e0**	83.67	83.7	83.67
	e85	6.61	6.66	6.61

Table.1. Average life expectancies for Sweden 2011

At the county level, in order to capture regional differences in mortality among the elderly, the model is also fitted using only the observed probabilities of death for the region at hand. However, the population in most counties is too small to appropriately apply the same method for the counties as for the national level. After extensive testing, it was decided that the fitting of the model would be based on observations in the age interval of 80 to 100. It was also decided that the smoothed probabilities of death would be used from the age of 90.

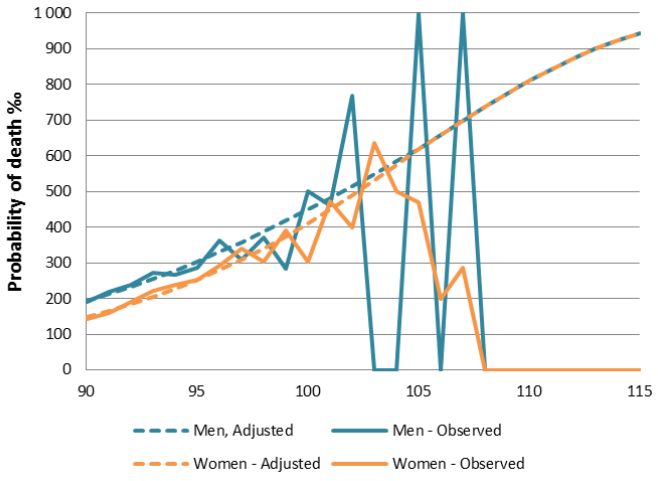

Fig.5. Observed and adjusted probabilities of death (‰) by sex and age (90 to 115) for Örebro county 2012

The updated smoothing method has a larger impact on the life expectancies for the counties than for the whole of Sweden, but the effects are not dramatic. Among the counties we noted the greatest change for the county of Norrbotten (2007-2011) where the updated method subtracts about a month from the mean total lifespan of women. Also for the counties, the updated method (compared with the old one) gives life expectancies which are closer to those gained if the life expectancy table were to be produced without any smoothing.

In the smoothing of the probabilities of death for municipalities, the population and hence the number of deaths are in many cases too small to use as basis for the fitting of the model. There are 290 municipalities In Sweden with populations ranging from just under 2 500 inhabitants to nearly 900 000 inhabitants. One-half of the municipalities have a population of around 15 000 inhabitants or less. Therefore, the smoothed probabilities of death at the corresponding county level are used for all the constituent municipalities from the age of 90. An exception is made for the three largest municipalities: Stockholm, Gothenburg and Malmö, where the adjustment of probabilities of death is based on the individual municipalities in the same way as for the counties.

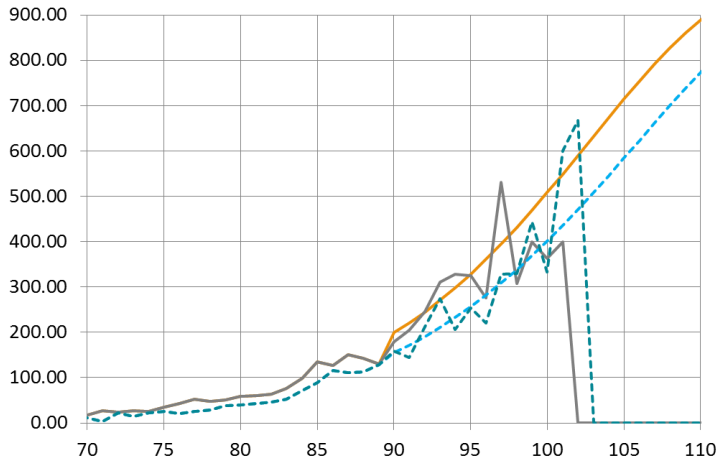

Fig.6. Observed and adjusted probabilities of death (‰) by sex and age for the municipality of Sandviken (population 40 000) 2013. The smoothing curves have been borrowed from the county of Gästrikland

The updated method has had a greater impact at the municipal level than at the national and county levels. Based on the period 2007-2011, the average life expectancy for newborn females is affected up to a shorter life expectancy of just over three months, compared with the old smoothing procedure. The largest

increase in average life expectancy for newborns in a municipality was an increase of about two months.
At the national level and for some of the counties the effect of the smoothing on the average life expectancies is marginal for the most ages, compared to results gained without smoothing. However, for many municipalities the smoothing of the probabilities of death is absolutely necessary. Without it, for some municipalities, we would end up with very unstable average life expectancies. For example, for the small municipality of Jokkmokk in the north of Sweden, the smoothing subtracts 150 days from e_0 for women.

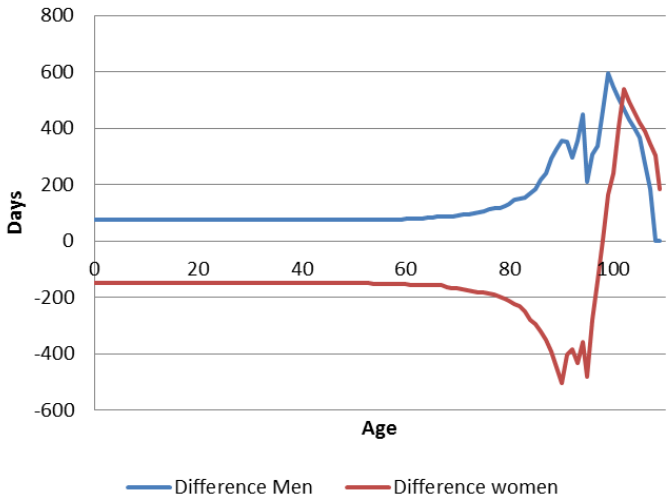

Fig.7. Difference in average life expectancy by age between smoothed and not smoothed results for Jokkmokk 2013

Conclusions

For the study of differences in mortality between time periods and between geographical regions it is important that the mortality data is analyzed using methods which preserve the differences. In this paper we have demonstrated a method for smoothing of mortality data for the elderly which does just that.
For the probabilities of death for the elderly the smoothing has a large effect for individual ages, and usable estimates of these probabilities are important in many applications. However, for large and stable regions like the whole of Sweden, the smoothing does not have a large effect on remaining life expectancies; actually our new updated method for smoothing gives results which are closer to 'non-smoothed' life expectancies than the old smoothing method. This is a good thing since we don't want to add model effects where they are not needed.

For smaller regions some form of model is necessary in the production of the life table and our smoothing procedure works well at the county level and for most of the municipalities. However for the smallest municipalities the methods needed to produce a reliable life table should be studied further.

References

1. R. E. Beard. Note on Some Mathematical Mortality Models, Colloquia on Ageing. CIBA Foundation, Vol 5. Churchill, London, 1959.
2. T. Johansson. G. Strandell. Slutrapport 2012 BVBE Livslängdstabeller. Statistics Sweden, 2012.
3. M. Martinelle. A Generalized Perks Formula for Old-Age Mortality, R&D Report, U/STM-38, Statistics Sweden, 1987.
4. W. Perks. On some Experiments in the Graduation of Mortality Statistics. Journal of the Institute of Actuaries. Vol LXIII, 1932.
5. A. Wienke. Frailty Models in Survival Analysis. Chapman &Hall/CRC Biostatistics Series, 2011.

Branching Processes: Forecasting Human Population

Plamen I. Trayanov[1] and Maroussia Slavtchova-Bojkova[2]

[1] Faculty of Mathematics and Informatics, Sofia University
Sofia, Bulgaria
(e-mail: plamentrayanov@gmail.com)
[2] Faculty of Mathematics and Informatics, Sofia University
Sofia, Bulgaria
(e-mail: bojkova@fmi.uni-sofia.bg)

Abstract. In this work we present a new technique using the Crump-Mode-Jagers branching process theory to model human population. We are addressing questions like: How the population grows according to given scenarios and how these results could be used in decision making to choose an appropriate demographic policy. Nowadays, such issues are especially important in view of the tasks before the knowledge-based society. Our aim is to estimate the growth of young population and the pensioners count and to forecast the development of the population structure in time.
Acknowledgements: This work is partially supported by the state funds allocated to the Sofia University, grant No 111/2013 and by funds of the National Project for supporting doctoral students and young scientists in Mathematics and Computer Science at Sofia University "St. Kliment Ohridski" and co-financed by the European Social Fund of EU, project No BG051PO001-3.3.06-0052.
Keywords: General Branching Process, Malthusian parameter, demography, population projections.

Introduction

Studying the population and forecasting its development and age structure is important for governments. It allows them to make an efficient policy so the negative developments are slowed down. It is important not only to make a policy to target the maximization of the total population count but to target the specific age groups that are important for the economy and the country as a whole. For example the study shows the working force in Bulgaria is diminishing, the number of young people finishing school and possibly going to universities is decreasing, which affects not only universities but businesses too. Less qualified specialists means some companies may struggle finding enough specialists in future and the less qualified work is less paid so the GDP of the country is affected. As a consequence the ability of the government to issue debt is more limited and more costly. This is an example that demographic

New Trends in Stochastic Modeling and Data Analysis (pp. 377-385)
Raimondo Manca - Sally McClean - Christos H Skiadas (Eds)

problems are something that affects many aspects of life in the country. Most demographic problems however take much time to be solved so the social policy and demographic strategy must be lingering and long term.

The empirical results are derived using General Branching Process Theory. We choose the General Branching Process (GBP) as a model because of its generality and flexibility (see Jagers [7]). Modelling human population however requires some additional tools presented in Trayanov [15] and Trayanov and Slavtchova-Bojkova [16]. These models however are developed for a population of women only so in this article we show how we can adjust them to include the population of men. In Section 1 we present a brief description of the proposed mathematical model of human population. In Section 2 we discuss the data we need and the available data. Then in Section 3 we present the empirical results and their implication for the population of Bulgaria.

1 Mathematical model.

A branching process is a model describing particles or individuals who live and die according to some probabilistic laws and give birth to one or more individuals in different moments of time according to probabilistic laws (see Slavtchova-Bojkova and Yanev [13] and Jagers [7]). The General Branching Process (GBP) gives the most flexible and close to reality stochastic model for a population and is general enough to incorporate the complex stochastic processes of birth and death. Women in this model can give birth to different number of children and in different moments of time. In addition the life length of women and men are modelled by random variables. This generality of the model is the reason the theory of Branching processes is a natural candidate for modelling human population.

In this section we present a brief description of the theory behind our model. First we define a GBP starting from a woman aged 0 at time 0. If x is an individual, we denote λ_x to be his/her life length and ξ_x to be her point process describing her the births in time. A point process is a random measure that represents the number of children born to a woman in a particular interval. The number of children born in interval $[a, b]$ is denoted by $\xi([a, b])$. An accurate mathematical definition of point process can be found in Jagers [7] and Feller [4]. We denote $\xi_x(t) = \xi([0, t])$ and $\mu_x(t) = \mathbb{E}\xi_x(t)$ which is the expected number of children that woman x gives birth to till age t.

Let $f(s) = \mathbb{E}(s^{\xi(\infty)})$, $|s| \leq 1$, $L(t) = \mathbb{P}(\lambda_x \leq t)$ and $\hat{\mu}$ is the Laplace-Stieltjes transformation of μ and $S(t) = 1 - L(t)$. We denote z_t^a to be the the number of people at time t on age less then a. The stochastic process z_t^a is called General Branching Process. A key mathematical result is that we can actually compute the expected number of individuals with the following theorem.

Theorem 1. *(see Jagers [7]) If $f(s) < \infty, |s| \leq 1$, then $m_t = \mathbb{E}(z_t) < \infty, \forall t$ and $m_t^a = \mathbb{E}(z_t^a)$ satisfies*

$$m_t^a = 1_{[0,a)}(t)\{1 - L(t)\} + \int_0^t m_{t-u}^a \mu(du). \tag{1}$$

If $m = \mu(\infty) < 1$, *then* $\lim_{t\to\infty} m_t = 0$. *If* $m = 1$ *and* μ *is non-lattice, then*

$$m_t^a \to \frac{\int_0^a \{1 - L(u)\}du}{\int_0^\infty u\mu(du)}.$$

If further $\int_0^\infty tL(dt) < \infty$, *then*

$$m_t^a \to \frac{\int_0^\infty uL(du)}{\int_0^\infty u\mu(du)}.$$

If $m > 1$, μ *is non-lattice and* $\alpha > 0$ *is the Malthusian parameter defined by* $\hat{\mu}(\alpha) = 1$, *then for* $0 \le a \le \infty$

$$m_t^a \sim e^{\alpha t} \frac{\int_0^a e^{-\alpha u}\{1 - L(u)\}du}{\int_0^\infty ue^{-\alpha u}\mu(du)}.$$

In the lattice cases corresponding assertions hold.

This theorem however gives us the expected population starting from a woman aged 0 at time 0. To calculate the expected population that starts from a woman aged b at time 0 we use the following theorem.

Theorem 2. *(see Trayanov [15]) If we denote* ${}_bm_t$ *to be the expected number of individuals started from a woman aged* b *and* ${}_b\mu(t)$ *to be her point process expectation then the following holds.*

$${}_bm_t = {}_bS(t) + \int_0^t m_{t-u}\ {}_b\mu(b + du), \tag{2}$$

where ${}_bS(t)$ *denotes the probability a woman of age* b *to survive to* $b + t$, *i.e.*

$${}_bS(t) = \frac{S(b + t)}{S(b)}. \tag{3}$$

To model real population however we need additional assumptions. We assume the fertility interval for each woman is $[12, 50]$ and women do not give birth outside it. In terms of GBP this means

$$\mathbb{P}(\xi\,[a, b) = 0)) = 1, when\,[a, b) \cap [12, 50] = \varnothing$$
$$\mathbb{P}(\xi[\lambda, \infty) = 0) = 1.$$

This assumption is made because we do not have data for births on ages less than 12 and greater than 50 and because births outside this age interval are very few and can be disregarded. The second assumption is that a woman could have 0 or 1 child during a year and each birth is a live birth. This means the number of live births is equal to the number of women who gave birth. The assumption is made because of missing data for the number of women that give birth and available data for the number of children born each year. In addition we do not have data for the sex of the child born, so we assume the probability for a girl is 100/205.

The model above gives us information of how a stationary population will change over time, but it is not sufficient to describe a dynamic population with changing birth and death laws. This problem could be easily avoided however (see Trayanov and Bojkova[16]). We achieve this varying environment by making population projection for only one year forward using the model and then change the birth and death laws according to what we forecast them to be and repeat the same for the next year. This gives us projections year after year incorporating the point process forecast and the life length forecast. For every year we know the number of men by age and we can model their contribution with the same equation 2 noting that their function $\mu(t)$ is actually zero for every t. The contribution of a single man aged b at time t is actually his survivability function ${}_bS(t)$. This small enhancement in the model allows us to include the men in predicting the age structure. We must note that their survivability function is different from women and is modelled separately.

2 Incorporating the available data into the model.

In order to calculate ${}_bm_t$ in Theorem 2 from real data we need the following mathematical result which reduces it to solving equation 1 in Theorem 1.

Theorem 3. *see Trayanov [15] If m_t has a continuous second derivative then a third order approximation of equation* (2) *is given by*

$$ {}_bm_t \approx {}_bS(t) + \sum_{k=1}^{n} m_{b+k-0.5} \cdot {}_b\mu(b+k-1, b+k), $$

where the expected number of births in $[b+k-1, b+k)$ of a woman aged b is

$$ {}_b\mu[b+k-1, b+k) = {}_bS(b+k-1) \cdot \mathbb{P}(\xi\,[b+k-1, b+k) = 1 | \lambda \geq b+k-1). $$

The probability $\mathbb{P}(\xi\,[b, b+1) = 1 | \lambda \geq b)$ can be calculated from the Age Specific Fertility Rate and the expected number of years lived by a woman in [b, b+1) (see Trayanov [15]).

The data we use can be seen in Eurostat database [3]. We use the number of births and deaths by age and sex, the population count by age and sex. We use data both by age reached during the year and by age of last birthday. There are some missing data about the death count for ages 80+ for some years so we need to fill them first and we use the Kannisto model (see Thatcher et al.

[14]) for this purpose. Then we calculate the fertility and mortality rates using the methodology described in Wilmoth et al. [17] and Shkolnikov [12] and then calculate the age specific fertility and mortality probabilities (see Chiang [2], Keyfitz [8] and Mode [9]) for every year since 1960. These probabilities however contain noise which we want to filter first and we achieve this with smoothing splines. The smoothing splines theory is explained more accurately in Ramsay [11] and de Boor [1].

3 Forecasting scenarios. Empirical results

In this section we will focus on forecasting the age structure and the population count. We discuss two scenarios for forecasting. The first scenario is called "No Change" because it assumes the current birth and death probabilities don't change in time. It projects the current state into the future. Although this projection gives us information about the future it gives us information about the present state too, answering the question if the the current state persists through time what development it expresses.

The second scenario is called "Dynamic Scenario" because it tries to capture trends in birth and death probabilities. This scenario requires several procedures to calculate:

- Principal Components Analysis (PCA) is used for decomposition of log-death probabilities and the point process density function for each year from 1980 to 2012. This gives us the main directions in which these function historically changed and reduces the forecasting of enormous amounts of points for each curve to forecasting only several parameters (see Hyndman [6]).
- ARIMA model is used to fit and forecast the principal components of birth and death probabilities. We find the best model according to AIC and use it to forecast the curves (see Hyndman [6]).
- We feed the forecasts into the General Branching Process model and compute the expected future population by age.

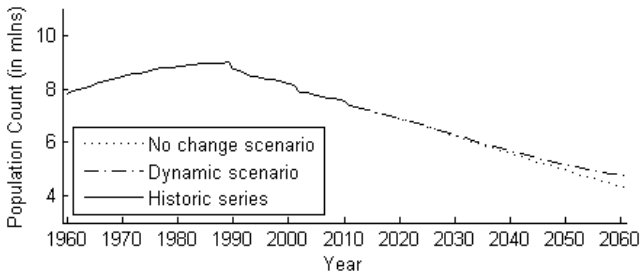

Fig. 1. Total population count.

The expected future total population count can be seen on Figure 1. We can see that according to both scenarios the population is decreasing rapidly in the

next 50 years. There are 3.57 mil men and 3.76 mil women by the beginning of year 2012. The "No Change" scenario is expecting this count to be reduced to 2.03 mil men and 2.21 mil women by the end of 2061. The "Dynamic" scenario gives us slightly less pessimistic expectations for 2.21 mil men and 2.48 mil women by the end of 2061. This is a reduction of 38% and 32% respectively.

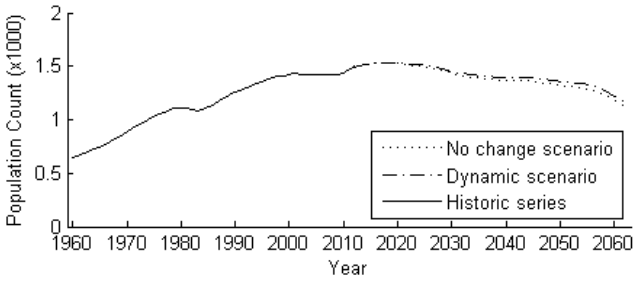

Fig. 2. Number of retired people.

The two scenarios give similar forecasts for the total population count but forecast different structure of the population. This can be seen in Figures 3 and 6. In Figure 3 we can see the number of retired women is far greater than the number of retired men as of 2012 and the model is expecting this ratio to continue to grow. This is partly due to the smaller retirement age of women in Bulgaria (age 63) than men (which retire on age 65) but it is also result of different mortality rates for men and women. Women traditionally live longer than men. In Bulgaria the expected life length of women is 77 as of 2012 and is greater than the expected life length of men (70). The Dynamic scenario expects the life length for men to stay the same and for women to live 3 years longer in year 2060.

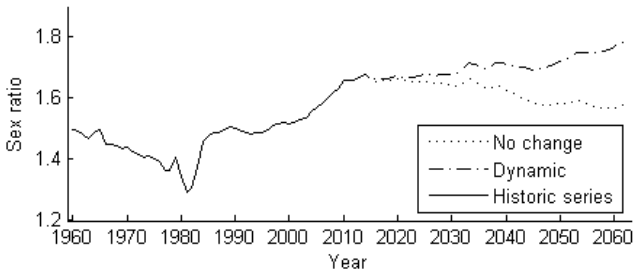

Fig. 3. Ratio of retired women against retired men.

An interesting feature in Figure 2 is that even though the percentage of pensioners is increasing in the past years it is expected to slow down in the near future and begin to decrease. It is interesting to see if this decrease of people on pension will help the economy recover. On Figure 4 is displayed the

percentage of working people and how it will change over time. It shows that even though people on pension will decrease, those on working age will decrease even more so the economy will be under even greater demographic stress than it is now.

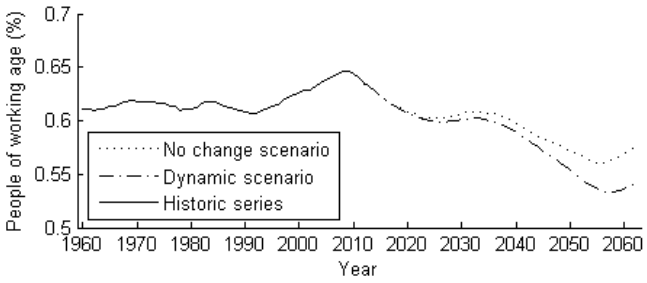

Fig. 4. Percentage of people on working age.

The "Dynamic" scenario shows that the population on working age is expected to decrease by 46%, whereas the people on pension are expected to decrease by 22%. This puts Bulgaria in a very difficult position because the working force will have to earn more to sustain the people on pension or the government will have to increase the retirement age. Calculations show that if we want to keep the current ratio of people on working age to people on pension in 2062, we need to gradually increase the retirement age of men by 4 years and to increase the retirement age of women even more - 6 years.

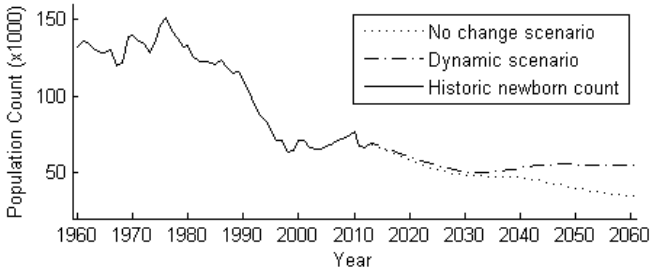

Fig. 5. Newborns count.

Another application of the model could be forecasting the number of newborns which can be used as a predictor of how many children will need kindergarten or the number of people on age 6 or 7 years which is a predictor of how many children will be beginning school in the future. Figure 6 shows the number of children beginning school is expected to decrease till 2035 but then it will start growing again. This change of trend is caused by the current age structure of the population that will change over time. The number of new-

borns is shown on Figure 5. It is expected to decrease till year 2030 due to the bad age structure but eventually it will start growing again.

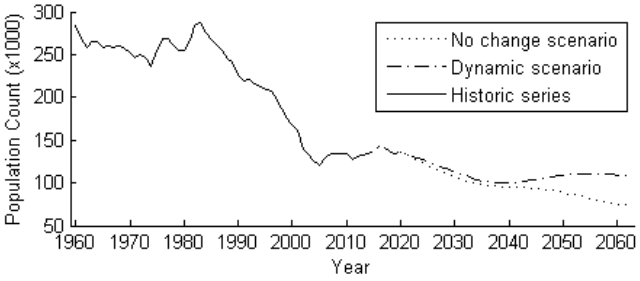

Fig. 6. People of age 6 or 7.

The number of people on age 18 and 19 is going to decrease till year 2017 by 25% and then start to increase for short while. This is important because the number of people on this age is the main source of students for universities. A decrease with 25% for 5 years puts the universities in difficult position. Calculations show that the number of young people of age between 18 and 30 is going to decrease too by 14% in year 2017 and continue decreasing till year 2026 by 34%. This results in fewer candidates for students and less young people in the economy.

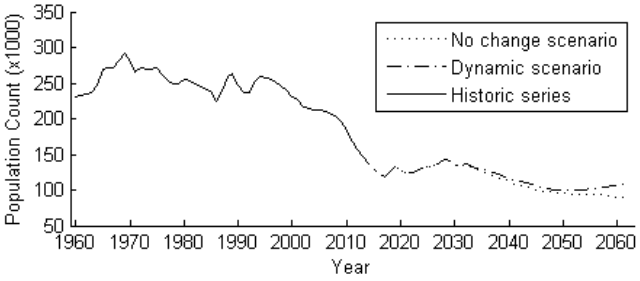

Fig. 7. People of age 18 and 19.

4 Final remarks

Modelling and forecasting the population is important for the country. It tells us about the current state and what is wrong with it so the government can make an efficient demographic policy. It tells us what to expect in the future so we can prepare. It gives us a tool to make social plans like how many new kindergartens we need to build in the future or can we expect a low number of students in the schools or universities. It answers economic questions - how

many people will be on working age and how many on pension so the government could adjust their policy appropriately and efficiently. The forecast results for Bulgaria should teach us that we need to pay attention to demography and make a social policy that counteracts these trends. The demographic problems are difficult to solve, affect many aspects of life in the country and require a long term strategy to be solved.

References

1. Boor, C., *A Practical Guide to Splines.* Springer, 2001.
2. Chiang, C., *Life Table and Its Applications.* Krieger Pub Co, 1983.
3. Eurostat Database, `http://epp.eurostat.ec.europa.eu/portal/page/portal/statistics/search_database`.
4. Feller, W. *An introduction to probability theory an its applications, vol. 2.* Wiley, 1971.
5. Hastie, T., gam: Generalized Additive Models. R package version 1.09-1, `http://CRAN.R-project.org/package=gam`, 2011.
6. Hyndman, R., Booth, H., Tickle, L. and Maindonald, J., demography: Forecasting mortality, fertility, migration and population data. R package version 1.09-1, `http://CRAN.R-project.org/package=demography`, 2011.
7. Jagers, P., Branching Processes with Biological Applications. John Wiley & Sons Ltd, 1975.
8. Keyfitz N. and Caswell, H., *Applied Mathematical Demography.* Springer, 2005.
9. Mode, C., *Stohastic Processes In Demography and Their Computer Implementation.* Springer, 1985.
10. R Development Core Team, R: A Language and Environment for Statistical Computing. `http://www.R-project.org/`, 2011.
11. Ramsay, J. and Silverman, B. *Functional Data Analysis.* Springer, 2005.
12. Shkolnikov, V., "Methodology Note on the Human Life-Table Database (HLD)". Unpublished Manuscript, `http://www.lifetable.de`
13. Slavtchova-Bojkova, M. and Yanev, N. M., *Branching Processes.* St. Kliment Ohridski University press, Sofia, 2007.
14. Thatcher, R., Kannisto, V. and Andreev, K., "The survivor ratio method for estimating numbers at high ages." *Demographic Research*, 6(1), 2-15. 2002.
15. Trayanov, P., "Crump-Mode-Jagers Branching Process: Modelling and Application for Human Population", *Pliska Stud. Math. Bulgar.*, 22, 207-224, 2013.
16. Trayanov, P. and Slavtchova-Bojkova, M., "Crump-Mode-Jagers Branching Processes: Application in Population Projections", , 2013.
17. Wilmoth, J. R., Andreev, K., Jdanov, D. and Glei, D. A., "Methods Protocol for the Human Mortality Database". Unpublished Manuscript, `http://www.mortality.org`, 2007

8 CHAPTER

Stochastic Processes, Copulas and Actuarial Applications

Multivariate Markov chain predictions adjusted with copula models

Mariela Fernández[1], Jesús. E. García[2], and Verónica A. González-López[3]

[1] University of Campinas, Campinas, Brazil
(e-mail: mariela@ime.unicamp.br)
[2] Department of Statistics
University of Campinas, Campinas, Brazil
(e-mail: jg@ime.unicamp.br)
[3] Department of Statistics
University of Campinas, Campinas, Brazil
(e-mail: veronica@ime.unicamp.br)

Abstract. In this paper we propose an estimator for the joint probability of Markov chains of finite order, with finite alphabet. First, the joint probabilities are found through a Partition Markov Model, using the Bayesian Information Criterion. Second, the corresponding discrete copula is computed and the Partition Markov estimation is applied to each marginal process. Finally, the copula is rearranged in the space defined by the marginal estimations and a new estimator is defined. Its efficiency is tested by simulations studies obtaining that it improves the predictions done through a Bayesian Information Criterion.
Keywords: Multivariate Markov chains, Copula theory, Model selection, Correction through the marginal.

1 Introduction

In this work we combine two statistical concepts with the purpose of defining a natural correction for the joint probabilities' estimation of multivariate Markovian processes. The first concept is the Partition Markov model and the second one is the Copula model.
The Partition Markov model was introduced in García and González-López[6] and it generalizes the Variable Length Markov Chains models. This model is based on the identification of a partition of the state space which allows to divide the space in parts, the elements inside each part are considered equivalents, where the equivalence between two elements is the equality of the transition probability from them to any other element in the alphabet of the process. The identification of the partition allows to reduce the number of parameters to be estimated for building the model when comparing with the estimation done without it. On the other hand, copula models describes the association among random variables independently of their marginal distributions. They have

New Trends in Stochastic Modeling and Data Analysis (pp. 389-394)
Raimondo Manca - Sally McClean - Christos H Skiadas (Eds)

been used for various purposes. Some recent results are García et al.[9], giving assistance for the development of new measures of dependence, García and González-López[7], classifying and discriminating between objects, Fernández and González-López[2] and [3], under the Bayesian assumptions developing estimators, between others. Indeed copulas and related concepts were also used recently in the construction of hypothesis tests, as shown in Genest and Remillard[10] and García and González-López[8]. And here, they are presented as a tool to improve the quality of the estimates of the joint probabilities in Markov processes.
The performance of the corrected estimation proposed here is illustrated by a simulation analysis.

2 Background

Let (Z_t) be a discrete time, Markov chain with memory M on a finite alphabet A, with state space $\mathcal{S} = A^M$. Denote the string $a_m a_{m+1} \dots a_n$ by a_m^n, where $a_i \in A$, $m \leq i \leq n$. This means that each string is a concatenation of elements from A. Also note that the state space is composed by strings of size M (concatenations of M elements from A). Denote by $P(a|s) = \text{Prob}(Z_t = a | Z_{t-M}^{t-1} = s)$ the transition probability from s to a, with $s \in \mathcal{S}$ and $a \in A$.
The following definitions are necessary to state the model that we estimate and apply in this work.

Definition 1. Given two strings $s, r \in \mathcal{S}$, s and r are equivalent (denoted by $s \sim_p r$) if $P(a|s) = P(a|r),\ \forall a \in A$.

Definition 2. Given (Z_t) a discrete time Markov chain with memory M, on a finite alphabet A, (Z_t) is a Markov chain with partition $\mathcal{L}$ if this partition is the one defined by the equivalence relationship $\sim_p$ introduced by Definition 1.

Then, given (Z_t) a discrete time Markov chain with memory M, on a finite alphabet A, the Partition Markov Model (PMM) is defined by $\left(\mathcal{L}, \{P(\cdot|L)\}_{L \in \mathcal{L}}\right)$, where the partition $\mathcal{L}$ was introduced in Definition 2 and the probability $P(a|L)$, for $L \in \mathcal{L}$ and $a \in A$, is defined by $P(a|s)$ for any string $s \in L$. The PMM were introduced in García and González-López[5] and explored in García and González-López[6] and García and Fernández[4]. Indeed, these models generalize the well-known models (i) variable length Markov chains of finite order and (ii) Markov chains of finite order.

What follows shows the construction of discrete copulas that the present study made use of. More details concerning this issue, as well as about continuous copulas, can be found in Joe[11]. Define $(Z_1, \dots, Z_K)$ as a vector of discrete random variables, where the variable Z_k takes values in the domain $D_k = \{z_{k1}, z_{k2}, \dots, z_{km_k}\}$ and m_k is some integer greater than 1, for $k = 1, \dots, K$. Suppose also that $\text{Prob}(Z_1 = z_{1i_1}, \dots, Z_K = z_{Ki_K}) = p_{z_{1i_1} \dots z_{Ki_K}}$. In addition we denote the univariate marginal distribution of Z_1 as being $p_{z_{1i_1} \bullet \dots \bullet} = \sum_{i_2} \dots \sum_{i_K} p_{z_{1i_1} z_{2i_2} \dots z_{Ki_K}}$, for each $z_{1i_1} \in D_1$. And the cumulative marginal distribution F_1, applied to an arbitrary point z, is given by

$F_1(z) = \sum_{z_{1i_1} \leq z} p_{z_{1i_1}\bullet\ldots\bullet}$. Similarly, it can be obtained the definitions for all other coordinates, $k = 2, \ldots, K$.
The K-variate copula density is given by

$$c(u_1, \ldots, u_K) = \begin{cases} \frac{p_{z_{1i_1}\ldots z_{Ki_K}}}{p_{z_{1i_1}\bullet\ldots\bullet}\times\ldots\times p_{\bullet\ldots\bullet z_{Ki_K}}}, \\ \qquad\qquad \text{if}(u_1, \ldots, u_K) \in \otimes_{k=1}^{K}[F_k(z_{ki_k-1}), F_k(z_{ki_k})[\\ 0, \qquad\qquad \text{otherwise}, \end{cases} \quad (1)$$

with $F_k(z_{k1-1}) = F_k(z_{k0}) = 0$, for $k = 1, \ldots, K$.
The function $c(u_1, \ldots, u_K)$ satisfies the following characteristics (i) it is a probability mass function, displayed in $[0, 1]^K$, (ii) the univariate marginal distributions are $U(0, 1)$ and (iii) the cumulative distribution C of c verifies

$$\text{Prob}(Z_1 \leq z_{1i_1}, \ldots, Z_K \leq z_{Ki_K}) = C\big(F_1(z_{1i_1}), \ldots, F_K(z_{Ki_K})\big), \quad (2)$$

for all $(z_{1i_1}, \ldots, z_{Ki_K}) \in \otimes_{k=1}^{K} D_k$. But, in opposition with the continuous case, c is not unique in the sense that there are other copula functions C which also satisfies (2).

3 Estimation proposed

In this section we introduce a strategy to estimate the joint conditional probabilities of stochastic processes. Given (Z_t) a discrete time Markov chain with memory M, on a finite alphabet A and state space $\mathcal{S} = A^M$, the estimation of the probabilities is traditionally performed by maximum likelihood with the help of some penalty criterion. Csiszár and Talata[1] and García and González-López[5] show that the Bayesian Information Criterion (BIC) enables, for a sample size big enough, a consistent estimate of the partition given in Definition 2 as well as for conditional probabilities. An efficient algorithm to find the partition can be found in García and González-López[6]. The goal of this work is to improve the predictive ability of the joint conditional probabilities estimated as suggested in García and González-López[5] and [6], by means of a marginal adjustment through the discrete copulas defined in Section 2.

Suppose that Z_t is a discrete time Markov chain with memory M_0 on a finite alphabet $A = \otimes_{k=1}^{K} B_k$, with state space $\mathcal{S} = \otimes_{k=1}^{K} B_k^{M_0}$. Suppose also that $Z_t = (Z_{1t}, \ldots, Z_{Kt})$, with marginal discrete time Z_{kt}, Markov chain with memory M_k on the finite alphabet B_k. In order to simplify the notation we assume $M_k = M$ and $M > M_0$. This last assumption ensures that, using marginal M_k memories, each joint string s can be decomposed into marginal strings, using these memories M_k.
Let us take an arbitrary string $s = z_1^M \in \mathcal{S}$, with $M > M_0$, recalling that $z_m^n = z_m z_{m+1} \ldots z_n$ where $z_j = (z_{1j}, \ldots, z_{Kj})$ and $a = (a_1, \ldots, a_K) \in A$. Then the joint probability $\text{Prob}(Z_t = a | Z_{t-M}^{t-1} = s)$ can be related to the one of order M_0 by means of

$$\text{Prob}(Z_t = a | Z_{t-M}^{t-1} = s) = \text{Prob}(Z_t = a | Z_{t-M_0}^{t-1} = z_{M-M_0+1}^{M}). \quad (3)$$

Hence, it can be computed efficiently from the PMM of memory M_0 built for the multidimensional process Z_t. From the estimated multidimensional probability, all the univariate marginal probabilities can be derived and, also, the estimated copula $c_{\mathcal{L}_Z|s}(u_1,\ldots,u_K)$ for each string s can be computed from the equation (1).

The marginal processes $Z_{kt}, k = 1,\ldots,K$ allow to build the PMM one by one. We will denote by $\hat{P}_{\mathcal{L}_{Z_k}}(a_k|z_{k1}^{kM})$ each marginal point probability estimated from the partition $\mathcal{L}_{Z_k}$, we also denote by $\hat{F}_{\mathcal{L}_{Z_k}}(a_k|z_{k1}^{kM})$ each cumulative distribution for $k = 1,\ldots,K$.
In the next equation we introduce the estimation of (3) proposed here

$$\hat{P}(a|s) = \int_{\hat{F}_{\mathcal{L}_{Z_1}}(a_1|z_{11}^{1M})}^{\hat{F}_{\mathcal{L}_{Z_1}}(a_1^+|z_{11}^{1M})} \ldots \int_{\hat{F}_{\mathcal{L}_{Z_K}}(a_K|z_{K1}^{KM})}^{\hat{F}_{\mathcal{L}_{Z_K}}(a_K^+|z_{K1}^{KM})} c_{\mathcal{L}_Z|s}(u_1,\ldots,u_K)du_K\ldots du_1 \quad (4)$$

where a_k^+ is the element immediately superior to a_k in the alphabet $B_k. k = 1,\ldots,K$.

4 Simulation study

In order to explore the performance of the technique proposed here, $\hat{P}$ (from equation (4)) with the standard method of estimation $\hat{P}_{\mathcal{L}_Z}$, there were investigated the models described in Table 4. For each model W and sample size T, there were randomly generated 100 datasets consisting of two parts. The first part, with size T, is used as training set. The second part, of size 10000, is used to test the prediction efficiency, commonly called testing set.
Models 1 and 2 represent processes with marginal alphabets of dimension 2, with $T \in \{50, 100, 150, 200, 300, 500, 1000\}$. Their probability of transition at time t depends on the value of the process at time $t - M$, where M is the order of the process. Model 1 is of order 2 and Model 2 has order $M = 4$. On the other hand, Model 3 has marginal alphabet of dimension 3. In this last case it was considered a sample size $T \in \{100, 250, 500, 750, 1000\}$ and a model showing a process in which the probability of transition at time t depends on the value of the process at time $t - 3$ as follows,

$$\text{Prob}(Z_t = z_t|Z_{t-3} = s) = 0.6 \text{ if } z_t = s \text{ and } 0.05 \text{ otherwise.} \quad (5)$$

The comparison of the hit rates of the method proposed here are presented in Figure (1). We note how the standard estimate worsens their hit rates by increasing the order of the process, while this increase of the order does not impact the hit rates when using equation (4).

Model 1 and 2				
s	$z_t = (0,0)$	$z_t = (1,0)$	$z_t = (0,1)$	$z_t = (1,1)$
$z_{t-2} = (0,0)$	0.7	0.1	0.05	0.15
$z_{t-2} = (1,0)$	0.25	0.65	0.05	0.05
$z_{t-2} = (0,1)$	0.05	0.1	0.8	0.05
$z_{t-2} = (1,1)$	0.05	0.05	0.1	0.8

Table 1. PMM's Transition probabilities used for the simulation study of dimension 2. The cells contain Prob$(Z_t = z_t | Z_{t-M}^{t-1} = s)$.

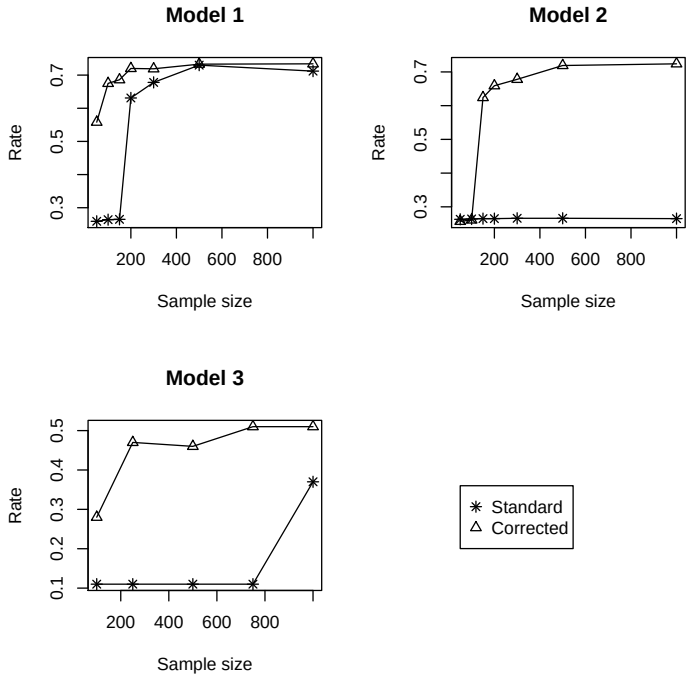

Fig. 1. Success Rates: settings with marginal alphabets of dimension 2 and 3, rates computed from $\hat{P}_{\mathcal{L}_Z}$ (Standard) and computed from $\hat{P}$-equation (4) (Corrected).

Acknowledgments

The authors acknowledge the support provided by USP project "Mathematics, computation, language and the brain. FAPESP projects "Portuguese in time and space: linguistic contact, grammars in competition and parametric change", 2012/06078-9 and "Research, Innovation and Dissemination Center for Neuromathematics - NeuroMat", 2013/07699-0 to Jesús E. García and V. A. González-López. Additionally, the authors acknowledge the financial support for this research provided by FAPESP Post-doctoral Grant 2011/18285-6 to M. Fernández.

References

1. I. Csiszár, and Z. Talata. Context tree estimation for not necessarily finite memory processes, via BIC and MDL. *IEEE Trans. Inform. Theory*, 52, 1007-1016, 2006.
2. M. Fernández and V. A. González-López. A Bayesian approach for convex combination of two Gumbel-Barnett copulas. *AIP Conference Proceedings*, 1558, 1491-1494, 2013.
3. M. Fernández and V. A. González-López. A copula model to analyze minimum admission scores. *AIP Conference Proceedings*, 1558, 1479-1482, 2013.
4. J. E. García and M. Fernández. Copula based model correction for bivariate Bernoulli financial series. *AIP Conference Proceedings*, 1558, 1487-1490, 2013.
5. J. E. García and V. A. González-López. Minimal Markov Models. *arXiv:1002.0729v1*, 2010.
6. J. E. García and V. A. González-López. Detecting regime changes in Markov Models. *Proceedings of The Sixth Workshop on Information Theoretic Methods in Science and Engineering*, 2013.
7. J. E. García and V. A. Gónzalez-López. Modeling of acoustic signal energies with a generalized Frank copula. A linguistic conjecture is reviewed. *Communications in Statistics - Theory and Methods*, 2013. Doi: 10.1080/03610926.2013.866248
8. J. E. García and V. A. Gónzalez-López. Independence tests for continuous random variables based on the longest increasing subsequence. *Journal of Multivariate Analysis* , 127, 126-146, 2014. Doi: 10.1016/j.jmva.2014.02.010
9. J. E. García, V. A. González-López and R. B. Nelsen. A new index to measure positive dependence in trivariate distributions. *Journal of Multivariate Analysis*, 115, 481-495, 2013.
10. C. Genest and B. Remillard. Tests of Independence or Randomness Based on the Empirical Copula Process. *Test*, 13, 335-369, 2004.
11. H. Joe. *Multivariate models and dependence concepts, Monographs on Statistics and Applied Probability, vol. 73*, Chapman & Hall/CRC, New York, 2001.

Modelling relations between returns of financial investments using perturbed copulas

Jozef Komorník[1], Magda Komorníková[2], and Jana Kalická[2]

[1] Faculty of Management, Comenius University, Odbojárov 10, P.O.BOX 95, 820 05 Bratislava, Slovakia
(E-mail: Jozef.Komornik@fm.uniba.sk)
[2] Faculty of Civil Engineering, Slovak University of Technology, Radlinského 11, 813 68 Bratislava, Slovakia
(E-mail: Magdalena.Komornikova@stuba.sk, Jana.Kalicka@stuba.sk)

Abstract. We have investigated the relations between 4 selected countries' (USA, Australia, Japan and UK) daily returns of the REIT (Real Estate Investment Trust) indexes in different time periods, determined by the recent global financial markets crises (July 1, 2008 – April 30, 2009). We have applied the fitting by copulas to the residuals of ARMA–GARCH filters. We considered models from strict Archimedean copulas (Joe, Frank, Clayton and Gumbel) families and their mixtures with corresponding survival copulas as well as their perturbation. For selecting the optimal models we have applied the Kolmogorov – Smirnov – Anderson – Darling (KSAD) test statistic (for which we also constructed a GoF simulation based test). We observed that for all 3 considered time periods, the minimal (considerably reduced) value of KSAD were received for perturbed copulas.
Keywords: Copula, Perturbed copulas, Real Estate Investment Trust (REIT) index, returns of REIT indexes.

1 Introduction

We have investigated the relations between 4 selected countries' (USA, Australia, Japan and UK) daily returns of the REIT (Real Estate Investment Trust) indexes in different time periods, determined by the recent global financial markets crises (July 1, 2008 – April 30, 2009). We have applied the fitting by copulas to the residuals of ARMA–GARCH filters. We fitted these residuals by suitable marginal distributions in one of the Normal, Logistic and Laplace classes of distributions. Next, for each considered time period and all six possible couples of filtered residuals, we investigated models from strict Archimedean copulas (Joe, Frank, Clayton and Gumbel) families and their mixtures with corresponding survival copulas (that have been applied e.g. in Patton's paper [15]) as well as their perturbations given in our paper Mesiar *et al.*[12]. We observed that for all three considered time periods, the minimal (considerably reduced) value of Kolmogorov–Smirnov–Anderson–Darling test statistic were received for perturbed model.

New Trends in Stochastic Modeling and Data Analysis (pp. 395-407)
Raimondo Manca - Sally McClean - Christos H Skiadas (Eds)

The paper is organized as follows. In the second section we present selected models of univariate (marginal) distributions as well as a brief overview of the theory of copulas including the methodology of their fitting to two–dimensional time series. The third section is devoted to perturbations of bivariate copulas. The fourth section, contains application to real data modelling. First we filter the considered group of REIT indexes (separately in the individual time sub–periods) by ARMA–GARCH models (in order to avoid a possible violation of the i.i.d. property). Then we fit the resulting time series of residuals by suitable marginal distributions and apply non–parametric correlation analyses (based on the Kendall coefficients) to all possible couples of the residual time series (for the individual time sub–periods). Next we provide an overview of the best copula models for different time sub–periods and selected significantly correlated pairs of returns of REIT indexes. Finally, some conclusions are presented.

2 Fitting univariate and bivariate distributions

2.1 Selected classes of univariate distributions

Recall that a *Logistic* distribution (see [5]) is determined by two parameters $(\mu,\ \beta)$ and its probability density function is given by

$$f(x,\mu,\beta) = \frac{e^{-\frac{x-\mu}{\beta}}}{\beta\left(e^{-\frac{x-\mu}{\beta}}+1\right)^2}.$$

Moreover, its theoretical parameters satisfy the relations

$$E[X]=\mu, \quad D[X]=\frac{\pi^2\beta^2}{3}, \quad \text{Skewness } =0, \quad \text{Kurtosis } =4.2.$$

Similarly a *Laplace* distribution (see [10]) is determined by two parameters $(\mu,\ \beta)$ and its probability density function is given by

$$f(x,\mu,\beta) == \begin{cases} \frac{e^{-\frac{x-\mu}{\beta}}}{2\beta} & x \geq \mu \\ \\ \frac{e^{-\frac{\mu-x}{\beta}}}{2\beta} & \text{otherwise} \end{cases}.$$

Its theoretical parameters satisfy the relations

$$E[X]=\mu, \quad D[X]=2\beta^2, \quad \text{Skewness } =0, \quad \text{Kurtosis } =6.$$

For all GoF tests with Logistic and Laplace distributions we applied the Anderson–Darling GoF test (see e.g. Anderson and Darling [3], Anderson [2]) that effectively uses a test statistic based on

$$A_n^2 = n\int_{-\infty}^{\infty} \frac{\left(\hat{F}(x)-F(x)\right)^2}{F(x))(1-F(x)}\, d\,F(x), \tag{1}$$

where n is the sample size, $\hat{F}(x)$ is the empirical distribution function and $F(x)$ is the specified distribution function. It was shown in Anderson and Darling [3] that (1) can be written as

$$A_n^2 = -n - \frac{1}{n}\sum_{k=1}^{n}(2k-1)\left(\log\left(1-u_{(-k+n+1)}\right)+\log u_{(k)}\right),$$

where $u_{(k)} = F(x_{(k)})$ and $x_{(1)} < ... < x_{(n)}$ is the ordered sample. The p-values of Anderson–Darling GoF test were calculated by the software Mathematica, version 9.

2.2 Copulas

Copula represents a multivariate distribution that capture the dependence structure among random variables. It is a great tool for building flexible multivariate stochastic models. Copula offers the choice of an appropriate model for the dependence between random variables independently from the selection of marginal distributions. This concept was introduced in the early 50's and became popular in several fields beyond statistics and probability theory, such as finance, actuarial science, fuzzy set theory, hydrology, etc.

Definition 1. A function $C : [0,1]^2 \to [0,1]$ is called a (bivariate) copula whenever it is

i) 2–increasing, i.e.,

$$V_C\left([u_1,u_2]\times[v_1,v_2]\right) = C(u_1,v_1)+C(u_2,v_2)-C(u_1,v_2)-C(u_2,v_1) \geq 0$$

for all $0 \leq u_1 \leq u_2 \leq 1$, $0 \leq v_1 \leq v_2 \leq 1$ (recall that $V_C\left([u_1,u_2]\times[v_1,v_2]\right)$ is the C–volume of the rectangle $[u_1,u_2]\times[v_1,v_2]$);

ii) grounded, i.e., $C(u,0) = C(0,v) = 0$ for all $u,v \in [0,1]$;

iii) it has a neutral element $e = 1$, i.e., $C(u,1) = u$ and $C(1,v) = v$ for all $u,v \in [0,1]$.

Sklar[16] proved in 1959 that $H(x,y) = C(F(x),G(y))$, where H is the joint distribution function of a random vector (X,Y) with marginal distribution functions F and G. If the marginals are continuous, the copula is unique. Thus, the copula function has other important interpretation as the joint distribution function.

For more details, examples and applications we recommend monographs Joe[9] and Nelsen[13]. The Table 1 provides a summary of some selected basic facts that are related to some classes of Archimedean copulas that we utilize in our analyses.

We follow the approach of Patton[15] and consider a so–called *survival copula* derived from a given copula $C(u,v)$ corresponding to the couple (X,Y) by

$$SC(u,v) = u+v-1+C(1-u,1-v) \tag{2}$$

which is the copula related to the couple $(-X,-Y)$ with the marginal distribution functions

$$F_{-X}(x) = 1-F_X(-x^+) \text{ and } F_{-Y}(y) = 1-F_Y(-y^+). \tag{3}$$

Family of copulas	Parameter	Bivariate copula $C(u,v)$
Gumbel	$\theta \geq 1$	$e^{-[(-ln(u))^\theta + (-ln(v))^\theta]^{\frac{1}{\theta}}}$
Clayton (strict)	$\theta > 0$	$(u^{-\theta} + v^{-\theta} - 1)^{-\frac{1}{\theta}}$
Frank	$\theta \in \Re$	$-\frac{1}{\theta}\ln(1 + \frac{(e^{-\theta u}-1)\,(e^{-\theta v}-1)}{(e^{-\theta}-1)})$
Joe	$\theta \in [1,\infty)$	$1 - \left((1-u)^\theta + (1-v)^\theta - (1-u)^\theta(1-v)^\theta\right)^{1/\theta}$
Ali-Mikhail-Haq	$\theta \in [-1,1]$	$\frac{uv}{1-\theta(1-u)(1-v)}$

Table 1. Some Archimedean copulas

2.3 Fitting of copulas

In practical fitting of the data we have utilized the *maximum pseudolikelihood method* (MPL) of parameter estimation with initial parameters estimates received by the minimalization of the mean square distance to the empirical copula C_n presented e.g. in Genest and Favre[7]

$$C_n(u,v) = \frac{1}{n}\sum_{i=1}^{n} \mathbf{1}\left(\frac{R_i}{n+1} \leq u, \frac{S_i}{n+1} \leq v\right)$$

where n is the sample size, R_i stands for the rank of X_i among $X_1,\ldots,X_n$, S_i stands for the rank of Y_i among $Y_1,\ldots,Y_n$ and $\mathbf{1}(\Omega)$ denoting the indicator function of set Ω. It requires that the copula $C_\theta(u,v)$ is absolutely continuous with density $c_\theta(u,v) = \frac{\partial^2}{\partial u\,\partial v}C_\theta(u,v)$. This method (described e.g. in Genest and Favre[7]) involves maximizing a rank-based log-likelihood of the form

$$L(\theta) = \sum_{i=1}^{n} \ln\left(c_\theta\left(\frac{R_i}{n+1}; \frac{S_i}{n+1}\right)\right).$$

where θ is vector of parameters in the model. Note that arguments $\frac{R_i}{n+1}$, $\frac{S_i}{n+1}$ equal to the corresponding values of the empirical marginal distributional functions of random variables X and Y.

For selecting the optimal models we applied the Kolmogorov – Smirnov – Anderson – Darling (KSAD, for which we use the abbreviation AD) test statistic defined e.g. in Berg and Bakken[6]

$$AD(\theta) = \sqrt{n}\ \max\left|\frac{C_n\left(\frac{R_i}{n+1},\frac{S_i}{n+1}\right) - C_\theta\left(\frac{R_i}{n+1},\frac{S_i}{n+1}\right)}{C_\theta\left(\frac{R_i}{n+1},\frac{S_i}{n+1}\right) * \left(1 - C_\theta\left(\frac{R_i}{n+1},\frac{S_i}{n+1}\right)\right)}\right| \tag{4}$$

for which we also constructed a GoF simulation based test, when comparing models with their submodels and different families of models.

3 Perturbation of bivariate copulas

Fitting of an appropriate copula to real data is one of major tasks in application of copulas. For this purpose, a large buffer of potential copulas is

necessary, preferably parametric families of copulas. Once we know approximately a copula C appropriate to model the observed data, we look for a minor perturbation of C which fit better then C itself. This is, e.g., the case of Farlie–Gumbel–Morgenstern (FGM) class of copulas, all of them being a perturbation of the independence copula Π, $\Pi(u,v) = u\,v$. Recall that FGM family $\left(C_\alpha^{FGM}\right)_{\alpha\in[-1,1]}$ of copulas is given by

$$C_\alpha^{FGM}(u,v) = u\,v + \alpha\,u\,(1-u)\,v\,(1-v). \tag{5}$$

Several generalizations of FGM approach to perturb the product copula Π can be found in literature, see, for example Amblard and Girard[1], Bairamov and Kotz [4], Rodríguez–Lallena and Úbeda–Flores[14].

For a given copula $C : [0,1]^2 \to [0,1]$, we will look for constraints on the noise $H : [0,1]^2 \to \Re$ so that the function $C_H : [0,1]^2 \to [0,1]$ given by

$$C_H(u,v) = \max\left(0,\ C(u,v) + H(u,v)\right) \tag{6}$$

is also a copula. Obviously FGM copulas given by (5) are linked to $C = \Pi$ and $H_\alpha(u,v) = \alpha * u * (1-u) * v * (1-v)$ (observe that in this case, no truncation is necessary).

For a fixed copula $C : [0,1]^2 \to [0,1]$, consider the function C_H given by (6). To satisfy the groundedness condition of copulas by C_H, necessarily $H(u,0) \le 0$ and $H(0,v) \le 0$ for all $u, v \in [0,1]$. Similarly, $e = 1$ is a neutral element of C_H only if $H(u,1) = H(1,v) = 0$ for all $u, v \in [0,1]$. The main problem to ensure that C_H is a copula is to guarantee the 2–increasingness of C_H, which depends both on C and H.

In general, if C is a singular copula, the function $H \neq 0$ cannot be absolutely continuous. Similarly, if C is an absolutely continuous copula, H cannot be singular. Therefore, as a special case of the perturbation (7), one can deal with perturbation related to functions $f, g : [0,1] \to [0,1]$ and constant $\lambda \in \Re$ in the form already discussed in Mesiar *et al.*[11], namely

$$C_{\lambda,f,g}(u,v) = \max\left(0,\ C(u,v) + \lambda\,C(f(u),f(v))\right). \tag{7}$$

Obviously, FGM family given in (5) can be seen as a special case of construction (6), considering $C = \Pi$, $\lambda \in [-1,1]$ and $f = g$ given by $f(x) = x - x^2$. Note that as a necessary condition to ensure that $e = 1$ is a neutral element of $C_{\lambda,f,g}$, one should consider $f(1) = g(1) = 0$. On the other hand, if $\lambda \le 0$, then $C_{\lambda,f,g}$ is always grounded. However, if $\lambda > 0$, then one should consider $C(f(0), g(0)) = 0$ (which is trivially satisfied for any copula C if $f(0) = g(0) = 0$).

In the case when no truncation is necessary, we have two general results.

Proposition 1. *Let $C : [0,1]^2 \to [0,1]$ be a copula and $H : [0,1]^2 \to [0,1]$ be a function so that $C + H \ge 0$ and C_H is a copula, i.e., $C_H = C + H$ is a copula. Then also $C_{\lambda\,H} = C + \lambda\,H$ is a copula for each $\lambda \in [0,1]$.*

Proposition 2. *Under the constraints of Proposition 1, the function $\hat{C}_{\bar{H}}$ is a copula, where $\hat{C} : [0,1]^2 \to [0,1]$ is the survival copula related to C,*

$$\hat{C}(u,v) = u + v - 1 + C(1-u, 1-v),$$

and $\bar{H} : [0,1]^2 \to [0,1]$ *is given by*

$$\bar{H}(u,v) = H(1-u, 1-v).$$

We have a next perturbation method valid for any copula C.

Theorem 1. *Let* $C : [0,1]^2 \to [0,1]$ *be a copula and define* $H_\lambda^C : [0,1]^2 \to [0,1], \lambda \in [0,1]$ *by*

$$H_\lambda^C(u,v) = \lambda\,(u - C(u,v))\,(v - C(u,v)).$$

Then $C_{H_\lambda^C} : [0,1]^2 \to [0,1]$ *given by*

$$C_{H_\lambda^C}(u,v) = C(u,v) + H_\lambda^C(u,v) \tag{8}$$

is a copula for each $\lambda \in [0,1]$ *and any copula* C.

4 Application to real data modelling

4.1 Real Estate Investment Trust

A REIT (**R**eal **E**state **I**nvestment **T**rust) is a company that mainly owns, and in most cases, operates income–producing real estate such as apartments, shopping centers, offices, hotels and warehouses. Some REITs also engage in financing real estate. The shares of many REITs are traded on major stock exchanges.

REIT Index Series is designed to present investors with a comprehensive family of REIT performance indexes that spans the commercial real estate space across the economy of the country. The index series provides investors with exposure to all investment and property sectors. In addition, the more narrowly focused property sector and sub–sector indexes provide the facility to concentrate commercial real estate exposure in more selected markets.

We have investigated the relations between 4 selected countries' (USA, Australia, Japan and UK) daily returns of the REIT (Real Estate Investment Trust) indexes in different time periods, determined by the recent global financial markets crises (July 1, 2008 – April 30, 2009) that can be also clearly identified from next Figure 1, presenting the parallel development of the considered REIT indexes.

We have performed filtering of the returns of all individual REIT indexes (in order to avoid a possible violation of the i.i.d. property) by ARMA–GARCH models (separately for the individual considered time sub-periods). Some basic descriptive statistical characteristics of 12 resulting time series are presented in Tables 2, 3 and 4 (mean values equal to 0 are in accordance to the expected properties of residuals of filtering).

The values of kurtosis for all 12 considered time series suggest that only the UK data during and after the crisis can be well fitted by Normal distributions

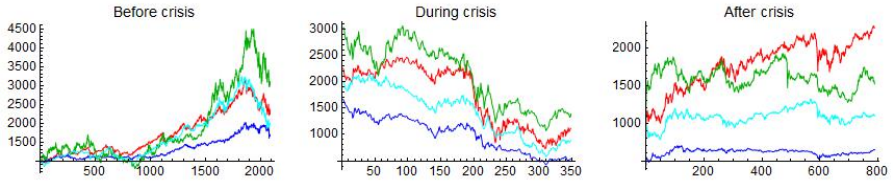

Fig. 1. Real Estate Investment Trust indexes in different time periods (USA = red, Australia = blue, Japan = green, UK = cyan)

Country	Mean	Standard deviation	Skewness	Kurtosis	Min	Max
USA	0.00	0.71	0.07	4.31	-3.85	3.31
Australia	0.00	0.39	0.14	4.83	-2.12	1.82
Japan	0.00	0.03	0.18	3.59	-0.09	0.11
U.K.	0.00	0.02	0.14	4.95	-0.07	0.08

Table 2. Descriptive statistics for filtered returns of the REIT indexes before crisis

Country	Mean	Standard deviation	Skewness	Kurtosis	Min	Max
USA	0.00	0.05	0.08	5.29	-0.23	0.24
Australia	0.00	0.08	-0.55	5.01	-0.49	0.26
Japan	0.00	0.05	-0.23	5.08	-0.29	0.16
U.K.	0.00	0.03	0.05	3.27	-0.10	0.11

Table 3. Descriptive statistics for filtered returns of the REIT indexes during crisis

Country	Mean	Standard deviation	Skewness	Kurtosis	Min	Max
USA	0.00	0.02	0.98	7.18	-0.11	0.44
Australia	0.00	0.01	0.90	6.97	-0.04	0.21
Japan	0.00	0.02	0.31	7.23	-0.12	0.29
U.K.	0.00	0.02	0.01	3.25	-0.08	0.08

Table 4. Descriptive statistics for filtered returns of the REIT indexes after crisis

(with the theoretical value of kurtosis equal to 3). This intuitive guess has been justified by the results of Jarque-Bera GoF test (see e.g. [8]) applied to all 12 time series. For fitting the remaining 10 time series, we utilized the Logistic and Laplace classes of distributions that have larger theoretical values of kurtosis.

Resulting types of distributions and their parameters for all 12 time series together with p-values are shown in Table 5, 6 and 7.

For all three time sub-periods and all couples of (filtered) returns of the REIT indexes we have performed the non–parametric correlation analyses based on the Kendall coefficients (see Table 8, 9 and 10). We have observed that the values of the correlation coefficients have dropped substantially between the first and the second considered time sub-periods and even more dramatically

Country	Type of distribution	Parameters	p–value
USA	Logistic	$\mu = 0,\ \beta = 0.3908$	0.97
Australia	Logistic	$\mu = 0,\ \beta = 0.2123$	0.49
Japan	Logistic	$\mu = 0,\ \beta = 0.0155$	0.21
U.K.	Logistic	$\mu = 0,\ \beta = 0.0082$	0.18

Table 5. Marginal distributions for filtered returns of the REIT indexes before crisis

Country	Type of distribution	Parameters	p–value
USA	Logistic	$\mu = 0,\ \beta = 0.0288$	0.09
Australia	Logistic	$\mu = 0,\ \beta = 0.0427$	0.11
Japan	Logistic	$\mu = 0,\ \beta = 0.0297$	0.33
U.K.	Normal	$\mu = 0,\ \sigma = 0.0344$	0.45

Table 6. Marginal distributions for filtered returns of the REIT indexes during crisis

Country	Type of distribution	Parameters	p–value
USA	Laplace	$\mu = 0,\ \beta = 0.0142$	0.12
Australia	Laplace	$\mu = 0,\ \beta = 0.0097$	0.16
Japan	Laplace	$\mu = 0,\ \beta = 0.0120$	0.15
U.K.	Normal	$\mu = 0,\ \sigma = 0.0247$	0.44

Table 7. Marginal distributions for filtered returns of the REIT indexes after crisis

for the third sub-period. These changes are illustrated in the scatter plots (see Figure 2 – Figure 7).

before crisis	USA	Australia	Japan	UK
USA	1	0.994	0.731	0.737
Australia	0.994	1	0.727	0.738
Japan	0.731	0.727	1	0.609
UK	0.737	0.738	0.609	1

Table 8. The values of the Kendall's correlation coefficient τ for the pre–crisis period

during crisis	USA	Australia	Japan	UK
USA	1	0.301	0.267	0.306
Australia	0.301	1	0.535	0.397
Japan	0.267	0.535	1	0.378
UK	0.306	0.397	0.378	1

Table 9. The values of the Kendall's correlation coefficient τ for the crisis period

after crisis	USA	Australia	Japan	UK
USA	1	0.111	0.061	0.221
Australia	0.111	1	0.222	0.087
Japan	0.061	0.222	1	0.073
UK	0.221	0.087	0.073	1

Table 10. The values of the Kendall's correlation coefficient τ for the post–crisis period

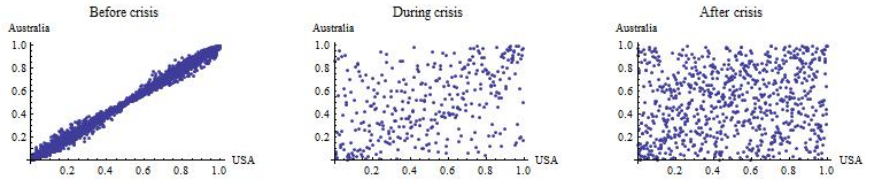

Fig. 2. USA & Australia

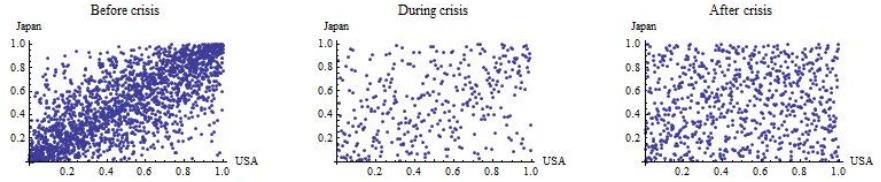

Fig. 3. USA & Japan

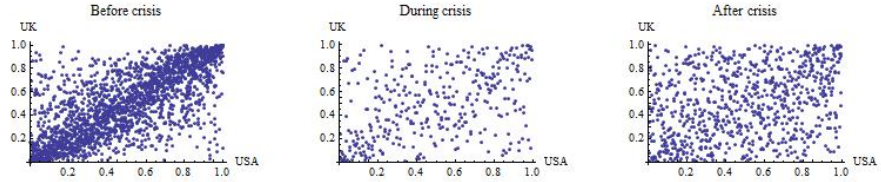

Fig. 4. USA & U.K.

We have applied the fitting by copulas to the residuals of ARMA–GARCH filters. We considered models from strict Archimedean copulas (Joe C^J, Frank C^F, Clayton C^{Cl} and Gumbel C^G) families and their mixtures with corresponding survival copulas $\hat{C}$ as well as their perturbations given by (8). We also tried the Farlie–Gumbel–Morgenstern (FGM) and Ali–Mikhail–Haq (AMH) copulas, but these had the greatest values of the AD for all the pairs and time periods.

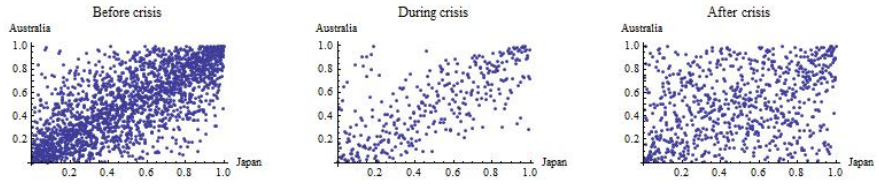

Fig. 5. Japan & Australia

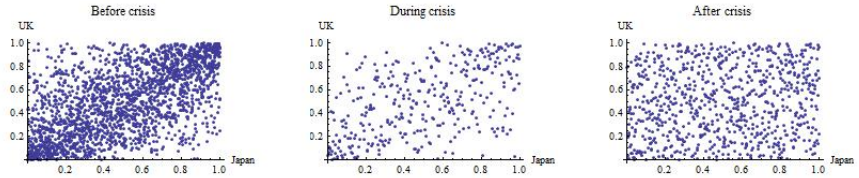

Fig. 6. Japan & U.K.

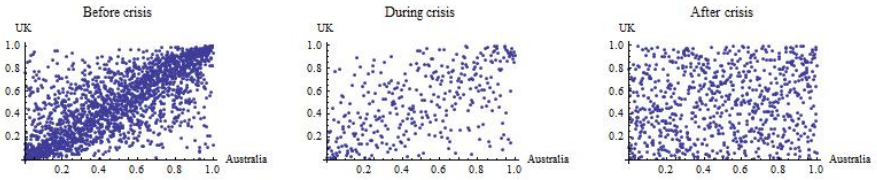

Fig. 7. Australia & U.K.

For estimation of parameters for each type of models we have used the maximum pseudo–likelihood method. For selecting the optimal models we have applied the Kolmogorov – Smirnov – Anderson – Darling (for which we have used the abbreviation AD) test statistic (4). For all of them, the simulation based GoF test yielded p–value > 0.1. Overview of optimal types of copulas for all couples and all time sub–periods of the filtered returns of REIT indexes is in Table 11 – Table 16.

5 Concluding remarks

We have found suitable marginal distribution models for all considered time series of filtered returns of REIT indexes and considered time period in one of Normal, Logistic or Laplace classes of distributions. We can observe that (although there is no clear relation between the pseudo likelihood functions and AD criterion) for all considered 6 couples of (filtered) returns of REIT indexes in 3 time periods and for all 6 couples of considered models the best perturbed models have lower values of AD criterion than the best models in the corresponding non–perturbed model classes. Moreover, for a great majority (16/18) of the considered 18 couples of (filtered) returns of REIT indexes, the non–perturbed models corresponding to the optimal perturbed ones attain the minimal values of the AD criterion among all considered non–perturbed classes

Type of copula	03.01.2000–31.07.2008			01.08.2008–30.04.2009			01.05.2009–08.05.2012		
	λ	θ	**AD**	λ	θ	**AD**	λ	θ	**AD**
C^G	x	1.99	4.42	x	1.31	2.56	x	1.05	8.81
$C^G + H_\lambda^{C^G}$	0.98	1.80	4.23	0.63	1.18	2.44	0.16	1.03	8.43
$0.5 * (C^G + \hat{C}^G)$	x	2.19	1.72	x	1.80	1.27	x	1.65	1.82
$0.5 * (C^G + \hat{C}^G) + H_\lambda^{0.5*(C^G+\hat{C}^G)}$	0.79	1.98	1.55	0.46	1.24	**1.03**	0.05	1.08	1.74
C^{Cl}	x	1.48	4.96	x	0.48	1.85	x	0.17	2.26
$C^{Cl} + H_\lambda^{C^{Cl}}$	0.97	1.18	3.72	0.76	0.24	1.45	0.04	0.17	2.19
$0.5 * (C^{Cl} + \hat{C}^{Cl})$	x	1.56	1.98	x	0.21	1.42	x	0.43	3.49
$0.5 * (C^{Cl} + \hat{C}^{Cl}) + H_\lambda^{0.5*(C^{Cl}+\hat{C}^{Cl})}$	0.98	1.71	**1.52**	0.53	0.42	1.69	0.03	0.16	3.27
C^J	x	2.25	12.09	x	1.40	4.09	x	1.04	10.32
$C^J + H_\lambda^{C^J}$	0.97	1.94	9.98	0.83	1.15	3.03	0.22	1.02	9.45
$0.5 * (C^J + \hat{C}^J)$	x	2.72	2.07	x	2.56	1.63	x	4.01	1.48
$0.5 * (C^J + \hat{C}^J) + H_\lambda^{0.5*(C^J+\hat{C}^J)}$	0.99	2.56	1.97	0.65	1.30	1.27	0.23	1.13	**1.34**

Table 11. The overview of optimal types of copulas for the couple USA & Japan of the (filtered) returns of REIT indexes

Type of copula	03.01.2000–31.07.2008			01.08.2008–30.04.2009			01.05.2009 – 08.05.2012		
	λ	θ	**AD**	λ	θ	**AD**	λ	θ	**AD**
C^G	x	2.21	3.75	x	1.42	3.54	x	1.27	6.05
$C^G + H_\lambda^{C^G}$	0.45	2.13	3.29	0.25	1.38	3.32	0.36	1.20	5.83
$0.5 * (C^G + \hat{C}^G)$	x	1.90	1.60	x	1.05	1.68	x	1.13	1.79
$0.5 * (C^G + \hat{C}^G) + H_\lambda^{0.5*(C^G+\hat{C}^G)}$	0.07	2.31	**1.47**	0.08	1.47	1.38	0.06	1.29	**1.58**
C^{Cl}	x	1.62	5.27	x	0.76	1.37	x	0.43	2.27
$C^{Cl} + H_\lambda^{C^{Cl}}$	0.98	1.32	4.22	0.41	0.65	**1.22**	0.62	0.24	1.93
$0.5 * (C^{Cl} + \hat{C}^{Cl})$	x	2.18	2.23	x	1.41	1.97	x	0.54	1.78
$0.5 * (C^{Cl} + \hat{C}^{Cl}) + H_\lambda^{0.5*(C^{Cl}+\hat{C}^{Cl})}$	0.54	2.17	2.12	0.02	0.87	1.71	0.05	0.59	1.62
C^J	x	2.60	10.00	x	1.51	6.46	x	1.34	12.05
$C^J + H_\lambda^{C^J}$	0.97	2.29	7.75	0.77	1.31	5.33	0.68	1.18	9.21
$0.5 * (C^J + \hat{C}^J)$	x	2.91	2.25	x	1.40	1.91	x	1.16	1.77
$0.5 * (C^J + \hat{C}^J) + H_\lambda^{0.5*(C^J+\hat{C}^J)}$	0.61	2.96	2.16	0.09	1.72	1.81	0.14	1.45	1.65

Table 12. The overview of optimal types of copulas for the couple USA & UK of the (filtered) returns of REIT indexes

Type of copula	03.01.2000–31.07.2008			01.08.2008–30.04.2009			01.05.2009–08.05.2012		
	λ	θ	**AD**	λ	θ	**AD**	λ	θ	**AD**
C^G	x	4.74	2.11	x	1.42	2.81	x	1.12	5.92
$C^G + H_\lambda^{C^G}$	0.95	4.18	1.92	0.08	1.41	2.49	0.06	1.11	5.58
$0.5 * (C^G + \hat{C}^G)$	x	7.03	1.67	x	1.27	1.57	x	1.04	2.05
$0.5 * (C^G + \hat{C}^G) + H_\lambda^{0.5*(C^G+\hat{C}^G)}$	0.97	6.64	**1.46**	0.05	1.44	**1.54**	0.05	1.14	1.98
C^{Cl}	x	5.94	4.07	x	0.59	1.95	x	0.22	1.53
$C^{Cl} + H_\lambda^{C^{Cl}}$	0.98	5.63	3.94	0.68	0.40	1.56	0.10	0.19	**1.27**
$0.5 * (C^{Cl} + \hat{C}^{Cl})$	x	11.08	1.58	x	0.56	1.88	x	0.80	2.19
$0.5 * (C^{Cl} + \hat{C}^{Cl}) + H_\lambda^{0.5*(C^{Cl}+\hat{C}^{Cl})}$	0.98	11.96	1.54	0.21	0.71	1.73	0.04	0.28	2.16
C^J	x	7.92	4.15	x	1.15	6.18	x	1.55	4.65
$C^J + H_\lambda^{C^J}$	0.95	7.07	3.78	0.26	1.09	5.51	0.59	1.39	3.75
$0.5 * (C^J + \hat{C}^J)$	x	13.81	1.58	x	2.15	1.88	x	1.39	1.80
$0.5 * (C^J + \hat{C}^J) + H_\lambda^{0.5*(C^J+\hat{C}^J)}$	0.99	13.65	1.54	0.03	1.24	1.58	0.30	1.59	1.57

Table 13. The overview of optimal types of copulas for the couple USA & Australia of the (filtered) returns of REIT indexes

of models for the (filtered) returns of REIT indexes (for 2 remaining couples they narrowly exceed the minimum values). Moreover, for 17 of 18 considered couples of (filtered) returns of REIT indexes the θ coefficients of the optimal

Type of copula	03.01.2000–31.07.2008			01.08.2008–30.04.2009			01.05.2009–08.05.2012		
	λ	θ	**AD**	λ	θ	**AD**	λ	θ	**AD**
C^G	x	1.97	3.77	x	1.97	3.70	x	1.28	4.54
$C^G + H_\lambda^{C^G}$	0.97	1.77	3.68	0.93	1.78	3.14	0.08	1.27	4.42
$0.5 * (C^G + \hat{C}^G)$	x	2.29	1.76	x	2.39	1.45	x	1.13	1.71
$0.5 * (C^G + \hat{C}^G) + H_\lambda^{0.5*(C^G+\hat{C}^G)}$	0.89	1.91	**1.52**	0.44	2.01	**1.32**	0.05	1.31	1.61
C^{Cl}	x	1.41	4.95	x	1.34	2.31	x	0.46	2.20
$C^{Cl} + H_\lambda^{C^{Cl}}$	0.95	1.11	3.65	0.98	1.04	1.93	0.45	0.33	1.76
$0.5 * (C^{Cl} + \hat{C}^{Cl})$	x	1.32	1.85	x	1.56	1.55	x	1.27	1.77
$0.5 * (C^{Cl} + \hat{C}^{Cl}) + H_\lambda^{0.5*(C^{Cl}+\hat{C}^{Cl})}$	0.97	1.65	1.76	0.76	1.75	1.47	0.05	0.60	1.65
C^J	x	2.21	11.53	x	2.25	12.41	x	1.36	7.35
$C^J + H_\lambda^{C^J}$	0.98	1.90	10.05	0.96	1.94	10.84	0.53	1.22	6.28
$0.5 * (C^J + \hat{C}^J)$	x	3.06	1.81	x	2.73	1.55	x	1.34	1.35
$0.5 * (C^J + \hat{C}^J) + H_\lambda^{0.5*(C^J+\hat{C}^J)}$	0.98	2.51	1.74	0.81	2.60	1.48	0.03	1.51	**1.18**

Table 14. The overview of optimal types of copulas for the couple Japan & Australia of the (filtered) returns of REIT indexes

Type of copula	03.01.2000–31.07.2008			01.08.2008–30.04.2009			01.05.2009–08.05.2012		
	λ	θ	**AD**	λ	θ	**AD**	λ	θ	**AD**
C^G	x	1.66	5.01	x	1.53	2.67	x	1.07	4.27
$C^G + H_\lambda^{C^G}$	0.98	1.46	4.66	0.85	1.36	2.57	0.23	1.0.	4.14
$0.5 * (C^G + \hat{C}^G)$	x	1.64	1.54	x	1.49	1.35	x	1.08	1.86
$0.5 * (C^G + \hat{C}^G) + H_\lambda^{0.5*(C^G+\hat{C}^G)}$	0.55	1.64	**1.37**	0.48	1.49	**1.23**	0.05	1.09	1.79
C^{Cl}	x	1.01	4.74	x	0.88	1.86	x	0.16	1.40
$C^{Cl} + H_\lambda^{C^{Cl}}$	0.97	0.71	3.07	0.93	0.61	1.24	0.02	0.15	**1.35**
$0.5 * (C^{Cl} + \hat{C}^{Cl})$	x	1.64	1.74	x	1.49	1.62	x	1.09	2.01
$0.5 * (C^{Cl} + \hat{C}^{Cl}) + H_\lambda^{0.5*(C^{Cl}+\hat{C}^{Cl})}$	0.71	1.16	1.58	0.79	0.76	1.54	0.03	0.18	1.94
C^J	x	1.83	5.99	x	1.66	4.50	x	1.07	5.10
$C^J + H_\lambda^{C^J}$	0.97	1.53	2.81	0.99	1.37	4.09	0.30	1.02	4.52
$0.5 * (C^J + \hat{C}^J)$	x	1.16	1.83	x	0.76	1.53	x	0.18	1.56
$0.5 * (C^J + \hat{C}^J) + H_\lambda^{0.5*(C^J+\hat{C}^J)}$	0.83	1.97	1.63	0.88	1.61	1.38	0.02	1.14	1.47

Table 15. The overview of optimal types of copulas for the couple Japan & U.K. of the (filtered) returns of REIT indexes

Type of copula	03.01.2000–31.07.2008			01.08.2008–30.04.2009			01.05.2009–08.05.2012		
	λ	θ	**AD**	λ	θ	**AD**	λ	θ	**AD**
C^G	x	2.26	3.94	x	1.59	2.78	x	1.08	2.98
$C^G + H_\lambda^{C^G}$	0.24	2.22	3.57	0.77	1.43	2.07	0.23	1.04	2.72
$0.5 * (C^G + \hat{C}^G)$	x	2.35	1.71	x	1.62	1.05	x	1.09	1.68
$0.5 * (C^G + \hat{C}^G) + H_\lambda^{0.5*(C^G+\hat{C}^G)}$	0.02	2.33	**1.67**	0.17	1.64	**0.93**	0.02	1.09	1.61
C^{Cl}	x	1.68	5.39	x	0.94	1.97	x	0.15	1.88
$C^{Cl} + H_\lambda^{C^{Cl}}$	0.98	1.38	4.44	0.98	0.66	1.65	0.24	0.08	**1.29**
$0.5 * (C^{Cl} + \hat{C}^{Cl})$	x	2.35	2.75	x	1.62	1.31	x	1.09	1.73
$0.5 * (C^{Cl} + \hat{C}^{Cl}) + H_\lambda^{0.5*(C^{Cl}+\hat{C}^{Cl})}$	0.42	2.26	2.63	0.72	0.89	1.08	0.02	0.21	1.57
C^J	x	2.68	5.22	x	1.73	6.08	x	1.10	3.69
$C^J + H_\lambda^{C^J}$	0.98	2.37	5.00	0.96	1.44	5.04	0.32	1.04	3.21
$0.5 * (C^J + \hat{C}^J)$	x	2.26	2.82	x	0.89	1.15	x	0.20	1.70
$0.5 * (C^J + \hat{C}^J) + H_\lambda^{0.5*(C^J+\hat{C}^J)}$	0.49	3.04	2.65	0.79	1.75	1.09	0.15	1.11	1.42

Table 16. The overview of optimal types of copulas for the couple U.K. & Australia of the (filtered) returns of REIT indexes

models do not considerably differ from the values of optimal models in the corresponding classes of non–perturbed models. The only exception to this

phenomenon could be attributed to very flat shapes of the respective pseudo likelihood functions around they minimum values.

Acknowledgement The support of the grants APVV–0073–10 and VEGA 1/0143/11 is kindly announced.

References

1. Amblard, C., Girard, S.: A new symmetric extension of FGM copulas. *Metrika* **70**, 1–17 (2009)
2. Anderson, T. W.: Anderson-Darling tests of goodness-of-fit. *International Encyclopedia of Statistical Science*, Springer (2011)
3. Anderson, T. W., Darling, D. A.: A Test of Goodness of Fit. *Journal of the American Statistical Association* Vol. **49**, No. 268, 765–769 (1954)
4. Bairamov, I., Kotz, S.: Dependence structure and symmetry of Huang-Kotz FGM distributions and their extensions. *Metrika* **56**, 55–72 (2002)
5. Balakrishnan, N.: *Handbook of the Logistic Distribution.* Marcel Dekker, New York (1992)
6. Berg, D., Bakken, H.: Copula Goodness-of-fit Tests: A Comparative Study. In: Working paper, University of Oslo and Norwegian Computing Center (2006)
7. Genest, C., Favre, A.C.: Everything you always wanted to know about copula modeling but were afraid to ask. *Journal of Hydrologic Engineering* **12**, 347–368 (2007)
8. Jarque, C.M., Bera, A.K.: A test for normality of observations and regression residuals. *International Statistical Review* **55** (2), 163-172 (1987)
9. Joe, H.: *Multivariate models and dependence concepts.* London : Chapman and Hall (1997)
10. Kotz, S., Kozubowski, T. J., Podgórski, K.: *The Laplace distribution and generalizations: a revisit with applications to Communications, Economics, Engineering and Finance.* Birkhauser. pp. 23 (Proposition 2.2.2, Equation 2.2.8) (2001)
11. Mesiar, R., Komorník, J., Komorníková, M.: On some construction methods for bivariate copulas. *Advances in Intelligent Systems and Computing*, **228**. Aggregation Functions in Theory and in Practise : Proceedings of the 7th International Summer School on Aggregation Operators at the Public University of Navarra, Pamplona, Spain, 16.-20.6.2013, 39–46 (2013)
12. Mesiar, R., Komorník, J., Komorníková, M.: Modification of bivariate copulas, *Fuzzy Sets and Systems* (2014), http://dx.doi.org/10.1016/j.fss.2014.04.016
13. Nelsen, R.B.: *An introduction to copulas.* Second Edition. Springer Series in Statistics, Springer-Verlag, New York (2006)
14. Rodríguez–Lallena, J. A., Úbeda–Flores, M.: A new class of bivariate copulas. *Statistics & Probability Letters* **66**, 315–325 (2004)
15. Patton, A.J.: Modelling Asymmetric Exchange Rate Dependence. *International Economic Review*, 47, **2**, 527–556 (2006)
16. Sklar, A.: Fonctions de répartition à n dimensions et leurs marges. *Publ. Inst. Statist. Univ. Paris* **8**, 229–231 (1959)

A survey on the isometry of certain orthogonal polynomial systems in martingale spaces

Edmundo J. Huertas[1] and Nuria Torrado[2]

[1] Centre for Mathematics, University of Coimbra (CMUC), Largo D. Dinis, Apartado 3008, EC Santa Cruz, 3001-501 Coimbra, Portugal
(E-mail: ehuertasce@mat.uc.pt, ehuertasce@gmail.com)
[2] Centre for Mathematics, University of Coimbra (CMUC), Largo D. Dinis, Apartado 3008, EC Santa Cruz, 3001-501 Coimbra, Portugal
(E-mail: nuria.torrado@mat.uc.pt, nuria.torrado@gmail.com)

Abstract. In this paper we survey how an inner product derived from an Uvarov transformation of the Laguerre weight function is used in the orthogonalization procedure of a sequence of martingales related to a Lévy process. The orthogonalization is done by isometry and it is based in previous works of Nualart and Schoutens (see [18] and [19]), where the resulting set of pairwise strongly orthogonal martingales involved are used as integrators in the so-called chaotic representation property. Finally, we give an idea of how to generalize the above works.
Keywords: Orthogonal polynomials; Laguerre-type polynomials; Krall-Laguerre polynomials; Inner products; Lévy processes; Stochastic processes.

1 Introduction

The Laguerre orthogonal polynomials are defined as the polynomials orthogonal with respect to the Gamma distribution. Therefore, they are orthogonal with respect to the inner product in the linear space $\mathbb{P}$ of polynomials with real coefficients (see [2])

$$\langle p, q\rangle_{\alpha} = \int_0^{\infty} pqx^{\alpha}e^{-x}dx, \quad \alpha > -1,\ p, q \in \mathbb{P}. \tag{1}$$

From now on, $\{\widehat{L}_n^{\alpha}(x)\}_{n\geq 0}$ stands for the sequence of monic Laguerre polynomials orthogonal with respect to (1). From the above inner product, let us introduce the modified inner product

$$\langle p, q\rangle = \int_0^{\infty} pqx^{\alpha}e^{-x}dx + \sigma^2 p(c)q(c), \quad \alpha > -1,\ p, q \in \mathbb{P} \tag{2}$$

where $\sigma^2 \in \mathbb{R}_+$, and $c \in (-\infty, 0]$. Notice that $\langle p, q\rangle = \langle p, q\rangle_{\alpha} + \sigma^2 p(c)q(c)$, so therefore (2) can be interpreted as a modification (or perturbation) of the

New Trends in Stochastic Modeling and Data Analysis (pp. 409-418)
Raimondo Manca - Sally McClean - Christos H Skiadas (Eds)

Laguerre measure $d\mu_\alpha(x) = x^\alpha e^{-x} dx$ with a discrete measure given by a mass point at $x = c$,

$$d\tilde{\mu}_\alpha(x) = x^\alpha e^{-x} dx + \sigma^2 \delta(x - c),$$

where $\delta(x - c)$ is the Dirac delta at $x = c$. This perturbation is known as the Uvarov perturbation of the measure $d\mu_\alpha(x)$ (see [5], [6], [7] and the references given there). The case $c = 0$ has been deeply studied in the literature (see [3], [4], [11] among others). These polynomials are called either Laguerre-type polynomials (see, for instance, [3] and [14]) or Krall-Laguerre polynomials (in [8]). They were also obtained by T.H. Koornwinder [12] as a special limit case of the Jacobi-Koornwinder (Jacobi type) orthogonal polynomials, and they are also known as Laguerre-Koornwinder polynomials.

A Lévy process is a stochastic process with independent and stationary increments which consists of three basic stochastically independent parts: a deterministic part, a pure jump part and a Brownian motion. Lévy processes play an important role in many fields of science. For example, in engineering, they are used for the study of networks; in the actuarial science, for the calculation of insurance and re-insurance risk and, in economics, for continuous time-series models. In the last decades, the study of the relation between orthogonal polynomials and Lévy processes have become increasing, see [17], [18], [21] and [22].

Consider a Lévy process and let σ^2 the constant of the Brownian motion part and ν its Lévy measure. Nualart and Schoutens [17] and Schoutens [19] have shown that there exists an isometry between the space of orthogonal polynomials with respect to the inner product (2) when $c = 0$ and the space of strongly orthogonal martingales which are the building blocks of a kind of chaotic representation of the square functionals of the Lévy process. The chaotic representation property (CRP) says that any square integrable random variable measurable with respect to normal martingales X can be expressed as an orthogonal sum of multiple stochastic integrals with respect to X. Based in the aforementioned previous works of Nualart and Schoutens, we are interested in finding new isometries that encompass the above cases using new families of orthogonal polynomials that generalize the Laguerre-type orthogonal polynomials used by Schoutens in [18]. Recently, several authors have begun to study the case when c is a negative number, i.e., the mass point is located outside the support of the Laguerre measure. The study of their asymptotic and analytic properties can be founded in [5], [6] or [7].

Our main goal is to consider a natural generalization of the work done in [18]. In other words, meanwhile Schoutens analyzed the connection between Lévy processes and Laguerre-type orthogonal polynomials with respect to the inner product (2) for the particular case $c = 0$, we study a more general case where $c \in (-\infty, 0)$. In our opinion, the differences between these two cases are sufficient to justify a new study of the isometry of these polynomials with certain sets of martingales.

The structure of the manuscript is as follows. In Section 2, we summarize some properties of Laguerre-type orthogonal polynomials to be used in the sequel. We briefly review the concept of Lévy process and study the orthogonalization procedure for a sequence of martingales related to the powers of the

jumps of this stochastic process in Section 3. As an original contribution that have not been published elsewhere, in Section 4 we provide the explicit coefficients of the generalize Laguerre-type orthogonal polynomials which eventually can lead to the desired isometry with some new space of Teugel martingales. We also discuss the work done so far and stress the problems founded to figure out the desired isometry, and give some few ideas that may help to find isometries for these new families of modified (standard and non standard) sequences of orthogonal polynomials.

2 Laguerre-type orthogonal polynomials

First, we review some basic properties of classical Laguerre polynomials $\widehat{L}_n^\alpha(x)$ useful in the sequel. Their corresponding norm is given by $||\widehat{L}_n^\alpha||_\alpha^2 = n!\Gamma(n+\alpha+1)$. Dealing with Laguerre polynomials, it is customary to use the normalization such that the leading coefficient of the n-th degree classical Laguerre polynomial (denoted by $L_n^{(\alpha)}(x)$) equals $\frac{(-1)^n}{n!}$, i.e., $L_n^{(\alpha)}(x) = \frac{(-1)^n}{n!}x^n +$ *lower degree terms,* and therefore

$$L_n^{(\alpha)}(x) = \frac{(-1)^n}{n!}\widehat{L}_n^\alpha(x).$$

It is very well known that these polynomials satisfy the following three term recurrence relation

$$x\widehat{L}_n^\alpha(x) = \widehat{L}_{n+1}^\alpha(x) + \beta_n\widehat{L}_n^\alpha(x) + \gamma_n\widehat{L}_{n-1}^\alpha(x), \quad n \geq 1, \tag{3}$$

with initial conditions $\widehat{L}_0^\alpha(x) = 1$, $\widehat{L}_1^\alpha(x) = x - (\alpha+1)$, and recurrence coefficients $\beta_n = 2n + \alpha + 1$, $\gamma_n = n(n+\alpha)$ for every $n \geq 1$ (see [16], [23] among others). They constitute a family of classical orthogonal polynomials (see [13] and [16]), and they are the eigenfunctions of a second order linear differential operator with polynomial coefficients. The kernel polynomials (see [2, Ch.I, Â§7]) associated with Laguerre polynomials will play a key role in order to obtain some conclusions of the manuscript. Let

$$K_n(x,y) = \sum_{k=0}^{n} \frac{\widehat{L}_k^\alpha(x)\widehat{L}_k^\alpha(y)}{||\widehat{L}_k^\alpha||_\alpha^2}$$

denotes the n-th kernel polynomial associated with the Laguerre orthogonal polynomials. Thus, according to the Christoffel-Darboux formula, for every $n \in \mathbb{N}$ we get the alternative expression

$$K_n(x,y) = \frac{\widehat{L}_{n+1}^\alpha(x)\widehat{L}_n^\alpha(y) - \widehat{L}_{n+1}^\alpha(y)\widehat{L}_n^\alpha(x)}{x-y}\frac{1}{||\widehat{L}_n^\alpha||_\alpha^2}.$$

The limit when $y \to x$ is known as the *confluent form* of the n-th kernel, and it reads

$$K_n(x,x) = \sum_{k=0}^{n} \frac{[\widehat{L}_k^\alpha(x)]^2}{||\widehat{L}_k^\alpha||_\alpha^2} = \frac{[\widehat{L}_{n+1}^\alpha(x)]'\,\widehat{L}_n^\alpha(x) - [\widehat{L}_n^\alpha(x)]'\,\widehat{L}_{n+1}^\alpha(x)}{||\widehat{L}_n^\alpha||_\alpha^2}.$$

From now on, $\{\widehat{L}_n^{\alpha,c,\sigma^2}(x)\}_{n\geq 0}$ denotes the sequence of monic polynomials orthogonal with respect to (2) when $c \in (-\infty, 0)$, and $\{\widehat{L}_n^{\alpha,\sigma^2}(x)\}_{n\geq 0}$ stands for the monic Laguerre-type orthogonal polynomials with $c = 0$.

We next present some specific properties of $\widehat{L}_n^{\alpha,c,\sigma^2}(x)$, showing the differences which appear when $c = 0$ or $c \in (-\infty, 0)$. The first remarkable fact is that the position of the first (or least) zero of the Laguerre-type polynomials, strongly depends on the value of the real and positive parameter σ^2, and the position of the mass point c (see [7] for detailed study). Obviously, if $\sigma^2 = 0$, the zeros of the Laguerre-type polynomials trivially reduces to the zeros of the classical Laguerre polynomials. Moreover, if $\sigma^2 > 0$ and $c \in (-\infty, 0)$, then one can find values of σ^2 for which the least zero of $\widehat{L}_n^{\alpha,c,\sigma^2}(x)$, $n \geq 1$, is located in the interval $(c, 0)$, i.e., outside of the support of the classic Laguerre measure, whereas if $\sigma^2 > 0$ and $c = 0$ this phenomenon does not occur at all, and all the zeros of $\widehat{L}_n^{\alpha,\sigma^2}(x)$, $n \geq 1$, are located inside the interval $(0, +\infty)$ for any value of σ^2. For every $n = 1, 2, \ldots$, the polynomials $\widehat{L}_n^{\alpha,c,\sigma^2}(x)$ satisfy as well a three term recurrence relation

$$x\widehat{L}_n^{\alpha,c,\sigma^2}(x) = \widehat{L}_{n+1}^{\alpha,c,\sigma^2}(x) + \tilde{\beta}_n \widehat{L}_n^{\alpha,c,\sigma^2}(x) + \tilde{\gamma}_n \widehat{L}_{n-1}^{\alpha,c,\sigma^2}(x), \quad n \geq 1,$$

with recurrence coefficients

$$\tilde{\beta}_n = \beta_n + \frac{\widehat{L}_{n+1}^{\alpha}(c)}{\widehat{L}_n^{\alpha}(c)}\left(1 - \frac{1 + \sigma^2 K_{n-1}(c,c)}{1 + \sigma^2 K_n(c,c)}\right) - \frac{\widehat{L}_n^{\alpha}(c)}{\widehat{L}_{n-1}^{\alpha}(c)}\left(1 - \frac{1 + \sigma^2 K_{n-2}(c,c)}{1 + \sigma^2 K_{n-1}(c,c)}\right),$$

$$\tilde{\gamma}_n = \frac{\left(1 + \sigma^2 K_n(c,c)\right)\left(1 + \sigma^2 K_{n-2}(c,c)\right)}{\left(1 + \sigma^2 K_{n-1}(c,c)\right)^2}\gamma_n.$$

where β_n and γ_n are the recurrence coefficients in (3) for the classical Laguerre polynomials. Notice that $\widehat{L}_n^{\alpha}(c) \neq 0$ for every $n = 0, 1, 2, \ldots$, because c does not belong to the support of the classical Laguerre measure. Finally, a very remarkable difference appear when we express the aforementioned families in terms of Gauss hypergeometric functions. The classical Laguerre polynomials $\widehat{L}_n^{\alpha}(x)$ can be expressed as hypergeometric functions of type ${}_1F_1$ (see [9], [23] among others). The addition of a mass point at $c = 0$ implies that the Laguerre-type polynomials $\widehat{L}_n^{\alpha,\sigma^2}(x)$, which are used in [18], are expressed in terms of ${}_2F_2$ hypergeometric functions (see, for example [10]), meanwhile moving the mass point to $c < 0$, as in our case, implies that the Laguerre-type polynomials $\widehat{L}_n^{\alpha,c,\sigma^2}(x)$ turn to be expressed in terms of ${}_3F_3$ hypergeometric functions (see [5]).

3 Lévy processes and Teugels martingales

Let $X = \{X_t, t \geq 0\}$ be a Lévy process (meaning that X has stationary and independent increments and is continuous in probability and that $X_0 = 0$), cadlag and centered, with moments of all orders. Let us remind that a stochastic process is cadlag if its sample paths are right continuous and have left-hand limits. Denote by σ^2 the variance of the Gaussian part of X and by ν its Lévy

measure. The existence of moments of all orders of X_t implies that the Lévy measure ν has moments of all orders ≥ 2. Write

$$m_n = \int_{\mathbb{R}} x^n \nu(dx) \quad \text{for} \quad n \geq 2.$$

For background on all these notions, we refer to Bertoin [1] and Sato [20]. Following Nualart and Schoutens [17], we introduce the square-integrable martingales (and Lévy processes) called Teugels martingales, related to the powers of the jumps of the process:

$$\begin{aligned} Y_t^{(1)} &= X_t, \\ Y_t^{(n)} &= \sum_{0<s\leq t} (\Delta X_t)^n - m_n t, \quad n \geq 2, \end{aligned}$$

where $\Delta X_t = X_t - X_{t^-}$ is the jump size at time t and

$$X_{t^-} = \lim_{s<t, s\to t} X_s, \ \ t > 0$$

is the left limit process. The compensated power jump process $Y^{(n)}$ of order n is a normal martingale.

An important question is the orthogonalization of the set $\left\{Y^{(n)},\, n = 1, 2, \ldots\right\}$ of martingales, called *Teugels Martingales*, as stochastic integrators of a kind of chaotic representation as we briefly discuss in the Introduction. Specifically, let $\mathcal{M}^2$ be the space of square-integrable martingales M such that $\sup_t E(M_t^2) < \infty$ and $M_0 = 0$ a.s. We recall that two martingales $M, N \in \mathcal{M}^2$ are strongly orthogonal if and only if their product MN is a uniform integrable martingale. Nualart and Schoutens [17] showed that every random variable F in $L^2(\Omega, \mathcal{F})$ has a representation of the form

$$F = E\left[F\right] +$$

$$\sum_{j=1}^{\infty} \sum_{(i_1,\ldots,i_j)\in N^j} \int_0^{\infty} \int_0^{t_1-} \cdots \int_0^{t_{j-1}-} f_{(i_1,\ldots,i_j)}(t_1, \ldots, t_j) dH_{t_j}^{(i_j)} \ldots dH_{t_2}^{(i_2)} dH_{t_1}^{(i_1)}$$

where $f_{(i_1,\ldots,i_j)}$'s are real deterministic functions, $N = \{1, 2, 3, \ldots\}$ and $\left\{H^{(i)}, i = 1, 2, \ldots\right\}$ is an orthogonalized set of martingales. A direct consequence is the weaker predictable representation property (PRP) with respect to the same set of orthogonalized martingales, saying that every random variable F in $L^2(\Omega, \mathcal{F})$ has a representation of the form

$$F = E\left[F\right] + \sum_{j=1}^{\infty} \int_0^{\infty} \Phi_s^{(i)} dH_s^{(i)},$$

where $\Phi_s^{(i)}$ is predictable (see [17] for more details).

Nualart and Schoutens[17], by using the measure $d\mu = x^r \nu(dx) + \sigma^2 \delta_0(dx)$, where δ_0 denotes the Dirac measure at point 0, σ^2 is the variance of the Gaussian part and ν the Lévy measure of a Lévy process, showed that the mapping

$x^{n-1} \longleftrightarrow Y^{(n)}$ defines an isometry between the space of polynomials $\mathbb{P} \subseteq L^2(\mu)$ and $\mathrm{Span}(\{Y^{(1)}, Y^{(2)}, Y^{(3)}, \ldots\}) \subseteq \mathcal{H}^2([0,1])$, where $\mathcal{H}^2([0,1])$ is the space of square integrable martingales on the time interval $[0,1]$. This isometry is given by the equality

$$\langle x^{i-1}, x^{j-1}\rangle_1 = m_{i+j} + \sigma^2 1_{\{i=j=1\}} = \langle Y^{(i)}, Y^{(j)}\rangle_2, \quad \text{for} i,j \geq 1.$$

Here the scalar product $\langle\cdot,\cdot\rangle_1$ in $L^2(\mu)$ is given by

$$\langle p(x), q(x)\rangle_1 = \int_{-\infty}^{+\infty} p(x)q(x)x^2\nu(dx) + \sigma^2 p(0)q(0),$$

whereas $\langle\cdot,\cdot\rangle_2$ denotes the scalar product in $\mathcal{H}^2([0,1])$. We observe that, because of the special structure of the Teugels martingales, for $M, N \in \mathrm{Span}(\{Y^{(1)}, Y^{(2)}, Y^{(3)}, \ldots\})$ the relation $\langle M, N\rangle_2 = 0$ is equivalent to the property that the martingales M and N are strongly orthogonal.

Nualart and Schoutens[17] and Schoutens[18] used this isometry for an orthogonalization procedure of the Teugels martingales: If the polynomials $P_0, P_1, \ldots$ are an orthogonalization of the monomials $\{1, x, x^2, \ldots\}$ in $L^2(\mu)$ and if these monomials $\{1, x, x^2, \ldots\}$ in $L^2(\mu)$ are substituted by $\{Y^{(1)}, Y^{(2)}, Y^{(3)}, \ldots\}$, then we obtain a system of strongly orthogonal martingales $\{H^{(1)}, H^{(2)}, H^{(3)}, \ldots\}$ with $\mathrm{Span}(\{H^{(1)}, H^{(2)}, H^{(3)}, \ldots\}) = \mathrm{Span}(\{Y^{(1)}, Y^{(2)}, Y^{(3)}, \ldots\})$. In particular, if the Lévy process is a Gamma process, then the obtained polynomials are just the Laguerre polynomials with parameter $\alpha = 1$. This makes it possible to find the coefficients for the above linear martingale transformation explicitly.

Here we consider a modified measure $d\mu^c = x^2\nu(dx) + \sigma^2\delta_c(dx)$, where δ_c denotes the Dirac measure at point $c < 0$, σ^2 is the variance of the Gaussian part and ν the Lévy measure of a Lévy process. In the concrete case of a Laguerre weight function this is related with the notion of the Uvarov transformation. In the case of the Gamma process this would lead to Laguerre-type polynomials also called Krall-Laguerre polynomials defined in Section 2.

Thus, we consider a new first space S_1^c as the space of all real polynomials on the positive real line endowed with the scalar product $\langle\cdot,\cdot\rangle_1$ given by

$$\langle p(x), q(x)\rangle_1 = \int_{-\infty}^{+\infty} p(x)q(x)x^2\nu(dx) + \sigma^2 p(c)q(c)$$

and a second space

$$S_2 = \{a_1Y^{(1)} + a_2Y^{(2)} + \cdots + a_nY^{(n)} : n \in \{1,2,\ldots\},\ a_i \in \mathbb{R},\ i = 1,\ldots,n\}$$

endowed with the scalar product

$$\langle X, Y\rangle_2 = E([X,Y]_1).$$

The elements of the space S_2 are linear combinations of Teugels martingales and the orthogonalization procedure produces a set of strongly pairwise orthogonal martingales

$$\{H^{(j)} = a_{1,j}Y^{(1)} + \cdots + a_{j,j}Y^{(j)}, \quad j = 1,2,\ldots\}$$

that can be used in the *chaotic representation property* defined above.

4 Coefficients in the orthogonalization procedure

As detailed in [18], the coefficients of the Laguerre-type polynomials when $c = 0$ are used in the orthogonalization process of the Teugels martingales. In this section, as an original contribution we give the coefficients of the modified Laguerre-type polynomials for $c < 0$ which, to the best of our knowledge, they have not been previously computed or published elsewhere. Our guess is that these coefficients will eventually be needed in new attempts to find the desired new isometries.

In order to find the coefficients $\{b_{k,n}\}_{k=0}^{n}$ of the Laguerre-type polynomials $L_n^{\alpha,c,\sigma^2}(x)$ when $c \in (-\infty, 0)$, we introduce the notation

$$\lambda_n^{\alpha,c} = \frac{L_{n+1}^{(\alpha)}(c)}{L_n^{(\alpha)}(c)}, \text{ and } \kappa_n^{\alpha,c} = 1 + \sigma^2 K_n(c,c).$$

Notice that $L_n^{(\alpha)}(c) \neq 0$ for every $n = 0, 1, 2, \ldots$, because c does not belong to the support of the classical Laguerre measure. In [5, Th. 1] the authors obtained a connection formula between the monic Laguerre-type orthogonal polynomials and the classical monic Laguerre orthogonal polynomials. Following [18], we will consider the alternative normalization of Laguerre-type polynomials with leading coefficient $\frac{(-1)^n}{n!}\kappa_{n-1}^{\alpha,c}$, and we will denote them by $L_n^{\alpha,c,\sigma^2}(x)$ when $c \in (-\infty, 0)$, and by $L_n^{\alpha,\sigma^2}(x)$ when $c = 0$. Using this normalization, the connection formula [5, Th. 1] between the Laguerre-type and the classical Laguerre polynomials reads

$$(x - c)\, L_n^{\alpha,c,\sigma^2}(x) = A_n L_{n+1}^{(\alpha)}(x) + B_n L_n^{(\alpha)}(x) + C_n L_{n-1}^{(\alpha)}(x), \tag{4}$$

where

$$\begin{aligned} A_n &= -(n+1)\kappa_{n-1}^{\alpha,c}, \\ B_n &= (n+1)\kappa_{n-1}^{\alpha,c}\lambda_n^{\alpha,c} + (n+\alpha)\frac{\kappa_n^{\alpha,c}}{\lambda_{n-1}^{\alpha,c}}, \\ C_n &= -(n+\alpha)\kappa_n^{\alpha,c}. \end{aligned}$$

Next, we would like to obtain the coefficients $\{b_{k,n}\}_{k=0}^{n}$ such that

$$L_n^{\alpha,c,\sigma^2}(x) = b_{n,n}x^n + b_{n-1,n}x^{n-1} + \cdots + b_{1,n}x + b_{0,n}.$$

Proposition 1. *Let*

$$L_n^{\alpha,c,\sigma^2}(x) = \sum_{k=0}^{n} b_{k,n}x^k$$

be the Laguerre-type polynomials, orthogonal with respect to the inner product (2). Then, the sequence $\{b_{k,n}\}_{k=0}^{n}$ *is given by*

$$\begin{cases} b_{n,n} = \dfrac{(-1)^n}{n!}\kappa_{n-1}^{\alpha,c}, \\ b_{k-1,n} = t_{k,n+1} + c b_{k,n}, \quad k = n, n-1, \ldots, 1, \end{cases}$$

where

$$t_{k,n+1} = \begin{cases} \dfrac{(-1)^n}{n!}\kappa_{n-1}^{\alpha,c}, & \text{for } k = n+1, \\ \dfrac{u_{k,n}(\alpha,c)}{n!k!}(-n)_k(\alpha+k+1)_{n-k}, & \text{for } 0 \le k \le n, \end{cases}$$

$$u_{k,n}(\alpha,c) = (n+1)\left(\lambda_n^{\alpha,c} + \frac{\alpha+(n+1)}{k-(n+1)}\right)\kappa_{n-1}^{\alpha,c} + \left((k-n) + \frac{(\alpha+n)}{\lambda_{n-1}^{\alpha,c}}\right)\kappa_n^{\alpha,c}$$

and

$$\sum_{k=0}^{n+1} t_{k,n+1}c^k = 0.$$

Proof. The proof will be divided into 2 steps. First, from (4) we will obtain the coefficients $\{t_{k,n+1}\}_{k=0}^{n+1}$ of the polynomial

$$T_{n+1}(x) = (x-c)\,L_n^{\alpha,c,\sigma^2}(x) = \sum_{k=0}^{n+1} t_{k,n+1}x^k, \tag{5}$$

which is obviously related with the Laguerre-type polynomials $L_n^{\alpha,c,\sigma^2}(x)$. Second, we obtain the desired coefficients $\{b_{k,n}\}_{k=0}^{n}$ from $\{t_{k,n+1}\}_{k=0}^{n+1}$.

From (4), and the explicit coefficients for the classical Laguerre polynomials with leading coefficient $\frac{(-1)^n}{n!}$, (see [18])

$$L_n^{(\alpha)}(x) = \frac{1}{n!}\sum_{k=0}^{n}(-n)_k(\alpha+k+1)_{n-k}\frac{x^k}{k!}, \quad \alpha > -1,$$

we get

$$(x-c)\,L_n^{\alpha,c,\sigma^2}(x) = \frac{(-1)^n}{n!}\kappa_{n-1}^{\alpha,c}x^{n+1} + \frac{1}{n!}\sum_{k=0}^{n} u_{k,n}(\alpha,c)(-n)_k(\alpha+k+1)_{n-k}\frac{x^k}{k!},$$

where

$$u_{k,n}(\alpha,c) = (n+1)\left(\lambda_n^{\alpha,c} + \frac{\alpha+(n+1)}{k-(n+1)}\right)\kappa_{n-1}^{\alpha,c} + \left((k-n) + \frac{(\alpha+n)}{\lambda_{n-1}^{\alpha,c}}\right)\kappa_n^{\alpha,c}.$$

Thus,

$$t_{k,n+1} = \begin{cases} \dfrac{(-1)^n}{n!}\kappa_{n-1}^{\alpha,c}, & \text{for } k = n+1, \\ \dfrac{u_{k,n}(\alpha,c)}{n!k!}(-n)_k(\alpha+k+1)_{n-k}, & \text{for } 0 \le k \le n. \end{cases} \tag{6}$$

Next, we deduce the sequence $\{b_{k,n}\}_{k=0}^{n}$ in terms of $\{t_{k,n+1}\}_{k=0}^{n+1}$. (5) makes it obvious that, for every $n \ge 0$

$$T_{n+1}(x) = (x-c)\,L_n^{\alpha,c,\sigma^2}(x),$$

$$t_{n+1,n+1}x^{n+1} + \sum_{k=1}^{n} t_{k,n+1}x^k + t_{0,n+1} = b_{n,n}x^{n+1} + \sum_{k=1}^{n}(b_{k-1,n} - cb_k)x^k - cb_{0,n},$$

being c a root of $T_{n+1}(x)$, i.e.

$$\sum_{k=0}^{n+1} t_{k,n+1} c^k = 0.$$

Hence, the following relations matching the coefficients of $T_{n+1}(x)$ and $L_n^{\alpha,c,\sigma^2}(x)$ hold

$$\begin{cases} t_{n+1,n+1} = b_{n,n}, \\ t_{k,n+1} = b_{k-1,n} - c b_{k,n}, \quad 1 \leq k \leq n, \\ t_{0,n+1} = -c b_{0,n}. \end{cases}$$

The above provide a simple recursive rule to obtain the n coefficients of $L_n^{\alpha,c,\sigma^2}(x)$, as follows

$$\begin{cases} b_{n,n} = t_{n+1,n+1}, \\ b_{k-1,n} = t_{k,n+1} + c b_{k,n}, \quad k = n, n-1, \ldots, 1. \end{cases}$$

From (6) the statement holds.

To give an idea of the work done so far, we mention our first attempt to get a new isometry for values of $c < 0$, we tried to construct a new family of martingales

$$\widetilde{Y}^{(i)} = \sum_{\ell=0}^{i-1} \binom{i-1}{\ell} \frac{1}{c^\ell} Y^{(\ell+1)}$$

that are suitable linear combinations of Teugels martingales. If we consider the basis

$$\{(\frac{x}{c} - 1)^n\}_{n \geq 0}$$

then we though that it could be possible to find that $(\frac{x}{c} - 1)^{n-1} \longleftrightarrow \widetilde{Y}^{(n)}$ works as an isometry between S_1 and S_2, but when one computes $\langle (\frac{x}{c} - 1)^{i-1}, (\frac{x}{c} - 1)^{j-1} \rangle_1$ and $\langle \widetilde{Y}^{(i)}, \widetilde{Y}^{(j)} \rangle_2$ one clearly sees that the above process fails. Work is currently underway on a new isometry and we hope to report these findings in a future paper.

By way of conclusion, we would like to remark that the substantial and recent advances (see the nice survey [15]) in these kind of modified inner products, such as the ones studied here, open the door to a vast mine of beautiful, interesting and accessible open problems.

Acknowledgements

The authors are thankful to professor Fabrizio Leisen at the School of Mathematics, Statistics and Actuarial Sciences of University of Kent (England) for useful discussions. This work was partially supported by the Centro de Matemática da Universidade de Coimbra (CMUC) under the project PEst-C/MAT/UI0324/2013. The research of N. Torrado was supported under the grant SFRH/BPD/91832/2012 and the research of E.J. Huertas under the grant SFRH/BPD/91841/2012 both by the Portuguese Government through the Fundação para a Ciência e a Tecnologia (FCT).

References

1. J. Bertoin, Lévy Processes. Cambridge University Press, Cambridge, 1996.
2. T.S. Chihara, *An Introduction to Orthogonal Polynomials*, Gordon and Breach, New York. (1978).
3. T.S. Chihara, *Orthogonal polynomials and measures with end point masses*, Rocky Mountain J. Math. **15** (1985), 705–719.
4. H. Dueñas and F. Marcellán, *Laguerre-Type orthogonal polynomials. Electrostatic interpretation*, Int. J. Pure and Appl. Math. **38** (2007), 345-358.
5. H. Dueñas, E.J. Huertas and F. Marcellán, *Analytic Properties of Laguerre-type Orthogonal Polynomials*, Integral Transforms Spec. Funct. **22** (2011), 107–122.
6. B.Xh. Fejzullahu and R.Xh. Zejnullahu, *Orthogonal polynomials with respect to the Laguerre measure perturbed by the canonical transformations*, Integral Transforms Spec. Funct. **17** (2010), 569–580.
7. E.J. Huertas, F. Marcellán, and F.R. Rafaeli, *Zeros of orthogonal polynomials generated by canonical perturbations of measures*, Appl. Math. Comput. **218** (2012), 7109–7127.
8. F.A. Grünbaum, L. Haine and E. Horozov, *Some functions that generalize the Krall-Laguerre polynomials*, J. Comput. Appl. Math. **106** (1999), 271–297.
9. M.E.H. Ismail, *Classical and Quantum Orthogonal Polynomials in one variable*, Encyclopedia of Mathematics and its Applications Vol **98**, Cambridge University Press, Cambridge, UK. (2005).
10. R. Koekoek, *Generalizations of classical Laguerre polynomials and some q-analogues*. Doctoral Dissertation, Technical University Delft.(1990)
11. J. Koekoek and R. Koekoek, *Differential equation for Koornwinder's generalized Laguerre polynomials*. Proc. Amer. Math. Soc. **112** (1991), 1045–1054.
12. T.H. Koornwinder, *Orthogonal polynomials with weight function* $(1-x)^{\alpha}(1+x)^{\beta}+M\delta(x+1)+N\delta(x-1)$, Canad. Math. Bull. **27** (1984), 205–214.
13. F. Marcellán, A. Branquinho, and J. C. Petronilho, *Classical Orthogonal Polynomials: A Functional Approach*, Acta Appl. Math. **34** (1994), 283–303.
14. F. Marcellán and A. Ronveaux, *Differential equations for classical type orthogonal polynomials*, Canad. Math. Bull. **32** (1989), 404-411.
15. F. Marcellán and Y. Xu, *On Sobolev orthogonal polynomials*, arXiv preprint arXiv:1403.6249 (2014).
16. A.F. Nikiforov and V.B. Uvarov, *Special Functions of Mathematical Physics: An Unified Approach*, Birkhauser Verlag, Basel. (1988).
17. D. Nualart and W. Schoutens, *Chaotic and predictable representations for Lévy processes*, Stochastic processes and their applications 90 (2000) 109–122.
18. W. Schoutens, *An application in stochastics of the Laguerre-type polynomials*, J. Comput. Appl. Math., **133**, Issues 1–2, (2001), 593–600.
19. W. Schoutens, *Stochastic processes and orthogonal polynomials*, in Lecture Notes in Statist., vol **146**, Springer-Verlag, New York, (2000).
20. K. Sato, Lévy processes and infinitely divisible distributions. Cambridge University Studies in Advanced Mathematics, Vol. 68. Cambridge University Press, Cambridge (1999).
21. J.L. Solé and F. Utzet, *Time-Space harmonic polynomials relative to a Lévy processes*, Bernoulli 14 (2008), 1–13.
22. J.L. Solé and F. Utzet, *On the orthogonal polynomials associated with a Lévy processes*, The Annals of Probability 36 (2008), 765–795.
23. G. Szegő, *Orthogonal Polynomials*, 4^{th} ed., Amer. Math. Soc. Colloq. Publ. Series, vol **23**, Amer. Math. Soc., Providence, RI. (1975).

Wald Test and Distance-Based Generalized Linear Models. Actuarial Application.

Eva Boj[1], Teresa Costa[1], Josep Fortiana[2], and Anna Esteve[3]

[1] Departament de Matemàtica Econòmica, Financera i Actuarial, Universitat de Barcelona, Avinguda Diagonal 690, 08034 Barcelona, Spain
(E-mails: evaboj@ub.edu and tcosta@ub.edu)

[2] Departament de Probabilitat, Lògica i Estadística, Universitat de Barcelona, Gran Via de les Corts Catalanes 595, 08007 Barcelona, Spain
(E-mail: fortiana@ub.edu)

[3] Centre d'Estudis Epidemiològics sobre les Infeccions de Transmissió Sexual i Sida de Catalunya (CEEISCAT). Hospital Universitari Germans Trias i Pujol. CIBER Epidemiologia i Salut Pública (CIBERESP), Ctra. de Caet, s/n, 08916 Badalona, Spain (E-mail: aesteve@iconcologia.net)

Abstract. The Distance-Based Generalized Linear Model (DB-GLM) is a generalization of the classical GLM to the DB framework. The DB-GLM is non-linear on original predictors because its information is entered in the model by means of a squared distances matrix. In a previous work, we defined influence coefficients for original factors in the DB-GLM to measure its importance. Now, with the aim to test the null hypothesis that each coefficient is equal to a fixed value, we define a t-like test statistic, we estimate its null hypothesis distribution by a bootstrapping pairs methodology and use it to obtain percentile confidence intervals. We make an example with actuarial data, and we fit the models with the `dbstats` package for `R`.
Keywords: Distance-based generalized linear model, Influence coefficients, Wald test, Confidence intervals, Actuarial science, `R`.

1 Introduction

The DB-GLM, defined in Boj et al.[2], extends the ordinary GLM (McCullagh and Nelder[14] allowing information on predictors to be entered as interdistances between observation pairs instead of as individual coordinates. In turn, these interdistances may have been computed from arbitrary, non-numerical observed predictors.

The estimation process of a DB-GLM is schematically as follows: a Euclidean configuration is obtained by a metric multidimensional scaling-like procedure, then the linear predictor of the underlying GLM is a linear combination of the resulting Euclidean coordinates, latent variables in the model. Therefore influence coefficients of the original observed predictors cannot be computed as in the ordinary GLM.

New Trends in Stochastic Modeling and Data Analysis (pp. 419-428)
Raimondo Manca - Sally McClean - Christos H Skiadas (Eds)

In Boj et al.[4] we proposed a definition of local influence coefficients for the DB-GLM depending on the nature of risk factors (numerical or categorical/binary). These coefficients measure the relative importance of each observed variable. In this paper, we study how to adapt the Wald test of predictor significance to the DB-GLM environment.

To this end, firstly we apply the definition of influence coefficients and the bootstrap by pairs methodology to estimate the distribution of coefficients, as is given in Boj et al.[4]. In this way we are able to estimate the coefficients of the DB-GLM and its associated standard errors. Then, we propose a procedure to adapt the Wald statistic to the DB-GLM. We construct *simple confidence intervals* by using a standard normal distribution, and *percentile t confidence intervals* by using a bootstrap t^* distribution, where both types of confidence intervals are understood in the sense defined in MacKinnon[12]. The t^* distribution of the percentile intervals follows the null hypothesis of the test in the bootstrap data generation process. In this way, the percentile t confidence intervals are useful to test the null hypothesis that a coefficient is equal to a fixed real value.

We illustrate the calculation of percentile t confidence intervals with a well known actuarial dataset. We estimate the related DB-GLM by using the dbglm function of the `dbstats R` package (Boj et al.[3], R Development Core Team[15]).

The paper is structured as follows. In Section 2 we describe the proposed procedure for the Wald test in the DB-GLM. Firstly, in Sub-section 2.1, we recall the definition of influence coefficients; secondly, in Sub-section 2.2, we construct simple and percentile t confidence intervals. In Section 3 we make an example. Finally, in Section 4, we conclude.

2 Hypothesis testing: the Wald test

The main objective of this work is to adapt the Wald test to the DB-GLM. The Wald test contrasts the null hypothesis $H_0 : \beta_j = \beta_0$. The statistic:

$$\tau_j = \frac{\hat{\beta}_j - \beta_0}{std\left(\hat{\beta}_j\right)} \tag{1}$$

follows (in the classical GLM) an asymptotically t distribution. In (1) $\hat{\beta}_j$ is the unrestricted estimate of the parameter $\hat{\beta}_j$ that is being tested and $std(\hat{\beta}_j)$ is its standard error.

In the next two subsections, we propose a procedure to estimate a bootstrapped t^* distribution for the DB-GLM that follows the null hypothesis, $H_0 : \beta_j = \beta_0$. First we recall the definition of influence coefficients and the bootstrap by pairs methodology to estimate coefficient distribution explained in Boj et al.[4]. Then, we show how to construct simple and percentile confidence intervals, taking into account the bootstrapped t^* distribution that follows the null hypothesis of the test.

2.1 Influence coefficients for the DB-GLM

Assume we have a response variable Y observed for n individuals, and a set of p risk factors F_j for $j = 1, \ldots, p$. In ordinary GLM the relation between response and linear predictor is

$$\hat{y} = g^{-1}(\hat{\eta}) = g^{-1}\left(\hat{\beta}_0 + F_1 \cdot \hat{\beta}_1 + F_2 \cdot \hat{\beta}_2 + \cdots + F_p \cdot \hat{\beta}_p\right),$$

where we can measure the influence of the predictor F_j by means of $\hat{\beta}_j$ for $j = 1, \ldots, p$. But in DB-GLM the relation of each observable predictor F_j with the prediction is not linear. The idea underlying our definition in Boj et al.[4] of influence is to mimic that of the $\hat{\beta}_j$ in GLM.

The influence of each F_j we want to quantify depends on a reference/virtual individual $\mathbf{f}^0$ which we take as reference or origin. Let $\mathbf{f}^0 = \left(f_1^0, f_2^0, \ldots, f_p^0\right)$ be the vector with the p predictor values of a reference individual. For instance $\mathbf{f}^0$ consists of mean or median in numerical coordinates and the mode in binary or qualitative coordinates.

For categorical (or binary) predictors we defined the influence coefficients $\hat{\beta}_j$ for $j = 1, \ldots, p$ as the increment in the estimated linear predictor $\hat{\eta}$ when the j-th predictor value of $\mathbf{f}^0$ changes to another level. As a short notation:

$$\beta_j = \Delta j\ \hat{\eta}|_{\mathbf{f}^0} \text{ for } j = 1, \ldots, p$$

For quantitative predictors we define the influence coefficients $\hat{\beta}_j$ for $j = 1, \ldots, p$ as:

$$\beta_j = \left.\frac{\partial \hat{\eta}}{\partial F_j}\right|_{\mathbf{f}0} \text{ for } j = 1, \ldots, p$$

the speed of the estimated linear predictor $\hat{\eta}$ changes as $\mathbf{f}^0$ moves along the curve:

$$\mathbf{f}0 + t \times s_j \left(0, \ldots, 0, \underset{j-th}{1}, 0, \ldots, 0\right), t \in (-\varepsilon, +\varepsilon)$$

where s_j is the standard deviation of the j-th quantitative predictor.

2.2 Bootstrap confidence intervals

There is an extensive literature on the numerous ways to construct bootstrap confidence intervals. MacKinnon[12] proposed that the simplest approach is to calculate the bootstrap standard error and use it to construct confidence intervals based on the normal distribution. A simple confidence interval for β_j at level $1 - \alpha$ is:

$$\left[\hat{\beta}_j - std^*\left(\hat{\beta}_j\right) \times z_{1-\alpha/2}, \hat{\beta}_j + std^*\left(\hat{\beta}_j\right) \times z_{1-\alpha/2}\right], \tag{2}$$

where $z_{1-\alpha/2}$ denotes the $1 - \alpha/2$ quantile of the standard normal distribution. If, e.g., $\alpha = 0.05$ this is equal to 1.96. The simple bootstrap confidence interval

can be modified so that it will be centred on a bias-corrected estimate of β_j by simply replacing $\hat{\beta}_j$ in (2) by $\tilde{\beta}_j = \hat{\beta}_j - \left(\bar{\hat{\beta}}^*_j - \hat{\beta}_j\right) = 2\hat{\beta}_j - \bar{\hat{\beta}}^*_j$.

In Boj et al.[4] we proposed a bootstrap by pairs methodology to estimate the distribution of β_j and its standard deviation, $std^*\left(\hat{\beta}_j\right)$, where we refer for a detailed description of the method.

The pairs bootstrap is easy to implement and it can be applied to a wide range of models. The resampling technique consists of n response-predictor pairs from the original data, see Boj et al.[1],[4], Davidson and Hinkley[5], Efron and Tibshirani[6] or Hall[9] among other references. Then, one can generate B bootstrap samples from which to estimate the statistic of interest. However, the bootstrap data generation process in the bootstrap by pairs does not impose any restrictions on β_j.

If we are testing some restrictions, e.g. $H_0 : \beta_j = \beta_0$, we need to modify the bootstrap data generation process in such a way that the given restrictions are enforced, yielding a valid bootstrap test statistic. A way to proceed is to use the modified bootstrap test statistic:

$$\hat{\tau}^b_j = \frac{\hat{\beta}^b_j - \hat{\beta}_j}{std^*\left(\hat{\beta}_j\right)} \tag{3}$$

where $\hat{\beta}^b_j$ is the estimate of β_j from the b-th bootstrap sample, for $b = 1, \ldots, B$ where B is the sample size, and the denominator $std^*\left(\hat{\beta}_j\right)$ is the standard error of the $\hat{\beta}_j$ distribution. As the estimate of β_j from the bootstrap samples should, on average, be equal to $\hat{\beta}_j$, the null hypothesis tested by $\hat{\tau}^b_j$ is true in the pairs bootstrap data generation process. In this way, we can compare the statistic of the original sample,

$$\hat{\tau}_j = \frac{\hat{\beta}_j - \beta_0}{std^*\left(\hat{\beta}_j\right)},$$

with the bootstrap t^* distribution given by (3), and calculate a p-value by:

$$\hat{p}^*\left(\hat{\tau}_j\right) = \frac{1}{B}\sum_{b=1}^{B} I\left(\left|\hat{\tau}^b_j\right| > \left|\hat{\tau}_j\right|\right),$$

or by,

$$\hat{p}^*\left(\hat{\tau}_j\right) = 2\min\left(\frac{1}{B}\sum_{b=1}^{B} I\left(\hat{\tau}^b_j \leq \hat{\tau}_j\right), \frac{1}{B}\sum_{b=1}^{B} I\left(\hat{\tau}^b_j > \hat{\tau}_j\right)\right).$$

An interval that has better properties than the simple bootstrap confidence interval is the percentile t confidence interval. A percentile t confidence interval for β_j at level $1-\alpha$ is defined as:

$$\left[\hat{\beta}_j - std^*\left(\hat{\beta}_j\right) \times t^*_{1-\alpha/2}, \hat{\beta}_j - std^*\left(\hat{\beta}_j\right) \times t^*_{\alpha/2}\right] \tag{4}$$

where t^*_δ is the δ quantile of the bootstrap distribution of the t^* statistic defined in (3). For example, if $\alpha = 0.05$ then $\alpha/2 = 0.025$ and $1-\alpha/2 = 0.975$ and $t^*_{\alpha/2}$ is the 0.025 quantile of the bootstrap t^* distribution and $t^*_{1-\alpha/2}$ is the 0.975 one. The t^* distribution given by (3) follows the null hypothesis, then the percentile t confidence interval (4) is usefully for the hypothesis testing $H_0 : \beta_j = \beta_0$ with β_0 a fixed real value. With these type of confidence intervals it is not necessary to repeat the calculations if we want to change the value of β_0, unlike what happens with p-values.

3 Application

We use a data set on Swedish third-party motor insurance in 1977 described in Hallin and Ingenbleek[10] and also used in Boj et al.[2],[4]. Data are included in the package `faraway` for `R` under the name *motorins*. The total number of observations is $n = 295$ corresponding to different non-empty risk groups. We analyze claim frequency, defined by the number of claims and the exposure variable number of insured in policy-years. There are three risk factors: Distance (kilometers travelled by year, with 5 levels), Bonus (level in the scale of Bonus, with continuous numerical values from 1 to 7) and Make (with 9 nominal categories). We code Bonus and Distance (using its class mark) as numerical variables and Make as categorical nominal. We assume a Poisson error distribution and the logarithmic link.

We fit DB-GLM to the main effects of the three risk factors, using the dbglm function in the `dbstats` package (see Boj et al.[3]. The similarity is computed with Gower's similarity index (`metric = "gower"`), taking into account all the geometric variability (`rel.gvar = 1`), i.e., the model named `dbglm1` in the Appendix A of Boj et al.[2], with a residual deviance of 454.1 on 276 degrees of freedom:

```
Call:
dbglm(formula = yfactor(MakeC) + KmC + BonC , data = Motor1, family
= poisson(link = "log"), method = "rel.gvar", metric = "gower",
weights = w, rel.gvar = 1)

family:  poisson
metric:  gower

Degrees of Freedom:  294 Total (i.e.  Null); 276 Residual 236
Null Deviance:  6978 237
Residual Deviance:  454.1
```

In Boj et al.[4] eleven coefficients were estimated: nine for the levels *Make1* to *Make9*, and two for the numerical factors *Distance* and *Bonus*. The linear predictor was:

$$\eta = \beta_0 + F_1 \cdot \beta_1 + F_2 \cdot \beta_2 + \cdots + F_{10} \cdot \beta_{10} + \varepsilon =$$
$$\beta_{Make1} + F_{Make2} \cdot \beta_{Make2} + F_{Make3} \cdot \beta_{Make3} + F_{Make4} \cdot \beta_{Make4} +$$
$$F_{Make5} \cdot \beta_{Make5} + F_{Make6} \cdot \beta_{Make6} + F_{Make7} \cdot \beta_{Make7} +$$
$$F_{Make8} \cdot \beta_{Make8} + F_{Make9} \cdot \beta_{Make9} + F_{Km} \cdot \beta_{Km} + F_{Bon} \cdot \beta_{Bon} + \varepsilon.$$

The reference individual chosen was:

$$\mathbf{f}^0 = \left(Make = 1, Km = \overline{Km}, Bon = \overline{Bon}\right) = (1, 9683.82, 5.58)\,,$$

being the class $Make = 1$ the corresponding to the intercept term β_0.

In Boj et al.[4] one can find, in Table 1, the results of the estimated influence coefficients for this model, `dbglm1`, and the corresponding standard errors using size $B = 1000$ for the bootstrap. Table 2 Table 2 contains simple bootstrap confidence intervals, (2), at level 0.95.

Now, we complete the example with a quantitative measure for the significance of predictors using the Wald test. We construct the corresponding percentile t confidence intervals, (4), at level 0.95. In Figures from 1 to 11 we show the histograms of the bootstrap t^* distributions given by (3) for the different predictors of the `dbglm1` model. In Table 1, one can find: in the first column the estimated betas; in the second column the 97.5 quantile of the bootstrapped null distribution given by the 1000 values of (3); in the third column the 2.5 quantile of the same bootstrap distribution; and in the fourth column the percentile t confidence intervals given by (4). As a result, we do not have the 0 value in any of the percentile t confidence intervals of Table 1, and it means that all the coefficients are significant in the `dbglm1` model.

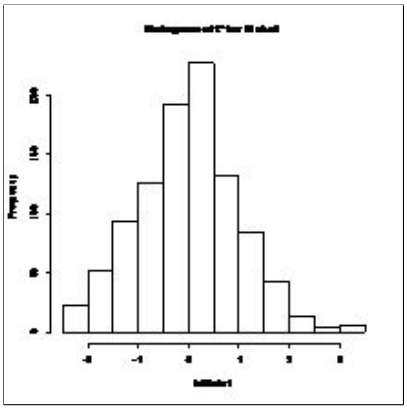

Fig. 1. Bootstrap t^* distribution of $\hat{\beta}_{Make1}$ for the `dbglm1` model.

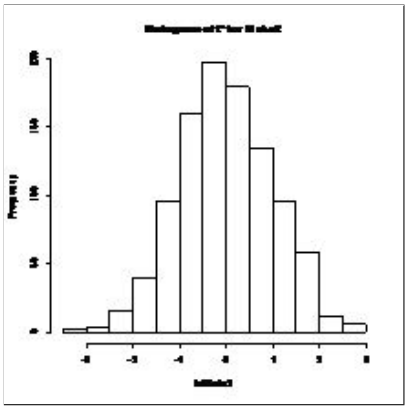

Fig. 2. Bootstrap t^* distribution of $\hat{\beta}_{Make2}$ for the `dbglm1` model.

4 Conclusions

In Boj et al.[4] we define -local valid- influence coefficients for the DB-GLM. Additionally, we propose a bootstrap methodology to estimate standard errors

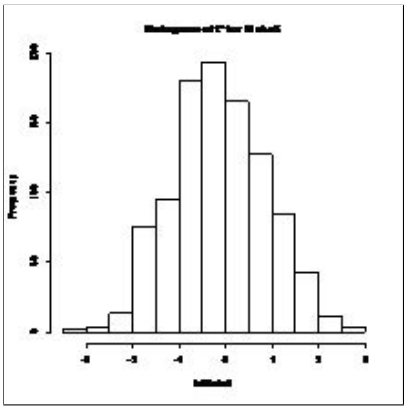

Fig. 3. Bootstrap t^* distribution of $\hat{\beta}_{Make3}$ for the `dbglm1` model.

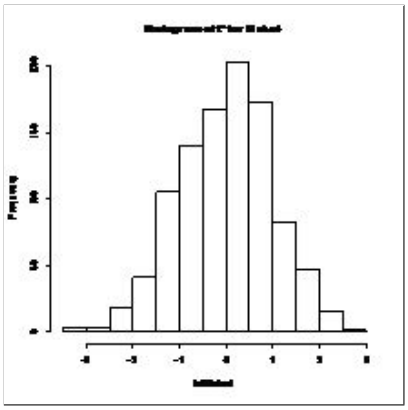

Fig. 4. Bootstrap t^* distribution of $\hat{\beta}_{Make4}$ for the `dbglm1` model.

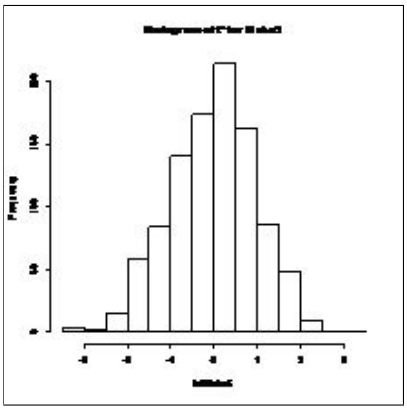

Fig. 5. Bootstrap t^* distribution of $\hat{\beta}_{Make5}$ for the `dbglm1` model.

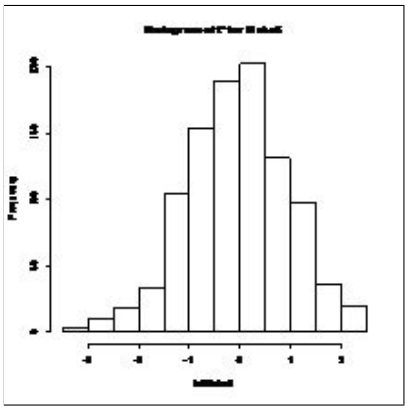

Fig. 6. Bootstrap t^* distribution of $\hat{\beta}_{Make6}$ for the `dbglm1` model.

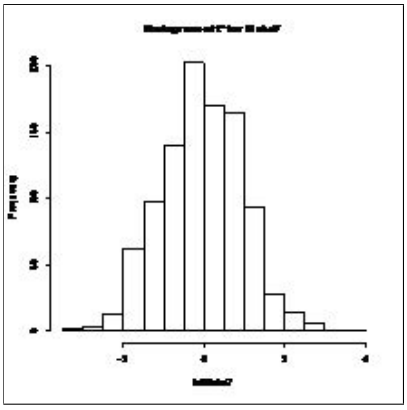

Fig. 7. Bootstrap t^* distribution of $\hat{\beta}_{Make7}$ for the `dbglm1` model.

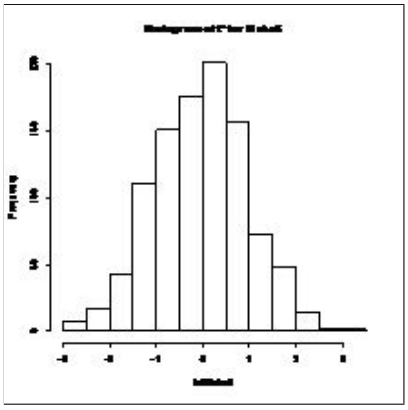

Fig. 8. Bootstrap t^* distribution of $\hat{\beta}_{Make8}$ for the `dbglm1` model.

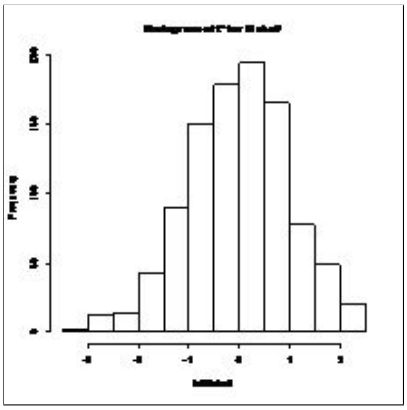

Fig. 9. Bootstrap t^* distribution of $\hat{\beta}_{Make9}$ for the `dbglm1` model.

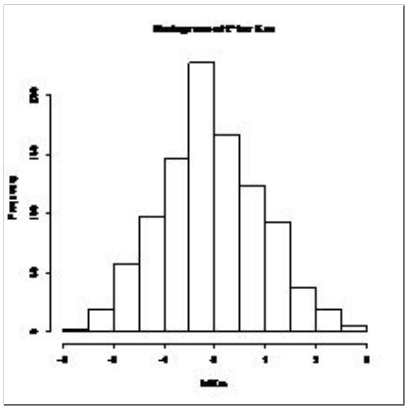

Fig. 10. Bootstrap t^* distribution of $\hat{\beta}_{Km}$ for the `dbglm1` model.

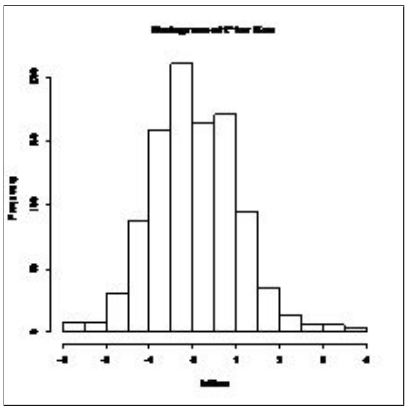

Fig. 11. Bootstrap t^* distribution of $\hat{\beta}_{Bon}$ for the `dbglm1` model.

and to calculate simple bootstrap confidence intervals as an informative measure. The proposed bootstrap methodology is bootstrapping pairs which could be adequate when we use DB regression models (see Boj et al.[1]).

The pairs bootstrap is very easy to implement and it can be applied to a wide range of models. However it sufers from two major deficiencies (see MacKinnon[11],[12],[13]). The first is that the bootstrap data generation process does not impose any restriction on β_j. Then, if we are testing restrictions on β_j, as opposed to estimating standard errors or forming simple confidence intervals, we need to modify the bootstrap test statistic so that it will test something that will be true in the bootstrap data generation process. Or, alternatively, we can modify the resampling scheme so that the null hypothesis will be respected in the bootstrap data generating process, see Boj et al.[1] and Flachaire[7],[8]. The other deficiency of the pairs bootstrap is that, compared with the residual bootstrap (when it is valid) and with the wild bootstrap, the pairs bootstrap generally does not yield very accurate results. But the pairs bootstrap is less

	$\hat{\beta}$	$t^*_{1-\alpha/2}$	$t^*_{\alpha/2}$	Percentile t confidence intervals
$\hat{\beta}_{Make1}$	$-1.857e+0$	1.962086	-1.908919	$[-1.860e+0, -1.853e+0]$
$\hat{\beta}_{Make2}$	$1.312e-01$	1.882888	-1.849325	$[1.251e-01, 1.371e-01]$
$\hat{\beta}_{Make3}$	$-2.142e-01$	1.828144	-1.976043	$[-2.260e-01, -2.014e-01]$
$\hat{\beta}_{Make4}$	$-4.977e-01$	1.930592	-2.144194	$[-5.028e-01, -4.919e-01]$
$\hat{\beta}_{Make5}$	$1.239e-01$	1.81118	-1.968902	$[1.178e-01, 1.305e-01]$
$\hat{\beta}_{Make6}$	$-3.880e-01$	1.916472	-2.03158	$[-3.926e-01, -3.832e-01]$
$\hat{\beta}_{Make7}$	$-1.304e-01$	1.968073	-1.909681	$[-1.410e-01, -1.200e-01]$
$\hat{\beta}_{Make8}$	$1.363e-01$	1.872734	-1.998162	$[1.081e-01, 1.664e-01]$
$\hat{\beta}_{Make9}$	$-2.361e-02$	1.799623	-2.038099	$[-2.597-02, -2.093e-02]$
$\hat{\beta}_{Km}$	$1.069e-05$	2.022189	-1.953856	$[1.050e-05, 1.087e-05]$
$\hat{\beta}_{Bon}$	$-3.733e-02$	2.113138	-1.685741	$[-4.111e-02, -3.431e-02]$

Table 1. Estimated coefficients; quantiles 97.5 and 2.5 of the t^* distributions; and percentile t confidence intervals assuming $\alpha = 0.05$, for the `dbglm1` model.

sensible to the hypotheses of the model than the residual bootstrap. And the estimated standard error via the pairs bootstrap offers reasonable results when some hypotheses of the model are not satisfied.

To complete the study of influence coefficients for the DB-GLM initiated in Boj et al.[4], in this work we propose a procedure to obtain an estimation of the Wald statistic. Our objective is to contrast the null hypothesis, $H_0 : \beta_j = \beta_0$. For this aim, we compute percentile t confidence intervals given by formula (4). The bootstrapped t^* distribution given by (3) follows the null hypothesis, then the percentile t confidence interval (4) is adequate for the hypothesis testing $H_0 : \beta_j = \beta_0$ given β_0 a fixed real value. With these type of confidence intervals it is not necessary to repeat the calculations if we want to contrast the null hypothesis for different values of β_0, unlike what happens when using p-values.

In the example, we have calculated percentile t confidence intervals for the coefficients of the *motorins* dataset related to the model with the main effects, named tt dbglm1. And we have obtained that all risk factors could be entered as a tariff variables in the final model.

The most important result of this work is that with the defined bootstrap percentile t confidence intervals we can study in an statistical way the significance of the influence coefficients defined in Boj et al.[4] for the DB-GLM. And this is an important question in actuarial rate-making, where the selection of risk factors is the basis of the problem.

Acknowledgments Work supported in part by the Spanish Ministerio de Educación y Ciencia and FEDER, grant MTM2010-17323, and by Generalitat de Catalunya, AGAUR grant 2014SGR152.

References

1. E. Boj, M.M. Claramunt and J. Fortiana. Selection of predictors in distance-based regression. *Communications in Statistics A. Theory and Methods*, 36, 87–98, 2007.

2. E. Boj, P. Delicado, J. Fortiana, A. Esteve and A. Caballé. Local distance-based generalized linear models using the dbstats package for R. *Documentos de Trabajo de la Xarxa de Referència en Economia Aplicada (XREAP)*, XREAP2012-11, 2012.
3. E. Boj, A. Caballé, P. Delicado, and J. Fortiana. *dbstats: Distance-Based Statistics (dbstats)*. `R` package version 1.0.3, 2013, URL `http://CRAN.R-project.org/package=dbstats`.
4. E. Boj, T. Costa, J. Fortiana and A. Esteve. Assessing the Importance of Risk Factors in Distance-Based Generalized Linear Models. *Methodology and Computing in Applied Probability*, `http://link.springer.com/article/10.1007/s11009-014-9415-6`, 2014.
5. A.C. Davidson and D.V. Hinkley. *Bootstrap methods and their application*, Cambridge University Press, New York, 1997.
6. B. Efron and J. Tibshirani. *An Introduction to the Bootstrap*, Chapman & Hall, New York, 1998.
7. E. Flachaire. A better way to bootstrap pairs. *Economics Letters*, 64, 257–262, 1999.
8. E. Flachaire. Bootstrapping heteroskedastic regression models: wild bootstrap vs. pairs bootstrap. *Computational Statistics & Data Analysis*, 49, 361–376, 2005.
9. P. Hall. *The Bootstrap and Edgeworth Expansion. Springer Series in Statistics.*, Springer, New York, 1992.
10. M. Hallin and J.F. Ingenbleek. The Swedish automobile portfolio in 1977. A statistical study. *Scandinavian Actuarial Journal*, 49–64, 1983.
11. J.G. MacKinnon. Bootstrap inference in econometrics. *The Canadian Journal of Economics* 35, 4, 615–645, 2002.
12. J.G. MacKinnon. Bootstrap methods in econometrics. *The Economic Record* 82, special issue, september 2006, s2–s18, 2006.
13. J.G. MacKinnon. Bootstrap hypothesis testing. *Queen's Economics Department Working Paper*, Number 1127, 2007.
14. P. McCullagh and J.A. Nelder. *Generalized Linear Models (2nd ed)*. Chapman and Hall, London, 1989.
15. `R` Development Core Team (2014). `R`*: A Language and Environment for Statistical Computing*. Vienna, Austria, URL `http://www.R-project.org/`.

Author Index

New Trends in Stochastic Modeling & Data Analysis

This is the first book devoted to the 3rd Stochastic Modeling Techniques and Data Analysis (SMTDA) International Conference held in Lisbon, Portugal, June 11-14, 2014. Revised and expanded forms of papers from the conference presentations are included.

The first Chapter includes papers on Asymptotic Analysis of Stochastic Systems with Complex Structure, whereas contributions on Markov and semi-Markov models are included in the second Chapter.

Papers on Clustering and Partitioning for particular cases are included in the third Chapter, and papers on Survival Analysis and Branching Processes are presented in the fourth Chapter.

Papers on Stochastics methods and techniques are presented in the fifth Chapter along with Data Analysis papers included in the sixth Chapter.

Chapter seven includes papers on Demography and Related Applications, whereas Stochastic Processes, Copulas and Actuarial Applications are analyzed in Chapter eight.

This book, like others in this SMTDA series, is directed towards researchers and others in the fields of probability and statistics, data analysis and forecasting, demography and insurance, finance and management. It is a valuable tool for demographers, actuaries, mathematicians and statisticians, economists and policy makers.

Raimondo Manca-Sally McClean-Christos H Skiadas, *Eds*

ISBN 978-6-18-518006-5

9 786185 180065

ISAST 2015